

4-1-2020

Isolation and Characterization of Potential Neurotoxic Cyanobacterial Metabolites Associated with Intoxication of Captive Bottlenose Dolphins in the Florida Keys

Christina Lydon

Department of Chemistry and Biochemistry, Florida International University, clydo002@fiu.edu

Follow this and additional works at: <https://digitalcommons.fiu.edu/etd>

 Part of the [Chemistry Commons](#)

Recommended Citation

Lydon, Christina, "Isolation and Characterization of Potential Neurotoxic Cyanobacterial Metabolites Associated with Intoxication of Captive Bottlenose Dolphins in the Florida Keys" (2020). *FIU Electronic Theses and Dissertations*. 4388.

<https://digitalcommons.fiu.edu/etd/4388>

This work is brought to you for free and open access by the University Graduate School at FIU Digital Commons. It has been accepted for inclusion in FIU Electronic Theses and Dissertations by an authorized administrator of FIU Digital Commons. For more information, please contact dcc@fiu.edu.

FLORIDA INTERNATIONAL UNIVERSITY

Miami, Florida

ISOLATION AND CHARACTERIZATION OF POTENTIAL NEUROTOXIC
CYANOBACTERIAL METABOLITES ASSOCIATED WITH INTOXICATION OF
CAPTIVE BOTTLENOSE DOLPHINS IN THE FLORIDA KEYS

A dissertation submitted in partial fulfillment of

the requirements for the degree of

DOCTOR OF PHILOSOPHY

in

CHEMISTRY

by

Christina A. Lydon

2020

To: Dean Michael R. Heithaus
College of Arts, Sciences and Education

This dissertation, written by Christina A. Lydon, and entitled Isolation and Characterization of Potential Neurotoxic Cyanobacterial Metabolites Associated with Intoxication of Captive Bottlenose Dolphins in the Florida Keys, having been approved in respect to style and intellectual content, is referred to you for judgment.

We have read this dissertation and recommend that it be approved.

Ligia Collado-Vides

Anthony P. DeCaprio

Piero R. Gardinali

Johanna Mejia-Fava

Yuk-Ching Tse-Dinh

John P. Berry, Major Professor

Date of Defense: April 1, 2020

The dissertation of Christina A. Lydon is approved.

Dean Michael R. Heithaus
College of Arts, Sciences and Education

Andrés G. Gil
Vice President for Research and Economic Development
and Dean of the University Graduate School

Florida International University, 2020

© Copyright 2020 by Christina A. Lydon

All rights reserved.

DEDICATION

I dedicate this dissertation to Valerie J. Paul, Ph.D., Director of the Smithsonian Marine Station at Fort Pierce, for being an amazing mentor and incredible philanthropist in the pursuit of marine science.

ACKNOWLEDGMENTS

Foremost, I extend my utmost gratitude to my family for their enduring love and patience, and for everything sacrificed for me to achieve this life goal. Secondly, I am indebted to the extreme altruism of Valerie Paul of the Marine Science Station at Fort Pierce, FL (SMS) for affording me invaluable mentoring and opportunities to complete this research project. Sarath Gunasekera at the SMS is also immensely appreciated for all the chemical analyses (LC-MS, NMR), separation science support and kind-hearted wisdom he provided. Sincere gratitude is given to Rina Dukor at BioTools Inc., for charitably providing the expertise of Juanita Sanchez to obtain the absolute configuration of my compound using Vibrational Circular Dichroism. Logesh Mathivathanan and Raphael Raptis (FIU) generously conducted single crystal x-ray crystallography. Kevin Montenegro and Ligia Collado-Vides (FIU Marine Macroalgae Lab) gratefully assisted with morphology-based macroalgae taxonomic assessments. I kindly thank my research advisor, John P. Berry, and the Dolphin Plus research team for this unique, collaborative project. Especially thanked from Dolphins Plus are Dr. Johanna Mejia-Fava, Holli Eskelinen and the staff who collected algal samples and dolphin data. I recognize each of my committee members, Ligia Collado-Vides, Anthony DeCaprio, Piero Gardinali, Yuk-Ching Tse-Dinh, and Dr. Johanna Mejia-Fava for their subject matter expertise, guidance and time.

I sincerely appreciate the Department of Chemistry and Biochemistry for funding me via continued Teaching Assistance Grants. I acknowledge the University Graduate School for generously awarding me the Spring 2018 Dissertation Year Fellowship. Lastly, I thank everyone at FIU who helped me along the way.

ABSTRACT OF THE DISSERTATION

ISOLATION AND CHARACTERIZATION OF POTENTIAL NEUROTOXIC
CYANOBACTERIAL METABOLITES ASSOCIATED WITH INTOXICATION OF
BOTTLENOSE DOLPHINS IN THE FLORIDA KEYS

by

Christina A. Lydon

Florida International University, 2020

Miami, Florida

Professor John P. Berry, Major Professor

Bottlenose dolphins (*Tursiops truncatus*) living in captivity in the Florida Keys have recently been observed grazing macrophytic algal communities, and particularly, filamentous cyanobacteria, within their enclosures, and subsequently presenting apparent signs of intoxication. Collections of a mixed assemblage of marine filamentous cyanobacteria were morphologically related to the taxonomically complex and toxigenic polyphyletic genus *Lyngbya*, *sensu lato*. Phylogenetic characterization, using 16S rDNA methods, identified an undescribed member of the recently accepted genus *Neolyngbya* (Oscillatoriales) among *Neolyngbya arenicola*, and an unknown Oscillatoriacean species within a poorly resolved clade clustering between the genera *Limnoraphis* and *Capilliphycus*.

A dual approach was subsequently utilized to identify a putative neurotoxic metabolite from cyanobacteria associated with the intoxication events. Initial chemical screening was unable to detect recognized algal and cyanobacterial neurotoxins including anatoxin-a, brevetoxin-2 (PbTx-2), domoic acid, β -methylamino-L-alanine and saxitoxin.

In tandem, however, toxicity testing – and concomitant bioassay-guided fractionation-based on early life stages (i.e., embryo, larvae) of the zebrafish (*Danio rerio*) as a vertebrate toxicological model, was employed to identify relevant metabolites from cyanobacterial collections. Using the latter approach, relevant toxicity including, particularly, endpoints of neurotoxicity were identified for extracts and subsequent fractions. Apparent neurotoxicity was comparatively assessed against the recognized algal neurotoxin, PbTx-2. Crude lipophilic extracts, and subsequent chemical fractions, notably aligned with observed neurotoxic effects of PbTx-2. Further bioassay-guided fractionation enabled purification and structural elucidation of a previously undocumented, neurotoxic metabolite, (4*S*,5*R*,6*R*,7*S*,10*S*)-eudesman-(4*S*,6*R*)-cyclocarbonate (i.e., eudesmacarbonate), from the mixed filamentous cyanobacteria (dominated by *Neolyngbya* sp.) which, may, in turn, contribute to the observed intoxications of captive dolphins.

TABLE OF CONTENTS

CHAPTER	PAGE
1. INTRODUCTION	1
1.1 Project Overview and Significance.....	1
1.1.1 Major Objective 1 – Algal Community Assessment	2
1.1.2 Major Objective 2 – Chemical Exploration for Potential Neurotoxin(s).....	2
1.2 Chapter Foci.....	2
1.3 Background and Theory.....	4
1.3.1 Marine Algal Community Diversity	5
1.3.2 Microalgae and Cyanobacteria Membership	7
1.3.3 Taxonomic Approaches	9
1.3.4 Eutrophication Issues	11
1.3.5 Harmful Algal Bloom (HAB) Potential.....	12
1.4 Zebrafish (<i>Danio rerio</i>) Bioassay Rationale.....	14
1.4.1 Developmental Toxicity Protocols for Cyanotoxins.....	15
1.4.2 Larval Neurobehavioral Assessments for Neurotoxicity	16
1.5 Key Questions to be Addressed	17
1.6 References.....	18
2. TAXONOMIC CHARACTERIZATION OF ALGAL AND CYANOBACTERIA COMMUNITIES	32
2.1 Introduction.....	32
2.1.1 Taxonomic Survey of Dominant Macroalgae and Cyanobacteria.....	36
2.1.2 Associated Neurotoxic Metabolites	36
2.2 Methodologies.....	36
2.2.1 Sampling of Dominant Macroalgae and Cyanobacteria	36
2.2.1.1 Sampling Process	37
2.2.1.2 Taxonomic Reference Samples.....	38
2.2.1.3 Cyanobacteria Phylogenetic Samples	39
2.2.1.4 Cyanobacteria Chemical Evaluation Samples	39
2.2.1.5 Microalgae Evaluation Samples	40
2.3 Taxonomic Characterization Procedures	41
2.3.1 Morphology-Based Identification.....	41
2.3.2 Chemical Analysis of Cyanobacteria by Low-Resolution LC-MS.....	42
2.3.3 Cyanobacteria Phylogeny	42
2.3.4 Microalgae Assessments.....	44
2.4 Results.....	44
2.4.1 Morphology-Based Identifications of Dominant Macroalgae and Cyanobacteria Taxonomies.....	45
2.4.2 Low-Resolution LC-MS Analysis of Dominant Cyanobacteria Morphotypes	54
2.4.3 Cyanobacteria Phylogenetic Characterization	57
2.4.4 Potential Neurotoxicogenic Microalgae Taxa Observations	57

2.4.5	Associated Neurotoxicogenic Taxa (Literature Search).....	62
2.5	Discussion.....	67
2.6	Conclusions.....	71
2.7	Acknowledgments.....	74
2.8	References.....	75
3.	CAPTIVE DOLPHIN ALGAL GRAZING AND INTOXICATION EVENTS.....	86
3.1	Introduction.....	86
3.2	Procedures.....	88
3.2.1	Process for Logging Observed Captive Dolphin Algal Grazing and Intoxications.....	88
3.2.2	Lagoon Water Quality Assessments.....	88
3.2.3	Correlation Assessments of Captive Dolphin Observations.....	88
3.3	Results.....	90
3.3.1	Captive Dolphin Observation Data and Correlation Assessments.....	90
3.3.2	Lagoon Water Quality Data and Correlation Assessments.....	108
3.4	Discussion.....	117
3.5	Conclusions.....	123
3.6	Acknowledgments.....	124
3.7	References.....	124
4.	CHEMICAL EVALUATION OF CYANOBACTERIA BIOMASS FOR KNOWN NEUROTOXINS.....	126
4.1	Introduction.....	126
4.1.1	Anatoxin-a (ATX-a).....	130
4.1.2	β -methylamino-L-alanine (BMAA).....	135
4.1.3	Saxitoxin (STX).....	140
4.1.4	Brevetoxin-2 (PbTx-2).....	145
4.1.5	Domoic Acid (DA).....	151
4.1.6	Investigation Targets.....	156
4.1.6.1	Known <i>Lyngbya</i> spp. Neurotoxins.....	156
4.1.6.2	Known Marine HAB-Microalgae Neurotoxins.....	156
4.2	Chemical Evaluation Methodologies.....	156
4.2.1	BMAA Analysis.....	157
4.2.1.1	BMAA Materials and Sample Preparation.....	157
4.2.1.2	BMAA Extraction and Mass Analysis Sample Preparation.....	158
4.2.1.3	BMAA MALDI-TOF-MS Analysis.....	159
4.2.1.4	BMAA LC-MS/MS Analysis.....	160
4.2.2	STX Analysis.....	161
4.2.2.1	STX Materials and Sample Preparation.....	161
4.2.2.2	STX Extraction and Mass Analysis Sample Preparation.....	162
4.2.2.3	STX LC-MS/MS Analysis.....	163
4.2.3	Commercial Chemical Evaluations.....	164
4.2.3.1	ATX-a Sample Preparation and LC-MS/MS Analysis.....	164
4.2.3.2	DA Sample Preparation and LC-MS/MS Analysis.....	165

4.2.3.3	STX Sample Preparation and ELISA Analysis	165
4.2.3.4	PbTx-2 Sample Preparation and ELISA Analysis	166
4.3	Results and Discussion	166
4.3.1	BMAA Results.....	166
4.3.2	STX Results	167
4.3.3	ATX-a Results	168
4.3.4	DA Results.....	168
4.3.5	PbTx-2 Results.....	169
4.3.6	Results Summary	169
4.4	Conclusions.....	172
4.5	Acknowledgments.....	173
4.6	References.....	174
5.	BIOASSAY-GUIDED INQUEST OF A MARINE FILAMENTOUS CYANOBACTERIAL ASSEMBLAGE ASSOCIATED WITH INTOXICATIONS OF CAPTIVE BOTTLENOSE DOLPHINS (<i>TURSIOPS TRUNCATUS</i>) IN THE FLORIDA KEYS USING ZEBRAFISH (<i>DANIO RERIO</i>) MODELS OF NEUROTOXICITY (in preparation for Harmful Algae)	194
5.1	Abstract.....	194
5.2	Introduction.....	195
5.3	Methods and Materials.....	198
5.3.1	Cyanobacteria Material.....	198
5.3.2	Chemical Explorations of Cyanobacteria Samples.....	199
5.3.2.1	Known Neurotoxin Evaluation of Cyanobacteria Samples	199
5.3.2.2	Bioassay-Guided Fractionation of Cyanobacteria Samples Using Zebrafish Neurotoxicological Models	200
5.4	Results.....	203
5.4.1	Average Percent Mortality of Embryos	206
5.4.2	Average Percent Deformed Embryos	208
5.4.3	Average 24-hpf Spontaneous Coiling Frequencies.....	214
5.4.4	Average Embryo Hatching Rates and Percentages.....	217
5.4.5	Average Day 2 and Day 3 Embryonic Heart Rate Measurements.....	220
5.4.6	Average Swimming-related Assessments of 5-dpf Larvae.....	227
5.4.6.1	Chronic Embryonic Exposure Swimming Assessments.....	227
5.4.6.2	Acute Larval Exposure Swimming Assessments	233
5.5	Discussion	241
5.6	Conclusions.....	248
5.7	Acknowledgments.....	249
5.8	References.....	250
6.	EUDESMACARBONATE AN EUDESMANE-TYPE SESQUITERPENE FROM MARINE FILAMENTOUS CYANOBACTERIAL MAT (OSCILLATORIALES) IN THE FLORIDA KEYS (submitted, Journal of Natural Products)	255
6.1	Abstract.....	255
6.2	Introduction.....	255

6.3	Methods.....	257
6.3.1	Biological Material	257
6.3.2	DNA Sequencing and Phylogenetics	257
6.3.3	Extraction and Isolation of Eudesmacarbonate.....	258
6.3.4	Chemical Characterization of Eudesmacarbonate	259
6.3.5	X-ray Crystallographic Analysis.....	260
6.3.6	Experimental VCD Analysis.....	261
6.3.7	Zebrafish Neurotoxicity Assays.....	261
6.3.7.1	Zebrafish Embryogenic Neurotoxicity Assay.....	262
6.3.7.2	Zebrafish Larval-Behavioral Neurotoxicity Assay	263
6.3.7.3	Statistical Analysis of Zebrafish Biological Assay Data	263
6.4	Results and Discussion	263
6.4.1	Purification of Eudesmacarbonate by Bioassay-Guided Fractionation	265
6.4.2	Structural Elucidation of Eudesmacarbonate.....	266
6.4.3	Biological Activity of Eudesmacarbonate	279
6.5	Conclusions.....	294
6.6	Acknowledgments.....	295
6.7	References.....	296
7.	SUMMARY AND PROSPECT	300
7.1	Summary Results of Research Project.....	300
7.2	Prospects of Cyanobacteria Biological and Chemical Diversity	302
7.3	Future Directions	304
7.4	References.....	305
	APPENDICES	306
	VITA.....	390

LIST OF TABLES

TABLE	PAGE
2.1 Dominant macrophyte taxa identified by morphology	46
2.2 Dominant cyanobacteria taxa identified by morphology.....	47
2.3 Algae and cyanobacteria sampling dates	47
2.4 Observed seasonality of dominant chlorophyte genera	48
2.5 Average measurements of representative cyanobacteria filaments collected December 2018	54
3.1 Summary of reported algal ingestions and intoxication events, by date(s) observed, for a mother-daughter captive dolphin pair	91
3.2 Frequency table of total intoxications observed between 2011 and 2014	95
3.3 Results of Shapiro-Wilk normality test of monthly intoxication observations during 2011-2014.....	95
3.4 Total days per month algal ingestions and intoxications were reported for the mother-daughter captive dolphin pair during 2013 and 2014.....	98
3.5 Summary of total days algal ingestions were observed, by algae type, for both captive dolphins during 2013 and 2014.....	99
3.6 Summary of algae-specific ingestions relevant to intoxication events.....	100
3.7 Overall diversity of observed intoxication incidents by algae type.....	101
3.8 Average algal grazing habits of the mother and daughter captive dolphins observed during 2013 and 2014.....	102
3.9 Summary results of Pearson’s Chi-Square test for independence between intoxications and algal ingestions for the mother-daughter captive dolphin pair...	107
3.10 Summary results of Pearson’s Chi-Square test for independence between intoxications and <i>Ulva</i> spp. ingestions for the mother-daughter captive dolphin pair	107
3.11 Summary results of Pearson’s Chi-Square test for independence between intoxications and seasonal algal ingestions for the mother-daughter captive dolphin pair	108

3.12	Average monthly site seawater quality parameters measured 2011-2014.....	109
3.13	Results of Shapiro-Wilk normality test of 2011-2014 AWT (°C) measurements ..	109
3.14	Results of Shapiro-Wilk normality test of 2011-2014 measured AFC (units per 100 mL seawater).....	109
4.1	Example neurotoxigenic HAB organisms	127
4.2	Correlation of HAB neurotoxins to compound class and source organism(s)	130
4.3	The prominent ATX-a producing cyanobacteria (Cyanophyceae) taxa	131
4.4	The prominent BMAA producing cyanobacteria (Cyanophyceae) taxa	136
4.5	The prominent STX producing cyanobacteria (Cyanophyceae) taxa.....	141
4.6	The cyanobacteria collections chemically screened for potential known neurotoxins.....	157
4.7	The cyanobacteria samples chemically evaluated for the presence of BMAA	158
4.8	The cyanobacteria samples chemically assessed for the presence of STX.....	162
4.9	Summary results for cyanobacteria samples chemically screened for known neurotoxins.....	172
6.1	NMR spectroscopic data for eudesmacarbonate (1) in (CD ₃) ₂ CO (¹ H 600 MHz, ¹³ C 151 MHz).....	270
6.2	Crystallographic data and structure refinement of eudesmacarbonate (1)	275
6.3	Numerical comparison between the calculated IR and VCD spectra for the (4 <i>S</i> ,5 <i>R</i> ,6 <i>R</i> ,7 <i>S</i> ,10 <i>S</i>) enantiomer of eudesmacarbonate (1)	276
6.4	Average 24-hpf embryo SCF as coils per minute (cpm) per exposure condition...281	
6.5	Average D2 HR (bpm) data of embryos per exposure condition	284
6.6	Average D3 HR (bpm) data of embryos per exposure condition	286
6.7	Average D5 percent SBD of embryos per exposure condition.....	289
6.8	Average D5 percent ASB of embryos per exposure condition.....	290
6.9	Average 2-hpe percent XSB data of larvae per treatment	293
6.10	Average 12-hpe percent XSB of larvae per treatment.....	294

LIST OF FIGURES

FIGURE	PAGE
2.1 Taxonomic composition as percentages of the dominant macroalgae and cyanobacteria phyla by a) genus biodiversity and b) species biodiversity	48
2.2 Dominant Chlorophyta: a <i>Caulerpa mexicana</i> , b <i>Ulva</i> spp. (e.g., <i>U. lactuca</i> , <i>U. rigida</i>), and c <i>Halimeda</i> spp. (e.g., <i>H. discoidea</i> , <i>H. scabra</i>). Photo credit: C. Lydon	49
2.3 Representative samples of epiphytic and dense, benthic mats of filamentous cyanobacteria collected during the study (e.g., October 2014): a red and green epiphytic, b yellow and purple tufts and c red, red-hairy and green benthic mats mixed, respectively within red and green macroalgae. Photo credit: C. Lydon	50
2.4 Light microscopy images of representative mixed assemblage filamentous cyanobacteria collections: (A) October 2014 benthic mat (10×) (B) October 2014 benthic mat (40×), (C) October 2014 purple tufts (10×), and (D) June 2015 yellow tufts (10×). Digital micrograph credit: C. Lydon.....	51
2.5 Digital micrographs of <i>Lyngbya</i> spp. morphotypes based on initial morphological examinations and comparisons with taxonomic classifications referenced from available field guides: a <i>L. polychroa</i> (63×), b-c <i>L. majuscula</i> (40×), d <i>L. majuscula</i> (63×), and e <i>L. confervoides</i> (40×). Digital image credit: C. Lydon	51
2.6 Mixed assemblage filamentous cyanobacteria collected December 2018 (20×). Digital micrograph courtesy of Michael J. Boyle (Smithsonian Marine Station at Fort Pierce, Fort Pierce, FL, USA)	53
2.7 Representative mixed assemblage cyanobacteria filament morphotypes collected December 2018 (40×): a-b dark green (V), c-d dark red (II), e from left to right - thin greens (TG), red beads (RB) and large red (FR), f-g epiphytic gray bead-like chains (GB) and h purple (P). Digital micrographs courtesy of Michael J. Boyle (Smithsonian Marine Station at Fort Pierce, Fort Pierce, FL, USA)	53
2.8 Low-resolution LC-MS of the dark green cyanobacteria morphotype (V) displaying the elution of the bioactive metabolite (i.e., eudesmacarbonate) at 10.30 minutes with MH indicating the [M+H] ⁺ peak	55
2.9 Low-resolution LC-MS of the dark red cyanobacteria morphotype (II) displaying the elution of a secondary metabolite at 10.13 minutes with MH indicating the [M+H] ⁺ peak and MNa indicating the [M+Na] ⁺ peak	56

2.10	Unidentified microalgae examples, epiphytic to the October 2014 <i>Lyngbya</i> spp. taxonomic reference sample (40×): a diatom and b dinoflagellate. Digital micrograph credit: C. Lydon.....	57
2.11	Epiphytic diatoms resembling <i>Pseudo-nitzschia</i> spp. versus literature image: a epiphytic diatoms on the October 2014 <i>Lyngbya</i> spp. taxonomic reference sample (40×) and b reference image of <i>P. cf. australis</i> . Digital image credits: a C. Lydon, b Gabriella Hannach (2014).....	58
2.12	Example FlowCam micrographs of 20-100 µm filtered particulates from the June 2015 site seawater collection. Digital image credit: C. Lydon.....	59
2.13	Comparative FlowCam images of unidentified dinoflagellates resembling <i>Karenia brevis</i> versus literature image: a-c FlowCam images from the June 2015 site seawater sample and d published FlowCam image of <i>K. brevis</i> . Digital image credits: a-c C. Lydon, d Campbell et al. (2013).....	59
2.14	Comparison of unidentified June 2015 site seawater dinoflagellate versus literature examples: A <i>Ceratium lineatum</i> , B FlowCam image, C <i>Ceratium pentagonum</i> and D <i>Neoceratium minutum</i> . Digital image credits: A Gómez et al. (2010), B C. Lydon, C-D Gómez et al. (2010)	60
2.15	Comparison of unidentified June 2015 site seawater dinoflagellate resembling <i>Ceratoperidinium falcatum</i> versus reference image: A FlowCam image and B C. <i>falcatum</i> reference image. Digital image credits: A C. Lydon, B Gárate-Lizárraga (2014).....	60
2.16	FlowCam images of diatoms observed in site seawater collected June 2015: a unidentified diatom (e.g., <i>Licmophora</i> spp.), b unidentified triradiate diatom (e.g., <i>Centronella</i> spp.), c unidentified diatom and d unidentified diatom (e.g., <i>Amorpha</i> spp., <i>Cymbella</i> spp.). Digital image credit: C. Lydon.....	61
2.17	Example diatoms observed by light microscopy in the October 2014 <i>Lyngbya</i> spp. taxonomic reference sample (40×): a unidentified diatom (e.g., <i>Bellerochea</i> spp.), b triradiate diatom form (e.g., <i>Centronella</i> spp.), c unidentified diatom similarly observed by FlowCam, and d unidentified diatom. Digital image credit: C. Lydon	62
3.1	Monthly intoxication intervals observed for the mother and daughter captive dolphins, plotted consecutively from 2011 through 2014	92
3.2	Comparison of monthly intoxication occurrences observed for the mother (M) and daughter (D) captive dolphins over 2011-2014	93
3.3	Histogram of intoxication frequencies observed during 2011 through 2014	95

3.4	Average monthly intoxication episodes observed per individual captive dolphin over 2011-2014: A mother and B daughter. Error bars are \pm SEM (n = 4).....	96
3.5	Combined monthly average intoxication episodes of both captive dolphins between 2011 and 2014. Error bars are \pm SEM (n = 8).....	97
3.6	Percentages of observed macroalgae and cyanobacteria ingestions by type	99
3.7	Percentages of intoxication-related algal ingestions per algae type	100
3.8	Overall percentages of intoxication events relative to overt, or otherwise “unobserved”, algal ingestions.....	101
3.9	Average grazing behaviors of both captive dolphins observed 2013-2014. Error bars are \pm SEM (n = 48 months)	103
3.10	Average grazing behaviors observed for the mother and daughter captive dolphins during 2013 and 2014: A two-year data for the mother and B two-year data for the daughter. Error bars are \pm SEM (n = 24 months)	104
3.11	The total number of days, per month, intoxication symptoms and algae-specific ingestions were reported for the mother and daughter captive dolphins during 2013 and 2014: A mother 2013 data, B mother 2014 data, C daughter 2013 data and D daughter 2014 data. Note: The numerical values indicate the number of days intoxication symptoms were observed for the specified dolphin	105
3.12	Average monthly site seawater quality parameters, plotted consecutively, from 2011 through 2014, with AFC indicating average maximum fecal coliform (units per 100 mL) and AWT indicating average seawater temperatures ($^{\circ}$ C). Error bars are \pm SEM (n = 3)	111
3.13	Box plot of 2011-2014 average site seawater temperature(AWT) measurements ($^{\circ}$ C) with error bars denoting \pm SD (n = 3) and \times indicating means	112
3.14	Box plot of 2011-2014 average maximum fecal coliform measurements (AFC) measured as units per 100 mL seawater with error bars denoting \pm SD (n = 3) and \times indicating means	113
3.15	Consecutive plot of 2011-2014 monthly observed intoxication days symptomatic for both captive dolphins and the north lagoon water quality parameters with FC indicating maximum fecal coliform units (per 100 mL) and WT indicating lagoon water temperatures ($^{\circ}$ C).....	114
3.16	Consecutive plot of 2011-2014 monthly observed intoxication events (IE), expressed as days symptomatic, for the mother and daughter captive dolphins, relevant to the north lagoon water quality parameters with FC indicating	

maximum fecal coliform units (per 100 mL) and WT indicating lagoon water temperatures (°C)	115
3.17 Comparison of annual maximum fecal coliform units per 100 mL north lagoon water (FC) versus annual frequencies of intoxication events observed for both captive dolphins relative to instances of no intoxications over the study period (2011-2014).....	117
4.1 The molecular structure of (+) anatoxin-a (ATX-a)	132
4.2 The molecular structure of β -methylamino-L-alanine (BMAA)	136
4.3 The molecular structure of saxitoxin (STX)	141
4.4 The molecular structures of the brevetoxin A class (PbTx-A) analogs denoted by R.....	146
4.5 The confirmed molecular structures of the brevetoxin B class (PbTx-B) analogs denoted by R	146
4.6 The molecular structures of the brevetoxin B class analogs PbTx-5 and PbTx-6..	146
4.7 The molecular structure of brevetoxin-2 (PbTx-2).....	147
4.8 The molecular structure of brevenal	148
4.9 The molecular structure of domoic acid (DA).....	151
5.1 Bioassay-guided fractionation scheme of invest cyanobacteria collected January 2016. The * denotes biologically active fractions exhibiting neurotoxicity aligned with PbTx-2 positive control in the zebrafish embryo-larvae neurotoxicological models.....	205
5.2 Percent mortality of crude cyanobacteria extracts through 5 dpf compared to controls. Error bars indicate \pm SEM (n = 5). The *, **, *** respectively denote p < 0.05, p < 0.01 and p < 0.001 significance derived by one-way ANOVA followed by the Tukey HSD multiple comparison test relative to untreated ASW control	207
5.3 The LD ₅₀ value of the cyanobacteria EtOAc extract at 5 dpf (Day 5) extrapolated by linear regression analysis of the Log ₁₀ concentration versus percent mortality plot with error bars indicating the \pm SEM (n = 5).....	207
5.4 Percent mortality of cyanobacteria EtOAc extract F29 fractions through 5 dpf compared to controls. Error bars are \pm SEM (n = 5). The *, **, *** denote the respective p < 0.05, p < 0.01 and p < 0.001 significance derived by one-way	

ANOVA followed by the Tukey HSD multiple comparison test relative to the untreated ASW control	208
5.5 Percentages of deformed embryos exposed to PbTx-2 positive control compared to the negative controls (i.e., ASW, MeOH) through 5 dpf: a) Day 1-2 results, b) Day 3 results, c) Day 4 results and d) Day 5 results. Error bars are \pm SEM (n = 3). The *, **, *** denote the respective p < 0.05, P < 0.01 and p < 0.001 significance relative to the MeOH solvent control derived from one-way ANOVA followed by the Tukey HSD multiple comparison test	209
5.6 Daily percentages of deformed embryos per cyanobacteria extract exposure condition compared to controls with error bars indicating \pm SEM (n = 5): a) Day 1, b) Day 2, c) Day 3 and d) Day 4-5. The *, **, *** denote the p < 0.05, p < 0.01 and p < 0.001 significance, respectively derived by one-way ANOVA followed by the Tukey HSD multiple comparison test relative to untreated ASW control	211
5.7 The 24-hpf (Day 1) dose-dependent trends of percent deformed embryos observed for crude cyanobacteria extracts with extrapolated ED ₅₀ values: a) Linear trend of crude cyanobacteria extract and b) Logarithmic trend for EtOAc extract. Error bars are \pm SEM (n = 5)	212
5.8 Daily percentages of deformed embryos per treatment with EtOAc-derived F29 fractions relative to controls with error bars indicating \pm SEM (n = 5): a) Day 1, b) Day 2, c) Day 3 and d) Day 4-5. The *, **, *** denote the p < 0.05, p < 0.01 and p < 0.001 significance, respectively derived by one-way ANOVA followed by the Tukey HSD multiple comparison test relative to untreated ASW control...	213
5.9 Linear dose dependency of lipophilic subfraction F29-2 deformed embryos through 5 dpf with error bars indicating \pm SEM (n = 5): a) Day 1, b) Day 2-3 and c) Day 4-5.....	214
5.10 Extrapolated Day 2 percent deformed embryos ED ₅₀ value for lipophilic subfraction F29-1 with error bars denoting \pm SEM (n = 5).....	214
5.11 The 24-hpf average spontaneous coiling frequencies of embryos exposed to PbTx-2 and cyanobacteria extracts, quantified as coils per minute: a) Plot of PbTx-2 test solutions compared to ASW and MeOH controls with error bars indicating \pm SEM (n = 15) and b) Plot of cyanobacteria extracts compared to controls with error bars indicating \pm SEM (n = 5). The *, **, *** denote the p < 0.05, p < 0.01 and p < 0.001 significance, respectively derived by one-way ANOVA followed by the Tukey HSD multiple comparison test. Note: Significance is relative to untreated ASW in a) and relative to PbTx-2 in b)	216
5.12 The 24-hpf average spontaneous coiling frequencies of embryos exposed to the lipophilic fractions of F29 compared to controls. Error bars are \pm SEM (n = 5).	

One-way ANOVA followed by the Tukey HSD multiple comparison test ($p < 0.001$) showed no significant differences between fractions and PbTx-2 positive control	216
5.13 Linear dose dependency of 24-hpf average spontaneous coiling frequencies for the lipophilic fractions a) F29-2 and b) F29-3 with error bars denoting \pm SEM (n = 5)	217
5.14 Percent hatch rates of controls and cyanobacteria extracts: a) Day 2 and Day 3 hatch rate data for PbTx-2 compared to ASW and MeOH negative controls with error bars indicating \pm SEM (n = 3) and b) Hatch rate data through Day 5 for the cyanobacteria extracts, compared to the PbTx-2 positive control, with error bars indicating \pm SEM (n = 5). The *, **, *** denote, respectively, $p < 0.05$, $p < 0.01$ and $p < 0.001$ significance derived from one-way ANOVA followed by the Tukey HSD multiple comparison test relative to untreated ASW control a) and PbTx-2 b).....	218
5.15 Determination of the cyanobacteria EtOAc extract Day 5 hatch rate (% H) ED ₅₀ value by linear regression analysis of the Log ₁₀ concentration versus % H plot with error bars denoting \pm SEM (n = 5)	219
5.16 Average percent hatch rates of lipophilic F29 related fractions compared to controls through 5 dpf with error bars indicating \pm SEM (n = 5). No significant differences were observed relative to untreated ASW control by one-way ANOVA followed by Tukey's HSD multiple comparison test at $p < 0.001$	220
5.17 Linear regression analysis determination of the Day 2 percent hatched ED ₅₀ values for embryos exposed to lipophilic fractions a) F29-2 and b) F29-3 with error bars denoting \pm SEM (n = 5).....	220
5.18 The Day 2 average heart rates (HR) quantified as beats per minute (bpm) per exposure condition: a) Box plot of PbTx-2 data compared to the ASW and MeOH controls and b) Box plot of cyanobacteria extracts compared to all three control conditions. Error bars are \pm SD with n = 15 for a) and n = 5 for b) and \times indicates the mean HR value. Significance levels, $p < 0.05$, $p < 0.01$ and $p < 0.001$, derived from one-way ANOVA followed by the Tukey HSD multiple comparison test, are respectively denoted by *, **, *** relative to the untreated ASW control	222
5.19 Day 2 average heart rate trends observed for the cyanobacteria a) crude and b) EtOAc extracts with error bars indicating \pm SEM (n = 5), quantified as beats per minute (bpm)	222
5.20 Box plot of the Day 2 average heart rates (HR) of the lipophilic F29 fractions, quantified as beats per minute (bpm) per treatment, compared to the controls. Error bars indicate \pm SD (n = 5) and \times indicates the mean HR value.	

Significance levels, $p < 0.05$, $p < 0.01$ and $p < 0.001$, derived from one-way ANOVA followed by the Tukey HSD multiple comparison test, are respectively denoted by *, **, *** relative to untreated ASW control	223
5.21 The Day 3 average heart rates (HR) quantified as beats per minute (bpm) per exposure condition: a) Box plot of PbTx-2 data compared to the ASW and MeOH controls and b) Box plot of cyanobacteria extracts compared to controls. Error bars are \pm SD with $n = 15$ for a) and $n = 5$ for b) and \times indicates the mean HR value. Significance levels, $p < 0.05$, $p < 0.01$ and $p < 0.001$, derived from one-way ANOVA followed by the Tukey HSD multiple comparison test, are respectively denoted by *, **, *** relative to untreated ASW control	225
5.22 Day 3 average heart rate trends observed for the cyanobacteria a) crude and b) EtOAc extracts with error bars indicating \pm SEM ($n = 5$), quantified as beats per minute (bpm)	225
5.23 Extrapolation of the Day 3 ED ₅₀ value for the percentage of embryos exposed to the cyanobacteria EtOAc extract exhibiting abnormal heart rates relative to normal controls	226
5.24 The Day 3 average heart rates (HR) of the lipophilic F29 fractions, quantified as beats per minute (bpm) per treatment. Error bars are \pm SD ($n = 5$) and \times indicates the mean HR value. Significance levels, $p < 0.05$, $p < 0.01$ and $p < 0.001$, derived from one-way ANOVA followed by the Tukey HSD multiple comparison test, are respectively denoted by *, **, *** relative to the PbTx-2 positive control	227
5.25 Day 3 dose dependency of average heart rates (bpm) for lipophilic fractions a) F29 and b) F29-1 with error bars indicating \pm SEM ($n = 5$).....	227
5.26 The Day 5 average percent swim bladder dysfunction of embryos chronically exposed to a) PbTx-2 and b) the cyanobacteria extracts compared to the ASW and MeOH controls. Error bars are \pm SEM with $n = 3$ for a) and $n = 5$ for b). Significance levels, $p < 0.05$, $p < 0.01$ and $p < 0.001$, derived from one-way ANOVA followed by the Tukey HSD multiple comparison test, are respectively denoted by *, **, *** relative to untreated ASW control for a) and PbTx-2 positive control for b)	229
5.27 Probit analysis determination of the D5 percent swim bladder dysfunction (% SBD) ED ₅₀ value for chronic PbTx-2 exposure: a) Concentration versus % SBD plot with error bars indicating \pm SEM with $n = 3$ and b) Probit analysis plot	229
5.28 Extrapolated D5 percent swim bladder dysfunction ED ₅₀ value for chronic cyanobacteria EtOAc extract exposure.....	230

5.29	The D5 average percent swim bladder dysfunction of embryos chronically exposed to the cyanobacteria lipophilic F29 fractions with error bars indicating \pm SEM (n = 5). Respectively, the *, **, *** denote significance levels $p < 0.05$, $p < 0.01$ and $p < 0.001$, relative to untreated ASW control, derived by one-way ANOVA followed by the Tukey HSD multiple comparison test	230
5.30	The Day 5 average percent aberrant swimming behaviors of embryos chronically exposed to a) PbTx-2 and b) the cyanobacteria extracts compared to the ASW and MeOH controls. Error bars are \pm SEM with n = 3 for a) and n = 5 for b). Significance levels, $p < 0.05$, $p < 0.01$ and $p < 0.001$, derived from one-way ANOVA followed by the Tukey HSD multiple comparison test, are respectively denoted by *, **, *** relative to untreated ASW control for a) and PbTx-2 positive control for b)	232
5.31	The Day 5 average percent aberrant swimming behaviors of embryos chronically exposed to the cyanobacteria lipophilic F29 related fractions with error bars indicating \pm SEM (n = 5) were not significantly different from the PbTx-2 treatment for $p < 0.05$, $P < 0.01$ and $p < 0.001$ significance levels derived by one-way ANOVA and the Tukey HSD multiple comparison test.....	232
5.32	Representative embryos chronically exposed to 27.9 nM (25 ppb) PbTx-2 through 5 dpf indicating irregular swim bladder development, laying on side, and head-up passive drift orientation (A) relative to normal development exhibited by MeOH solvent control embryos examined at 5 dpf (B).....	233
5.33	Representative embryos chronically exposed to 10 ppm concentrations of cyanobacteria extracts and fractions versus controls, examined at 5 dpf: a ASW untreated control, b MeOH solvent control, c 0.025 ppm PbTx-2 positive control, d crude cyanobacteria extract, e EtOAc extract, f BuOH extract, g Aq extract, h F29, i F29-1, j F29-2, k F29-3. Shown are irregular swim bladder development in c, d, f-h and j-k and bent body axis in f, h and k. Aberrant swimming behaviors are indicated by laying on side in c, d and g and head-up passive drifting in e, f, and h-k relative to upright orientation and normal swim bladder development in controls a and b	233
5.34	Lethality of the 24-hpe (t24) acute PbTx-2 larval exposures compared to negative controls, with error bars indicating \pm SEM (n = 24). Significance levels, $p < 0.05$, $p < 0.01$ and $p < 0.001$, derived from one-way ANOVA followed by the Tukey HSD multiple comparison test, are respectively denoted by *, **, *** relative to untreated ASW control	235
5.35	Probit analysis determination of the 24-hpe (t24) LD ₅₀ value for acute PbTx-2 larval exposure: a) Concentration versus percent mortality plot and b) Probit analysis plot. Error bars are \pm SEM with n = 20, 21, 21 and 24 replicate embryos for the respective 2.79, 5.59, 11.2 and 27.9 nM PbTx-2 treatments.....	235

5.36	Lethality of acute larval exposures to the cyanobacteria extracts compared to controls with error bars indicating \pm SEM (n = 12 for extracts and n = 24 for controls). Significance levels, p < 0.05, p < 0.01 and p < 0.001, derived from one-way ANOVA followed by the Tukey HSD multiple comparison test, are respectively denoted by *, **, *** relative to untreated ASW control	236
5.37	Lethality of acute larval exposures to the cyanobacteria lipophilic F29 fractions compared to controls. Error bars indicate \pm SEM (n = 5 for fractions and n = 24 for controls). Significance levels, p < 0.05, p < 0.01 and p < 0.001, derived from one-way ANOVA followed by the Tukey HSD multiple comparison test, are respectively denoted by *, **, *** relative to untreated ASW control	237
5.38	Percentages of larvae acutely exposed to cyanobacteria extracts exhibiting swimming issues at 24 hpe (t24) relative to controls. Error bars indicate \pm SEM (n = 12 for extracts and n = 24 for controls). Significance levels, p < 0.05, p < 0.01 and p < 0.001, derived from one-way ANOVA followed by the Tukey HSD multiple comparison test, are respectively denoted by *, **, *** relative to untreated ASW control	238
5.39	Linear regression analysis extrapolation of the 24-hpe (t24) percent swimming issues ED ₅₀ values for the cyanobacteria a) crude and b) BuOH extracts with error bars denoting \pm SEM (n = 12).....	238
5.40	Percentages of larvae acutely exposed to lipophilic F29 fractions exhibiting swimming issues at 1-hpe (t1) relative to controls. Error bars indicate \pm SEM (n = 5 for extracts and n = 24 for controls). Significance levels, p < 0.05, p < 0.01 and p < 0.001, derived from one-way ANOVA followed by the Tukey HSD multiple comparison test, are respectively denoted by *, **, *** relative to PbTx-2 control.....	240
5.41	Determination of the 1-hpe (t1) percent swimming issues (% SI) ED ₅₀ values for acute larval exposure to lipophilic fractions F29-1 and F29-2: a) F29-1 concentration versus % SI, b) F29-1 probit analysis plot and c) F29-2 concentration versus % SI plot. Error bars are \pm SEM (n = 5).....	240
5.42	Percentages of larvae acutely exposed to lipophilic F29 fractions exhibiting swimming issues at 24 hpe (t24) compared to controls. Error bars indicate \pm SEM (n = 5 for extracts and n = 24 for controls). Significance levels, p < 0.05, p < 0.01 and p < 0.001, derived from one-way ANOVA followed by the Tukey HSD multiple comparison test, are respectively denoted by *, **, *** relative to untreated ASW control	241
5.43	Probit analysis determination of the 24-hpe (t24) percent swimming issues ED ₅₀ values for acute larval exposure to lipophilic fraction F29-2 with error bars denoting \pm SEM (n = 5).....	241

6.1	The 16S rDNA maximum likelihood tree showing the phylogenetic position of three Oscillatoriacean species found in the eudesmacarbonate-producing cyanobacterial mat CAL-V (shaded in grey and with clone abundance in parenthesis). Note the overall lack of the backbone of the tree for clarity	264
6.2	The molecular structure of eudesmacarbonate (1).....	265
6.3	High-resolution LC-MS spectrum of eudesmacarbonate (1) with MH indicating the $[M+H]^+$ peak and MNa indicating the $[M+Na]^+$ peak.....	266
6.4	FTIR spectrum of eudesmacarbonate (1).....	267
6.5	The 1H NMR spectrum of eudesmacarbonate (1). The peaks observed between 2.01 and 2.05 ppm, respectively indicate the $(CD_3)_2CO$ solvent. Water contamination is indicated by the peaks at 2.81 and 2.84 ppm respectively	268
6.6	The ^{13}C NMR spectrum of eudesmacarbonate (1). The $(CD_3)_2CO$ solvent peaks are indicated between 28.6-29.4 ppm and at 205.3 and 205.4 ppm, respectively ..	269
6.7	The DQF-COSY 2D-NMR spectrum of eudesmacarbonate (1).....	271
6.8	The HMBC 2D-NMR spectrum of eudesmacarbonate (1).....	272
6.9	The NOESY 2D-NMR spectrum of eudesmacarbonate (1)	273
6.10	Key 1H - 1H COSY (bold lines) and HMBC (arrows) correlations of eudesmacarbonate (1)	274
6.11	The single crystal X-ray structure of eudesmacarbonate (1)	274
6.12	The molecular structure of eudesmacarbonate (1) with assigned relative configuration.....	275
6.13	Comparison of experimental and calculated VCD and IR spectra of eudesmacarbonate (1) and the respective enantiomers for (4 <i>S</i> ,5 <i>R</i> ,6 <i>R</i> ,7 <i>S</i> ,10 <i>S</i>) in black and (4 <i>R</i> ,5 <i>S</i> ,6 <i>S</i> ,7 <i>R</i> ,10 <i>R</i>) in red obtained from the CompareVOA software ...	277
6.14	The molecular structure of the lowest-energy conformer of eudesmacarbonate (1).....	278
6.15	The structures of referenced compounds (2)-(5). The structures of (+)-5 α ,7 β (H)-eudesm-4 α ,6 α -diol (2) and its sulfurous ester (3) were adapted from Toyota and Asakawa (1990). The structures of torilen (4), now known as germacrene-D, and torilensulfat (5), now known as eudesmane-4,6-diol cyclic sulfate, were adapted by Itokawa et al. (1988)	279

6.16	Comparative results of average 24-hpf spontaneous coils per minute. Data are the mean and SD of the total number of embryos for three replicate samples. Respectively, the *, **, *** denote $p < 0.05$, $p < 0.01$ and $p < 0.001$ significance derived by one-way ANOVA followed by the Tukey HSD multiple comparison test relative to the negative control.....	281
6.17	Logarithmic dose dependence of eudesmacarbonate (1) with respect to spontaneous coiling frequency per minute. Error bars are \pm SEM for the total number of embryos of three replicate test solutions with $n = 14, 15$ and 14 , respectively, for the low, mid and high treatments.....	282
6.18	Comparative embryo morphologies observed at 24-hpf for untreated control (A) versus PbTx-2 treatments of $0.0045 \mu\text{M}$ (B) and $0.0223 \mu\text{M}$ (C) and treatment with eudesmacarbonate (1) at $9.4 \mu\text{M}$ (D), $38 \mu\text{M}$ (E) and $94 \mu\text{M}$ (F), respectively	282
6.19	Comparative results of Day 2 average heart rates measured as beats per minute (bpm). Data are the mean and SD of the total number of embryos for three replicate samples. The *, ** and ***, respectively denote $p < 0.05$, $p < 0.01$ and $p < 0.001$ significance derived by one-way ANOVA followed by the Tukey HSD multiple comparison test relative to the negative control.....	284
6.20	Dose dependence of eudesmacarbonate (1) with respect to D2 average heart rates (HR) in bpm. Error bars are \pm SEM of the total number of embryos per exposure concentration of 1 ($n = 14, 15$ and 14 for the respective low, mid and high treatments)	285
6.21	Comparative results of D3 average heart rates measured as beats per minute (bpm). Data are the mean and SD of the total number of embryos for three replicate samples. The *, **, and *** respectively denote $p < 0.05$, $p < 0.01$ and $p < 0.001$ significance derived by one-way ANOVA followed by the Tukey HSD multiple comparison test relative to the negative control.....	287
6.22	Logarithmic dose dependence of eudesmacarbonate (1) with respect to D3 average heart rates in bpm with error bars denoting \pm SEM for the total number of embryos per treatment ($n = 14, 15$ and 14 for the respective low, mid and high treatments)	287
6.23	Comparative embryo development observed at D3 for untreated control (A) versus PbTx-2 treatments of $0.0045 \mu\text{M}$ (B) and $0.0223 \mu\text{M}$ (C) and treatment with eudesmacarbonate (1) at $9.4 \mu\text{M}$ (D), $38 \mu\text{M}$ (E) and $94 \mu\text{M}$ (F), respectively	288
6.24	Comparative results of D5 average percent swim bladder dysfunction per chronic exposure concentration. Data are the mean and \pm SEM of three replicate samples. Respectively, the *, **, and * denote $p < 0.05$, $p < 0.01$ and	

	p < 0.001 significance derived by one-way ANOVA followed by the Tukey HSD multiple comparison test relative to the negative control	290
6.25	Comparative results of D5 average percent aberrant swimming behaviors per chronic exposure concentration. Data are the mean and ± SEM of three replicate samples. The *, **, and *** denote the respective p < 0.05, p < 0.01, and p < 0.001 significance derived by one-way ANOVA followed by the Tukey HSD multiple comparison test relative to the negative control	291
6.26	Day 5 logarithmic dose dependence of eudesmacarbonate (1) with respect to a) average percent swim bladder dysfunction and b) average percent aberrant swimming behaviors with error bars denoting ± SEM (n = 3 replicate test solutions).....	291
6.27	Comparative embryo development observed at D5 for untreated control (A) versus chronic exposure to 0.0045 µM PbTx-2 (B) and eudesmacarbonate (1) at 9.4 µM (C), 38 µM (D) and 94 µM (E), respectively	292
6.28	Comparative results of the percent ataxia-related swimming behaviors per acute exposure concentration. Data are the mean and SEM of 12 replicate larvae. The *, **, and *** denote the respective p < 0.05, p < 0.01, and p < 0.001 significance derived by one-way ANOVA followed by the Tukey HSD multiple comparison test relative to the negative control	293

LIST OF ABBREVIATIONS AND ACRONYMS

AEG	N-(2-aminoethyl)-glycine
AFC	Average Fecal Coliforms
AMSF	Analytical Mass Spectrometry Facility
AOAC	Association of Official Analytical Chemists - International
ASP	Amnesic Shellfish Poisoning
ASW	Aquaria System Water
ATX	Anatoxins
ATX-a	Anatoxin-a
AWT	Average Water Temperature
BLAST	Basic Local Alignment Search Tool
BMAA	β -methylamino-L-alanine
bpm	beats per minute
BuOH	2-butanol
C ₈	Octylsilane
C ₁₈	Octadecylsilane
(CD ₃) ₂ CO	Deuterated acetone
cpm	Coils per minute
DA	Domoic Acid
DAB	2,4-diaminobutyric acid
dpf	Days post-fertilization
ELSD	Evaporative Light Scattering Detection

EPA	Environmental Protection Agency
EtOAc	Ethyl Acetate
FC	Fecal Coliforms
FIU	Florida International University
HAB	Harmful Algal Bloom
HILIC	Hydrophobic Interaction Ligand Chromatography
hpe	Hour(s) post-exposure
hpf	Hour(s) post-fertilization
HSD	Honestly Significant Difference
LFB	Lab Fortified Blank
LFM	Lab Fortified Matrix
LOD	Limit of Detection
LOQ	Limit of Quantification
MBA	Mouse Bioassay
MeOH	Methanol
MS/MS	Tandem Mass Spectrometry
NSP	Neurotoxic Shellfish Poisoning
p	pProbability
PbTx	Brevetoxins
PbTx-2	Brevetoxin-2 (standard)
SCF	Spontaneous Coiling Frequency
SPE	Solid Phase Extraction

1. INTRODUCTION

1.1 Project Overview and Significance

Bottlenose dolphins (*Tursiops truncatus*) living in captivity in the Florida Keys were recently observed to graze on macroalgae including cyanobacteria (i.e., epiphytic, filamentous), occurring within their enclosures, followed by apparent signs of intoxication, and specifically seeming, neurotoxicity. Cyanobacteria, ubiquitous photosynthetic bacteria, commonly referred to as “blue-green” algae, yield a multifarious portfolio of toxic or otherwise bioactive metabolites (e.g., neurotoxins, hepatotoxins, dermatotoxins) that have been linked to intoxication of humans and wildlife (Buratti et al., 2017; Ferrão-Filho and Koslowsky-Suzuki, 2011). The overarching intent of the research project was to investigate the presence of toxigenic alga, including cyanobacteria, that captive dolphins may be consuming within their enclosures, the possible contribution of these toxigenic algae to the observed intoxication events, and to provide dolphin facility staff the tools to improve prophylactic health monitoring. In addition, the study represented, more generally, an unprecedented opportunity to explore the potential for exposure of marine mammals, such as dolphins, to algal and/or cyanobacterial toxins present in a representative natural environment (i.e., chain-link fenced enclosures), and the possible health impacts of these toxins. Thus, the dissertation research specifically aimed to examine the role of potential neurotoxic algal and/or cyanobacterial metabolites in the observed captive dolphin intoxication events via the following two, parallel and interrelated Major Objectives:

1.1.1 Major Objective 1 - Algal Community Assessment

To conduct a taxonomic survey of the dominant macroalgal and cyanobacteria genera present in the captive dolphin enclosures and subsequently evaluate the potential presence of neurotoxic, known or otherwise relevant bioactive, metabolites associated, particularly, with identified neurotoxigenic cyanobacterial taxa.

1.1.2 Major Objective 2 – Chemical Explorations for Potential Neurotoxin(s)

To use the zebrafish (*Danio rerio*), as an aquatic, vertebrate neurotoxicological model (e.g., developmental neurotoxicity, larval behavioral neurotoxicity), during the isolation, characterization and identification of potential neurotoxic metabolites in the relevant cyanobacteria samples collected from within the captive dolphin enclosures.

1.2 Chapter Foci

Seven chapters comprise this dissertation, the first of which provides an in-depth background for the research project. The next five chapters detail the relevant background information, applied methodologies including materials, reagents, instrumentation and protocol development, and results discussions relative to the two major objectives. Specifically, the second chapter encompasses the taxonomic characterization and biodiversity of the dominant macroalgae, and cyanobacteria, communities observed growing within the captive dolphin enclosures and introduces a zoopharmacognosy hypothesis. Chapter Three distills the relevance of the captive dolphins' algal grazing behaviors to the intoxications observed by the facility staff and augurs a zoopharmacognostic rationale. Observational data and historical water quality

measurements, collected during the study period of 2011 through 2014, were statistically analyzed for potential correlations that could help predict and/or assuage future intoxication events. Chapter Four presents the rationale and results for the chemical evaluation of the relevant cyanobacteria samples collected from within the captive dolphin enclosures for the possible presence of known, culpable marine Harmful Algal Bloom (HAB) associated neurotoxins, specifically anatoxin-a (ATX-a), brevetoxin-2 (PbTx-2), domoic acid (DA), β -methylamino-L-alanine (BMAA) and saxitoxin (STX), to augment the first major objective. The fifth and sixth chapters detail the bioassay-guided chemical investigation of the involved cyanobacteria, completing the major objectives of this dissertation. The fifth chapter describes the comparative zebrafish neurotoxicological models used in the bioassay-guided investigation of the cyanobacteria collections for the presence of a neurotoxic metabolite potentially associated with the observed captive dolphin intoxications. Particularly, Chapter Five, written as a manuscript for submission to Harmful Algae, communicates the zebrafish embryogenic neurotoxicity and larval neurobehavioral bioassays used to assess neurotoxicity in the crude extracts and relevant bioactive fractions compared to the known marine, HAB-related neurotoxin, PbTx-2 (e.g., standard), produced by the marine dinoflagellate *Karenia brevis*. The neurotoxicity of PbTx-2 in zebrafish had not been previously reported in the available literature. Whilst, Chapter Six details the analytical methods used to isolate, purify and structurally characterize a previously undescribed and biologically active eudesmane-type sesquiterpene, eudesmacarbonate, as the putative secondary metabolite, possibly associated with the observed intoxications. The compound was obtained from the lipophilic extract of a cyanobacterial mat comprised of closely related Oscillatoriacean

species including an undescribed *Neolyngbya* sp., sampled from within the captive dolphin enclosures and associated with the observed algal ingestions. Also presented in Chapter Six were the neurotoxic effects of eudesmacarbonate, compared to the PbTx-2 standard. A manuscript, prepared from the results of Chapter Six, was submitted as a Note to the Journal of Natural Products to publicly disseminate the scientific approaches and major findings of this dissertation. Lastly, a summary chapter discussing the combined outcomes, relevant significances, and possible future direction(s) concludes the dissertation.

1.3 Background and Theory

Bottlenose dolphins are generally recognized as piscivores, preying primarily on seasonally available native fish, crustaceans and other living marine invertebrates. In contrast, the availability of specific, sustainable fish from fisheries and the manpower required for fish preparation, necessitate feeding captive dolphins, living in human-controlled marine aquaria, stricter diets of two or three major varieties including herring and capelin. Indeed, a marine mammal zoological facility, located in the Florida Keys, further supports their dolphins' health by providing an increased variety of fish (e.g., capelin, sprat, herring, mackerel, whiting, mullet) and squid as well as dietary supplements (e.g., vitamins, antioxidants, beta-glucans, carotenoids) and freshwater to ensure proper nutrition and hydration (Koutsos et al., 2013; Mejia-Fava and Colitz, 2014). Proof of concept clinical trial pilot study data in human-managed, immunocompromised (e.g., cancers, papillomas) cetaceans have shown promising results for the use of propriety nutraceuticals (i.e., beta-glucans) developed for humans (Rodriguez et al., 2007, 2008) to stimulate immune responses. Recently, the staff at the

Florida Keys marine mammal facility observed their captive bottlenose dolphins occasionally grazing on macroalgae, including cyanobacteria, growing within the enclosures. Reports of direct algal ingestion by wild or captive bottlenose dolphins are unprecedented in the available scientific literature. However, wild bottlenose, particularly reproducing females amongst the Western Australian Shark Bay population, are presumed ingesting sponges as a means of supplementing calcium and self-medicating from the available bioactive (e.g., antimicrobial, anticancer) secondary metabolites produced by the sponges (Smolker et al., 1997; Meylan 1988; Anjum et al., 2016). After feeding on macroalgae and cyanobacteria, the Florida Keys captive dolphins exhibited signs of intoxication as evidenced by ataxia and other neurological symptoms (e.g., uncoordinated swimming, disorientation, respiratory issues, blepharospasms, ocular dysfunctions) after which the dolphins seemed to fully recover, typically within several days, as determined by the staff veterinarian. Facility staff have observed intermittent grazing of macroalgae and cyanobacteria by the captive dolphins and apparent intoxication events of varying intensity between 2011 and 2014, suggesting a possible link to seasonal variability.

1.3.1 Marine Algal Community Diversity

Collectively, algae refer to an umbrella category for several oxygenic, photosynthesizing organisms, primarily excluding terrestrial plants, as most recently defined by Cavalier-Smith (2018). Representative members include multicellular macroalgae (i.e., seaweeds) and various microscopic microalgae (e.g., phytoplankton) ranging from unicellular individuals to colonial and filamentous assemblages (Metting Jr., 1996). Andersen (1992) and Whitton (1992) each provided a comprehensive update

of the taxonomic biodiversity and complexity among algae constituents using photosynthetic attributes, revised molecular phylogenetic classifications and evolutionary pathways, respective of their specific domains, Eukaryota (i.e., eukaryotes) and Bacteria (i.e., prokaryotes). Sapp (2005) reasserted that the major distinction between eukaryotes and bacteria is the cellular organization first ascribed by Chatton in 1925; i.e., -eukaryotic cells contain a nucleus encased by a membrane, whereas the nucleus of bacterial cells has no membrane boundary.

Best known as seaweeds, macroalgae are multicellular, eukaryotic, and appear more plant-like. The “green,” the “red” and the “brown” common names for the three major marine seaweeds describe the colors of their respective taxonomic divisions; Chlorophyta, Rhodophyta, Phaeophyta. Microalgae comprise a wide array of polyphyletic, primarily eukaryotic, photosynthetic organisms having essential light harvesting and accessory pigments, typically chlorophylls, carotenoids (e.g., carotenes, xanthophylls), phaeophytins and/or phycobillins (Rowan, 1989). Prokaryotic cyanobacteria are also included under the algae umbrella due to their photosynthetic pigments (i.e., phycobillins) and capabilities (Nowicka and Kruk, 2016). In general, algae, most typically, inhabit water bodies, that afford enough sunlight for photosynthesis (Raven and Giordano, 2014). Although, some algal communities exist, often symbiotically or as biofilms, in other moisture-rich terrestrial habitats (e.g., snow, sea-ice, soil), living organisms (e.g., animals, plants), and on artificial substrates made from organic (e.g., wood) and synthetic (e.g., plastic, metal, concrete, building) materials as respectively described by Gosselin et al. (1986), Pandey et al. (2004), Pauli et al. (2014), Neustupa and Škaloud (2010), Raven and Giordano (2014), Häubner et al. (2006), and

Samad and Adhikary (2008). Whilst, still other microalgae and cyanobacteria can withstand living in some of the most extreme environmental conditions ranging over desiccated and hypersaline (Perera et al., 2018; Wierzchos et al., 2006), frozen (Thomas and Dieckmann, 2002; Lyon and Mock, 2014; Christmas et al., 2015), volcanic and geothermal (Hsieh et al., 2018; López-Rodas et al., 2009), and chemically toxic (Cohen et al., 1986; Ward et al., 1998; Beatty et al., 2005) environs as reviewed by Varshney et al. (2015).

1.3.2 Microalgae and Cyanobacteria Membership

Marine phytoplankton, as previously surveyed, and particularly relevant, herein, to the representative estuarine Florida coasts of Florida Bay (Phlips and Badylak, 1996), Indian River Lagoon (Badylak and Phlips, 2004; Phlips et al., 2004), and Tampa Bay (Badylak et al., 2007), consist predominantly of HAB-forming diatoms (Bacillariophyceae, Haeckel, 1878), dinoflagellates (Dinophyceae, Fritsch, 1927) and cyanobacteria (Cyanophyceae, Schaffner, 1909).

Specifically, marine diatoms are phototrophic eukaryotes, subsisting as free-living, unicellular individuals which may also aggregate to form filaments and/or colonies. Their unique opaline cell walls, called frustules, demonstrate that it is possible to live within glass-walls. Vast deposits of their fossilized remains, best known as diatomaceous earth, are economically exploited (Desikachary and Dweltz, 1961). Given their abundance, diatoms play major roles in earth's biogenic silicon and carbon transport cycles (Leblanc et al., 2012; Bozarth et al., 2009; Sarthou et al., 2005; Nelson et al., 1995).

Marine dinoflagellates are, typically, free-living unicellular, mixotrophic organisms (e.g., photoautotrophic, parasitic, predatory) currently taxonomically classified as eukaryotes (Jeong et al., 2010; Ismael, 2003; Gomez, 2012). Moreover, some dinoflagellates possess a unique nuclear organelle, (i.e., dinokaryon), structurally bridging eukaryotes and prokaryotes (Gomez, 2012). Whilst, certain photosynthetic marine dinoflagellates, known as zooxanthellae (e.g., *Symbiodinium* spp.), live symbiotically within various marine invertebrate hosts including corals (LaJeunesse, 2002; Rowan, 1998; Muscatine and Porter, 1977) and bivalve mollusks (Carlos et al., 2000; Klumpp et al., 1992). Consequently, the dinoflagellates provide up to 90% of their host's nutrients while mutualistically receiving respiration products for photosynthesis and safe harbor (Schnepf and Elbrächter, 1992; Falkowski et al., 1984). These zooxanthellae symbionts play a major role in the growth and development of coral reef ecosystems (Dubinsky and Jokiel, 1994; Muscatine and Porter, 1977).

Primarily autotrophic, cyanobacteria are often referred to as “blue-green” algae relative to their photosynthetic-enabling bluish pigment phycocyanin (MacColl, 1998). Ubiquitous on earth, cyanobacteria exist as free-living unicellular individuals, colonial aggregates, or multicellular filaments and assemblages, surviving in nearly every habitat including the extreme conditions of desert (Bahl et al., 2011; Wierzchos et al., 2006), hypersaline (Wieland and Kühl, 2000), polar/alpine (Comte et al., 2007; Christmas et al., 2015), and alkaline hot spring (Ward et al., 1998; Steunou et al., 2006) environments. Unlike eukaryotic diatoms and most dinoflagellates, cyanobacteria cells lack any membrane-bound organelles including the nucleus (Stainer and Cohen-Bazire, 1977). Currently, cyanobacteria comprise a phylum of prokaryotes classified under the Bacteria

domain (Ruggiero et al., 2015; Komárek et al., 2014; Margulis et al., 1999; Cavalier-Smith, 1998; Woese and Fox, 1977). Whilst mostly oxygenic, carbon-fixing photoautotrophs, some cyanobacteria, under dark, anaerobic conditions, act as chemotrophs, to fix carbon and/or respire at night using sulfur (Oren and Paden, 1978; Cohen et al., 1986), akin to green sulfur bacteria that inhabit deep, hydrothermal sea vents (Beatty et al., 2005). Still others, acting as diazotrophs during anoxic conditions, are capable of fixing nitrogen from inorganic nitrites, nitrates and ammonia as well as from organic sources including urea and amino acids (Bergman et al., 2012; Kashiyama et al., 2008). Cyanobacteria play a major role in earth's global biogenic carbon and nitrogen cycles (Lea-Smith et al., 2015; Schneider and Le Campion-Alsumard, 1999; Latysheva et al., 2012). Known to be some of earth's earliest photosynthetic life forms, marine cyanobacteria are also credited with oxygenating earth's atmosphere (Bekker et al., 2004; Rasmussen et al., 2008; Lyons et al., 2014).

1.3.3 Taxonomic Approaches

Classic taxonomy primarily identified algal and cyanobacterial species using morphological differentiation (Metting Jr., 1996; Manoylov 2014). For example, Litaker et al. (2009) used light microscopy and scanning electron microscopy to detail the morphological differentiations between several species of the dinoflagellate genera *Gambierdiscus* (Gonyaulacales) affording the identification of four new species (i.e., *G. caribaeus*, *G. carolinianus*, *G. carpenter*, *G. ruetzleri*). Gene sequencing and molecular taxonomic identification techniques such as Polymerase Chain Reaction (PCR), DNA probes and barcoding, and Fluorescence *in situ* Hybridization (FISH), provide more precise classification of cyanobacteria and algae species compared to morphology-based

characterizations (Moreira et al., 2013; Engene et al., 2013, 2010; Palinska et al., 2015; Grossman, 2005; Leliaert et al., 2012; Hajibabaei et al., 2007). The specificity of current ribosomal genetic biomarkers (e.g., 16S rRNA, 16S-23S rRNA Internal Transcribed Signal [ITS], Phycocyanin-Intergenic Spacer [PC-IGS]) has been shown to facilitate the taxonomic identification and toxigenicity of some cyanobacteria directly from source samples, including *Microcystis* and *Anabaena*, as described by Neilan et al. (1997), Otsuka et al. (1999), Beltran and Neilan (2000), and Tillet et al. (2001). Whilst, using 18S rRNA gene sequencing, Suutari et al. (2010) showed that the fur of Central and South American two- and three-toed sloths, *Choloepus* spp. and *Bradypus* spp. respectively, provides microcosms for Ulvophyceae (green microalgae), unique to the sloths (e.g., *Trichophilus welckeri*) and seasonal environmental conditions (e.g., *Trentepholia* spp., *Myrmecia* spp.), among other observed eukaryotic microalgal (e.g., dinoflagellates, rhodophytes) symbionts.

Recent applications of Matrix-Assisted Laser Desorption Ionization (MALDI) – Time-of-Flight (TOF)-mass spectrometry (MS) afford rapid, taxonomic characterization of cyanobacteria species and ability to differentiate between toxic and non-toxic strains (e.g., *Lyngbya*, *Microcystis*) with minimal sample preparation (Engene et al., 2011; Sun et al., 2016). Specifically, Grindberg et al. (2011) used MALDI-TOF-MS analysis to quickly assess the presence of known neurotoxins (e.g., apratoxin A) in crude extracts of *Lyngbya bouillonii* toward identifying the responsible biosynthetic gene cluster. Likewise, Barbano et al. (2015) characterized 31 microalgae species, individually and prepared as mixtures, using MALDI-TOF-MS (e.g., proteome, gene-expression) for direct comparison against gene-sequenced (e.g., 16S rDNA, 18S rDNA) taxonomic

classification and clustering organization toward more definitive phylogenetic identifications. Moreover, the obtained MALDI-TOF-MS results showed species level distinctions and identified potential biomarker data within mixtures useful for future applications, including taxonomic differentiation between species and within-community biodiversity characterizations.

1.3.4 Eutrophication Issues

Eutrophication can occur naturally from environmental impacts (e.g., drought, fire, flooding, hurricanes) that temporarily alter nutrient loads from normal ecological cycles (e.g., carbon, nitrogen, water) as described by Mesnage et al. (2002). Whilst, anthropological activity from agribusiness practices (e.g., deforestation, monoculture, chemical use, animal use), urban development (e.g., sewage, chemical use, land manipulation), and industrialization pollutants (e.g., fossil fuels consumption, manufacturing, chemical synthesis) steadily inject nutrients directly into the environment, often above natural flux levels and capacities, to the detriment of ecosystems (Rhind, 2009). Zimmerman and Canuel (2000) showed, using lipid and photolithic biomarkers (i.e., phytoplankton) in the estuarine system of Chesapeake Bay, that rapidly increased human related activity directly correlated to rapidly increased total organic matter leading to eutrophication. Ecosystem health typically declines as eutrophication progresses due to increased nutrients, particularly nitrogen and phosphorus from natural and anthropogenic sources. Excessive nutrient loading promotes unregulated algal growth to the point of inhibiting photosynthesis across different trophic levels, leading to the successive death of plants, macroalgae, microalgae, and cyanobacteria. Resultant dissolved oxygen levels

decline, adversely impacting resident fauna survival and further changing the biotic dynamics to life limiting, anoxic conditions (O'Neil et al., 2012).

1.3.5 Harmful Algae Bloom (HAB) Potential

Within the Florida Keys estuarine habitats, natural and anthropogenic eutrophication influence the taxonomic composition and diversity of the dominating algal inhabitants from healthy seagrass beds (e.g., *Thalassia testudinum*) and macroalgae to proliferations of microalgae and cyanobacteria (Lapointe et al., 1994; Gilbert et al., 2004). Harmful algal blooms (HAB) result when rapid toxin-producing algae and cyanobacteria growth leads to extensive release of toxic metabolites during subsidence. Subsequently, large declines often overwhelm many marine organisms (e.g., shellfish, fish, birds, marine mammals) with fatal doses (Anderson et al., 2008).

Twiner et al. (2012) reported wild dolphins living in southwest Florida have been routinely subjected to HAB events involving two different neurotoxin-producing microalgae. One is the dinoflagellate, *Karenia brevis*, associated with red-tides, responsible for Neurotoxic Shellfish Poisoning (NSP) from brevetoxins (PbTx). The other is the domoic acid (DA)-producing diatom, *Pseudo-nitzschia* spp., responsible for Amnesic Shellfish Poisoning. Various aquatic (e.g., marine) cyanobacteria produce numerous toxic secondary metabolites (Golubic et al., 2010), often associated with neurotoxicity. The most notorious cyanobacterial neurotoxins for which standards and established analytical methodologies exist include anatoxin-a (ATX-a), associated with several freshwater species including *Anabaena* spp. and *Oscillatoria* spp. (Sivonen et al., 1989; Méjean et al., 2014) and *Phormidium* sp. (Faassen et al., 2012), β -methylamino-L-alanine (BMAA) detected in numerous species including *Lyngbya* spp. (Cox et al., 2005), and saxitoxin

(STX) produced by several species including *Lyngbya wollei* (Onodera et al., 1997; Mihali et al., 2011). Recently, BMAA production has been observed in the dinoflagellate *Heterocapsa triquerta* (Jiang and Ilag, 2014) and in cultures of the diatoms *Phaeodactylum tricornutum*, *Chaetoceros* spp., *Thalassiosira pseudonana* and their associated bacteria (Réveillon et al., 2016). Whilst, the neurotoxic analog of ATX, homo-ATX, was detected in the marine cyanobacteria, *Hydrocoleum lyngbyaceum* by Méjean et al. (2010). These microalgae and cyanobacterial neurotoxins can bio-magnify, cause neurodegenerative illnesses and be fatal (Aráoz et al., 2010; Brand et al., 2010).

Cyanobacteria proliferations within Florida estuaries (e.g., Indian River Lagoon, Caloosahatchee River), due to anthropogenic effects, increase harmful exposure risks to humans and wildlife (Lapointe et al., 2015; Milbrandt et al., 2012; Philips et al., 2011; Bloetscher et al., 2010; Lapointe and Bedford, 2007). The captive dolphin facility is located within residential boating communities subject to runoff associated with human activity (e.g., sewage, agriculture, petroleum). These nitrogen and phosphorus rich pollutants are known to promote HAB development and transport, affecting major aquatic ecosystems (e.g., freshwater, estuarine, marine). Indeed, abundant growth of cyanobacteria within the captive dolphin enclosures has been observed. Thus, cyanobacteria biomass sampling at discrete intervals (e.g., seasonal), warranted chemical evaluations for the potential presence of known HAB-associated neurotoxins, specifically ATX-a, BMAA, STX, PbTx-2 and DA using applicable standards (e.g., synthetic, certified reference material [CRM]) and established analyte-specific methodologies including Liquid Chromatography-Mass Spectrometry (LC-MS, LC-MS/MS) and Enzyme-Linked Immunosorbent Assay (ELISA).

1.4 Zebrafish (*Danio rerio*) Bioassay Rationale

The zebrafish (*Danio rerio*) has become an increasingly important and widely accepted vertebrate model for in vivo toxicological characterization studies of chemicals (Ali et al., 2011; Sipes et al., 2011). As a fast maturing, small, freshwater species able to breed frequently with high fecundity in the laboratory setting, zebrafish provide a cost-effective, easily maintained in-house, high-throughput toxicological platform toward investigating and identifying bioactive metabolites causing impairment or inhibition of developmental pathways (Fraysse et al., 2006). Having a lucent chorion facilitates monitoring of development and other relevant endpoints in embryonic stages by light microscopy. Kimmel et al. (1995) describes the 72-hour embryogenesis progression in full details for standardization. A variety of measurable endpoints (e.g., hatching time, heart rate, organ development, locomotor function, behavior) exist to assess developmental toxicity and neurotoxicity (García-Camero et al., 2012; Ali et al., 2012; Padilla et al., 2011; Parng et al., 2006).

The same endpoints were used to investigate developmental neurotoxicity (Selderslaghs et al., 2010; Drapeau et al., 2002). These criteria have recently been reviewed by de Esch et al. (2012), to help standardize endpoint measurements. Likewise, various biological assays (e.g., heart rate, photomotor response, vibration response, swimming behaviors) have been developed for larval fish stages and, specifically with respect to the proposed research, in terms of identification and characterization of neurotoxicity (Long et al., 2014). Kalueff et al. (2013) meticulously summarized and indexed observed zebrafish behaviors according to several characterized behavioral domains providing a very descriptive and useful reference tool. Moreover, genome

sequencing advances, and recently developed mutant zebrafish lines - analogous to discrete human gene functions - offer rapid, precise bioassay tools to study specific toxicological effects (Das et al., 2013; Howe et al., 2012, 2013; Zhang et al., 2003; Fan et al., 2010; Linney et al., 2004).

1.4.1 Developmental Toxicity Protocols for Cyanotoxins

The zebrafish model of developmental toxicity has been used to investigate freshwater HAB-related cyanobacterial hepatotoxins (e.g., cylindrospermopsin, microcystins, nodularin), typically associated with *Cylindrospermopsis raciborskii*, *Aphanizomenon ovalisporum* and *Microcystis* spp. as shown by Berry et al. (2009) and Faltermann et al. (2016). Whilst Wu et al. (2016) evaluated the neurotoxicity effects of microcystin-LR in developing zebrafish embryos. Likewise, the effects of HAB-related neurotoxins on zebrafish embryogenesis have also been studied. For example, Purdie et al. (2009), Tiedeken et al. (2005) and Lefebvre et al. (2004) each, independently, assessed the neurotoxicity of one specific marine HAB-associated neurotoxin, respectively, β -methylamino-L-alanine (i.e., synthetic), domoic acid (i.e., synthetic) and saxitoxin (i.e., certified reference material), on zebrafish development. Briefly, to appropriately assess zebrafish developmental toxicity (Berry et al., 2007) and neurotoxicity during embryogenesis (Chen et al., 2011), relevant developmental stages (e.g., 24-hours post-fertilization [hpf] spontaneous coiling, heart rate, hatching success and rate, morphological deformities, survival rate) were monitored over a range of test sample (e.g., extracts, chemical standards) concentrations from initial exposure, typically 2-6 hpf (i.e., 4-64 cell stage), through 120 hpf, and in accordance with an Institutional Animal Care and Use Committee (IACUC) approved protocol (Appendix).

1.4.2 Larval Behavioral Assessments for Neurotoxicity

Recent focus has shifted toward quantifiable behavioral endpoints (e.g., avoidance and preferential behaviors, sensorimotor responses, learning and memory) to evaluate the effects of neurotoxins on neurological pathways in zebrafish embryos and larvae, reviewed by Best and Alderton (2008), and further described by Selderslaghs et al. (2013), Tierney (2011), and Mueller and Neuhauss (2010). Moreover, automated systems designed to monitor concurrent endpoints have emerged (Pelkowski et al., 2011; Creton, 2009). Sagaciously, Jonas et al. (2015) specifically evaluated the neurotoxicity and teratogenicity of three different cultured cyanobacteria (i.e., *Planktothrix agardhii*, *Aphanizomenon gracile*, *Microcystis aeruginosa*) using *Danio rerio* Teratogenicity Assay (DarT) morphological endpoints established by Nagel (2002) and the zebrafish eleuthero-larvae locomotor activity described by Irons et al. (2010). Kalueff et al. (2013) compiled a detailed guide to uniformly identify and characterize quantifiable neurotypical behaviors in larval zebrafish suitable for assessing neurotoxicity. Investigations of neurotoxicity-induced behavioral effects (e.g., survival rate, morphologic deformation, swim bladder inflation changes, abnormal swimming behavior), monitored in zebrafish eleuthero-larvae exposed to test samples over 5-10 days post-fertilization (dpf), as described by Legradi et al. (2015), also required an approved IACUC protocol (Appendix). Thus, the zebrafish embryogenesis and neurobehavioral models of toxicity afford diverse applications toward identifying neurotoxic metabolites and their neurobiological target(s) as shown, respectively, by Berry et al. (2007) and Legradi et al. (2015).

1.5 Key Questions to be Addressed

To conclude, marine algal communities are represented by diverse members of macroalgae (i.e., seaweeds), microalgae (e.g., diatoms, dinoflagellates) and cyanobacteria. Microalgae and cyanobacteria are known to produce potent, neurotoxic secondary metabolites that can adversely impact wildlife and humans, particularly when prolific. A Florida Keys marine mammal zoological facility houses captive bottlenose dolphins within enclosures (i.e., chain-linked fences) representative of a natural environment. The facility staff have observed the captive dolphins intermittently grazing the algae (i.e., macroalgae, cyanobacteria) growing within their enclosure and exhibiting behaviors symptomatic of neurotoxicity. Accepted methods and standards exist to a) taxonomically classify the dominant extant macroalgae and cyanobacteria genera and to b) evaluate collected algal samples for the presence of specific HAB-related neurotoxins. The zebrafish (*Danio rerio*) afford a rapid, bioassay-guided approach toward a) isolating and identifying potential neurotoxic metabolites present in the cyanobacteria and/or algae, associated with captive dolphin ingestions, collected from within the habitats and b) the toxicological characterization of relevant bioactive metabolites. Thus, the dissertation research attempted to identify the source of the dolphin intoxications by addressing the following key questions relevant to the two a priori major objectives:

- A. What are the dominant, potentially HAB-associated, macroalgae and/or cyanobacteria taxa, possibly being ingested by the captive dolphins, observed growing within the enclosures?

- B. What potential neurotoxin(s) is/are present in collected samples of cyanobacteria, possibly associated with algal ingestions by the captive dolphins? particularly:
- i) are any observed cyanobacteria producing known neurotoxins, specifically, anatoxin-a (ATX-a), β -methylamino-L-alanine (BMAA), and/or saxitoxin (STX)?
 - ii) are the known epiphytic HAB-related neurotoxins, brevetoxin-2 (PbTx-2) and/or domoic acid (DA), present?
 - iii) is a previously uncharacterized neurotoxin, or otherwise bioactive metabolite, being produced?

1.6 References

- Ali, S., van Mil, H.G.J., Richardson, M.K., 2011. Large-scale assessment of the zebrafish embryo as a predictive model in toxicity testing. *PLoS One* 6(6), e21076. doi:10.1371/journal.pone.0021076
- Ali, S., Champagne, D.L., Richardson, M.K., 2012. Behavioral profiling of zebrafish embryos exposed to a panel of 60 water-soluble compounds. *Behav. Brain Res.* 228, 272-283. doi:10.1016/j.bbr.2011.11.020
- Andersen, R.A., 1992. Diversity of eukaryotic algae. *Biodivers. Conserv.* 1, 267-292.
- Anderson, D.M., Burkholder, J.M., Cochlan, W.P., Gilbert, P.M., Gobler, C.J., Heil, C.A., Kudela, R., Parsons, M.L., Rensel, J.E.J., Townsend, D.W., Trainer, V.L., Vargo, G.A., 2008. Harmful algal blooms and eutrophication: Examining linkages from selected coastal regions of the United States. *Harmful Algae* 8(1), 39-53. doi:10.1016/j.hal.2008.08.017
- Anjum, K., Abbas, S.Q., Shah, S.A.A., Akhter, N., Batool, S., Hassan, S.S., 2016. Marine sponges as a drug treasure. *Biomol. Ther.* 24(4), 347-362. doi:10.4062/biomolther.2016.067
- Aráoz, R., Molgo, J., de Marsac, N.T., 2010. Neurotoxic cyanobacterial toxins. *Toxicon* 56(5), 813-828. doi:10.1016/j.toxicon.2009.007.036

- Badylak, S., Phlips, E.J., 2004. Spatial and temporal patterns of phytoplankton composition in a subtropical coastal lagoon, the Indian River Lagoon, Florida, USA. *J. Plankton Res.* 26(10), 1229-1247. doi:10.1093/plankt/fbh114
- Badylak, S., Phlips, E.J., Baker, P., Fajans, J., Boler, R., 2007. Distributions of phytoplankton in Tampa Bay estuary, U.S.A. 2002-2003. *B. Mar. Sci.* 80(2), 295-317.
- Bahl, J., Lau, M.C.Y., Smith, G.J.D., Vijaykrishna, D., Cary, C., Lacap, D.C., Lee, C.K., Papke, R.T., Warren-Rhodes, K.A., Wong, F.K.Y., McKay, C.P., Pointing, S.B., 2011. Ancient origins determine global biogeography of hot and cold desert cyanobacteria. *Nat. Commun.* 2, 163. doi:10.1038/ncomms1167
- Barbano, D., Diaz, R., Zhang, L., Sandrin, T., Gerken, H., Dempster, T., 2015. Rapid characterization of microalgae and microalgae mixtures using Matrix-Assisted Laser Desorption Ionization Time-of-Flight Mass Spectrometry (MALDI-TOF MS). *PLoS One* 10(8), e0135337. doi:10.1371/journal.pone.0135337
- Beatty, J.T., Overmann, J., Lince, M.T., Manske, A.K., Lang, A.S., Blankenship, R.E., Van Dover, C.L., Martinson, T.A., Plumley, F.G., 2005. An obligately photosynthetic bacterial anaerobe from a deep-sea hydrothermal vent. *PNAS* 102(26), 9306-9310. doi:10.1073/pnas.0503674102
- Bekker, A., Holland, H.D., Wang, P.L. Rumble III, D., Stein, H.J., Hannah, J.L., Coetsee, L.L., Beukes, N.J., 2004. Dating the rise of atmospheric oxygen. *Nature* 427(6790), 117-120. doi:10.1038/nature02260
- Beltran, E.C., Neilan, B.A., 2000. Geographical segregation of the neurotoxin-producing cyanobacterium *Anabaena circinalis*. *Appl. Environ. Microbiol.*, 66(10), 4468-4474. doi:10.1128/aem.66.10.4468-4474.2000
- Bergman, B., Sandh, G., Lin, S., Larsson, J., Carpenter E.J., 2012. *Trichodesmium* – a widespread cyanobacterium with unusual nitrogen fixation properties. *FEMS Microbiol. Rev.* 37, 286-302. doi:10.1111/j.1574-6976.2012.00352.x
- Berry, J.P., Gantar, M., Gibbs, P.D.L., Schmale, M.C., 2007. The zebrafish (*Danio rerio*) embryo as a model system for identification and characterization of developmental toxins from marine and freshwater microalgae. *Comp. Biochem. Physiol. C Toxicol. Pharmacol.* 145(1), 61-72. doi:10.1016/j.cbpc.2006.07.011
- Berry, J.P., Gibbs, P.D.L., Schmale, M.C., Saker, M.L., 2009. Toxicity of cylindrospermopsin, and other apparent metabolites from *Cylindrospermopsis raciborskii* and *Aphanizomenon ovalisporum*, to the zebrafish (*Danio rerio*) embryo. *Toxicon* 53(2), 289-299. doi:10.1016/j.toxicon.2008.11.016
- Best, J.D., Alderton, W.K., 2008. Zebrafish: An in vivo model for the study of neurological diseases. *Neuropsychiatr. Dis. Treat.* 4(3), 567-576. PMID:18830398

- Bloetscher, F., Meeroff, D.E., Plummer, J.D., 2010. Environmental reviews and case studies: evaluation of coastal ocean discharges and environmental impacts in southeast Florida. *Environmental Practice* 12(4), 285-303.
- Bozarth, A., Maier, U.-G., Zauner, S., 2009. Diatoms in biotechnology: modern tools and applications. *Appl. Microbiol. Biotechnol.* 82, 195-201. doi:10.1007/s00253-008-1804-8
- Brand, L.E., Pablo, J., Compton, A., Hammerschlag, N., Mash, D.C., 2010. Cyanobacterial blooms and the occurrence of the neurotoxin beta-N-methylamino-L-alanine (BMAA) in South Florida aquatic food webs. *Harmful Algae* 9(6), 620-635. doi:10.1016/j.hal.2010.05.002
- Buratti, F.M., Manganelli, M., Vichi, S., Stefanelli, M., Scardala, S., Testai, E., Funari, E., 2017. Cyanotoxins: producing organisms, occurrence, toxicity, mechanism of action and human health toxicological risk evaluation. *Arch. Toxicol.* 91, 1049-1130. doi:10.1007/s00204-016-1913-6
- Carlos, A.A., Baillie, B.K., Maruyama, T., 2000. Diversity of dinoflagellate symbionts (zooxanthellae) in a host individual. *Mar. Ecol. Prog. Ser.* 195, 93-100.
- Cavalier-Smith, T., 1998. A revised six-kingdom system of life. *Biol. Rev.* 73, 203-266.
- Cavalier-Smith, T., 2018. Kingdom Chromista and its eight phyla: a new synthesis emphasizing periplastid protein targeting cytoskeletal and periplastid evolution, and ancient divergences. *Protoplasma* 255, 297-357. doi:10.1007/s00709-017-1147-3
- Chen, J., Huang, C., Zheng, L., Simonich, M., Bai, C., Tanguay, R., Dong, Q., 2011. Trimethyltin chloride (TMT) neurobehavioral toxicity in embryonic zebrafish. *Neurotoxicol. Teratol.* 33, 721-726. doi:10.1016/j.ntt.2011.09.03
- Christmas, N.A.M., Anesio, A.M., Sánchez-Baracaldo, P., 2015. Multiple adaptations to polar and alpine environments within cyanobacteria: a phylogenomic and Bayesian approach. *Front. Microbiol.* 6, 1070. doi:10.3389/fmicb.2015.01070
- Cohen, Y., Jørgensen, B.B., Revsbech, N.P., Poplawski, R., 1986. Adaptation to hydrogen sulfide of oxygenic and anoxygenic photosynthesis among cyanobacteria. *Appl. Environ. Microbiol.* 51, 398-407.
- Comte, K., Šabacká, M., Carré-Mlouka, A., Elster, J., Komárek, J., 2007. Relationships between the Arctic and Antarctic cyanobacteria; three *Phormidium*-like strains evaluated by a polyphasic approach. *FEMS Microbiol. Ecol.* 59, 366-376. doi:10.1111/j.1574-6941.2006.00257.x
- Cox, P.A., Banack, S.A., Murch, S.J., Rasmussen, U., Tien, G., Bidigare, R.R., Metcalf, J.S., Morrison, L.F., Codd, G.A., Bergmen, B., 2005. Diverse taxa of cyanobacteria produce β -N-methylamino-L-alanine, a neurotoxic amino acid. *PNAS* 102(14), 5074-5078. doi:10.1073/pnas.0501526102

- Creton, R., 2009. Automated analysis of behavior in zebrafish larvae. *Behav. Brain Res.* 203(1), 127-136. doi:10.1016/j.bbr.2009.04.030
- Das, B.C, McCormick, L., Thapa, P., Karki, R., Evans, T., 2013. Use of zebrafish in chemical and biology drug discovery. *Future Med. Chem.* 5(17), 2103-2116. doi:10.4155/fmc.13.170
- de Esch, C., Sleiker, R., Wolterbeek, A., Woutersen, R., de Groot, D., 2012. Zebrafish as potential model for developmental neurotoxicity testing: A mini review. *Neurotoxicol. Teratol.* 34(6), 545-553. doi:10.1016/j.ntt.2012.08.006
- Desikachary, T.V., Dweltz, N.E., 1961. The chemical composition of the diatom frustule. In *P. Indian Acad. Sci. B* 53(4), 157-165. Springer India.
- Drapeau, P., Saint-Armant, L., Buss, R.R., Chong, M., McDearmid, J.R., Brustein, E., 2002. Development of the locomotor network in zebrafish. *Prog. Neurobiol.* 68(2), 85-111. doi:10.1016/s0301-0082(02)00075-8
- Dubinsky, Z., Jokiel, P.L., 1994. Ratio of energy and nutrient fluxes regulates symbiosis between zooxanthellae and corals. *Pac. Sci.* 48(3), 313-324.
- Engene, N., Coates, R.C., Gerwick, W.H., 2010. 16S rRNA gene heterogeneity in the filamentous marine cyanobacteria genus *Lyngbya*. *J. Phycol.* 46(3), 591-601. doi:10.1111/j.1529-8817.2010.00840.x
- Engene, N., Choi, H., Esquenazi, E., Rottacker, E.C., Ellisman, M.H., Dorrestein, P.C., Gerwick, W.H., 2011. Underestimated biodiversity as a major explanation for the perceived rich secondary metabolite capacity of the cyanobacterial genus *Lyngbya*. *Environ. Microbiol.* 13(6), 1601-1610. doi:10.1111/j.1462-2920.2011.02472.x
- Engene, N., Gunasekera, S.P., Gerwick, G.H., Paul, V.J., 2013. Phylogenetic inferences reveal large extent of novel biodiversity in chemically rich tropical marine cyanobacteria. *Appl. Environ. Microbiol.* AEM-03793. doi:10.1128/aem.03793-12
- Faassen, E.J., Harkema, L., Begeman, L., Lurling, M., 2012. First report of (homo)anatoxin-a and dog neurotoxicosis after ingestion of benthic cyanobacteria in the Netherlands. *Toxicon* 60, 378-384. doi:10.1016/j.toxicon.2012.04.335
- Falkowski, P.G., Dubinsky, Z., Muscatine, L., Porter, J.W., 1984. Light and the bioenergetics of a symbiotic coral. *Bioscience* 34(11), 705-709. doi:10.2307/1309663
- Faltermann, S, Grundler, V., Gademann, K., Pernthaler, J., Fent, K., 2016. Comparative effects of nodularin and microcystin-LR in zebrafish: 2. Uptake and molecular effects in eleuthero-embryos and adult liver with focus on endoplasmic reticulum stress. *Aquat. Toxicol.* 171, 77-87. doi:10.1016/j.aquatox.2015.12.001

- Fan, C.-Y., Cowden, J., Simmons, S.O., Padilla, S., Ramabhadran, R., 2010. Gene expression changes in developing zebrafish as potential markers for rapid developmental neurotoxicity screening. *Neurotoxicol. Teratol.* 32(1), 91-98. doi:10.1016/j.ntt.2009.04.065
- Ferrão-Filho, A.S., Koslowsky-Suzuki, B., 2011. Cyanotoxins: Bioaccumulation and Effects on Aquatic Animals. *Mar. Drugs* 9, 2729-2772. doi:10.3390/md9122729
- Fraysse, B., Mons, R., Garric, J., 2006. Development of a zebrafish 4-day embryo-larval bioassay to assess toxicity of chemicals. *Ecotox. Environ. Safe.* 63(2), 253-267. doi:10.1016/j.ecoenv.2004.10.015
- García-Camero, J.P., Catalá, M., Valcárcel, Y., 2012. River waters induced neurotoxicity in an embryo-larval zebrafish model. *Ecotox. Environ. Safe.* 84, 84-91. doi:10.1016/j.ecoenv.2012.06.029
- Gilbert, P.M., Heil, C.A., Hollander, D., Revilla, M., Hoare, A., Alexander, J., Murasko, S., 2004. Evidence for dissolved organic nitrogen and phosphorus uptake during a cyanobacteria bloom in Florida Bay. *Mar. Ecol. Prog. Ser.* 280, 73-83.
- Golubic S., Abed, R.M.M., Palinska, K., Pauillac, S., Chinain, M., Laurent, D., 2010. Marine toxic cyanobacteria: Diversity, environmental responses and hazards. *Toxicon* 56, 836-841. doi:10.1016/j.toxicon.2009.07.023
- Gomez, F., 2012. A checklist and classification of living dinoflagellates (Dinoflagellata, Alveolata). *CICIMAR Océánides* 27(1), 65-140.
- Gosselin, M., Legendre, L., Therriault, J.-C., Demers, S., Rochet, M., 1986. Physical control of the horizontal patchiness of sea-ice microalgae. *Mar. Ecol. Prog. Ser.* 29, 289-298.
- Grindberg, R.V., Ishoey, T., Brinza, D., Esquenazi, E., Coates, R.C., Liu, W., Gerwick, L., Dorrestein, P. C., Pevzner, P., Lasken, R., Gerwick, W.H., 2011. Single cell genome amplification accelerates identification of the apratoxin biosynthetic pathway from a complex microbial assemblage. *PLoS One* 6(4), e18565. doi:10.1371/journal.pone.0018565
- Grossman, A.R., 2005. Paths toward algal genomics. *Plant Physiol.* 137(2), 410-427. doi:10.1104/pp.104.053447
- Hajibabaei, M., Singer, G.A.C., Hebert, P.D.N., Hickey, D.A., 2007. DNA barcoding: how it complements taxonomy, molecular phylogenetics and popular genetics. *TRENDS Genet.* 23(4), 167-172. doi:10.1016/j.tig.2007.02.001
- Häubner, N., Schumann, R., Karsten, U., 2006. Aeroterrestrial microalgae growing in biofilms on facades-response to temperature and water stress. *Microbial Ecol.* 51, 285-293. doi:10.1007/s00248-006-9016-1

- Howe, D.G., Bradford, Y.M., Conlin, T., Eagle, A.E., Fashena, D., Frazer, K., Knight, J., Mani, P., Martin, R., Moxon, S.A.T., Paddock, H., 2012. ZFIN, the zebrafish model organism database: Increased support for mutants and transgenics. *Nucleic Acids Res.* 41(D1), D854-D860. doi:10.1093/nar/gks938
- Howe, K., Clark, M.D., Torroja, C.F., Berthelot, C., Muffato, M., Collins, J.E., Humphray, S., McLaren, K., Matthews, L., McLaren, S., 2013. The zebrafish reference genome sequence and its relationship to the human genome. *Nature* 496(7446), 498-503. doi:10.1038/nature12111
- Hsieh, C.J., Zhan, S.H., Liao, C.P., Tang, S.L., Wang, L.C., Watanabe, T., Geraldino, P.J.L., Liu, S.L., 2018. The effects of contemporary selection and dispersal limitation on the community assembly of acidophilic microalgae. *J. Phycol.*, 54(5), 720-733. doi:10.1111/jpy.12771
- Irons, T.D., MacPhail, R.C., Hunter, D.L., Padilla, S., 2010. Acute neuroactive drug exposures alter locomotor activity in larval zebrafish. *Neurotoxicol. Teratol.* 32(1), 84-90. doi:10.1016/j.ntt.2009.04.066
- Ismael, A.A., 2003. Succession of heterotrophic and mixotrophic dinoflagellates as well as autotrophic microplankton in the harbor of Alexandria, Egypt. *J. Plankton Res.* 25(2), 193-202.
- Jeong, H.J., Yoo, Y.D., Kim, J.S., Seong, K.A., Kang, N.S., Kim, T.H., 2010. Growth, feeding and ecological roles of the mixotrophic and heterotrophic dinoflagellates in marine phytoplanktonic food webs. *Ocean Sci. J.* 45(2), 65-91. doi:10.1007/s12601-010-0007-2
- Jiang, L., Ilag, L.L., 2014. Detection of endogenous BMAA in dinoflagellate (*Heterocapsa triquetra*) hints at evolutionary conservation and environmental concern. *PubRaw Sci.* 1(2), 1-8.
- Jonas, A., Scholz, S., Fetter, E., Sychrova, E., Novakova, K., Ortmann, J., Benisek, M., Adamovsky, O., Giesy, J. P., Hilscherova, K., 2015. Endocrine, teratogenic and neurotoxic effects of cyanobacteria detected by cellular in vitro and zebrafish embryo assays. *Chemosphere* 120, 321-327. doi:10.1016/j.chemosphere.2014.07.074
- Kalueff, V., Gebhardt, M., Stewart, A.M., Cachat, J.M., Brimmer, M., Chawla, J.S., Craddock, C., Kyzar, E.J., Roth, A., Landsman, S., Gaikward, S., Robinson, K., Baatrup, E., Tierney, K., Shamchuk, A., Norton, W., Miller, N., Nicolson, T., Braubach, O., Gilman, C. P., Pittman, J., Rosemberg, D.B., Gerlai, R., Echevarria, D., Lamb, E., Neuhaus, S.C.F., Weng, W., Bally-Cuif, L., Schneider, H., 2013. Towards a comprehensive catalog of zebrafish behavior 1.0 and beyond. *Zebrafish* 10(1), 70-86. doi:10.1089/zeb.2012.0861

- Kashiyama, Y., Ogawa, N.O., Kuroda, J., Shiro, M., Nomoto, S., Tada, R., Kitazato, H., Ohkouchi, N., 2008. Diazotrophic cyanobacteria as the major autotrophs during mid-Cretaceous oceanic anoxic events: Nitrogen and carbon isotopic evidence from sedimentary porphyrin. *Org. Geochem.* 39(5), 532-549.
doi:10.1016/j.orggeochem.2007.11.010
- Kimmel, C.B., Ballard, W.W., Kimmel, S.R., Ullmann, B., Schilling, T.F., 1995. Stages of embryonic development of the zebrafish. *Dev. Dynam.* 203, 253-310.
- Klumpp, D.W., Bayne, B.L., Hawkins, A.J.S., 1992. Nutrition of the giant clam *Tridacna gigas* (L.) I. Contribution of filter feeding and photosynthates to respiration and growth. *J. Exp. Mar. Biol. Ecol.* 155(1), 105-122. doi:10.1016/022-0981(92)90030-e
- Komárek, J., Kaštovský, J., Mareš, J., Johansen, J.R.J., 2014. Taxonomic classification of cyanoprokaryotes (cyanobacterial genera) 2014, using a polyphasic approach. *Preslia* 86, 295-335.
- Koutsos, E.A., Schmitt, T., Colitz, C.M., Mazzaro, L., 2013. Absorption and ocular deposition of dietary lutein in marine mammals. *Zoo Biol.* 32(3), 316-323.
doi:10.1002/zoo.21033
- LaJeunesse, T.C., 2002. Diversity and community structure of symbiotic dinoflagellates from Caribbean coral reefs. *Mar. Biol.* 141, 687-400. doi:10.1007/s00227-002-0829-2
- Lapointe, B.E., Tomasko, D.A., Matzie, W.R., 1994. Eutrophication and trophic state classification of seagrass communities in the Florida Keys. *B. Mar. Sci.* 54(3), 696-717.
- Lapointe, B.E., Bedford, B.J., 2007. Drift rhodophyte blooms emerge in Lee County, Florida, USA: Evidence of escalating coastal eutrophication. *Harmful Algae* 6(3), 421-437. doi:10.1016/j.hal.2006.12.005
- Lapointe, B.E., Herren, L.W., Debortoli, D.D., Vogel, M.A., 2015. Evidence of sewage-driven eutrophication and harmful algal blooms in Florida's Indian River Lagoon. *Harmful Algae* 43, 82-102. doi:10.10116/j.hal.2015.01.004
- Latysheva, N., Junker, V.L., Palmer, W.J., Codd, G.A., Barker, D., 2012. The evolution of nitrogen fixation in cyanobacteria. *Bioinformatics* 28(5), 603-606.
doi:10.1093/bioinformatics/bts008
- Lea-Smith, D.J., Biller, S.J., Davey, M.P., Cotton, C.A.R., Perez Sepulveda, B.M., Turchyn, A.V., Scanlan, D.J., Smith, A.G., Chisholm, S.W., Howe, C.J., 2015. Contribution of cyanobacterial alkane production to the ocean hydrocarbon cycle. *PNAS* 112(44), 13591-13596. doi:10.1073/pnas.1507274112
- Leblanc, K., Arístegui, J., Armand, L., Assmy, P., Beker, B., Bode, A., Breton, E., Cornet, V., Gibson, J., Gosselin, M.-P., Kopczynska, E., Marshall, H., Peloquin, J., Pointkovski, S., Poulton, A.J., Quéguiner, B., Schiebel, R., Shipe, R., Stefels, J., van

- Leeuwe, M.A., Varela, M., Widdicombe, C., Yallop., M., 2012. A global diatom database – abundance, biovolume and biomass in the world ocean. *Earth Syst. Sci. Data* 4, 149-165. doi:10.5194/essd-4-149-2012
- Lefebvre, K.A., Trainer, V.L., Scholz, N.L., 2004. Morphological abnormalities and sensorimotor deficits in larval fish exposed to dissolved saxitoxin. *Aquat. Toxicol.* 66, 159-170. doi:10.1016/j.aquatox.2003.08.006
- Legradi, J., el Abdellaoui, N., van Pomeran, M., Legler, J., 2015. Comparability of behavioral assays using zebrafish larvae to assess neurotoxicity. *Environ. Sci. Pollut. Res.* 22, 16277-16289. doi:10.1007/s11356-014-3805-8
- Leliaert, F., Smith, D., Moreau, H., Herron, M., Verbruggen, H., Delwiche, C., De Clerck, O., 2012. Phylogeny and molecular evolution of the green algae. *Crit. Rev. Plant Sci.* 31(1), 1-46. doi:10.1080/07352689.2011.615705
- Linney, E., Upchurch, L., Donerly, S., 2004. Zebrafish as a neurotoxicological model. *Neurotoxicol. Teratol.* 26(6), 709-718. doi:10.1016/j.ntt.2004.06.015
- Litaker, R.W., Vandersea M.W., Faust, M.A., Kibler, S. R., Chinain, M., Holmes, M.J., Holland, W.C., Tester, P.A., 2009. Taxonomy of *Gambierdiscus* including four new species, *Gambierdiscus caribaeus*, *Gambierdiscus carolinianus*, *Gambierdiscus carpenteri* and *Gambierdiscus ruetzleri* (Gonyaulacales, Dinophyceae). *Phycologia* 48, 344-390. doi:10.2216/07-15.1
- Long, S.-M., Liang, F.-Y., Wu, Q., Lu, X.-L., Yao, X.-L., Li, S.-C., Li, J., Su, H., Pang, J.-Y., Pei, Z., 2014. Identification of marine neuroactive molecules in behavior-based screens in the larval zebrafish. *Mar. Drugs* 12(6), 3307-3322. doi:10.3390/md12063307
- López-Rodas, V., Costas, E., Maneiro, E., Marva, F., Rouco, M., Delgado, A., Flores-Moya, A., 2009. Living in Vulcan's forge: Algal adaptation to stressful geothermal ponds on Vulcano Island (southern Italy) as a result of pre-selective mutations. *Phycol. Res.* 57(2), 111-117. doi:10.1111/j.1440-1835.2009.00527.x
- Lyon, B.R., Mock, T., 2014. Polar microalgae: new approaches towards understanding adaptations to an extreme and changing environment. *Biology*, 3(1), 56-80. doi:10.3390/biology3010056
- Lyons, T.W., Reinhard, C.T., Planavsky, N.J., 2014. The rise of oxygen in Earth's early ocean and atmosphere. *Nature* 506, 307-315. doi:10.1038/nature13068
- MacColl, R., 1998. Cyanobacteria phycobilisomes. *J. Struct. Biol.* 124(2-3), 311-334. doi:10.1006/jsbi.1998.4062
- Manoylov, K.M., 2014. Taxonomic identification of algae (morphological and molecular): Species concepts, methodologies, and their implications for ecological bioassessment. *J. Phycol.* 50, 409-424. doi:10.1111/jpy.12183

- Margulis, L., Schwartz, K.V., Dolan, M., 1999. Diversity of Life: The illustrated guide to the five kingdoms. Jones and Bartlett Learning.
- Méjean, A., Paci, G., Gautier, V., Ploux, O., 2014. Biosynthesis of anatoxin-a and analogues (anatoxins) in cyanobacteria. *Toxicon* 91, 15-22. doi:10.1016/j.toxicon.2014.07.016
- Méjean, A., Peyraud-Thomas, C., Kerbrat, A.S., Golubic, S., Pauillac, S., Chinain, M. Laurent, D., 2010. First identification of the neurotoxin homo-anatoxin-a from mats of *Hydrocoleum lyngbyaceum* (marine cyanobacteria) possibly linked to giant clam poisoning in New Caledonia. *Toxicon* 56, 829-835. doi:10.1016/j.toxicon.2009.10.029
- Mejia-Fava, J., Colitz, C.M.H., 2014. Supplements for Exotic Pets. *Vet. Clin. North Am. Exot. Anim. Pract.* 17(3), 503-525. Doi::10.1016/j.cvex.2014.05.001
- Mesnage, V., Bonneville, S., Laignel, B., Lefebvre, D., Dupont, J.-P., Mikes, D., 2002. Filling of a wetland (Seine estuary, France): natural eutrophication or anthropogenic process? A sedimentological and geochemical study of wetland organic sediments. *Hydrobiologia* 475/476, 423-435. doi:10.1023/A:1020355812786
- Metting Jr., F.B., 1996. Biodiversity and application of microalgae. *J. Ind. Microbiol.* 17, 477-489.
- Meylan A., 1988. Spongivory in hawksbill turtles: a diet of glass. *Science* 239(4838), 393-5.
- Mihali, T.K., Carmichael, W.W., Neilan, B.A., 2011. A putative gene cluster from a *Lyngbya wollei* bloom that encodes Paralytic Shellfish Toxin biosynthesis. *PLoS One* 6(2), e14657. doi:10.1371/journal.pone.0014657
- Milbrandt, E.C., Bartleson, R.D., Coen, L.D., Rybak, O., Thompson, M.A., DeAngelo, J.A., Stevens, P.W., 2012. Local and regional effects of reopening a tidal inlet on estuarine water quality, seagrass habitat, and fish assemblages. *Cont. Shelf Res.* 41, 1-16. doi:10.1016/j.csr.2012.03.012
- Moreira, C., Vasconcelos, V., Antunes, A., 2013. Phylogeny and biogeography of cyanobacteria and their produced toxins. *Mar. Drugs* 11(11), 4350-4369. doi:10.3390/md11114350
- Mueller, K.P., Neuhauss, S.C.F., 2010. Behavioral neurobiology: How larval fish orient to the light. *Curr. Biol.* 20(4), R59-R161. doi:10.1016/j.cub.2009.12.028
- Muscatine, L.E., Porter J.W., 1977. Reef corals: mutualistic symbioses adapted to nutrient-poor environments. *Bioscience* 27(7), 454-460. doi:10.2307/1297526
- Nagel, R., 2002. *DarT*: The embryo test with the zebrafish *Danio rerio* – a general model in ecotoxicology and toxicology. *Altex* 19(Suppl 1), 38-48.

- Neilan, B.A., Jacobs, D., Del Dot, T., Blackall, L.L., Hawkins, P.R., Cox, P.T., Goodman, A.E., 1997. rRNA sequences and evolutionary relationships among toxic and nontoxic cyanobacteria of the genus *Microcystis*. *Int. J. Syst. Bacteriol.* 47(3), 693-697.
- Nelson, D.M., Tréguer, P., Brzezinski, M.A., Leynaert, A., Quéguiner, B., 1995. Production and dissolution of biogenic silica in the ocean: revised global estimates, comparison with regional data and relationship to biogenic sedimentation. *Global Biogeochem. Cy.* 9(3), 359-372.
- Neustupa, J., Škaloud, P., 2010. Diversity of subaerial algae and cyanobacteria growing on bark and wood in the lowland tropical forests of Singapore. *Plant Ecol. Evol.* 143(1), 51-62. doi:10.5091/plecevo.2010.417
- Nowicka, B., Kruk, J., 2016. Powered by light: Phototrophy and photosynthesis in prokaryotes and its evolution. *Microbiol. Res.* 186-187, 99-118. doi:10.1016/j.micres.2016.04.001
- O'Neil, J.M., Davis, T.W., Burford, M.A., Gobler, C.J., 2012. The rise of harmful cyanobacteria blooms: The potential roles of eutrophication and climate change. *Harmful Algae* 14, 313-334. doi:10.1016/j.hal.2011.10.027
- Onodera, H., Satake, M., Oshima, Y., Yasumoto, T., Carmichael, W.W., 1997. New saxitoxin analogues from the freshwater filamentous cyanobacteria *Lyngbya wollei*. *Nat. Toxins* 5(4), 146-151. doi:10.1002/19970504nt4
- Oren, A., Padan, E., 1978. Induction of Anaerobic, photoautotrophic growth in the cyanobacterium *Oscillatoria limnetica*. *J. Bacteriol.* 133(2), 558-563.
- Otsuka, S., Suda, S., Li, R., Watanabe, M., Oyaizu, H., Matsumoto, S., Watanabe, M.M., 1999. Phylogenetic relationships between toxic and non-toxic strains of the genus *Microcystis* based on 16S to 23 S internal transcribed spacer sequence. *FEMS Microbiol. Lett.* 172(1), 15-21. doi:10.1111/j.1574-6968.1999.tb13443.x
- Padilla, S., Hunter, D.L., Padnos, B., Frady, S., McPhail, R.C., 2011. Assessing locomotor activity in larval zebrafish: Influence if extrinsic and intrinsic variables. *Neurotoxicol. Teratol.* 33(6), 624-630.
- Palinska, K.A., Abed, R.M.M., Charpy, L., Langlade, M.-J., Beltrán-Magos, Y., Golubic, S., 2015. Morphological, genetic and physiological characterization of *Hydrocoleum*, the most common benthic cyanobacterium in tropical oceans. *Eur. J. Phycol.* 50(2), 139-154. doi:10.1080/09670262.2051.1010239
- Pandey, K.D., Shukla, S.P., Shukla, P.N., Giri, D.D., Singh, J.S., Singh, P., Kashyap, A.K., 2004. Cyanobacteria in Antarctica: Ecology, physiology and cold adaptation. *Cell. Mol. Biol.* 50(5), 575-584. doi:10.1170/T547

- Parng, C., Roy, N.M., Ton, C., Lin, Y., McGrath, P., 2006. Neurotoxicity assessment using zebrafish. *J. Pharmacol. Tox. Met.* 55(1), 103-112. doi:10.1016/j.vascn.2006.04.004
- Pauli, J.N., Mendoza, J.E., Steffan, S.A., Carey, C.C., Weimer, P.J., Peery, M.Z., 2014. A syndrome of mutualism reinforces the lifestyle of a sloth. *Proc. R. Soc. B* 281, 20133006. doi:10.1098/rspb.2013.3006
- Pelkowski, S.D., Kappoor, M., Richendrfer, H.A., Wang, X., Colwill, R.M., Creton, R., 2011. A novel high-throughput imaging system for automated analyses of avoidance behavior in zebrafish larvae. *Behav. Brain Res.* 223(1), 135-144. doi:10.1016/j.bbr.2011.04.033
- Perera, I., Subashchandrabose, R.R., Venkateswarlu, K., Naidu, R., Megharaj, M., 2018. Consortia of cyanobacteria/microalgae and bacteria in desert soils: an underexplored microbiota. *Appl. Microbiol. Biot.* 102(17), 7351-7363.
- Phlips, E.J., Badylak, S., 1996. Spatial variability in phytoplankton standing crop and composition in a shallow inner-shelf lagoon, Florida Bay, Florida. *B. Mar. Sci.* 58(1), 203-216.
- Phlips, E.J., Badylak, S., Youn, S., Kelley, K., 2004. The occurrence of potentially toxic dinoflagellates and diatoms in a subtropical lagoon, the Indian River Lagoon, Florida, USA. *Harmful Algae* 3, 39-49. doi:10.1016/j.hal.2003.08.003
- Phlips, E.J., Badylak, S., Christman, M., Wolny, J., Brame, J., Garland, J., Hall, L., Hart, J., Landsberg, J., Lasi, M., Lockwood, J., Paperno, R., Scheidt, D., Staples, A., Steidinger, K., 2011. Scales of temporal and spatial variability in the distribution of species in the Indian River Lagoon, Florida, USA. *Harmful Algae* 10(3), 277-290. doi:10.1016/j.hal.2010.11.001
- Purdie, E.L., Samsudin, S., Eddy, F.B., Codd, G.A., 2009. Effects of the cyanobacterial neurotoxin β -N-methylamino-L-alanine on the early-life stage development of zebrafish (*Danio rerio*). *Aquat. Toxicol.* 95(4), 279-284. doi:10.1016/j.aquatox.2009.02.009
- Rasmussen, B., Fletcher, I.R., Brocks, J.J., Kilburn, M.R., 2008. Reassessing the first appearance of eukaryotes and cyanobacteria. *Nature* 455, 1101-1105. doi:10.1038/nature07381
- Raven, J.A., Giordano, M., 2014. *Algae*. *Curr. Biol.* 24(13), R590-R595.
- Réveillon, D., Séchet, V., Hess, P., Amzil, Z., 2016. Production of BMAA and DAB by diatoms (*Phaeodactylum tricorutum*, *Chaetoceros* sp., *Chaetoceros calcitrans* and *Thalassiosira pseudonana*) and bacteria isolated from a diatom culture. *Harmful Algae* 58, 45-50. doi:10.1016/j.hal.2016.07.008

- Rhind, S.M., 2009. Anthropogenic pollutants: a threat to ecosystem sustainability? *Phil. Trans. R. Soc. B* 364, 3391-3401. doi:10.1098/rstb.2009.0122
- Rodriguez, M.M., Mejia, J.C., Blanchard, M.T., Stott, J., Pestano, N., Perez, P.P., 2007. Pilot study: The affects of Natramune™ (PDS-2865®), a new immunostimulatory supplement on different cetacean species; *Tursiops truncatus*, *Lagenorhynchus obliquidens*, and *Orcinus orca*. In: Proceedings from the 38th Annual IAAAM Conference; May 17-22, 2007; Orlando, FL, USA.
- Rodriguez, M.M., Mejia, J.C., Blanchard, M.T., Stott, J., Pestano, N., Perez, P. Natramune™ (PDS-2865®), an immuno-stimulator supplement in cetaceans. In: Proceedings from the 39th Annual IAAAM Conference; May 10–14, 2008; Pomezia, Rome, Italy.
- Rowan, K.S., 1989. Photosynthetic Pigments of algae. CUP Archive.
- Rowan, R., 1998. Diversity and ecology of zooxanthellae on coral reefs. *J. Phycol.* 34(3), 407-417. doi:10.1046/j.1529-8817.1998.340407.x
- Ruggiero, M.A., Gordon, D.P., Orrell, T.M., Bailly, N., Bourgoin, T., Brusca, R.C., Cavalier-Smith, T., Guiry, M.D., Kirk, P.M., 2015. A higher level classification of all living organisms. *PLoS One* 10(4), e0119248.
- Samad, L.K., Adhikary, S.P., 2008. Diversity of micro-algae and cyanobacteria on building facades and monuments in India. *Algae* 23(2), 91-114.
- Sapp, J., 2005. The prokaryote-eukaryote dichotomy: Meanings and mythology. *Microbiol. Mol. Biol. Rev.* 69(2), 292-305. doi:10.1128/jmbr.69.2.292-305.2005
- Sarthou, G., Timmermans, K.R., Blain, S., Tréguer, P., 2005. Growth physiology and fate of diatoms in the ocean: a review. *J. Sea Res.* 53, 25-42. doi:10.1016/j.seares.2004.01.007
- Schneider, J. Le Campion-Alsumard, T., 1999. Construction and destruction of carbonates by marine and freshwater cyanobacteria. *Eur. J. Phycol.* 34(4), 417-426. doi:10.1080/09670269910001736472
- Schnepf, E., Elbrächter, M., 1992. Nutritional strategies in dinoflagellates: a review with emphasis on cell biological aspects. *Europ. J. Protistol.* 28(1), 3-24.
- Selderslaghs, I.W.T., Hooyberghs, J., De Coen, W., Witters, H.E., 2010. Locomotor activity in zebrafish embryos: A new method to assess developmental neurotoxicity. *Neurotoxicol. Teratol.* 32(4), 460-471. doi:10.1016/j.ntt.2010.03.002
- Selderslaghs, I.W.T., Hooyberghs, J., Blust, R., Witter, H.E., 2013. Assessment of the developmental neurotoxicity of compounds by measuring locomotor activity in zebrafish embryos and larvae. *Neurotoxicol. Teratol.* 37, 44-56. doi:10.1016/j.ntt.2013.01.003

- Smolker, R., Richards, A., Conner R., Mann, J., Berggren, P., 1997. Sponge carrying by dolphins (Delphinidae, *Tursiops* sp.): A foraging specialization involving tool use? *Ethology* 103, 454-465.
- Sipes, N.S., Padilla, S., Knudsen, T.B., 2011. Zebrafish-as an integrative model for twenty-first century toxicity testing. *Birth Defects Res. C* 93(3), 256-267. doi:10.1002/bdrc.20214
- Sivonen, K., Himberg, K., Luukkainen, R., Niemelä, S.I., Poon, G.K., Codd, G.A., 1989. Preliminary characterization of neurotoxic cyanobacteria blooms and strains from Finland. *Toxic. Assess.* 4(3), 339-3352. doi:10.1002/tox.2540040310
- Stanier, R.Y., Cohen-Bazire, G., 1977. Phototrophic prokaryotes: The cyanobacteria. *Ann. Rev. Microbiol.* 31, 225-274. doi:10.1146/annurev.mi.31.100177.001301
- Steunou, A.-S., Bhaya, D., Bateson, M.M., Melendrez, M.C., Ward, D.M., Brecht, E., Peters, J.W., Köhl, M., Grossman, A.R., 2006. *In situ* analysis of nitrogen fixation and metabolic switching in unicellular thermophilic cyanobacteria inhabiting hot spring microbial mats. *PNAS* 103(7), 2398-2403. doi:10.1073/pnas.0507513103
- Sun, L.-W., Jiang, W.-J., Sato, H., Kawachi, M., Lu, X.-W., 2016. Rapid classification of *Microcystis aeruginosa* strains using MALDI-TOF MS and phylogenetic analysis. *PLoS One* 11(5), e0156275. doi:10.1371/journal.pone.0156275
- Suutari, M., Majaneva, M., Fewer, D.P., Voinin, B., Friedl, T., Chiarello, A.G., Blomster, J., 2010. Molecular evidence for a diverse green algal community growing in the hair of sloths and a specific association with *Trichophilus welckeri* (Chlorophyta, Ulvophyceae). *BMC Evol. Biol.* 10, 86.
- Thomas, D.N., Dieckmann, G.S., 2002. Antarctic sea ice--a habitat for extremophiles. *Science*, 295(5555), 641-644. doi:10.1126/science.1063391
- Tiedeken, J.A., Ramsdell, J.S., Ramsdell, A.F., 2005. Developmental toxicity of domoic acid in zebrafish (*Danio rerio*). *Neurotoxicol. Teratol.* 27, 711-717.
- Tierney, K.B., 2011. Behavioural assessments of neurotoxic effects and neurodegeneration in zebrafish. *BBA-Mol. Basis Dis.* 1812(3), 381-389. doi:10.1016/j.bbadis.2010.10.011
- Tillet, D., Parker, D.L., Neilan, B.A., 2001. Detection of toxigenicity by a probe for the microcystin synthetase A gene (mcyA) of the cyanobacterial genus *Microcystis*: Comparison of toxicities with 16S rRNA and Phycocyanin Operon (Phycocyanin Intergenic Spacer) phylogenies. *Appl. Environ. Microbiol.* 67(6), 2810-2818. doi:10.1128/aem.67.6.2810-2818.2001
- Twiner, M.J., Flewelling, L.J., Fire, S.E., Bowen-Stevens, S.R., Gaydos, J.K., Johnson, C.K., Landsberg, J.H., Leighfield, T.A., Mase-Guthrie, B., Schwacke, L., Van Dolah,

- F.M., Wang, Z., Rowles, T.K., 2012. Comparative analysis of three brevetoxin-associated Bottlenose dolphin (*Tursiops truncatus*) mortality events in the Florida Panhandle region (USA). PLoS One 7(8), e42974. doi:10.1371/journal.pone.0042974
- Varshney, P., Mikulic, P., Vonshak, A., Beardall, J., Wangikar, P.P., 2015. Extremophilic micro-algae and their potential contribution in biotechnology. Bioresource Technol. 184, 363-372. doi:10.1016/j.biortech.2014.11.040
- Ward, D.M., Ferris, M.J., Nold, S.C., Bateson, M.M., 1998. A natural view of microbial biodiversity within hot spring cyanobacterial mat communities. Microbiol. Mol. Biol. Rev. 32(4), 1353-1370.
- Whitton, B.A., 1992. Diversity, ecology, and taxonomy of the cyanobacteria. In Photosynthetic prokaryotes. 1-51. Springer, Boston, MA
- Wieland, A., Köhl, M., 2000. Short-term temperature effects on oxygen and sulfide cycling in a hypersaline cyanobacterial mat (Solar Lake, Egypt). Mar. Ecol. Prog. Ser. 196, 87-102.
- Wierzchos, J.W., Ascaso, C., McKay, C.P., 2006. Endolithic cyanobacteria in halite rocks from the hyperarid core of the Atacama Desert. Astrobiology 6(3), 415-422.
- Woese, C.R., Fox, G.E., 1977. Phylogenetic structure of the prokaryotic domain: The primary kingdoms. PNAS 74(11), 5088-5090. doi:10.1073/pnas.74.11.5088
- Wu, Q., Yan, W., Liu, C., Li, L., Yu, L., Zhao, S., Li, G., 2016. Microcystin-LR exposure induces developmental neurotoxicity in zebrafish embryo. Environ. Pollut. 213, 793-800. doi:10.1016/j.envpol.2016.03.048
- Zhang, C., Willett, C., Fremgen, T., 2003. Zebrafish: An animal model for toxicological studies. Curr. Protoc. Toxicol. 17(1), 1-7. doi:10.1002/0471140856.tx0107s17
- Zimmerman, A.R., Canuel, E.A., 2000. A geochemical record of eutrophication and anoxia in Chesapeake Bay sediments: anthropogenic influence on organic matter composition. Mar. Chem. 69, 117-137.

2. TAXONOMIC CHARACTERIZATION OF ALGAL AND CYANOBACTERIA COMMUNITIES

2.1 Introduction

As described in Chapter One, captive bottlenose dolphins (*Tursiops truncatus*), managed in Florida Keys marine mammal zoological facility were recently observed by facility staff to occasionally graze the marine flora (e.g., macroalgae, cyanobacteria) growing within their habitats, followed by apparent neurotoxic seeming intoxications. The available scientific literature holds no accounts of wild or captive bottlenose dolphins ingesting algae. At the marine mammal facility, the captive bottlenose dolphins are fed a strict, human-controlled diet consisting of previously frozen fish (e.g., sprat, herring, mackerel, menhaden, whiting) and squid. Their diet is augmented with freshwater, vitamins, and prophylactic holistic supplements to ensure proper nutrition and health. Following the observed ingestions of macroalgae and cyanobacteria, the captive dolphins displayed signs of intoxication with seemingly neurological symptoms (e.g., ataxia, disorientation, uncoordinated swimming, respiratory issues, blepharospams) as described by the staff veterinarian. Every case of apparent intoxication was addressed and resolved by the veterinarian staff.

The marine mammal zoological facility, located in the Florida Keys, is within the coastal system of the Florida Bay estuary and the Atlantic Ocean. The captive bottlenose dolphin enclosures (i.e., chain-linked fencing) therein afford a more representative natural environment including habitat for local marine flora (i.e., sea grasses, algae, cyanobacteria). However, the facility is part of a residential boating community subject to nutrient rich anthropogenic effluence (e.g., sewage, fertilizer, petroleum) as described by

Lapointe and Clark (1992). Historically, seagrass communities comprised of turtle grass (*Thalassia testudinum*), shoal grass (*Halodule wrightii*), widgeon grass (*Ruppia maritima*) and manatee grass (*Syringodium filiforme*), replete with a biodiverse food web (e.g., invertebrates, fish, mammals, birds), dominated the estuarine bay and keys of Florida (Fourqurean and Robblee, 1999; Lapointe, 1989). However, over the last century, Florida Bay and the interconnected Florida Keys have become increasingly subject to episodic eutrophication from increasing urban development and associated human activities, as described by Lapointe and Clark (1992), Lapointe et al. (1994) and Corbett et al. (1999). Butler et al. (1995) also documented the observed decline of the Florida Bay estuary to eutrophic conditions resulting from the anthropogenic alterations of the Florida Everglades watershed. Such anthropogenic eutrophication allows for uncontrolled propagation of marine algae and cyanobacteria (O'Neil et al., 2012) relevant to the Florida Keys and the marine mammal zoological facility. Indeed, dense macroalgae and cyanobacterial growth was observed at the captive bottlenose dolphin facility.

Marine microalgae, particularly diatoms and dinoflagellates, and cyanobacteria are known to produce multifarious, toxic secondary metabolites. Harmful algal blooms (HAB) result from overgrowth of these toxin-producing algae and cyanobacteria (Heisler et al., 2008). Rapid releases of toxic metabolites occur as blooms abate adversely impacting local wildlife (e.g., shellfish, fish, birds, mammals) and humans (Anderson et al., 2008). For example, Fire et al. (2007) and Twiner et al. (2011) reported recurring episodes of HAB events in southwest Florida (i.e., Sarasota Bay) resulting in high mortalities in the wild bottlenose dolphin population. In these cases, the mortalities were directly associated with environmental exposures from aerosols and consuming prey that

were contaminated with two different HAB-related neurotoxins (e.g., brevetoxins, domoic acid). Bricelj et al. (2012) reported bioaccumulations of brevetoxins in primary vector organisms can directly and adversely impact trophic transfer to higher level consumers and predators. Brevetoxins (PbTx) are produced by the marine dinoflagellate, *Karenia brevis*, and are associated with red tides. Brevetoxicosis is more commonly known as Neurotoxic Shellfish Poisoning (NSP) in humans. Domoic acid (DA) is produced by the marine diatom, *Pseudo-nitzschia* spp., and is responsible for Amnesic Shellfish Poisoning (ASP) in humans.

Freshwater and marine cyanobacteria, particularly *Lyngbya* spp. (e.g., *L. wollei*, *L. majuscula*), also produce a series of potent neurotoxins leading to rapid death (e.g., anatoxins), neurodegeneration (e.g., β -methylamino-L-alanine) and potentially fatal Paralytic Shellfish Poisoning (PSP) (e.g., saxitoxins). These neurotoxins can bio-magnify, cause neurodegenerative illnesses, and be fatal (Ar oz et al., 2010; Brand et al., 2010). A host of neurotoxic secondary metabolites including the jamaicamide family of polyketide-peptides (Edwards et al., 2004) and the lipopeptides, antillatoxins and kalkitoxins (Berman et al., 1999; Wu et al., 2000; Nogle et al., 2001; Nogle and Gerwick, 2003), have been isolated and biochemically characterized from the Caribbean marine cyanobacteria *Lyngbya majuscula*. A comprehensive review, by Liu and Rein (2010) describes the prolific suite of biologically active peptides isolated, over a three-year period, specifically from the tropical marine genus *Lyngbya sensu lato* (*s.l.*) throughout the Caribbean, tropical Western Atlantic and Gulf of Mexico. Mi et al. (2017) recently provided an updated review, covering the last ten years, of novel, bioactive peptides derived from marine cyanobacteria.

A first step toward assessing the potential contribution of algal and/or cyanobacterial toxins to intoxication events was to taxonomically characterize the dominant macroalgal and cyanobacterial communities growing within the captive dolphin enclosures to at least the genus level. Subsequently, targeted chemical evaluations of known neurotoxins associated with identified relevant toxigenic taxa could be performed. A second factor considered possible seasonal effects shifting resident cyanobacteria and algal population dominance, leading to overgrowth and the potential release of neurotoxic metabolites during periods of decline and associated HAB events. Lastly, facility staff began an active monitoring program during normal business hours, to log directly observed dolphin algal ingestions including cyanobacteria, appraising the frequency, genus identity and any associated health impacts (i.e., intoxication). Thus, characterizing the dominant macroalgae and cyanobacteria (e.g., taxonomy, diversity, seasonality, toxigenicity) observed growing within the captive dolphin enclosures was the primary focus of this study with the goal of identifying potential neurotoxigenic varieties.

Classical taxonomy tools (e.g., morphology, microscopy) remain informative, and generally essential to preliminary taxonomic identification. Modern taxonomy methods (i.e., molecular phylogeny, gene sequencing), as described in Chapter One, have become particularly useful for more precise species identification and differentiation of algae and cyanobacteria (Moreira et al., 2013; Engene et al., 2011; Grossman, 2005). For example, Engene et al. (2010, 2013a) applied the genetic biomarker 16S rRNA and mass spectrometry (i.e., MALDI-TOF-MS, LC-MS/MS) to characterize the molecular phylogeny of *Lyngbya* spp. Specifically, the phylogenetic and molecular evaluation of *L. majuscula* revealed two new genera, *Okeania* gen. nov. (Engene et al., 2013b) and

Moorea gen. nov. (Engene et al., 2012). More recently, phylogenetic approaches were coupled with liquid chromatography-mass spectrometry (LC-MS) analysis to taxonomically characterize cyanobacteria species using specific secondary metabolite composition (Salvador-Reyes et al., 2015). Herein, classical and modern taxonomic approaches were applied, as much as possible, to characterize the dominant macroalgae and cyanobacteria relevant to identifying the algal community composition and relevant neurotoxic genera. Thus, this chapter focused on the following two main objectives:

2.1.1 Taxonomic Survey of Dominant Macroalgae and Cyanobacteria

The first objective was to survey the macroalgal and cyanobacteria communities growing within the captive dolphin habitats to assess the composition, dominance, seasonality, and presence of harmful algae genera using qualitative observations and morphology-based taxonomic methods to at least the genus level.

2.1.2 Associated Neurotoxic Metabolites

The second objective was to ascertain if the identified algae and cyanobacteria taxa, growing at the site, and possibly being ingested by the captive dolphins, have the potential to produce neurotoxic secondary metabolites based on their taxonomic identity.

2.2 Methodologies

2.2.1 Sampling of Dominant Macroalgae and Cyanobacteria

The cyanobacteria and macroalgae communities present within the captive dolphin enclosures, located at 25.084192° N, 80.442295° W, were examined quarterly to determine seasonal dominance and variability toward subsequent evaluation of neurotoxic, or otherwise relevant, bioactive compounds associated with these taxa. Qualitative assessments of the macroalgae and cyanobacteria growing within the captive

dolphin habitats occurred at least seasonally (e.g., spring, summer, fall, winter) by visual observations from above and below the water to estimate the prevalence, absence, and diversity of Chlorophyta (greens), Rhodophyta (reds), Phaeophyta (browns), and Cyanophyta (blue-greens). Relative abundances of the dominant macroalgae and cyanobacteria were estimated and recorded at each timepoint.

2.2.1.1 Sampling Process

Samples of the dominant macroalgae and cyanobacteria were collected, by snorkeling from within the captive dolphin habitats, at least quarterly, from July 2013 through January 2016, for taxonomic characterization and to identify the presence of harmful algae species (e.g., cyanobacteria, macroalgae, microalgae) being ingested by the captive dolphins. A final collection occurred in December 2018 to assess the impact of Hurricane Irma on the algal community and gather additional cyanobacteria specimens for more precise taxonomic identification (i.e., molecular, genetic). At each timepoint, the collections of representative macroalgae and cyanobacteria samples were pre-sorted by phylum and obvious physical differences to avoid possible cross contamination prior to analysis (i.e., taxonomic characterization, chemical evaluation). Samples of site seawater were collected, from within the captive dolphin enclosures, twice to qualitatively assess the presence of HAB related microalgae. Taxonomic characterization of the macroalgae community relied primarily on physical examination using morphology-based identification techniques (i.e., light microscopy, reference field guides). More precise taxonomic methods using molecular-based phylogenetic techniques were applied to the cyanobacteria specimens.

2.2.1.2 Taxonomic Reference Samples

Individual voucher specimens of macroalgae and cyanobacteria were preserved at each collection event and coded as Lydon: DP-MMMYYYY to represent the collection date by month and year. Collection of reference specimens included lightly rinsing with site seawater to sort and remove debris (e.g., sand, rocks, macro-fauna/flora) before placing in labeled 15mL or 50mL Falcon polypropylene conical centrifuge tubes (Fisher Scientific, Fair Lawn, NJ, USA) filled with site seawater and packed on ice for immediate transport to the laboratory for preservation and morphological examination. A Leica Zoom 2000 dissecting microscope (Leica-Microsystems, Wetzlar, Germany) allowed the removal of remaining macro-flora/fauna from each voucher sample. The 2013 through 2016 reference samples were preserved in 4% formaldehyde (Fisher) aqueous solution for morphological identification. The 2018 macroalgae reference samples were preserved in 90% ethanol (Fisher) after rinsing with 20 μ m filtered seawater. The 2018 cyanobacteria specimens were culled from the mixed assemblage and morphologically differentiated by filament color and dimensions (e.g., width, cell length) using a Wild Heerbrugg MS dissecting microscope (Wild Heerbrugg, Heerbrugg, Germany) equipped with a 150-watt light source (Fiberoptic Solutions, Peabody, MA, USA). Representative cyanobacteria morphotypes (approximately 0.5 mg) were rinsed well with 20 μ m filtered seawater and prepared with 1.5 mL *RNAlater* (Ambion, Austin, TX, USA) in 1.5 mL Eppendorf Safe-Lock (Fisher) micro-centrifuge tubes for voucher specimens. All 2013-2016 voucher specimens and the 2018 macroalgae voucher specimens were foil-wrapped and held in the Marine Macroalgae Research Laboratory collection at Florida International University, Miami, FL, respectively identified to the

genus or species level (e.g., Lydon: DP-OCT2014-*Lyngbya* spp., Lydon: DP-OCT2014-*Caulerpa mexicana*). The 2018 cyanobacteria voucher specimens were preserved in RNAlater and stored (-80 °C) at the Smithsonian Marine Station at Fort Pierce in Fort Pierce, FL, respectively as Lydon-DP2018: CAL-II, CAL-V and CAL-FR.

2.2.1.3 Cyanobacteria Phylogenetic Samples

Since 2015, representative individual filamentous cyanobacteria samples (e.g., 1-2 mg each) were visually sorted, by their morphological differences (e.g., color, dimensions) from bulk cyanobacteria assemblages during field collections for molecular phylogenetic characterization. Sample preparation included light rinsing with 20 µm filtered site seawater followed by deionized water and immediate preservation in 1.5mL Eppendorf Safe-Lock (Fisher Scientific) micro-centrifuge tubes filled with RNAlater (Ambion). The phylogenetic analysis samples were secured in a zippered plastic bag and placed with dry-ice in a Styrofoam cooler for transport to the laboratory where stored at -80 °C until analyzed.

Representative cyanobacteria morphotypes of CAL-II, CAL-V and CAL-FR (approximately 0.2 mg each), culled from the mixed assemblage, were cleaned with 20 µm filtered seawater. The samples were then preserved in 1.5 mL RNAlater (Ambion) in 1.5 mL Eppendorf Safe-Lock (Fisher Scientific) micro-centrifuge tubes and stored frozen (-80 °C) until phylogenetic analysis.

2.2.1.4 Cyanobacteria Chemical Evaluation Samples

Large quantities (ca. 10 gallons) of cyanobacteria biomass were collected at each sampling timepoint for chemical evaluation of neurotoxic metabolites. All bulk cyanobacteria samples were lightly rinsed on site with seawater to remove major debris

(e.g., sand, rocks, macro fauna), then placed in labeled, zippered 1-gallon plastic bags filled with site seawater and set in a cooler with ice for direct transport to the laboratory for immediate processing or storage at -20 °C until processed. Laboratory processing of the biomass material included lightly rinsing with distilled water, removal of remaining visible debris, gently patting dry with paper towels, lyophilizing and blender pulverizing to prepare samples for chemical evaluations and bioassay-guided fractionation.

Subsequent biomass collections occurred on an as-needed basis and were treated as previously described. The 2018 filamentous cyanobacteria collection was cleaned with 20 µm filtered seawater and apportioned by the dominant morphotypes (i.e., red, green), using light microscopy, before lyophilization and chemical analysis by LC-MS to evaluate the specific secondary metabolite composition relevant to the isolated compound of interest.

2.2.1.5 Microalgae Evaluation Samples

To assess the presence of potential HAB microalgae, approximately 10 liters (L) of site seawater (i.e., North Lagoon) were passed through consecutive 100 µm and 20 µm sieves to collect microalgae. The filtered seawater was reserved and used to quantitatively transfer the captured 20-100 µm particulates into two separately labeled 50 mL Falcon polypropylene conical centrifuge tubes (Fisher Scientific) to a pre-concentrated volume of 45 mL. The total volume of each sample was brought up to 50 mL with 8:2 deionized water/ethanol (Fisher Scientific), as preservative and to retard proliferation until analysis. Two timepoints, June 2015 and January 2016, were chosen to evaluate seasonality differences between summer and winter, respectively. Reference samples of 100 mL unfiltered seawater were also retained at each sampling timepoint in

labeled 50 mL Falcon polypropylene conical centrifuge tubes (Fisher Scientific) and stored at -20 °C for possible future analysis.

2.3 Taxonomic Characterization Procedures

2.3.1 Morphology-based Identification

Taxonomic characterization methods included physical, morphology-based identification, using the Leica dissecting microscope, a Leica CM E compound light microscope equipped with an eyepiece digital camera (ScopeTek, Hangzhou, China) and relevant taxonomic guides (e.g., Littler and Littler, 2000; Guiry and Guiry, 2014-2018, [www.algaebase.org]; Littler et al., 2008). Macroalgae and cyanobacteria reference samples were identified to the genus level, at a minimum, and species level where definitive morphological characterizations allowed. The calibrated microscope ocular micrometer provided comparative measurements as needed. Digital micrographs afforded physical comparisons with taxonomic literature. A Microsoft Excel spreadsheet was used to catalog the representative dominant macroalgae and cyanobacteria community taxa with their respective authorities. Morphological evaluations performed at the Smithsonian Marine Station at Fort Pierce utilized the Wild Heerbrugg dissecting microscope equipped with a light kit and a Nikon Eclipse E8000 Differential Interference Contrast compound microscope (Nikon Instruments Inc., Melville NY, USA) for digital micrographs. Morphological measurements were calculated as the mean \pm SD of cell dimensions of three representative filaments for each winnowed cyanobacterial morphotype. More precise taxonomic identification of the macroalgae was not pursued and further taxonomic characterization of the cyanobacteria required phylogenetic techniques.

2.3.2 Chemical Analysis of Cyanobacteria by Low-Resolution LC-MS

Mass analysis of the 2018 cyanobacteria morphotype samples was conducted using the low-resolution LC-MS method, detailed in Chapter Five of this dissertation, to identify the specific secondary metabolite composition (e.g., eudesmacarbonate). Briefly, a Thermo Finnegan LC electrospray ionization MS system equipped with an LTQ Advantage Max mass spectrometer was employed. Chromatographic separation was achieved using a Grace (Alltech) Vyadac C₁₈ (Grace Division Discovery Science, Deerfield, IL, USA) column (100 o.d. × 2.1 i.d. mm, 5 μm) set at 30 °C. A binary mobile phase system consisted of (A) 0.1% aqueous formic acid in LC-MS grade water and (B) 0.1% formic acid in LC-MS grade acetonitrile. Elution of 10 μL injections occurred via a 22-min step gradient at 0.5 L/min flow rate ramped from 10% to 100% B in 15 min and held at 100% B for 6 min, then returned to 10% B in 4 min and re-equilibrated at 10% B for 2 min. The mass spectra were examined for the presence of the isolated bioactive metabolite (i.e., eudesmacarbonate) by its characteristic ions observed at m/z 267.2 [M+H]⁺, 289.2 [M+Na]⁺, 533.4 [2M+H]⁺, 555.4 [2M+Na]⁺, and 205.2 [M+H-62]⁺ (see Chapter Six, section 6.4.2 Structural Elucidation of Eudesmacarbonate).

2.3.3 Cyanobacteria Phylogeny

The RNA*later* - fixed and cryopreserved (-80 °C) cyanobacteria specimens, collected through 2016, were transferred, in their respective vials, under dry-ice, to the Engene laboratory at FIU for taxonomic identification following the molecular-phylogenetic protocol (i.e., 16S rRNA genetic biomarker) established by Engene et al. (2013a). Briefly, the genomic DNA of each cryopreserved specimen sample was extracted using the Wizard Genomic DNA Purification Kit (Promega, Madison, WI,

USA), according to the manufacturer's specifications. The concentration and purity of the DNA extracts were assessed using a NanoDrop-1000 spectrophotometer (Thermo Scientific, Waltham, MA, USA). Further attempts to phylogenetically characterize the cyanobacteria specimens were not pursued because insufficient DNA extracted material was obtained.

The December 2018 RNA*later* preserved (-80 °C) cyanobacteria specimens (i.e., CAL-II, CAL-V) underwent DNA extraction, at the Smithsonian Marine Station at Fort Pierce, using a DNeasy Plant Mini Kit (Qiagen, Hilden, Germany) as specified by the manufacturer. The concentration and purity of the extracted DNA were measured using a NanoDropOne spectrophotometer (ThermoScientific). The PCR-amplification of the 16S rDNA gene with the respective forward and reverse cyanobacterial primers, CY106F and CY781R (Nübel et al. 1997). The PCR products were cloned with a pGEM-T Easy Vector Systems (Promega Corp., Madison, WI, USA) according to the manufacturer's specifications. Clones were grown on Luria Broth (LB) agar plates containing 100 µg/mL Ampicillin, 0.1 mM isopropyl β-D-1-thiogalactopyranoside (IPTG) and 40 µg/mL 5-bromo-4-chloro-3-indolyl β-D-galactopyranoside (X-Gal) (GOLDBIO, St Louis, MO, USA). The PCR was conducted on white colonies with pUC/M13 primers (Promega Corp.). Colony PCR products of the correct size (i.e., ≥ 1 mm diameter) were then Sanger sequenced at the Laboratories of Analytical Biology (National Museum of History, Washington DC, USA). The resulting chromatograms were assembled using Sequencher v5.1. Phylogenetic analyses were performed using Randomized Axelerated Maximum Likelihood (RAXML) (Stamatakis, 2014) and relied on datasets from recent taxonomic revisions combined with GenBank searches via BLASTn (Altschul et al., 1997) to

retrieve closely related matches to CAL-V. The best phylogenetic tree was reconstructed from 1000 tree search restarts and branch support assessed with 1000 bootstrap replicates. The 16S rDNA sequences, obtained via cloning of the PSC products, were deposited in GenBank and the remaining portion of the CAL-V isolate is maintained at the Smithsonian Marine Station as a voucher.

2.3.4 Microalgae Assessments

Generally, morphology-based light microscopy was used to examine the relevance of the microalgae and epiphytes, observed in the taxonomic reference samples, with respect to possible HAB taxa. A qualitative assessment to identify potential HAB microalgae was attempted using a FlowCam Benchtop II Model particle analyzer (Fluid Imaging Technologies, Scarborough, ME, USA), courtesy of the FIU Fisheries Ecology and Acoustics Lab. Digital photographs were captured on the computer while a 5 mL aliquot of the preserved, pre-concentrated, 20-100 μm filtered site lagoon water passed through the FlowCam system. The system was flushed with 5 mL of ethanol, followed by 5 mL of distilled water between each sample. The software-processed images were sorted by size (e.g., phytoplankton enumeration). Despite the low-resolution of the captured digital images, an attempt was made to assess the presence of HAB related microalgae by qualitatively comparing published images of known HAB microalgae.

2.4 Results

The research project, initiated July 2013, was put on hold (i.e., algal collections, observational data) in December 2013, by the marine mammal zoological facility until the required Research Collaboration Agreement with FIU was approved by the facility research committee. The research agreement was drafted by this researcher and submitted

for approval to the Project Principal Investigator and the FIU Research Development Unit in January 2014. Significant delays occurred in the FIU approval process and the agreement was not approved by FIU until August 2014. Subsequently, the facility research committee approved the research agreement in September 2014 and the project resumed (i.e., algal collections, observational data) in October 2014. Although no official sampling of algae or cyanobacteria was permitted by FIU researchers during the interim, the facility staff, acting in good faith, collected some macroalgae and cyanobacteria samples between December 2013 and August 2014. The various samples were stored in a freezer (ca -20 °C) at the facility until the project was reinstated and samples could be retrieved by FIU (i.e., October 2014). The archived samples were excluded from taxonomic characterization (i.e., morphological, phylogenetic) due to degradation issues. Renewed sampling and analyses by FIU, began in October 2014 through January 2016. A final sampling occurred in December 2018 to assess possible impacts of recent hurricanes to the algal community within the captive dolphin habitats and to collect additional cyanobacteria samples for more precise phylogenetic characterizations.

2.4.1 Morphology-Based Identifications of Dominant Macroalgae and Cyanobacteria Taxonomies

The representative macroalgal communities, including cyanobacteria, observed growing within the captive dolphin enclosures at the facility year-round are listed with their morphology-based taxonomic and bibliographic references in Table 2.1 (i.e., macroalgae) and Table 2.2 (i.e., cyanobacteria) whilst, the specific sampling dates are recorded in Table 2.3.

Table 2.1 Dominant macrophyte taxa identified by morphology.

CLASS	ORDER	FAMILY	GENUS	SPECIES	AUTHORITY*
<i>Bryopsidophyceae</i>	<i>Bryopsidales</i>	<i>Bryopsidaceae</i>	<i>Bryopsis</i>	<i>hypnoides</i>	J.V. Lamouroux 1809: 333 [135]
		<i>Caulerpaceae</i>	<i>Caulerpa</i>	<i>mexicana</i>	Sonder ex Kützing 1849: 496
				<i>sertularioides</i>	(S. G. Gmelin) M. Howe 1905b: 576
				<i>verticillata</i>	J. Agardh 1847: 6
		<i>Derbesiaceae</i>	<i>Derbesia</i>	<i>vaucheriiformis</i> <i>xix. vaucheriaeformis</i>	(Harvey) J. Agardh 1887: 34
		<i>Halimedaceae</i>	<i>Halimeda</i>	<i>discoidea</i>	Decaisne 1842: 102
				<i>scabra</i>	M. Howe 1905a: 241, pls. 11, 12
		<i>Udoteaceae</i>	<i>Penicillus</i> <i>Udotea</i>	<i>capitatus</i>	Lamarck 1813: 299
				<i>dixonii</i>	D.S. Littler & M.M. Littler 1990a: 220, fig. 8
				<i>flabellum</i>	(J. Ellis & Solander) M. Howe 1904: 94, pl. 6
<i>Ulvophyceae</i>	<i>Ulvales</i>	<i>Ulvaceae</i>	<i>Ulva</i>	<i>lactuca</i>	Linnaeus 1753: 1163
				<i>rigida</i>	C. Agardh 1823: 410
<i>Florideophyceae</i>	<i>Ceramiales</i>	<i>Rhodomelaceae</i>	<i>Acanthophora</i>	<i>muscooides</i>	(Linnaeus) Bory de Saint-Vincent 1828 [1826-1829]: 156
				<i>spicifera</i>	(M. Vahl) Börgesen 1910: 201, figs. 18, 19; syn. <i>Fucus spiciferus</i> Vahl 1802: 44
		<i>Dasyaceae</i>	<i>Heterosiphonia</i>	<i>crispella</i>	(C. Agardh) M.J. Wynne 1985a: 87 * <i>Callithamnion crispellum</i> C. Agardh 1828: 183
	<i>Ceramiaceae</i>	<i>Polysiphonia</i>	<i>binneyi</i>	Harvey 1853: 37	
	<i>Gigartinales</i>	<i>Cystoloniaceae</i>	<i>Hypnea</i>	<i>valentiae</i>	(Turner) Montagne 1841 [1839-1841]: 161
		<i>Solieriaceae</i>	<i>Solieria</i>	<i>filiformis</i>	(Kützing) P.W. Gabrielson 1985: 278, figs. 1b, 1d; syn. <i>Euhymenia filiformis</i> Kützing 1863: 15
	<i>Halymeniales</i>	<i>Halymenaceae</i>	<i>Halymenia</i>	<i>pseudofloresii</i> <i>xix. pseudofloresia</i>	Collins & M. Howe 1916: 177
<i>Phaeophyceae</i>	<i>Dictyotales</i>	<i>Dictyoceae</i>	<i>Padina</i>	<i>gymnospora</i>	(Kützing) Sonder 1871: 47
<i>Angiospermae</i>	<i>Alismatales</i>	<i>Hydrocharitaceae</i>	<i>Thalassia</i>	<i>testudinum</i>	Banks ex Soland ex K. D. König 1805: 96

*The available reference field guides used for morphology-based identifications were Littler and Littler (2000) and Littler et al. (2008).

Table 2.2 Dominant cyanobacteria taxa identified by morphology.

CLASS	ORDER	FAMILY	GENUS	SPECIES	AUTHORITY ^a
<i>Cyanophyceae</i>	<i>Oscillatoriales</i>	<i>Oscillatoriaceae</i>	<i>Lyngbya s.l.</i> ^b	<i>confervoides</i>	C. Agardh ex Gomont 1892: 136, pl. III [3]: figs 5, 6
				<i>majuscula</i> ^b	Harvey ex Gomont 1892:131, pl. III: figs 3, 4
				<i>polychroa</i> ^c	(Meneghini) Rabenhorst 1846:83

^a The available reference field guides used for morphology-based identifications were Littler and Littler (2000) and Littler et al. (2008).
^b The *Lyngbya sensu lato* genus is currently undergoing taxonomic revisions using molecular genotyping to include the newly accepted genera of *Moorea* and *Okeania* formerly classified as the species *L. majuscula* (Engene et al., 2012, 2013b).
^c The currently accepted name is *L. sordida* Gomont ex Gomont (Guiry and Guiry, 2018, [www.algaebase.org]).

Table 2.3 Algae and cyanobacteria sampling dates.

COLLECTION YEAR	MONTH	SEASON	SAMPLES COLLECTED		
			Macroalgae	Cyanobacteria	Microalgae
2013	July	Summer	Y	Y	N
	October	Fall	Y	Y	N
	December*	Winter	Y	Y	N
2014	January-March*	Spring	Y	Y	N
	August*	Summer	Y	Y	N
	October	Fall	Y	Y	N
2015	January	Winter	Y	Y	N
	June	Spring	Y	Y	Y
2016	January	Winter	Y	Y	Y
2018	December	Winter	Y	Y	N

* Facility staff collected samples and stored (-20 °C) on site until October 2014. These samples were limited in size and combined and labeled December 2014 for subsequent processing.

Algae diversity changed little between collections based on the qualitative visual observations of prevalence, absence, and diversity of chlorophytes, rhodophytes, phaeophytes and cyanobacteria. The overall taxonomic composition is depicted in Figure 2.1.

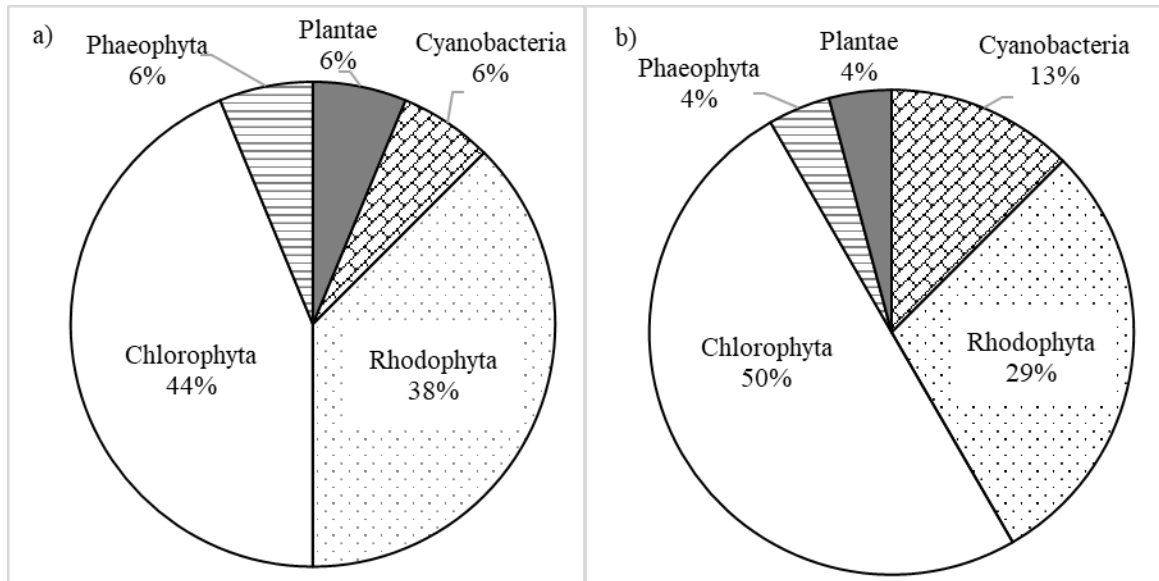


Figure 2.1 Taxonomic composition as percentages of the dominant macroalgae and cyanobacteria phyla by a) genus biodiversity and b) species biodiversity.

The qualitative abundance assessments, using visual inspections at four seasonal timepoints (e.g., summer, fall, winter, spring), deemed the three most abundant Chlorophyta genera to be *Caulerpa*, *Ulva* and *Halimeda* (Table 2.4).

Table 2.4 Observed seasonality of dominant chlorophyte genera.

Collection Date	Season	Primary genus	Secondary genus
July 2013	Summer	<i>Ulva</i>	<i>Halimeda</i>
October 2013	Fall	<i>Caulerpa</i>	<i>Halimeda</i>
October 2014	Fall	<i>Caulerpa</i>	<i>Halimeda</i>
January 2015	Winter	<i>Caulerpa</i>	<i>Halimeda</i>
June 2015	Spring	<i>Caulerpa</i>	<i>Halimeda</i>
January 2016	Winter	<i>Caulerpa</i>	<i>Halimeda</i>
December 2018	Winter	<i>Caulerpa</i>	<i>Halimeda</i>

Generally, *Caulerpa mexicana* proliferated during the fall through spring and *Ulva* spp. (e.g., *U. lactuca*, *U. rigida*) flourished in the summer months, while *Halimeda* spp. (e.g., *H. discoidea*, *H. scabra*) abundance remained essentially the same throughout the year. Figure 2.2 displays collected specimens of the dominant green macroalgae.

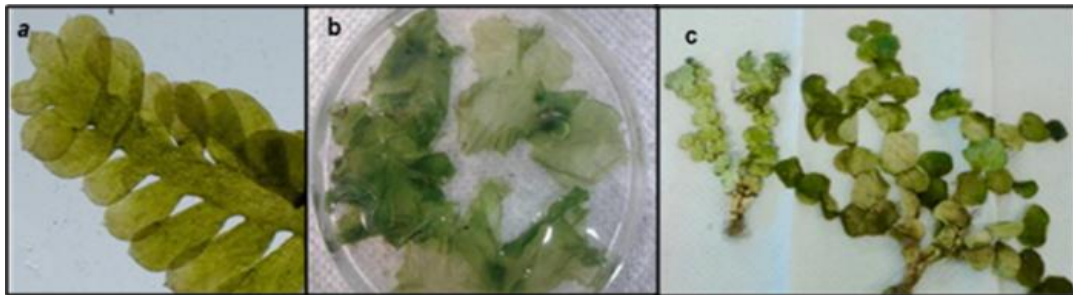


Figure 2.2 Dominant Chlorophyta: a *Caulerpa mexicana*, b *Ulva* spp. (e.g., *U. lactuca*, *U. rigida*), and c *Halimeda* spp. (e.g., *H. discoidea*, *H. scabra*). Photo credit: C. Lydon

Rhodophyta, or red seaweeds, were represented by seven species within six identified genera including *Acanthophora* (i.e., *A. muscoides*, *A. spicifera*), *Halymenia pseudofloresii*, *Heterosiphonia crispella*, *Hypnea valentiae*, *Polysiphonia binneyi*, and *Solieria filiformis*. The prevalence of Rhodophyta remained essentially the same at each collection timepoint. Phaeophyta, or brown seaweeds, were the least diverse group. Dominated by *Padina gymnospora*, their abundance also varied little across the study period. The seagrass, *Thalassia testudinum* was observed growing sparsely within the enclosures during the study as well. Cyanobacteria grew, copiously and continuously, throughout the enclosures (e.g., walls, fences, bottoms) with little variation in abundance during the study. Both epiphytic and dispersed within the red and green macroalgae, dense assemblages of filamentous cyanobacteria appeared as thick, red, green and red-hairy mats and tufts of purple and yellow (Figure 2.3).



Figure 2.3 Representative samples of epiphytic and dense, benthic mats of filamentous cyanobacteria collected during the study (e.g., October 2014): a red and green epiphytic, b yellow and purple tufts, and c red, red-hairy and green benthic mats mixed, respectively, within red and green macroalgae. Photo credit: C. Lydon

The physical appearances of the cyanobacterial mats observed in the captive dolphin enclosures were comparable to physical descriptions of benthic cyanobacteria mats (e.g., red mat, red hairy, purple tuft) collected from coral reefs near the Caribbean island of Curaçao detailed by Brocke et al. (2018). The captive dolphin enclosures were separated by chain-linked style fences, opposite a narrow canal permitting twice daily tidal flushing from the nearby Atlantic Ocean. Notably, the cyanobacteria proliferated to a much greater extent in the North enclosure than in the South enclosure. The qualitative, physical inspections of the captive dolphin habitats, over the study period, suggested the most prolific episodes of cyanobacteria growth occurred during the July and October 2013 collections. Initial morphological inspections under the light microscope revealed the epiphytic and dense, benthic mats of cyanobacteria comprised mixed assemblages of

the toxigenic, filamentous, polyphyletic genus *Lyngbya* (Agardh ex Gomont, 1892) including previously classified *L. confervoides* (i.e., yellow tufts, red and green filaments), *L. majuscula* (i.e., purple tufts, red and green filaments), and *L. polychroa* (red and red-hairy filaments) shown in Figures 2.4 and 2.5 and cross-referenced with the available field guides containing comparative images.

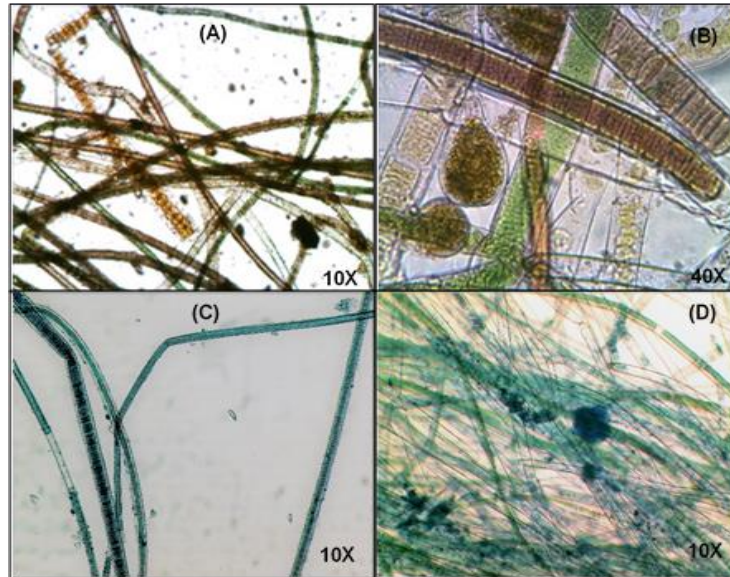


Figure 2.4 Light microscopy images of representative mixed assemblage filamentous cyanobacteria collections: (A) October 2014 benthic mat (10×), (B) October 2014 benthic mat (40×), (C) October 2014 purple tufts (10×), and (D) June 2015 yellow tufts (10×). Digital micrograph credit: C. Lydon

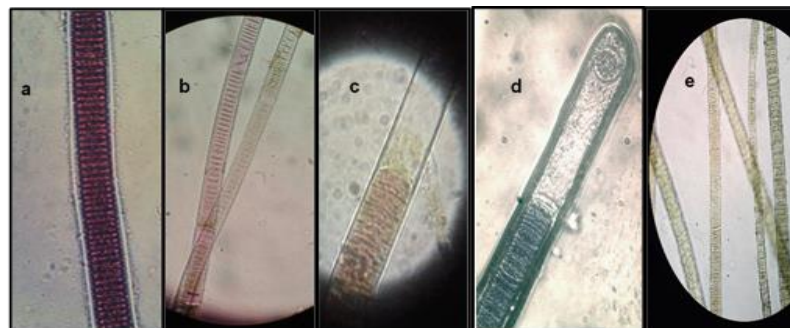


Figure 2.5 Digital micrographs of *Lyngbya* spp. morphotypes based on initial morphological examinations and comparisons with taxonomic classifications referenced from available field guides: a *L. polychroa* (63×), b-c *L. majuscula* (40×), d *L. majuscula* (63×), and e *L. confervoides* (40×). Digital image credit: C. Lydon

Taxonomic reference samples of the cyanobacteria, specifically grazed by the captive dolphins, were collected separately during the October 2014 sampling date and morphologically identified as *Lyngbya* spp. using available taxonomic reference guides (Littler and Littler, 2000; Littler et al., 2008). Recent revisions to the taxonomic characterization of the genus *Lyngbya s.l.* warranted an attempt to apply molecular phylogenetic techniques to more precisely discern the species level. The RNA^{later} (Ambion) prepared cyanobacteria specimens, collected in 2015, at the respective January and June sampling intervals, were submitted to the Engene laboratory (FIU Biology Department, Miami, FL) for phylogenetic and toxicological characterization as outlined in Engene et al. (2013a). However, insufficient genetic material was obtained to complete the phylogenetic analysis. Continuing the taxonomic designation of *Lyngbya* spp. was deemed appropriate, and in keeping with literature classifications, until phylogenetic characterization could be accomplished.

Morphological inspection of the filamentous cyanobacteria collected in December 2018 by light microscopy (Figure 2.6) revealed a similar mixed assemblage of red and green filaments as previously described. Upon closer examination at 40 \times , individual filaments could be differentiated primarily by color and trichome cell width (Figure 2.7). Most abundant were long (> 100 μm), dark red (II) and dark green (V) filaments, encased in clear sheaths averaging 25 μm wide, and having average cellular dimensions of 22 μm wide by 3 μm length (Table 2.5). Interspersed were larger red filaments (e.g., FR, RB), also encased in clear sheaths, a few purple (P) filaments and a small chain of gray bead-like cyanobacteria (GB) looped around a green filament (Figure 2.7).



Figure 2.6 Mixed assemblage filamentous cyanobacteria collected December 2018 (20×). Digital micrograph courtesy of Michael J. Boyle (Smithsonian Marine Station at Fort Pierce, Fort Pierce, FL USA).

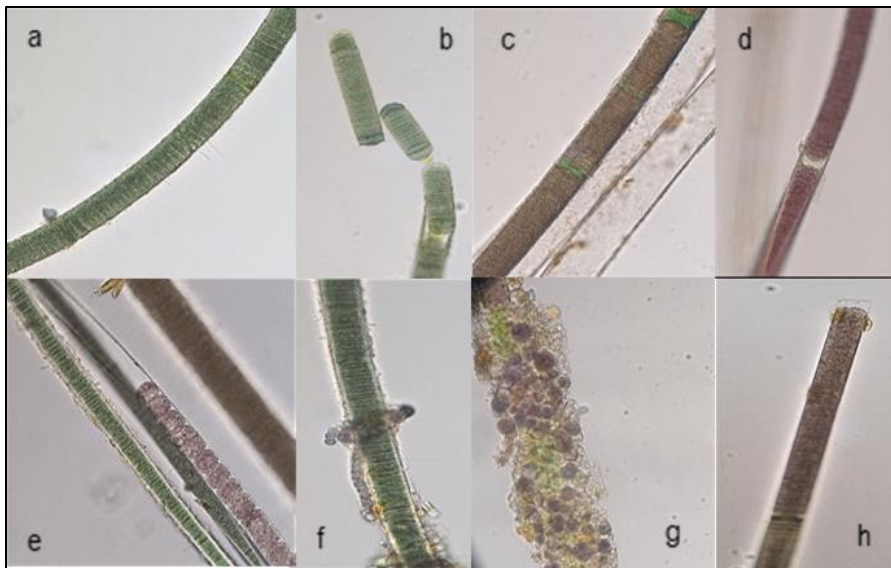


Figure 2.7 Representative mixed assemblage cyanobacteria filament morphotypes collected December 2018 (40×). a-b dark green (V), c-d dark red (II), e from left to right - thin greens (TG), red beads (RB) and large red (FR), f-g epiphytic gray bead-like chains (GB) and h purple (P). Digital micrographs courtesy of Michael J. Boyle (Smithsonian Marine Station at Fort Pierce, Fort Pierce, FL USA).

Table 2.5 Average measurements of representative cyanobacteria filaments collected December 2018.

Filament Description	ID Code	Sheath Width (µm), SD	Cell Width (µm), SD	Cell Length (µm), SD	Segment Length (µm), SD
Dark Red	II	24.6, 1.9	22.1, 1.9	2.9, 0.7	104, 44
Dark Green	V	25.0, 1.3	22.1, 0.7	2.5, 1.3	90, 16
Large Red	FR	37.9, 2.6	32.1, 1.9	3.8, 1.3	69, 18
Red Beads	RB	25.4, 0.7	22.9, 0.7	17.5, 1.3	62, 18
Thin Green	TG	15.4, 0.7	13.8, 1.3	2.9, 0.7	125, 13
Purple	P	47.5, 2.5	39.2, 3.8	3.8, 1.3	88, 1
Gray Bead-Like Chains	GB	NA	5.3, 0.3	5.3, 0.3	24, 3
ID Code = Strain morphotype identification label SD = Standard Deviation					

2.4.2 Low-Resolution LC-MS Analysis of Dominant Cyanobacteria Morphotypes

Comparative mass analysis of the cyanobacteria as the mixed assemblage and the morphotypes II (dark red) and V (dark green), by LC-MS, indicated that the filamentous dark green morphotype was the primary producer of the isolated bioactive metabolite (i.e., eudesmacarbonate) described in Chapter Six of the dissertation. As shown in the mass spectrum obtained for the dark green morphotype (i.e., CAL-V), eudesmacarbonate eluted at 10.3 minutes exhibiting characteristic ions at m/z 267.1 $[M+H]^+$, 205.2 $[M+H-62]^+$, 533.2 $[2M+H]^+$, and 555.2 $[2M+Na]^+$ (Figure 2.8). The acquired mass spectra also showed that the filamentous dark red strain (i.e., CAL-II) produced a secondary metabolite (i.e., 10.1 minutes retention time) having a different ion profile observed at m/z 299.3 $[M+H]^+$, 321.2 $[M+Na]^+$, 596.7 $[2M+H]^+$, and 619.1 $[2M+Na]^+$ with the implied molecular formula $C_{17}H_{27}O$ that was most likely an eudesmane derivative (Figure 2.9).

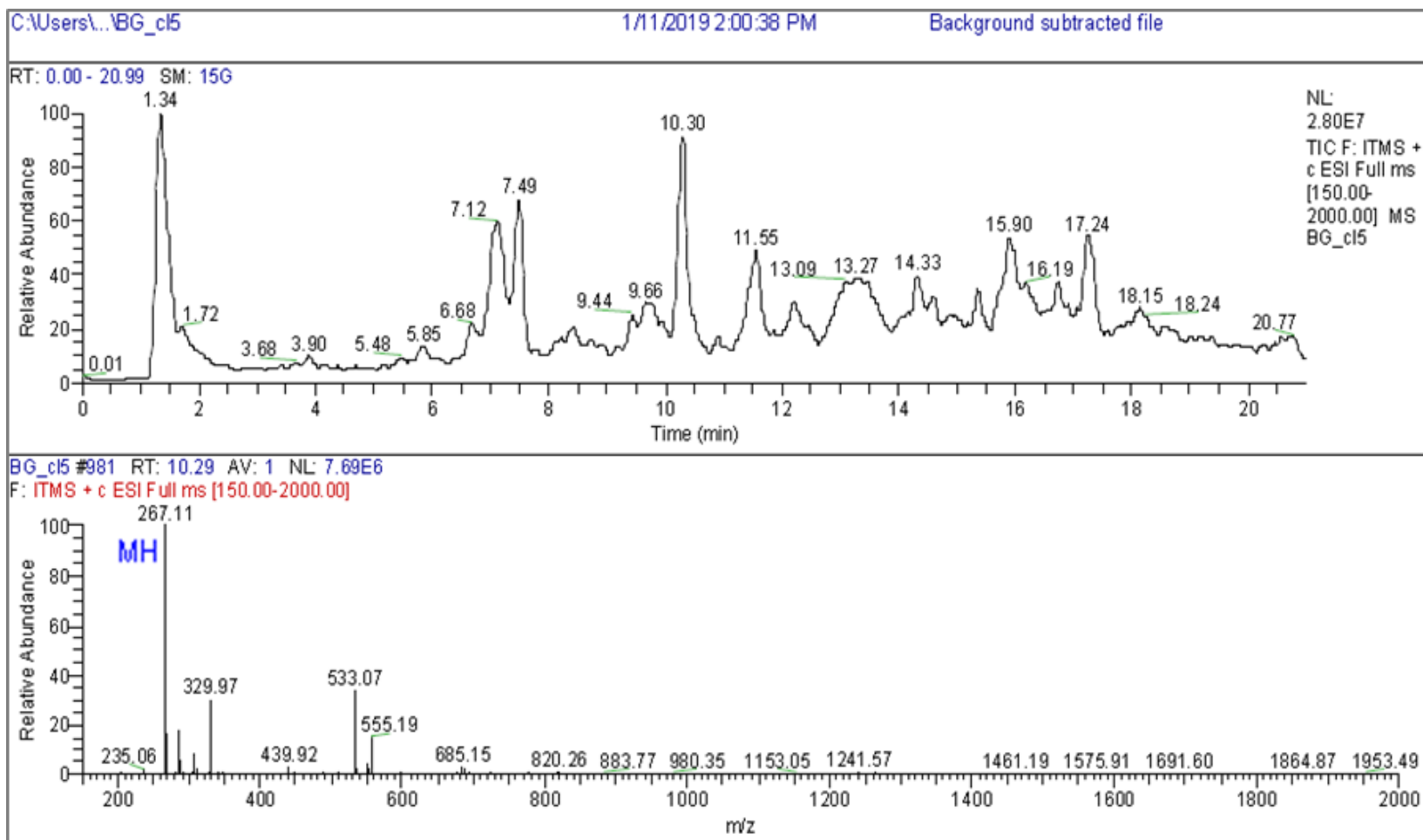


Figure 2.8 Low-resolution LC-MS of the dark green cyanobacteria morphotype (V) displaying the elution of the bioactive metabolite (i.e., eudesmacarbonate) at 10.30 minutes with MH indicating the $[M+H]^+$ peak.

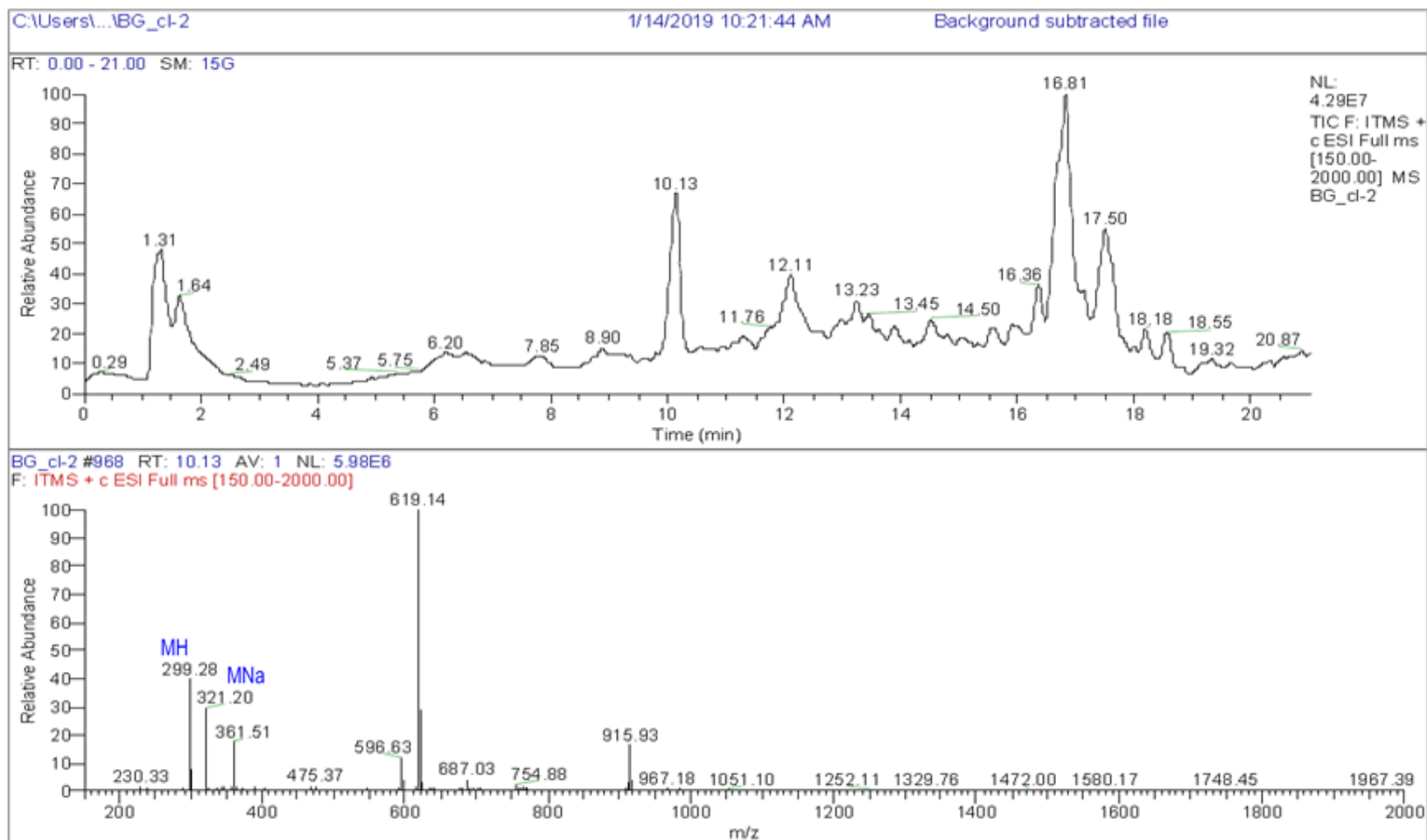


Figure 2.9 Low-resolution LC-MS of the dark red cyanobacteria morphotype (II) displaying the elution of a secondary metabolite at 10.13 minutes with MH indicating the $[M+H]^+$ peak and MNa indicating the $[M+Na]^+$ peak.

2.4.3 Cyanobacteria Phylogenetic Characterization

The CAL-V isolate 16S rDNA sequences, obtained via cloning of the PCR products and Sanger sequencing, were deposited under accession numbers MN845141-MN845143 in GenBank. Phylogenetic analysis of the sequences retrieved from BLASTn searches showed the filamentous, dark green CAL-V cyanobacteria represents closely related members of the family Oscillatoriaceae (Oscillatoriales). The reconstructed phylogenetic tree (See Figure 6.1, Chapter Six) revealed a novel member of the recently described genus *Neolyngbya* T.A. Caires, C.L. Sant’Anna et J.M.C. Nunes gen. nov. (Caires et al., 2018a), as the potentially dominating putative taxa, among *Neolyngbya arenicola* and a species found in a poorly resolved clade, clustering between the genera *Limnoraphis* (Komárek et al., 2013) and *Capilliphycus* (Caires et al., 2018b, Caires et al., 2019). The significant findings described herein, regarding the Oscillatoriacean membership comprising the CAL-V cyanobacteria morphotype and the isolated bioactive metabolite (i.e., eudesmacarbonate), are detailed in Chapter Six.

2.4.4 Potential Neurotoxicogenic Microalgae Taxa Observations

Reexamination, by light microscopy at 40×, of the grazed cyanobacteria reference samples (i.e., *Lyngbya* spp.), collected October 2014, revealed the presence of unidentified, epiphytic diatoms and dinoflagellates (Figure 2.10).

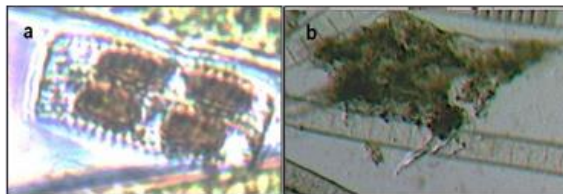


Figure 2.10 Unidentified microalgae examples, epiphytic to the October 2014 *Lyngbya* spp. taxonomic reference sample (40×): a diatom and b dinoflagellate. Digital micrograph credits: C. Lydon

Further scrutiny of the sampled filamentous cyanobacteria (i.e., *Lyngbya s.l.*), observed being ingested by the captive dolphins during the October 2014 collection, suggested the presence of the neurotoxic diatom, *Pseudo-nitzschia* spp. Figure 2.11 provides a visual comparison of the microscopically imaged epiphytic diatom, a, with the digital image of *Pseudo-nitzschia*. cf. *australis*, b, identified by Cusack et al. (2002) as a domoic acid producer.

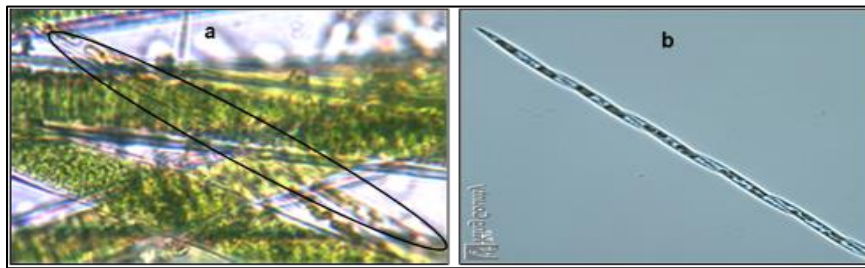


Figure 2.11 Epiphytic diatoms resembling *Pseudo-nitzschia* spp. versus literature image: a epiphytic diatoms on the October 2014 *Lyngbya* spp. taxonomic reference sample (40×) and b reference image of *P.* cf. *australis*. Digital image credits: a C. Lydon, b Gabriella Hannach (2014).

Digital imaging by light microscopy was limited to 10× and 40× magnifications as higher resolution images (e.g., 63×, 100×) were often blurred. The site seawater samples were subsequently collected at two timepoints (e.g., summer, winter) and filtered to capture 20-100 µm particulates (i.e., diatoms, dinoflagellates). A FlowCam apparatus (Fluid Imaging Technologies) was used to qualitatively screen the pre-concentrated filtrate and collect visible evidence (i.e., digital images) of the microorganisms present in the samples, particularly *K. brevis* and *Pseudo-nitzschia* spp. Generally, the digital images captured by the FlowCam were blurry and of low resolution, making definitive identifications of observed microalgae impossible. Image distortion was correlated to fine sediments in the samples, improper flow, and optical limitations. The January 2016

sample contained very few organisms. The June 2015 sample was more turbid than the January 2016 sample, consistent with the observed fine sediments. The June 2015 sample also held a greater enumeration and heterogeneity of captured microorganisms than the January 2016 sample. Thus, the FlowCam digital images, obtained from the June 2015 sample, afforded the best evidence of potential HAB-related phytoplankton. Figure 2.12 exemplifies a sampling of the digital images captured by the FlowCam system from the June 2015 collection.

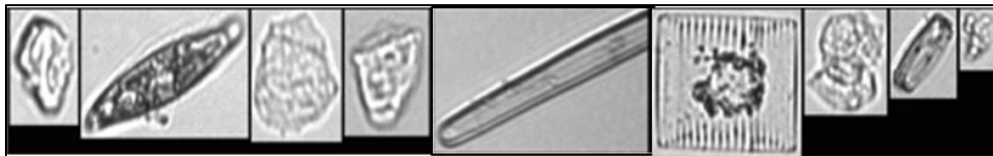


Figure 2.12 Example FlowCam micrographs of 20–100 μm filtered particulates from the June 2015 site seawater collection. Digital image credit: C. Lydon

The turbidity of the June 2015 collection samples compromised the quality of the FlowCam digital images. At best, only a couple of marine dinoflagellates could be potentially discerned by their distinguishable characteristics. As shown in Figure 2.13, a few images (i.e., a, b, c), captured by the FlowCam system, remotely resembled the brevetoxin-producing dinoflagellate, *Karenia brevis*, when directly compared to d, a FlowCam acquired image of *K. brevis*, published by Campbell et al. (2013).

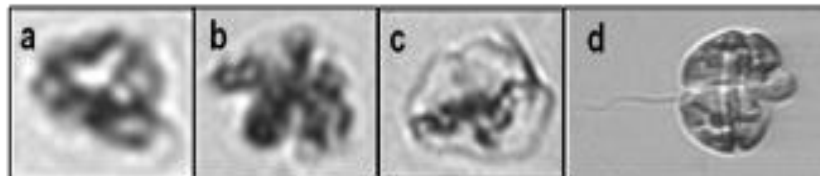


Figure 2.13 Comparative FlowCam images of unidentified dinoflagellates resembling *Karenia brevis* versus literature image: a-c FlowCam images from the June 2015 site seawater sample and d published FlowCam image of *K. brevis*. Digital image credits: a-c C. Lydon, d Campbell et al. (2013).

A visual comparison (Figure 2.14) of the June 2015 digital image of a dinoflagellate acquired by FlowCam (B), suggested the possible observance of a *Ceratium* species (A), or a *Neoceratium* spp. (C, D) imaged by Gómez et al. (2010).

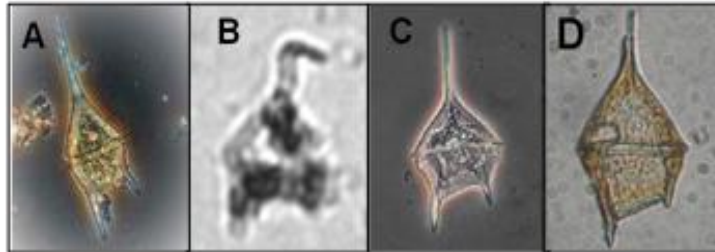


Figure 2.14 Comparison of unidentified June 2015 site seawater dinoflagellate versus literature examples: A *Ceratium lineatum*, B FlowCam image, C *Ceratium pentagonum* and D *Neoceratium minutum*. Digital image credits: A Gómez et al. (2010), B C. Lydon, C-D Gómez et al. (2010)

As depicted in Figure 2.15, another imaged dinoflagellate (A) appeared very similar to a mature *Ceratoperidinium falcatum* specimen (B), identified by Gárate-Lizárraga (2014) and formerly known as *Gyrodinium falcatum* (Kofoid and Swezy, 1921) Reñé et de Salas.

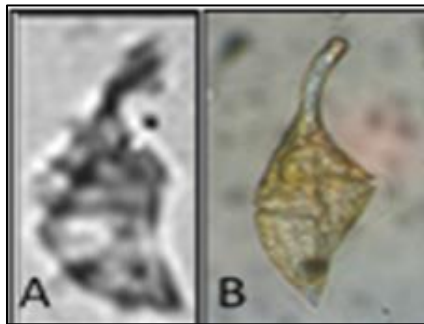


Figure 2.15 Comparison of unidentified June 2015 site seawater dinoflagellate resembling *Ceratoperidinium falcatum* versus reference image: A FlowCam image and B *C. falcatum* reference image. Digital image credits: A C. Lydon, B Gárate-Lizárraga (2014).

The FlowCam digital camera also captured the presence of several individual pennate diatoms sized between 20–100 μm (Figure 2.16). One diatom (a) appeared to be a member of the *Licmophora* (C. Agardh, 1827) genus and another (b) could only be identified as being a triradiate form, possibly associated to the *Centronella* (M. Voigt, 1901) genus (Echenique and Guerrero, 2004). Whilst, the other two images (c) and (d) were too blurry to attempt any definitive level of recognition, image (d) suggested the observed diatom possibly belonged to the genera *Amphora* (Ehrenberg ex Kützing, 1844) or *Seminavis* (D. G. Mann in Round et al., 1990), both extant in the FL Bay estuary (Wachnicka and Gaiser, 2007). The appearances of *Amphora* spp. have similar morphological characteristics to *Cymbella* spp. (C. Agardh). Currently, numerous diatoms species are undergoing taxonomic reclassifications via enhanced morphology-based microscopic approaches (e.g., scanning electron microscopy [SEM]). For example, Cavalcante et al. (2014) recently characterized a Brazilian coastal diatom as *Halamorpha* spp. ([Cleve] Levkov, 2009) using SEM and the revised classifications. The FlowCam images of the four example diatoms observed in the June 2015 sampled site seawater are shown for illustrative purposes only (Figure 2.16).



Figure 2.16 FlowCam images of diatoms observed in site seawater collected June 2015: a unidentified diatom (e.g., *Licmophora* spp.), b unidentified triradiate diatom (e.g., *Centronella* spp.), c unidentified diatom, and d unidentified diatom (e.g., *Amorpha* spp., *Cymbella* spp.). Digital image credit: C. Lydon

Light microscopy analysis of cyanobacteria and macroalgae taxonomic reference specimens, from each collection, revealed similar pennate diatoms when viewed at 40 \times

magnification (Figure 2.17). The microscopic images had slightly better resolution than the FlowCam images. One diatom (a) was recognized belonging to the genus *Bellerochea* (van Heurck, 1885), such as *B. malleus*, as described by Hernández-Becerril et al. (2013). Two of the microscopy imaged diatoms (b) and (c) appeared to be the same types as captured by the FlowCam imaging (e.g., Figure 2.16 b, c). Whilst, a fourth diatom (d), although more clearly resolved, also remained unidentified.

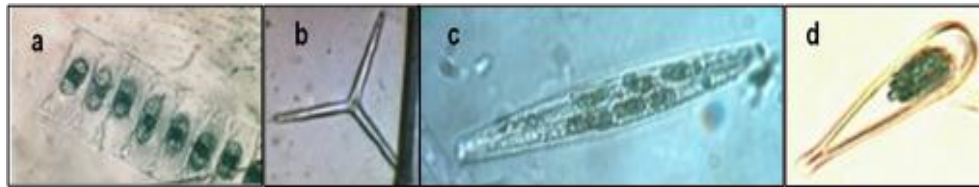


Figure 2.17 Example diatoms observed by light microscopy in the October 2014 *Lyngbya* spp. taxonomic reference sample (40×): a unidentified diatom (e.g., *Bellerochea* spp.), b triradiate diatom form (e.g., *Centronella* spp.), c unidentified diatom similarly observed by FlowCam, and d unidentified diatom. Digital image credit: C. Lydon

Neither of the two neurotoxic HAB microalgae species of interest (i.e., *Karenia brevis*, *Pseudo-nitzschia* spp.) could be positively identified by morphology-based techniques from digital images captured using either light microscopy or the FlowCam apparatus.

2.4.5 Associated Neurotoxic Taxa (Literature Search)

A literature search for neurotoxins produced by the identified macroalgae genera returned few results. Only two genera of the identified chlorophytes (i.e., *Ulva*, *Caulerpa*) were reported to have toxic effects. The *Caulerpa* (J. V. Lamouroux, 1809, Caulerpaceae) genus has been established to produce an array of bioactive secondary metabolites. Particularly, the secondary metabolite, caulerpenyne, a linear sesquiterpene isolated from *Caulerpa* spp. (i.e., *C. prolifera*, *C. racemosa*, *C. taxifolia*) as described by Amico et al. (1978), Valls et al. (1994) and Dumay et al. (2002), has shown

developmental toxicity in sea urchins (Pesando et al., 1996) and neurotoxic effects (e.g., excitatory, neurite inhibition), respectively, in leeches (Brunelli et al., 2000; Mozzachiodi et al., 2001) and the murine neuroblastoma cell line, NA2B, (Kurt et al., 2009).

Investigated allelopathic properties include seagrass phytotoxicity activity and chemical defense responses to herbivory. For example, Raniello et al. (2007) observed *C.*

racemosa exhibited phytotoxicity against the Mediterranean seagrass, *Cynodocea nodosa*. Whilst Ferrer et al. (1997) reported *C. taxifolia* seasonally inhibits the growth of the Mediterranean phaeophyte, *Cystoseira barbata* f. *aurantia* during the springtime.

Antifeedant activity was also shown when caulerpenyne, serving as the monomer precursor, is quickly, enzymatically biopolymerized into an unpalatable cicatrizant (Jung and Pohnert, 2001; Adolph et al., 2005; Weissflog et al., 2008). Conversely, caulerpenyne has shown promise as an anticancer therapy against several human cancer cell lines (Fischel et al., 1995; Barbier et al., 2001). To date, caulerpenyne has not been isolated from *C. mexicana*, *C. sertularioides*, or *C. verticillata*, - the species observed growing in the captive dolphin habitats.

The *Ulva* (Linnaeus, 1753, Ulvophyceae) genus is regularly consumed throughout the world as sea lettuce (i.e., *U. lactuca*) for its nutritional content and is not generally considered to produce toxins (Fleurence, 1999; Ortiz et al., 2006; Abirami and Kowsalya, 2011; Banu and Umamageswari, 2011). For example, Guedes et al. (2013) reported the crude aqueous extract of *U. lactuca* is relatively non-toxic to human cancer cell lines (e.g., larynx, leukemia, lung). However, in 2009, massive decaying *Ulva* spp. blooms along the French Coast were implicated with animal and human deaths caused by the release of toxic hydrogen sulfide gas (Smetacek and Zingone, 2013; Nedergaard et al.,

2002). Van Alstyne (2008) reviewed the toxicity of the *Ulva* spp. secondary metabolite, dimethyl sulfoniopropionate (DMSP), and its degradants (e.g., hydrogen sulfide gas). Paul and Van Alstyne (1992) previously reported that DMSP acts as a precursor allelochemical to deter grazing. Whilst, Tang and Gobler (2011) reported the rapid, allelopathic nutrient uptake exhibited by *U. lactuca* acts as an anti-fouling mechanism, against at least seven HAB epiphytes, including *Karenia brevis* and *Pseudo-nitzschia multiseriis*, which flourish in eutrophic conditions, corroborating the findings of Fong et al. (1994). Recently, Van Alstyne et al. (2015) provided an updated review of the allelochemicals and their proposed chemical defense mechanisms associated with *U. lactuca*. For example, reactive oxygen species have been shown to aid in regulating environmental parameters more favorable for the growth of *U. lactuca* at the expense of competitors (e.g., seagrasses, grazers) as described by Nelson et al. (2008) and by van Hees and Van Alstyne (2013). Moreover, Sly (2013) reported significant trophic transport of toxic (e.g., neurotoxicity, developmental toxicity), lipophilic polychlorinated biphenyls (PCBs) readily absorbed by *Ulva* spp. (i.e., *U. rigida*) from heavily contaminated sediments (i.e., New Bedford Harbor Superfund Site, Massachusetts, USA).

Literature abounds with neurotoxic secondary metabolites isolated from the marine, filamentous cyanobacteria, formerly classified as *Lyngbya* spp., and particularly, *L. majuscula* as reviewed by Aráoz et al. (2010). Recently, Kerbrat et al. (2010) investigated the possible role of marine filamentous cyanobacteria as the causative agents in seafood related poisonings in New Caledonia, and previously suggested by Hahn and Capra (1992) and Endean et al. (1993). Biological assays indicated the cyanobacteria,

Trichodesmium spp., *Hydrocoleum* spp., *Oscillatoria* spp., and *Phormidium* spp. may very well produce secondary metabolites akin to ciguateratoxins and paralytic shellfish toxins. However, further chemical investigation was warranted to structurally identify the observed potential neurotoxins. Whilst, Méjean et al. (2010) confirmed *Hydrocoleum lyngbyaceum* produces homoanatoxin-a, a neurotoxic analog of the very potent neurotoxin, anatoxin-a.

Globally, macroalgae (Déléris et al., 2016; Kiliç et al., 2013) and cyanobacteria (Gantar and Svirčev, 2008) are incorporated into human diets (e.g., food additives, nutraceuticals, supplements) from local farming to industrial scale production (Martinez-Hernández et al., 2018). Example edible, nutrient-rich green macroalgae include sea lettuce (*Ulva lactuca*) and sea grapes (*Caulerpa lentillifera*) as described by Pereira (2016). The food additives, agar and carrageenan, are obtained from red macroalgae (e.g., *Acanthophora spicifera*, *Hypnea valentiae*). Whilst the cyanobacteria genus *Arthrospira* (i.e., *A. maxima*, *A. platensis*) comprise the dietary supplement, spirulina. Most chemical investigations of macroalgae and cyanobacteria focused on exploiting therapeutic secondary metabolites (Baker, 1984; Smit, 2004) and beneficial nutrients (MacArtain et al., 2007). Screening crude extracts for cytotoxicity against human carcinoma cell lines and other health benefits (e.g., antimicrobial, anticoagulant, gastrointestinal stimulation, neuroprotection) were primary targets toward drug development (Lee et al., 2013; Barbosa et al., 2014). Fitzgerald et al. (2011) described the potential of macroalgae-derived peptides as pharmaceutical agents to combat cardiovascular disease (e.g., obesity, anticoagulant). Likewise, the Vijayakumar et al. (2016) review shows the burgeoning cannabinoid receptor binding studies offer novel therapeutics for pain management,

obesity and antiemetics. The renewed search for marine-sourced drugs has revisited toxigenic cyanobacteria to chemically mine metabolites for potential therapeutic uses (Tan 2013). For example, in the independent reviews by Vijayakumar and Menakha (2015) and Swain et al. (2015), the cytotoxicity screening of *Lyngbya* spp. offered promising anticancer leads. For example, apratoxins, isolated from *L. majuscula*, showed cytotoxicity against several human carcinoma cell lines including bone, colorectal, cervical and lung cancers (Luesch et al., 2001; Chen et al., 2011). Still, other studies gauged the chemical defenses of secondary metabolites against herbivory (Paul and Fenical, 1986; Paul and Van Alstyne, 1992; Fong et al., 1994).

Indeed, numerous bioactive secondary metabolites derived from marine macroalgae have shown promise toward improving current drug therapies as reviewed by Smit (2004) and Pal et al. (2014). For example, the anticoagulant, anti-inflammatory and pain-relieving effects of sulfated polysaccharides derived from crude aqueous extracts from *Solieria filiformis* and *Halymenia floresia* were studied by de Araújo et al. (2011) and das Neves Amorim et al. (2011), respectively. Whilst, Graça et al. (2011), explored gastrointestinal motor functions in rats using similar *H. floresia* extracts as an aid to digestive disorders. Zakaria et al. (2011) investigated the hexane extracts of *Acanthophora spicifera* for phytochemicals potentially exhibiting antibacterial and antioxidant properties. Moreover, Banu and Umamageswari (2011) determined that *A. spicifera* was not toxic to rats at levels typical of normal consumption. Antimicrobial activity was observed by crude lipophilic extracts of *Halimeda discoidea* (Supardy et al., 2012). Guedes et al. (2013), observed the crude lipophilic (e.g., chloroform, methylene chloride) extracts from *Padina gymnospora* were selectively cytotoxic against human

lung cancer cells. The crude methanolic extract from *P. gymnospora* showed positive antimicrobial properties (Chander et al., 2014). Recently, Shanmuganathan et al. (2015), reported the *P. gymnospora* crude acetone extract offers potential neuroprotection against Alzheimer's Disease by preventing and reversing aggregation of β -amyloid plaques. The crude acetone extract of *P. gymnospora* was also selectively cytotoxic to the human leukemia cells tested by Guedes et al. (2013).

2.5 Discussion

The taxonomies of the dominant macroalgal and cyanobacteria communities, observed growing within the captive dolphin enclosures at the marine mammal zoological facility in the Florida Keys, were morphologically identified to at least the genus level, and species, where possible, using comparative, bibliographic references. The results are listed in Table 2.1. Qualitative visual assessments throughout the study period revealed overall diversity changed little over time. Chlorophyta, represented by twelve species across seven genera, dominated the algal community diversity at 50% (see Figure 2.1). Most physically abundant were *Ulva* spp. (e.g., *U. lactuca*, *U. rigida*) and *Caulerpa* spp. (e.g., *C. mexicana*, *C. sertularioides*, *C. verticillata*). The *Ulva* spp. flourished during the summer months, as anticipated (Teichberg et al., 2010). Although an abundance of *Ulva* spp. (e.g., *U. lactuca*) grew within the captive dolphin enclosures, no noxious bloom decay (e.g., hydrogen sulfide) was observed at any time during the study period. Whilst, *Caulerpa* spp., mainly *C. mexicana* thrived in the fall, as expected (O'Neal and Prince, 1982). Important to this research, the neurotoxigenic species, *C. taxifolia*, was not present during any collection. Other identified Chlorophyta members included *Bryopsis hypnoides*, *Derbesia vaucheriiformis*, *Halimeda* spp. (e.g., *H.*

discoidea, *H. scabra*), *Penicillus capitatus* and *Udotea* spp. (e.g., *U. dixonii*, *U. flabellum*). Rhodophyta were slightly less diverse than Chlorophyta, having seven species within six genera, accounting for 29% of the total algal species diversity. Specifically identified were *Acanthophora* spp. (e.g., *A. muscoides*, *A. spicifera*), *Halymenia pseudofloresii*, *Heterosiphonia crispella*, *Hypnea valentiae*, *Polysiphonia binneyi* and *Solieria filiformis*. The available literature reported no associated neurotoxins with any of the identified Rhodophytes. The presence of Phaeophyta, represented primarily by *Padina gymnospora* equated to 4% of the total algal species diversity. The literature search held no accounts of neurotoxins isolated from *P. gymnospora*.

In general, the literature search for neurotoxin-producing macroalgae returned limited information. Worldwide, humans regularly consume macroalgae as part of their natural diet including *Ulva lactuca* (i.e., sea lettuce), *Caulerpa lentillifera* (i.e., sea grapes), and commercially extracted agar, alginate and carrageenan from Rhodophytes (e.g., *Acanthophora spicifera*, *Hypnea valentiae*) for use in food processing (McHugh, 1991). Moreover, in the last few decades, the quest for new and improved drug therapies has returned to harvesting bioactive secondary metabolites from the sea (i.e., macroalgae) as compiled by Déléris et al. (2016). Indeed, most chemical investigations of macroalgae focused on chemically screening crude extracts (e.g., *Solieria filiformis*, *Padina gymnospora*, *Udotea discoidea*, *Ulva lactuca*) towards improving available therapies (e.g., anticancer, anticoagulant, anti-inflammatory, antimicrobial, neuroprotective) as described by de Araújo et al. (2011), Supardy et al. (2012), Guedes et al. (2013), Chander et al. (2014) and Shanmuganathan et al. (2015). The Florida Keys human-managed bottlenose dolphin facility is open to tidal inputs from the Atlantic Ocean and the Florida

Bay watershed, often harboring HAB organisms (e.g., *K. brevis*, *Pseudo-nitzschia* spp.). Thus, the captive dolphin residents may well be ingesting macroalgae and particularly *Ulva* spp., growing with the enclosures, to exploit available medicinal natural products to self-medicate against HAB infestations. If so, these observed algal grazing behaviors may be the first documented evidence of an example of oral ingestion zoopharmacognosy (Mejia-Fava and Colitz, 2014) among captive bottlenose dolphins publicly presented in scientific literature.

Cyanobacteria consistently proliferated year-round, throughout the captive dolphin enclosures, as large, dense mats of mixed filamentous assemblages. These cyanobacteria represented 13% of the algal community species variety. The filamentous cyanobacteria were morphologically identified, by light microscopy, as the polyphyletic, neurotoxigenic genus *Lyngbya*, including the formerly classified species, *L. majuscula*. In keeping with literature references, previously associated with the neurotoxigenic species, *L. majuscula*, the mixed assemblage mats of filamentous cyanobacteria were taxonomically classified as “*Lyngbya* spp.”, until a more refined genetic identification could be realized. The mixed assemblage filamentous cyanobacteria, collected in December 2018, were differentiated and morphologically characterized by trichome size and color. Chemical evaluation by LC-MS of the filamentous mixed assemblage and the primary morphotypes, dark red (II) and dark green (V), established that the dark green (V) filaments produced the bioactive metabolite of interest (i.e., eudesmacarbonate). Phylogenetic inference of a subsample of the dark green filamentous cyanobacteria voucher specimen (CAL-V), preserved in RNAlater, determined this morphotype comprised three closely-related Oscillatoriacean members including an undocumented

species of the recently recognized *Neolyngbya* genus as detailed in Chapter Six of this dissertation.

The diversity and inventory of the microalgae samples (i.e., diatoms, dinoflagellates) collected in the summer showed more diversity than the winter collection, as anticipated (Okolodkov et al., 2014). A few, blurry digital images acquired using the FlowCam apparatus suggested *Karenia brevis* was potentially present in the site seawater samples. However, positive identification by visual comparison with literature images of *K. brevis* could not be achieved. Nor were *Pseudo-nitzschia* spp. definitively discerned in any of the FlowCam captured images or light microscopy digital images. Thus, the potential presence of two neurotoxin producing HAB microalgae remained dubious. Moreover, the presence of other HAB-related neurotoxigenic dinoflagellates (e.g., *Alexandrium* spp., *Gymnodinium* spp., *Lingulodinium* spp., *Protoperdinium* spp., *Pyrodinium* spp.) found throughout the Gulf of Mexico and the Caribbean Sea as described by Hernández-Becerril et al. (2007) and Wang (2008), could not be definitively determined using FlowCam or light microscopy.

The seagrass, *Thalassia testudinum*, was sparsely present, accounting for 4% of the total marine flora species diversity. Notably, macroalgae (e.g., *Caulerpa sertularioides*, *Halimeda* spp., *Penicillus capitatus*) and marine plants (e.g., *T. testudinum*) have recently been identified as preferred hosts for colonization by epiphytic HAB-related dinoflagellates (e.g., *Gambierdiscus toxicus*, *Ostreopsis* spp.) in the Caribbean Sea (Rodriguez et al., 2010) and the Gulf of Mexico (Almazán-Becerril et al., 2015), known to also produce neurotoxins (e.g., ciguatoxins, palytoxins). Moreover, Réveillon et al. (2016) recently established that the pennate (e.g., *Phaeodactylum*

tricornutum) and centric (e.g., *Chaeotoceros* spp., *Thalassiosira pseudonana*) marine diatoms produce the known neurotoxins, BMAA and 2,4 diaminobutyric acid (DAB), a structural isomer. Indeed, during the morphological taxonomic characterizations of the reference samples collected from within the captive dolphin closures, diatoms, dinoflagellates and cyanobacteria (i.e., *Lyngbya s.l.*) including *Neolyngbya* spp., were observed as epiphytes on *Halimeda* spp. (*H. discoidea*, *H. scabra*), and *T. testudinum*. Thus, monitoring for the potential presence of neurotoxicogenic HAB-related microalgae (e.g., *K. brevis*, *Pseudo-nitzschia* spp., *G. toxicus*) was recommended to the staff of the marine mammal zoological facility in the event of subsequent intoxications.

2.6 Conclusions

The results of this chapter addressed the key question “What are the dominant macroalgae and/or HAB-associated cyanobacteria taxa, possibly being ingested by the captive dolphins, observed growing within the enclosures?” posed in Chapter One. Additionally, the results provide insight to postulate that the captive dolphins may be displaying zoopharmacognosy by ingesting macroalgae, particularly *Ulva* spp., shown by Abirami and Kowsalya (2011) to be nutrient-rich (i.e., protein, micronutrients) and to produce exploitable, therapeutic secondary metabolites (e.g., nutraceuticals, pharmaceuticals). In summary, the diversity of the macroalgal and cyanobacteria community was established at the marine mammal zoological facility by collecting representative specimens at least quarterly during the study period. The morphology-based taxonomy studies allowed for generalizing the representative macroalgal and cyanobacteria communities growing within the dolphin enclosures throughout the study period. Chlorophyta were most diverse with the *Ulva* spp. (e.g., *U. lactuca*, *U. rigida*),

Caulerpa spp. (e.g., *C. Mexicana*, *C. sertularioides*, *C. verticillata*), and *Halimeda* spp. (e.g., *H. discoidea*, *H. scabra*) being most abundant. Notably, the neurotoxigenic *Caulerpa* spp. (e.g., *C. prolifera*, *C. racemosa*, *C. taxifolia*) were not observed any time during the study period. Rhodophyta were less diverse and the least represented macroalgae were Phaeophyta. None of the identified macroalgae species were known to overtly produce neurotoxic secondary metabolites. However, pervasive thick, benthic mats of filamentous Oscillatoriacean cyanobacteria, including an undescribed, potentially neurotoxigenic species of recently classified *Neolyngbya* spp., proliferated throughout the captive dolphin enclosures all year long as well. Attempts to determine the presence of potential neurotoxin-producing microalgae (e.g., *K. brevis*, *Pseudo-nitzschia* spp.) were inconclusive by light microscopy and the FlowCam apparatus.

The persistent preponderance of cyanobacteria year-round and concurrent taxonomic reclassifications, using emergent, molecular phylogenetic techniques, warranted an attempt to more precisely characterize the cyanobacteria to the species level. Morphology-based taxonomic identification of the cyanobacteria specimens, using light microscopy and reference field guides, was conducted to assign the preliminary genus-level classification. The cyanobacteria comprised a mixed assemblage resembling members of the polyphyletic and toxigenic genus *Lyngbya* s.l. More precise taxonomic identification of the macroalgae taxa was deemed irrelevant to the scope of the dissertation and not pursued since no neurotoxigenic species were detected. Thus, the focus of the dissertation shifted to chemically evaluate the cyanobacteria for potential neurotoxic metabolites. Further taxonomic characterization of the cyanobacteria required phylogenetic techniques.

The morphological identification of the neurotoxigenic genus *Lyngbya s.l.* and its likely association with intoxication events occurring at the marine mammal zoological facility drove the focus of this investigation toward identifying potential cyanobacteria-related neurotoxic (e.g., known, unrecognized) metabolites. The constant presence of the neurotoxin-producing *Lyngbya s.l.* morphotypes and the potential presence of HAB-related microalgae (e.g., *K. brevis*, *Pseudo-nitzschia* spp.) warranted chemical investigations, specifically, for the known neurotoxic metabolites ATX-a, BMAA, STX, PbTx and DA. The absence of neurotoxigenic *Caulerpa taxifolia* and no observed grazing of *Caulerpa* spp. by the captive dolphins deemed chemical evaluations of these taxa irrelevant to the scope of this project.

To conclude, no known neurotoxin-producing macroalgae were identified growing within the dolphin enclosures or observed being grazed by the captive dolphins. Epiphytic microalgae were detected but could not be decisively identified as HAB species. A mixed assemblage of filamentous cyanobacteria was omnipresent in the captive dolphin enclosures. The morphological identification of toxigenic *Lyngbya s.l.* shifted the focus of this research to chemically investigate cyanobacteria collections for known, or otherwise uncharacterized, neurotoxic metabolites, possibly related to the observed captive dolphin intoxications as detailed in next three chapters. Phylogenetic characterization of the cyanobacteria mat identified a dark green filamentous morphotype within the assemblage dominated by an undescribed species of the recently accepted genus *Neolyngbya* (Caires et al., 2018a) (see Chapter Six section 6.4 Results and Discussion). Chemical analysis of the cyanobacteria mat, by low-resolution LC-MS, suggested the production of a secondary metabolite (i.e., eudesmacarbonate) exhibiting

neurotoxicity in the zebrafish toxicological models comparable to PbTx-2 (see Chapter Six section 6.4.3 Biological Activity of Eudesmacarbonate).

After assessing the taxonomic results, described herein, the recommendation to periodically remove excessive cyanobacteria growth was proposed to the facility staff as a prophylactic measure to support the overall health of their resident captive dolphins. Likewise, monitoring for the potential presence of HAB-related microalgae (e.g., *Karenia brevis*, *Pseudo-nitzschia* spp., *Gambierdiscus toxicus*) was also suggested, especially if future intoxications occur. Lastly, chemical analysis of biological samples collected from subsequently intoxicated dolphins, for HAB-related neurotoxins, particularly brevetoxins, may be prudent (Maucher et al., 2007).

Future work should include more precisely identifying the various strains of filamentous cyanobacteria growing within the captive dolphin enclosures to species level using molecular genetics and chemically evaluating these strains for other potential neurotoxic metabolites.

2.7 Acknowledgments

This chapter was completed with the enormous assistance and expert guidance of Ligia Collado-Vides, who literally jumped into this project to physically collect macroalgae and cyanobacteria samples as well as providing her lab facilities and associates to help sort, label and morphologically identify the various algal and cyanobacteria specimens. Kevin Montenegro deserves great appreciation for his instrumental contribution by performing the morphological taxonomic identification for most of the macroalgae collected at each timepoint during the project. Mark Barton of Kevin Boswell's Lab is thanked for affording the instruction and FlowCam equipment

used for the microalgae assessments. Hernán Vázquez-Miranda of Heather Bracken-Grissom's Lab generously donated RNA*later*. Appreciation is extended to Niclas Engene. and his lab associates for attempting the cyanobacteria molecular phylogenetic characterization. Immense gratitude is given to Valerie Paul of the Smithsonian Marine Station at Fort Pierce for generously providing the expertise of Larissa Dos Santos, Thomas Sauvage and Michael Boyle to characterize the relevant cyanobacteria taxa. Holli Eskelinen and Dr. Johanna Mejia-Fava of Dolphin's Plus are thanked for making this project a reality by affording open access to staff, facilities, data, knowledge, and biomass collections whenever needed.

2.8 References

- Abirami, R.G., Kowsalya, S., 2011. Nutrient and nutraceutical potentials of seaweed biomass *Ulva lactuca* and *Kappaphycus alvarezii*. J. Agr. Sci. Technol. 5(1), 109-115.
- Adolph, S., Jung, V., Rattke, J., Pohnert, G., 2005. Wound closure in the invasive green alga *Caulerpa taxifolia* by enzymatic activation of a protein cross-linker. Angew. Chem. Int. Edit. 44(18), 2806-2808. doi:10.1002/anie.200462276
- Almazán-Becerril, A., Escobar-Morales, S., Rosiles-González, G., Valadez, F., 2015. Benthic-epiphytic dinoflagellates from the northern portion of the Mesoamerican reef system. Bot. Mar. 58(2), 115-120.
- Altschul, S.F., Madden, T.L., Schaffer, A.A., Zhang J., Zhang, Z, Miller, W., Lipman, D. J., 1997. Gapped BLAST and PSI-BLAST: a new generation of protein database search programs. Nucleic Acids Res. 25, 3389-3402.
- Amico V., Oriente, G., Piattelli, M., Tringali, C., Fattorusso, E., Magno, S., Mayol, L., 1978. Caulerpenyne, an unusual sesquiterpenoid from the green alga *Caulerpa prolifera*. Tetrahedron Lett. 19(38), 3593-3596. doi:10.1016/s0040-4039(01)95003-8
- Anderson, D.M., Burkholder, J.M., Cochlan, W.P., Gilbert, P.M., Gobler, C.J., Heil, C. A., Kudela, R., Parsons, M.L., Rensel, J.E.J., Townsend, D.W., Trainer, V.L., Vargo, G.A., 2008. Harmful algal blooms and eutrophication: Examining linkages from selected coastal regions of the United States. Harmful Algae 8(1), 39-53. doi:10.1016/j.hal.2008.08.017

- Aráoz, R., Molgo, J., de Marsac, N.T., 2010. Neurotoxic cyanobacterial toxins. *Toxicon* 56(5), 813-828. doi:10.1016/j.toxicon.2009.007.036
- Baker, J.T., 1984. Seaweeds in pharmaceutical studies and applications. *Hydrobiologia* 116(1), 29-40.
- Banu, A.T., Umamageswari, S., 2011. Toxicity study of seaweeds in rat. *CJFST*. 5(2), 23-31.
- Barbier, P., Guise, S., Huitorel, P., Amade, P., Pesando, D., Briand, C., Peyro, V., 2001. Caulerpenyne from *Caulerpa taxifolia* has an antiproliferative activity on tumor cell line SK-N-SH and modifies the microtubule network. *Life Sci.* 70, 415-429.
- Barbosa, M., Valentão, P., Andrade, P.B., 2014. Bioactive compounds from macroalgae in the new millennium: Implications for neurodegenerative diseases. *Mar. Drugs* 12, 4934-4972. doi:10.3390/md12094934
- Berman, F.W., Gerwick, W.H., Murray, T.F., 1999. Antillatoxin and kalkitoxin, ichthyotoxins from the tropical cyanobacterium *Lyngbya majuscula*, induce distinct temporal patterns of NMDA receptor-mediated neurotoxicity. *Toxicon* 37(11), 1645-1648. doi:10.1016/s0041-0101(99)00108-7
- Brand, L.E., Pablo, J., Compton, A., Hammerschlag, N., Mash, D.C., 2010. Cyanobacterial blooms and the occurrence of the neurotoxin beta-N-methylamino- α -alanine (BMAA) in South Florida aquatic food webs. *Harmful Algae* 9(6), 620-635. doi:10.1016/j.hal.2010.05.002
- Bricelj, V.M., Haubois, A.-G., Sengco, M.R., Pierce, R.H., Cutler, J.K., Anderson, D.M., 2012. Trophic transfer of brevetoxins to the benthic macrofaunal community during a bloom of the harmful dinoflagellate *Karenia brevis* in Sarasota Bay, Florida. *Harmful Algae* 16, 27-34.
- Brocke, H.J., Piltz, B., Herz, N., Abed, R.M. M., Palinska, K.A., John, U., den Haan, J., de Beer, D., Nugues, M.M., 2018. Nitrogen fixation and diversity of benthic cyanobacterial mats on coral reefs in Curacao. *Coral Reefs* 37(3), 861-874. doi:10.1007/s00338-018-1713-y
- Brunelli, M., Garcia-Gil, M., Mozzachiodi, R. Scuri, M.R.R., Traina, G., Zaccardi, M.L., 2000. Neurotoxic effects of caulerpenyne. *Prog. Neuro-Physchoph.* 24(6), 939-954. doi:10.1016/s0278-5848(00)00112-3
- Butler IV, M.J., Hunt, J.H., Herrnkind, W.F., Childress, M.J., Bertelsen, R., Sharp, W., Matthews, T., Field, J.M., Marshall, H.G., 1995. Cascading disturbances in Florida Bay, USA: cyanobacterial blooms, sponge mortality, and implications for juvenile spiny lobsters *Panulirus argus*. *Mar. Ecol. Prog. Ser.* 129, 119-125. doi:10.3354/meps129119

- Caires, T.A., de Mattos Lyra, G., Hentschke, G.S., de Gusmão Pedrini, A., Sant'Anna, C.L., de Castro Nunes, J.M., 2018a. *Neolyngbya* gen. nov. (Cyanobacteria, Oscillatoriaceae): A new filamentous benthic marine taxon widely distributed along the Brazilian Coast. *Mol. Phylogenet. Evol.* 120, 196-211. doi:10.1016/j.ympev.2017.12.009
- Caires, T.A., Lyra, G.D.M., Hentschke, G.S., Silva, A.M.S.D., Araújo, V.L.D., Anna, C.L.S., Nunes, J.M.D.C., 2018b. Polyphasic delimitation of a filamentous marine genus, *Capillus* gen. nov. (Cyanobacteria, Oscillatoriaceae) with the description of two Brazilian species. *Algae* 33(4), 291-304. doi:10.4490/algae.2018.33.11.25
- Caires, T.A., Sant'Anna, C.L., Nunes, J.M., 2019. *Capilliphycus* gen. nov.; validation of "Capillus T.A.Caires, Sant'Anna & J.M.Nunes," inval. (Oscillatoriaceae, Cyanobacteria). *Notulae Algarum* 95: 1-2
- Campbell, L., Henrichs, D.W., Olson, R.J., Sosik, H.M., 2013. Continuous automated imaging-in-flow cytometry for detection and early warning of *Karenia brevis* blooms in the Gulf of Mexico. *Environ. Sci. Pollut. Res.* 20, 6896-6902. doi:10.1007/s11356-012-1437-4
- Cavalcante, K.P., Tremarin, P.I., Ludwig, T.A.V., 2014. New records of amphoroid diatoms (Bacillariophyceae) from Cachoeira River, Northeast Brazil. *Braz. J. Biol.* 74(1), 257-263. doi:10.1590/1519-6984.24512
- Chander, M.P., Veeraragavam, S., Vijayachari, P., 2014. Antimicrobial and hemolytic activity of seaweed *Padina gymnospora* from South Andaman, Andaman, and Nicobar Islands of India. *Int. J. Curr. Microbiol. App. Sci.* 3(6), 364-369.
- Chen, Q.Y., Liu, Y., Luesch, H., 2011. Systematic chemical mutagenesis identifies a potent novel, apratoxin A/E hybrid with improved in vivo antitumor activity. *ACS Med. Chem. Lett.* 2(11), 861-865. doi:10.1021/ml200176m
- Corbett, D.R., Chanton, J., Burnett, W., Dillon, K., Rutkowski, C, Fourqurean, J.W., 1999. Patterns of groundwater discharge into Florida Bay, *Limnol. Oceanogr.* 44(4), 1045-1055.
- Cusack, C.K., Bates, S.S., Quilliam, M.A., Patching, J.W., Raine, R., 2002. Confirmation of domoic acid production by *Pseudo-nitzschia australis* (Bacillariophyceae) isolated from Irish waters. *J. Phycol.* 38, 1106-1112. doi:10.1046/j.1529-8817.2002.01054.x
- das Neves Amorim, R.C., Gurgel Rodrigues, J.A., Lima Holanda, M., de Souza Mourão, P.A., Barros Benevides, N.M., 2011. Anticoagulant properties of a crude sulfated polysaccharide from the red marine alga *Halymenia floresia* (Clemente) C. Agardh. *Acta Sci. Biol.* 33(3), 255-261. doi:10.4025/actascibiolsci.v33i3.6402
- de Araújo, I.W.F., Vanderlei, E.S.O. Rodrigues, J.A.G., Coura, C.O., Quinderé, A.L.G., Fontes, B.P., de Queiroz, I.N.L., Jorge, R.J.B., Bezerra, M.M., e Silva, A.A.R., Chaves,

- H.V., Monterio, H.S.A., de Paula, R.C.M., Benevides, N.M.R., 2011. Effects of a sulfated polysaccharide isolated from the red seaweed *Solieria filiformis* on models of nociception and inflammation. *Carbohydr. Polym.* 86(3), 1207-1215. doi:10.1016/j.carbpol.2011.06.016
- Déléris, P., Nazih, H., Bard, J.-M., 2016. Seaweeds in human health. In *Seaweed in Health and Disease Prevention* 319-367. doi:10.1016/b978-0-12-802772-1.00010-5
- Dumay, O., Pergent, G., Pergent-Martini, C., Amade, P., 2002. Variations in caulerpenyne contents in *Caulerpa taxifolia* and *Caulerpa racemosa*. *J. Chem. Ecol.* 28(2), 343-352. doi:10.1023/a:1017938225559
- Echenique, R.O., Guerrero, J.M., 2004. Morphology of the symmetrical morphotypes of *Centronella reicheltii* Voigt (Fragilariaceae, Bacillariophyceae) from Patagonian environments. *Gayano Bot.* 61(1), 18-26.
- Edwards, D.J., Marques, B.L., Nogel, L.M., McPhail, K., Goeger, D.E., Roberts, M.A., Gerwick, W.H., 2004. Structure and biosynthesis of the jamaicamides, new mixed polyketide-peptide neurotoxins from the marine cyanobacterium *Lyngbya majuscula*. *Chem. Biol.* 11, 817-833. doi:10.1016/j.chembiol.2004.03.030
- Endean, R., Monks, S.A., Griffith, J.K., Llewellyn, L.E., 1993. Apparent relationships between toxins elaborated by the cyanobacterium *Trichodesmium erythraeum* and those present in the flesh of the narrow-barred Spanish mackerel *Scomberomorus commersoni*. *Toxicon* 31, 1155–1165.
- Engene, N., Coates, R.C., Gerwick, W.H., 2010. 16S rRNA gene heterogeneity in the filamentous marine cyanobacteria genus *Lyngbya*. *J. Phycol.* 46(3), 591-601. doi:10.1111/j.1529-8817.2010.00840.x
- Engene, N., Choi, H., Esquenazi, E., Rottacker, E.C., Ellisman, M.H., Dorrestein, P.C., Gerwick, W.H., 2011. Underestimated biodiversity as a major explanation for the perceived rich secondary metabolite capacity of the cyanobacterial genus *Lyngbya*. *Environ. Microbiol.* 13(6), 1601-1610. doi:10.1111/j.1462-2920.2011.02472x
- Engene N., Rottacker, E.C., Kaštovský, J., Byrum, T., Choi, H., Ellisman, M.H., Komárek, J., Gerwick, W.H., 2012. *Moorea producens* gen. nov., sp. nov. and *Moorea bouillonii* comb. nov., tropical marine cyanobacteria rich in bioactive secondary metabolites. *Int. J. Syst. Evol. Micr.* 62, 1171-1178. doi:10.1099/ijs.0.033761-0
- Engene, N., Gunasekera, S.P., Gerwick, W.H., Paul, V.J., 2013(a). Phylogenetic inferences reveal large extent of novel biodiversity in chemically rich tropical marine cyanobacteria. *Appl. Environ. Microbiol.* AEM-03793. doi:10.1128/aem.03793-12
- Engene, N., Paul, V.J., Byrum, T., Gerwick, W.H., Thor, A., Ellisman, M.H., 2013(b). Five chemically rich species of tropical marine cyanobacteria of the genus *Okeania* gen.

nov. (Oscillatoriales, Cyanoprokaryota). J. Phycol. 49(6), 1095-1106.
doi:10.1111/jyp.12115

Ferrer, E., Gómez Garreta, A., Ribera, M.A., 1997. Effect of *Caulerpa taxifolia* on the productivity of two Mediterranean macrophytes. Mar. Ecol. Prog. Ser. 149, 279-287.
doi:10.3354/meps149279

Fire, S.E., Fauquier, D., Flewelling, L.J., Henry, M., Naar, J., Pierce, R., Wells, R.S., 2007. Brevetoxin exposure in Bottlenose dolphins (*Tursiops truncatus*) associated with *Karenia brevis* blooms in Sarasota Bay, Florida. Mar. Biol. 152(4), 827-834.
doi:10.1007/s00227-007-0733-x

Fischel, J.L., Lemee, R., Formento, P., Caldani, C., Moll, J.L., Pesando, D., Meinesz, A., Grelier, P., Guerriero, A., Milano, G., 1995. Cell growth inhibitory effects of caulerpenyne, a sesquiterpenoid from the marine alga *Caulerpa taxifolia*. Anticancer Res. 15, 2155-2160.

Fitzgerald, C., Gallagher, E., Tasdemir, D., Hayes, M., 2011. Heart health peptides from macroalgae and their potential functional foods. J. Agric. Food Chem. 59(13), 6829-6836. doi:10.1021/jf201114d

Fleurence, J., 1999. Seaweed proteins: biochemical, nutritional aspects and potential uses. Trends Food Sci. Tech. 10, 25-28.

Fong, P., Foin, T.C., Zedler, J.B., 1994. A simulation model of lagoon algae based on nitrogen competition and internal storage. Ecol. Monogr. 64(2), 225-247.

Fourqurean, J.W., Robblee, M.B., 1999. Florida Bay: A history of recent ecological changes. Estuaries 22(28), 345-357.

Gantar, M., Svirčev, Z., 2008. Microalgae and cyanobacteria: Food for thought. J. Phycol. 44(2), 260-268. doi:10.1111/j.1529-8817.2008.00469.x

Gárate-Lizárraga I., Muñetón-Gómez, Ma. S. Pérez-Cruz, B., Diaz-Ortiz, J.A., 2014. Bloom of *Gonyaulax spinifera* (Dinophyceae: Gonyaulacales) in Ensenada de la Paz Lagoon, Gulf of California. CICMAR Oceánides 29(1), 11-18.

Graça, J.R.V., Bezerra, M.M., Lima, V., Rodrigues J.A.G., Monteiro, D.L.S., Quinderé, A.L.G., Amorim, R.C.d.N., Paula, R.C. M, Benevides, N.M.B., 2011. Effect of a crude sulfated polysaccharide from *Halymenia floresia* (Rhodophyta) on gastrointestinal smooth muscle contractility. Braz. Arch. Biol. Techn. 54(5), 907-916.
doi:10.1590/s1516-89132011000500008

Grossman, A.R., 2005. Paths toward algal genomics. Plant Physiol. 137(2), 410-427.
doi:10.1104/pp.104.053447

- Gómez, F., Moreira, D., López-García P., 2010. *Neoceratium* gen. nov., a new genus for all marine species currently assigned to *Ceratium* (Dinophyceae). *Protist* 161(1), 35-54. doi:10.1016/j.protis.2009.06.004
- Guedes, E.A.C., da Silva, T.G., Aguiar, J.S., de Barros, L.D., Pinotti, L.M., Sant'Ana, A.E.G., 2013. Cytotoxic activity of marine algae against cancerous cells. *Rev. Bras. Farmacogn.* 23(4), 668-673. doi:10.1590/s0102-695x2013005000060
- Guiry, M.D., Guiry, G.M., 2018. *AlgaeBase*. World-wide electronic publication, National University of Ireland, Galway. <http://www.algaebase.org>; searched on 18 September 2018.
- Hahn, S.T., Capra, M., 1992. The cyanobacterium *Oscillatoria erythraea* – a potential source of toxin in the ciguatera food-chain. *Food Addit. Contam.* 9 (4), 351–355.
- Heisler, J., Gilbert, P.M., Burkholder, J.A.M., Anderson, D.M., Cochlan, W., Dennison, W.C., Dortch, Q., Gobler, C.J., Heil, C.A., Humphries, E., Lewitus, A., 2008. Eutrophication and harmful algal blooms: a scientific consensus. *Harmful Algae* 8(1), 3-13. doi:10.1016/j.hal.2008.08.006
- Hernández-Becerril, D.U., Alonso-Rodríguez, R., Álvarez-Góngora, C. Barón-Campis, S. A., Ceballos-Corona, G., Herrera-Silveira, J., Meave del Castillo, M. E., Juárez-Ruiz, Merino-Virgilio, F., Morales-Blake, A., Ochoa, J.L., Orellana-Cepeda, E., Ramirez-Camarena, C., Rodríguez-Salvador, R., 2007. Toxic and harmful marine phytoplankton and microalgae (HABs) in Mexican coasts. *J. Environ. Sci. Heal. A* 42(10), 1349-1363 doi:10.1080/10934520701480219
- Hernández-Becerril, D.U., Nelson Navarro, R., Barón-Campis, S.A., Moreno-Guiférrez, S.P., 2013. Morphological study of two closely related marine planktonic diatoms: *Bellerochea malleus* and *Helicotheca tamesis*. *Cryptogamie Algol.* 34(3), 245-254. doi:10.7872/crya.v34.iss3.2013.245
- Jung, V., Pohnert, G., 2001. Rapid wound-activated transformation of the green algal defensive metabolite caulerpenyne. *Tetrahedron* 57(33), 7169-7172. doi:10.1016/s0040-4020(01)00692-5
- Kerbrat, A., Dariu, H.T., Pauillac, S., Chinain, M., Laurent, D., 2010. Detection of ciguatoxin-like and paralyzing toxins in *Trichodesmium* spp. from New Caledonia lagoon. *Mar. Pollut. Bull.* 61, 360-366. doi:10.1016/j.marpolbul.2010.06.017
- Kiliç B., Cirik, S., Turan, G., Tekogul, H., Koru, E., 2013. Seaweeds for food and industrial applications. In *Food Industry. InTech*. doi:10.5772/53172
- Komárek, J., Zapomelová, E., Smarda, J., Kopecký, J., Rejmanková, E. Woodhouse, J., Neilan, B.A., Komárková, J., 2013. Polyphasic evaluation of *Limnoraphis robusta* a

water-bloom forming cyanobacterium from Lake Atitlán, Guatemala, with a description of *Limnoraphis* gen. nov. *Fottea* 13(1), 39-52.

Kurt, O., Özdal-Kurt, F., Tuglu, I., Deliloglu-Gurhan, S. I., Ozturk, M., 2009. Neurotoxic effect of *Caulerpa racemosa* var. *cylindracea* by neurite inhibition on the neuroblastoma cell line. *Russ. J. Mar. Biol.* 35(4), 342-350. doi:10.1134/s1063074009040105

Lapointe, B.E., 1989. Macroalgal production and nutrient relations in oligotrophic areas of Florida Bay. *B. Mar. Sci.* 44(1), 312-323.

Lapointe, B.E., Clark, M.W., 1992. Nutrient input from the watershed and coastal eutrophication in the Florida Keys. *Estuaries* 15(4), 465-476.

Lapointe, B.E., Tomasko, D.A., Matzie, W.R., 1994. Eutrophication and trophic state classification of seagrass communities in the Florida Keys. *B. Mar. Sci.* 54(3), 696-717.

Lee, J.C., Hou, M.F., Huang, H.W., Chang, F.R., Yeh, C.C., Tang, J.Y., Chang, H.W., 2013. Marine algal natural products with anti-oxidative, anti-inflammatory, and anti-cancer properties. *Cancer Cell Int.* 13(1), 55. doi:10.1186/1475-2867-13-55

Littler, D.S., Littler, M.M., 2000. Caribbean reef plants. Offshore Graphics.

Littler, D.S., Littler, M.M., Hanisak, M.D., 2008. Submerged plants of the Indian River Lagoon: A floristic inventory and field guide. Washington, DC: Offshore Graphics.

Liu, L., Rein, K.S., 2010. New peptides isolated from *Lyngbya* species: A review. *Mar. Drugs* 8(6), 1817-1837. doi:10.3390/md8061817

Luesch, H., Yoshida, W.Y., Moore, R.E., Paul, V.J., Corbett, T.H., 2001. Total structural determination of Apratoxin A, a potent novel cytotoxin from the marine cyanobacterium *Lyngbya majuscula*. *J. Am. Chem. Soc.* 123(23), 5418-5423. doi:10.1021/ja010453j

MacArtain, P., Gill, C.I.R., Brooks, M., Campbell, M., Rowland, I.R., 2007. Nutritional value of edible seaweeds. *Nutr. Rev.* 65(12), 535-543. doi:10.1111/j.1753-4887.2007.tb.00278.x

Martinez-Hernández, G.B., Castillejo, N., Carrion-Montegudo, M.D.M., Artés, F., Artés - Hernández, F., 2018. Nutritional and bioactive compounds of commercialized algae powders used as food supplements. *Food Sci. Technol. Int.* 24(2), 172-182. doi:10.1177/1082013217740000

Maucher, J.M., Briggs, L., Podmore, C., Ramsdell, J.S., 2007. Optimization of Blood Collection Card Method/Enzyme-Linked Immunoassay for Monitoring Exposure of Bottlenose Dolphin to Brevetoxin-Producing Red Tides. *Environ. Sci. Technol.* 41(2), 563 -567. doi:10.1021/es0612605

- McHugh, D.J., 1991. Worldwide distribution of commercial resources of seaweeds including *Gelidium*. In International workshop on *Gelidium*. 19-29. Springer, Dordrecht.
- Méjean, A., Peyraud-Thomac, C., Kerbrat, A.S., Golubic, S., Pauillac, S. Chinain, M., Laurent, D., 2010. First identification of the neurotoxin homoanatoxin-a from mats of *Hydrocoleum lyngbyaceum* (marine cyanobacterium) possibly linked to giant clam poisonings in New Caledonia. *Toxicon* 56(5), 829-835.
doi:10.1016/j.toxicon.2009.10.029
- Mejia-Fava, J., Colitz, C.M.H., 2014. Supplements for Exotic Pets. *Vet. Clin. North Am. Exot. Anim. Pract.* 17(3), 503-525. Doi::10.1016/j.cvex.2014.05.001
- Mi, Y., Zhang, J., He, S., Yan, X., 2017. New peptides isolated from marine cyanobacteria, an overview over the past decade. *Mar. Drugs* 15(5), 132.
doi:10.3390/md15050132
- Moreira, C., Vasconcelos, V., Antunes, A., 2013. Phylogeny and biogeography of cyanobacteria and their produced toxins. *Mar. Drugs* 11(11), 4350-4369.
doi:10.3390/md11114350
- Mozzachiodi, R., Scuri, R., Roberto, M., Brunelli, M., 2001. Caulerpenyne, a toxin from the seaweed *Caulerpa taxifolia*, depresses afterhyperpolarization in invertebrate neurons. *Neuroscience* 107(3), 519-528. doi:10.1016/s0306-4522(01)00365-7
- Nedergaard, R.I., Risgaard-Petersen, N., Finster, K., 2002. The importance of sulfate reduction associated with *Ulva lactuca* thalli during decomposition: A mesocosm experiment. *J. Exp. Mar. Biol. Ecol.* 275(1), 15-29. doi:10.1016/s0022-0981(02)00211-3
- Nelson, T.A., Haberlin, K., Nelson, A.V., Ribarich, H., Van Alstyne, K.L., Buckingham, L., Simunds, D.J, Frederickson, K., 2008. Ecological and physiological controls of species of green macroalgal blooms. *Ecology* 89(5), 1287-1298. doi:10.1890/07-0494.1
- Nogle, L.M., Okino, T., Gerwick, W.H., 2001. Antillatoxin B, a neurotoxic lipopeptide from the marine cyanobacterium *Lyngbya majuscula*. *J. Nat. Prod.* 64(7), 983-985.
doi:10.1021/np010107f
- Nogle, L.M., Gerwick, W.H., 2003. Diverse secondary metabolites from a Puerto Rican collection of *Lyngbya majuscula*. *J. Nat. Prod.* 66(2), 217-220 doi:10.1021/np020332c
- Nübel, U., Garcia-Pichel F., Muyzer, G., 1997. PCR primers to amplify 16S rRNA genes from cyanobacteria. *Appl. Environ. Microbiol.* 63, 3327-3332
- Okolodkov, Y.B., Virgilio F.D.C.M., Castillo, J.A.A., Trujillo, A.C.A., Espinosa-Matias, S., Silveira, A.H., 2014. Seasonal changes in epiphytic dinoflagellate assemblages near the northern coast of the Yucatan Peninsula, Gulf of Mexico. *Acta Bot. Mex.* 107, 121-151.

- O'Neal, S.W., Prince, J.S., 1982. Relationship between seasonal growth, photosynthetic production and apex mortality of *Caulerpa paspaloides* (Chlorophyceae). *Mar. Biol.* 72, 61-67.
- O'Neil, J.M., Davis, T.W., Burford, M.A., Gobler, C.J., 2012. The rise of harmful cyanobacteria blooms: The potential roles of eutrophication and climate change. *Harmful Algae* 14, 313-334 doi:10.1016/j.hal.2011.10.027
- Ortiz, J., Romero, N., Robert, P., Araya, J., Lopez-Hernandez, J., Bozzo, C., Navarrete, E., Osorio, A., Rios, A., 2006. Dietary fiber, amino acid, fatty acid and tocopherol contents of the edible seaweeds *Ulva lactuca* and *Durvillaea antarctica*. *Food Chem.* 99(1), 98-104 doi:10.1016/j.foodchem.2005.07.027
- Pal, A., Kamthania, M., Kumar, A., 2014. Bioactive compounds and properties of seaweeds – A review. *OALib Journal* 1(4), 1-17. doi:10.4236/oalib.1100752
- Paul, V.J., Fenical, W., 1986. Chemical defense in tropical green algae, order Caulerpales. *Mar. Ecol. Prog. Ser.* 34, 157-169.
- Paul, V.J., Van Alstyne, K.L., 1992. Activation of chemical defenses in the tropical green algae *Halimeda* spp. *J. Exp. Mar. Biol. Ecol.* 160(2), 191-203. doi:10.1016/0022-0981(92)90237-5
- Pereira, L., 2016. Edible seaweeds of the world. Boca Raton: CRC Press.
- Pesando, D., Lemée, R., Ferrua, C., Amade, P., Girard, J.P., 1996. Effects of caulerpenyne, the major toxin from *Caulerpa taxifolia* on mechanisms related to sea urchin egg cleavage. *Aquat. Toxicol.* 35(3-4), 139-155. doi:10.1016/0166-455x(96)00013-6
- Phlips, E.J., Badylak, S., 1996. Spatial variability in phytoplankton standing crop and composition in a shallow inner-shelf lagoon, Florida Bay, Florida. *B. Mar. Sci.* 58(1), 203-216.
- Raniello, R., Mollo, E., Lorenti, M., Gavagnin, M., Buia, M.C., 2007. Phytotoxic activity of caulerpenyne from the Mediterranean invasive variety of *Caulerpa racemosa*: A potential allelochemical. *Biol. Invasions* 9, 361-368. doi:10.1007/s10530-006-9044-2
- Réveillon, D., Séchet, V., Hess, P., Amzil, Z., 2016. Production of BMAA and DAB by diatoms (*Phaeodactylum tricornutum*, *Chaetoceros* sp., *Chaetoceros calcitrans* and, *Thalassiosira pseudonana*) and bacteria isolated from a diatom culture. *Harmful Algae*, 58, pp.45-50. doi:10.1016/j.hal.2016.07.008
- Rodriguez, E.A., Mancera Pineda, J.E., ad Gavio, B., 2010. Survey of benthic dinoflagellates associated to beds of *Thalassia testudinum* in San Andres Island, Seaflower Biosphere Reserve, Caribbean Colombia. *Acta Biol. Colomb.* 15(2), 229-246

- Salvador-Reyes, L.A., Engene, N., Paul, V.J., Luesch, H., 2015. Targeted natural products discovery from marine cyanobacteria using combined phylogenetic and mass spectrometric evaluation. *J. Nat. Prod.* 78(3), 486-492. doi:10.1021/np500931q
- Shanmuganathan, B., Malar, D.S., Sathya, S., Devi., K.P., 2015. Antiaggregation potential of *Padina gymnospora* against the toxic Alzheimer's beta-amyloid peptide 25-35 and cholinesterase inhibitory property of its bioactive compounds. *PLoS One* 10(11), e0141708. doi:journal.pone.0141708
- Sly, E., 2013. Dietary contribution of polychlorinated biphenyl contaminated *Ulva* to *Fundulus heteroclitus* in the New Bedford Harbor, MA, Superfund site (Doctoral dissertation, Northeastern University).
- Smetacek, V., Zingone, A., 2013. Green and golden seaweed tides on the rise. *Nature* 504(7478), 84-88. doi:10.1038/nature12860
- Smit, A.J., 2004. Medicinal and pharmaceutical uses of seaweed natural products: A review. *J. Appl. Phycol.* 16, 245-262. doi:10.1023/b:japh.0000047783.36600.ef
- Stamatakis, A., 2014. RAxML version 8: a tool for phylogenetic analysis and post-analysis of large phylogenies. *Bioinformatics* 30(9), 1312-1313. doi:10.1093/bioinformatics/btu033
- Supardy, N.A., Ibrahim, D., Sulaiman, S.F., Zakaria, N.A., 2012. Inhibition of *Klebsiella pneumoniae* ATCC 13883 cells by hexane extract of *Halimeda discoidea* (Decaisne) and the identification of its potential bioactive compounds. *J. Microbiol. Biotechnol.* 22(6), 872-881. doi:10.4014/jmb.1111.11053
- Swain, S.S., Padhy, R.N., Singh, P.K., 2015. Anticancer compounds from cyanobacterium *Lyngbya* species: A review. *Anton. Leeuw. Int. J. G.* 108(2), 223-265. doi:10.1007/s10482-015-0487-2
- Tan, L.T., 2013. Pharmaceutical agents from filamentous marine cyanobacteria. *Drug Discov. Today* 18(17-18), 863-871. doi:10.1016/j.drudis.2013.05.010
- Tang, Y.Z., Gobler, C.J., 2011. The green macroalga, *Ulva lactuca*, inhibits the growth of seven common harmful algal bloom species via allelopathy. *Harmful Algae* 10(5), 480-488. doi:10.1016/j.hal.2011.03.003
- Teichberg, M., Fox, S.E., Olsen, Y.S., Valiela, I., Martinetto, P., Iribarne, O., Muto, E.Y., Petti, M.A.V., Corbisier, T.N., Soto-Jiménez, M., Páez-Osuna, F., Castro, P., Freitas, H., Zitelli, A., Carninaletti, M., Tagliapietra, D., 2010. Eutrophication and macroalgal blooms in temperate and tropical coastal waters: nutrient enrichment experiments with *Ulva* spp. *Global Change Biol.* 16, 2624-2637. doi:10.1111/j.1365-2486.2009.02108.x
- Twiner, M.J., Fire, S., Schwacke, L., Davidson, L., Wang, Z., Morton, S., Roth, S., Rowles, T.K., Wells, R.S., 2011. Concurrent exposure of Bottlenose dolphins (*Tursiops*

- truncatus*) to multiple algal toxins in Sarasota Bay, Florida, USA. PLoS One
doi:10.1371/journal.pone.0017394
- Valls, R., Artaud, J., Amade, P., Vincente, N., Piovetti, L., 1994. Determination of caulerpenyne, a toxin from the *Caulerpa taxifolia* (Caulerpaceae). J. Chromatogr. A 663, 114-118.
- Van Alstyne, K.L., 2008. Ecological and physiological roles of dimethylsulfoniopropionate and its products in marine macroalgae. In Algal Chemical Ecology 173-194. Springer, Berlin, Heidelberg.
- Van Alstyne, K.L., Nelson, T.A., Ridway, R.L., 2015. Environmental chemistry and chemical ecology of “green tide” seaweed blooms. Integr. Comp. Biol. 55(3), 518-532. doi:10.1093/icb/icv035
- van Hees, D.H., Van Alstyne K.L., 2013. Effects of emersion, temperature, dopamine, and hypoxia on the accumulation of extracellular oxidants surrounding the bloom-forming seaweeds *Ulva lactuca* and *Ulvaria obscura*. J. Exp. Mar. Biol. Ecol. 448, 207-213 doi:10.1016/j.embe.2013.07.013
- Vijayakumar, S., Menakha, M., 2015. Pharmaceutical applications of cyanobacteria – A review. J. Acute Med. 5, 15-23. doi:10.1016/j.jacmc.2015.02.004
- Vijayakumar, S., Manogar, P., Prabhu, S., 2016. Potential therapeutic targets and the role of technology in developing cannabinoid drugs from cyanobacteria. Biomed. Pharmacother. 83, 362-371. doi:10.1016/j.biopha.2016.06.052
- Wachnicka, A.H., Gaiser, E.E., 2007. Characterization of *Amphora* and *Seminavis* from South Florida, U.S.A. Diatom Res. 22(2), 387-455. doi:10.1080/0269249x.2007.9705722
- Wang, D.Z., 2008. Neurotoxins from marine dinoflagellates: A brief review. Mar. Drugs 6(2), 349-371. doi:10.3390/md20080016
- Weissflog, J., Adolph, S., Weisemeier, T., 2008. Reduction of herbivory through wound-activated protein cross-linking by the invasive macroalga *Caulerpa taxifolia*. ChemBioChem 9(1), 29-32. doi:10.1002/cbic.200700443
- Wu, M., Okino, T., Nogle, L.M., Marquez, B.L., Williamson, T., Sitachitta, N., Berman, F.W., Murray, T.F., McGough, K., Jacobs, R., Colsen, K., Asano, T., Yokokawa, F., Shioiri, T., Gerwick, W.H., 2000. Structure, synthesis, and biological properties of kalkitoxin, a novel neurotoxin from the marine cyanobacterium *Lyngbya majuscula*. J. Am. Chem. 122, 12041-12042. doi:10.1021/ja005526y
- Zakaria, N.A., Ibrahim, D., Shaida, S.F., Supardy, N.A., 2011. Phytochemical composition and antibacterial potential of hexane extract from Malaysian red algae, *Acanthophora spicifera* (Vahl) Borgeson. World Appl. Sci. J. 15(4), 496-501.

3. CAPTIVE DOLPHIN ALGAL GRAZING AND INTOXICATION EVENTS

3.1 Introduction

As described in Chapter One, human-managed bottlenose dolphins (*Tursiops truncatus*) live in a marine mammal zoological facility in the Florida Keys influenced by the tidal flux of the Atlantic Ocean and Florida Bay. The dolphin management program includes a vitamin-fortified, piscivorous diet of various fish and squid, supplemental hydration, and veterinarian care. Rarely, reports exist of captive dolphins experiencing adverse effects from HAB-related poisonings (Hokama et al., 1990). Contemporary scientific literature does not include accounts of wild bottlenose dolphins intentionally consuming macroalgae or cyanobacteria. Only one instance of zoopharmacognostic-related behaviors involved female (i.e., gestating, lactating) Shark Bay dolphins of Western Australia using sponges, presumably, to supplement dietary calcium needs and to self-medicate by exploiting antimicrobial and anticancer natural products produced by the sponges (Meylan, 1988; Smolker et al., 1997). In this research study, captive bottlenose dolphins have been observed grazing macroalgae, including cyanobacteria, growing copiously within their enclosures since 2011. The cyanobacteria comprised a mixed assemblage of filamentous cyanobacteria, morphologically resembling previously classified, neurotoxigenic *Lyngbya sensu lato* (*s.l.*) and the genetically identified genus *Neolyngbya* (Caires et al., 2018a) as previously described in Chapter Two of this dissertation (See Chapter Two section 2.4.1 Morphology-Based Identifications of Dominant Macroalgae and Cyanobacteria Taxonomies, section 2.4.3 Cyanobacteria Phylogenetic Characterization). Moreover, these captive dolphins periodically presented apparent neurotoxicity manifested by neurological symptoms including ataxia,

incoordination, respiratory issues and blepharospasms from which they fully recover under the care of the facility's veterinarian. Chapter Three, herein, details the specific algal (e.g., macroalgae, cyanobacteria) ingestions and intoxication events documented by the facility staff with the primary goal of identifying any relationship(s) of the observed algal ingestions to intoxications and zoopharmacognosy (Mejia-Fava and Colitz, 2014).

Fecal coliform serves as an anthropological contaminant indicator in aquatic systems. Although contamination includes fecal material from humans and animals, pollution from human sewage and associated pathogens are often inferred from the presence of FC (Paul et al., 1995; Mill et al., 2006; Mallin et al., 2007). Eutrophic conditions, caused by increased nutrient loading from anthropological influences (i.e., sewage effluents, fertilizer runoff), can lead to algal blooms, including HAB-related species, inducing deleterious effects on the ecosystem inhabitants (Anderson et al., 2008; Rhind, 2009; O'Neil et al., 2012). The seawater quality at the marine mammal zoological facility was periodically tested by an independent contractor between 2011 and 2014 for maximum fecal coliform units (FC) and water temperature (WT) in °F. The reported data, from 2011 through 2014, were furnished to FIU with the secondary goal of identifying any potential correlations between the measured water quality parameter(s) and the observed dolphin intoxications and/or the algal ingestions.

The overall intent of Chapter Three was to evaluate the facility's observation records of the captive dolphin intoxication episodes relevant to the observed algal ingestions and/or site seawater quality measurements during the study period to identify any causative or predictable correlations.

3.2 Procedures

3.2.1 Process for Logging Observed Captive Dolphin Algal Grazing and Intoxications

Facility staff recorded, to the best of their ability, incidents of captive dolphin algal grazing and/or intoxication events, observed within normal daily operational hours, typically between 8 A.M. and 6 P.M. Pertinent data logged by facility staff included date(s) of observed ingestion(s), dolphin name(s), algal identification(s), and observed symptom(s) and date(s) of any neurological impairment(s). Facility staff identified algae by morphological similarity to the available reference guide provided by the FIU Macroalgae Laboratory using relevant common names. To facilitate identification for the staff observers, the FIU algae guide simplified classification of the mixed assemblage cyanobacteria as “*Lyngbya* spp.” to include morphologically similar species of the genera *Neolyngbya*, *Limnoraphis* and *Capilliphycus*.

3.2.2 Lagoon Water Quality Assessments

Historical data for FC and WT measurements, sampled within the north and south enclosures (i.e., lagoons) and the connecting canal, were obtained from the marine mammal facility site between 2011 and 2014. The water quality parameters were statistically evaluated to identify potential trends.

3.2.3 Correlation Assessments of Captive Dolphin Observations

Two captive dolphins, a mother-daughter pair, were chosen as the subjects of the investigation because of their observed algae-grazing behaviors and reported intoxication episodes. The observed algae ingestions were first sorted by algae-type and the number of days per month was determined for each type grazed. The number of days per month

each dolphin experienced intoxication symptoms was also calculated. Total monthly durations for specifically grazed algae types and intoxications for the dolphins (e.g., individual, combined) were plotted over time to assess any obvious patterns. The percentage of intoxication events relevant to each type of algae grazed was also determined. The seawater quality data (i.e., FC, WT) were averaged, for the three collection areas at the site, and plotted over time to assess any obvious patterns (e.g., seasonal). The north lagoon water quality parameters were also plotted over the study period. The FC and WT data collected from the north enclosure, where the captive dolphins resided, were used to statistically compare the intoxication observations for possible correlations.

Statistical analyses were performed using a combination of the Real Statistics Resource Pack (Release 5.4.2), copyright (2013-2019) Charles Zaiontz, www.real-statistics.com (last accessed 23JAN2018) statistical software add-in for Microsoft Excel (RealStats for Excel), and the IBM Corp. Released 2017. IBM SPSS Statistics for Macintosh, Version 25.0 (IBM Corp., Armonk, NY, USA) statistical software (IBM SPSS). Data amassed between 2011 through 2014 for the captive dolphin (i.e., individual, combined) intoxication episodes versus observed algal grazing behaviors and the FC data were statistically evaluated to identify potential correlations. The Shapiro-Wilk test for normality was applied to the intoxication events, observed for both captive dolphins between 2013 and 2014, and the seawater quality data (i.e., FC and WT) collected over the four-year period (i.e., 2011-2014). Non-parametric, two-tailed, Spearman's rho correlation tests were performed to compare the observed captive dolphin intoxications with FC measurements. Chi Square tests of association were conducted to assess any

relationships between the observed algal ingestions and intoxication episodes of the captive dolphins (e.g., individual, combined).

3.3 Results

3.3.1 Captive Dolphin Observation Data and Correlation Assessments

Initially, the facility staff provided an historical almanac of dolphin intoxication events (e.g., dolphin identification, dates and symptoms of observed neurological impairment) observed in 2011 through 2012. Additional detailed record keeping occurred between 2013 through 2014 for the purpose of this study. Staff continued to monitor the captive dolphins for algal grazing behaviors and intoxication symptoms through 2016. Since none of the captive dolphins experienced subsequent intoxications, algae-specific ingestions were not reported between 2015 and 2016. Using the FIU macroalgae field guide, facility staff descriptively logged, to the best of their ability, individual dolphin ingestions (i.e., macroalgae, cyanobacteria) and intoxication events (e.g., date, symptoms), when directly witnessed. Photocopies of the observation logs were provided to FIU. The apposite data were transcribed into a Microsoft Excel spreadsheet and analyzed using statistical software (i.e., RealStats for Excel, IBM SPSS) to identify potential correlations between algal ingestions and subsequent intoxications.

Two related captive dolphins (i.e., mother, daughter) were identified as the animals that predominantly grazed macroalgae, including cyanobacteria, and experienced apparent intoxication symptoms and became the focus of the investigation to determine any possible relationships between observed algal ingestions and subsequent intoxication events. The recorded observations, obtained for the mother and daughter captive dolphins during the study were first summarized (Table 3.1, Appendix).

Table 3.1 Summary of reported algal ingestions and intoxication events, by date(s) observed, for a mother-daughter captive dolphin pair.

Mother	JAN	FEB	MAR	APR	MAY	JUN	JUL	AUG	SEP	OCT	NOV	DEC
2011*	NA	NA	NA	22	NA	6	16-25	NA	NA	NA	18	NA
2012*	NA	NA	NA	18	25	12-22	17-19	31	NA	22	NA	NA
2013	28	NR	NR	NR	NR	NO	NO	NR	NO	NO	NO	NR
2014	NR	NR	NR	NR	NO	5-22, 30	1-8, 28-31	1,12	12	2-3	NO	NR
2015	NR	NR	NR	NR	NR	NR	NR	NR	NR	NR	NR	NR
2016	NR	NR	NR	NR	NR	NR	NR	NR	NR	NR	NR	NR
Daughter	JAN	FEB	MAR	APR	MAY	JUN	JUL	AUG	SEP	OCT	NOV	DEC
2011*	NA	NA	NA	NA	NA	NA	NA	NA	NA	NA	18	NA
2012*	NA	15	16	NA	NA	NA	NA	NA	NA	NA	NA	NA
2013	NO	NR	NR	NR	NO	NA	NA	NA	27,29	NA	NA	NA
2014	NR	4	11, 21-28	15,23	NR	5-15	31	8-12	NR	NR	NR	NR
2015	NR	NR	NR	NR	NR	NR	NR	NR	NR	NR	NR	NR
2016	NR	NR	NR	NR	NR	NR	NR	NR	NR	NR	NR	NR

* Compiled from previous intoxication event data prior to reporting algal ingestions
 NA = no algae ingestion data available
 NR = no neurological symptoms observed associated with reported ingestions
 NO = no observed ingestions or symptoms
 Note: Blue bolded entries represent simultaneously occurring dates of observations for both the mother and daughter captive bottlenose dolphins.

To assess possible correlations of observed intoxication events between the two related dolphins, the data from Table 3.1 were graphically summarized as the total number of days each captive dolphin exhibited intoxication symptoms per month for each calendar year. The study period included the four consecutive years from 2011 through 2014 as no further intoxications occurred and logging of algae ingestions discontinued. The monthly intoxication event data observed for the mother and daughter captive dolphins were plotted consecutively over the four-year period (Figure 3.1).

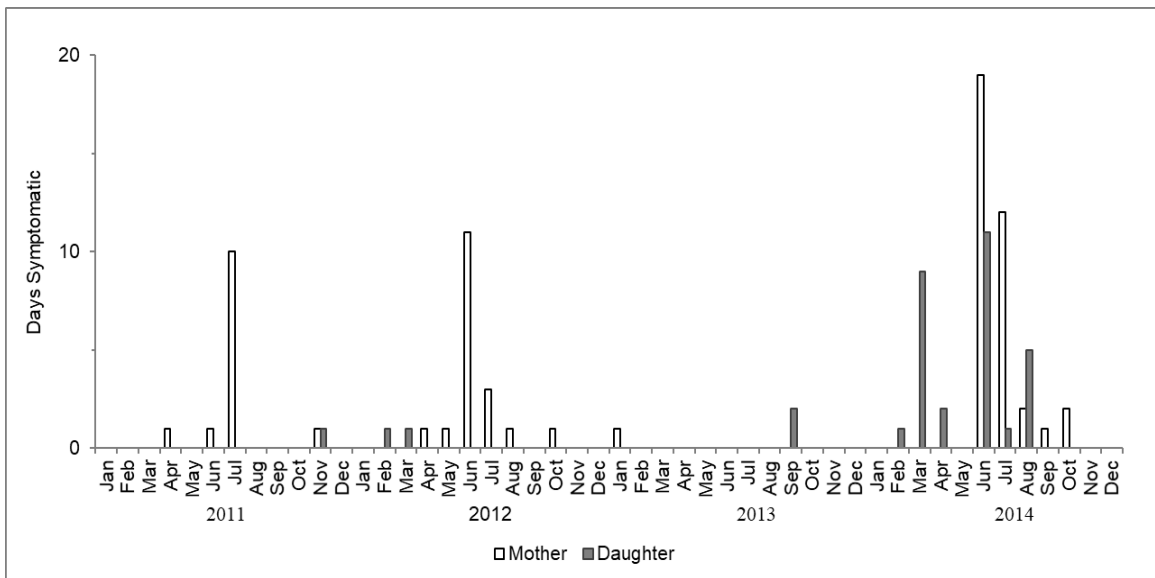


Figure 3.1 Monthly intoxication intervals observed for the mother and daughter captive dolphins, plotted consecutively from 2011 through 2014.

The intoxication episodes seemed to occur most often during the summer months (i.e., June, July, August) between 2011 and 2014. The graphed data also showed a longer duration of intoxication symptoms during the summer months, especially during the summer of 2014. The fewest reported intoxication events occurred during 2013, with a total of three symptomatic days observed between the mother and daughter captive dolphins. During 2014, the daughter captive dolphin exhibited more frequent intoxication

events compared to the mother. Specifically, the daughter captive dolphin experienced three episodes lasting five days or more between March and August of 2014, whilst the mother endured two consecutive episodes during June and July 2014 lasting longer than 10 days. The elder captive dolphin typically experienced intoxication symptoms of longer duration than the daughter. For example, the mother exhibited signs of apparent intoxication ranging from one to 19 days per month, whilst the daughter experienced symptoms ranging from one to 11 days per month.

The intoxication episodes for each dolphin were also compared over the four-year period from 2011 through 2014 to identify any potential trends (Figure 3.2).

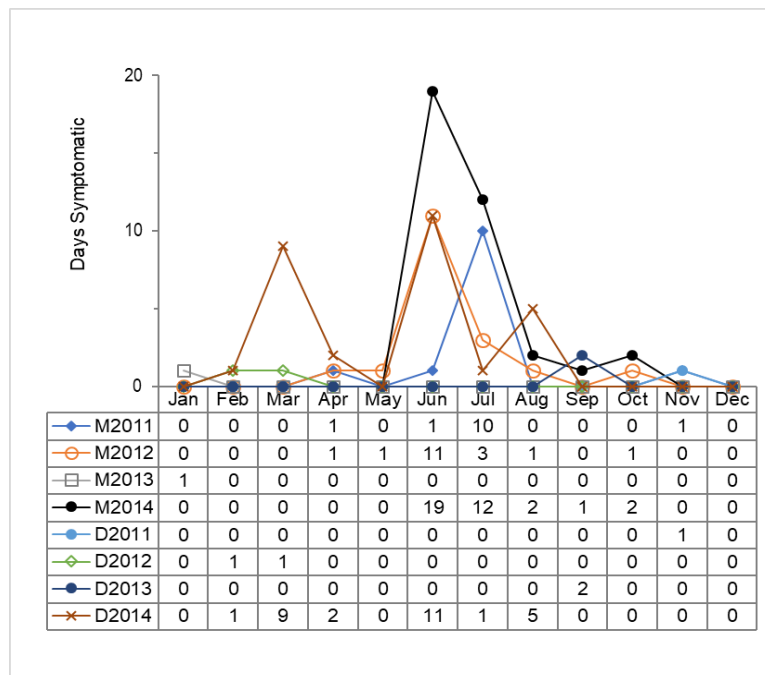


Figure 3.2 Comparison of monthly intoxication occurrences observed for the mother (M) and daughter (D) captive dolphins over 2011-2014.

The graphed data in Figure 3.2 showed increased intoxication events associated during the late spring and summer months, May through August, and peaking between June and July, every year except 2013. During 2011, 2012 and 2014, the total days the

mother captive dolphin showed signs of apparent intoxications tended to increase annually. Specifically, in 2011, the number of days the captive mother dolphin exhibited neurological symptoms totaled 13 days and increased to 18 days in 2012, whilst 2013 was relatively intoxication free with only one symptomatic day observed. However, in 2014, the total number of days the captive mother dolphin experienced neurological symptoms doubled to 36, compared to 2012. The daughter captive dolphin experienced only one or two days of intoxication symptoms annually until 2014 when a total of 29 symptomatic days were observed. The mother captive dolphin also appeared to have the longest consecutive durations of intoxication symptoms each year compared to the daughter, exclusive of 2013. Particularly, in the summer of 2014, the mother experienced symptoms lasting a total of 36 days, more than twice that of the daughter's 17 consecutive symptomatic days. Moreover, the mother captive dolphin continued to exhibit intoxication symptoms in September and October 2014.

Overall, intoxications occurred infrequently between 2011 and 2014 as interpreted from the histogram analysis of observed frequencies (Figure 3.3, Table 3.2). The probability of the captive dolphins experiencing intoxication symptoms lasting more than three days was approximately 1% compared to the 73% probability that no symptoms would be observed (Table 3.6). Whilst, the prospect for staff observed episode durations of 11 days was 2%. The likelihood of a captive dolphin exhibiting neurological symptoms lasting at least one day increased to 15%, whilst the chance of an episode lasting two days was 4%. Moreover, the monthly observed intoxication episodes were not normally distributed when statistically analyzed using the Shapiro-Wilk test for normality (Table 3.3).

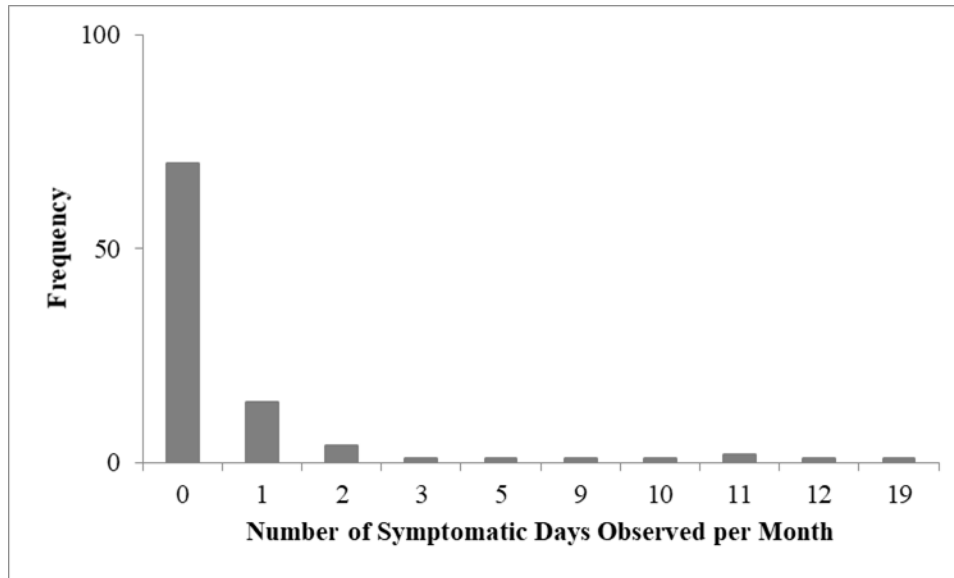


Figure 3.3 Histogram of intoxication frequencies observed during 2011 through 2014.

Table 3.2 Frequency table of total intoxications observed between 2011 and 2014.

Days Symptomatic per Month	Frequency	% Probability
0	70	73%
1	14	15%
2	4	4%
3	1	1%
5	1	1%
9	1	1%
10	1	1%
11	2	2%
12	1	1%
19	1	1%
	96	100%

Table 3.3 Results of Shapiro-Wilk normality test of monthly intoxication observations during 2011-2014.

Month	Jan	Feb	Mar	Apr	May	Jun	Jul	Aug	Sep	Oct	Nov	Dec
W-stat	0.42	0.57	0.48	0.72	0.42	0.75	0.71	0.67	0.60	0.60	0.57	NA
p-value	0.000	0.000	0.000	0.004	0.000	0.01	0.003	0.001	0.000	0.000	0.000	NA
normal	no	no	no	no	no	no	no	no	no	no	no	NA

alpha = 0.05

Intoxication episodes, lasting two or more consecutive days per month, appeared to cluster during June and July for the mother during the four-year period (Figure 3.4). Similar episodes observed for the daughter captive dolphin clustered during March, June

and August. The observed monthly intoxication events, averaged for both captive dolphins, also displayed a general trend of one or more consecutive symptomatic days occurring in spring and summer (Figure 3.5). Over the four-year period, the month of March showed a brief period of intoxication symptoms followed by a symptom-free period in late spring (i.e., May). Intoxication events peaked in the summer months of June and July. Overall, intoxication symptoms were experienced by one, or both, of the captive dolphins nearly every month over the four-year period except December.

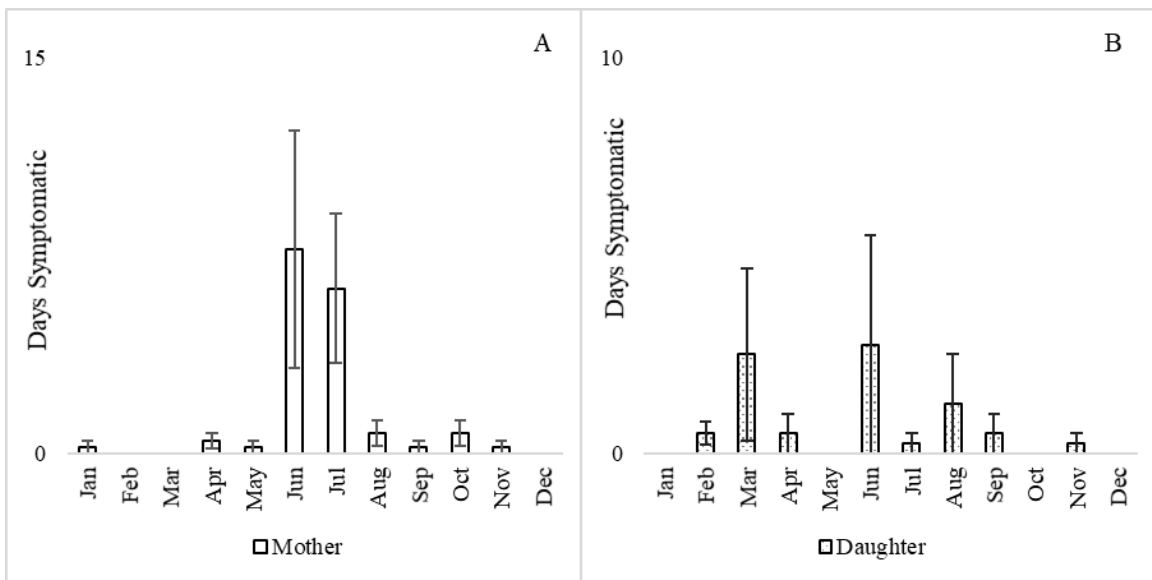


Figure 3.4 Average monthly intoxication episodes observed per individual captive dolphin over 2011-2014: A mother and B daughter. Error bars are \pm SEM (n = 4).

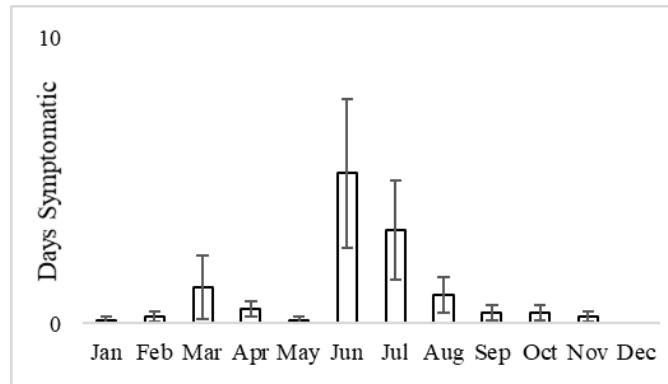


Figure 3.5 Combined monthly average intoxication episodes of both captive dolphins between 2011 and 2014. Error bars are \pm SEM (n = 8).

During 2013 and 2014, the facility staff recorded the dates and common names of the various types of macroalgae, including cyanobacteria, observed being ingested by the captive dolphins, as well as the dates and symptoms of observed intoxications. Staff observers identified the algal specimens (i.e., macroalgae, cyanobacteria, seagrass), to the best of their ability, using visual inspection, cross-referenced to the FIU provided algae field guide. The *Lyngbya* spp. nomenclature, used in the FIU field guide, simplified the mixed assemblage cyanobacteria classification and included potential species from the morphologically similar genera *Neolyngbya*, *Limnoraphis* and *Capilliphycus*. Table 3.4 lists the relevant algal-specific ingestion and intoxication data observed for the mother-daughter pair of captive dolphins, extracted from the 2013-2014 facility records.

Table 3.4 Total days per month algal ingestions and intoxications were reported for the mother-daughter captive dolphin pair during 2013 and 2014.

2013	Total Days	Jan	Feb	Mar	Apr	May	Jun	Jul	Aug	Sep	Oct	Nov	Dec	Sum
Mother	symptomatic	1	0	0	0	0	0	0	0	0	0	0	0	1
	<i>Lyngbya</i> spp.	0	0	0	0	1	0	0	1	0	0	0	0	2
	<i>Ulva</i> spp.	0	13	6	3	2	0	0	0	0	0	0	3	27
	Rhodophyta	0	0	1	0	0	0	0	0	0	0	0	0	1
	<i>T. testudinum</i>	0	0	0	0	0	0	0	1	0	0	0	2	3
	unobserved*	1	0	0	0	0	0	0	0	0	0	0	0	1
Daughter	symptomatic	0	0	0	0	0	0	0	0	2	0	0	0	2
	<i>Lyngbya</i> spp.	0	0	0	0	0	0	1	0	1	2	0	0	4
	<i>Ulva</i> spp.	0	5	1	0	0	0	1	0	0	0	0	3	10
	Rhodophyta	0	3	0	0	0	0	1	0	0	0	0	0	4
	<i>T. testudinum</i>	0	0	0	0	0	0	0	1	1	0	0	1	3
	unobserved*	0	0	0	0	0	0	0	0	0	0	0	0	0
2014	Total Days	Jan	Feb	Mar	Apr	May	Jun	Jul	Aug	Sep	Oct	Nov	Dec	Sum
Mother	symptomatic	0	0	0	0	0	19	12	2	1	2	0	0	36
	<i>Lyngbya</i> spp.	0	0	0	0	0	0	0	1	0	0	0	0	1
	<i>Ulva</i> spp.	3	1	7	3	0	1	0	0	0	0	0	3	18
	Rhodophyta	0	1	1	0	0	0	0	0	0	0	0	0	2
	<i>T. testudinum</i>	1	0	0	0	0	0	0	1	0	0	0	2	4
	unobserved*	0	0	0	0	0	18	12	1	1	2	0	0	34
Daughter	symptomatic	0	1	9	2	0	11	1	5	0	0	0	0	29
	<i>Lyngbya</i> spp.	0	0	0	0	0	0	0	1	0	0	0	0	1
	<i>Ulva</i> spp.	4	1	2	1	0	0	0	0	0	0	0	0	8
	Rhodophyta	1	1	0	0	0	0	1	0	0	0	0	0	3
	<i>T. testudinum</i>	2	0	0	0	0	0	0	0	0	0	0	0	2
	unobserved*	0	0	0	1	0	11	0	0	0	0	0	0	12

*No overt algal ingestions were reported by staff; the total duration of the observed intoxication symptoms may have resulted from undocumented algal ingestions while captive dolphins were not monitored by staff.

The diversity of the algae ingested, by both dolphins, was summarized, as percentages of the total recorded grazing occurrences (Table 3.5, Figure 3.6) inferred from the observed frequencies each type of algae grazed in Table 3.4.

Table 3.5 Summary of total days algal ingestions were observed, by algae type, for both captive dolphins during 2013 and 2014.

Algae type ingested	<i>Lyngbya spp.</i>	<i>Ulva spp.</i>	Rhodophyta	<i>T. testudinum</i>	Total
Total number of days ingested	8	63	10	12	93
Percent algae ingested by type	8	68	11	13	100

The captive dolphins, predominately, grazed sea lettuce, previously identified in Chapter Two of this dissertation, as *Ulva spp.* (e.g., *U. lactuca*, *U. rigida*) 68% of the time, followed by the seagrass, *Thalassia testudinum* (13%), red macroalgae (Rhodophyta) not typically identified (11%), and cyanobacteria, categorized as *Lyngbya spp.*, including *Neolyngbya spp.* and potential members of the *Limnoraphis* and *Capilliphyucus* genera, least often at 8%.

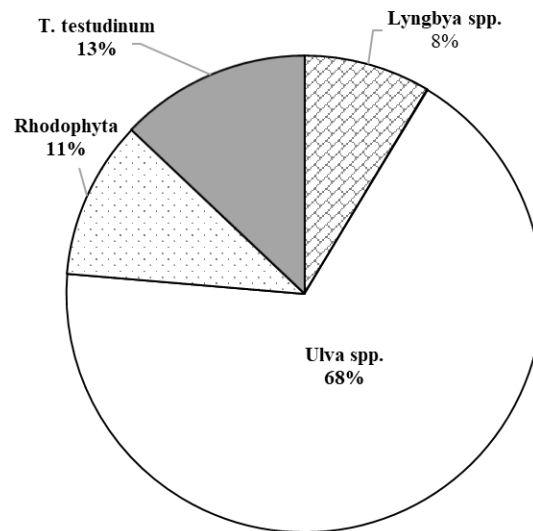


Figure 3.6 Percentages of observed macroalgae and cyanobacteria ingestions by type.

The number of days intoxication symptoms were concomitant to specific algal ingestions (Table 3.6) was calculated from the data presented in Table 3.4 and shown as percentages of the total ingestions for each type of algae (Figure 3.7).

Table 3.6 Summary of algae-specific ingestions relevant to intoxication events.

Algae Type	<i>Lyngbya</i> spp.	<i>Ulva</i> spp.	Rhodophyta	<i>T. testudinum</i>
Number of days ingestions related to intoxication events	3	5	2	1
Total number of days algae ingested	8	63	10	12
Percent of intoxication relevance	38	8	20	8

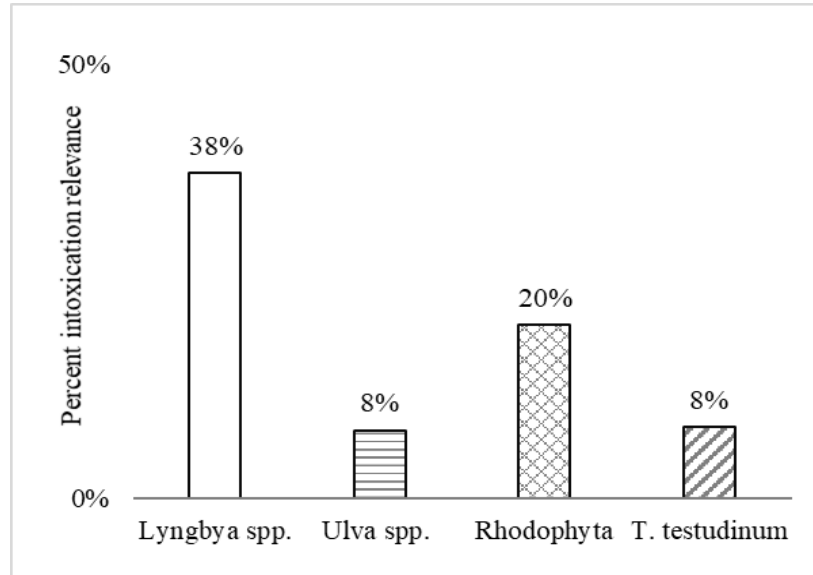


Figure 3.7 Percentages of intoxication-related algal ingestions per algae type.

The highest incidence of intoxication symptoms concomitant to ingestions, 38%, was observed for the filamentous cyanobacteria (i.e., *Lyngbya* spp.), the algae type least often consumed by the captive dolphins. The most frequently ingested macroalgae, sea lettuce (i.e., *Ulva* spp.), was associated 8% of the time with intoxications. Whilst, intoxications observed with red macroalgae (Rhodophyta) and turtle grass (i.e., *Thalassia testudinum*), grazed with similar frequency, were affiliated 20% and 8% of the time, respectively. As previously described in Chapter Two of the dissertation, the filamentous cyanobacteria often entangled and/or were epiphytic to the macroalgae specimens (e.g., Rhodophyta, *T. testudinum*). Moreover, staff observations of algal grazing by the captive

dolphins were constrained to normal business hours. Thus, as previously shown in Table 3.4, the facility staff logged incidents of apparent intoxications with, and without, directly observing concurrent algal ingestions. The algae ingestion category “unobserved” was added to account for intoxication events for which specific algal ingestions were not directly observed by the facility staff, particularly outside normal business hours (Table 3.7, Figure 3.8).

Table 3.7 Overall diversity of observed intoxication incidents by algae type.

Algae Type	<i>Lyngbya</i> spp.	<i>Ulva</i> spp.	Rhodophyta	<i>T. testudinum</i>	“Unobserved”	Total
Number of days intoxications related to algae ingestions	8	12	2	1	47	70
Percent of algae-specific intoxications relative to total intoxication days	12	17	3	1	67	100

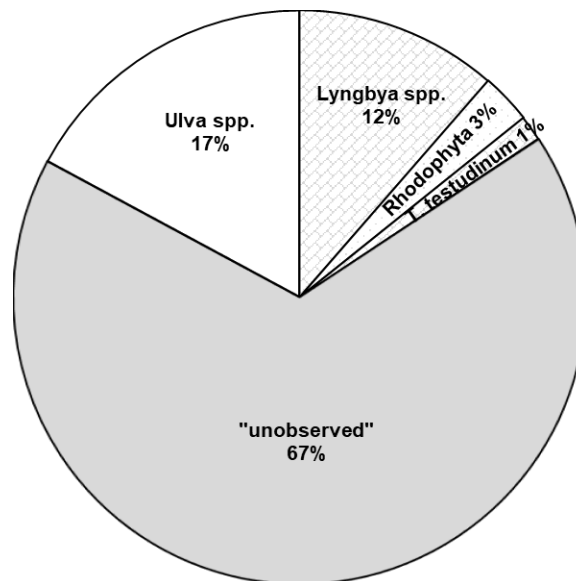


Figure 3.8 Overall percentages of intoxication events related to overt, or otherwise “unobserved”, algal ingestions.

Nearly 70% of the time, reported intoxication symptoms could not be associated with any specifically observed algal ingestions. Whereas, grazing of *Ulva* spp. related to

intoxications 17% of the time and *Lyngbya* spp. ingestions associated with 12% of the intoxication episodes. Observed grazing of red macroalgae and turtle grass accounted for fewer instances of intoxication at 4% and 1%, respectively. The grazing patterns of the captive dolphins were also examined over time (Table 3.8, Figure 3.9, Appendix). During the two-year period that algal ingestions were logged by facility staff (i.e., 2013, 2014), the mother and daughter dolphins grazed sea lettuce (*Ulva* spp.) an average of 5.3 ± 1.0 (SEM, n = 48 months) days, compared to turtle grass (*T. testudinum*) grazed an average of 1.1 ± 0.2 days. Cyanobacteria and Rhodophyta grazing averaged less than one day during 2013 and 2014, at 0.7 ± 0.1 day and 0.8 ± 0.2 day, respectively.

Table 3.8 Average algal grazing habits of the mother and daughter captive dolphins observed during 2013 and 2014.

2013-2014 Observations	<i>Ulva</i> spp.	<i>Lyngbya</i> spp.	Rhodophyta	<i>T. testudinum</i>
Average both	5.3	0.7	0.8	1.1
SEM, n = 48 months	1.0	0.1	0.2	0.2
Mother Average	3.8	0.3	0.3	0.6
SEM, n = 24 months	1.0	0.1	0.1	0.3
Daughter Average	1.5	0.4	0.6	0.5
SEM, n = 24 months	0.4	0.1	0.3	0.1
SEM = Standard Error of the Mean				

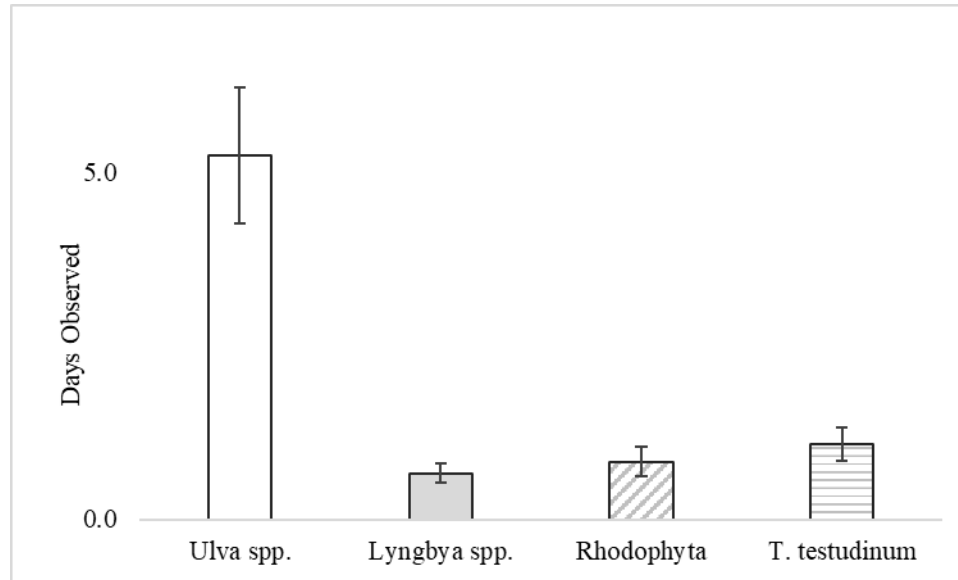


Figure 3.9 Average grazing behaviors of both captive dolphins observed 2013-2014. Error bars are \pm SEM (n = 48 months).

The mother captive dolphin grazed sea lettuce and turtle grass more frequently than the daughter, and the daughter appeared to preferentially graze cyanobacteria and red macroalgae (Table 3.8, Figure 3.10). Over the two-year period, staff observed the mother grazing sea lettuce an average of 3.8 ± 1.0 days, nearly four times more often than the average of 1.5 ± 0.4 days by the daughter. compared to the daughter. Observed ingestions of turtle grass by the mother averaged 0.6 ± 0.3 days compared to the daughter's average of 0.5 ± 0.1 day. The daughter was observed grazing cyanobacteria and red macroalgae respectively averaging 0.4 ± 0.1 day and 0.6 ± 0.3 day. Whilst, the average grazing behavior of the mother appeared uniform for both cyanobacteria and red algae at 0.3 ± 0.1 day.

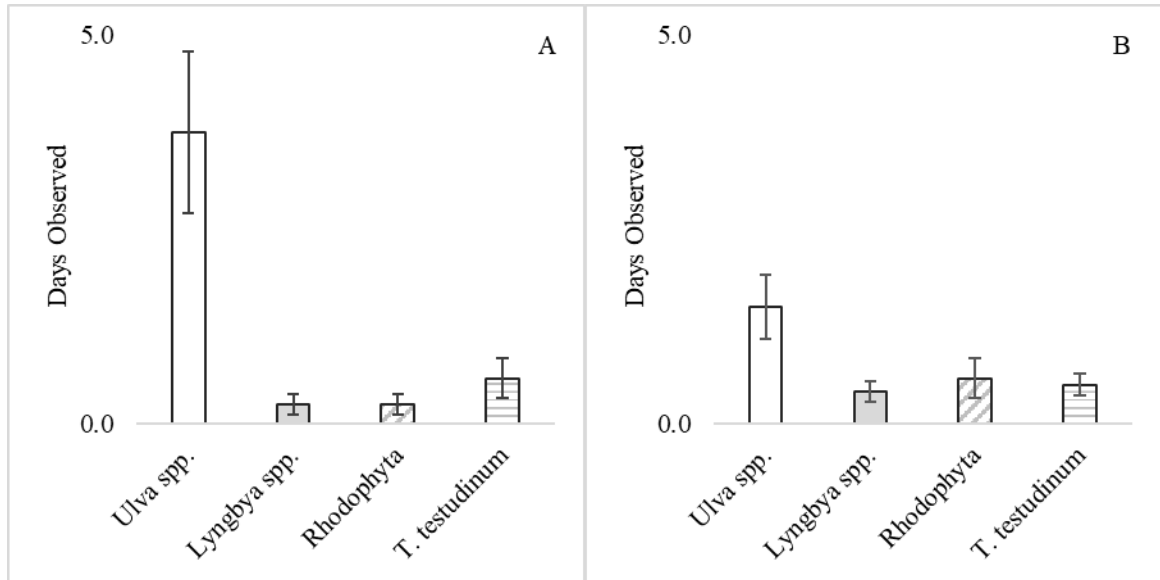


Figure 3.10 Average grazing behaviors observed for the mother and daughter captive dolphins during 2013 and 2014: A two-year data for the mother and B two-year data for the daughter. Error bars are \pm SEM ($n = 24$ months).

The monthly durations of intoxications and algae-specific ingestions, observed for the mother and daughter captive dolphin pair between 2013 and 2014 (see Table 3.4), were also compared over time to identify potential trends (Figure 3.11).

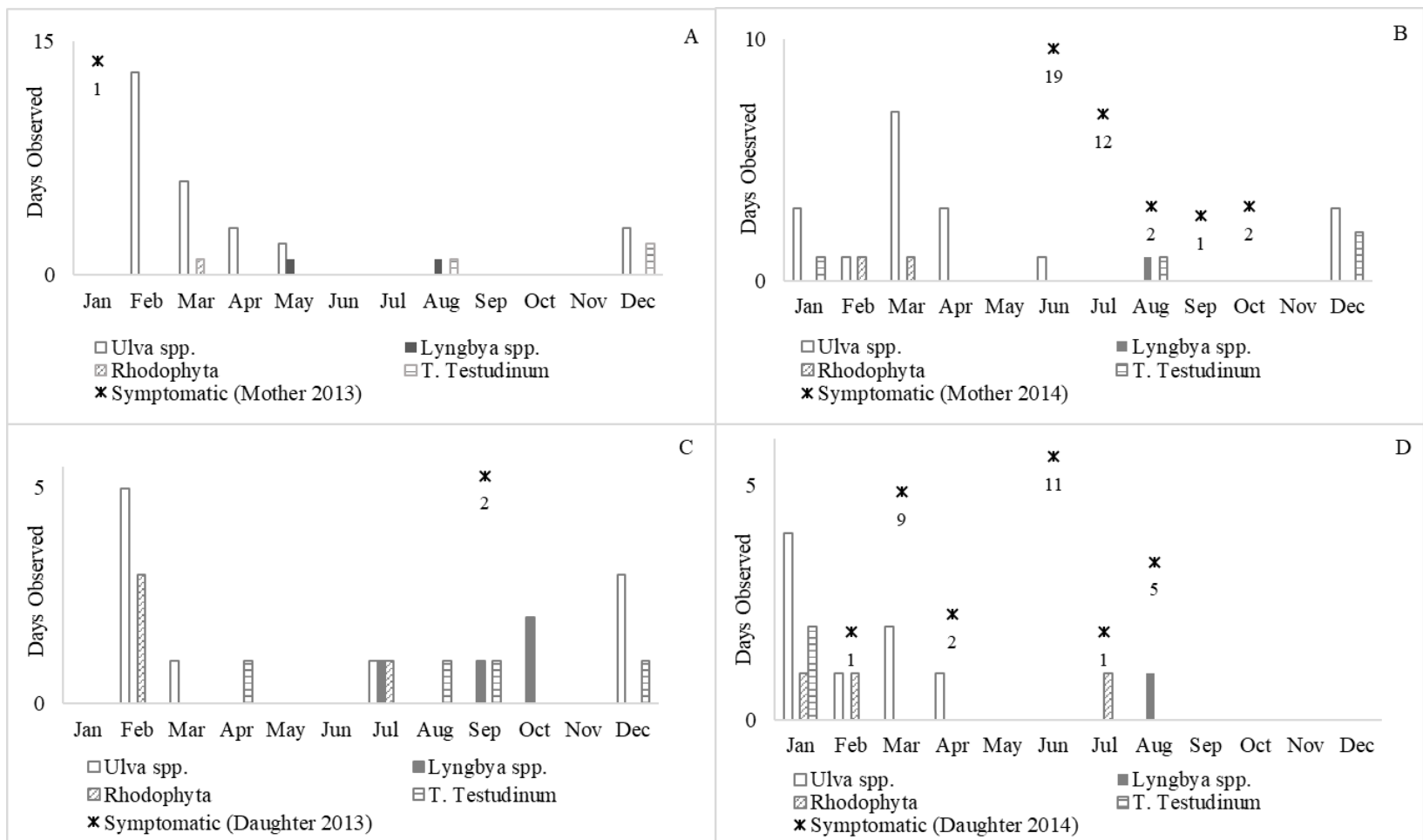


Figure 3.11 The total number of days, per month, intoxication symptoms and algae-specific ingestions were reported for the mother and daughter captive dolphins during 2013 and 2014: A mother 2013 data, B mother 2014 data, C daughter 2013 data and D daughter 2014 data. Note: The numerical values indicate the number of days intoxication symptoms were observed for the specified dolphin.

Statistical analyses of the 2013 and 2014 data, previously presented in Table 3.8, was performed using IBM SPSS could not establish any significant correlations between the monthly observed algal ingestions and intoxications per year shown in Figure 3.11 A-D. The statistical results are included in the Appendix. Two instances of ingesting cyanobacteria and subsequent intoxication symptoms occurred during the study period, one for the daughter captive dolphin in September 2013 and one involving both captive dolphins in August 2014. The daughter 2013 and mother 2014 incidents coincided with reported ingestions of *T. testudinum*. Macroalgal ingestions, particularly *Ulva* spp., during 2014, appeared to correlate with intoxications between February and April for the daughter and in June for the mother. Rhodophyta ingestions related to intoxications observed for the daughter captive dolphin in February and July 2014. Cyanobacteria and macroalgae ingestions were logged for both captive dolphins without subsequent intoxications during 2013 and January 2014. Moreover, intoxications were reported without observed algal ingestions. For example, neither the single January 2013 intoxication episode nor the 2014 September and October intoxications, reported for the mother, could be attributed to any known algal ingestion. During June 2014, both captive dolphins exhibited intoxications lasting longer than 10 days for which no algal ingestions were recorded prior to the onset of symptoms. Notably, in late June 2014, the mother was observed ingesting *Ulva* spp. followed by at least one day of intoxication symptoms and perhaps early July (see Table 3.1, Appendix). However, no overt alga-specific ingestions were observed by the staff relative to the intoxication symptoms exhibited by the mother captive dolphin at the end of July 2014. Thus, the recorded symptoms of intoxication,

attributed to unknown sources, may reflect potential unobserved algal and/or cyanobacteria ingestions occurring outside normal hours of operations.

Statistical evaluations of the observed captive dolphin data (i.e., individually, combined) were conducted, using the Pearson’s chi-square test for independence, to identify potential correlations between algal ingestions and intoxications (see Appendix). Specifically, the intoxication observations were compared to algal ingestions relative to algae type (e.g., *Ulva* spp.) and seasonal effects (i.e., winter, spring, summer, fall) (see Appendix). No significant correlations (e.g., $p < 0.05$) were identified for any of the statistical comparisons as summarized in Table 3.9 through Table 3.11 from the results data provided in the Appendix of this dissertation.

Table 3.9 Summary results of Pearson’s Chi-Square test for independence between intoxications and algal ingestions for the mother-daughter captive dolphin pair.

Intoxications versus Algal Ingestions	Mother	Daughter	Both
Pearson’s Chi-Square value	1.433	3.048	2.49
Probability value	0.231	0.081	0.115

Chi-Square critical value = 3.841 for 1 degree of freedom and alpha (p) = 0.05

Table 3.10 Summary results of Pearson’s Chi-Square test for independence between intoxications and *Ulva* spp. ingestions for the mother-daughter captive dolphin pair.

Intoxications versus <i>Ulva</i> spp. Ingestions	Mother	Daughter	Both
Pearson’s Chi-Square value	2.741	0.509	0.738
Probability value	0.098	0.476	0.390

Chi-Square critical value = 3.841 for 1 degree of freedom and alpha = 0.05

Table 3.11 Summary results of Pearson’s Chi -Square test for independence between intoxications and seasonal algal ingestions for the mother-daughter captive dolphin pair.

Intoxications versus Seasonal Algae Ingestions	Mother	Daughter	Both
Pearson’s Chi-Square value	4.444	2.218	4.536
Probability value	0.217	0.528	0.209
Chi-Square critical value = 7.815 for 3 degrees of freedom and alpha = 0.05			

3.3.2 Lagoon Water Quality Data and Correlation Assessments

A next step toward assessing the possible causes of the apparent intoxication symptoms exhibited by the captive dolphins involved reviewing the lagoon water quality data (i.e., FC, WT) measured between 2011 and 2104. The FC and WT were measured from 100 mL of seawater sampled from the north and south captive dolphin enclosures (i.e., lagoon) and the adjoining residential canal, periodically (e.g., bi-annually, monthly), by an independent contractor from 2011 through 2014. The compiled raw data reports, provided to FIU, were then transcribed into a Microsoft Excel spreadsheet for data analysis. First, the WT data were converted from °F to °C. Both water quality parameter data sets were respectively averaged from the three sampling areas per timepoint as tallied in Table 3.12. The raw data and graphical analysis are provided in the Appendix of this dissertation.

Table 3.12 Average monthly site seawater quality parameters measured 2011-2014.

Year	2011		2012		2013		2014	
Data	AFC	AWT (°C)	AFC	AWT (°C)	AFC	AWT (°C)	AFC	AWT (°C)
JAN	-	-	-	-	-	-	-	-
FEB	5.8 ± 1.7	21.9 ± 0.2	-	-	-	-	19.7 ± 3.8	23.0 ± 1.3
MAR	-	-	-	-	5.7 ± 3.2	23.3 ± 0.0	7.3 ± 0.9	26.3 ± 0.4
APR	-	-	-	-	-	-	17.3 ± 10.5	26.1 ± 0.0
MAY	-	-	9.2 ± 4.4	27.8 ± 0.0	-	-	25.7 ± 11.0	25.9 ± 0.2
JUN	-	-	3.3 ± 1.9	29.4 ± 0.0	2.0 ± 0.0	24.4 ± 0.0	5.7 ± 1.2	28.4 ± 0.6
JUL	-	-	2.7 ± 1.2	29.4 ± 0.0	-	-	4.0 ± 0.8	29.4 ± 0.0
AUG	17.5 ± 0.0	29.4 ± 0.0	5.0 ± 4.0	29.4 ± 0.0	-	-	8.7 ± 1.3	29.8 ± 0.2
SEP	-	-	30.0 ± 2.0	29.4 ± 0.0	-	-	5.7 ± 0.9	28.5 ± 0.4
OCT	-	-	16.0 ± 0.6	26.1 ± 0.0	16.0 ± 0.0	24.4 ± 0.0	8.7 ± 0.9	26.5 ± 0.2
NOV	-	-	-	-	-	-	7.7 ± 0.9	24.3 ± 0.2
DEC	-	-	5.0 ± 1.4	23.3 ± 0.0	-	-	3.0 ± 1.5	26.1 ± 0.0

AFC = Average maximum fecal coliform units per 100 mL seawater
 AWT = Average seawater temperature (°C)
 - = seawater quality parameter was not measured.
 Error values are ± SEM (Standard Error of the Mean), n = 3

Application of the Shapiro-Wilk test for normality indicated the monthly average WT data (AWT), were not typically normally distributed over the four-year period, except for March (Table 3.13). The monthly average FC measurements (AFC), overall, showed normal distributions during the study (Table 3.14).

Table 3.13 Results of Shapiro-Wilk normality test of 2011-2014 AWT (°C) measurements.

Month:	Jan	Feb	Mar	Apr	May	Jun	Jul	Aug	Sep	Oct	Nov	Dec
W-stat	NA	0.70	0.92	NA	0.78	0.78	2E-33	0.54	0.77	0.72	0.75	0.68
p-value	NA	0.01	0.49	NA	0.04	0.01	0.00	2E-05	0.03	0.01	-9E-07	0.004
normal	NA	no	yes	NA	no	no	no	no	no	no	no	no

alpha = 0.05

Table 3.14 Results of Shapiro-Wilk normality test of 2011-2014 measured AFC (units per 100 mL seawater).

Month:	Jan	Feb	Mar	Apr	May	Jun	Jul	Aug	Sep	Oct	Nov	Dec
W-stat	NA	0.95	0.97	0.88	0.89	0.85	0.89	0.88	0.81	0.93	0.96	0.94
p-value	NA	0.71	0.88	0.32	0.30	0.08	0.38	0.15	0.08	0.58	0.64	0.65
normal	NA	yes	yes	yes	yes	yes	yes	yes	yes	yes	yes	yes

alpha = 0.05

The measured water quality parameters (i.e., WT and FC) were respectively averaged for the three sampling stations during 2011 through 2014 (Figure 3.12) and examined by descriptive statistics and Box plot analysis using RealStats for Excel – the raw data and summary results are provided in the Appendix. Overall, the average site seawater temperatures tended to increase, from February lows of 22 °C through spring, reaching a maximum of 29 °C sustained during the summer months of June through August, followed by progressive cooling throughout fall as was expected (Figure 3.13, Appendix). Annual average site seawater temperatures, measured over the four years, ranged between a minimum of $21.9 \pm 0.2^{\circ}\text{C}$ (SEM, $n = 3$) in February 2011 and a maximum of $29.8 \pm 0.2^{\circ}\text{C}$ (SEM, $n = 3$) in August 2014. Site seawater temperatures, over the four years, averaged $26.9 \pm 0.3^{\circ}\text{C}$ (SEM, $n = 66$ total measurements) with minima of 21.7 °C observed in February 2011 and 2012 and an absolute maximum of 30.0 °C in August 2014. Whilst the monthly AWT (°C), averaged over the four years, ranged between the February minimum of $23.1 \pm 0.8^{\circ}\text{C}$ (SEM, $n = 6$) and the August maximum of $29.6 \pm 0.1^{\circ}\text{C}$ (SEM, $n = 9$) with an overall average for the year of $26.6 \pm 0.6^{\circ}\text{C}$ (SEM, $n = 11$ months) (Figure 3.13, Appendix).

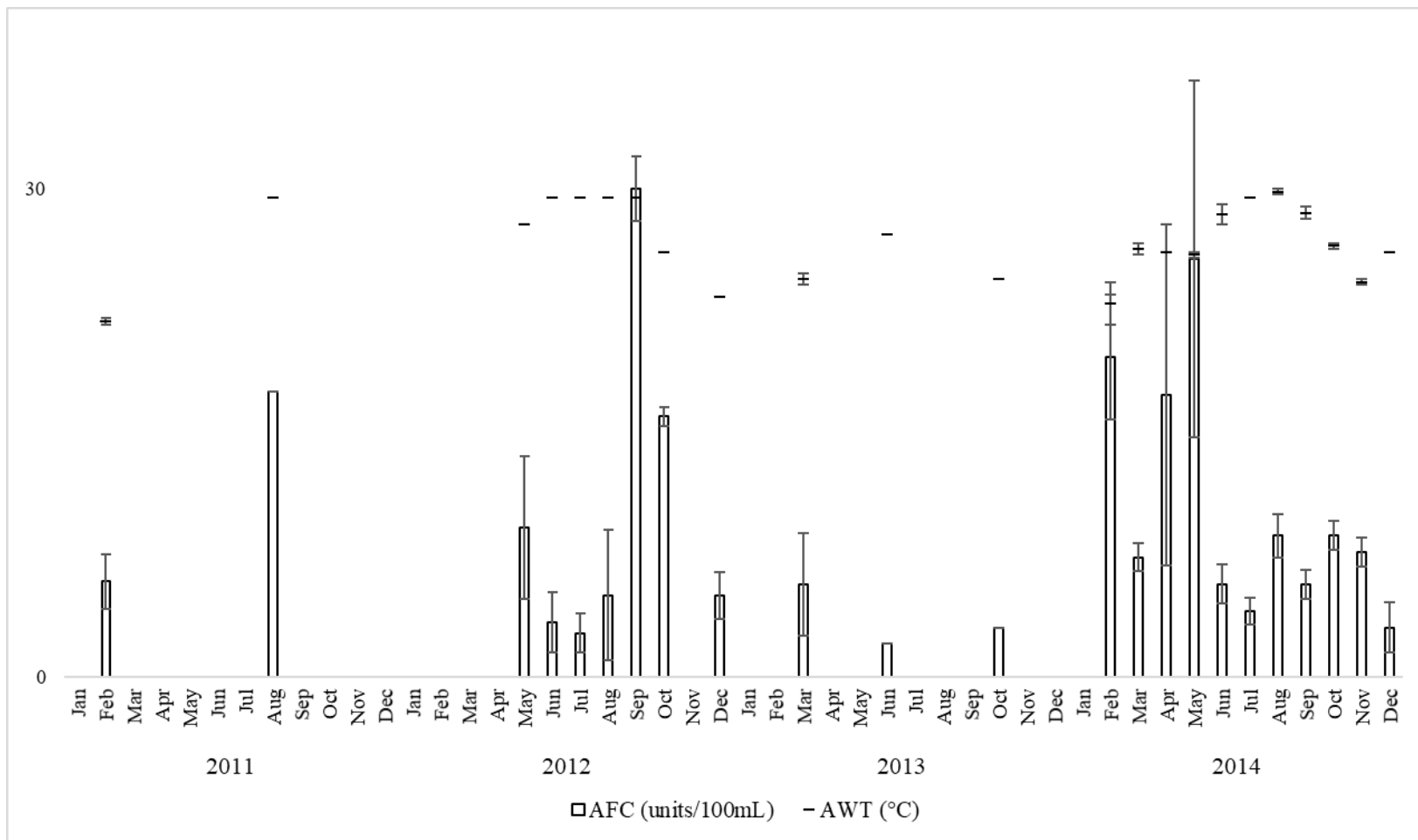


Figure 3.12 Average monthly site seawater quality parameters, plotted consecutively, from 2011 through 2014, with AFC indicating average maximum fecal coliform (units per 100 mL) and AWT indicating average seawater temperatures (°C). Error bars are ± SEM (n = 3).

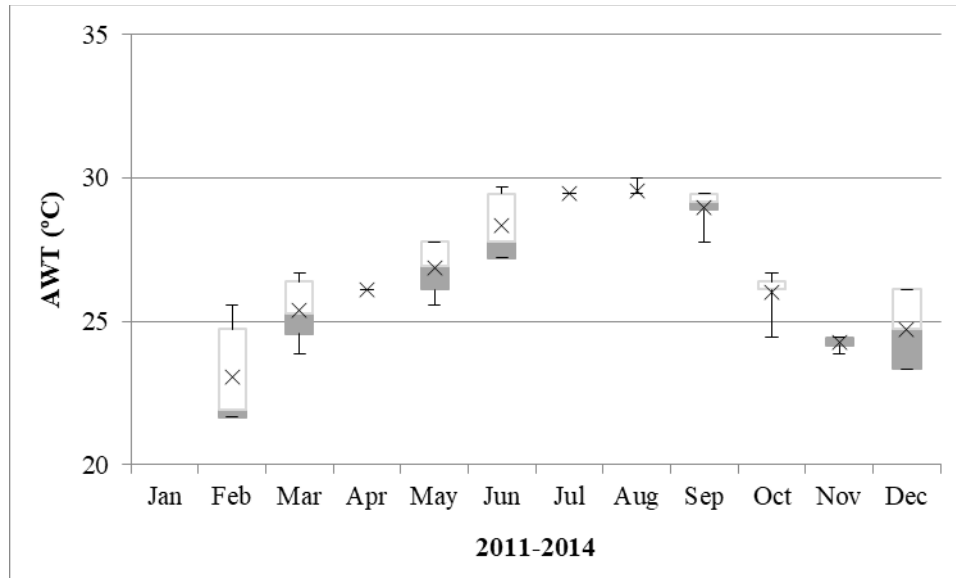


Figure 3.13 Box plot of 2011-2014 average site seawater temperature (AWT) measurements (°C) with error bars denoting \pm SD ($n = 3$) and \times indicating means.

The average fecal coliform measurements appeared to generally follow the same trend as the average seawater temperatures (Figure 3.14, Appendix). The monthly AFC measurements generally averaged 10.2 ± 1.6 FC (SEM, $n = 11$ months) during the study period, ranging from a July average minimum of 3.2 ± 0.8 FC (SEM, $n = 5$) to a September average maximum of 17.8 ± 5.5 FC (SEM, $n = 6$) and. Overall, fecal coliforms averaged 9.8 ± 1.2 FC (SEM, $n = 66$) during 2011 through 2014 and ranged from 1.0 to 45.0 FC. The timing of the absolute minima and maxima varied each year. For example, minimum measurements of 1.0 FC clustered between June through August of 2012 and occurred once more in December of 2014. Whilst, measurements greater than 30 FC were observed in September 2012 and then in April and May of 2014. Moreover, the variability of the AFC measurements obtained from the north and south enclosures and canal areas ranged from consistent (± 0.0) to inconsistent (± 11.0), as determined by the SEM values for the three sampling areas over time (Figure 3.14,

Appendix). Thus, the focus of the statistical inquiry shifted to water quality measurements, particularly FC, from the north lagoon where the affected captive dolphins resided to evaluate any potential historical or predictable trends observed for the pair (Figure 3.15) or each individual (Figure 3.16) during the study period.

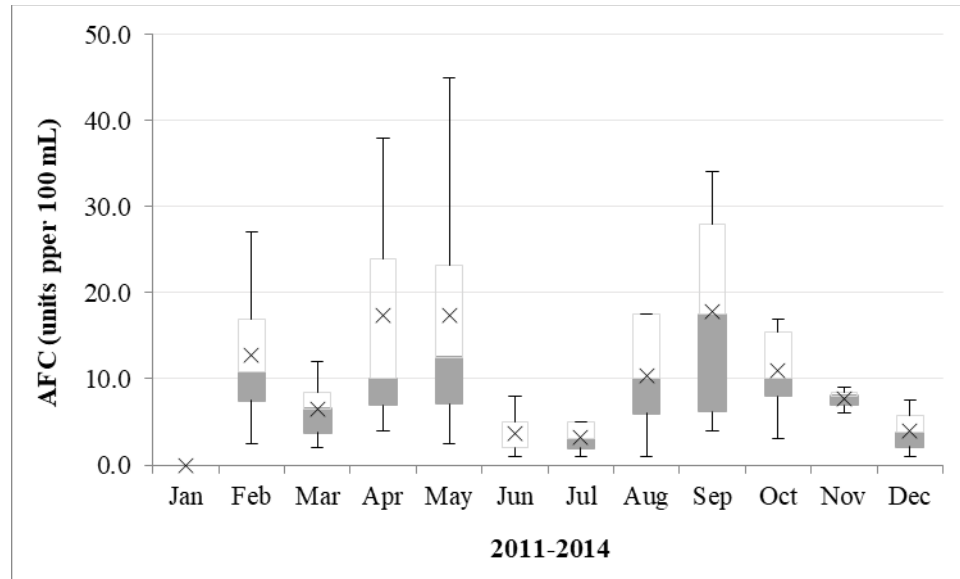


Figure 3.14 Box plot of 2011-2014 average maximum fecal coliform measurements (AFC) measured as units per 100 mL seawater with error bars denoting \pm SD ($n = 3$) and \times indicating means.

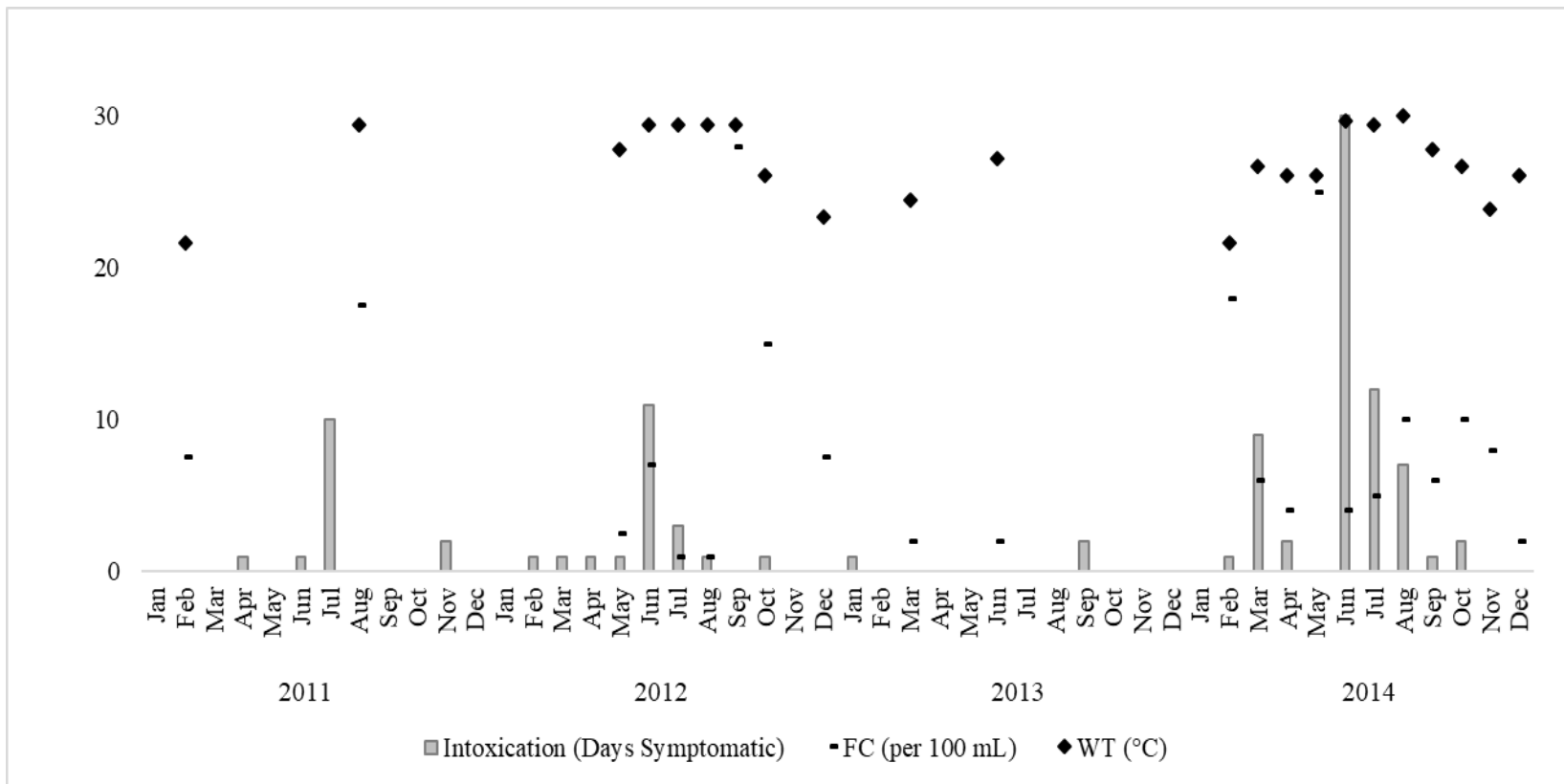


Figure 3.15 Consecutive plot of 2011-2014 monthly observed intoxication days symptomatic for both captive dolphins and the north lagoon water quality parameters with FC indicating maximum fecal coliform units (per 100 mL) and WT indicating lagoon water temperatures (°C).

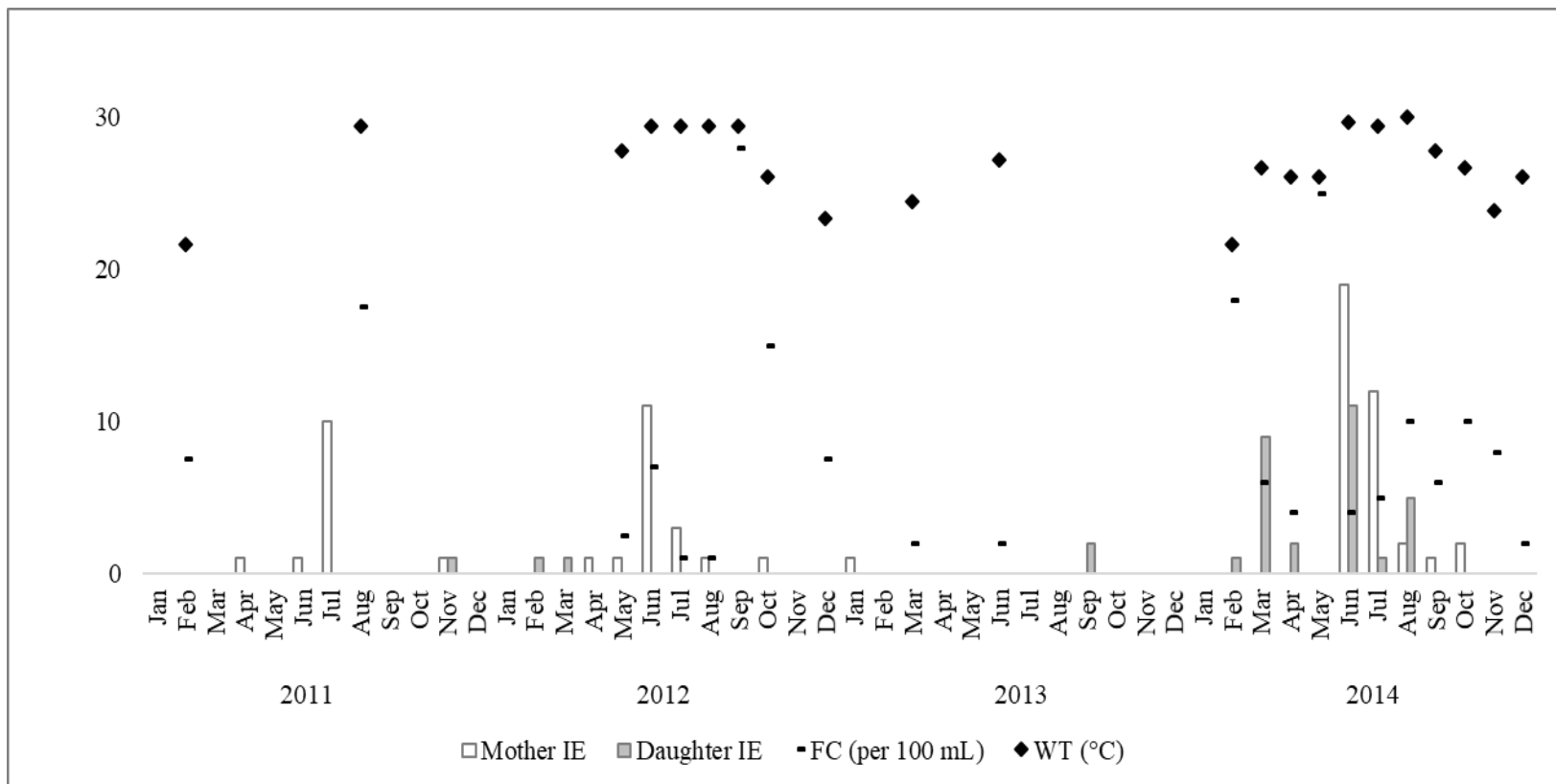


Figure 3.16 Consecutive plot of 2011-2014 monthly observed intoxication events (IE), expressed as days symptomatic, for the mother and daughter captive dolphins, relevant to the north lagoon seawater quality parameters with FC indicating maximum fecal coliform units (per 100 mL) and WT indicating lagoon water temperatures (°C).

The seawater temperatures for the north lagoon ranged from the February 2011 minimum of 21.7 °C (71.0 °F) to the August 2014 maximum of 30.0 °C (86.0 °F) with an average temperature of 26.9 ± 0.6 °C (80.4 ± 1.0 °F) over the four-year study period (Figure 3.15). The average of the 2011 to 2014 FC measurements for the north lagoon was 8.6 ± 1.6 FC and ranged from the 1.0 FC minima observed during July and August of 2012 to the 28.0 FC maximum measured in September 2012 (Figure 3.15). The maxima of monthly observed intoxications, expressed as days symptomatic for the mother-daughter captive dolphin pair, individually and combined, occurred in June 2011, 2012 and 2014 (Figure 3.15 and Figure 3.16). These intoxication maxima did not appear to coincide with the FC maxima observed during 2011 through 2014. Statistical analysis of the individual captive dolphin intoxication data and the FC data did not indicate any significant correlations, using a non-parametric, Spearman's rho two-tailed test for significance (Appendix) between the north lagoon FC data and the combined dolphin intoxication observations when averaged annual over the study (Figure 3.17).

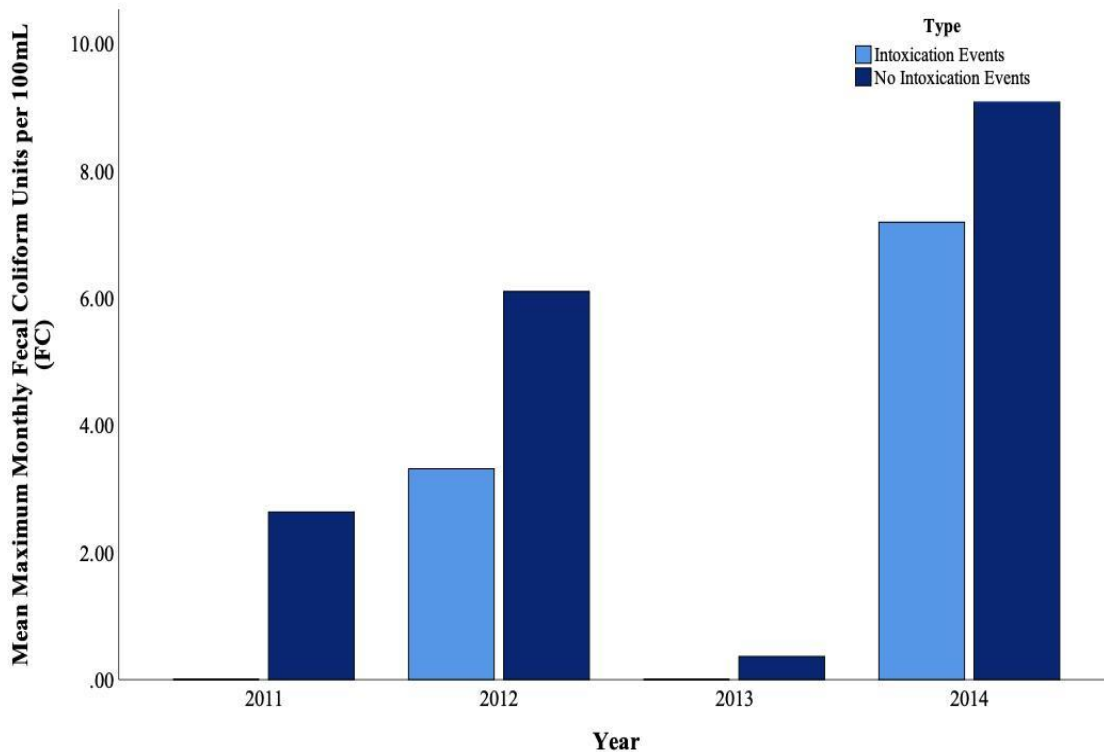


Figure 3.17 Comparison of annual maximum fecal coliform units per 100 mL north lagoon water (FC) versus annual frequencies of intoxications events observed for both captive dolphins relative to instances of no intoxications over the study period (2011-2014).

Overall, the data for the site water quality and the captive dolphin observations were either too limited or too varied to determine a more causative relationship via rigorous statistical analyses using IBM SPSS. (see Appendix)

3.4 Discussion

During the study period, the facility staff directly observed several captive dolphins playing with and/or ingesting macroalgae, primarily *Ulva* spp. (e.g., *U. lactuca*, *U. rigida*) and cyanobacteria (i.e., *Lyngbya* spp.) with and without, subsequently exhibiting apparent intoxication. The observed captive dolphin algal grazing, perhaps indicative of active pharmacognosy-related behaviors, are reported here for the first time for public dissemination. The observed grazing behaviors, overall, estimated *Ulva* spp.

was ingested 68% of the time followed by *T. testudinum*, unspecified Rhodophyta, and cyanobacteria, respectively at 13%, 11% and 8% of the time (see Figure 3.6). Notably, as described in Chapter Two, the captive dolphins most often ingested *Ulva* spp., generally recognized as a nutritionally valuable, non-toxic genus (Abirami and Kowsalya, 2011). However, *Ulva* spp. are also known to inhibit epiphytism by the HAB organisms *Karenia brevis* and *Pseudo-nitzschia* spp. and to produce therapeutic secondary metabolites including antioxidants (Tang and Gobler, 2011; Ratnayake et al., 2013). Concomitant intoxications were observed relative to algae-specific ingestions (see Figure 3.7). Particularly, intoxications were 38% related to cyanobacteria ingestions, compared to 20% for red macroalgae and 8% each for sea lettuce (*Ulva* spp.) and turtle grass (i.e., *T. testudinum*). The facility staff also logged the captive dolphins exhibiting episodic intoxications for which no algal ingestions were reported. These “unobserved” sources accounted for 67% of the overall intoxications when compared with algae-related incidents (see Figure 3.8). Intoxications were then associated to ingestions of *Ulva* spp. and *Lyngbya* spp., including *Neolyngbya* spp., at 17% and 12%, respectively. Whilst, approximately 3% of Rhodophyta and 1% of *T. testudinum* ingestions were related to intoxications. Direct observations of the captive dolphins grazing the cyanobacteria and macroalgae were limited to staff availability during normal hours of operation. Thus, the actual grazing behaviors of the captive dolphins are likely underestimated.

The prolific and persistent abundance of neurotoxicogenic *Lyngbya s.l.*, observed growing within the captive dolphin enclosures throughout the study, suggested that the captive dolphins were ingesting the cyanobacteria at a higher frequency than witnessed by the facility staff. Moreover, the neurological symptoms (e.g., ataxia, uncoordinated

swimming, seizure-like behavior, blepharospasms) associated with the apparent intoxication events remained consistent overall, regardless of the type of algal ingestions observed (e.g., macroalgae, cyanobacteria). As previously discussed in Chapter Two, microalgae observed to be epiphytic on the algae and cyanobacteria samples associated with the reported algal consumptions. However, neither of the neurotoxin-producing (e.g., brevetoxin, domoic acid) HAB-related epiphytes (e.g., *Karenia brevis*, *Pseudo-nitzschia* spp.) were positively identified. Thus, the observed intoxication events could be attributed to ingesting the known, neurotoxin-producing cyanobacteria (i.e., *Lyngbya s.l.*), overtly and incidentally, via grazing the macroalgae, particularly Rhodophyta. The findings herein led to chemical investigations of the cyanobacteria sampled from the captive dolphin lagoon for the presence of known or otherwise, uncharacterized, neurotoxic metabolites described in Chapters Four through Six.

From the staff observational records, a mother-daughter pair of related dolphins appeared to preferentially graze *Ulva* spp. and cyanobacteria (i.e., *Lyngbya s.l.*) and most often presented intoxication symptoms. The observational data logs indicated a general pattern of independent grazing and symptoms of intoxication between the mother-daughter pair of captive dolphins (see Figure 3.10 and Figure 3.11). However, both captive dolphins simultaneously experienced episodes of intoxications in November 2011 and during the summer of 2014 (i.e., June, July, August) as previously shown in Figure 3.1. Overall, the mother captive dolphin exhibited at least one major intoxication event, lasting up to 10 or more days per month, typically during the summer months of June through August in 2011, 2012 and 2014. During 2014, both captive dolphins experienced the most intoxications reported for the study. The mother dolphin endured a total of 33

symptomatic days between June and July. Comparatively, the daughter dolphin was symptomatic for 17 days during the summer. However, the daughter dolphin experienced 12 additional days of intoxication symptoms between February and April of 2014, whilst the mother dolphin was symptom-free during that time.

Specifically, both captive dolphins concurrently exhibited ataxia, uncoordinated swimming behaviors, ocular dysfunctions (i.e., blepharospasms), and respiratory issues (i.e., unspecified) between June and August of 2014. However, no immediate sampling or chemical investigations of macroalgae or cyanobacteria could be performed since the FIU-marine mammal zoological facility research agreement was still pending. A small amount of biomass, collected by the facility staff in August 2014, was stored on site at -20 °C, until retrieval in October 2014. However, the samples were too degraded and limited for either taxonomic characterizations or comprehensive chemical analyses (see Chapter Four).

From the observed cyanobacteria ingestion and subsequent intoxication data, combined for both captive dolphins, a general trend was elaborated. Intoxication events appeared to increase in the spring, peak during the summer months (e.g., June, July), and decline in the fall as typically expected with annual HAB bloom growth and subsidence trends. Notably, 2013 was a year relatively devoid of any reported intoxication symptoms despite reported algal ingestions. However, no statistically significant correlations could be determined between algal ingestions and apparent intoxications. The facility's veterinarian addressed and typically resolved each intoxication case within several days.

An examination of site seawater quality data, particularly fecal coliform, measured as the average maximum fecal coliform counts per 100 mL of collected lagoon

seawater, suggested an anticipated cyclic, seasonal trend. Periods of high nutrient input are often reflected by elevated AFC and indicative of eutrophic conditions. The observed AFC maxima could be attributed to anthropogenic-related inputs associated with increased human activities during the summertime. Likewise, spikes in AFC measurements greater than 9.8 ± 1.2 (SEM, $n = 66$) observed during the winter (e.g., February 2014) and spring months (e.g., April 2014) were possibly attributed to the “wintering over” effect resulting from the influx of seasonal residents escaping colder climates (see Figure 3.12 and Figure 3.15). Anthropogenic eutrophication likely contributed to the increased FC measurements in late summer through early fall between 2011 and 2012. Moreover, individual AFC seawater samples could have been collected very near a release of captive dolphin fecal matter, thus accounting for the large variability observed in the calculated averages. For example, the maximum value of 30.0 ± 2.0 AFC (SEM, $n = 3$), obtained in September 2012, was less variable than the May 2014 observed maximum of 25.7 ± 11.0 AFC (SEM, $n = 3$). Statistically, the water quality data (i.e., AWT, AFC) were too sporadic to establish any causal relationships (e.g., long-term, seasonal). Nor were statistical correlations (i.e., Spearman’s rho, Pearson Chi-Square) established between the observed captive dolphin intoxications and the FC data sampled specifically from their lagoon.

The fecal coliform measurements were graphically compared to the observed algal ingestions and intoxication events experienced by the captive dolphins during 2013 and 2014 (see Figure 3.15 and Figure 3.16). Episodic eutrophic conditions occurred throughout the study period. The proliferation of *Ulva* spp. generally coincided with the seasonal elevation of AFC during the summer months as expected. The captive dolphins

appeared to graze *Ulva* spp. (e.g., *U. lactuca*) more frequently during the winter and the spring, with and without subsequently exhibiting apparent signs of intoxications. The copious and continuous growth of cyanobacteria growth throughout the year did not appear to be correlated with either temperature or fecal coliform measurements. Moreover, statistical analyses of these data could not determine any definitive causal relationships between water quality parameters, algal growth, reported grazing behaviors or intoxications (see Appendix).

Notably, the mother and daughter dolphins were subsequently relocated in 2015 from the North enclosure to the opposing South enclosure. The staff continued to observe the pair ingesting cyanobacteria, without displaying any further intoxication symptoms since their move. Additionally, the fencing along the canal of each enclosure was replaced and a general clean up (e.g., removal of debris, cyanobacteria) of both enclosures occurred.

The facility staff observations of captive dolphins intermittently grazing of macroalgae and cyanobacteria, followed by apparent intoxications, led to the collection and subsequent morphology-based taxonomic characterizations of the algal community growing within the habitats. The facility staff observed the captive dolphins ingesting the cyanobacteria qualitatively identified as neurotoxigenic *Lyngbya* spp. Staff also observed a related pair of captive dolphins exhibiting symptoms of seemingly neurological impairment (e.g., ataxia, uncoordinated swimming) subsequent to the algal grazing. The staff observations led to chemically evaluating collections of the cyanobacteria for known or otherwise, previously uncharacterized, neurotoxic metabolites detailed in Chapters Four through Six of this dissertation.

3.5 Conclusions

The results of this chapter primarily sought to establish correlations between the apparent intoxication episodes and observed algal grazing behaviors of the captive dolphins. Overt algal grazing has not yet been reported in the available literature and is presented here to bring public attention to the phenomenon. Herein, zoopharmacognosy is hypothesized to rationalize the observed algal ingestions. Facility staff observed and recorded captive dolphins occasionally grazing macroalgae, primarily *Ulva* spp., and significant to this research, cyanobacteria identified as the neurotoxigenic, polyphyletic genus *Lyngbya*. A mother-daughter pair of captive dolphins were most-often observed ingesting *Ulva* spp. and the cyanobacteria. Subsequently, these captive dolphins presented neurotoxicity seeming intoxications as evidenced by neurological impairments (i.e., ataxia, uncoordinated swimming, blepharospasms). Each case of apparent intoxication was addressed by the facility's veterinarian, and all cases were resolved. The observations logged by the facility staff during the summer of 2014 suggested a positive, causal relationship indicative of the possible presence of neurotoxic agent related to the material ingested. However, in general, any observed intoxication events could not be well correlated (i.e., statistically) to specific ingestion observations due to the uncontrolled variability with overall monitoring (e.g., daily staff changes, staff assessment abilities, hours of facility operation).

The summer 2014 simultaneous intoxication events of two related dolphins correlated to ingesting cyanobacteria (i.e., *Lyngbya* spp.) including *Neolyngbya* spp. fueled the chemical evaluations of collected cyanobacteria for the presence of known, or

otherwise unidentified, neurotoxic metabolites described in Chapters Four through Six, respectively.

Future work should include continued monitoring of the captive dolphin grazing behaviors and subsequent intoxications to acquire a more statistically robust data set to better establish and/or predict future intoxication events. In addition, the results herein, provide an unprecedented opportunity to investigate the zoopharmacognosy hypothesis to explain the observed algal and cyanobacteria ingestions.

3.6 Acknowledgments

Express gratitude is given to Holli Eskelinen and Dr. Johanna Mejia-Fava of Dolphin's Plus for generously amassing the captive dolphin behavioral data and site water quality measurements needed to construct this chapter. Holli is especially thanked for providing her statistical prowess with IBM SPSS.

3.7 References

- Abirami, R.G., Kowsalya, S., 2011. Nutrient and nutraceutical potentials of seaweed biomass *Ulva lactuca* and *Kappaphycus alvarezii*. *J. Agr. Sci. Technol.* 5(1), 109-115.
- Anderson, D.M., Burkholder, J.M., Cochlan, W.P., Gilbert, P.M., Gobler, C.J., Heil, C. A., Kudela, R., Parsons, M.L., Rensel, J.E.J., Townsend, D.W., Trainer, V.L., Vargo, G.A., 2008. Harmful algal blooms and eutrophication: Examining linkages from selected coastal regions of the United States. *Harmful Algae* 8(1), 39-53. doi:10.1016/j.hal.2008.08.017
- Hokama, Y., Asahina, A.Y., Hong, T.W.P., Katsura, K., Miyahara, J.T., Sweeney, J.C., Stone, R., 1990. Causative Toxins(s) in the Death of Two Atlantic Dolphins. *J. Clin. Lab. Anal.* 4, 474-478. doi:10.1002/jcla.1860040615
- Mallin, M.A., Cahoon, L.B., Toothman, B.R., McIver, M.R., Ortwine, M.L., Parsons, D.C., Harrington, R.N., 2007. Impacts of a raw sewage spill on water and sediment quality in an urbanized estuary. *Mar. Pollut. Bull.* 54, 81-88. doi:10.1016/j.marpolbul.2006.09.003
- Mejia-Fava, J., Colitz, C.M.H., 2014. Supplements for Exotic Pets. *Vet. Clin. North Am. Exot. Anim. Pract.* 17(3), 503-525. doi:10.1016/j.cvex.2014.05.001

Meylan A., 1988. Spongivory in hawksbill turtles: a diet of glass. *Science* 239(4838), 393–5.

Mill, A., Schlacher, T., Katouli, M., 2006. Tidal and longitudinal variation of faecal indicator bacteria in an estuarine creek in south-east Queensland, Australia. *Mar. Pollut. Bull.* 52, 881-891. doi:10.1016/j.marpolbul.2005.11.018.

O’Neil, J.M., Davis, T.W., Burford, M.A., Gobler, C.J., 2012. The rise of harmful cyanobacteria blooms: The potential roles of eutrophication and climate change. *Harmful Algae* 14, 313-334. doi:10.1016/j.hal.2011.10.027

Paul, J.H., Rose, J.B., Jiang, S., Kellog, C., Shinn, E.A., 1995. Occurrence of Fecal Indicator Bacteria in Surface Waters and the Subsurface Aquifer in Key Largo, Florida. *Appl. Environ. Microb.* 61(6), 2235-2241

Ratnayake, R., Liu, Y., Paul, V.J., Luesch, H., 2013. Cultivated sea lettuce is a multiorgan protector from oxidative stress and inflammatory stress by enhancing the endogenous antioxidant defense mechanism. *Cancer Prev. Res. (Phila)* 6(9), 989-999. doi:10.1158/1940-6207.capr-13-0014

Rhind, S.M., 2009. Anthropogenic pollutants: a threat to ecosystem sustainability? *Phil. Trans. R. Soc. B* 364, 3391-3401. doi:10.1098/rstb.2009.0122

Smolker, R., Richards, A., Conner R., Mann, J., Berggren, P., 1997. Sponge carrying by dolphins (*Delphinidae*, *Tursiops* sp.): A foraging specialization involving tool use? *Ethology* 103, 454-465.

Tang, Y.Z., Gobler, C.J., 2011. The green macroalga, *Ulva lactuca*, inhibits the growth of seven common harmful algal bloom species via allelopathy. *Harmful Algae* 10(5), 480-488. doi:10.1016/j.hal.2011.03.003

4. CHEMICAL EVALUATION OF CYANOBACTERIA BIOMASS FOR KNOWN NEUROTOXINS

4.1 Introduction

Literature abounds with chemical investigations of bioactive secondary metabolites produced by aquatic cyanobacteria (e.g., dermatoxins, hepatotoxin, neurotoxins) and marine phytoplankton (e.g., diatoms, dinoflagellates) associated with shellfish poisonings (e.g., amnesic, diarrhetic, neurotoxic, paralytic) as reviewed by Aráoz et al. (2010). Human activity often impacts environmental conditions to favor proliferation of toxin-producing algae. Harmful algal blooms (HAB) result from the release of high concentrations of toxins into the ecosystem during bloom subsidence. Erdner et al. (2008) presented an excellent overview of concerns and challenges imposed on human health by HAB events. Release of puissant, deleterious neurotoxins including anatoxins (ATX), brevetoxins (PbTx), domoic acid (DA), β -methylamino-L-alanine (BMAA) and saxitoxins (STX) occurs during the subsidence of specific HAB cyanobacteria, diatom, and dinoflagellate species. Indeed, as a result of the serious health implications posed by human exposures, the USA Food and Drug Administration (U.S. FDA) developed guidance concerning several fisheries-related HAB toxins describing sources, control strategies, tolerable limits and detection methods per U.S. FDA UCM252395 Chapter 6 (U.S. FDA, 2011). Table 4.1 précises some of the culprit neurotoxicogenic HAB genera with their respective aquatic habitats.

Table 4.1 Example neurotoxicogenic HAB organisms.

Neurotoxin	Habitat	Organism	Genus	Reference
ATX	freshwater, marine	cyanobacteria	<i>Anabaena</i>	Devlin et al. (1977) Onodera et al. (1997)
			<i>Aphanizomenon</i>	Wood et al. (2007)
			<i>Cylindrospermopsis</i>	Lagos et al. (1999)
			<i>Oscillatoria</i>	Aráoz et al. (2005)
			<i>Phormidium</i>	Cadel-Six et al. (2007)
			<i>Planktothrix</i>	Viaggiu et al. (2004)
			<i>Tychonema</i>	Shams et al. (2015)
STX	freshwater, estuarine,	cyanobacteria	<i>Cylindrospermopsis</i>	Lagos et al. (1999) Filho et al. (2008)
			<i>Lyngbya*</i> (e.g., <i>L. wollei</i>)	Carmichael et al. (1997)
			<i>Anabaena</i> <i>Aphanizomenon</i>	Mihali et al. (2009)
	marine, estuarine	dinoflagellate	<i>Planktothrix</i>	Pomati et al. (2000)
			<i>Alexandrium</i>	Anderson et al. (1990) Lilly et al. (2007)
			<i>Gymnodinium</i>	Oshima et al. (1987)
			<i>Pyrodinium</i>	Harada et al. (1982)
BMAA	freshwater, estuarine, marine, desert	cyanobacteria	<i>Aphanizomenon</i> <i>Chroococciopsis</i> <i>Cylindrospermopsis</i> <i>Lyngbya*</i> <i>Myxosarcina</i> <i>Nostoc</i> <i>Symploca</i> <i>Trichodesmium</i>	Cox et al. (2005)
			marine	diatom
	marine	dinoflagellate	<i>Heterocapsa</i> (e.g., <i>H. triquetra</i>)	Jiang and Ilag (2014)
PbTx	marine	dinoflagellate	<i>Karenia</i> (e.g., <i>K. brevis</i>) formerly <i>Ptychodiscus brevis</i> , <i>Gymnodinium breve</i>	Lin and Risk (1981) Haywood et al. (2007)
DA	marine	diatom	<i>Pseudo-nitzschia</i>	Wright et al. (1989)

* Taxonomic revisions include *Moorea* spp. and *Okeania* spp. (Engene et al., 2012 and 2013a, b) and *Neolyngbya* spp. (Caires et al., 2018a)

Reviews by Stewart et al. (2008) and Backer et al. (2013) and, most recently, by Wood (2016) indicate that HAB-related neurotoxin contaminations are particularly worrisome because of the adverse health outcomes for exposed people and animals (e.g., companion, wildlife, farm). Economic concerns arise when agricultural, aquacultural,

recreational and potable water resources are negatively impacted by the presence of HAB-organisms as described by Anderson et al. (2000), Anderson (2004), and Hoagland et al. (2002). Allelopathic reactions to environmental stressors feasibly stimulate production of neurotoxic secondary metabolites in a variety of marine algae and cyanobacteria. For example, herbivory of *Caulerpa taxifolia* elicits a chemical defense response to produce an unpalatable (e.g., neurotoxic) cicatrizant (Weissflog et al., 2008). Thus, a variety of chemical classes have been biologically synthesized to elicit adverse neurotoxic responses within afflicted organisms via specifically targeted metabolic pathways and modes of action. As such, structure activity relationship studies (SAR), through in vitro and in vivo testing, help identify the pathway(s) at risk to neurotoxicity affronts.

As described in Chapter Two, captive bottlenose dolphins (*Tursiops truncatus*) living in the Florida Keys were observed grazing algae, and cyanobacteria, growing within their enclosure followed by apparent intoxications (e.g., ataxia, uncoordinated swimming, blepharospasms). The staff veterinarian addressed and generally resolved each instance of intoxication within several days. The facility staff logged the captive dolphins primarily ingesting sea lettuce, (e.g., *Ulva* spp.) and the omnipresent cyanobacteria. The algal ingestion-related manifestations of apparent neurotoxicity led to evaluating the algal community for potential neurotoxigenic taxa. None of the identified macroalgae were reported to produce neurotoxins. The initial taxonomic characterizations (e.g., morphology, light microscopy) of the pervasive, dense mats of mixed assemblage, filamentous cyanobacteria, collected from within the captive dolphin enclosures, recognized the known, neurotoxigenic, polyphyletic genus, *Lyngbya* C. Agardh ex

Gomont (Cyanophyceae). As shown in Table 4.1, *Lyngbya* spp. produce a variety of potent neurotoxins including BMAA and STX. The genus *Lyngbya* is undergoing taxonomic revisions since the advent of molecular phylogenetic techniques. Indeed, the phylogenetic characterization of dark green, filamentous morphotypes within the collected cyanobacteria assemblage recently identified three closely related members of the family Oscillatoriaceae, including the genus *Neolyngbya* (Caires et al., 2018a). To date, *Neolyngbya* spp. have not been chemically profiled for production of neurotoxic secondary metabolites associated with *Lyngbya* spp. Positive identifications of the neurotoxic HAB-related dinoflagellate, *Karenia brevis* (Davis) G. Hansen et Moestrup (Dinophyceae), and the diatom *Pseudo-nitzschia* spp. (Cleve) Peragallo (Bacillariophyceae), were inconclusive during the morphological examinations of the algae and cyanobacteria collected from within the dolphin habitat. Hence, their presence remains plausible. As shown in Table 4.1, *Karenia* spp. are known to produce the neurotoxic PbTx, whilst the neurotoxin DA is produced by *Pseudo-nitzschia* spp. Likewise, other HAB-related microalgae (e.g., diatoms, dinoflagellates) may be present (Zingone and Enevoldsen, 2000; Jiang et al., 2014a; Lage et al., 2014; Jiang and Ilag, 2014). A recommendation was proposed to the marine mammal zoological facility to periodically remove excessive cyanobacteria growth and monitor for HAB-related organisms (e.g., cyanobacteria, diatoms, dinoflagellates), especially during any future dolphin intoxication event.

The taxonomic diversity within the captive dolphin habitats inferred the potential for HAB-related neurotoxin production as detailed in Chapter Two and summarized herein. No statistical correlations could confirm that overt captive dolphin ingestions of

the cyanobacteria morphologically categorized as the neurotoxigenic, polyphyletic *Lyngbya* spp. led to subsequent intoxication events. Thus, inadvertent ingestions of neurotoxigenic HAB-related microalgae (i.e., diatoms, dinoflagellates) were possible. These observations warranted the subsequent collection and chemical investigation of the cyanobacterial biomass for known, or otherwise uncharacterized, neurotoxins. Specifically evaluated were the HAB-related neurotoxins, anatoxin-a (ATX-a), BMAA, STX, brevetoxin-2 (PbTx-2) and DA for which standards and validated analytical methodologies exist. The results of the known neurotoxin screenings are summarily presented herein. The rationale and salient aspects of each HAB-related neurotoxin are briefly discussed below. Table 4.2 ascribes the neurotoxic secondary metabolites to the respective compound classes and representative source organisms with a descriptive sobriquet relating the noxious human health effect.

Table 4.2 Correlation of HAB neurotoxins to compound class and source organism(s).

HAB Neurotoxin	Compound Class	Associated Ailment	Source Organism
Anatoxin-a (ATX-a)	Alkaloid	Very Fast Death Factor (VFDF)	cyanobacteria
β -methylamino-L-alanine (BMAA)	Amino acid	Neurodegeneration (ND)	cyanobacteria, diatoms, dinoflagellates
Saxitoxin (STX)	Alkaloid	Paralytic Shellfish Poisoning (PSP)	cyanobacteria, dinoflagellates
Brevetoxin-2 (PbTx-2)	Polycyclic ether	Neurotoxic Shellfish Poisoning (NSP)	dinoflagellates (<i>Karenia</i> spp.)
Domoic Acid (DA)	Amino acid	Amnesic Shellfish Poisoning (ASP)	Diatoms (<i>Pseudo-nitzschia</i> spp.)

4.1.1 Anatoxin-a (ATX-a)

Of the known anatoxin analogues, naturally occurring (+)-anatoxin-a (ATX-a), is considered the most potent neurotoxin. Freshwater cyanobacteria of the filamentous genera *Anabaena* spp. (Devlin et al., 1977; Onodera et al., 1997), *Aphanizomenon* spp.

(Wood et al., 2007), *Cylindrospermopsis* spp. (Kiss et al., 2002), *Oscillatoria* spp. (Aráoz et al., 2005, 2008), and *Planktothrix* spp. (Viaggiu et al., 2004) chiefly produce ATX-a. The homologue, homoanatoxin-a, another potent neurotoxin, is produced by the pantropic marine, filamentous cyanobacteria, *Hydrocoleum* spp. (Méjean et al., 2010) and both marine and freshwater, filamentous *Oscillatoria* spp. (Skulberg et al., 1992; Aráoz et al., 2005, 2008). The current taxonomic classification of ATX-a producing filamentous cyanobacteria, as displayed in Table 4.3, blends traditional morphology-based and the more recently phylogenetic (e.g., 16S rRNA, molecular) revisions of genera described by Komárek et al. (2014) and Aguilera et al. (2018).

Table 4.3 The prominent ATX-a producing cyanobacteria (Cyanophyceae) taxa.

Order	Family	Genus	Authority
Nostocales	Nostocaceae	<i>Anabaena</i>	Bory ex Bornet and Flahault 1886; Komárek et al. 2014
	Aphanizomenonaceae	<i>Aphanizomenon</i>	Morren ex Bornet and Flahault 1886; Komárek et al. 2014
		<i>Cylindrospermopsis</i>	Seenayya and Subba Raju 1972; Aguilera et al. 2018
Oscillatoriales	Microcoleaceae	<i>Planktothrix</i>	Anagnostidis and Komárek 1988; Suda et al. 2002; Lin et al. 2010; Komárek et al. 2014
	Oscillatoriaceae	<i>Oscillatoria</i>	Vaucher ex Gomont 1892; Komárek et al. 2014

Noteworthy, Takada et al. (2000) isolated a similarly potent ATX derivative (e.g., pinnamine) from an Okinawan marine clam (e.g., *Pinna muricata*). Expanding ATX research continues to identify additional ATX producing cyanobacteria genera (e.g., *Raphidiopsis*, *Phormidium*, *Tychonema*) as reported by Namikoshi et al. (2004), Hodoki et al. (2013), Gugger et al. (2005), Harland et al. (2013, 2014), and Shams et al. (2015).

As shown in Figure 4.1, ATX-a is a small, water-soluble, secondary bicyclic alkaloid stereoisomer derivative of glutamic acid having a molecular mass of 165.23 grams/mole (g/mol).

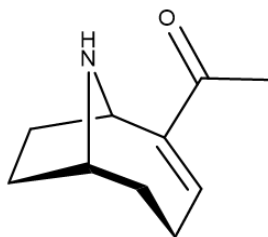


Figure 4.1 The molecular structure of (+) anatoxin-a (ATX-a).

A strong neurotransmitter mimic of acetylcholine, ATX-a irreversibly activates nerve cell voltage-gated sodium channels of nicotinic acetylcholine receptors causing overstimulation of the respiratory muscles leading to rapid paralysis and, ultimately, asphyxiation. Death can occur within minutes of drinking water contaminated with ATX-a, hence its moniker “Very Fast Death Factor.” Wonnacott and Gallagher (2006) presented an in-depth review of the neurotoxicity mechanisms of ATX-a and its related analogues. First isolated in 1972 by Devlin et al. (1977), ATX-a has been implicated in globally reported fatalities involving companion animals (e.g., dogs, horses), livestock (e.g., cattle, sheep pigs), wildlife (e.g., deer, elk) and waterfowl (e.g., ducks, flamingos). Bioaccumulation and biomagnification of ATX-a occurs within aquatic fauna (e.g., mussels, snails, fish) as reported by Osswald et al. (2008, 2011) and Pawlik-Skowrońska et al. (2012). Little definitive toxicological data exists to clearly establish an accurate daily permissible level of ATX-a ingestion from water or food sources. Upon evaluating the available data, the Washington State Department of Ecology estimated a reference dose of 1 µg/L as the threshold concentration of ATX-a in recreational waters in 2012

(Trainer and Hardy, 2015). Several dog deaths related to ATX-a exposures in 2008-2010 (Puschner et al., 2008, 2010) prompted the Oregon Health Authority to derive Tolerable Daily Intake (TDI) guideline values for humans and dogs at 0.1 µg/kg/day, 3.0 µg/L for human drinking water, 20.0 µg/L for human recreational freshwater, and dog-specific recreational freshwater at 0.4 µg/L, respectively (Farrer et al., 2015). California, Ohio, Vermont and Washington have proposed similar guidelines for recreational freshwater only. Considerable variability of measured water-volume concentrations observed across sampled water bodies relevant to detection methods also confounds the ability to propose suitable safety levels by U.S. regulators and the World Health Organization (WHO).

Primarily produced by aquatic cyanobacteria genera of *Anabaena* spp., *Oscillatoria* spp. and *Planktothrix* spp., under eutrophic conditions, high concentrations of the neurotoxin can be released into the ecosystem during bloom decline. In addition, cyanobacteria production of ATX-a is directly proportional to increased water temperature, solar radiation (e.g., UV), and alkalinity which are all environmental conditions favorable for cyanobacteria growth. Thus, toxic blooms are most often associated with the summer season and, especially, tropical water bodies according to the recent U.S. Environmental Protection Agency (EPA) report, EPA_820-R-15-104 (U.S. EPA, June 2015, D'Anglada et al., 2015). The same environmental conditions that amplify ATX-a production also cause its rapid hydrolytic and photolytic degradation (e.g., hours to days) as shown by Yang (2007) into less noxious products (e.g., dihydroanatoxin-a, epoxyanatoxin-a). Conversely, dense cyanobacteria proliferations retard environmental degradation processes, allowing ATX-a to persist over time (e.g., weeks, months) as reported by Smith and Sutton (1993). Dynamic (e.g., diurnal,

seasonal) environmental conditions (e.g., insolation, water temperature, pH) affect rates of cyanobacteria growth, decline, toxin production and degradation further impeding accurate quantification of ATX-a concentrations in real time. Thus, there is often a lag time between HAB observation, reporting, sample collection, and analysis.

The major analytical methods used for detection and quantification of ATX-a include enzyme-linked immunosorbent assay (ELISA), high performance liquid chromatography (HPLC) with fluorescence detection (FD), and liquid chromatography-tandem mass spectrometry (LC-MS/MS) as reviewed by Osswald et al. (2007), and by Al-Sammack et al. (2013). Most recently, Fayad et al. (2015), developed an on-line solid phase extraction-liquid chromatography-tandem mass spectrometry (SPE-LC-MS/MS) to expedite analysis time. The ELISA method provides a fast, economical, high throughput, qualitative, screening tool with high enough sensitivity to allow quantitation. Although, cross reactivity and matrix effects can yield false positive results, requiring additional analysis for confirmation. The less specific HPLC-FD methods often requires post-column derivatization to enhance detection and are also subject to matrix effects. Very specific and sensitive LC-MS and LC-MS/MS methods afford high throughput, unambiguous confirmation, but are more time consuming (e.g., analysis time) and costly (e.g., instrumentation, specialty columns, operator training). The approved U.S. EPA Method 545, U.S. EPA_815-R-15-009, employs LC-MS/MS with the electrospray ionization technique and the use of internal standards over a range of 0.029-5.87 ng/mL ATX-a (U.S. EPA, April 2015). Applying emergent Matrix-Assisted Laser Desorption/Ionization Time-of-Flight (MALDI-TOF-MS) technology, Aráoz et al. (2008) developed a rapid, high-resolution MS method to directly analyze cyanobacteria

filaments (e.g., lyophilized, fresh) with minimal sample preparation for the presence of secondary metabolites.

The Florida Everglades, sourced from central Florida's East Lake Tohopekaliga emptying into Lake Okeechobee approximately 100 miles south via the Kissimmee River, comprise a vast drainage basin covering much of south Florida with outflow directly into Florida Bay and continuing through the Florida Keys into the Atlantic Ocean. Heavy anthropogenic activities throughout this watershed during the last century (e.g., urbanized land development, agriculture enterprises, water flow manipulations) have led to deleterious water quality and ecosystem declines stimulating episodic HAB events. Although, to date, no estuarine or marine cyanobacteria have been shown to produce ATX-a, it remains plausible that the neurotoxin could be present if associated with a persistent bloom in and around Florida Bay. The interconnectedness of the Everglades watershed with the Florida Keys warranted testing the cyanobacteria mats collected from the eutrophic captive dolphin lagoons for the presence of ATX-a.

4.1.2 β -methylamino-L-alanine (BMAA)

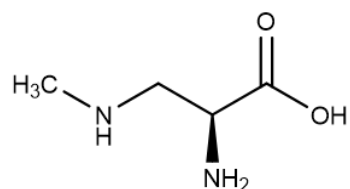
Although an amino acid secondary metabolite produced by cyanobacteria, lichen and plants worldwide (Cox et al., 2005), β -methylamino-L-alanine (BMAA) is not found in any genetic sequences. As a neurotoxin, BMAA purportedly induces neurodegeneration (Delcourt et al., 2018). Marine cyanobacteria known to produce BMAA include species of the genera *Lyngbya* spp., *Nostoc* spp., *Prochlorococcus* spp., *Symploca* spp., and *Trichodesmium* spp., (Cox et al., 2005). Table 4.4 shows the current taxonomies of BMAA-producing cyanobacteria (e.g., aquatic, marine) genera including classifications by molecular phylogeny.

Table 4.4 The prominent BMAA producing cyanobacteria (Cyanophyceae) taxa.

Order	Family	Genus	Authority
Nostocales	Nostocaceae	<i>Nostoc</i>	Vaucher ex Bornet and Flahault 1886; Rajaniemi et al. 2005a, b; Komérek et al. 2014
Oscillatoriales	Microcoleaceae	<i>Symploca</i>	Kützing ex Gomont 1892; Thacker and Paul 2004; Komérek et al. 2014
		<i>Trichodesmium</i>	Ehrenberg ex Gomont 1892, nom. Cons.; Abed et al. 2006; Komérek et al. 2014
	Oscillatoriaceae	<i>Lyngbya</i> *	C. Agardh ex Gomont 1892; Komárek et al. 2014
Synechococcales	Prochloraceae	<i>Prochlorococcus</i>	Chisholm et al. 1992; Komérek et al. 2014

* Taxonomy revisions include *Moorea* spp. and *Okeania* spp. (Engene et al., 2012, 2013a, b) and *Neolyngbya* spp. (Caires et al., 2018a)

As shown in Figure 4.2, BMAA is a small, water-soluble, amino acid derivative of alanine having a molecular mass of 118.14 g/mol.

**Figure 4.2** The molecular structure of β -methylamino-L-alanine (BMAA).

A non-protein amino acid, current research postulates that BMAA is misencoded for the naturally occurring amino acid, L-serine during protein synthesis (Dunlop et al., 2013). Glover et al. (2014) revealed BMAA is capable of substituting for L-alanine during neuroprotein synthesis in humans. The misincorporated BMAA activates receptors involved with sodium and calcium channel regulation (e.g., NMDA, AMPA, glutamate, kainite) leading to potential neural protein (e.g., tau, neurofibrillary) entanglements and β -amyloid plaques within the central nervous system, motor neuron damage and apoptosis, and, eventually, irreversible tauopathies (e.g., neurodegeneration). Especially

targeted are neurons involved with cognition, movement, and regulatory receptors (e.g., dopamine, serotonin) as described by Lindström et al. (1990). Cox et al. (2003) and Bradley and Mash (2009) implicated acute and chronic BMAA exposures to subsequent development of neurodegenerative diseases such as Alzheimer's Disease (AD), Parkinson's Dementia Complex (PDC), and Amyotrophic Lateral Sclerosis (ALS), also known as Lou Gehrig's Disease.

The high prevalence of neurodegenerative disease (e.g., AD, ALS, PDC) symptoms observed in the isolated Chamorra population of Guam spurred the initial investigations of BMAA. Recognition of dietary BMAA exposures led to identifying sources, causes, effects, and roles of BMAA production, and specifically, by HAB forming cyanobacteria as reported by Lobner et al. (2007), Dunlop et al. (2013) and Masseret et al. (2013). Additional studies showed BMAA both bioaccumulates and biomagnifies in humans and animals (e.g., mollusks, crustaceans, sharks, birds, rats, flying foxes) including rodent maternal transfer through nursing neonates (e.g., rats) as described by Cox and Sacks (2002), Banack and Cox (2003), Banack, et al. (2006), Mondo et al. (2012), Andersson et al. (2013), Andersson (2015) and Karlsson et al. (2009). Karlsson et al. (2009, 2011) observed acute and chronic neonatal exposure of BMAA impaired learning and memory in both neonate and adult rats. Further studies by Karlsson et al. (2014, 2017) subsequently linked learning and memory deficiencies in rats to BMAA activation of glutamate receptors (e.g., NMDA) and calcium channels using mass spectrometry imaging techniques in rodent models. Cox et al. (2016) implicated chronic BMAA exposure (e.g., dietary, environmental) in progressive neurodegenerative disease over a lifetime. However, in some case studies of neurodegeneration (e.g.,

human, mice), BMAA was anticipated but not detected (Snyder et al., 2009; Montine et al., 2005; Cruz-Agado et al., 2006). These conflicting reports stirred debate (Faassen, 2014; Jiang et al., 2014b) revealing inconsistencies with organism sampling (e.g., species), preparation (e.g., tissues), quantification techniques (e.g., wet weight, dry weight, derivatization) and the targeted analyte (e.g., free versus protein-bound BMAA). The Jiang et al. (2014b) study focused on localized seafood (e.g., fish, crustaceans, bivalve mollusks) consumed in Sweden. Their results confirmed that BMAA levels vary with organisms (e.g., species, age), sampled tissues (i.e., edible), and targeted analyte (e.g., free, bound). The BMAA levels also varied with environmental factors (e.g., eutrophication, location, season). As expected, elevated BMAA levels in lower trophic species, consistent with filter feeders (e.g., blue mussel, oyster) and planktonic feeders (e.g., shrimp, flatfish), compared to higher trophic species, verified bioaccumulation. Trophic transfer was also observed in farmed and wild fish (Jonasson et al., 2010; Al-Sammak et al., 2014). Most recently, Banack et al. (2014) correlated the development of ALS in a Florida fisherman directly to chronic (e.g., 30 years) consumption of BMAA contaminated shellfish (e.g., lobsters). Davis et al. (2019) detected elevated levels of BMAA in the brains of coastal bottlenose dolphins that stranded in Florida and pelagic common dolphins stranded in Massachusetts using chromatographic and hyphenated mass analysis methods (e.g., HPLC, LC-MS/MS). Increased β -amyloid plaques observed in brain tissue samples collected from the common dolphins were not directly correlated to measured BMAA concentrations. Currently, no conclusively positive correlation exists between BMAA exposure and neurodegeneration. Thus, health authorities (e.g., Oregon,

U.S. EPA) require more definitive dose-response data to set appropriate BMAA guideline limits (Farrer et al., 2015).

In contrast with ATX-a, many cyanobacteria symbionts (e.g., lichens, plants) produce BMAA across several ecosystems (e.g., terrestrial, desert, aquatic, marine) as described by Cox et al. (2005). More recently, diatoms (Jiang et al., 2014a) and dinoflagellates (Jiang and Ilag, 2014; Lage et al., 2014) were reported to produce BMAA. Thus, BMAA exposure may be much more prevalent than previously expected. Laboratory culturing of pure cyanobacteria (e.g., *Microcystis* spp., *Synechocystis* spp.) by Downing et al. (2011) suggest BMAA production varies with species, strain and tends to accelerate in nitrogen poor environments (i.e., oligotrophic) versus eutrophic conditions. However, increased anthropological activity in and around the South Florida watersheds during the 1980s resulted in large, episodic cyanobacteria blooms stimulated by considerable eutrophication (Brand et al., 2002). Significant environmental impacts caused by human activities and hurricanes during 2005 enriched the Florida Bay ecosystem with phosphorus perpetuating cyanobacteria blooms (Gilbert et al., 2009). Subsequently, Brand et al. (2010), observed elevated levels of BMAA in crustaceans (e.g., pink shrimp) compared to fish (e.g., grey snapper) relevant to the cyanobacteria subsidence occurring in the Florida Bay watershed. Noteworthy, Jiang et al. (2014b) measured elevated BMAA levels in shrimp fished from the Northern Atlantic Ocean near Sweden. Investigations of BMAA levels present in cyanobacteria are limited to the studies by Downing et al. (2011), Spáčil et al. (2010) and Réveillon et al. (2014).

Evaluation of BMAA entails analyte extraction (e.g., acid hydrolysis), concentration, detection and quantification. The analytical methods most commonly used

to detect and quantify BMAA include HPLC-FD and LC-MS/MS. Without specialized hydrophilic interaction liquid chromatography (HILIC) column stationary phases used for HPLC, both techniques require post-column derivatization to enhance BMAA detection (Eriksson et al., 2009; Salomonsson et al., 2013). Regardless of method choice, addition of isomeric internal standards (e.g., DAB, BAMA, AEG) confirmed BMAA identification and quantitation for mass spectrometry methods by reducing isobaric interferences from phenylalanine (Kubo et al., 2008; Faassen et al., 2009; Spáčil et al., 2010; Al-Sammak et al., 2013; Réveillon et al., 2014). Currently, detection limits are method specific because of the varied analytical approaches. The advent of MALDI-TOF-MS allowed fast, high-resolution analyses of cyanobacteria metabolites from minimally prepared extracts or intact specimens (Esquenazi et al., 2008).

The elevated levels of BMAA detected within Florida Bay crustaceans (e.g., shrimp, lobster), by Brand et al. (2010) and Banack et al. (2014) and particularly, wild dolphins (Davis et al., 2019) warranted the chemical evaluation for the presence of BMAA in the cyanobacteria growing within the Florida Keys captive dolphin enclosures by LC-MS/MS and MALDI-TOF-MS, techniques available at the Analytical Mass Spectrometry Facility at Florida International University (FIU-AMSF).

4.1.3 Saxitoxin (STX)

Saxitoxin (STX), akin to ATX-a, exhibits the most neurotoxic effects within its chemical family of more than 55 analogues. Being the parent molecule, STX was assigned a relative toxicity value of 1.000 to facilitate direct toxicity equivalence comparisons between the less potent derivatives. Marine dinoflagellates known to specifically produce STX include species in the genera of *Alexandrium* spp.,

Cochlodinium spp., *Gymnodinium* spp. and *Pyrodinium* spp. (Phlips et al., 2006; Zingone and Enevoldsen, 2000). Several aquatic cyanobacteria species also produce STX (Deeds et al., 2008a; Filho et al., 2008; Moustafa et al., 2009) as shown in Table 4.5.

Table 4.5 The prominent STX producing cyanobacteria (Cyanophyceae) taxa.

Order	Family	Genus	Authority
Nostocales	Aphanizomenonaceae	<i>Aphanizomenon</i>	Morren ex Bornet and Flahault 1886; Komárek et al. 2014
		<i>Cylindrospermopsis</i>	Seenayya and Subba Raju 1972; Aguilera et al. 2018
	Nostocaceae	<i>Anabaena</i>	Bory ex Bornet and Flahault 1886; Komárek et al. 2014
	Rivulariaceae	<i>Rivularia</i>	C. Agardh ex Bornet et Flahault 1886
Oscillatoriales	Microcoleaceae	<i>Planktothrix</i>	Anagnostidis and Komárek 1988; Suda et al. 2002; Lin et al. 2010; Komárek et al. 2014
	Oscillatoriaceae	<i>Lyngbya</i> * (e.g., <i>wollei</i>)	C. Agardh ex Gomont 1892; (e.g., Farlow ex Gomont, 1892); Komárek et al. 2014
* Taxonomy revisions include <i>Moorea</i> spp. and <i>Okeania</i> spp. (Engene et al., 2012, 2013a, b) and <i>Neolyngbya</i> spp. (Caires et al., 2018a)			

As shown in Figure 4.3, STX is a small, water-soluble, alkaloid having a molecular mass of 299.29 g/mol.

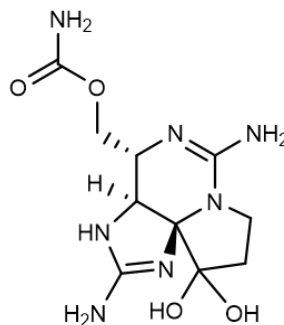


Figure 4.3 The molecular structure of saxitoxin (STX).

Another voltage-gated sodium channel neurotransmitter mimic, STX reversibly inhibits nerve cell sodium channels indiscriminately causing nerve signal transmission

failure leading to paralysis of the affected area, and even death. Discrete neurological symptoms including ataxia, localized numbness and tingling, gastrointestinal, respiratory and speech issues can occur within 30 minutes of ingestion, causing death by respiratory paralysis within 2-12 hours. The suite of STX analogues exhibits similar, less potent neurotoxicity, hence, the collective moniker “Paralytic Shellfish Poisoning” (PSPs). No antidote is currently available for STX. A comprehensive review by Cusick and Sayler (2013) concisely captured the salient ion channel biochemistry of PSPs (e.g., Na⁺, K⁺, Ca²⁺). Most recently, Diehl et al. (2016) implicated chronic exposure to STX with memory impairment in rats when drinking water was contaminated with a known PSP producing cyanobacteria (e.g., *Cylindrospermopsis raciborskii*).

Saxitoxin is aptly named for being first isolated from the butter clam, *Saxidomus giganteus* by Shantz et al. (1957). Bioaccumulation and biomagnification of STX chiefly occurs within lower trophic levels (e.g., crustaceans, gastropods, fish, shellfish) in most tissues (Landsberg et al., 2006; Shearn-Bochsler et al., 2014). Thus, marine mammals (e.g., seals, sea lions, dolphins, whales) are susceptible to morbidity and/or mortality events via trophic transfer from STX contaminated prey sources (Zingone and Enevoldsen, 2000). Ingestions of contaminated mollusks (e.g., clams, gastropods, mussels, oysters,) and puffer fish are the primary vector for human poisonings (Deeds et al., 2008b). Worldwide, health authorities have set stringent guidelines pertaining to PSP exposure and food contamination limits. The U.S. FDA and EPA jointly established an action limit of 80 µg STX-eq/100 g, using the official mouse bioassay method (MBA), for all marine and aquatic organisms (e.g., fin fish, crustaceans, mollusks) intended for human consumption per Appendix 5 of the FDA and EPA Safety Levels in Regulations

and Guidance, UCM252448 (U.S. FDA, 2011). Wild and domesticated birds and mammals were excluded from this list. However, fowl and animal consumers of contaminated prey can also be adversely affected by STX poisoning. Prudently, the Oregon Health Authority calculated Tolerable Daily Intake (TDI) guideline values for humans at 0.05 µg/kg/day and for dogs at 0.005 µg/kg /day, 1.0 µg/L for human drinking water, 10.0 µg/L for human recreational freshwater, and dog-specific recreational freshwater at 0.02 µg/L based on the European Food Safety Authority 2009 STX-eq data as reported by Farrer et al. (2015).

Globally, dinoflagellates comprise the main STX producers. Whilst, STX production is limited to freshwater cyanobacteria species, especially where anthropogenic nutrient enrichment occurs. Ballast water transport also introduces STX-producing, and other invasive, HAB species. Eutrophic conditions, inducing HAB formations, are especially problematic when copious amounts of toxins are subsequently released during subsidence. Akin to ATX-a, environmental conditions and warmer climates favor STX HAB organism proliferations, impacting the level of PSPs present, except in suppressive, alkaline environs. Bioaccumulation and metabolite stability (e.g., heat, polar solvent, biological pH) allow STX to remain detectable in contaminated organisms for long periods (Wiese et al., 2010). Landsberg et al. (2006) detected STX, after 12 months of captivity, in wild puffer fish (e.g., skin mucous, liver, muscle, ovaries) captured from the Florida Indian River Lagoon.

The major analytical methods employed to achieve STX detection and quantification include biological (e.g., MBA) and chemical (e.g., ELISA) assays (Codd et al., 2001), hyphenated chromatographic methods such as HPLC-UV/FD, LC-MS, LC-

MS/MS, LC-ion trap (IT)-MS (Harju et al., 2015a, 2015b), LC-TOF-MS (Fang et al., 2004). Although considered the official test method, the MBA lacks specificity and requires animals. Whereas ELISA (e.g., AOAC 2011.27) relies on antibody specificity to improve confirmatory results. Alternative AOAC official methods (e.g., EU-2005.06, US/Canada-2011.02) use HPLC-FD with pre- or post- column derivatization (Van De Riet et al., 2011). Among the chromatographic methods, high-resolution techniques (e.g., LC-TOF-MS and LC-IT-MS) are most specific. The U.S. EPA recently sanctioned a compilation of analytical methods for official use for selected biotoxins prepared by Campisano et al. (2017). Most often used is LC-MS/MS because of instrumentation availability and selectivity. Specialized HILIC HPLC column stationary phases significantly enhanced separation and specificity of LC-MS methods (Dell'Aversano et al., 2005; Foss et al., 2012a, 2012b). Most recently, Boundy et al. (2015) employed graphitized carbon SPE to improve specificity with LC-MS methods. Detection and quantitation limits, expressed in STX-eq values, vary by method choice and sample matrix. Other challenges include the sheer number of chemical variants (e.g., more than 30) and lack of standards to confirm detection and quantification as reviewed by Humpage et al. (2010). Resultant, no official LC-MS method currently exists for STX resulting from validation issues (e.g., sensitivity differences, matrix interferences, lack of applicable standards) as shown by Costa et al. (2009).

The transient neurological symptoms exhibited by the captive dolphins, evokes causative non-lethal ingestion of PSP contamination (i.e., STX) from epiphytic PSP producers (e.g., dinoflagellates) and/or other biota (e.g., gastropods, fish) present within the enclosures. Akin to ATX-a, proximity to the Everglades watershed, coupled with the

tidal flux from the Atlantic Ocean, warranted testing the cyanobacteria mats collected from the eutrophic captive dolphin lagoons for the presence of saxitoxin.

4.1.4 Brevetoxin-2 (PbTx-2)

Brevetoxin-2 (PbTx-2) belongs to a suite of analogous neurotoxic metabolites termed brevetoxins (PbTx). Primarily produced by the marine dinoflagellate, *Karenia brevis*, formerly *Gymnodinium breve* (Davis cf. Hansen et Moestrup), PbTx are most associated with HAB mortality events afflicting coastlines of the Gulf of Mexico (Flewelling et al., 2005; Fire et al., 2007; Twiner et al., 2012). Although, Bourdelais et al. (2002) implicated the phytoflagellate, *Chattonella cf. verruculosa* (Raphidophyceae), with the fish kills along the U.S. Eastern seaboard (e.g., Delaware) during the fall of 2000 (e.g., September, October). Previously, Khan et al. (1996) reported brevetoxin production (i.e., PbTx-2, PbTx-3) by *Chattonella antiqua*.

Along Florida's Gulf Coast, the HAB events associated with significant marine fauna (e.g., fish, birds, mammals) mortalities are referred to as "Florida red tides." Two distinct structural classes of PbTx exist, as the A form (Figure 4.4) and the B form (Figure 4.5), consisting of large, polycyclic, polyethers with molecular masses around 900 Daltons (Hua et al., 1996). Each class exhibits neurotoxicity with the parent structures, PbTx-1 (i.e., A) and PbTx-2 (i.e., B) being the most potent (Baden et al., 2005). Individual derivatives in both classes typically differ by common moiety interchanges at the terminal ether ring labeled "R" in the figures below (Figure 4.4, Figure 4.5). The PbTx B class includes two additionally modified analogues (e.g., PbTx-5, PbTx-6) having the confirmed structures (Figure 4.6). The unconfirmed structure of the B class PbTx-4 analog was not included.

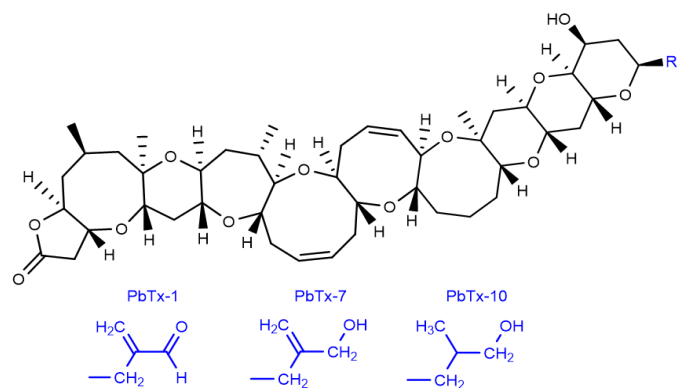


Figure 4.4 The molecular structures of the brevetoxin A class (PbTx-A) analogs denoted by R.

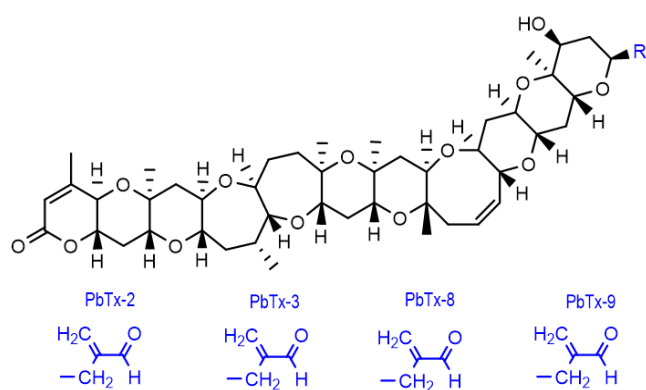


Figure 4.5 The confirmed molecular structures of the brevetoxin B class (PbTx-B) analogs denoted by R.

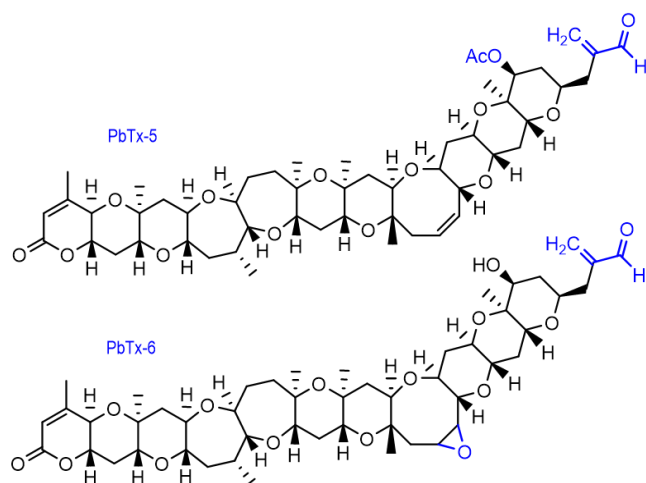


Figure 4.6 The molecular structures of brevetoxin B class analogs PbTx-5 and PbTx-6.

Of the PbTx-B class, PbTx-2 is the most potent and abundantly produced metabolite. As shown in Figure 4.7, PbTx-2 is a large, lipophilic, polycyclic polyether having a molecular mass of 895 g/mol.

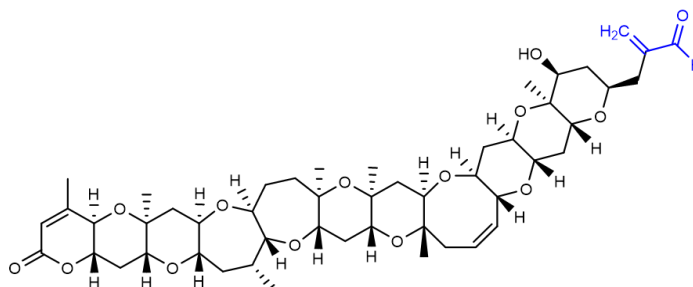


Figure 4.7 The molecular structure of brevetoxin-2 (PbTx-2).

Akin to ATX, brevetoxins activate voltage-gated sodium channels, however, indiscriminately and irreversibly, inducing STX-like neuron overstimulation primarily afflicting gastrointestinal, neurological and respiratory systems as reviewed by Baden et al. (2005). Additionally, being lipophilic, PbTx can cross the blood-brain barrier to effect a host of neurological conditions (e.g., temperature reversal, ataxia, incoordination). Symptoms reported by human cases describe similar, less severe PSP symptoms and not usually life threatening. On average, symptom onset occurs within 3-4 hours with seemingly full recovery within 2-3 days. Baden et al. (2005) provides an overview of the structure activity relationships observed within the PbTx analogs with respect to inhalation toxicities. Whilst, Pierce and Henry (2008) examined PbTx analog diversities and concentrations within various marine environmental (e.g., water, aerosols) and biological (e.g., shellfish) samples relevant to ecosystem stress causing marine animal (e.g., fish, mammals, birds, turtles) kills. Akin to PSPs, PbTx were first affiliated with consumption of contaminated lower trophic marine life, particularly, shellfish (e.g.,

gastropods, mollusks). Thus, collectively, PbTx earned the moniker “Neurological Shellfish Poisoning” (NSP) in humans. The term brevetoxicosis denotes PbTx poisoning in marine mammals and birds. Cocilova and Milton (2016) confirmed the PbTx neurotoxic pathway (i.e., PbTx-3) in freshwater turtle brain cells is analogous to mammals. Akin to STX, PbTx are quite stable for long periods. Unlike STX, a non-toxic, annotated derivative (i.e., brevenal), shown in Figure 4.8, exists that inhibits PbTx binding and has potential as a pulmonary therapeutic (Gold et al., 2013).

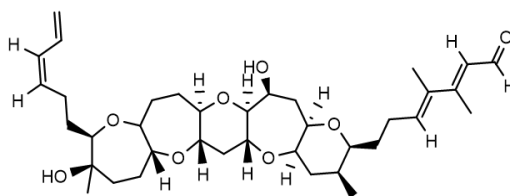


Figure 4.8 The molecular structure of brevenal.

The primary, culprit dinoflagellate, *K. brevis*, resides in the Gulf of Mexico, Caribbean Sea, and New Zealand coastal waters, but *K. brevis* can be transported globally via currents and shipping ballast water impacting areas as far away as the United Kingdom (Turner et al., 2015). Eutrophic conditions and El Niño weather patterns contribute to noxious *K. brevis* HAB blooms (Vargo et al., 2008; Vargo 2009). Trophic transfer (e.g., bioaccumulation, biomagnification) of PbTx parallels that of STX (Plakas et al., 2002; Naar et al., 2007; Perrault et al., 2016). More recently, PbTx have been shown to accumulate in marine vertebrates (e.g., fish, dolphins, manatee) as described by Fire et al. (2007). Major marine vertebrate die offs (e.g., birds, dolphins, fish, manatees) observed since the 1840s, have been attributed now to excessive *K. brevis* HAB events, occurring mostly seasonally, especially along the Florida Gulf Coast *K. brevis* HAB

(Flewelling et al., 2005; Twiner et al., 2011, 2012). Moreover, bloom declines create anoxic conditions further contributing to marine life mortalities (e.g., fish). Notably, HAB frequencies and persistence have increased in step with Florida's urban and agricultural development (Brand and Compton, 2007). Significant to the research herein are the reports of PbTx-producing epiphytes persisting on the seagrass, *Thalassia testudinum*, throughout Florida (Sotka et al., 2009; Hitchcock et al., 2012). The marine mammal zoological facility staff recently noted their captive bottlenose dolphins occasionally grazing the *T. testudinum* growing within their habitats. Additionally, morphological taxonomic evaluations detected the presence of epiphytic cyanobacteria (e.g., *Lyngbya* spp.) and microalgae (e.g., diatoms, dinoflagellates) growing on the collected reference specimens.

Along the Florida Gulf Coast, background levels of 1000-5000 *K. brevis* cells/L are common, thus the threshold for shellfish bed contamination was set at the upper limit. Ingestion of PbTx contaminated shellfish is the primary vector for humans, although reports of aerosolized NSPs exist (Backer et al., 2003). In Florida's wild bottlenose dolphin populations, the primary vectors of brevetoxicosis are feeding on PbTx contaminated marine life (e.g., fish, crustaceans) and inhaling aerosolized PbTx at the water surface (Naar et al., 2007; Fire et al., 2008; Twiner et al., 2012). Inhalation of aerosolized PbTx causes respiratory complications resembling asthma. As PbTx-2 is the major congener of the B class of brevetoxins, environmental detection methods often measure relative PbTx-2 concentrations in similar fashion to STX-eq values. However, living marine mammals (e.g., dolphins, manatees) can metabolize PbTx-2 into the PbTx-3 analogue, as previously shown in Figure 4.5, having similar neurotoxic potency

(Watkins et al., 2008). Thus, PbTx-3 is used for detecting PbTx levels in marine mammals (e.g., dolphins). Akin to STX, insufficient toxicological data and the numerous analogues prevent setting applicable human exposure limits. However, the U.S. FDA established a PbTx-2 action level of 80 µg PbTx-2/100 g of tissue for shellfish intended for human consumption using the official MBA method per the National Shellfish Sanitation Program Guide for the Control of Molluscan Shellfish, UCM2006754 (U.S. FDA, 2015) and the U.S. FDA UCM252448 Appendix 5 (U.S. FDA, 2011).

The major analytical methods used include the AOAC official methods for MBA and ELISA (Naar et al., 2002), and LC-MS/MS (Twiner et al., 2007). However, the in vivo MBA method lacks specificity while incurring costs, analysis time and ethical concerns. The increased specificity of ligand receptor binding analyses (e.g., ELISA, radiochemical) allows quantifiable detection of PbTx (e.g., PbTx-2, PbTx-3) in crude extracts, thus affording a more efficient, in vitro, method. Among the three methods, LC-MS/MS is highly specific but requires advanced instrumentation and laboratory skills. Moreover, method detection limits vary with method choice, sample type (e.g., extract purity, liquid, biological) and any matrix effects. For example, Twiner et al. (2012) demonstrated detection limit variability between the ELISA and LC-MS/MS methods for BTX-3 levels analyzed in biological samples collected from the wild bottlenose dolphin mortality events in Sarasota, FL. The LC-MS/MS method detection limit of 1.0 ng/mL proved more sensitive than the 2-8 ng/mL detection limit range observed for the ELISA method.

The transient neurological symptoms exhibited by the FL Keys captive bottlenose dolphins suggested the possibility of sub-lethal brevetoxicosis. The captive dolphins may

have inadvertently ingested potential PbTx-producing organisms, including epiphytes, associated with grazing the algae (e.g., *T. testudinum*, *Lyngbya* spp.) growing within their habitats. The FL Keys susceptibility to red tide HAB events also warranted testing the cyanobacteria, collected from the eutrophic dolphin enclosures, for the presence of PbTx-2. Additionally, PbTx-2 served as the positive control for the zebrafish larvae neurobehavioral studies used for the bioassay-guided investigation of the cyanobacteria detailed in Chapter Five.

4.1.5 Domoic Acid (DA)

Domoic acid (DA), is a native amino acid secondary metabolite derived from proline. Mimicking glutamic acid, DA acts as an irreversible excitatory neurotransmitter targeting glutamate receptors in the brain (Rao et al., 1988). Globally produced by marine pennate diatoms, the primary neurotoxic species is *Pseudo-nitzschia* spp. H. Peragallo (Bacillariaceae). Smida et al. (2014) reported increased awareness of domoic acid monitoring and more precise taxonomic characterization methods are leading to the discovery of additional *P.* species and diatom genera (e.g., *Nitzschia* spp., *Halamphora* spp.) with pending taxonomic revisions.

As shown in Figure 4.9, DA is a small, water-soluble, amino acid derivative of proline having a molecular mass of 311.33 grams/mole.

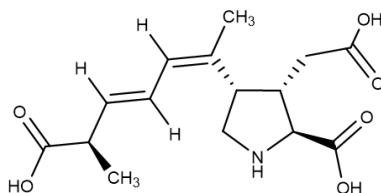


Figure 4.9 The molecular structure of domoic acid (DA).

Structurally and neurotoxicologically akin to kainic acid, also produced by marine microalgae, DA acts as an irreversible agonist to glutamate receptors including the kainite (KA) and α -amino-3-hydroxy-5-methyl-4-isoxazolepropionate (AMDP) subtypes (Cendes et al., 1995). Neurotoxicity results from overstimulation of Na^+ , K^+ , and Ca^{2+} channels, particularly targeting the hippocampus (e.g., short-term memory, learning), as studied in rats (Debonnel et al., 1989; Teitelbaum et al., 1990; Strain and Tasker 1991). A classic symptom observed with human DA poisonings includes transient to permanent short-term memory loss, giving rise to the moniker Amnesic Shellfish Poisoning (ASP).

To date, eleven DA isomers (A-H) have been isolated, although neurotoxic characterization data was limited to non-mammalian toxicological and KA binding affinity studies of isomers D-F (Hampson et al., 1992). Recently, Sawant et al. (2010, 2008) investigated the isomers for KA and AMPA binding affinities and seizure potential within rats to assess predictive structure-potency relationships. Despite being water-soluble and readily excreted via urine, DA can cross the blood-brain barrier to effect deleterious neurological damage to the hippocampal region (Teitelbaum et al., 1990). Manifestations of DA poisonings include motor incoordination, disorientation, copious mucosal secretions, seizures, and death in humans and marine mammals. Akin to BMAA, DA is quite stable, resisting thermal degradation, and has no known antidote.

Bates et al. (1989) and Wright et al. (1989) correlated the first reported cases of human ASP, in 1987, to consuming contaminated Canadian shellfish (e.g., Prince Edward Island blue mussels). Early toxicology studies in mice, via intraperitoneal injections, established a no observable adverse effect level (NOAEL) of 0.59 mg/kg-body weight (bw) and corresponding LD_{50} of 2.4 mg/kg-bw (Iverson et al., 1989). Neurotoxicity was

expressed, increasingly, as stereotypic behaviors from scratching, trembling, seizing and culminating in death. Although oral doses required 35-60 mg/kg-bw to induce similar outcomes, no LD₅₀ value is currently available. Likewise, simian (e.g., *Macaca fascicularis*) and rat DA studies, by Tryphonas et al. (1990 a-c) and Tryphonas and Iverson (1990), yielded analogous neurobehavioral and toxicological effects over comparable dose ranges and administration routes (e.g., intraperitoneal injection, oral), targeting the limbic system (e.g., hippocampus, amygdala) and thalamus.

The U.S. EPA regulates DA levels to not exceed 20 ppm in aquatic (e.g., fresh, marine) organisms intended for human consumption per the U.S. FDA UCM252448 Appendix 5 (U.S. FDA, 2011). Although, DA levels up to 30 ppm are permissible in Dungeness crab viscera. Birds and mammals are excluded from the list. Scholin et al. (2000), Sherman (2000), and Fire et al. (2010) affirmed marine and coastal vertebrate (e.g., whales, dolphins, birds, raccoons) DA poisonings led to acute mortality events along the western U.S. coastline. During blooms of *Pseudo-nitzschia* spp., DA pervasively contaminates prey foods at the lower trophic levels (e.g., plankton, krill, clams, crabs) through upper level consumers (e.g., sardines, anchovies, menhaden) contributing to massive DA poisoning among apex predators and scavengers (Costa and Garrido, 2004; Del Rio et al., 2010). Recently, Twiner et al. (2011) and Fire et al. (2009) observed increased DA production and frequency of DA poisoning events within aquatic habitats (e.g., estuarine, mangrove, aquaculture), symptomatic of increased anthropological activities. Similar occurrences, including newly identified DA producing *P.* species, have been reported in Northern Gulf of Mexico estuaries (Liefer et al., 2013; Del Rio et al., 2010) and globally. Worldwide reports include Mediterranean Sea

aquaculture (Smida et al., 2014), Malaysian mangroves (Tan et al., 2016), along Australian coasts (Ajani et al., 2017), and European Union waters (McNamee et al., 2016). Production and distribution of DA varies with nutrient loading from upwelling along western US and Spanish coasts (Trainer et al., 2010; Dittami et al., 2013), coastal eutrophication (Parsons and Dortch, 2002; Shanks et al., 2016), and seasonal conditions including temperature, photoperiod and solar flux (Downes-Tettmar et al., 2013; Thorel et al., 2014). Studies involving marine mammal DA poisonings improved analytical methodologies affording quantification of trace amounts (Barbaro et al., 2013; Frame and Lefebvre, 2013). Akin to STX, insufficient toxicological data and the numerous analogues prevent setting applicable human exposure limits.

He et al. (2010) provided a thorough review of the major analytical methods (e.g., AOAC PSP MBA, ELISA, HPLC-DAD/FD, LC-MS/MS) used to quantify DA contamination in a variety of shellfish (e.g., clams, mussels, scallops), microalgae, and seawater samples. The AOAC PSP official MBA 40 mg/g limit of detection exceeded the 20 mg/g regulatory limit, rendering the MBA method inapplicable. Thus, alternative methods were adopted and validated for screening by ELISA (e.g., AOAC 2006.02) and detection by HPLC-UV (e.g., AOAC 991.26, AOAC 2000b) as reviewed by Quilliam (2003). The European Union Harmonization Commission generated a DA Standard Operating Procedure adopted from the 1995 HPLC-UV method developed by Quilliam et al. (1995), requiring careful desalting of shellfish samples. Domoic acid, extracted from seawater using reversed-phase extraction disks, was accomplished by de la Iglesia et al. (2008) for subsequent chemical analysis by LC-MS/MS. Whilst, Mafra et al. (2009) achieved chemical detection (e.g., HPLC-UV, LC-MS) of trace amounts of domoic acid

from marine samples (e.g., seawater planktonic) without using derivatization techniques. Recently, Iglesia et al. (2011) developed and validated an ultra-fast (e.g., 2.5 min total run time) and sensitive (e.g., 0.06 mg/kg LOD, 0.2 mg/kg LOQ) LC-MS/MS method for AOAC screening of shellfish (e.g., clam, mussels, scallops). Although, any positive results still required confirmation via the official HPLC-UV method. Emergent technologies including polymeric molecular imprinting (Lin et al., 2016) and high-resolution MS using laser ablation (Beach et al., 2016) are being developed as alternatives to current AOAC methods. These promising techniques afford DA determinations with increased specificity, sensitivity and throughput for shellfish samples. Urgent needs for rapid, detection of DA poisoning in marine mammal (e.g., seals, sea lions) body fluids (e.g., blood, urine, feces, gastric and amniotic fluid) have driven improvements in ELISA (Seubert et al., 2014) and LC-MS/MS (Zhang et al., 2016) extraction techniques.

The frequency, distribution and co-occurrence of DA-producing organisms in the Gulf of Mexico, resulting in marine vertebrate (e.g., fish, mammals, birds) DA poisonings, along the Florida Gulf Coast, justified prudent examination of the cyanobacteria collected from the captive dolphin habitats for the presence of DA.

In summary, the literature evidence, reviewed herein, identified five plausible HAB-specific neurotoxins, having comparative analytical standards. Thus, the sampled neurotoxigenic cyanobacteria (i.e., *Lyngbya* spp.), and potential for epiphytic HAB microalgae (e.g., *Karenia brevis*, *Pseudo-nitzschia* spp.), growing within the captive dolphin habitats and subject to grazing by the captive dolphins, warranted chemical evaluation for the presence of the five known neurotoxins, ATX-a, BMAA, STX, PbTx-2

and DA. These potent neurotoxins are also most associated with relevant marine mammal intoxications observed in Florida marine ecosystems (e.g., Florida Bay, Sarasota Bay).

4.1.6 Investigation Targets

This chapter focused on the following two investigational targets to address the key question regarding the possible presence of known HAB-related neurotoxins posed in Chapter One:

4.1.6.1 Known *Lyngbya* spp. Neurotoxins

The first target to chemically investigate was the cyanobacteria *Lyngbya s.l.* taxa, persistently growing within the captive dolphin habitats, for the presence of neurotoxins (i.e., ATX-a, BMAA, STX) associated with this toxigenic, polyphyletic genus.

4.1.6.2 Known Marine HAB-Microalgae Neurotoxins

The second targeted investigation was to chemically explore these mixed assemblage cyanobacteria for the presence of the known neurotoxins, PbTx-2 and DA, produced, respectively, by *K. brevis*, *Pseudo-nitzschia* spp., and other HAB-related microalgae, perhaps epiphytic to the cyanobacteria mat.

4.2 Chemical Evaluation Methodologies

Dense mats of mixed cyanobacteria assemblages, including *Neolyngbya* spp., were sampled, as previously described in Chapter Two, from the captive dolphin enclosures, for taxonomic and chemical investigations at timepoints associated with HAB species blooms and declines when toxins, if present, would be at higher concentrations (e.g., summer, winter). Briefly, previously prepared cyanobacteria samples were lyophilized and homogenized prior to chemical analysis (see Chapter Two, section 2.2.1.4 Cyanobacteria Chemical Evaluation Samples). Subsamples (ca. 25 g) of the

lyophilized material, from each collection, were retained for separate extraction and detection of the selected neurotoxins of interest, according to previously published analytical methods. Method choice depended on neurotoxin specificity and compatibility with the facilities and equipment available at FIU (e.g., HPLC-UV/FD, LC-MS/MS), respective of the neurotoxin of interest (e.g., ATX-a, BMAA, STX, PbTx-2, DA).

Chemical investigations of BMAA and STX over three cyanobacteria collection timepoints were conducted at the FIU-AMSF. GreenWater Laboratories/CyanoLab was contracted to chemically evaluate the presence of ATX-a, PbTx-2, DA and STX from one sample of the cyanobacteria collected in January 2016. The aliquots from each collection point were analyzed for the respective neurotoxin as listed in Table 4.6.

Table 4.6 The cyanobacteria collections chemically screened for potential known neurotoxins.

Collection Date	Neurotoxin Analyzed				
	BMAA	STX	ATX-a	PbTx-2	DA
October 2014	FIU-AMSF	FIU-AMSF	NT	NT	NT
December 2014	FIU-AMSF	FIU-AMSF	NT	NT	NT
January 2015	NT	FIU-AMSF	NT	NT	NT
June 2015	FIU-AMSF	NT	NT	NT	NT
January 2016	NT	GWL	GWL	GWL	GWL
FIU-AMSF = Florida International University-Analytical Mass Spectrometry Facility, Miami, FL GWL = GreenWater Laboratories/CyanoLab, Palatka, FL NT = Not Tested					

Individual method details for each neurotoxin chemical analysis are summarized below, respective of analyte tested.

4.2.1 BMAA Analyses

4.2.1.1 BMAA Materials and Sample Preparation

Reference standards of L-BMAA hydrochloride and DL-2,4-DAB dihydrochloride were respectively purchased from Sigma Aldrich (St. Louis, MO, USA)

and Alfa Aesar (Ward Hill, MA, USA). LC-MS grade solvents (e.g., acetonitrile, water), reagent grade chloroform, concentrated hydrochloric acid (HCl), and concentrated formic acid (FA) were purchased from Fisher Scientific (Fair Lawn, NJ, USA).

Aliquots of approximately 5 grams (dry weight) were removed from each of the lyophilized, bulk cyanobacteria samples, stored at -20 °C, and homogenized using a mini food chopper, prior to extraction and mass spectrometric analysis for total BMAA. As shown in Table 4.7, the samples were chosen from the three seasonally different collection timepoints for the chemical evaluation for the presence of BMAA by MALDI-TOF-MS and/or LC-MS/MS. Specific sample preparation and chemical analyses were adapted from the previously published analytical methods for MALDI-TOF-MS (Esquenazi et al., 2008) and LC-MS/MS (Réveillon et al., 2014) using DL-2,4-DAB as an internal standard.

Table 4.7 The cyanobacteria samples chemically evaluated for the presence of BMAA.

Collection Date	Sample Identification	Sample Code	Analysis Method
October 2014	DP19OCT2014 BMAA XTN	SE-O14	MALDI-TOF-MS, LC-MS/MS
		SE-O14 LFM* (10 ppm)	LC-MS/MS
December 2014	DP24DEC2014 BMAA XTN	CMX-D14	MALDI-TOF-MS, LC-MS/MS
January 2015	DP19JAN2015 BMAA XTN	21A	LC-MS/MS
		21AS* (20 ppm)	LC-MS/MS
* Post-extraction, BMAA spiked replicate to confirm LC-MS/MS detection of BMAA. Note: The MALDI-TOF-MS and LC-MS/MS analyses were adapted from the previously published methods by Esquenazi et al. (2008) and Réveillon et al. (2014), respectively.			

4.2.1.2 BMAA Extraction and Mass Analysis Sample Preparation

From each timepoint sample, duplicate 2 g (± 0.1 g) aliquots were each extracted with 20 mL of 6 M aqueous HCl by acid hydrolysis for 24 hours at 110 °C (± 1 °C). Once

cooled, each crude extract underwent vacuum filtration (Whatman 42.5 mm 0 circles, 11 μm porosity) to remove residual particulates. Each filtrate was successively passed through 0.45 μm polyvinylidene fluoride (PVDF) syringe filters (VWR, Radnor, PA, USA) into 20 mL scintillation vials (VWR) for lyophilization. The dried extracts were reconstituted with 0.1% aqueous formic acid to 2 mL volumes while quantitatively transferring 1 mL aliquots into individual 1.5 mL amber glass vials (ThermoScientific, Rockwood, TN, USA). Each sample was partitioned with 500 μL of chloroform to dissolve remaining lipids and dried under nitrogen after removing the organic layer. After drying, each sample solution was reconstituted with LC-MS grade water and spiked with an isobaric internal standard (e.g., 25 ppm DAB) to a final 1 mL volume, comprising 1 ppm DAB, for mass analyses by MALDI-TOF-MS and LC-MS/MS. For the LC-MS/MS analysis, duplicate 300 μL aliquots were prepared by passing each solution through 0.2 μm polyvinylidene fluoride (PVDF) syringe filters (VWR) into a glass insert within a 1.5 mL amber glass vial (ThermoScientific). To confirm mass detection, a 20 ppm BMAA spiked lab fortified sample (21AS) was prepared from a 0.2 μm filtered aliquot of 200 μL taken from the JAN 2105 LC-MS/MS sample. In addition, an aqueous blank sample of 1 ppm DAB (BE5A IS) was prepared in 1 mL of LC-MS grade water. All samples were stored at $-20\text{ }^{\circ}\text{C}$ until analyzed at the FIU-AMSF.

4.2.1.3 BMAA MALDI-TOF-MS Analysis

A Bruker Autoflex III Smartbeam MALDI-TOF/TOF (Bruker Daltronics Inc., Billerica, MA, USA), operated in positive ion reflector mode, acquired spectral data for two of the hydrolyzed cyanobacteria samples (e.g., SE-O14, CMX-D14, CHCA matrix blank) using a BMAA selective method, previously developed and validated by the FIU-

AMSF (Conklin, 2015). Briefly, individual 1 μ L aliquots of each sample were deposited by the dried droplet technique, using 1 μ L of α -cyano-4-hydroxycinnamic acid (CHCA) matrix (i.e., blank), onto separate wells of the MALDI target plate (e.g., MTP384 ground steel). Data acquisition covered the 80-143 m/z mass range. Monitoring of the protonated isobaric molecular ion, $[M+H]^+$, m/z 119.0815 was performed. Processing of raw spectral data by the Bruker Daltronics flexAnalysis software (version 3.4, build 70) generated mass specific peak data (e.g., height, area S/N, resolution), exported as a Microsoft Excel spreadsheet, and analyte-specific (e.g., BMAA) chromatograms for each sample analyzed. The full FIU-AMSF MALDI-TOF-MS Sample Analysis Report is attached to the Appendix of this dissertation.

4.2.1.4 BMAA LC-MS/MS Analysis

One LC-MS/MS prepared extraction sample, spiked with 1 ppm DAB IS, from the three timepoints (i.e., SE-O14, CMX-D14, 21A), the 20 ppm BMAA spiked LC-MS/MS prepared sample (21AS), spiked with 1 ppm DAB IS, and the 1 ppm DAB blank sample (BE5A IS) were submitted to the FIU-AMSF for mass analysis. The FIU-AMSF prepared an additional 10 ppm BMAA lab fortified matrix (LFM) sample from the SE-O14 sample. The HILIC LC-MS/MS analytical method previously developed by Réveillon et al. (2014) was adapted for the chromatographic equipment and mass spectrometer at the FIU-AMSF (Conklin, 2015). Briefly, a Shimadzu Prominence LC-20AD Ultra-Fast Liquid Chromatograph (Shimadzu Corporation, Kyoto, Japan) achieved chromatographic separation using a Kinetix HILIC (Phenomenex, Torrance, CA, USA) column (100 x 4.6 mm, 2.6 μ m) set at 40 °C. A binary mobile phase system consisted of (A) 0.1% aqueous formic acid in LC-MS grade water and (B) 0.1% formic acid in LC-

MS grade acetonitrile. Elution of 20 μ L injections occurred via a 10-min step gradient at 0.5 mL/min flow rate from 30% A held for 0.5 min, ramped to 95% A in 5 min, held at 95% A for 0.75 min, ramped to 5% A in 0.25 min, held at 5% A for 1.5 min to flush the column, then ramped back to 30% A in 1.5 min and re-equilibrated at 30% A for 1.75 min.

Mass analysis of BMAA employed the AB Sciex (AB Sciex LLC, Framingham, MA, USA) QTRAP 5500 Triple-Quadrupole mass spectrometer, equipped with a Turbospray ESI ion source, tuned to detect the $[M+H]^+$ ion (m/z 119.0) and fragmentation product ions (m/z 76.1, 87.9) by Selective Ion Monitoring (SIM) and Multiple Reaction Monitoring (MRM), respectively as described by Réveillon et al. (2014). Previous interference from the isobaric internal standard, DAB IS, determined the choice of fragment ions monitored. As such, MRM detected the DAB IS transitions of m/z 119.005 $>$ 101.200 and 119.005 $>$ 56.300. Sample analysis was performed in conjunction with the method validation of another BMAA related study (Conklin, 2015) using their previously prepared calibration standards. The full FIU AMSF Sample Analysis Report was attached to the Appendix.

4.2.2 STX Analysis

4.2.2.1 STX Materials and Sample Preparation

Reference standards of saxitoxin were purchased from Abraxis, Inc. (Warminster, PA, USA). LC-MS grade solvents (e.g., acetonitrile, water), and concentrated acetic acid (HOAc) were purchased from Fisher Scientific (Fair Lawn, NJ, USA).

Aliquots of approximately 5 grams (dry weight) were removed from each of the lyophilized, -20 $^{\circ}$ C stored, cyanobacteria samples and homogenized using a mini food

chopper, prior to extraction and mass spectrometric analysis for STX. As shown in Table 4.8, the samples were chosen from the three seasonally different collection timepoints for the chemical evaluation for the presence of STX by LC-MS/MS. Specific sample preparation, extraction and analytical methodology were adapted from the protocol detailed by Foss et al. (2012b), for STX analysis of the freshwater cyanobacteria, *Lyngbya wollei*.

Table 4.8 The cyanobacteria samples chemically assessed for the presence of STX.

Collection Date	Sample Identification	Sample Code
October 2014	DP19OCT2014 STX XTN	SE-O14
December 2014	DP24DEC2014 STX XTN	CMX-D14
January 2015	DP19JAN2015 STX XTN	21A
	DP19JAN2015 STX-SPIKED*	21AS
* Post-extraction, 20ppm STX spiked replicate to confirm LC-MS/MS detection of STX.		

4.2.2.2 STX extraction and Mass Analysis Sample Preparation

In triplicate, 1 g (± 0.1 g) aliquots were each extracted with 50 mL of 0.1 M aqueous HOAc, by boiling (c.a. 100 °C) in a beaker on a hot plate for at least 5 minutes, with constant stirring. Once cooled, the total volume of each crude extract was replenished to 50 mL with 0.1 M HOAc. Triplicate, 1 mL aliquots, from each extraction sample, were prepared for MS analysis, by passing the extract solution sequentially through 0.45 μ m and 0.20 μ m polyvinylidene fluoride (PVDF) syringe filters (VWR) into 1.5 mL glass vials (Fisher Scientific). Each aliquot was dried under nitrogen, at room temperature, and reconstituted with 0.003 M HCl, prepared with LC-MS grade water, to a final 20 mg/mL concentration for LC-MS/MS analysis. A fourth aliquot was similarly prepared from the January 2015 timepoint extraction solution. This reconstituted aliquot

was then spiked with 20 ppm STX standard (21AS) for use as a post-extraction LFM to confirm STX detection above the 10 µg/mL anticipated LC-MS/MS method LOD.

4.2.2.3 STX LC-MS/MS Analysis

One replicate LC-MS/MS prepared STX extraction aliquot, from each sampled timepoint (i.e., SE-O14, CMX-D14, 21A), and the 20 ppm LFM prepared aliquot (21AS), were submitted to the FIU-AMSF for qualitative mass analysis. The Foss et al. (2012) analytical method was adapted for the Shimadzu Prominence LC-20AD Ultra-Fast Liquid Chromatograph coupled to the AB Sciex QTRAP 5500 Triple-Quadrupole mass spectrometer, equipped with a Turbospray ESI ion source. Briefly, the previously described Kinetix HILIC column, maintained at 40 °C, afforded chromatographic separation via a binary mobile phase step gradient system. Mobile phases consisted of (A) LC-MS grade (A) aqueous buffer containing 2 mM formic acid and 3.6 mM ammonium formate and (B) 95:5 (v/v) LC-MS grade acetonitrile and LC-MS grade aqueous buffer. Elution of 20µL injections followed a 10-min step gradient at 0.5 mL/min flow rate from 10% A held for 0.5 min, ramped to 90% A in 5 min, held at 90% A for 0.75 min, ramped to 10% A in 0.25 min, held at 10% A for 1.5 min to flush the column, then ramped back to 90% A in 1.5 min to re-equilibrate the column at 90% A for 1.75 min. Mass detection utilized the STX [M+H]⁺ ion (m/z 300.046) and fragmentation product ion transitions (m/z 282.100, 204.100) by SIM and MRM, respectively. Each extract was qualitatively analyzed for the detection of STX. Thus, only positive results would warrant further quantitative analysis (e.g., calibration data, LOD, LOQ). The full FIU-AMSF Sample Analysis Report is attached in the Appendix.

4.2.3 Commercial Chemical Evaluations

An aliquot of approximately 25 grams (dry weight) was removed from the bulk, lyophilized, -20 °C stored, cyanobacteria collected January 2016. This sample was overnight shipped, frozen, to GreenWater Laboratories/CyanoLab (Palatka, FL, USA) for chemical evaluations for the presence of ATX-a, PbTx-2, DA, and STX. The full report provided by the commercial marine biotoxin laboratory is attached in the Appendix of this chapter and describes all the protocols used for subsample preparations, detection analysis, and results obtained for each of the neurotoxin analytes.

Briefly, the bulk lyophilized sample was homogenized using a coffee grinder. Appropriate subsamples were removed to prepare duplicate samples, including an LFM sample, for each neurotoxin analyte. For mass analyses, a lab fortified blank (LFB) was also prepared using the neurotoxin of interest. The analytes of ATX-a and DA were analyzed using previously developed, neurotoxin-specific LC-MS/MS methods, whilst PbTx-2 and STX were analyzed using commercially available, neurotoxin-selective ELISA kits (Abraxis Inc., Warminster, PA, USA).

4.2.3.1 ATX-a Sample Preparation and LC-MS/MS Analysis

Duplicate 100 mg (± 5 mg) samples were extracted with 75% acidified methanol solution. One of the samples was spiked with ATX-a as a 100 ng/g ATX-a LFM sample. Both samples were sonicated for 25 minutes, using a water bath, then centrifuged for 10 minutes at 3000 rpm. For each sample, the supernatant was collected, and the remaining pellet extracted again with the 75% acidified methanol solution. The resultant supernatants were respectively pooled, for each sample. The methanol was removed using heat and nitrogen gas. Sample clean-up employed Strata-X (Phenomenex,

Torrence, CA, USA) solid phase extraction (SPE), followed by 0.45 μm PVDF filtration. A sample concentration of 0.1 g/mL was prepared for LC-MS/MS analysis for the ATX-a $[\text{M}+\text{H}]^+$ ion (m/z 166) and fragmentation product ions (m/z 43.5, 91.5, 107.3, 131.1). The 10 ng/g method limit of detection was based on the current instrument sensitivity and the LFM.

4.2.3.2 DA Sample Preparation and LC-MS/MS Analysis

Duplicate 100 mg (± 5 mg) samples were extracted twice with 80% methanol solution. One of the samples was spiked with DA standard as a 500 ng/g LFM. Both samples were sonicated for 25 minutes using a water bath then centrifuged for 10 minutes at 3000 rpm. For each sample, the respectively collected supernatants were pooled and the methanol solution was removed. Sample clean-up employed Strata-X SPE followed by 0.45 μm PVDF filtration. A sample concentration of 0.1 g/mL was prepared for LC-MS/MS analysis for the DA $[\text{M}+\text{H}]^+$ ion (m/z 312) and fragmentation product ions (m/z 145.5, 220.3, 248.5, 266.2) with a 50 ng/g method limit of detection (e.g., LFM, instrument sensitivity)

4.2.3.3 STX Sample Preparation and ELISA Analysis

Duplicate 500 mg (± 5 mg) samples were used for STX extraction. One sample was spiked with STX standard as a 100 ng/g LFM sample. Each sample was extracted with 7.5 mL of 0.1 M HOAc solution and placed in a boiling water bath for 5 minutes. The samples were cooled and centrifuged. For each sample, the supernatant was retained, and the remaining pellet rinsed with 2.5 mL 0.1 M HOAc solution. The resultant supernatant for each sample was pooled, respectively. Sample clean-up employed Strata-X SPE followed by 0.45 μm PVDF filtration. The LFB sample was also prepared using

0.2 ng STX/mL LFM. Sample aliquots of 10 mg/mL, in kit diluent, were analyzed using a Saxitoxin ELISA kit (Abraxis, Inc.). The 5 ng/g detection and quantification limits were based on the LFM dilution factors and 0.05 µg/L kit sensitivity.

4.2.3.4 PbTx-2 Sample Preparation and ELISA Analysis

Duplicate 500 mg (± 5 mg) samples were extracted twice with an 80% methanol solution. One of the samples was spiked with PbTx-2 as a 1 µg/g PbTx-2 (e.g., dry weight) LFM. Both samples were sonicated for 25 minutes using a water bath then centrifuged for 10 minutes at 3000 rpm. For each extracted sample, the resultant supernatants were, respectively pooled, and the methanol removed. Sample clean-up employed Strata-X SPE followed by 0.45 µm PVDF filtration. An LFB sample was also prepared using as 1.0 ng PbTx-2/mL LFM. Sample aliquots of 1 mg/mL in 5% methanol were analyzed using a Brevetoxin (NSP) ELISA kit (Abraxis Inc., Warminster, PA, USA). The 50 ng/g detection and quantification limits were based on the LFM dilution factors and 50 µg/L kit sensitivity. The calibration curve was prepared from a PbTx-3 standard solution (e.g., 5% MeOH), while PbTx-2 was used to prepare the quality control samples.

4.3 Results and Discussion

4.3.1 BMAA Results

Analysis by MALDI-TOF-MS conducted at the FIU-AMSF, did not detect BMAA as $[M+H]^+$ ($m/z = 119.0815$ m/z) in either of the two 2014 cyanobacteria sample extracts (e.g., SE-O14, CMX-D14) above the S/N of 3 or below the calibrants' mass errors of ≤ 3 ppm. Notably, mass spectral data revealed < 3 S/N ion peaks, at $m/z =$

119.0566 (mass error 209.1 ppm) and 119.0384 (mass error 361.9 ppm), respectively, for the SE-O14 and CMX-D14 extracts.

Moreover, BMAA was not detected by the LC-MS/MS analysis acquired at the FIU-AMSF in the SE-O14, CMX-D14, 21A extracts. The LC-MS/MS method required the use of 1 ppm DAB internal standard (IS), BMAA calibration standards (e.g., 0.25-50 ppm), 10 ppm BMAA quality control samples (e.g., CS4) and the LFM and 21AS samples, respectively spiked with BMAA at 10 ppm and 20 ppm. The 0.25 ppm calibration standard defined the limit of detection. Due to isobaric interference from DAB IS, the BMAA multiple reaction monitoring (MRM) m/z transitions were set at 119>76 (main) and 119>88 (secondary), whilst the main DAB IS MRM was set at 119>101. The 10 ppm and 20 ppm BMAA spiked samples showed respective recoveries of 89% and 70% for SE-O14 LFM and 21AS when compared to the 10 ppm CS4 calibration standard.

4.3.2 STX Results

Analysis by LC-MS/MS, conducted at the FIU-AMSF, did not detect STX in any of the cyanobacteria samples extracts (e.g., SE-O14, CMX-D14, 21A) when qualitatively compared to a 20 ppm STX spiked extract (21AS) and blank sample (e.g., LC-MS Water). Positive identification in the spiked extract by LC-MS/MS employed the STX MRM m/z transitions at (300>204) and (300>282). The qualitative absence of STX in the three un-spiked extract samples warranted no further analytical quantitation (e.g., calibration standards, detection limits).

Analysis by STX-selective ELISA, conducted at GreenWater Laboratories/CyanoLab, did not detect STX in the respective subsample extract derived

from the January 2016 cyanobacteria collection. A sample concentration of 10 mg/mL was prepared with the STX ELISA (Abraxis, Inc.) kit diluent for analysis at 10 mg/mL sample concentration with a detection/quantification limit of 5 ng/g based on the dilution factors and 0.05 µg/L kit sensitivity. Pre-extraction and post-extraction results of the LFM resulted were 55% and 70%, respectively. The low LFM pre-extraction result suggested the possible loss of STX to the matrix and/or destruction due to the extraction process. Thus, STX was not observed in any of the cyanobacteria samples using either LC-MS/MS or ELISA.

4.3.3 ATX-a Results

A sample concentration of 0.1 g/mL was prepared for LC-MS/MS analysis for the ATX-a [M+H]⁺ ion (m/z 166) and fragmentation product ions (m/z 43.5, 91.5, 107.3, 131.1). The 10 ng/g method limit of detection was based on the current instrument sensitivity and the LFM. Analysis by LC-MS/MS of the January 2016 cyanobacteria sample, conducted by GreenWater Laboratories/CyanoLab, did not detect the presence of ATX-a above the 10 ng/g detection limit defined by the LFM sample.

4.3.4 DA Results

A sample concentration of 0.1 g/mL was prepared from the respective January 2016 cyanobacteria subsample for LC-MS/MS analysis of the DA [M+H]⁺ ion (m/z 312) and fragmentation product ions (m/z 145.5, 220.3, 248.5, 266.2). The results, obtained by GreenWater Laboratories/CyanoLab, did not detect the presence of DA above the 50 ng/g detection limit established from the LFM sample and instrument sensitivity.

4.3.5 PbTx-2 Results

Using an Abraxis PbTx-selective ELISA kit, GreenWater Laboratories/CyanoLab did not detect PbTx (e.g., PbTx-2, PbTx-3) in the respective January 2016 cyanobacteria extract. Pre-extraction and post-extraction results for the PbTx-2 spiked LFM sample were 64% and 110%, respectively. The lower LFM pre-extraction result suggested possible loss of PbTx-2 to the matrix and/or destruction due to the extraction process.

4.3.6 Results Summary

As previously described in Chapter Two, the green macroalgae, *Ulva* spp., and cyanobacteria, morphologically identified as the neurotoxicogenic, polyphyletic *Lyngbya s.l.*, including *Neolyngbya* spp., were observed growing abundantly within the enclosures of the marine mammal zoological facility located in the Florida Keys. Moreover, the facility staff observed their captive bottlenose dolphins intermittently grazing the *Ulva* spp. and, important to this study, potential HAB-related cyanobacteria (e.g., *Lyngbya s.l.*, *Neolyngbya* sp.). Occasionally, after these algal ingestions, the captive dolphins exhibited apparent intoxications of seemingly neurotoxicity (e.g., ataxia, uncoordinated swimming, blepharospasms). Each apparent intoxication case was addressed and typically resolved within several days by the facility's veterinarian. Numerous neurotoxic secondary metabolites have been isolated from freshwater, estuarine and marine *Lyngbya* spp. including ATX, BMAA and STX. The cyanobacteria were sampled, seasonally during the study, for taxonomic characterization and comparative chemical analysis to determine the presence of ATX-a, BMAA and STX using conventional analytical methods (e.g., ELISA, LC-MS/MS, MALDI-TOF-MS). The known neurotoxin-producing HAB-related microalgae, *Karenia brevis* (i.e., PbTx) and *Pseudo-nitzschia* spp. (i.e., DA) were not

conclusively identified among the epiphytes observed during the algal (e.g., macroalgae, cyanobacteria) morphology examinations. However, these HAB organisms are frequently associated with wild bottlenose dolphin intoxications and mortalities along the Florida Gulf Coast. Thus, one cyanobacteria sample was also chemically evaluated for the known HAB neurotoxins, PbTx-2 and DA.

Each neurotoxin was chemically analyzed using an adapted, previously published neurotoxin-specific method (i.e., mass spectrometry, ELISA) from an applicably extracted aliquot of the relevant cyanobacteria collections. For chemical investigations of BMAA and STX, conducted at FIU, two seasonally representative (e.g., fall, winter) cyanobacteria collection timepoints were chosen, after the captive dolphins exhibited intoxication events over the summer of 2014. Specifically, the October 2014 cyanobacteria sample (SE-O14) was known to be ingested by one of the afflicted captive bottlenose dolphins and represented the near maximum of potential HAB-neurotoxin presence. The January 2015 cyanobacteria sample (21A) represented the near minimum of HAB-neurotoxin potential. Whilst, the December 2014 cyanobacteria collection (CMX-D14) consisted of all the cyanobacteria the facility staff had collected from January through August 2014; the year multiple intoxication events were observed for the captive dolphins. These three cyanobacteria samples were chemically investigated at FIU for the presence of BMAA and STX using mass spectrometry (e.g., MALDI-TOF-MS, LC-MS/MS). The LC-MS/MS method served to confirm the absence of BMAA in the extracted samples evaluated by MALDI-TOF-MS. Whilst, the January 2016 cyanobacteria sample, was chemically evaluated for the presence of ATX-a, PbTX-2, DA and STX by a commercial analytical laboratory specializing in biotoxins. The negative

ELISA results further confirmed the absence of STX as observed in extracts analyzed using the FIU-ASMF LC-MS/MS method.

The results of this chapter provided a snapshot answer to the key question originally presented in Chapter One regarding the potential presence of HAB-related neurotoxin(s) present in collected samples of cyanobacteria and possibly associated with algal ingestions by the captive dolphins. Specifically, cyanobacteria samples were chemically evaluated for the potential presence of the neurotoxic cyanotoxins ATX-a, BMAA, and STX and the marine microalgae neurotoxins, PbTx-2 and DA. As summarized in Table 4.9, none of the known neurotoxins were detected above the respective method limit of detection, where applicable, in any of the cyanobacteria samples collected from within the captive dolphin enclosures. However, a recommendation to monitor for the presence of the HAB-related neurotoxins during any future captive dolphin algal ingestion related intoxication events was proposed to the marine mammal zoological facility staff.

Table 4.9 Summary results for cyanobacteria samples chemically screened for known neurotoxins.

Collection Date	Sample Code	Neurotoxin Analyzed	Detection Method	LOD (ng/g)	Analytical Results (ppm)	Analytical Test Facility
January 2016	DP16	ATX-a	LC-MS/MS	10	ND	GreenWater Laboratories /CyanoLab
		PbTx-2	ELISA	50	ND	
		DA	LC-MS/MS	50	ND	
		STX	ELISA	5	ND	
January 2015	21A-LFM (20 ppm)	STX	LC-MS/MS	NA	6.0	FIU-AMSF
	21A				ND	
October 2014	SE-O14				ND	
December 2014 ^a	CMX-D14				ND	
January 2015	BE5A IS	BMAA	LC-MS/MS ^b	0.25	ND	FIU-AMSF
	21AS (20 ppm)				19.8	
	21A				ND	
October 2014	SE-O14 LFM (10 ppm)		LC-MS/MS ^b		8.9	
	SE-O14		LC-MS/MS ^b		ND	
			MALDI-TOF-MS		≥ 3 S/N ^c	
December 2014 ^a	CMX-D14		LC-MS/MS ^b		0.25	
		MALDI-TOF-MS	≥ 3 S/N ^c	ND		

^a DEC2014 represents the combined biomass collected by DP staff during 2014 except for OCT2014.
^b Samples were spiked with internal standard (IS) DAB to 1 ppm prior to LC-MS/MS analysis.
^c The MALDI-TOF-MS LOD was expressed as a Signal to Noise ratio (S/N) greater than or equal to 3 and mass error less than 3 ppm based on calibrant mass errors.

LFM = Laboratory Fortified Matrix (analyte spiked)
LOD = Method Limit of Detection
ND = Not Detected above Method LOD
NA = Not Available/Applicable
FIU-AMSF = Florida International University-Advanced Mass Spectrometry Facility

4.4 Conclusions

To conclude, none of the known neurotoxins, specifically ATX-a, BMAA, PbTx-2, DA, and STX, were detected above the limit of detection for their respective methods in any

of the cyanobacteria samples chemically evaluated. Thus, the dissertation research focus returned to chemically investigating the cyanobacteria for other potentially neurotoxic secondary metabolites, known or otherwise uncharacterized, as guided by the zebrafish embryo-larvae neurobehavioral model of toxicity. Results are detailed in the next two chapters, Chapter Five and Chapter Six.

Despite the absence of known neurotoxins, the potential remains for future HAB related events to occur as favorable growing conditions arise within the captive dolphin enclosures. As such, a prudent recommendation advised the marine mammal zoological facility staff to continue monitoring dolphin algae ingestions, particularly cyanobacteria, and any subsequent symptoms of intoxication to allow for more-timely chemical evaluations of HAB-related neurotoxins. Likewise, as no definitive correlation could statistically link algal and cyanobacteria ingestions to intoxication episodes as described previously in Chapter Three of this dissertation, the staff were cautioned to be cognizant for HAB contaminated dietary fish supplies, especially those derived from the Gulf of Mexico (e.g., menhaden), as a further step to identify the intoxication source.

4.5 Acknowledgments

Cesar Ramirez and Mario Fernandez-Gomez of the FIU-AMSF are greatly appreciated for their help with the BMAA and STX by LC-MS/MS method development and analyses. Gratitude is given to John P. Berry for providing access to the FIU-AMSF service for this unfunded project. Mark T. Aubel, Amanda Foss, and Kamil Ceslik, of GreenWater Laboratories/CyanoLab, are especially thanked for providing rapid ELISA (i.e., PbTx-2, STX) and LC-MS/MS (i.e., ANTX-a, DA) analyses. Sincere appreciation is extended to the marine mammal zoological facility staff, especially Dr. Johanna Mejia-

Fava and Holli Eskelinen, for providing this research project and their assistance with all the cyanobacteria collections.

4.6 References

- Aguilera, A., Berrendero Gómez, E., Kastovsky, J., Echenique, R.O., Salerno, G.L., 2018. The polyphasic analysis of two native *Raphidiopsis* isolates supports the unification of the genera *Raphidiopsis* and *Cylindrospermopsis* (Nostocales, Cyanobacteria). *Phycologia* 57(2), 130-146.
- Ajani, P., Harwood, D.T., Murray, S.A., 2017. Recent trend in marine phycotoxins from Australian coastal waters. *Mar. Drugs* 15(2), 33. doi:10.3390/md15020033
- Al-Sammak, M.A., Hoagland, K.D., Snow, D.D., Cassada, D., 2013. Methods for simultaneous detection of the cyanotoxins BMAA, DABA, and anatoxin-a in environmental samples. *Toxicon* 76, 316-325. doi:10.1016/j.toxicon.2013.10.015
- Al-Sammak, M.A., Hoagland, K.D., Cassada, D. Snow, D.D., 2014. Co-occurrence of the cyanotoxins BMAA, DABA and anatoxin-a in Nebraska reservoirs, fish, and aquatic plants. *Toxins* 6(2), 488-508. doi:10.3390/toxins6020488
- Anderson, D.M., Kulis, D.M., Sullivan, J.J., Hall, S., Lee, C., 1990. Dynamics and physiology of saxitoxin production by the dinoflagellates *Alexandrium* spp. *Mar. Biol.* 104, 511–524.
- Anderson, D.M., Hoagland, P., Kaoru, Y., White, A.W., 2000. Estimated annual economic impacts from harmful algal blooms (HABs) in the United States (No. WHOI-2000-11). NOAA Norman OK National Severe Storms Lab.
- Anderson, D.M., 2004. Prevention, control and mitigation of harmful algal blooms: multiple approaches to HAB management. *Harmful Algae Management and Mitigation* 123-130.
- Andersson, M., Karlsson, O., Bergström, U., Brittebo, E.B., Brandt, I., 2013. Maternal transfer of the cyanobacterial neurotoxin β -N-methylamino-L-alanine (BMAA) via milk to suckling offspring. *PLoS One* 8(10), e78133. doi:10.1371/journal.pone.0078133
- Andersson, M., 2015. Cellular transport and secretion of the cyanobacterial neurotoxin BMAA into milk and egg: Implications for developmental neurotoxicity (Doctoral dissertation, Acta Universitatis Upsaliensis).
- Anon, A.O.A.C., 2005. Official method 959.08. Paralytic shellfish poison. Biological method. Final action. In: Truckses, M. W. (Ed.). *Natural Toxins* 18th ed., chapter 49, 79-80. AOAC International, Gaithersburg, MD, USA.

Anon., A.O.A.C., 2005. Official method 2005.06 Quantitative determination of paralytic shellfish poisoning toxins in shellfish using pre-chromatographic oxidation and liquid chromatography with fluorescence detection. AOAC International, Gaithersburg, MD, USA.

Anon, A.O.A.C., 2011. Official method 2011.02 Determination of paralytic shellfish poisoning toxins in mussels, clams, oysters and Scallops. Post-column Oxidation Method (PCOX). First Action 2011 AOAC International, Gaithersburg, MD, USA.

Anon, A.O.A.C., 2011. Official Method 2011.27. Paralytic Shellfish Toxins (PSTs) in Shellfish, Receptor Binding Assay. AOAC International, Gaithersburg, MD, USA.

Aráoz, R., Nghiê, H.-O., Rippka, R. Palibroda, N., de Marsac, N.T., Herdman, M., 2005. Neurotoxins in axenic Oscillatorian cyanobacteria: Coexistence of anatoxin-a and homoanatoxin-a determined by ligand-binding assay and GC/MS. *Microbiology* 151, 1263-1273. doi:10.1099/mic.0.27660-0

Aráoz, R., Guérineau, V., Rippka, R., Palibroda, N., Herdman, M., Laprevote, O., Von Döhren, H., de Marsac, N.T., Erhard, M., 2008. MALDI-TOF-MS detection of the low molecular weight neurotoxins anatoxin-a and homoanatoxin-a on lyophilized and fresh filaments of axenic *Oscillatoria* strains. *Toxicon* 51(7), 1308-1315. doi:10.1016/j.toxicon.2008.02.018

Aráoz, R., Molgó, J., de Marsac, N.T., 2010. Neurotoxic cyanobacterial toxins. *Toxicon* 56(5), 813-828. doi:10.1016/j.toxicon.2009.07.036

Backer, L.C., Fleming, L.E., Rowan, A., Cheng, Y.S., Benson, J., Pierce, R.H., Zaias, J., Bean, J., Bossart, G.D., Johnson, D., Quimbo, R., 2003. Recreational exposure to aerosolized brevetoxins during Florida red tide events. *Harmful Algae* 2(1), 19-28. doi:10.1016/S1568-9883(03)00005-2

Backer, L.C., Landsberg, J.H., Miller, M., Keel, K., Taylor, T. K., 2013. Canine cyanotoxin poisonings in the United States (1920s–2012): Review of suspected and confirmed cases from three data sources. *Toxins* 5(9),1597-1628. doi:10.3390/toxins5091597

Baden, D.G., Bourdelais, A.J., Jacocks, H., Michelliza, S., Naar, J., 2005. Natural and derivative brevetoxins: Historical background, multiplicity, and effects. *Environ. Health Persp.* 113(5), 621-625. doi:10.1289/ehp.7499

Banack, S.A., Cox, P.A., 2003. Distribution of the neurotoxic nonprotein amino acid BMAA in *Cycas micronesica*. *Bot. J. Linn. Soc.* 143(2), 165-168. doi:10.1046/j.1095-8339.2003.00217.x

- Banack, S.A., Murch, S.J., Cox, P.A., 2006. Neurotoxic flying foxes as dietary items for the Chamorro people, Marianas Islands. *J. Ethnopharmacol.* 106(1), 97-104. doi:10.1016/j.jep.2005.12.032
- Banack, S.A., Metcalf, J.S., Bradley, W.G., Cox, P.A., 2014. Detection of cyanobacterial neurotoxin β -N-methylamino-l-alanine within shellfish in the diet of an ALS patient in Florida. *Toxicon* 90, 167-173. doi:10.1016/j.toxicon.2014.07.018
- Barbaro, E., Zangrando, R., Rossi, S., Cairns, W.R.L., Piazza, R., Corami, F., Barbante, C., Gambaro, A., 2013. Domoic acid at trace levels in lagoon waters: assessment of a method using internal standard quantification. *Anal. Bioanal. Chem.* 405(28), 9113-9123. doi:10.1007/s00216-013-7348-5
- Bates, S.S., Bird, C.J., Freitas, A.D., Foxall, R., Gilgan, M., Hanic, L. A., Johnson, G.R., McCulloch, A.W., Odense, P., Pocklington, R., Quilliam, M.A., Sim, P.G., Smith, J.C., Subba Rao, D.V., Todd, E.C.D., Walter, J.A., Wright, J.L.C., 1989. Pennate diatom *Nitzschia pungens* as the primary source of domoic acid, a toxin in shellfish from eastern Prince Edward Island, Canada. *Can. J. Fish Aquat. Sci.* 46(7), 1203-1215. doi:10.1139/f89-156
- Beach, D.G., Walsh, C.M., Cantrell, P., Rourke, W., O'Brien, S., Reeves, K., McCarron, P., 2016. Laser ablation electrospray ionization high-resolution mass spectrometry for regulatory screening of domoic acid in shellfish. *Rapid Commun. Mass Sp.* 30(22), 2379-2387. doi:10.1002/rcm.7725
- Boundy, M.J., Selwood, A.I., Harwood, D.T., McNabb, P.S., Turner, A.D., 2015. Development of a sensitive and selective liquid chromatography–mass spectrometry method for high throughput analysis of paralytic shellfish toxins using graphitised carbon solid phase extraction. *J. Chrom. A* 1387, 1-12. doi:10.1016/j.chroma.2015.01.086
- Bourdelais, A.J., Tomas, C.R., Naar, J., Kubanek, J., Baden, D.G., 2002. New fish-killing alga in coastal Delaware produces neurotoxins. *Environ. Health Persp.* 110(5), 465. doi:10.1289/ehp.02110465
- Bradley, W.G., Mash, D.C., 2009. Beyond Guam: the cyanobacteria/BMAA hypothesis of the cause of ALS and other neurodegenerative diseases. *Amyotroph. Lateral Sc.* 10(sup2), 7-20. doi:10.3109/17482960903286009
- Brand, L.E., 2002. The transport of terrestrial nutrients to South Florida coastal waters. In: *The Everglades, Florida Bay, and Coral Reefs of the Florida Keys*, CRC Press; Boca Raton, Florida, USA, 353-406
- Brand, L.E., Comptom, A., 2007. Long-term increase in *Karenia brevis* abundance along the Southwest Florida coast. *Harmful Algae* 6(2), 232–252. doi:10.1016/j.hal.2006.08.005

- Brand, L.E., Pablo, J., Compton, A., Hammerschlag, N., Mash, D.C., 2010. Cyanobacterial blooms and the occurrence of the neurotoxin, beta-N-methylamino-L-alanine (BMAA), in South Florida aquatic food webs. *Harmful Algae* 9(6), 620–635. doi:10.1016/j.hal.2010.05.002
- Cadel-Six, S., Peyraud-Thomas, C., Brient, L., Rippka, R., Méjean, A., 2007. Different genotypes of anatoxin-producing cyanobacteria coexist in the Tarn River, France. *Appl. Environ. Microbiol.* 73(23), 7605-7614. doi:10.1128/aem.01225-07
- Campisano, R., Hall, K., Griggs, J., Willison, S., Reimer, S., Mash, H., Magnuson, M., Boczek, L., Rhodes, E., 2017. Selected Analytical Methods for Environmental Remediation and Recovery (SAM) 2017. U.S. EPA, Washington, DC, EPA/600/R-17/356, 2017.
- Carmichael, W.W., Evans, W.R., Yin, Q.Q., Bell, P., Moczydlowski, E., 1997. Evidence for paralytic shellfish poisons in the freshwater cyanobacterium *Lyngbya wollei* (Farlow ex Gomont) comb. nov. *Appl. Environ. Microbiol.* 63(8), 3104–3110.
- Cendes, F., Andermann, F., Carpenter, S., Zatorre, R.J., Cashman, N.R., 1995. Temporal lobe epilepsy caused by domoic acid intoxication: Evidence for glutamate receptor-mediated excitotoxicity in humans. *Ann. Neurol.* 37, 123-126.
- Cocilova, C.C., Milton, S.L., 2016. Characterization of brevetoxin (PbTx-3) exposure in neurons of the anoxia-tolerant freshwater turtle (*Trachemys scripta*). *Aquat. Toxicol.* 180, 115-122. doi:10.1016/j.aquatox.2016.09.016
- Codd, G.A., Metcalf, J.S., Ward, J.C., Beattie, K.A., Bell, S.G., Kaya, K., Poon, G.K., 2001. Analysis of cyanobacterial toxins by physicochemical and biochemical methods. *J. AOAC Int.* 84(5), 1626-1635.
- Conklin, L.M., 2015. Development of a MALDI-TOF-MS Method for the Analysis of Cyanobacterial Neurotoxin β -N-Methylamino-L-alanine (BMAA) in Search of BMAA Incorporation in Biological Samples. FIU Electronic Theses and Dissertations. doi:10.25148/etd.FIDC000172
- Costa, P.R., Garrido, S., 2004. Domoic acid accumulation in the sardine *Sardina pilchardus* and its relationship to *Pseudo-nitzschia* diatom ingestion. *Mar. Ecol. Prog. Ser.* 284, 261-268. doi:10.3354/meps284261
- Costa, P.R., Baugh, K.A., Wright, B., RaLonde, R., Nance, S.L., Tatarenkova, N., Etheridge, S.M., Lefebvre, K.A., 2009. Comparative determination of paralytic shellfish toxins (PSTs) using five different toxin detection methods in shellfish species collected in the Aleutian Islands, Alaska. *Toxicon*, 54(3), 313-320. doi:10.1016/j.toxicon.2009.04.023
- Cox, P.A., Sacks, O.W., 2002. Cycad neurotoxins, consumption of flying foxes, and ALS-PDC disease in Guam. *Neurology* 58(6), 956-959. doi:10.1212/WNL.58.6.956

Cox, P.A., Banack, S.A., Murch, S.J., 2003. Biomagnification of cyanobacterial neurotoxins and neurodegenerative disease among the Chamorro people of Guam. *PNAS* 100(23), 13380-13383. doi:10.1073/pnas.2235808100

Cox, P.A., Banack, S.A., Murch, S.J., Rasmussen, U., Tien, G., Bidigare, R.R., Metcalf, J.S., Morrison, L.F., Codd, G. A., Bergman, B., 2005. Diverse taxa of cyanobacteria produce β -*N*-methylamino-L-alanine, a neurotoxic amino acid. *PNAS* 102(14), 5074-5078. doi:10.1073/pnas.05101526102

Cox, P.A., Davis, D.A., Mash, D.C., Metcalf, J.S., Banack, S.A., 2016. Do vervets and macaques respond differently to BMAA?. *Neurotoxicology* 57, 310-311. doi:10.1016/j.neuro.2016.04.017

Cruz-Aguado, R., Winkler, D., Shaw, C.A., 2006. Lack of behavioral and neuropathological effects of dietary [beta]-methylamino-L-alanine (BMAA) in mice. *Pharmacol. Biochem. Behav.* 84, 294-299.

Cusick, K.D., Sayler, G.S., 2013. An overview on the marine neurotoxin, saxitoxin: genetics, molecular targets, methods of detection and ecological functions. *Mar. Drugs* 11(4), 991-1018. doi:10.3390/md11040991

D'Anglada, L., Donohue, J.M., Strong, J., 2015. Health Effects Support Document for the Cyanobacterial Toxin Anatoxin-A (EPA- 820R15104). U.S. EPA, Office of Water (4304T), Health and Ecological Criteria Division. Washington, DC, USA.

Davis, D.A., Mondo, K., Stern, E., Annor, A.K., Murch, S.J., Coyne, T.M., Brand, L.E., Niemeyer, M.E., Sharp, S., Bradley, W.G., Cox, P.A., 2019. Cyanobacterial neurotoxin BMAA and brain pathology in stranded dolphins. *PloS One*, 14(3) e0213346. doi:10.1371/journal.pone.0213346.

de la Iglesia, P., Giménez, G., Diogène, J., 2008. Determination of dissolved domoic acid in seawater with reversed-phase extraction disks and rapid resolution liquid chromatography tandem mass spectrometry with head-column trapping. *J. Chrom. A* 1215(1-2), 116-124. doi:10.1016/j.chroma.2008.10.123

Debonnel, G., Beauchesne, L., Montigny, C.D., 1989. Domoic acid, the alleged "mussel toxin," might produce its neurotoxic effect through kainate receptor activation: an electrophysiological study in the rat dorsal hippocampus. *Can. J. Physiol. Pharm.* 67(1), 29-33. doi:10.1139/y89-005

Deeds, J.R., Landsberg, J.H., Etheridge, S.M., Pitcher, G.C., Longan, S.W., 2008a. Non-traditional vectors for paralytic shellfish poisoning. *Mar. Drugs* 6(2), 308-348. doi:10.3390/md20080015

Deeds, J.R., White, K.D., Etheridge, S.M., Landsberg, J.H., 2008b. Concentrations of saxitoxin and tetrodotoxin in three species of puffers from the Indian River Lagoon,

Florida, the location for multiple cases of saxitoxin puffer poisoning from 2002 to 2004. T. Am. Fish. Soc. 137(5), 1317-1326. doi.org/10.1577/T07-204.1

Del Rio, R., Bargu, S., Baltz, D., Fire, S., Peterson, G., Wang, Z., 2010. Gulf menhaden (*Brevoortia patronus*): a potential vector of domoic acid in coastal Louisiana food webs. Algae 10(1), 19-29. doi:10.1016/j.hal.2010.05.006

Delcourt, N., Claudepierre, T., Maignien, T., Arnich, N., Mattei, C., 2018. Cellular and Molecular Aspects of the β -methylamino-L-alanine (BMAA) Mode of Action within the Neurodegenerative Pathway: Facts and Controversy. Toxins 10(1), 6. doi:10.3390/toxins10010006

Dell'Aversano, C., Hess, P., Quilliam, M.A., 2005. Hydrophilic interaction liquid chromatography–mass spectrometry for the analysis of paralytic shellfish poisoning (PSP) toxins. J. Chrom. A 1081(2), 190-201. doi:10.1016/j.chroma.2005.05.056

Devlin, J.P., Edwards, O.E., Gorham, P.R., Hunter, N.R., Pike, R.K., Stavric, B., 1977. Anatoxin-a, a toxic alkaloid from *Anabaena flos-aquae* NRC-44h. Can. J. Chem. 55(8), 1367-1371.

Diehl, F., Ramos, P.B., dos Santos, J.M., Barros, D.M., Yunes, J.S., 2016. Behavioral alterations induced by repeated saxitoxin exposure in drinking water. J. Venom. Anim. Toxins. 22, 18. doi:10.1186/s40409-016-0072-9

Dittami, S.M., Pazos, Y., Laspra, M., Medlin, L.K., 2013. Microarray testing for the presence of toxic algae monitoring programme in Galicia (NW Spain). Environ. Sci. Pollut. Res. 20(10), 6778-6793. doi:10.1007/s11356-012-1295-0

Downes-Tettmar, N., Rowland, S., Widdicombe, C., Woodward, M., Llewellyn, C., 2013. Seasonal variation in *Pseudo-nitzschia* spp. and domoic acid in the Western English Channel. Cont. Shelf Res. 53, 40-49. doi:10.1016/j.csr.2012.10.011

Downing, S., Banack, S.A., Metcalf, J.S., Cox, P.A., Downing, T.G., 2011. Nitrogen starvation of cyanobacteria results in the production of β -N-methylamino-L-alanine. Toxicon 58(2), 187-194. doi:10.1016/j.toxicon.2011.05.017

Dunlop, R.A., Cox, P.A., Banack, S.A., Rodgers, K.J., 2013. The non-protein amino acid BMAA is misincorporated into human proteins in place of L-serine causing protein misfolding and aggregation. PloS One 8(9), e75376. doi.org/10.1371/journal.pone.0075376

Engene, N., Rottacker, E.C., Kaštovský, J., Byrum, T., Choi, H., Ellisman, M.H., Komárek, J., Gerwick, W.H., 2012. *Moorea producens* gen. nov., sp. nov. and *Moorea bouillonii* comb. nov., tropical marine cyanobacteria rich in bioactive secondary metabolites. Int. J. Syst. Evol. Micr. 62(5), 1171-1178. doi:10.1099/ijs.0.033761-0

- Engene, N., Paul, V.J., Byrum, T., Gerwick, W.H., Thor, A., Ellisman, M.H., 2013a. Five chemically rich species of tropical marine cyanobacteria of the genus *Okeania* gen. nov. (Oscillatoriales, Cyanoprokaryota). *J. Phycol.* 49(6), 1095-1106. doi:10.1111/jpy.12115
- Engene, N., Gunasekera, S.P., Gerwick, W.H., Paul, V.J., 2013b. Phylogenetic inferences reveal large extent of novel biodiversity in chemically rich tropical marine cyanobacteria. *Appl. Environ. Microbiol.* AEM-03793. doi:10.1128/AEM.03793-12
- Erdner, D.L., Dyble, J., Parsons, M.L., Stevens, R.C., Hubbard, K.A., Wrabel, M.L., Moore, S.K., Lefebvre, K.A., Anderson, D.M., Bienfang, P., Bidigare, R.R., 2008. Centers for Oceans and Human Health: a unified approach to the challenge of harmful algal blooms. *Environ. Health* 7, S2. doi:10.1186/1476-069X-7-S2-S2
- Eriksson, J., Jonasson, S., Papaefthimiou, D., Rasmussen, U., Bergman, B., 2009. Improving derivatization efficiency of BMAA utilizing AccQ-Tag® in a complex cyanobacterial matrix. *Amino Acids* 36(1), 43-48. doi:10.1007/s00726-007-0023-4
- Esquenazi, E., Coates, C., Simmons, L., Gonzalez, D., Gerwick, W.H., Dorrestein, P.C., 2008. Visualizing the spatial distribution of secondary metabolites produced by marine cyanobacteria and sponges via MALDI-TOF imaging. *Mol. Biosyst.* 4(6), 562-570. doi:10.1039/b720018h.
- Faassen, E.J., Gillissen, F., Zweers, H.A., Lüring, M., 2009. Determination of the neurotoxins BMAA (β -N-methylamino-L-alanine) and DAB (α -, γ -diaminobutyric acid) by LC-MSMS in Dutch urban waters with cyanobacterial blooms. *Amyotroph. Lateral Sc.* 10(sup2), 79-84. doi:10.3109/17482960903272967
- Faassen, E.J., 2014. Presence of the neurotoxin BMAA in aquatic ecosystems: What do we really know? *Toxins* 6(3), 1109-1138. doi:10.3390/toxins6031109
- Fang, X., Fan, X., Tang, Y., Chen, J., Lu, J., 2004. Liquid chromatography/quadrupole time-of-flight mass spectrometry for determination of saxitoxin and decarbamoylsaxitoxin in shellfish. *J. Chrom. A* 1036(2), 233-237. doi:10.1016/j.chroma.2004.02.075
- Farrer, D., Counter, M., Hillwig, R., Cude, C., 2015. Health-based cyanotoxin guideline values allow for cyanotoxin-based monitoring and efficient public health response to cyanobacterial blooms. *Toxins* 7, 457-477. doi:10.3390/toxins7020457
- Fayad, P.B., Roy-Lachapelle, A., Duy, S.V., Prévost, M., Sauv e, S., 2015. On-line solid-phase extraction coupled to liquid chromatography tandem mass spectrometry for the analysis of cyanotoxins in algal blooms. *Toxicon* 108, 167-175. doi:10.1016/j.toxicon.2015.10.010
- Filho, A.D.S.F., da Costa, S.M., Ribeiro, M.G.L., Azevedo, S.M., 2008. Effects of a saxitoxin-producer strain of *Cylindrospermopsis raciborskii* (cyanobacteria) on the

swimming movements of cladocerans. Environ. Toxicol. 23(2), 161-168.
doi:10.1002/tox.20320

Fire, S.E., Fauquier, D., Flewelling, L.J., Henry, M., Naar, J., Pierce, R., Wells, R.S., 2007. Brevetoxin exposure in Bottlenose dolphins (*Tursiops truncatus*) associated with *Karenia brevis* blooms in Sarasota Bay, Florida. Mar. Biol. 152(4), 827-834.
doi:10.1007/s00227-007-0733-x

Fire, S.E., Flewelling, L.J., Naar, J., Twiner, M.J., Henry, M.S., Pierce, R.H., Gannon, D.P., Wang, Z., Davidson, L., Wells, R.S., 2008. Prevalence of brevetoxins in prey fish of Bottlenose dolphins in Sarasota Bay, Florida. Mar. Ecol. Prog. Ser. 368, 283-294.
doi:10.3354/meps07643

Fire, S.E., Wang, Z., Leighfield, T.A., Morton, S.L., McFee, W.E., McLellan, W.A., Litaker, R.W., Tester, P.A., Hohn, A.A., Lovewell, G., Harms, C., 2009. Domoic acid exposure in pygmy and dwarf sperm whales (*Kogia* spp.) from southeastern and mid-Atlantic US waters. Harmful Algae 8(5), 658-664. doi:10.1016/j.hal.2008.12.002

Fire, S.E., Wang, Z., Berman, M., Langlois, G.W., Morton, S.L., Sekula-Wood, E., Benitez-Nelson, C.R., 2010. Trophic transfer of the harmful algal toxin domoic acid as a cause of death in a minke whale (*Balaenoptera acutorostrata*) stranding in Southern California. Aquat. Mamm. 36(4), 342-350. doi:10.1578/AM.36.4.2010.342

Flewelling, L.J., Naar, J.P., Abbott, J.P., Baden, D.G., Barros, N.B., Bossart, G.D., Bottein, M.Y.D., Hammond, D.G., Haubold, E.M., Heil, C.A., Henry, M.S., 2005. Brevetoxicosis: red tides and marine mammal mortalities. Nature 435(7043), 755-756.
doi:10.1038/nature435755a.

Foss, A.J., Philips, E.J., Yilmaz, M., Chapman, A., 2012a. Characterization of paralytic shellfish toxins from *Lyngbya wollei* dominated mats collected from two Florida springs. Harmful Algae 16, 98-107. doi:10.1016/j.hal.2012.02.004

Foss, A.J., Philips, E.J., Aubel, M.T., Szabo, N.J., 2012b. Investigation of extraction and analysis techniques for *Lyngbya wollei* derived Paralytic Shellfish Toxins. Toxicon 60(6), 1148-1158. doi:10.1016/j.toxicon.2012.07.009

Frame, E.R., Lefebvre, K.A., 2013. ELISA methods for domoic acid quantification in multiple marine mammal species and sample matrices. U.S. Dept. Commer., NOAA Tech. Memo. NMFS-NWFSC-122, 20 p.

Hokama, Y., Asahina, A.Y., Hong, T.W.P., Katsura, K., Miyahara, J.T., Sweeney, J.C., Stone, R., 1990. Causative Toxin(s) in the Death of Two Atlantic Dolphins. J. Clin. Lab. Anal. 4, 474-478. doi:10.1002/jcla.1860040615

Gilbert, P.M., Heil, C.A., Rudnick, D.T., Madden, C.J., Boyer, J.N., Kelly, S.P., 2009. Florida Bay: Water Quality Status and Trends, Historic and Emerging Bloom Problems. *Contrib. Mar. Sci.* 38, 5-17.

Glover, W.B., Mash, D.C., Murch, S.J., 2014. The natural non-protein amino acid N- β -methylamino-L-alanine (BMAA) is incorporated into protein during synthesis. *Amino Acids*, 46(11), 2553-2559.

Gold, E.P., Jacocks, H.M., Bourdelais, A.J., Baden, D.G., 2013. Brevenal, a brevetoxin antagonist from *Karenia brevis*, binds to a previously unreported site on mammalian sodium channels. *Harmful Algae* 26, 12–19. doi:10.1016/j.hal.2013.03.001.

Gugger, M., Lenoir, S., Berger, C., Ledreux, A., Druart, J.C., Humbert, J.F., Guette, C., Bernard, C., 2005. First report in a river in France of the benthic cyanobacterium *Phormidium favosum* producing anatoxin-a associated with dog neurotoxicosis. *Toxicon* 45(7), 919-928. doi:10.1016/j.toxicon.2005.02.031

Hampson, D.R., Huang, X.P., Wells, J.W., Walter, J.A., Wright, J.L., 1992. Interaction of domoic acid and several derivatives with kainic acid and AMPA binding sites in rat brain. *Eur. J. Pharmacol.* 218(1), 1-8. doi:10.1016/0014-2999(92)90140-Y

Harada, T., Oshima, Y., Yasumoto, T., 1982. Structure of two paralytic shellfish toxins, gonyautoxins V and VI, isolated from a tropical dinoflagellate *Pyrodinium bahamense* var. *compressa*. *Agric. Biol. Chem.* 46(7), 1861–1864. doi:10.1080/00021369.1982.10865327

Harju, K., Rapinoja, M.L., Avondet, M.A., Arnold, W., Schär, M., Luginbühl, W., Kremp, A., Suikkanen, S., Kankaanpää, H., Burrell, S., Söderström, M., 2015a. Results of a saxitoxin proficiency test including characterization of reference material and stability studies. *Toxins* 7(12), 4852-4867. doi:10.3390/toxins7124852

Harju, K., Rapinoja, M. L., Avondet, M. A., Arnold, W., Schär, M., Burrell, S., Luginbühl, W., Vanninen, P., 2015b. Optimization of sample preparation for the identification and quantification of saxitoxin in proficiency test mussel sample using liquid chromatography-tandem mass spectrometry. *Toxins* 7(12), 4868-4880. doi:10.3390/toxins7124853

Harland, F.M., Wood, S.A., Moltchanova, E., Williamson, W.M., Gaw, S., 2013. *Phormidium autumnale* growth and anatoxin-a production under iron and copper stress. *Toxins* 5(12), 2504-2521. doi:10.3390/toxins5122504

Harland, F.M.J., Wood, S.A., Broady, P.A., Gaw, S., Williamson, W.M., 2014. Polyphasic studies of cyanobacterial strains isolated from benthic freshwater mats in Canterbury, New Zealand. *New Zeal. J. Bot.* 52(1), 116-135.

- Haywood, A.J., Scholin, C.A., Marin III, R., Steidinger, K.A., Heil, C., Ray, J., 2007. Molecular detection of the brevetoxin-producing dinoflagellate *Karenia brevis* and closely related species using rRNA-targeted probes and a semiautomated sandwich hybridization assay. *J. Phycol.* 43(6),1271-1286. doi:10.1111/j.1529-8817.2007.00407.x
- He, Y., Fekete, A., Chen, G., Harir, M., Zhang, L., Tong, P., Schmitt-Kopplin, P., 2010. Analytical approaches for an important shellfish poisoning agent: domoic acid. *J. Agric. Food Chem.* 58(22), 11525-11533. doi:10.1021/jf1031789
- Hitchcock, G.L., Fourqurean, J.W., Drake, J.L., Mead, R.N., Heil, C.A., 2012. Brevetoxin persistence in sediments and seagrass epiphytes of east Florida coastal waters. *Harmful Algae* 13, 89-94. doi:10.1016/j.hal.2011.10.008
- Hoagland, P., Anderson, D.M., Kaoru, Y., White, A.W., 2002. The economic effects of harmful algal blooms in the United States: estimates, assessment issues, and information needs. *Estuaries* 25(4), 819-837.
- Hodoki, Y., Ohbayashi, K., Kobayashi, Y., Takasu, H., Okuda, N., Nakano, S.I., 2013. Anatoxin-a-producing *Raphidiopsis mediterranea* Skuja var. *grandis* Hill is one ecotype of non-heterocytous *Cuspidothrix issatschenkoi* (Usačev) Rajaniemi et al. in Japanese lakes. *Harmful Algae* 21-22, 44-53. doi:10.1016/j.hal.2012.11.007
- Hua, Y., Lu, W., Henry, M.S., Pierce, R.H., Cole, R.B., 1996. On-line liquid chromatography-electrospray ionization mass spectrometry for determination of the brevetoxin profile in natural "red tide" algae blooms. *J. Chrom. A*, 750(1-2), 115-125. doi:10.1016/0021-9673(96)00470-0
- Humpage, A.R., Magalhaes, V.F., Froscio, S.M., 2010. Comparison of analytical tools and biological assays for detection of paralytic shellfish poisoning toxins. *Anal. Bioanal. Chem.* 397, 1655-1671. doi:10.1007/s00216-010-3459-4
- Iglesia, P.D.L., Barber, E., Gimenez, G., Rodriguez-Velasco, Mara, L., Villar-Gonzalez, A., Diogne, J., 2011. High-throughput analysis of amnesic shellfish poisoning toxins in shellfish by ultra-performance rapid resolution LC-MS/MS. *J. AOAC Int.* 94(2), 555-564.
- Iverson, F., Truelove, J., Nera, E., Tryphonas, L., Campbell, J., Lok, E., 1989. Domoic acid poisoning and mussel-associated intoxication: Preliminary investigations into the response of mice and rats to toxic mussels. *Food Chem. Toxicol.* 27(6), 377-384. doi:10.1016/0278-6915(89)90143-9
- Jiang L., Eriksson J., Lage S., Jonasson S., Shams S., Mehine, M., Ilag, L.L., Rasmussen, U., 2014a. Diatoms: A novel source for the neurotoxin BMAA in aquatic environments. *PLoS One* 9(1), e84578. doi:10.1371/journal.pone.0084578

- Jiang, L., Ilag, L.L., 2014. Detection of endogenous BMAA in dinoflagellate (*Heterocapsa triquetra*) hints at evolutionary conservation and environmental concern. *PubRaw Sci.* 1(2), 1-8.
- Jiang, L., Kiselova, N., Rosén, J., Ilag, L.L., 2014b. Quantification of neurotoxin BMAA (β -N-methylamino-L-alanine) in seafood from Swedish markets. *Scientific Reports* 4, srep06931.
- Jonasson, S., Eriksson, J., Berntzon, L., Spáčil, Z., Ilag, L.L., Ronnevi, L.O., Rasmussen, U., Bergman, B., 2010. Transfer of a cyanobacterial neurotoxin within a temperate aquatic ecosystem suggests pathways for human exposure. *PNAS* 107(2), 9252-9257. doi:10.1073/pnas.0914417107
- Karlsson, O., Lindquist, N.G., Brittebo, E.B., Roman, E., 2009. Selective brain uptake and behavioral effects of the cyanobacterial toxin BMAA (β -N-Methylamino-L-alanine) following neonatal administration to rodents. *Toxicol. Sci.* 109(2), 286–295 doi:10.1093/toxsci/kfp062
- Karlsson O., Roman E., Berg, A.L., Brittebo, E.B., 2011. Early hippocampal cell death, and late learning and memory deficits in rats exposed to the environmental toxin BMAA (β -N-methylamino-L-alanine) during the neonatal period. *Behav. Brain Res.* 219(2), 310-320. doi:10.1016/j.bbr.2011.01.056.
- Karlsson, O., Jiang, L., Andersson, M., Ilag, L.L., Brittebo, E.B., 2014. Protein association of the neurotoxin and non-protein amino acid BMAA (β -N-methylamino-l-alanine) in the liver and brain following neonatal administration in rats. *Toxicol. Lett.* 226(1), 1-5. doi:10.1016/j.toxlet.2014.01.027
- Karlsson, O., Mincho, W., Ransome, Y., Hanreider, J., 2017. MALDI imaging delineates hippocampal glycosphingolipid changes associated with neurotoxin induced proteopathy following neonatal BMAA exposure. *BBA-Proteins Proteom.* 1865(7), 740–746. doi:10.1016/j.bbapap.2016.12.004.
- Khan, S., Arakawa, O., Onoue, Y., 1996. A toxicological study of the marine phytoflagellate, *Chattonella antiqua* (Raphidophyceae). *Phycologia* 35(3), 239–244. doi:10.2216/i0031-8884-35-3-239.1
- Kiss, T., Vehovszky, A., Hiripi, L., Kovacs, A., Vörös, L., 2002. Membrane effects of toxins isolated from a cyanobacterium, *Cylindrospermopsis raciborskii*, on identified molluscan neurones. *Comp. Biochem. Phys. C*, 131(2), 167-176. doi:10.1016/S1532-0456(01)00290-3
- Komárek, J., Kastovsky, J., Mares, J., Johansen, J.R., 2014. Taxonomic classification of cyanoprokaryotes (cyanobacterial genera) 2014, using a polyphasic approach. *Preslia* 86, 295-335.

- Kubo, T., Kato, N., Hosoya, K., Kaya, K., 2008. Effective determination method for a cyanobacterial neurotoxin, β -N-methylamino-L-alanine. *Toxicon* 51(7), 1264-1268. doi:10.1016/j.toxicon.2008.02.015
- Lage, S., Costa, P.R., Moita, T., Eriksen, J., Rasmussen, U., Rydberg, S.J., 2014. BMAA in shellfish from two Portuguese transitional water bodies suggests the marine dinoflagellate *Gymnodinium catenae* as a potential BMAA source. *Aquat. Toxicol.* 152, 131-138. doi:10.1016/j.aquatox.2014.03.029
- Lagos, N., Onodera, H., Zagatto, P.A., Andrinolo, D., Azevedo, S.M.F.Q., Oshima, Y., 1999. The first evidence of paralytic shellfish toxins in the freshwater cyanobacterium *Cylindrospermopsis raciborskii*, isolated from Brazil. *Toxicon* 37, 1359–1373.
- Landsberg, J.H., Hall, S., Johannessen, J.N., White, K.D., Conrad, S.M., Abbott, J.P., Flewelling, L.J., Richardson, R.W., Dickey, R.W., Jester, E.L., Etheridge, S.M., 2006. Saxitoxin puffer fish poisoning in the United States, with the first report of *Pyrodinium bahamense* as the putative toxin source. *Environ. Health Persp.* 114(10), 1502-1507.
- Liefer, J.D., Robertson, A., MacIntyre, H.L., Smith, W.L., Dorsey, C.P., 2013. Characterization of a toxic *Pseudo-nitzschia* spp. bloom in the Northern Gulf of Mexico associated with domoic acid accumulation in fish. *Harmful Algae* 26, 20-32. doi:10.1016/j.hal.2013.03.002
- Lilly, E.L., Halanych, K.M., Anderson, D.M., 2007. Species boundaries and global biogeography of the *Alexandrium tamarens* complex (Dinophyceae). *J. Phycol.* 43, 1329-1338. doi:10.1111/j.1529-8817.2007.00420.x
- Lin, Y.-Y., Risk, M., 1981. Isolation and structure elucidation of brevetoxin B from the “red tide” dinoflagellate *Ptychodiscus brevis* (*Gymnodinium breve*). *J. Am. Chem. Soc.* 103, 6773-6775. doi:10.1021/ja00412a053
- Lin, Z., Wang, D., Peng, A., Huang, Z., Lin, Y., 2016. Determination of domoic acid in shellfish extracted by molecularly imprinted polymers. *J. Sep. Sci.* 39(16), 3254-3259. doi:10.1002/jssc.201600393
- Lindström, H., Luthman, J., Mouton, P., Spencer, P., Olson, L., 1990. Plant-Derived Neurotoxic Amino Acids (β -N-Oxalylamino-l-Alanine and β -N-Methylamino-l-Alanine): Effects on Central Monoamine Neurons. *J. Neurochem.* 55(3), 941-949. doi:10.1111/j.1471-4159.1990.tb04582.x
- Lobner, D., Piana, P.M.T., Salous, A.K., Peoples, R.W., 2007. β -N-methylamino-L-alanine enhances neurotoxicity through multiple mechanisms. *Neurobiol. Dis.* 25(2), 360-366. doi:10.1016/j.nbd.2006.10.002
- Mafra Jr., L.L., Léger, C., Bates, S.S., Quilliam, M.A., 2009. Analysis of trace levels of domoic acid in seawater and plankton by liquid chromatography without derivatization,

using UV or mass spectrometry detection. *J. Chrom. A* 1216, 6003-6011.
doi:10.1016/j.chroma.2009.06.050

Masseret, E., Banack, S., Boumédiène, F., Abadie, E., Brient, L., Pernet, F., Juntas-Morales, R., Pageot, N., Metcalf, J., Cox, P., Camu, W., 2013. Dietary BMAA exposure in an amyotrophic lateral sclerosis cluster from southern France. *PloS One* 8(12), e83406. doi:10.1371/journal.pone.0083406

McNamee, S.E., Medlin, L.K., Kegel, J., McCoy, G.R., Raine, R., Barra, L., Ruggiero, M.V., Kooistra, W.H.C.F., Montresor, M., Hagstrom, J., Blanco, E.P., Graneli, E., Rodríguez, F., Escalera, L., Reguera, B., Dittami, S., Edvardsen, B., Taylor, J., Lewis, J.M., Pazos, Y., Elliott, C.T., Campbell, K., 2016. Distribution, occurrence and biotoxin composition of the main shellfish toxin producing microalgae within European waters: A comparison of methods of analysis. *Harmful Algae* 55, 112-120. doi:10.1016/j.hal.2016.02.008

Méjean, A., Peyraud-Thomas, C., Kerbrat, A.S., Golubic, S., Pauillac, S., Chinain, M., Laurent, D., 2010. First identification of the neurotoxin homoanatoxin-a from mats of *Hydrocoleum lyngbyaceum* (marine Cyanobacteria) possibly linked to giant clam poisoning in New Caledonia. *Toxicon* 56(5), 829-835. doi:10.1016/j.toxicon.2009.10.029

Mihali, T.K., Kellmann, R., Neilan, B.R., 2009. Characterisation of the paralytic shellfish toxin biosynthesis gene clusters in *Anabaena circinalis* AWQC131C and *Aphanizomenon* sp. NH-5. *BMC Biochem.* 10(1), 8. doi:10.1186/1471-2091-10-8

Mondo, K., Hammerschlag, N., Basile, M., Pablo, J., Banack, S.A., Mash, D.C., 2012. Cyanobacterial Neurotoxin β -N-Methylamino-L-alanine (BMAA) in Shark Fins. *Mar. Drugs* 10, 509-520. doi:10.3390/md10020509

Montine, T.J., Li, K., Perl, D.P., Galasko, D., 2005. Lack of β -methylamino-L-alanine in brain from controls, AD, or Chamorro with PDC. *Neurology* 65(5), 768-769. doi:10.1212/01.wnl.0000174523.62022.52

Moustafa, A., Loram, J.E., Hackett, J.D., Anderson, D.M., Plumley, F.G., Bhattacharya, D., 2009. Origin of saxitoxin biosynthetic genes in cyanobacteria. *PLoS One* 4(6), e5758. doi:10.1371/journal.pone.0005758

Naar, J., Bourdelais, A., Tomas, C., Kubanek, J., Whitney, P.L., Flewelling, L., Steidinger, K., Lancaster, J., Baden, D.G., 2002. A competitive ELISA to detect brevetoxins from *Karenia brevis* (formerly *Gymnodinium breve*) in seawater, shellfish, and mammalian body fluid. *Environ. Health Persp.* 110(2), 179.

Naar, J.P., Flewelling, L.J., Lenzi, A., Abbott, J.P., Granholm, A., Jacocks, H.M., Gannon, D., Henry, M., Pierce, R., Baden, D.G., Wolny, J., 2007. Brevetoxins, like ciguatoxins, are potent ichthyotoxic neurotoxins that accumulate in fish. *Toxicon* 50(5), 707-723. doi:10.1016/j.toxicon.2007.06.005

- Namikoshi, M., Murakami, T., Fujiwara, T., Nagai, H., Niki, T., Harigaya, E., Watanabe, M.F., Oda, T., Yamada, J., Tsujimura, S., 2004. Biosynthesis and transformation of homoanatoxin-a in the cyanobacterium *Raphidiopsis mediterranea* Skuja and structures of three new homologues. *Chem. Res. Toxicol.* 17(12), 1692-1696. doi:10.1021/tx0498152
- Onodera, H., Oshima, Y., Henriksen P., Yasumoto, T., 1997. Confirmation of anatoxin-a(s), in the cyanobacterium *Anabaena lemmermannii*, as the cause of bird kills in Danish lakes. *Toxicon* 35, 1645–1648.
- Oshima, Y., Hasegawa, M., Yasumoto, T., Hallegaeff, G., Blackburn, S., 1987. Dinoflagellate *Gymnodinium catenatum* as the source of paralytic shellfish toxins in Tasmanian shellfish. *Toxicon* 25(10), 1105–1111.
- Osswald, J., Rellán, S., Gago, A., Vasconcelos, V., 2007. Toxicology and detection methods of the alkaloid neurotoxin produced by cyanobacteria, anatoxin-a. *Environ. Int.* 33(8), 1070-1089. doi:10.1016/j.envint.2007.06.003
- Osswald, J., Rellán, S., Gago, A., Vasconcelos, V., 2008. Uptake and depuration of anatoxin-a by the mussel *Mytilus galloprovincialis* (Lamarck, 1819) under laboratory conditions. *Chemosphere* 72(9), 1235-1241. doi:10.1016/j.chemosphere.2008.05.012
- Osswald, J., Azevedo, J., Vasconcelos, V., Guilhermino, L., 2011. Experimental determination of the bioconcentration factors for anatoxin-a in juvenile rainbow trout (*Oncorhynchus mykiss*). *Proc. Int. Acad.* 1(2), 77-86.
- Parsons, M.L., Dortch, Q., 2002. Sedimentological evidence of an increase in *Pseudo-nitzschia* (Bacillariophyceae) abundance in response to coastal eutrophication. *Limnol. Oceanogr.* 47(2), 551-558. doi:10.4319/lo.2002.47.2.0551
- Pawlik-Skowrońska, B., Toporowska, M., Rechulicz, J., 2012. Simultaneous accumulation of anatoxin-a and microcystins in three fish species indigenous to lakes affected by cyanobacterial blooms. *Oceanol. Hydrobiol. St.* 41(4), 53-65. doi:10.2478/s13545-012-0039-6
- Perrault, J.R., Bauman, K.D., Greenan, T.M., Blum, P.C., Henry, M.S., Walsh, C.J., 2016. Maternal transfer and sublethal immune system effects of brevetoxin exposure in nesting loggerhead sea turtles (*Caretta caretta*) from western Florida. *Aquat. Toxicol.* 180, 131-140. doi:10.1016/j.aquatox.2016.09.020
- Phlips, E.J., Badylak, S., Bledsoe, E., Cichra, M., 2006. Factors affecting the distribution of *Pyrodinium bahamense* var. *bahamense* in coastal waters of Florida. *Mar. Ecol. Prog. Ser.* 322, 99-115. doi:10.3354/meps322099

- Pierce, R.H., Henry, M.S., 2008. Harmful algal toxins of the Florida red tide (*Karenia brevis*): Natural chemical stressors in South Florida coastal ecosystems. *Ecotoxicology* 17(7), 623–631. doi:10.1007/s10646-008-0241-x
- Plakas, S.M., El Said, K.R., Jester, E.L., Granade, H.R., Musser, S.M., Dickey, R.W., 2002. Confirmation of brevetoxin metabolism in the Eastern oyster (*Crassostrea virginica*) by controlled exposures to pure toxins and to *Karenia brevis* cultures. *Toxicon* 40(6), 721-729. doi:10.1016/S0041-0101(01)00267-7
- Pomati, F.; Sacchi, S.; Rossetti, C.; Giovannardi, S.; Onodera, H.; Oshima, Y.; Neilan, B.A., 2000. The freshwater cyanobacterium *Planktothrix* sp. FP1: Molecular identification and detection of paralytic shellfish poisoning toxins. *J. Phycol.* 36, 553–562.
- Puschner, B., Hoff, B., Tor, E.R., 2008. Diagnosis of anatoxin-a poisoning in dogs from North America. *J. Vet. Diagn. Invest.* 20(1), 89-92. doi:10.1177/104063870802000119
- Puschner, B., Pratt, C., Tor, E.R., 2010. Treatment and diagnosis of a dog with fulminant neurological deterioration due to anatoxin-a intoxication. *J. Vet. Emerg. Crit. Car.* 20(5), 518-522. doi:10.1111/j.1476-4431.2010.00578.x
- Quilliam, M.A., Xie, M., Hardstaff, W.R., 1995. Rapid extraction and cleanup for liquid chromatographic determination of domoic acid in unsalted seafood. *J. AOAC Int.* 78, 543-543.
- Quilliam, M.A., 2003. The role of chromatography in the hunt for red tide toxins. *J. Chrom. A* 1000(1-2), 527-548. doi:10.1016/S0021-9673(03)00586-7
- Rao, D.S., Quilliam, M.A., Pocklington, R., 1988. Domoic acid—a neurotoxic amino acid produced by the marine diatom *Nitzschia pungens* in culture. *Can. J. Aquat. Sci.* 45(12), 2076-2079. doi:10.1139/f88-241
- Réveillon, D., Abadie, E., Séchet, V., Brient, L., Savar, V., Bardouil, M., Hess, P., Amzil, Z., 2014. Beta-N-methylamino-L-alanine: LC-MS/MS optimization, screening of cyanobacterial strains and occurrence in shellfish from Thau, a French Mediterranean lagoon. *Mar. Drugs* 12, 5441-5467. doi:10.3390/md12115441
- Réveillon, D., Séchet, V., Hess, P., Amzil, Z., 2016. Production of BMAA and DAB by diatoms (*Phaeodactylum tricorutum*, *Chaetoceros* sp., *Chaetoceros calcitrans* and, *Thalassiosira pseudonana*) and bacteria isolated from a diatom culture. *Harmful Algae* 58, 45-50. doi:10.1016/j.hal.2016.07.008
- Salomonsson, M.L., Hansson, A., Bondesson, U., 2013. Development and in-house validation of a method for quantification of BMAA in mussels using dansyl chloride derivatization and ultra performance liquid chromatography tandem mass spectrometry. *Anal. Methods-UK* 5(18), 4865-4874. doi:10.1039/C3AY40657A

- Sawant, P.M., Holland, P.T., Mountfort, D.O., Kerr, D.S., 2008. In vivo seizure induction and pharmacological preconditioning by domoic acid and isodomoic acids A, B and C. *Neuropharmacology* 55(8), 1412-1418. doi:10.1016/j.neuropharm.2008.09.001
- Sawant, P.M., Tyndall, J.D., Holland, P.T., Peake, B.M, Mountfort, D.O., Kerr, D.S., 2010. In vivo seizure induction and affinity studies of domoic acid and isodomoic acids-D,-E and-F. *Neuropharmacology* 59(3), 129-38. doi:10.1016/j.neuropharm.2010.03.019
- Scholin, C.A., Gulland, F., Doucette, G.J., Benson, S., Busman, M., Chavez, F.P., Cordaro, J., DeLong, R., De Vogelaere, A., Harvey, J., Haulena, M. Lefebvre, K., Lipscomb, T., Loscutoff, S., Lowenstine, L. J., Marin, R., Miller, P. E., McLellan, W. A., Moeller, P.D.R., Powell, C.L., Rowles, T., Silvagni, P. Silver, M., Spraker, R., Trainer, T., Van Dolah, F.M., 2000. Mortality of sea lions along the central California coast linked to a toxic diatom bloom. *Nature* 403(6765), 80.
- Seubert, E.L., Howard, M.D., Kudela, R.M., Stewart, T.N., Litaker, R.W., Evans, R., Caron, D.A., 2014. Development, comparison and validation using ELISAs for the analysis of domoic acid in California sea lion body fluids. *J. AOAC Int.* 97(345), e355. doi:10.5740/jaoacint.SGSESeubert
- Shams, S., Capelli, C., Cerasino, L., Ballot, A., Dietrich, D.R., Sivonen, K., Salmaso, N., 2015. Anatoxin-a producing *Tychonema* (Cyanobacteria) in European waterbodies. *Water Res.* 69, 68-79. doi:10.1016/j.watres.2014.11.006
- Shanks, A.L., Morgan, S.G., MacMahan, J., Reniers, A.J., Kudela, R., Jarvis, M., Brown, J., Fujimura, A., Ziccarelli, L., Griesemer, C., 2016. Variation in the abundance of *Pseudo-nitzschia* and domoic acid with surf zone type. *Harmful Algae* 55, 172-178. doi:10.1016/j.jhal.2016.03.004
- Shantz, E.J., Mold, J.D., Stanger, D.W., Shavel, J. Lynch, J.M., Wyler, R.S., Riegel, B., Sommer, H., 1957. Paralytic Shellfish Poison. VI. A procedure for the isolation and purification of the poison from toxic clam and mussel tissues. *J. Am. Chem. Soci.* 79(19), 5230-5235. doi:10.1021/ja01576a044
- Shearn-Bochsler, V., Lance, E.W., Corcoran, R., Piatt, J., Bodenstein, B., Frame, E., Lawonn, J., 2014. Fatal paralytic shellfish poisoning in Kittlitz's murrelet (*Brachyramphus brevirostris*) nestlings, Alaska, USA. *J. Wildlife Dis.* 50(4), 933-937. doi:10.7589/2013-11-296
- Sherman, B.H., 2000. Marine ecosystem health as an expression of morbidity, mortality and disease events. *Mar. Pollut. Bull.* 41(1-6), 232-254. doi:10.1016/S0025-326x(00)00113-2
- Skulberg, O.M., Carmichael, W.W., Andersen, R.A., Matsunaga, S., Moore, R.E., Skulberg, R., 1992. Investigations of a neurotoxic Oscillatorialean strain (Cyanophyceae)

and its toxin. Isolation and characterization of homoanatoxin-a. *Environ. Toxicol. Chem.* 11, 321–329.

Smida, D.B., Lundholm, N., Kooistra, W.H., Sahraoui, I., Ruggiero, M.V., Kotaki, Y., Ellegaard, M., Lambert, C., Mabrouk, H.H., Hlaili, A.S., 2014. Morphology and molecular phylogeny of *Nitzschia bizertensis* sp. nov.—a new domoic acid-producer. *Harmful Algae* 32, 49-63. doi:10.1016/j.hal.2013.12.004

Smith, C., Sutton, A., 1993. The persistence of anatoxin-a in reservoir water. Foundation for Water Research, UK Report No. FR0427.

Snyder, L.R., Cruz-Aguado, R., Sadilek, M., Galasko, D., Shaw, C.A., Montine, T.J., 2009. Lack of cerebral BMAA in human cerebral cortex. *Neurology* 72(15), 1360-1361. doi:10.1212/wnl.0b013e3181a0fed1

Sotka, E.E., McCarty, A., Monroe, E.A., Oakman, N., Van Dolah, F.M., 2009. Benthic Herbivores are not Deterred by Brevetoxins Produced by the Red Tide Dinoflagellate *Karenia Brevis*. *J. Chem. Ecol.* 35, 851-859. doi:10.1007/s10886-009-9658-9

Spáčil, Z., Eriksson, J., Jonasson, S., Rasmussen, U., Ilag, L.L., Bergman, B., 2010. Analytical protocol for identification of BMAA and DAB in biological samples. *Analyst* 135(1), 127-132. doi:10.1039/b921048b

Stewart I., Seawright A.A., Shaw G.R., 2008. Cyanobacterial poisoning in livestock, wild mammals and birds—an overview. In: *Cyanobacterial harmful algal blooms: state of the science and research needs.* 613-637. Springer, New York, NY.

Strain, S.M., Tasker, R.A.R., 1991. Hippocampal damage produced by systemic injections of domoic acid in mice. *Neuroscience* 44(2), 343-352. doi:10.1016/0306-4522(91)90059-W

Takada, N., Iwatsuki, M., Suenaga, K., Uemura, D., 2000. Pinnamine, an alkaloidal marine toxin, isolated from *Pinna muricata*. *Tetrahedron Lett.* 41(33), 6425-6428. doi:10.1016/s0040-4039(00)00931-x

Tan, S.N., Teng, S.T., Lim, H.C., Kotaki, Y., Bates, S.S., Leaw, C.P., Lim, P.T., 2016. Diatom *Nitzschia navis-varingica* (Bacillariophyceae) and its domoic acid production from the mangrove environments of Malaysia. *Harmful Algae* 60, 139-149. doi:10.1016/j.hal.2016.11.003

Teitelbaum, J.S., Zatorre, R.J., Carpenter, S., Gendron, D., Evans, A.C., Gjedde, A., Cashman, N.R., 1990. Neurologic sequelae of domoic acid intoxication due to the ingestion of contaminated mussels. *N. Engl. J. Med.* 322,1781-1787 doi:10.1056/NEJM199006213222505

Thorel, M., Fauchot, J., Morelle, J., Raimbault, V., Le Roy, B., Miossec, C., Kientz-Bouchart, V., Claquin, P., 2014. Interactive effects of irradiance and temperature on

- growth and domoic acid production of the toxic diatom *Pseudo-nitzschia australis* (Bacillariophyceae). *Harmful Algae* 39, 232-241. doi:10.1016/j.hal.2014.07.010
- Trainer, V.L., Pitcher, G.C., Reguera, B., Smayda, T.J., 2010. The distribution and impacts of harmful algal bloom species in eastern boundary upwelling systems. *Prog. Oceanogr.* 85(1-2), 33-52. doi:10.1016/j.pocean.2010.02.003
- Trainer, V.L., Hardy, F.J., 2015. Integrative monitoring of marine and freshwater harmful algae in Washington state for public health protection. *Toxins* 7, 1206-1234. doi:10.3390/toxins7041206
- Tryphonas, L., Truelove, J., Iverson, F., 1990a. Acute parenteral neurotoxicity of domoic acid in cynomolgus monkeys (*M. fascicularis*). *Toxicol. Pathol.* 18(2), 297-303. doi:10.1177/019262339001800208
- Tryphonas, L., Truelove, J., Todd, E., Nera, E., Iverson, F., 1990b. Experimental oral toxicity of domoic acid in cynomolgus monkeys (*Macaca fascicularis*) and rats.: Preliminary investigations. *Food Chem. Toxicol.* 28(10), 707-715. doi:10.1016/0278-6915(90)90147-f
- Tryphonas, L., Truelove, J., Nera, E., Iverson, F., 1990c. Acute neurotoxicity of domoic acid in the rat. *Toxicol. Pathol.* 18(1), 1-9. doi:10.1177/019262339001800101
- Tryphonas, L., Iverson, F., 1990. Neuropathology of excitatory neurotoxins: the domoic acid model. *Toxicol. Pathol.* 18(1_part_2), 165-169. doi:10.1177/019262339001800122
- Turner, A.D., Higgins, C., Davidson, K., Veszelovszki, A., Payne, D., Hungerford, J., Higman, W., 2015. Potential threats posed by new or emerging marine biotoxins in UK waters and examination of detection methodology used in their control: brevetoxins. *Mar. Drugs* 13(3), 1224-1254. doi:10.3390/md13031224
- Twiner, M.J., Dechraoui, M.Y.B., Wang, Z., Mikulski, C.M., Henry, M.S., Pierce, R.H., Doucette, G.J., 2007. Extraction and analysis of lipophilic brevetoxins from the red tide dinoflagellate *Karenia brevis*. *Anal. Biochem.* 369(1), 128-135. doi:10.1016/j.ab.2007.06.031
- Twiner, M.J., Fire, S., Schwacke, L., Davidson, L., Wang, Z., Morton, S., Roth, S., Balmer, B., Rowles, T. K., Wells, R.S., 2011. Concurrent exposure of bottlenose dolphins (*Tursiops truncatus*) to multiple algal toxins in Sarasota Bay, Florida, USA. *PLoS One* 6(3), e17394. doi:10.1371/journal.pone.0017394
- Twiner, M.J., Flewelling, L.J., Fire, S.E., Bowen-Stevens, S.R., Gaydos, J.K., Johnson, C. K., Landsberg, J.H., Leighfield, T.A., Mase-Guthrie, B., Schwacker, L., Van Dolah, F.M., Wang, Z., Knowles, T.K., 2012. Comparative analysis of three brevetoxin-associated Bottlenose dolphin (*Tursiops truncatus*) mortality events in the Florida Panhandle Region (USA). *PLoS One* 7(8), e42974. doi:10.1371/journal.pone.0042974

U.S. EPA. April 2015. Method 545: Determination of cylindrospermopsin and anatoxin-a in drinking water by liquid chromatography electrospray ionization tandem mass spectrometry (LC/ESI-MS/MS), EPA 815-R-15-009. Washington DC: U.S. Environmental Protection Agency. https://www.epa.gov/sites/production/files/2017-10/documents/epa_815-r-15-009_method_545.pdf

U.S. EPA. June 2015. Health effects support document for the cyanobacterial toxin anatoxin-a, EPA 820-R-15-104. Washington DC: U.S. Environmental Protection Agency. <https://www.epa.gov/sites/production/files/2015-06/documents/anatoxin-a-report-2015.pdf>

U.S. FDA. 2011. U.S. FDA Hazards Guide: Fish and Fishery Products Hazards, and Controls Guidance (SGR-129, 4th edition, April 2011), Chapter 6-Natural Toxins. Washington DC: U.S. Food and Drug Administration. <https://www.fda.gov/downloads/food/guidanceregulation/ucm252395.pdf>

U.S. FDA. 2011. U.S. FDA Hazards Guide: Fish and Fishery Products Hazards, and Controls Guidance (SGR-129, 4th edition, April 2011), Appendix 5. Washington DC: U.S. Food and Drug Administration. <https://www.fda.gov/downloads/food/guidanceregulation/ucm252448.pdf>

U.S. FDA. 2015. U.S. FDA National Shellfish Sanitation Program: Guide for the Control of Molluscan Shellfish, Rev. 2015: 260–263. Washington DC: U.S. Food and Drug Administration. <https://www.fda.gov/downloads/food/guidanceregulation/federalstatefoodprograms/ucm505093.pdf>

Van De Riet, J., Gibbs, R.D., Muggah, P.M., Rourke, W.A., MacNeil, J.D., Quilliam, M.A., 2011. Liquid chromatography post-column Oxidation (PCOX) method for the determination of paralytic shellfish toxins in mussels, clams, oysters, and scallops: Collaborative study. *J. AOAC Int.* 94(4), 1154-1176.

Vargo, G.A., Heil, C.A., Fanning, K.A., Dixon, L.K., Neely, M.B., Lester, K., Ault, D., Murasko, S., Havens, J., Walsh, J., Bell, S., 2008. Nutrient availability in support of *Karenia brevis* blooms on the central West Florida Shelf: What keeps *Karenia* blooming?. *Cont. Shelf Res.* 28(1), 73-98. doi:10.1016/j.csr.2007.04.008

Vargo, G.A., 2009. A brief summary of the physiology and ecology of *Karenia brevis* Davis (G. Hansen and Moestrup comb. nov.) red tides on the West Florida Shelf and of hypotheses posed for their initiation, growth, maintenance, and termination. *Harmful Algae* 8(4): 573-584. doi:10.1016/j.hal.2008.11.002

Viaggiu, E., Melchiorre, S., Volpi, F., Di Corcia, A., Mancini, R., Garibaldi, L., Crichigno, G., Bruno, M., 2004. Anatoxin-a toxin in the cyanobacterium *Planktothrix rubescens* from a fishing pond in northern Italy. *Environ. Toxicol.* 19, 191–197.

- Watkins, S.M., Reich, A., Fleming, L.E., Hammond, R., 2008. Neurotoxic shellfish poisoning. *Mar. Drugs* 6(3), 431-455. doi:10.3390/md20080021
- Weissflog, J., Adolph, S., Weisemeier, T., 2008. Reduction of herbivory through wound-activated protein cross-linking by the invasive macroalga *Caulerpa taxifolia*. *ChemBioChem* 9(1), 29-32. doi:10.1002/cbic.200700443
- Wiese, M., D'Agostino, P.M., Mihali, T.K., Moffit, M.C., Neilan, B.A., 2010. Neurotoxic alkaloids: Saxitoxin and its analogs. *Mar. Drugs* 8, 2185-2211. doi:10.3390/md8072185
- Wonnacott, S., Gallagher, T., 2006. The chemistry and pharmacology of anatoxin-a and related homotropans with respect to nicotinic acetylcholine receptors. *Mar. Drugs* 4(3), 228-254. doi:10.3390/md403228
- Wood, R., 2016. Acute animal and human poisonings from cyanotoxin exposure—A review of the literature. *Environ. Int.* 91, 276-282. doi:10.1016/j.envint.2016.02.026
- Wood, S.A., Rasmussen, J.P., Holland, P.T., Campbell, R., Crowe, A.L.M., 2007. First report of cyanotoxin anatoxin-a from *Aphanizomenon issatschenkoi* (cyanobacteria). *J. Phycol.* 43, 356–365.
- Wright, J.L.C., Boyd, R.K., de Freitas, A.D., Falk, M., Foxall, R.A., Jamieson, W.D., Laycock, M.V., McCulloch, A.W., McInnes, A.G., Odense, P., Pathak, V.P., McQuilliam, A.W., Ragan, M.A., Sim, P.G., Thibault, P., Walter, J.A., Gilgan, M., Richard, D.J.A., Dewar, D., 1989. Identification of domoic acid, a neuroexcitatory amino acid, in toxic mussels from eastern Prince Edward Island. *Can. J. Chem.* 67(3), 481-490. doi:10.1139/v89-075
- Yang, X., 2007. Occurrence of the cyanobacterial neurotoxin, anatoxin-a. New York state waters. Ph. D. Thesis, State University of New York, Syracuse.
- Zhang, Y., Chen, D., Hong, Z., 2016. A rapid LC-HRMS method for the determination of domoic acid in urine using a self-assembly pipette tip solid-phase extraction. *Toxins* 8(1), 10 doi:10.3390/toxins8010010
- Zingone, A., Enevoldsen, H.O., 2000. The diversity of harmful algal blooms: a challenge for science and management. *Ocean Coast. Manage.* 43, 725-748. doi:10.1016/S0964-5691(00)00056-9

**5. BIOASSAY-GUIDED INQUEST OF A MARINE FILAMENTOUS
CYANOBACTERIAL ASSEMBLAGE ASSOCIATED WITH
INTOXICATIONS OF CAPTIVE BOTTLENOSE DOLPHINS (*TURSIOPS
TRUNCATUS*) IN THE FLORIDA KEYS USING ZEBRAFISH (*DANIO
RERIO*) MODELS OF NEUROTOXICITY (in preparation for Harmful Algae)**

5.1 Abstract

A marine filamentous cyanobacterial assemblage (i.e., mat) was recently implicated in apparent ingestion-related intoxications of captive bottlenose dolphins (*Tursiops truncatus*) in the Florida Keys. The cyanobacterial mat morphologically resembled the formerly classified, toxigenic, polyphyletic genus *Lyngbya* (Oscillatoriales). Phylogenetic characterization of the cyanobacterial assemblage inferred Oscillatoriacean membership including species from the genus *Neolyngbya*. Chemical analysis of the cyanobacterial mat determined the absence of plausible HAB-related neurotoxins: anatoxin-a, saxitoxin, brevetoxin-2 and domoic acid. Successive classical bioassay-guided fractionation of the cyanobacteria assemblage led to the isolation and characterization of a previously undocumented eudesmane-type sesquiterpene as a secondary metabolite exhibiting neurotoxic effects in the zebrafish (*Danio rerio*) embryo-larvae toxicological model, adapted to comparatively assess neurotoxicity against brevetoxin-2. Herein, the zebrafish neurotoxicological model used to investigate the biological activity of the cyanobacteria fractions are described relative toward exploring potential new HAB cyanoneurotoxins and understanding the role of cyano-HABs on marine mammals more generally.

5.2 Introduction

Florida's vast coastal and estuaries provide major habitats for bottlenose dolphins (*Tursiops truncatus*), often sustaining discrete residential groups of these apex predators considered the sentinels for these ecosystems (Bossart, 2011). These environments are particularly vulnerable to eutrophication related to Florida's rapid urbanization and agricultural growth over the last century (Lapointe and Clark, 1992; Wang et al., 1999; Sigua et al., 2000). The unique dolphin pods have been deleteriously afflicted (e.g., mass mortalities, diseases) by recurring Harmful Algal Bloom (HAB) events involving neurotoxin poisonings from brevetoxins (PbTx), domoic acid (DA) and saxitoxins (STX), particularly within Sarasota Bay along Florida's Gulf Coast and within the Atlantic Intercoastal Waterway (Twiner et al., 2011; Fire et al., 2015; Landsberg et al., 2006). Increased anthropogenic inputs to Florida's waterways have contributed to the rise in HAB frequencies and intensities (Phlips et al., 2011; Milbrandt et al., 2012; Lapointe et al., 2015). Consequently, estuarine residential bottlenose dolphins have been increasingly subjected to co-occurring marine and freshwater HAB-related toxins, particularly cyanotoxins, with detrimental outcomes including mortality, organ damage (i.e., internal, dermal) and neurodegeneration (Fire et al., 2008; Brown et al., 2018; Davis et al., 2019). Moreover, only recently has the co-occurrence of marine and freshwater HAB species been investigated (Bukaveckas et al., 2018; Peacock et al., 2018).

The Florida Keys, interfaced between Florida Bay and the Atlantic Ocean, are home to wild and human-managed bottlenose dolphins. The commercial marine mammal zoological facilities are connected to the surrounding native ecosystems via man-made canals and/or water pumping stations allowing for adequate flushing of their aquaria.

Wild bottlenose dolphins, known to primarily prey on seasonally available native fish, crustaceans and other living marine invertebrates, are fed, in captivity, strict piscivorous diets including sprat, herring, mackerel and squid, supplemented with prophylactic vitamins and freshwater to ensure proper nutrition and hydration. Recently, some captive bottlenose dolphins were observed, by staff, occasionally grazing members of the macrophytic algal community, including filamentous cyanobacteria, growing within their enclosures. The dolphins presented ensuing intoxication events of seemingly transient neurotoxicity, manifested by neurological symptoms of ataxia, blepharospasms and respiratory stress, as evaluated by the staff veterinarian. The facility's veterinarian addressed and typically resolved each apparent case of intoxication within several days. Although the macrophytic algal communities within the enclosures comprised several diverse taxa, and the dolphins grazed multiple members, the apparent intoxication events were generally linked to ingestions of the filamentous cyanobacteria.

Among the recognized cyanobacterial taxa associated with HABs, members of the polyphyletic, filamentous genus, *Lyngbya* (Oscillatoriales), are frequently linked to toxigenic blooms in freshwater, estuarine and marine ecosystems worldwide, including Florida (Capper et al., 2016; Foss et al., 2012; Burns, 2008). In freshwater habitats, *Lyngbya wollei* (Farlow ex Gomont) Speziale & Dyck 1992 has been associated with the production of multiple, water-soluble toxins, and specifically, the potent neurotoxic alkaloid, saxitoxin (STX) and its analogues (Carmichael et al., 1997). Moreover, the previously classified marine, filamentous species *Lyngbya majuscula* (Harvey ex Gomont) afforded copious biologically active, secondary metabolites, notably including several neurotoxic lipopeptides (Aráoz et al., 2010) and the non-proteinogenic amino

acid, β -methylamino-L-alanine (BMAA), controversially linked to neurodegenerative disease (Rodgers et al., 2018). The neurotoxin homoanatoxin-a, a potent analogue of the deadly anatoxin-a (ATX-a), primarily associated with freshwater cyanobacteria taxa, was identified in the marine, mat-forming filamentous cyanobacteria *Hydrocoleum lyngbyaceum* (Oscillatoriales) (Méjean et al., 2010).

More generally, *Lyngbya sensu lato (s.l.)* is, arguably, one of the most prodigious cyanobacterial producers of a largely unequalled diversity of bioactive metabolites including, several compounds which have been explored as leads to novel drugs (Swain et al., 2015). The potential role, however, of these biologically active metabolites as “toxins”, aside from the recognized “cyanotoxins” (e.g., STX, ATX-a, BMAA), has been relatively unexplored. Moreover, the genus *Lyngbya* is now recognized as a polyphyletic, mixed assemblage comprising multiple, closely related species, making morphological differentiation nearly impossible (Jones et al., 2011). Recent molecular and phylogenetic characterizations of *Lyngbya* spp. identified several new genera including *Limnoraphis* (Komárek et al., 2013), *Microseira* (McGregor et al., 2015), *Neolyngbya* (Caires et al., 2018a), and *Capilliphycus* (Caires et al., 2018b; Caires et al., 2019). Indeed, the cyanobacteria mixed assemblage (i.e., mat), chemically explored herein, resembled the polyphyletic, toxigenic *Lyngbya s.l.*, thus requiring a molecular and genetic identification approach (Lydon et al., submitted), was dominated by an undescribed species of *Neolyngbya*.

The present study used a dual strategy to identify neurotoxic metabolites from collections of the marine filamentous cyanobacteria mat affiliated with the captive dolphin intoxications. Collections of the cyanobacterial mat were chemically investigated

for the presence of the known HAB neurotoxins ATX-a, STX, PbTx-2 and DA, possibly contributing to the dolphin intoxications, and for which there are available standards and established analytical methods. In tandem, classical bioassay-guided fractionation techniques were used to explore known, or otherwise, uncharacterized neurotoxic metabolites. The biological assays, described herein, adapted the well-established zebrafish (*Danio rerio*) embryo developmental (Berry et al., 2007) and larval behavioral (Legradi et al., 2015) toxicological modes to comparatively assess the neurotoxicity of extracts and subsequent fractions against PbTx-2 as the positive control and negative controls of the untreated aquaria system water (ASW) and the methanolic (MeOH) solvent control.

5.3 Methods and Materials

5.3.1 Cyanobacteria Material

The mixed assemblage cyanobacteria sampled for the study were collected by snorkeling at a depth of 2-5 m (8-16 ft) at the marine mammal zoological facility in the Florida Keys, Florida, United States (25.084192° N, 80.442295° W), in January 2016. Initial morphology-based examination by light microscopy, of a small portion of the sample, associated the filamentous cyanobacteria with the polyphyletic, toxigenic genus *Lyngbya*. Aliquots of the main morphotypes were cleaned with deionized water and stored in 5 mL RNAlater (Ambion, Austin, TX, USA) at (-80 °C) for phylogenetic characterization. Voucher specimens (Lydon-DP2016-*Lyngbya* spp.) were prepared with 4% formalin (Fisher Scientific, Fair Lawn, NJ, USA) in ethanol (Fisher) and stored at the Marine Macroalgae Research Laboratory at Florida International University, Miami, FL, as previously described in Chapter Two of this dissertation (see 2.2.1.2 Taxonomic

Reference Samples). The remaining sample of mixed assemblage cyanobacteria mat was cleaned of obvious debris, fauna and macroalgae, excess moisture removed, then lyophilized and stored frozen (-20 °C) until chemically explored.

5.3.2 Chemical Explorations of Cyanobacteria Samples

Wet samples (ca. 5 gallons) of the mixed assemblage cyanobacteria mat, collected January 2016, were rinsed well with site seawater to remove obvious debris, fauna and macroalgae and prepared as previously described in Chapter Two of this dissertation (see 2.2.1.4 Cyanobacteria Chemical Evaluation Samples). Briefly, the cyanobacteria biomass was lightly rinsed with deionized water and patted dry with paper towels to remove excess moisture. The semi-dried material was then frozen (-80 °C) and lyophilized in preparation for chemical exploration of known or otherwise, previously uncharacterized neurotoxic secondary metabolites. The lyophilized cyanobacteria material was stored frozen (-20 °C) until chemical analyses were performed.

5.3.2.1 Known Neurotoxin Evaluation of Cyanobacteria Samples

A 25 g portion of the lyophilized cyanobacteria was shipped, frozen, to a commercial analytical laboratory (GreenWater Laboratories/CyanoLab, Palatka, FL, USA) for chemical analysis of the harmful algal neurotoxins ATX-a, STX, PbTx-2, and DA. The analytical detection (i.e., LC-MS/MS, ELISA) methods are detailed in Chapter Four (see 4.2.3 Commercial Chemical Evaluation, Appendix). Briefly, for each neurotoxin investigated, an appropriate sample (ca., 5 mg) was aliquoted from the lyophilized cyanobacteria material to prepare replicate extracts. One replicate of each extract was spiked with the applicable analyte standard, as a Laboratory Fortified Matrix LFM, to establish the relevant method detection limit. Neurotoxin-specific ELISA kits

(Abraxis, Inc., Warminster, PA, USA) were used to evaluate the presence of STX and PbTx-2. Previously established, neurotoxin-specific LC-MS/MS methods were used to detect the presence of ATX-a and DA.

5.3.2.2 Bioassay-Guided Fractionation of Cyanobacteria Samples Using Zebrafish Neurotoxicological Models

As described in Chapter Six (see 6.3.7 Zebrafish Neurotoxicity Assays), Wild-type AB, embryonic (4-6 hours post-fertilization [hpf]) and larval (3-5 days post-fertilization [dpf]) zebrafish (*Danio rerio*), were purchased from the Zebrafish Core Facility, University Miami, Miami, FL. All experiments were performed according to IACUC approved animal protocols (Appendix). Existing toxicological methods were adapted to evaluate developmental (Berry et al., 2007) and behavioral (Legradi et al., 2015) neurotoxicity endpoints including percent mortality, 24-hpf spontaneous coiling frequency, hatching rate, heart rate, and the percentage of embryos exhibiting swimming-related issues (i.e., irregular swim bladder, abnormal swim behavior) as described by Henry et al. (1997) and Kalueff et al. (2013). The experiments were conducted in solvent-resistant, polypropylene 24-well (embryos) and 96-well (larvae) plates (Evergreen Scientific, Caplugs CA, Rancho Domingo, CA, USA). Test concentrations were added to individual wells and allowed to air-dry prior to exposing test subjects. Replicate zebrafish test subjects (i.e., embryos) were exposed to three concentrations of cyanobacteria extracts at 10, 25 or 50 ppm, respectively, or the positive control, PbTx-2 standard (Sigma Aldrich, Saint Louis, MO, USA), at 2.79, 5.59, 11.17 and 27.93 nM respectively, or the negative control, aquarium system water (ASW). Five embryos (4-6 hpf) per 1 mL of ASW per well (24-well plate) were used for the ZDN studies. The ZLNB studies used

one, 5-dpf larva, with its swim bladder inflated and exhibiting normal beat and glide swim behavior, per 100 μ L ASW per well (96-well plate), with 6 or 12 replicate test subjects per concentration. Herein, additional (e.g., up to 24) test subjects were used to evaluate larval behavioral neurotoxicity of PbTx-2 and cyanobacteria material (i.e., extracts, fractions) at four exposure concentrations, respectively 2.5 ppb, 5 ppb, 10 ppb and 25 ppb over 24 hpe. All experiments were conducted at 28 °C and a 14-h light and 10-h dark photoperiod. A Spot Imaging Solutions TLB-4000 equipped with a Fisher Bioblock Scientific Carl Zeiss Microimaging STEMI 2000-C stereomicroscope and an Optronics Microcast HD Studio 3CCD 1080P 2MP digital camera was used to examine the zebrafish embryo-larva development and behavior at selected timepoints. Daily monitoring of embryogenesis, through 5 dpf, included percentages of adverse neurotoxic and developmental effects including mortality, atypical 24-hpf spontaneous coiling frequencies, abnormal growth and hatching rates, irregular heart rhythms, and abnormal swimming behaviors, relative to ASW negative controls. Larva were monitored over 24 hours for percentages of mortality, aberrant swimming behaviors and swim bladder irregularities compared to the untreated controls. Data were statistically analyzed by one-way ANOVA followed by Tukey's Honestly Significant Difference (HSD) multiple comparison test, using the Real Statistics Resource Pack software (Release 5.4.2), copyright (2013-2019) Charles Zaiontz www.real-statistics.com (last accessed 23JAN2018). Statistical significance was defined by p values of ≤ 0.05 , ≤ 0.01 , and/or ≤ 0.001 .

Fractionation of the lyophilized cyanobacteria biomass began after preliminary exposure concentrations of 25, 75, and 100 ppm, prepared from a 1 mg aliquot of

lyophilized cyanobacteria biomass, dissolved in 1 mL MeOH, indicated biological activity using the zebrafish developmental neurotoxicity (ZDN) and larval neurobehavioral (ZLNB) assays. The bioassay-guided fractionation methodology is fully detailed in Chapter Six (see 6.3.3 Bioassay-Guided Fractionation of Eudesmacarbonate). At each fractionation step, neurotoxicological activity was assessed using the ZDN and ZLNB assays until the putative metabolite (i.e., compound 1) was obtained as (4*S*,5*R*,6*R*,7*S*,10*S*)-eudesman-(4*S*,6*R*)-cyclocarbonate (i.e., eudesmacarbonate). Briefly, 50 g (dry weight) of lyophilized cyanobacteria biomass, sampled in January 2016, was systematically extracted with EtOAc-MeOH (1:1), concentrated in vacuo, and thrice partitioned between EtOAc-H₂O (3:1). The pooled, lipophilic (i.e., EtOAc) crude extract was concentrated in vacuo whilst, the pooled polar crude extract immediately partitioned between 2-butanol (BuOH) and HPLC-grade water (H₂O). The BuOH crude extract and the aqueous (Aq) crude extract were concentrated in vacuo. Aliquots (ca. 2 mg) of the crude cyanobacteria extract and the solvent partitioned extracts were removed and resuspended in methanol to prepare 1 mg/mL bioassay samples. The EtOAc crude extract bioassay sample exhibited neurotoxicological activity comparable to PbTx-2. Thus, a 500 mg aliquot of the EtOAc crude extract was dissolved in EtOAc and concentrated onto a Büchi Reveleris HP silica gel, 60-75 Å mesh, 16-24 µm cartridge and subjected to normal-phase semi-preparative flash chromatography using a Büchi Reveleris X2 automated flash chromatography system equipped with UV/ELSD detection (Büchi Corp., Flawil, Switzerland). A stepwise solvent gradient of n-hexanes-EtOAc-MeOH from 95:5:0 to 0:0:100 at 20 mL/min was used to collect fractions at approximately 20 mL intervals over 80 min. Fractions were monitored for purity by normal-phase thin layer

chromatography (TLC). Aluminum-backed silica gel TLC plates with UV 254 nm fluorescence, 250 μ M (Whatman LTD, Maidstone, Kent, England) were developed using 65:30:5 n-hexanes-EtOAc-EtOH. Fractions with multiple retention factors were pooled by similar retention factor (R_f) values, dried in vacuo, and retained for potential future separation. Semi-pure fractions were dried in vacuo and reconstituted with EtOAc to 1 mg/mL concentrations to comparatively assess neurotoxicity against PbTx-2 (see below). A semi-pure fraction (i.e., F29), eluted with 50:50:0 n-hexanes-EtOAc-MeOH, exhibited bioactivity aligned with PbTx-2. Further separation, using reversed-phase C₁₈ (Varian BondElut, 1.6 g) vacuum assisted column chromatography, with a step gradient of 20-0% aqueous methanol, yielded the bioactive fraction F29-1 in the first eluent. Isocratic elution using C₁₈ with 20% aqueous methanol isolated the bioactive metabolite in the first fraction. Subsequently purified with MeOH, the structural elucidation of the neurotoxic metabolite was determined, by the chemical analysis methods, to be the novel, cyclic carbonate ester of an eudesmane-type sesquiterpene, (4*S*,5*R*,6*R*,7*S*,10*S*)-eudesman-(4*S*,6*R*)-cyclocarbonate (i.e., eudesmacarbonate) as detailed in Chapter Six of this dissertation (see 6.3.4 Chemical Characterization of Eudesmacarbonate). All solvents were HPLC or LC-MS grade (Fisher Scientific, OmniSolv).

5.4 Results

Commercial analysis (GreenWater Laboratories/CyanoLab, Palatka, FL, USA) of the 2016 collected cyanobacteria biomass did not detect any of the known HAB-related neurotoxins (i.e., ATX-a, STX, PbTx-2, DA) at levels above the respective method limit of detection. The full report is attached in the appendix (See Appendix). The absence of these neurotoxins prompted the bioassay-guided fractionation of a portion of the

remaining lyophilized cyanobacteria biomass (50 g, dry weight) for the potential presence of neurotoxic secondary metabolites. Bioactivity was established if extracts exhibited neurotoxicity in the zebrafish embryo and larval-behavioral toxicological models compared to the recognized, marine HAB-neurotoxin, PbTx-2. Embryo development and behaviors over five days and larval behaviors over 24 hours were monitored for key endpoints associated with neurotoxicity. Quantitative developmental neurotoxicity assessments were based on abnormal spontaneous coiling frequencies, percent mortality and deformity, abnormal hatching rates and heart rhythms, and swim bladder dysfunction (e.g., irregular swim bladder inflation, aberrant swimming behaviors). Larval behaviors, indicative of neurotoxicity, were monitored including percent mortality, ataxia-related swimming behaviors and swim bladder dysfunction (i.e., irregular swim bladder morphologies). Biological activity (i.e., neurotoxicity, teratogenicity) was assessed at each fractionation step until a putative, compound exhibiting neurotoxic effects aligned with PbTx-2, was isolated and structurally identified as eudesmacarbonate (Figure 5.1).

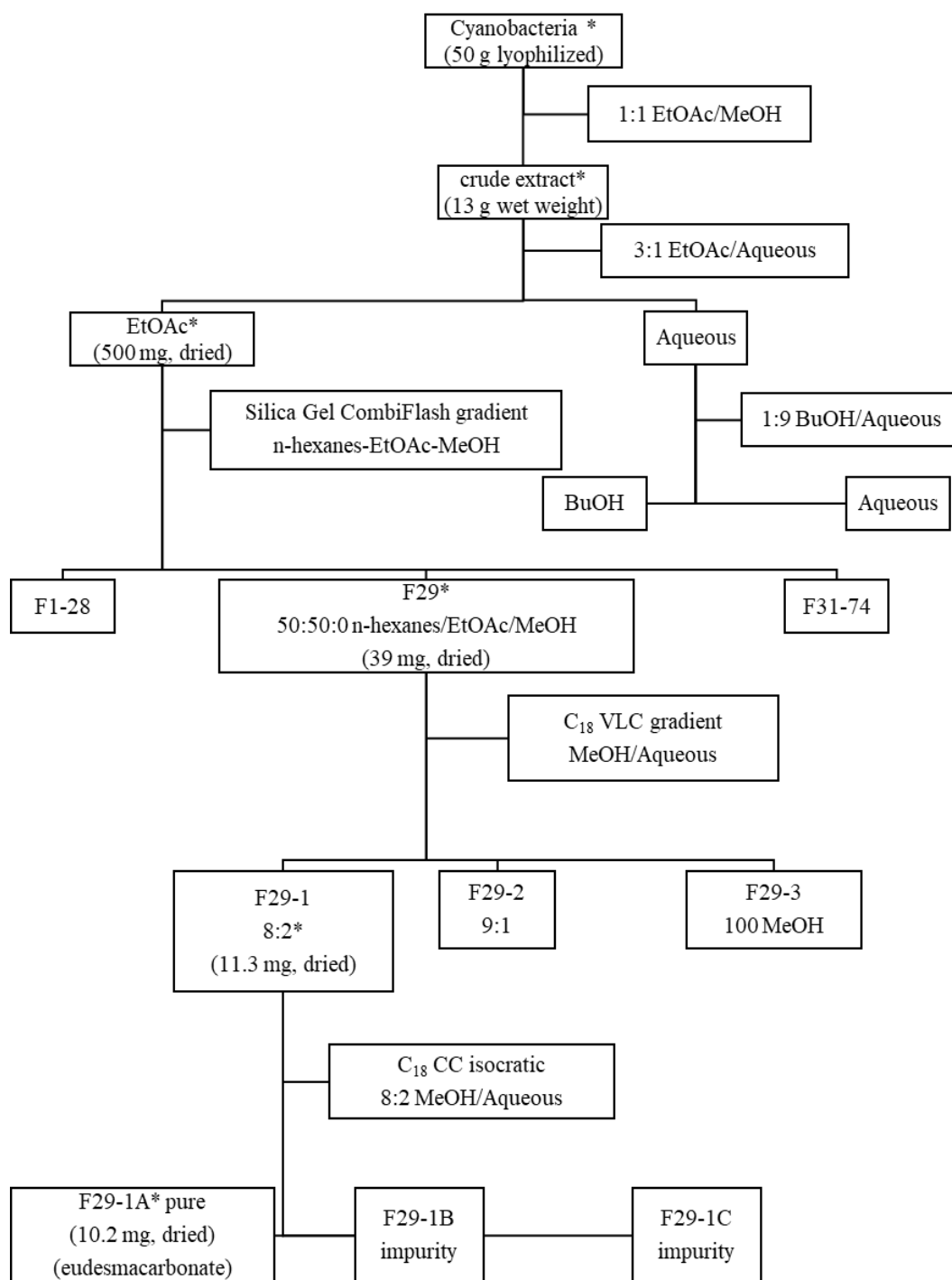


Figure 5.1 Bioassay-guided fractionation scheme of invest cyanobacteria collected January 2016. The * denotes biologically active fractions exhibiting neurotoxicity aligned with PbTx-2 positive control in the zebrafish embryo-larvae neurotoxicological models.

Developmental neurotoxicity was assessed for three concentrations of each fraction compared to the ASW negative control, the MeOH solvent control and four concentrations of PbTx-2 standard used as the positive controls. Fractions were tested at the respective exposure concentrations of 10, 25 and 50 ppm based on the results of preliminary exposures to the crude cyanobacteria extract exhibiting 100% lethality at concentrations of 75 ppm and higher. The larval neurotoxicity assessments of cyanobacteria fractions included the additional exposure concentration of 2.5 ppm. Exposures to PbTx-2 were evaluated using 2.5, 5, 10 and 25 ppb, respectively for the embryo bioassay. Larvae were respectively exposed to 2.5, 10, 25 and 50 ppb PbTx-2 or cyanobacterial material (i.e., extracts, fractions) at 2.5, 10, 25 and 50 ppm or the negative controls (i.e., ASW, MeOH). The fractions exhibiting neurotoxicity, relevant to PbTx-2, guided the ultimate isolation and purification of eudesmacarbonate (F29-1A) and are reported herein. The biological activity of eudesmacarbonate are detailed in Chapter Six (see 6.4.3 Biological Activity of Eudesmacarbonate, Appendix).

5.4.1 Average Percent Mortality of Embryos

No mortalities were observed through Day Five (5) for any of the four PbTx-2 standard exposure concentrations or either of the negative controls (i.e., ASW, MeOH). Bioassays of the crude extracts obtained from the initial fractionation of the lyophilized cyanobacteria indicated neurotoxicity in the non-polar (i.e., EtOAc) fraction, lethality in the mid-polar BuOH fraction, and inconclusive (i.e., variable) biological activity in the polar (i.e., Aq) fraction (Figure 5.2, Appendix). Thus, the EtOAc crude extract was pursued due to the sublethal biological activity observed (Figure 5.2). The LD₅₀ value of 36.1 ppm for the EtOAc crude extract was extrapolated by linear regression analysis of

the logarithmic (Log_{10}) concentration versus percent mortality plot through five dpf (Figure 5.3).

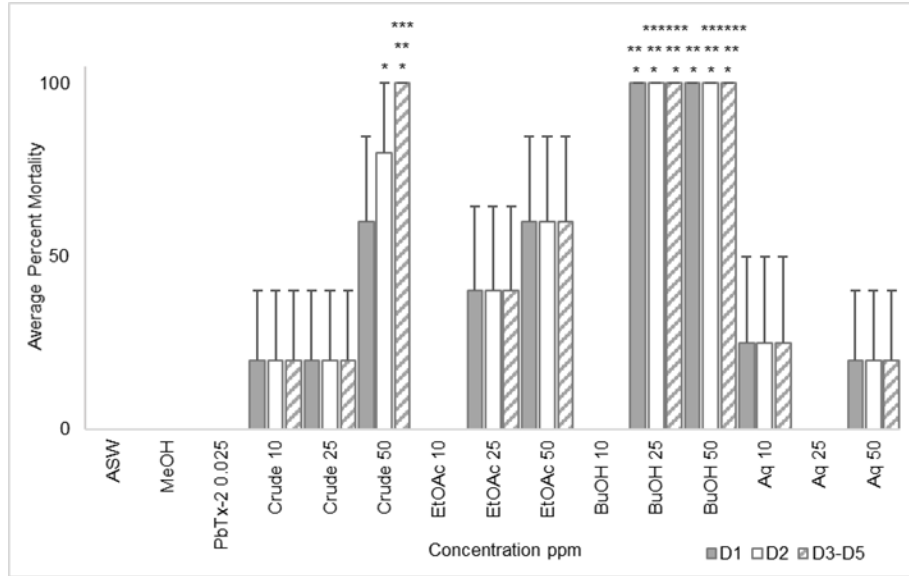


Figure 5.2 Percent mortality of crude cyanobacteria extracts through 5 dpf compared to controls. Error bars indicate \pm SEM ($n = 5$). The *, **, *** respectively denote $p < 0.05$, $p < 0.01$ and $p < 0.001$ significance derived by one-way ANOVA followed by the Tukey HSD multiple comparison test relative to untreated ASW control.

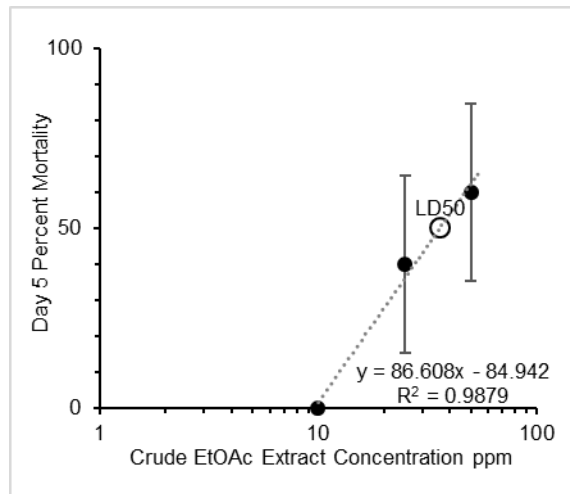


Figure 5.3 The LD_{50} value of the cyanobacteria EtOAc extract at 5 dpf (Day 5) extrapolated by linear regression analysis of the Log_{10} concentration versus percent mortality plot with error bars indicating the \pm SEM ($n = 5$).

Automated, normal phase (i.e., Si-gel) chromatographic separation of the EtOAc crude extract yielded 74 fractions of which fraction F29 exhibited potential neurotoxicity in the ZFNT bioassay. Subsequent, orthogonal reversed-phase (i.e., C₁₈) chromatographic separation of F29 afforded three fractions that were tested for neurotoxicity against PbTx-2 (see Appendix). Only subfraction F29-2 exhibited 20% ± 20% (SEM, n = 5) mortality within 24 hours and increased to 100% by Day 3 compared to the controls (Figure 5.4).

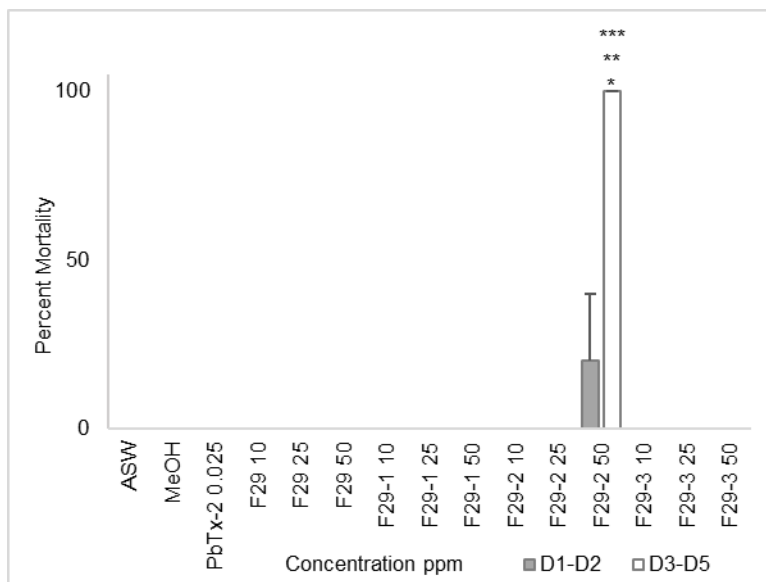


Figure 5.4 Percent mortality of cyanobacteria EtOAc extract F29 fractions through 5 dpf compared to controls. Error bars are ± SEM (n = 5). The *, **, *** denote the respective p < 0.05, p < 0.01 and p < 0.001 significance derived by one-way ANOVA followed by the Tukey HSD multiple comparison test relative to the untreated ASW control.

5.4.2 Average Percent Deformed Embryos

Within 24 hpe, significant deformities, quantified by the percentage of deformed embryos (%D), were observed in all PbTx-2 treatments above 2.79 nM (2.5 ppb) compared to the ASW and MeOH controls, indicating neurotoxic and/or teratogenic effects (Figure 5.5, Appendix). During the first two exposure days, the percentages of deformed embryos remained consistent at approximately 30% for the three highest PbTx-

2 treatments (Figure 5.5a). Deformities occurred in the lowest PbTx-2 exposure condition by Day 3 (Figure 5.5b). The percentages of deformed embryos of the two highest PbTx-2 exposure conditions significantly increased to 40% and 93%, respectively, by Day 4 (Figure 5.5c). By Day 5, all embryos exposed to 2.79 nM (25 ppb) PbTx-2 were deformed (Figure 5.5d). The 5 dpf ED₅₀ was approximated by the 46.7 ± 6.7% (SEM, n = 3 replicates of 5 embryos each) of deformed embryos observed in the 11.2 nM treatment.

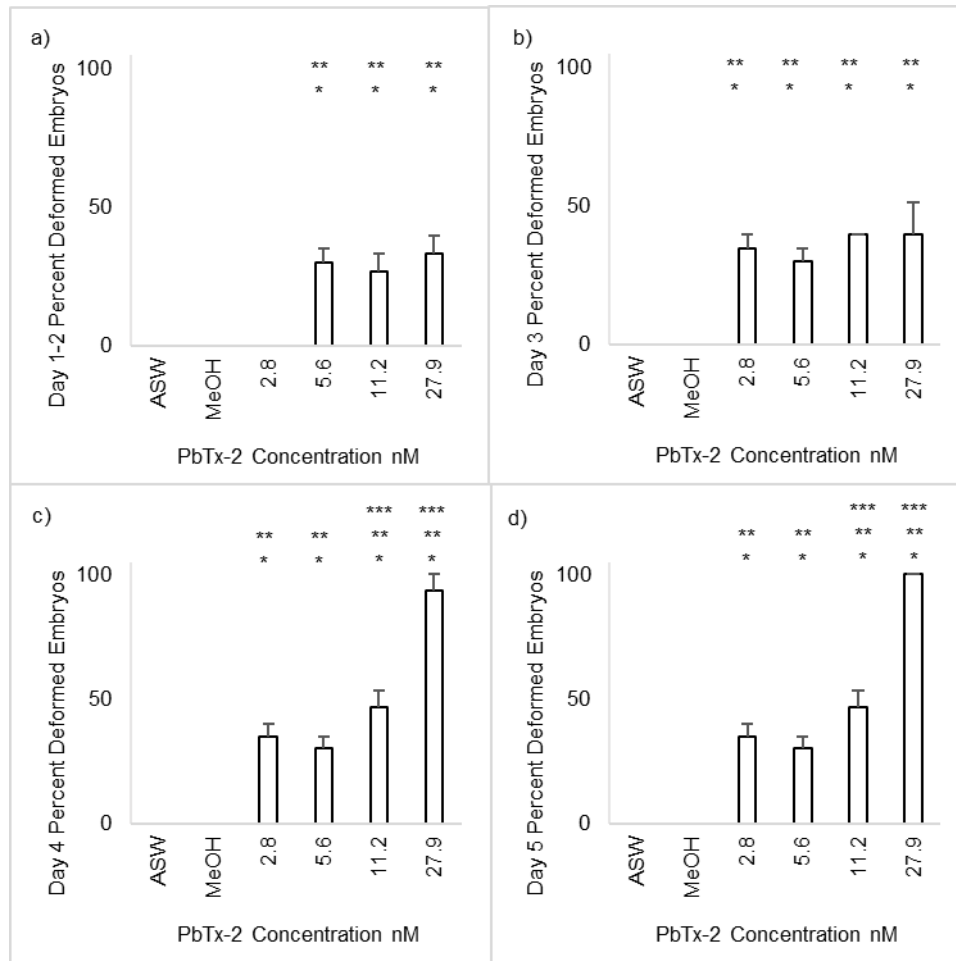


Figure 5.5 Percentages of deformed embryos exposed to PbTx-2 positive control compared to the negative controls (i.e., ASW, MeOH) through 5 dpf: a) Day 1-2 results, b) Day 3 results, c) Day 4 results and d) Day 5 results. Error bars are ± SEM (n = 3). The *, **, *** denote the respective $p < 0.05$, $P < 0.01$ and $p < 0.001$ significance relative to the MeOH solvent control derived from one-way ANOVA followed by the Tukey HSD multiple comparison test.

Thus, the highest test concentration of PbTx-2 standard (i.e., 0.025 ppm) was chosen as the positive control to comparatively assess the potential neurotoxicity of the crude cyanobacteria and subsequent fractions against the ASW and MeOH negative controls (Figure 5.6, Appendix). Within 24 hpf, embryos exposed to the positive control (i.e., 0.025 ppm PbTx-2) and the cyanobacteria extracts, except the lowest BuOH extract treatment, exhibited deformities compared to the negative controls (i.e., ASW, MeOH), indicative of neurotoxicity (Figure 5.6). Embryos exposed to the 25 and 50 ppm crude cyanobacteria crude and lipophilic (i.e., EtOAc, BuOH) extracts and the 50 ppm EtOAc-derived fraction F29-2 exhibited significant deformities relative to the negative controls through Day 5 (Figure 5.6). However, no significant differences in the average percentages of deformed embryos were observed between the 0.025 ppm PbTx-2 positive control and any of the cyanobacteria test solutions through Day 5 (Figure 5.6). Dose-dependent trends were observed at 24 hpf (Day 1) for the crude cyanobacteria and EtOAc extracts with respective ED₅₀ values determined to be 17.3 and 16.6 ppm (Figure 5.7). Results obtained for the aqueous extract were variable and generally not significantly different than the untreated ASW control (see Figure 5.6).

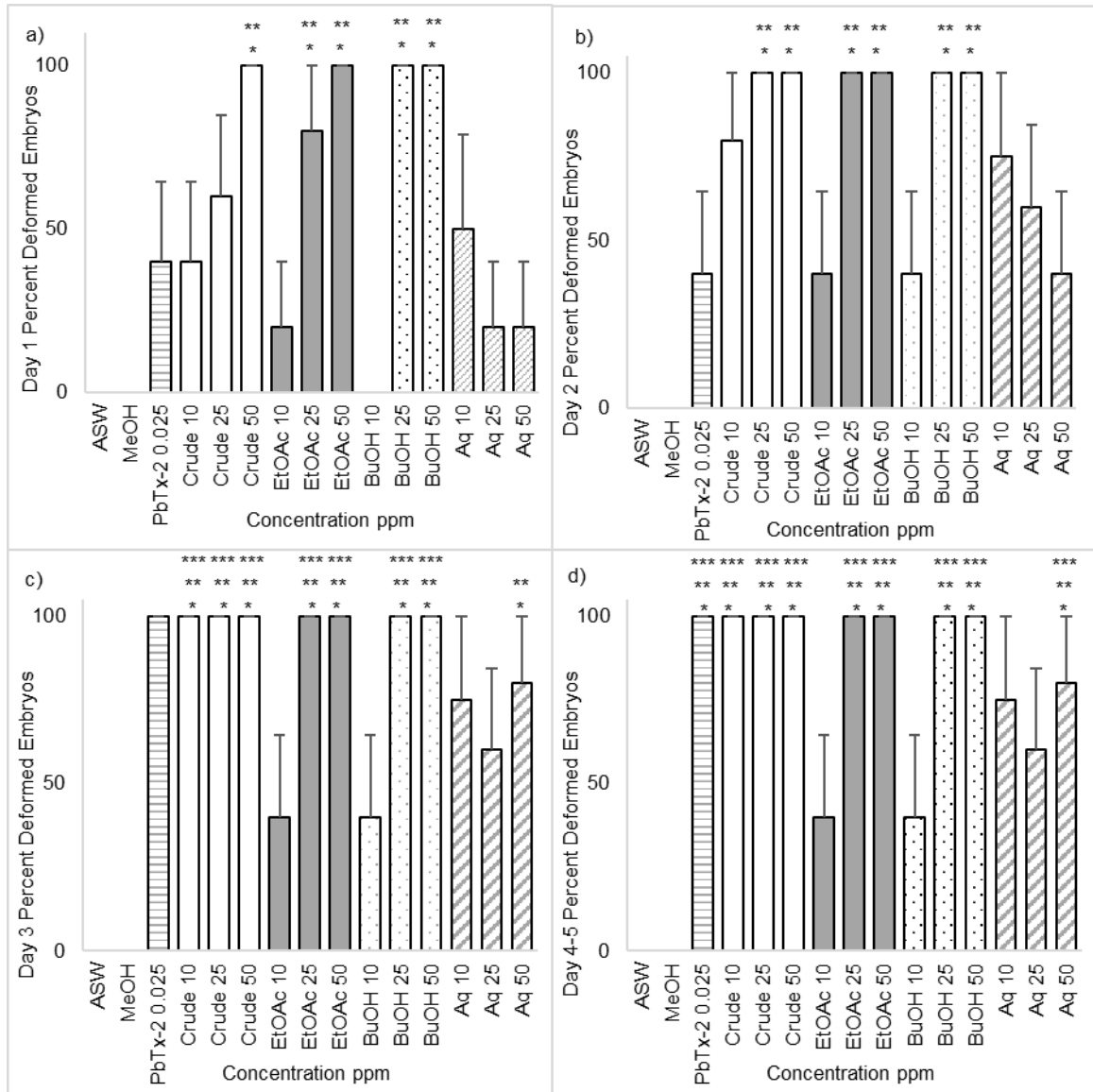


Figure 5.6 Daily percentages of deformed embryos per cyanobacteria extract exposure condition compared to controls with error bars indicating \pm SEM ($n = 5$): a) Day 1, b) Day 2, c) Day 3 and d) Day 4-5. The *, **, *** denote the $p < 0.05$, $p < 0.01$ and $p < 0.001$ significance, respectively derived by one-way ANOVA followed by the Tukey HSD multiple comparison test relative to untreated ASW control.

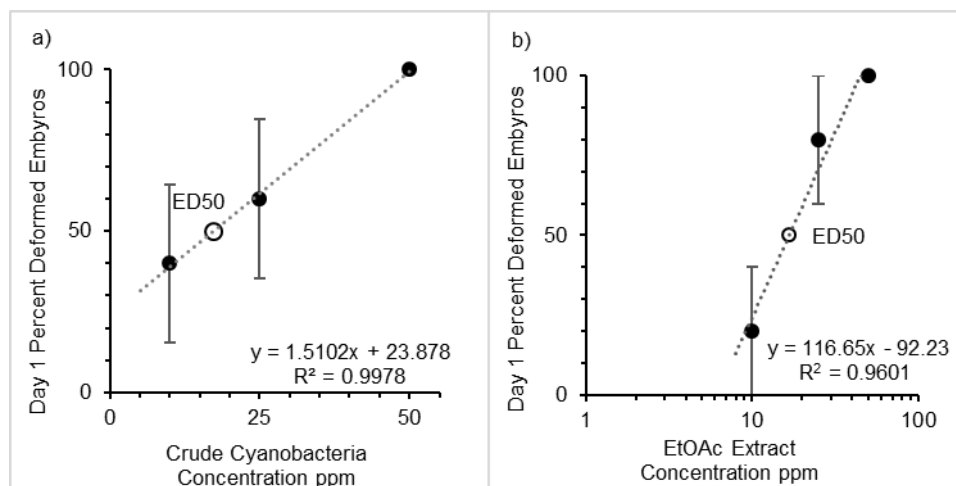


Figure 5.7 The 24-hpf (Day 1) dose-dependent trends of percent deformed embryos observed for crude cyanobacteria extracts with extrapolated ED₅₀ values: a) Linear trend of cyanobacteria crude extract and b) Logarithmic trend for EtOAc extract. Error bars are \pm SEM (n = 5).

Embryonic exposure to the lipophilic (i.e., EtOAc) F29 subfractions induced deformities through Day 5 with only the 50 ppm F29-2 subfraction exhibiting significantly more deformed embryos than the untreated ASW control (Figure 5.8). Subfraction F29-2 exhibited a linear trend on Day 1 with an extrapolated ED₅₀ value of 29.7 ppm that continued through 5 dpf allowing extrapolation of the respective ED₅₀ values of 26.7 and 23.2 ppm observed for Days 2-3, Days 4-5 (Figure 5.9). An ED₅₀ value of 78.2 ppm was extrapolated from the logarithmic dose-dependent trend observed on Day 2 for subfraction F29-1 (Figure 5.10). By Day 3, $40 \pm 24.5\%$ (SEM, n = 5) of the embryos exposed to 25 and 50 ppm F29-1 were deformed, persisting through Day 5 (see Appendix).

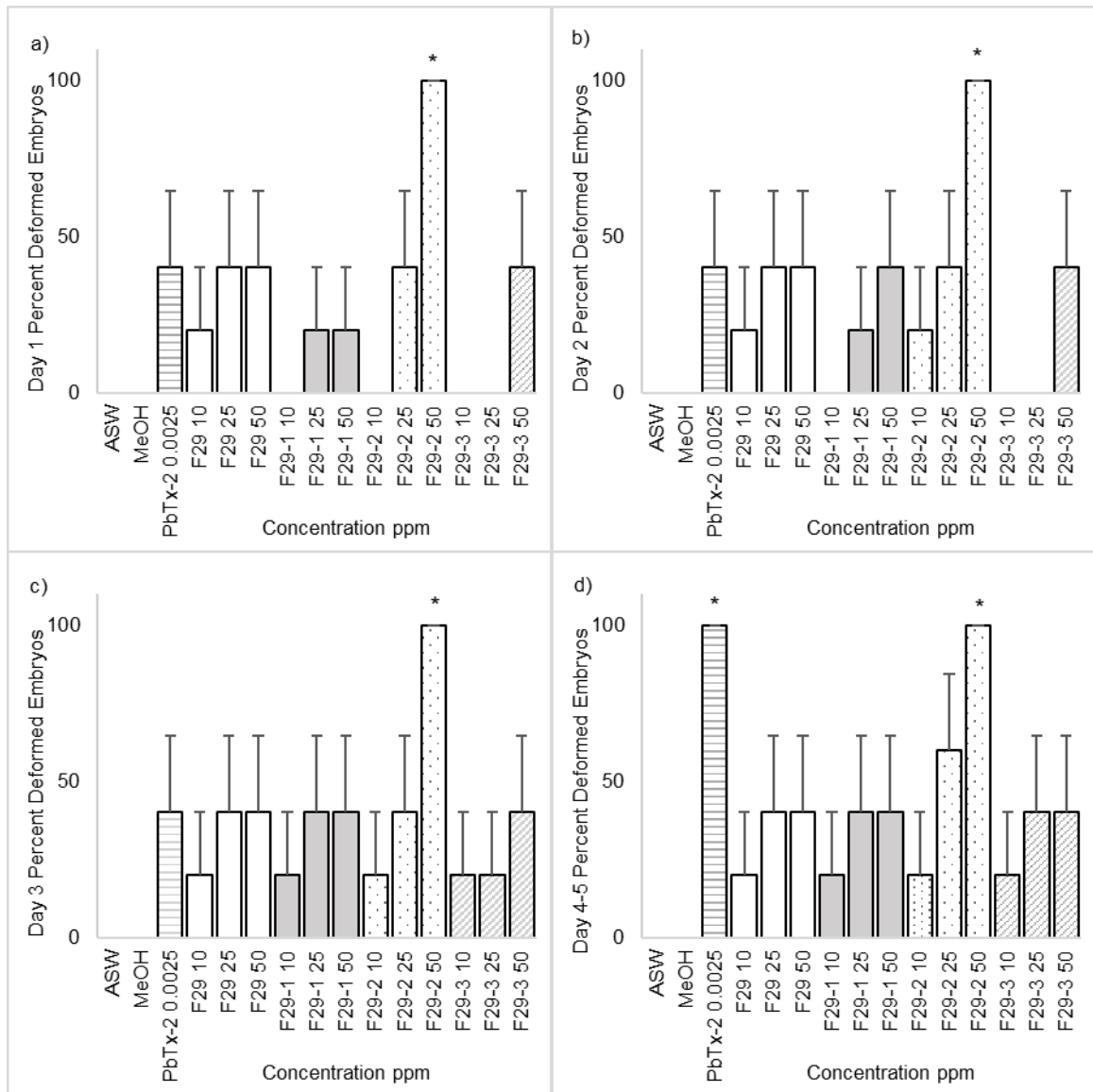


Figure 5.8 Daily percentages of deformed embryos per treatment with EtOAc-derived F29 fractions relative to controls with error bars indicating \pm SEM (n = 5): a) Day 1, b) Day 2, c) Day 3 and d) Day 4-5. The *, **, *** denote the $p < 0.05$, $p < 0.01$ and $p < 0.001$ significance, respectively derived by one-way ANOVA followed by the Tukey HSD multiple comparison test relative to untreated ASW control.

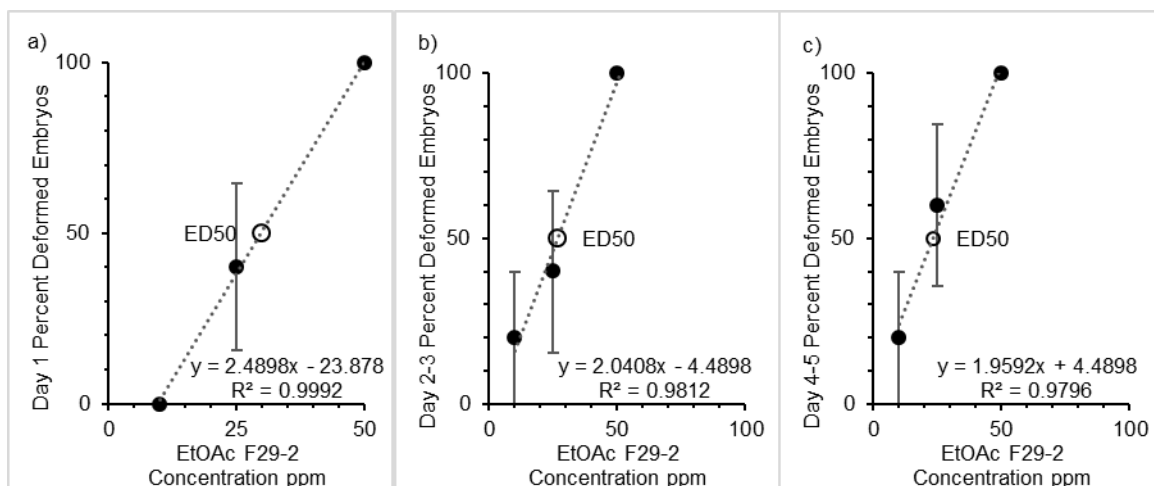


Figure 5.9 Linear dose dependency of lipophilic subfraction F29-2 deformed embryos through 5 dpf with error bars indicating \pm SEM (n = 5): a) Day, b) Day 2-3 and c) Day 4-5.

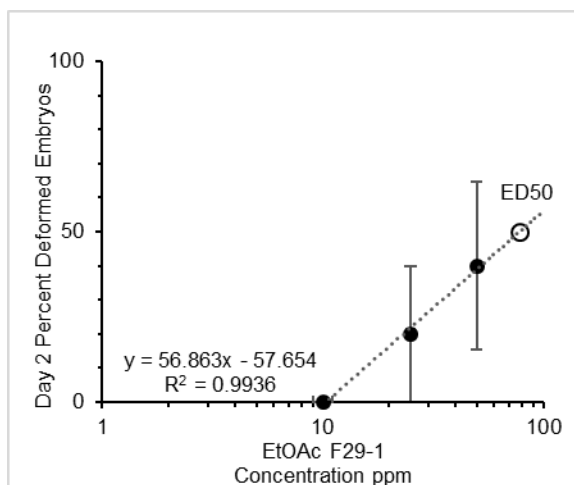


Figure 5.10 Extrapolated Day 2 percent deformed embryos ED₅₀ value for lipophilic subfraction F29-1 with error bars denoting \pm SEM (n = 5).

5.4.3 Average 24-hpf Spontaneous Coiling Frequencies

The average 24-hpf spontaneous coiling frequencies (SCF) were quantified as the number of coils per minute (cpm) per embryo per test solution after 24 hours of exposure (see Appendix). The 3.5 ± 0.4 cpm (\pm SEM, n = 15) average SCF of the ASW negative control did not significantly differ from the MeOH solvent control average of 3.2 ± 0.3 cpm (SEM, n = 15) (Figure 5.11a). Of the PbTx-2 exposure conditions, only the 11.2 nM

concentration exhibited a significantly slower average SCF than the ASW and MeOH controls, indicative of neurotoxicity (Figure 5.11a, Appendix). The average SCF for all PbTx-2 exposed embryos varied between a minimum of 1.3 ± 0.3 cpm (SEM, n = 15) for the 11.2 nM concentration and a maximum of 3.2 ± 0.4 cpm (SEM, n = 13) for the 5.59 nM concentration. None of the embryos exposed to the cyanobacteria extracts or subsequent lipophilic subfractions exhibited significantly different average SCF values compared to the 2.79 nM (0.025 ppm) PbTx-2 positive control average of 2.0 ± 0.6 cpm (SEM, n = 5) (Figure 5.11b, Figure 5.12, Appendix). The average SCF values of all cyanobacteria test solutions with surviving embryos, ranged between 0.0 ± 0.0 cpm (SEM, n = 5) and 3.2 ± 0.8 cpm (SEM, n = 5), suggesting neurotoxicity. Although no specific dose-dependent trends were observed for the cyanobacteria extracts, the average SCF values for the were generally aligned with that of the PbTx-2 positive control, implying neurotoxic effects (Figure 5.11b). Linear dose-dependent trends were observed for the average SCF values for the lipophilic F29-2 and F29-3 fractions (Figure 5.13). Specifically, embryos exposed to increasing concentrations of fraction F29-2 exhibited reduced average SCF values (Figure 5.13a) whilst F29-3 exposure induced a positive trend (Figure 5.13b).

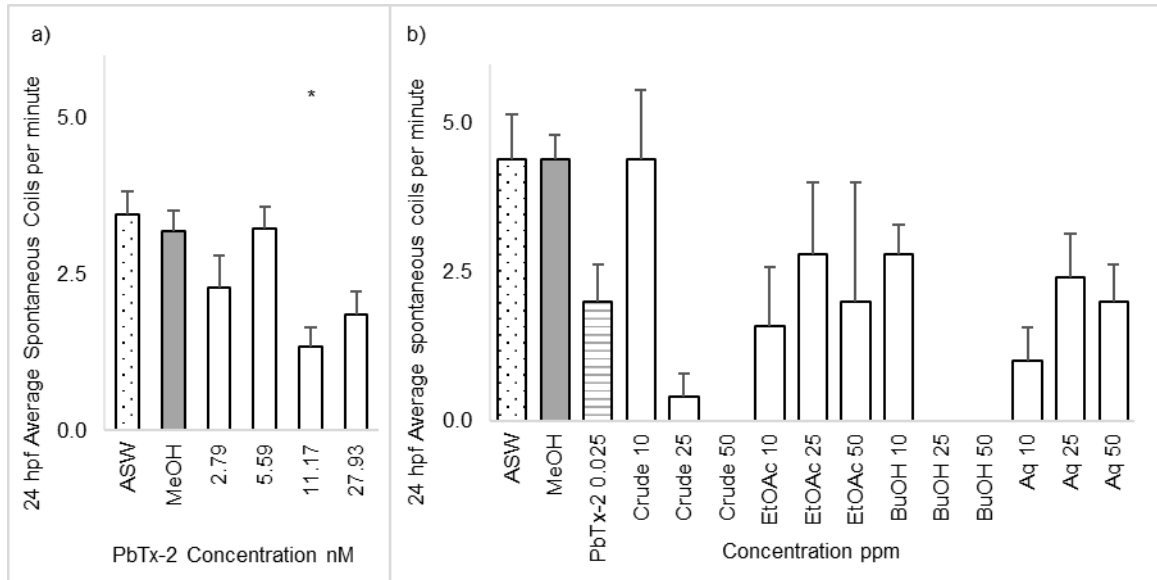


Figure 5.11 The 24-hpf average spontaneous coiling frequencies of embryos exposed to PbTx-2 and cyanobacteria extracts, quantified as coils per minute: a) Plot of PbTx-2 test solutions compared to ASW and MeOH controls with error bars indicating \pm SEM ($n = 15$) and b) Plot of cyanobacteria extracts compared to controls with error bars indicating \pm SEM ($n = 5$). The *, **, *** denote the $p < 0.05$, $p < 0.01$ and $p < 0.001$ significance, respectively derived by one-way ANOVA followed by the Tukey HSD multiple comparison test. Note: Significance is relative to untreated ASW in a) and relative to PbTx-2 in b).

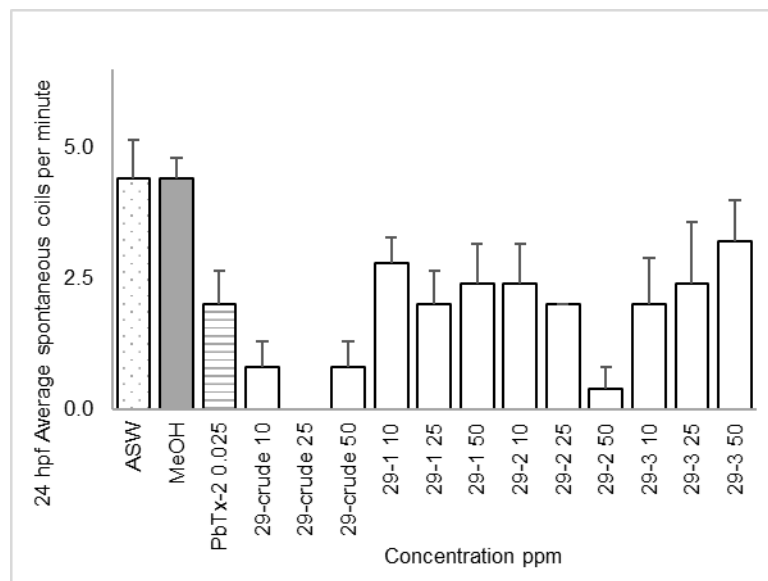


Figure 5.12 The 24-hpf average spontaneous coiling frequencies of embryos exposed to the lipophilic fractions of F29 compared to controls. Error bars are \pm SEM ($n = 5$). One-way ANOVA followed by the Tukey HSD multiple comparison test ($p < 0.001$) showed no significant differences between fractions and PbTx-2 positive control.

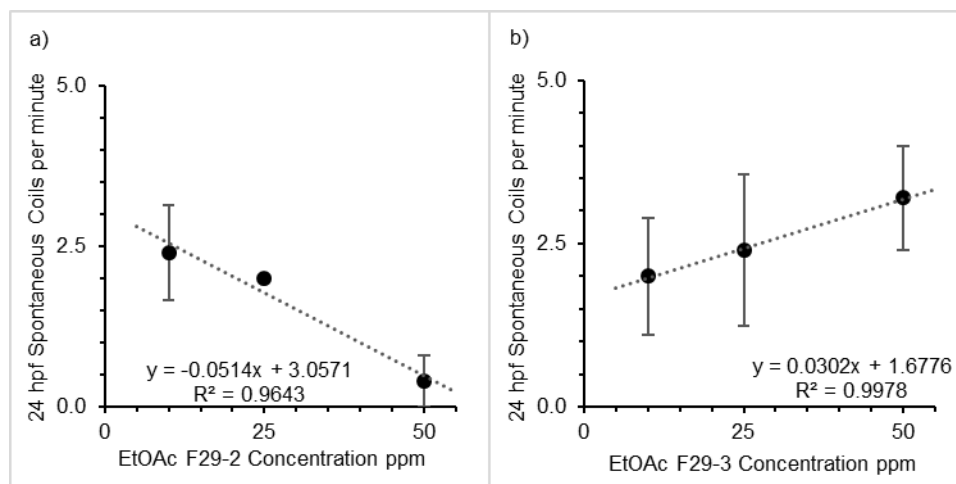


Figure 5.13 Linear dose-dependency of 24-hpf average spontaneous coiling frequencies for the lipophilic fractions a) F29-2 and b) F29-3 with error bars denoting \pm SEM (n = 5).

5.4.4 Average Embryo Hatching Rates and Percentages

As anticipated, no embryos in any of the solutions tested had hatched at the 24-hpf (Day 1) monitoring interval. The Day 2 and Day 3 average hatching rates (%H), quantified as the percentage of hatched embryos, of all four PbTx-2 test concentrations were not significantly different from those of the ASW and MeOH controls (Figure 5.14a). The average Day 2 %H for the ASW and MeOH controls were $46.7 \pm 6.7\%$ (SEM, n = 3) and $40.0 \pm 11.5\%$ (SEM, n = 3). The average %H for the PbTx-2 treatments ranged between $41.7 \pm 22.0\%$ (SEM, n = 3) for 55.9 nM PbTx-2 and $68.3 \pm 22.4\%$ (SEM, n = 3) for 2.79 nM PbTx-2, with no specific trend observed. All control embryos were 100% hatched by Day 3. No specific hatching trends were observed for PbTx-2 exposed embryos, implying any neurotoxic effects related to PbTx-2 exposure during embryogenesis do not affect hatching time or success. In contrast, exposures to the cyanobacteria extracts and fractions generally adversely affected hatching rates through five dpf (Figure 5.14b). The average %H of surviving embryos exposed to the cyanobacteria crude extracts were delayed, compared with embryos exposed to 27.9 mM

(0.025 ppm) PbTx-2 through Day 5, excepting the 10 ppm BuOH and 25 ppm aqueous (Aq) exposure conditions (Figure 5.14b). The crude EtOAc extract displayed a logarithmic dose-dependent hatching rate, suggesting teratogenicity, perhaps associated with neurotoxicity, and an extrapolated ED₅₀ value of 36.1 ppm (Figure 5.15).

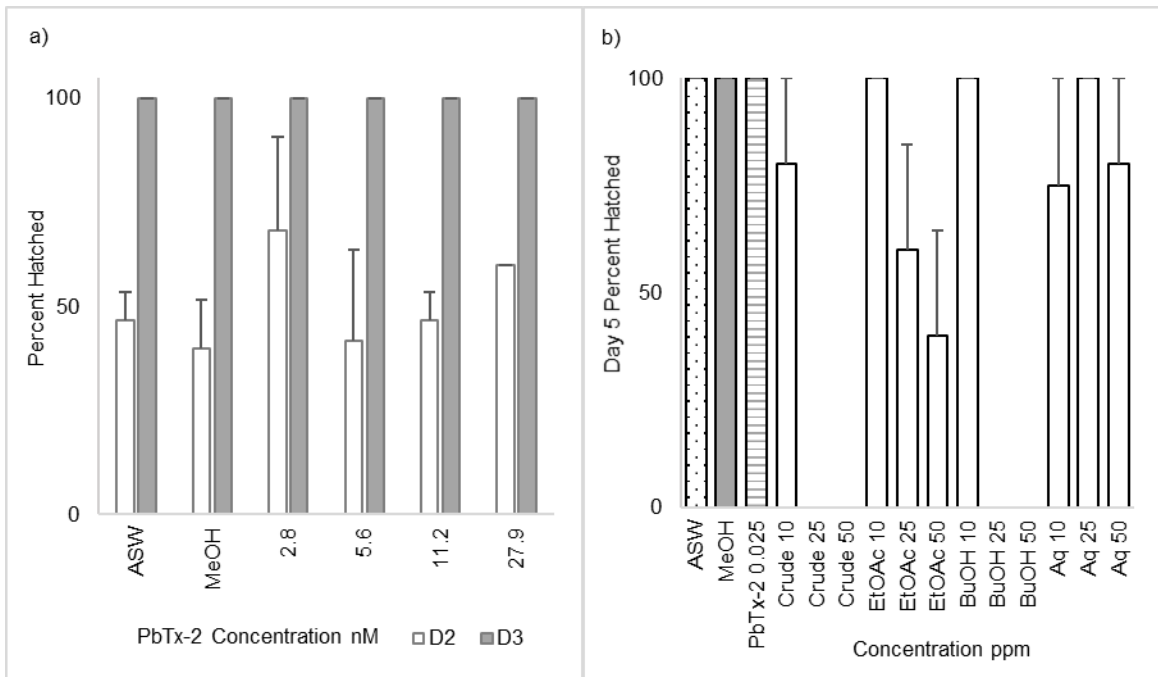


Figure 5.14 Percent hatch rates of controls and cyanobacteria extracts: a) Day 2 and Day 3 hatch rate data for PbTx-2 compared to ASW and MeOH negative controls with error bars indicating \pm SEM ($n = 3$) and b) Hatch rate data through Day 5 for the cyanobacteria crude extracts, compared to the PbTx-2 positive control, with error bars indicating \pm SEM ($n = 5$). The *, **, *** denote, respectively, $p < 0.05$, $p < 0.01$ and $p < 0.001$ significance derived from one-way ANOVA followed by the Tukey HSD multiple comparison test relative to untreated ASW control a) and PbTx-2 b).

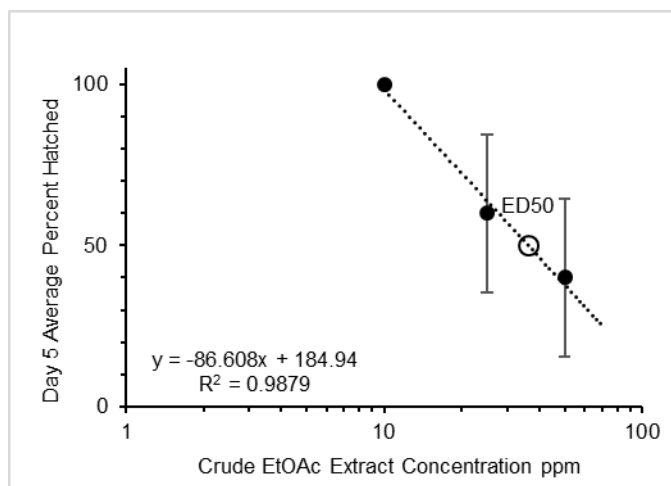


Figure 5.15 Determination of the cyanobacteria EtOAc extract Day 5 hatch rate (% H) ED₅₀ value by linear regression analysis of the Log₁₀ concentration versus % H with error bars denoting ± SEM (n = 5).

The %H of the surviving embryos exposed to the lipophilic fraction F29 and subfractions were not significantly different compared to any of the controls at Day 2 and Day 3 (Figure 5.16, Appendix). Moreover, the %H of embryos exposed to the F29 fractions, particularly F29-1 and F29-2, were aligned with those of PbTx-2, suggesting similarity of any potential neurotoxic effects. Dose dependent hatch rates were observed for fractions F29-2 and F29-3 on Day 2 (Figure 5.17), with respective ED₅₀ values extrapolated to be 6.9 ppm and 26.7 ppm.

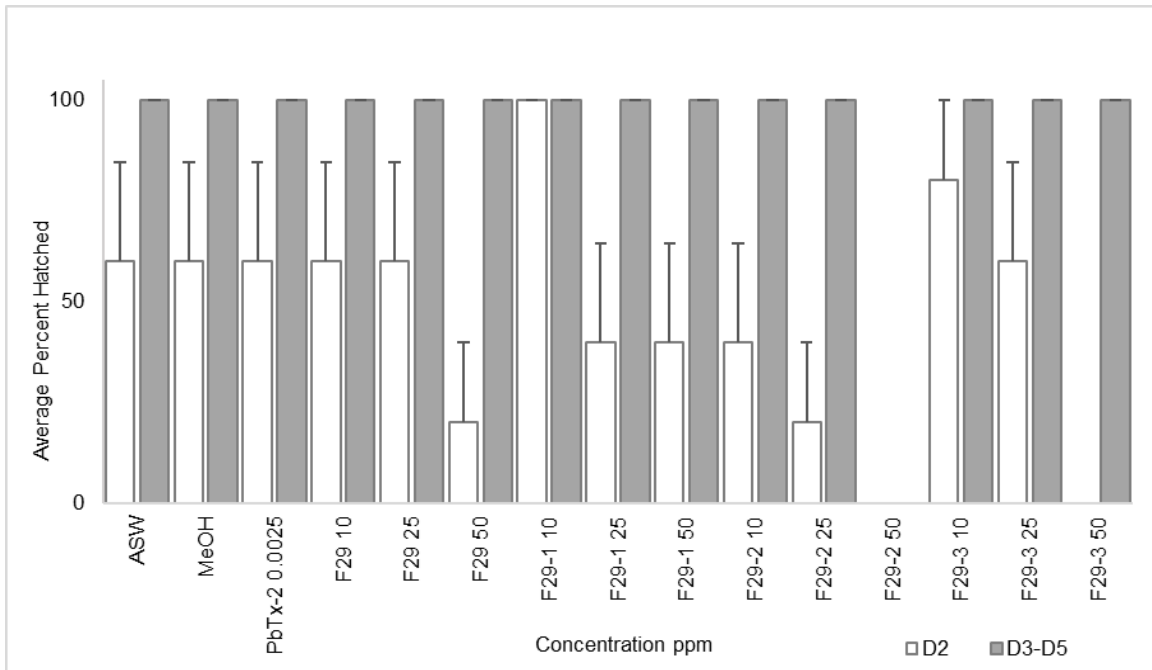


Figure 5.16 Average percent hatch rates of lipophilic F29 related fractions compared to controls through 5 dpf with error bars indicating \pm SEM (n = 5). No significant differences were observed relative to untreated ASW control by one-way ANOVA followed by Tukey's HSD multiple comparison test at $p < 0.001$.

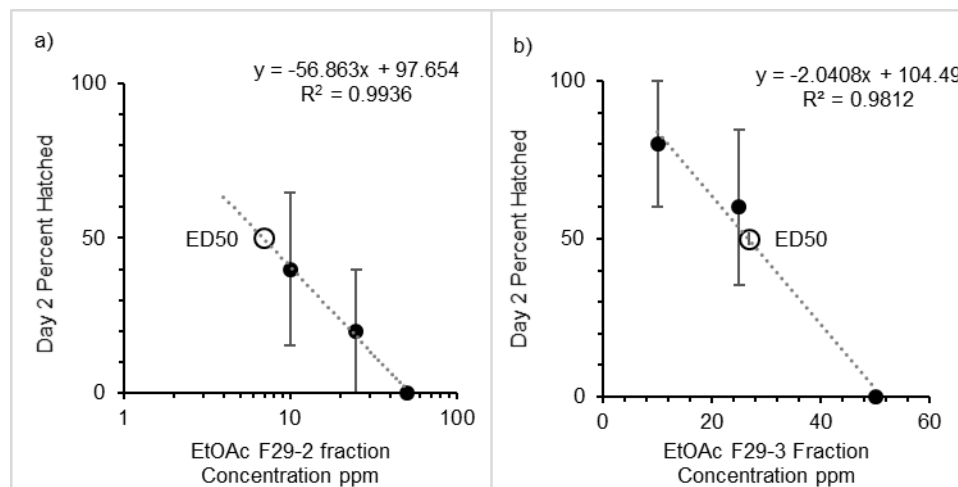


Figure 5.17 Linear regression analysis determination of the Day 2 percent hatched ED₅₀ values for embryos exposed to lipophilic fractions a) F29-2 and b) F29-3 with error bars denoting \pm SEM (n = 5).

5.4.5 Average Day 2 and Day 3 Embryonic Heart Rate Measurements

Embryo heart rates (HR) were measured as beats per minute (bpm) on Day 2 and Day 3 and the average heart rates determined per test condition (see Appendix). All

control data were normally distributed using the d'Agostino-Pearson test for normality (see Appendix). Deceased embryos were counted as exhibiting no heartbeat and thus, contributed to significant differences in average heart rates observed between the cyanobacteria exposed embryos and controls. All PbTx-2 exposure concentrations induced significant tachycardia of approximately 30 bpm faster than the ASW and MeOH controls (Figure 5.18a), indicating neurotoxicity (Sarmah and Marrs, 2016, Henry et al., 1997). The Day 2 HR of the ASW negative control embryos ranged from 132 to 146 bpm with an average of 138.4 ± 1.0 bpm (SEM, n = 15). For the MeOH solvent control, the Day 2 HR averaged 132.3 ± 1.5 bpm (SEM, n = 15), ranging between 120 and 140 bpm. The Day 2 average HR of the PbTx-2 exposure conditions varied from 168.9 ± 4.2 bpm (SEM, n = 15) to 178.1 ± 1.3 bpm (SEM, n = 14), respectively, for 27.9 nM and 2.79 nM, with no observed trend in the data (Figure 5.18a). Heart rates of the PbTx-2 exposed embryos ranged between 140 and 188 bpm. Overall, the crude cyanobacteria extracts, exhibited bradycardia compared to the controls, except for the aqueous extract test solutions (Figure 5.18b). A linear dose dependent decrease in average HR was observed for the crude cyanobacteria extract (Figure 5.19a), whilst the crude EtOAc extract displayed a logarithmic dose dependent decreasing trend (Figure 5.19b). No ED₅₀ values could be determined from the cyanobacteria crude extract D2 HR measurements.

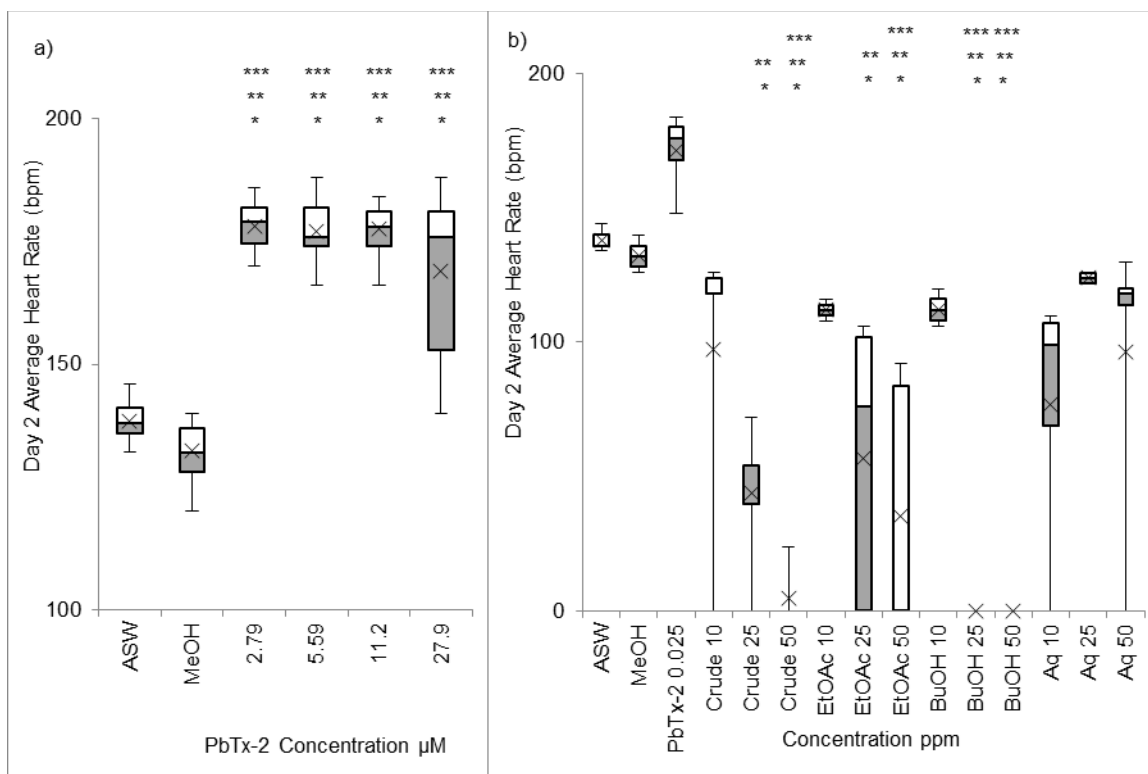


Figure 5.18 The Day 2 average heart rates (HR) quantified as beats per minute (bpm) per exposure condition: a) Box plot of PbTx-2 data compared to the ASW and MeOH controls and b) Box plot of cyanobacteria extracts compared to all three control conditions. Error bars are \pm SD with $n = 15$ for a) and $n = 5$ for b) and \times indicates the mean HR value. Significance levels, $p < 0.05$, $p < 0.01$ and $p < 0.001$, derived from one-way ANOVA followed by the Tukey HSD multiple comparison test, are respectively denoted by *, **, *** relative to the untreated ASW control.

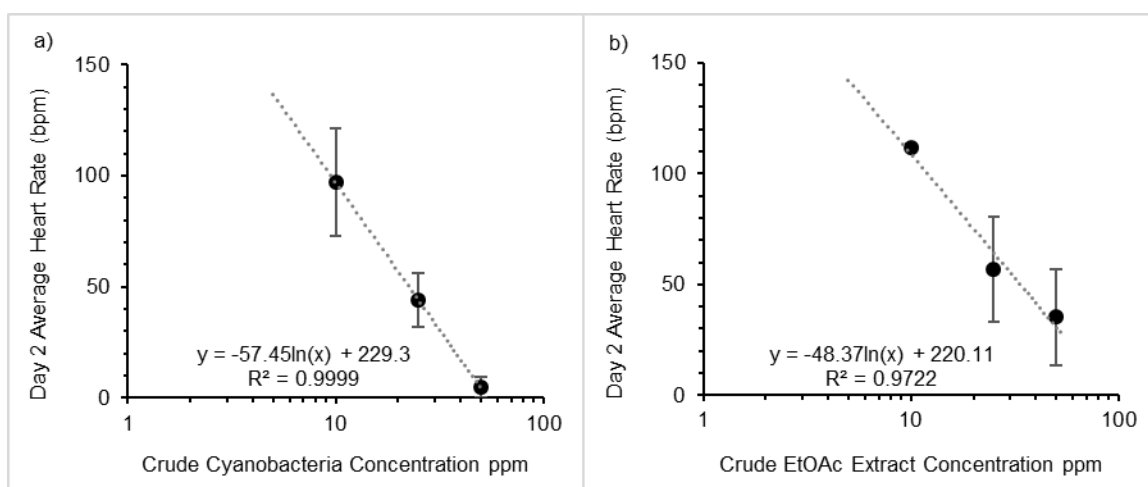


Figure 5.19 Day 2 average heart rate trends observed for the cyanobacteria a) crude and b) EtOAc extracts with error bars indicating \pm SEM ($n = 5$), quantified as beats per minute (bpm).

Generally, treatments with the lipophilic (i.e., EtOAc) F29-related fractions, at Day 2 of development, were consistent with the negative controls, implying any potentially associated neurotoxicity did not affect embryo heart rates (Figure 5.20). However, exposure to 50 ppm of subfraction F29-2 induced significant bradycardia, in contrast to the tachycardia associated with exposure to 0.025 ppm PbTx-2 (Figure 5.20). The average D2 HR of embryos exposed to 50 ppm subfraction F29-2 was 85.6 ± 21.6 bpm (SEM, n = 5). Average D2 HR for all other F29 related treatments ranged between 128.4 ± 3.1 bpm (SEM, n = 5) and 145.6 ± 2.3 bpm (SEM, n = 5) with no specific dose-dependent trends observed (see Appendix).

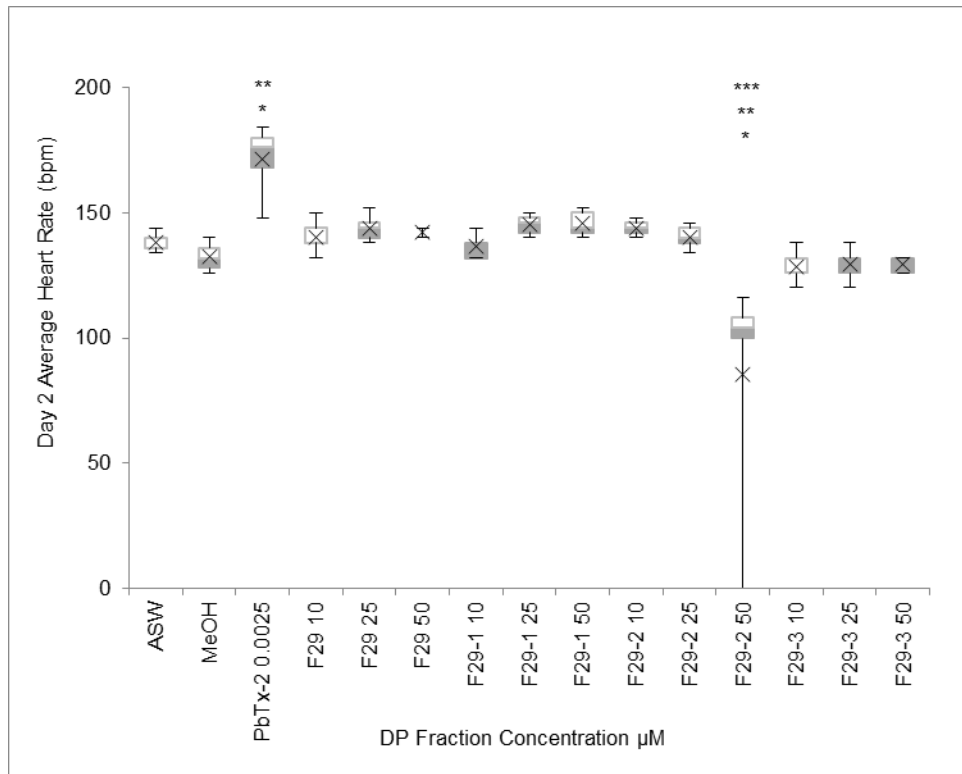


Figure 5.20 Box plot of the Day 2 average heart rates (HR) of the lipophilic F29 fractions, quantified as beats per minute (bpm) per treatment, compared to the controls. Error bars indicate \pm SD (n = 5) and \times indicates the mean HR value. Significance levels, $p < 0.05$, $p < 0.01$ and $p < 0.001$, derived from one-way ANOVA followed by the Tukey HSD multiple comparison test, are respectively denoted by *, **, *** relative to untreated ASW control.

Overall, embryos exposed to PbTx-2 through Day 3 exhibited average heart rates (HR) consistent with those of the ASW and MeOH controls, perhaps suggesting a developmental recovery (Figure 5.21a, Appendix). Heart rate measurements ranged from 162 to 192 bpm across all control conditions. The D3 average HR of the PbTx-2 exposed embryos, ranging between 180.4 ± 1.2 bpm (SEM, $n = 14$) and 183.7 ± 0.8 bpm (SEM, $n = 13$), were overall not significantly (i.e., $p < 0.01$, $p < 0.001$) higher than the respective D3 average HR and of 175.2 ± 2.3 bpm (SEM, $n = 15$) and 176.0 ± 2.1 bpm (SEM, $n = 15$) for the ASW and MeOH controls (Figure 5.21a, Appendix). However, the D3 average HR of embryos exposed to 5.59 nM PbTx-2 was significantly elevated compared to the controls, for $p < 0.05$ significance (Figure 5.21a). Generally, embryos exposed to the crude cyanobacteria extracts continued to exhibit bradycardia at Day 3 compared to the controls, indicative of lingering teratogenic and/or neurotoxic effects (Figure 5.21b). The significantly lower average D3 HR of the mid and high treatments of cyanobacteria crude extracts relative to the control averages were largely attributed to the increased mortalities observed at Day 3. Logarithmic dose dependency was observed for the crude cyanobacteria and EtOAc extracts (Figure 5.22). An extrapolated ED₅₀ value of 22.0 ppm for the EtOAc crude extract was derived from the number of embryos per treatment exhibiting abnormal HR relative to the controls (Figure 5.23). Embryo heart rates below 162 bpm and above 192 bpm were considered abnormal. No other trends or ED₅₀ values could be determined for the other crude extracts.

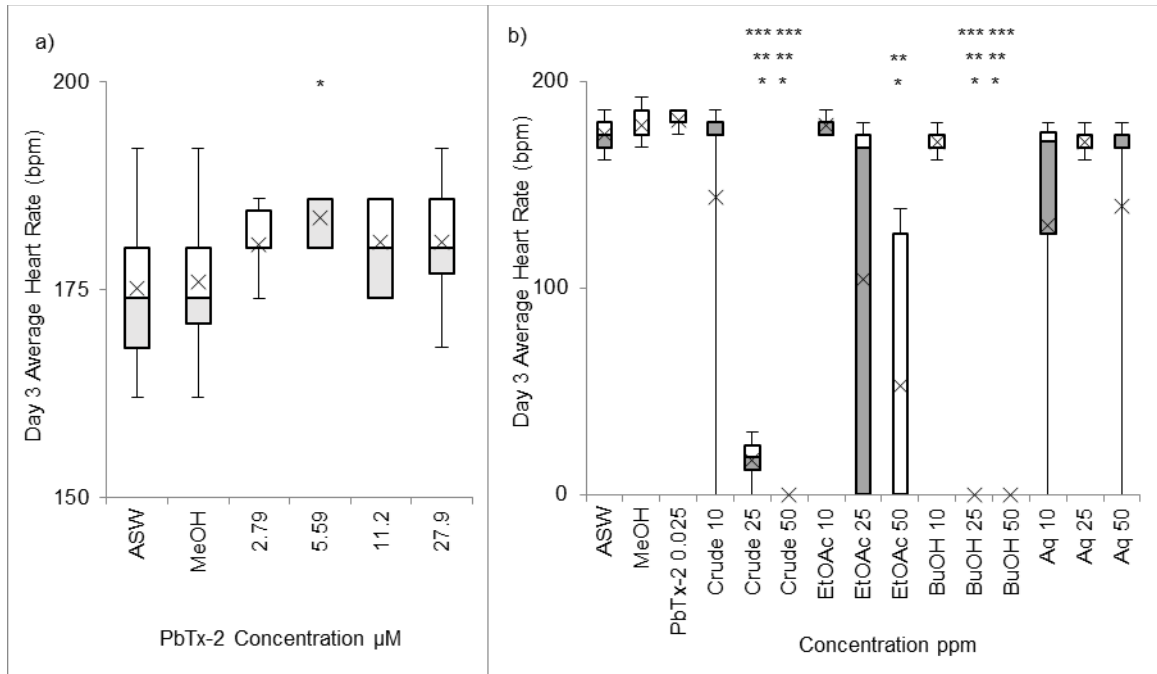


Figure 5.21 The Day 3 average heart rates (HR) quantified as beats per minute (bpm) per exposure condition: a) Box plot of PbTx-2 data compared to the ASW and MeOH controls and b) Box plot of cyanobacteria extracts compared to controls. Error bars are \pm SD with $n = 15$ for a) and $n = 5$ for b) and \times indicates the mean HR value. Significance levels, $p < 0.05$, $p < 0.01$ and $p < 0.001$, derived from one-way ANOVA followed by the Tukey HSD multiple comparison test, are respectively denoted by *, **, *** relative to untreated ASW control.

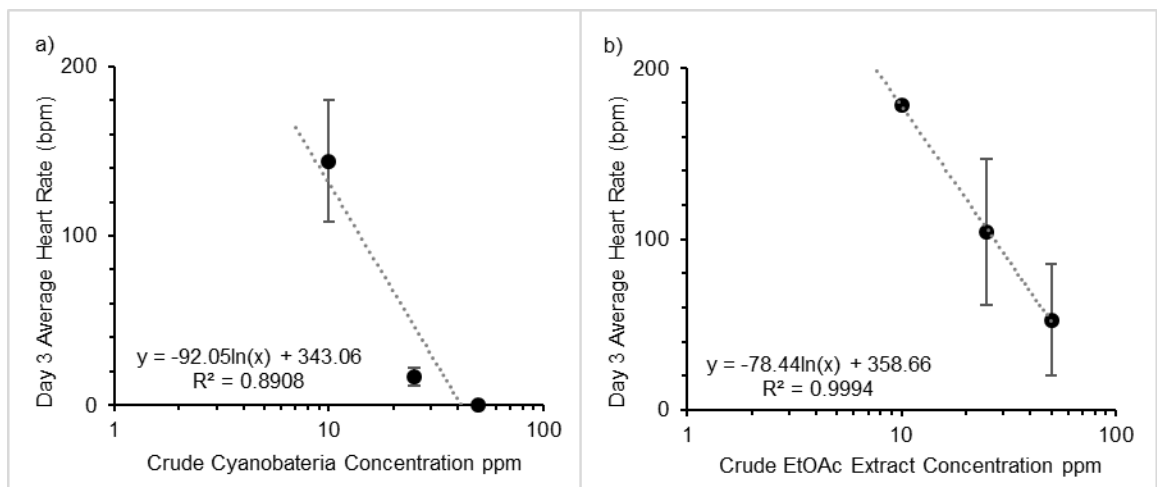


Figure 5.22 Day 3 average heart rate trends observed for the cyanobacteria a) crude and b) EtOAc extracts with error bars indicating \pm SEM ($n = 5$), quantified as beats per minute (bpm).

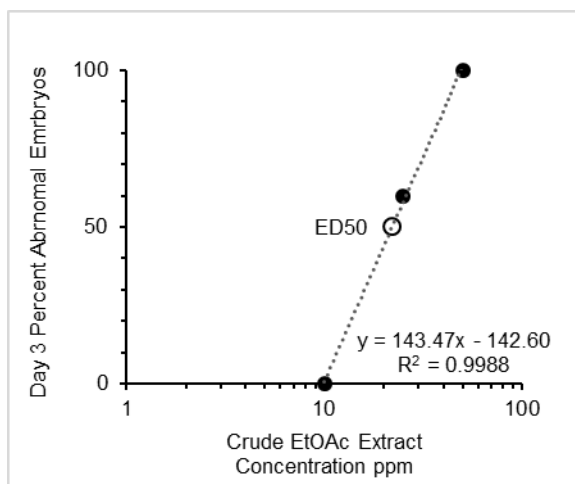


Figure 5.23 Extrapolation of the Day 3 ED₅₀ value for the percentage of embryos exposed to the cyanobacteria EtOAc extract exhibiting abnormal heart rates relative to normal controls.

Average D3 HR for surviving embryos exposed to the lipophilic (i.e., EtOAc) F29 subfractions remained consistent with the controls (Figure 5.24). Notably, all embryos exposed to the 50 ppm F29-2 subfraction were deceased by 3 dpf. The average D3 HR of all F29 related fractions ranged between 166.8 ± 5.2 bpm (SEM, n = 5) and 186.0 ± 4.2 bpm (SEM, n = 5), within the range of the heart rates measured for controls. Bradycardia dose dependency was observed at 3 dpf in embryos treated with fraction F29 and subfraction F29-1 (Figure 5.25). However, no ED₅₀ values could be determined from these data.

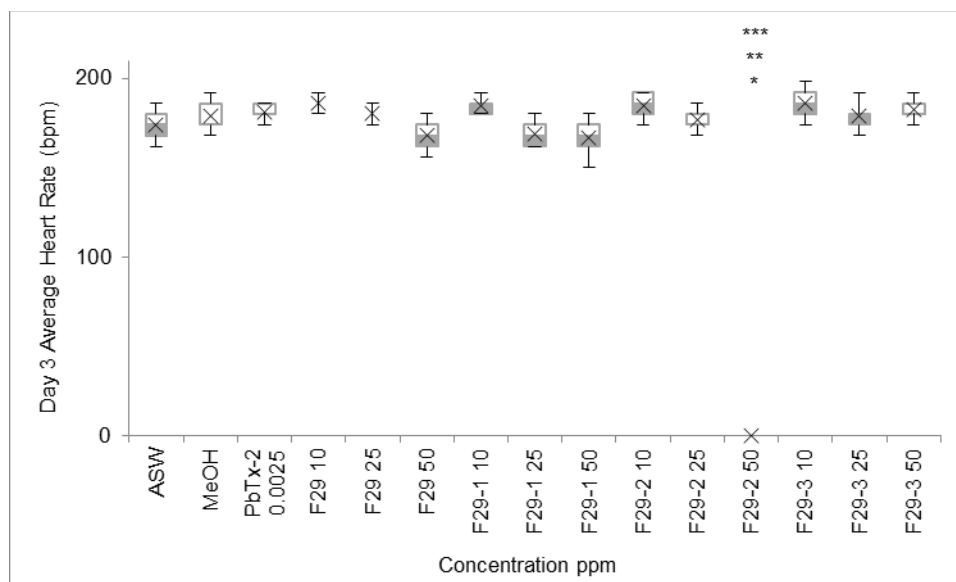


Figure 5.24 The Day 3 average heart rates (HR) of the lipophilic F29 fractions, quantified as beats per minute (bpm) per treatment. Error bars are \pm SD ($n = 5$) and \times indicates the mean HR value. Significance levels, $p < 0.05$, $p < 0.01$ and $p < 0.001$, derived from one-way ANOVA followed by the Tukey HSD multiple comparison test, are respectively denoted by *, **, *** relative to the PbTx-2 positive control.

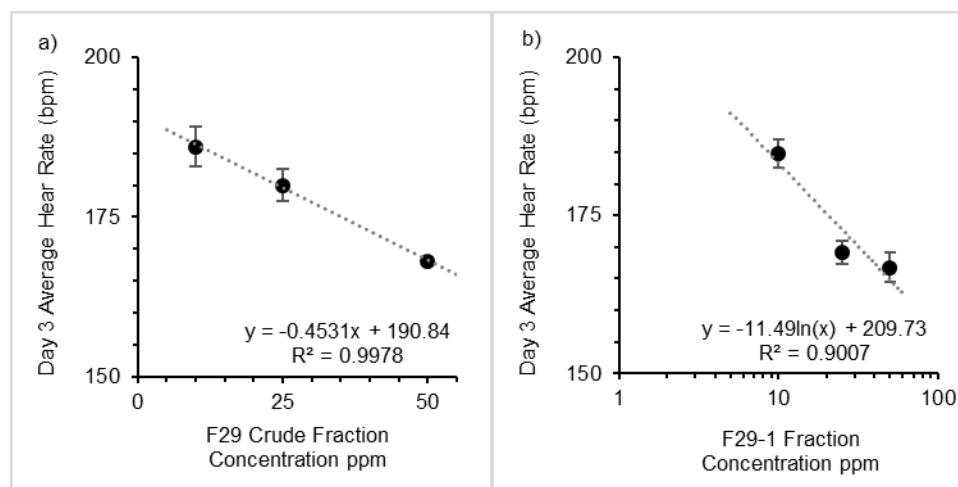


Figure 5.25 Day 3 dose dependency of average heart rates (bpm) for the lipophilic fractions a) F29 and b) F29-1 with error bars indicating \pm SEM ($n = 5$).

5.4.6 Average Swimming-related Assessments of 5-dpf Larvae

5.4.6.1 Chronic Embryogenic Exposure Swimming Assessments

Swim bladder development and swimming behaviors were assessed in all exposure conditions at Day 5 with deceased embryos counted as abnormal (Appendix).

Swim bladder dysfunction (SBD) was quantified as the percentage of embryos, per treatment, having irregular swim bladder development (e.g., inflation issues, misshapen, undeveloped) compared to ASW negative controls. Aberrant swimming behaviors (ASB) were quantified as the percentage of embryos, per exposure condition, exhibiting movements characteristic of neurotoxicity associated ataxia (e.g., laying on side, spasms, titling) relative to swimming patterns exhibited by the negative controls (e.g., beat-and-glide) as described by Kalueff et al. (2013). None of the embryos in the ASW and MeOH solvent controls exhibited any issues with swim bladder development on Day 5 (Figure 5.26a, Appendix). However, significant, dose dependent SBD was observed in all PbTx-2 treatments at 5 dpf, consistent with neurotoxic effects (Figure 5.26a, Appendix). An ED₅₀ value of 1.12 nM PbTx-2 was determined by probit analysis (Figure 5.27). Embryonic exposures to the cyanobacterial extracts through 5 dpf also caused significant SBD, relative to the negative controls, and qualitatively aligned with the 0.025 ppm PbTx-2 treatment, implying neurotoxicity (Figure 5.26b, Appendix). Moreover, all embryos exposed to 0.025 ppm PbTx-2 and all cyanobacteria crude extract treatments exhibited irregular swim bladder development (Appendix). The cyanobacteria EtOAc extract displayed logarithmic dose dependency allowing the extrapolation of an ED₅₀ value of 6.9 ppm (Figure 5.28). Significant SBD, analogous to PbTx-2, was also observed in embryos exposed to the lipophilic F29 related fractions compared to the negative controls, suggesting neurotoxic effects (Figure 5.29). However, no dose-related trends were observed for the F29 fractions.

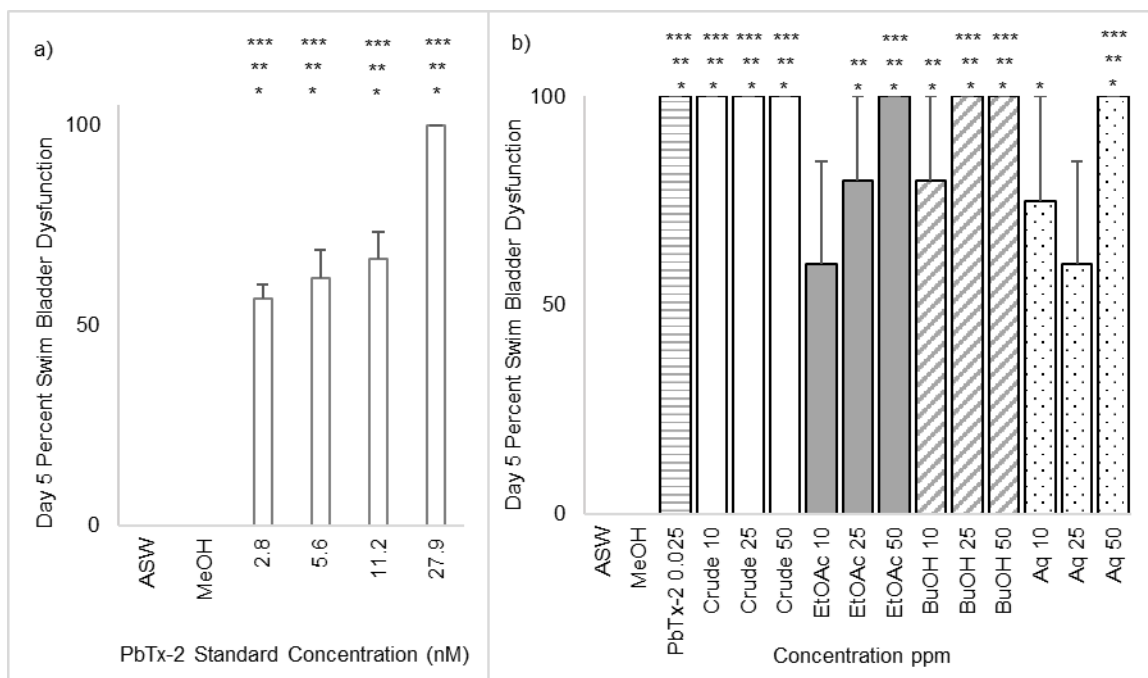


Figure 5.26 The Day 5 average percent swim bladder dysfunction of embryos chronically exposed to a) PbTx-2 and b) the cyanobacteria extracts compared to the ASW and MeOH controls. Error bars are \pm SEM with $n = 3$ for a) and $n = 5$ for b). Significance levels, $p < 0.05$, $p < 0.01$ and $p < 0.001$, derived from one-way ANOVA followed by the Tukey HSD multiple comparison test, are respectively denoted by *, **, *** relative to untreated ASW control for a) and PbTx-2 positive control for b).

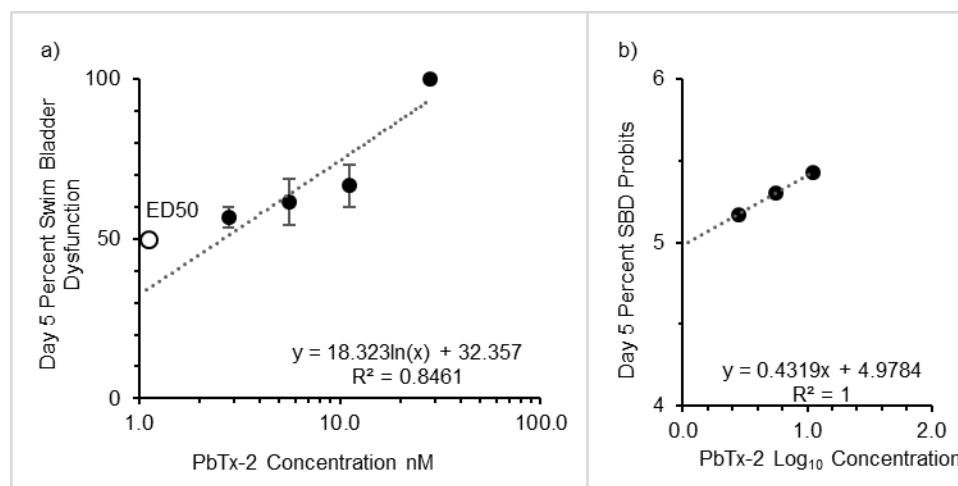


Figure 5.27 Probit analysis determination of the D5 percent swim bladder dysfunction (% SBD) ED₅₀ value for chronic PbTx-2 exposure: a) Concentration versus %SBD plot with error bars denoting \pm SEM ($n = 3$) and b) Probit analysis plot.

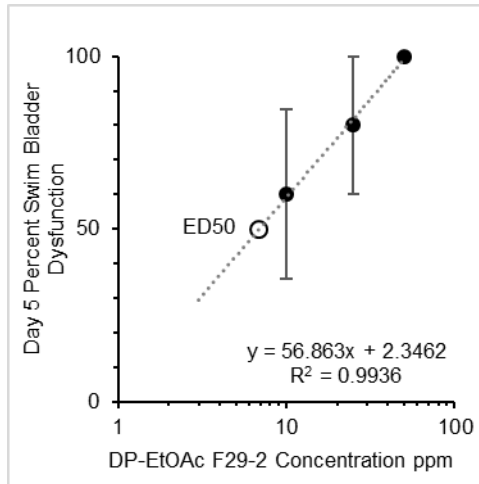


Figure 5.28 Extrapolated D5 percent swim bladder dysfunction ED₅₀ value for chronic cyanobacteria EtOAc extract exposure.

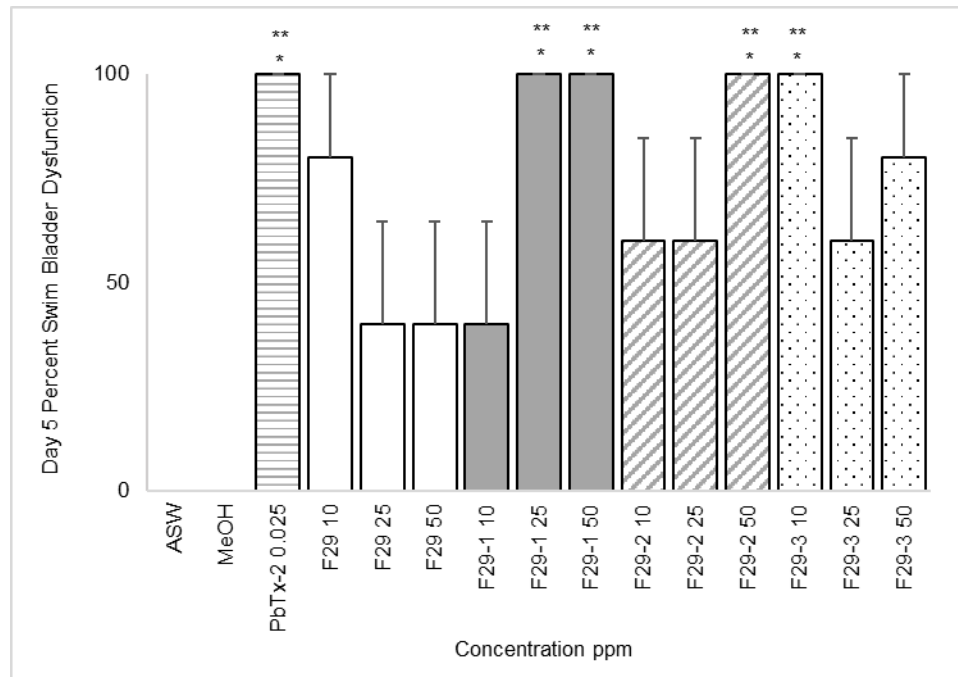


Figure 5.29 The D5 average percent swim bladder dysfunction of embryos chronically exposed to the cyanobacteria lipophilic F29 fractions with error bars indicating \pm SEM ($n = 5$). Respectively, the *, **, *** denote significance levels $p < 0.05$, $p < 0.01$ and $p < 0.001$, relative to untreated ASW control, derived by one-way ANOVA followed by the Tukey HSD multiple comparison test.

All embryos in the ASW and MeOH solvent controls displayed normal swimming behaviors indicated by maintaining upright postures and typical beat-and-glide swimming patterns with no buoyancy issues when examined at 5 dpf (Figure 5.30a). In contrast, embryos exposed to all PbTx-2 treatments exhibited significant aberrant swimming behaviors associated with neurotoxic effects including ataxia manifested by the inability to stay upright, laying on side, and spasms. Buoyancy issues, expressed as head up or down drifting, were also detected in PbTx-2 exposed embryos and most likely associated with swim bladder dysfunctions. No specific concentration-related trend was observed for PbTx-2 as over 60% of embryos in each PbTx-2 treatment exhibited significant ASB compared to the negative controls (Figure 5.30a). Embryos exposed to cyanobacteria extracts and the lipophilic F29 related fractions also displayed significant ASB, aligned with PbTx-2 behaviors, relative to the negative controls (Figure 5.30b, Figure 5.31). Significantly fewer embryos exhibited ASB when exposed to the 10 ppm EtOAc extract compared to the 0.025 ppm PbTx-2 treatment (Figure 5.30b). However, no dose dependency was observed for any of the cyanobacteria treatments.

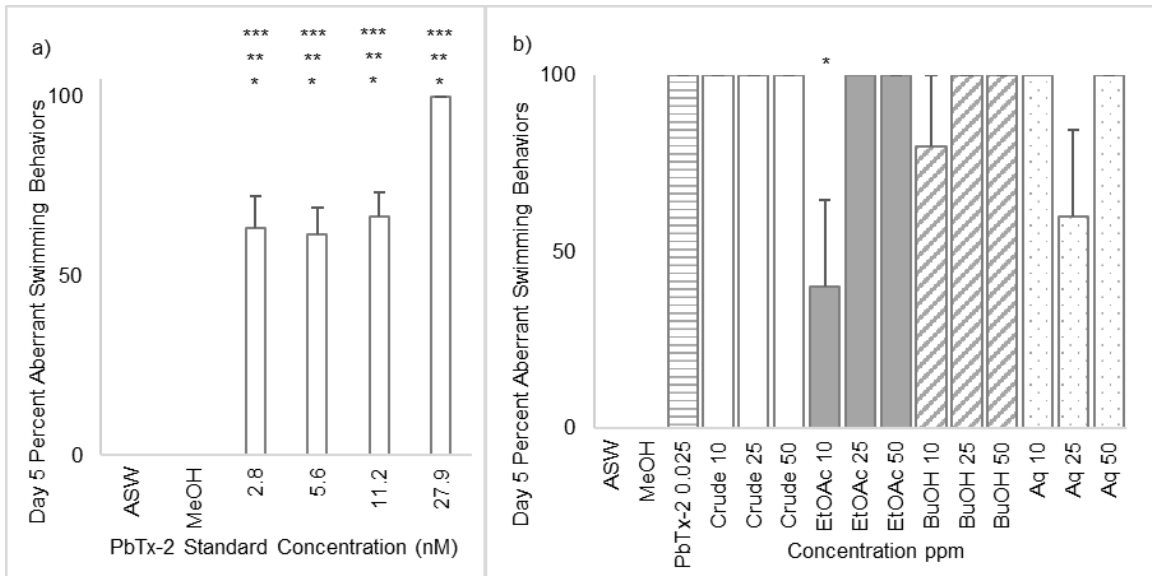


Figure 5.30 The Day 5 average percent aberrant swimming behaviors of embryos chronically exposed to a) PbTx-2 and b) the cyanobacteria extracts compared to the ASW and MeOH controls. Error bars are \pm SEM with $n = 3$ for a) and $n = 5$ for b). Significance levels, $p < 0.05$, $p < 0.01$ and $p < 0.001$, derived from one-way ANOVA followed by the Tukey HSD multiple comparison test, are respectively denoted by *, **, *** relative to untreated ASW control for a) and PbTx-2 positive control for b).

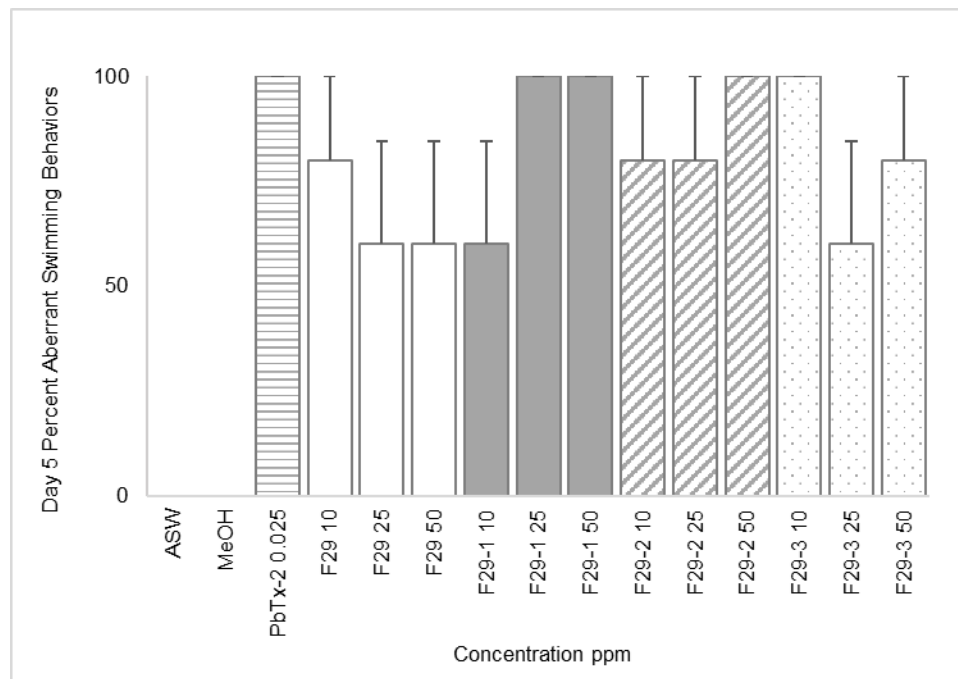


Figure 5.31 The Day 5 average percent aberrant swimming behaviors of embryos chronically exposed to the cyanobacteria lipophilic F29 fractions with error bars indicating \pm SEM ($n = 5$) were not significantly different from the PbTx-2 treatment for $p < 0.05$, $P < 0.01$ and $p < 0.001$ significance levels derived by one-way ANOVA and the Tukey HSD multiple comparison test.

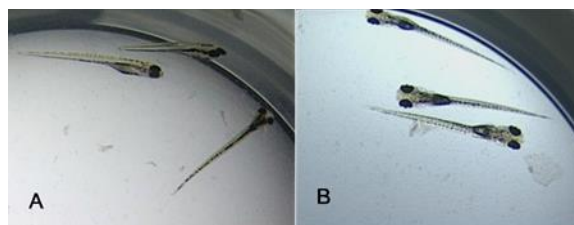


Figure 5.32 Representative embryos chronically exposed to 27.9 nM (25 ppb) PbTx-2 through 5 dpf indicating irregular swim bladder development, laying on side, and head-up passive drift orientation (A) relative to normal development exhibited by MeOH solvent control embryos examined at 5 dpf (B).

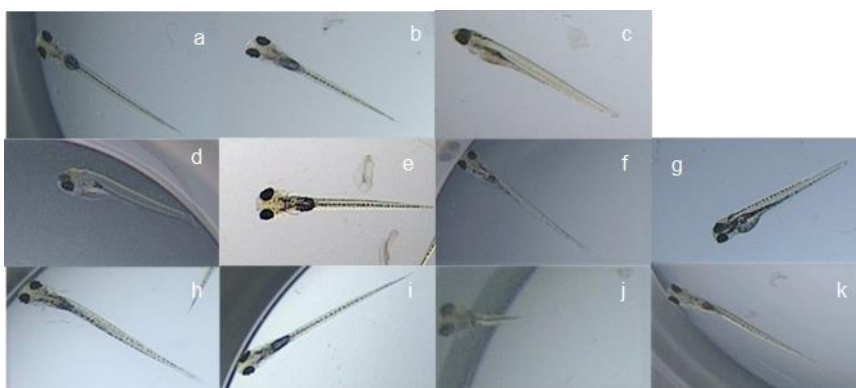


Figure 5.33 Representative embryos chronically exposed to 10 ppm concentrations of cyanobacteria extracts and fractions versus controls, examined at 5 dpf: a ASW untreated control, b MeOH solvent control, c 0.025 ppm PbTx-2 positive control, d crude cyanobacteria extract, e EtOAc extract, f BuOH extract, g Aq extract, h F29, i F29-1, j F29-2, k F29-3. Shown are irregular swim bladder development in c, d, f-h and j-k and bent body axis in f, h and k. Aberrant swimming behaviors are indicated by laying on side in c, d and g and head-up passive drifting in e, f, and h-k relative to upright orientation and normal swim bladder development in controls a and b.

5.4.6.2 Acute Larval Exposure Swimming Assessments

During the bioassay-guided fractionation process, 24-hour acute exposure studies were conducted to assess potential neurotoxicity induced effects of PbTx-2 and the cyanobacteria extracts and subsequent fractions on otherwise normally developed 5-dpf larvae. Larvae with fully inflated swim bladders and displaying appropriate swimming behaviors (e.g., beat-and-glide, upright orientation) were exposed to four different concentrations of test material (i.e., PbTx-2, cyanobacteria fraction) and compared to the

negative controls (i.e., ASW, MeOH). Percent mortality (%M) and the percentage of larvae exhibiting swimming issues (SI) related to neurotoxicity (e.g., ataxia, irregular swim bladder morphologies, aberrant swimming behaviors) were quantified at five timepoints after initial exposure (see Appendix). Deceased embryos were considered to have swimming issues. These observational data were used to help guide the cyanobacteria fractionation and not statistically analyzed.

Larval mortalities were first observed in the 11.2 nM PbTx-2 treatment within 2 hpe, possibly related to hyperactivity. At 6 hpe, mortalities occurred in all but the lowest PbTx-2 treatment and continued through 24 hpe (Figure 5.34). The 18.5 nM LD₅₀ value for PbTx-2 exposure was established at 24 hpe by probit analysis (Figure 5.34). An increasing linear trend in %M was observed for the 27.9 nM PbTx-2 treatment from 23.8 %M at 6 hpe to 57.1 %M at 24 h. At 1 hpe, all larvae in each PbTx-2 treatment displayed swimming issues including hyperactivity at lower concentrations, lethargy at higher concentration, tilting, and spasms, characteristic of neurotoxicity. Buoyancy issues also occurred, manifested by altered swim bladder morphologies including diminished inflation and deemed a swimming issue. Quantitation of swim bladder irregularities could not be achieved due to larval mobility. Active larvae generally appeared to have normal responses to light and tap exposures. All larvae remained 100% affected by PbTx-2 exposure at all concentrations through 24 hpe (see Appendix). No larvae appeared to recover from any PbTx-2 treatment during the 24-hour study. The 0.025 ppm (27.9 nM) PbTx-2 concentration was chosen as the positive control treatment used to evaluate the cyanobacteria fraction based on the %M data.

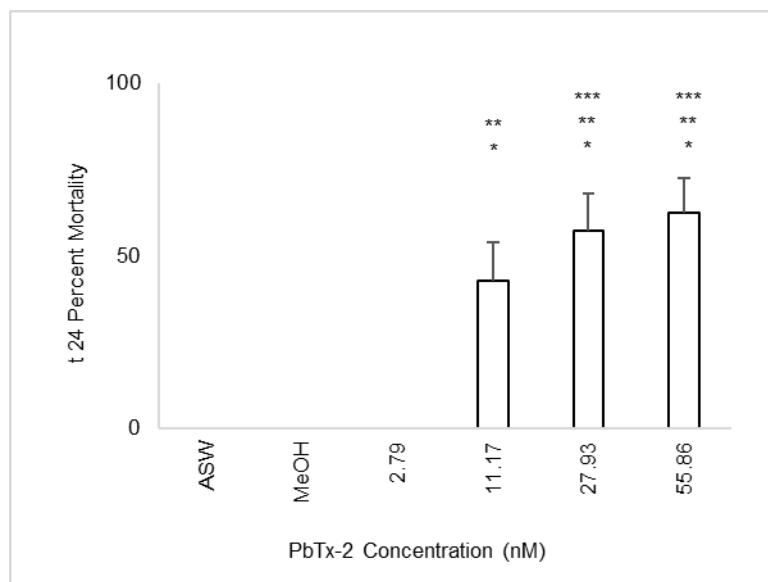


Figure 5.34 Lethality of the 24-hpe (t24) acute PbTx-2 larval exposures compared to negative controls, with error bars indicating \pm SEM ($n = 24$). Significance levels, $p < 0.05$, $p < 0.01$ and $p < 0.001$, derived from one-way ANOVA followed by the Tukey HSD multiple comparison test, are respectively denoted by *, **, *** relative to untreated ASW control.

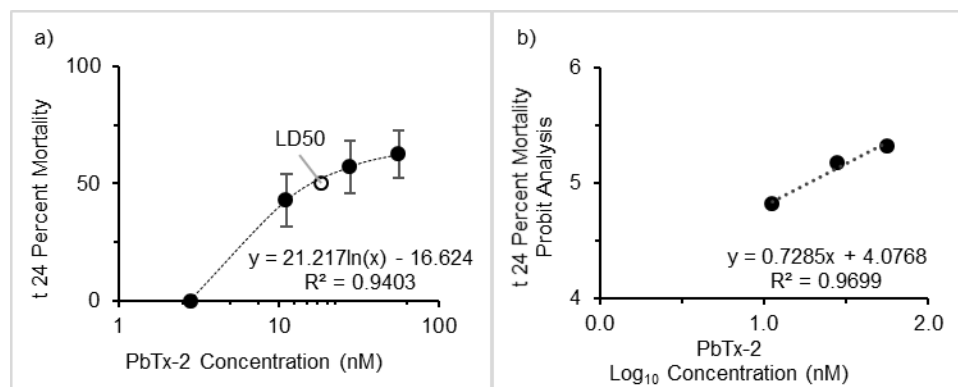


Figure 5.35 Probit analysis determination of the 24-hpe (t24) LD₅₀ value for acute PbTx-2 larval exposure: a) Concentration versus percent mortality plot and b) Probit analysis plot. Error bars are \pm SEM with $n = 20, 21, 21$ and 24 replicate embryos for the respective 2.79, 5.59, 11.2 and 27.9 nM PbTx-2 treatments.

No specific dose dependency was observed for the percent mortality of larvae exposed to any of the cyanobacteria extracts or lipophilic (i.e., EtOAc) F29 fractions at 24 hpe (Figure 5.36). Generally, cyanobacterial extract concentrations less than 50 ppm were not as lethal as the positive control, and particularly, no larval mortality was

observed from exposures to the lipophilic fractions F29-2 and F29-3. Moreover, fractions F29 and F29-1 most aligned with PbTx-2 lethality. No LD₅₀ values could be determined for the cyanobacteria extracts or lipophilic F29 fractions.

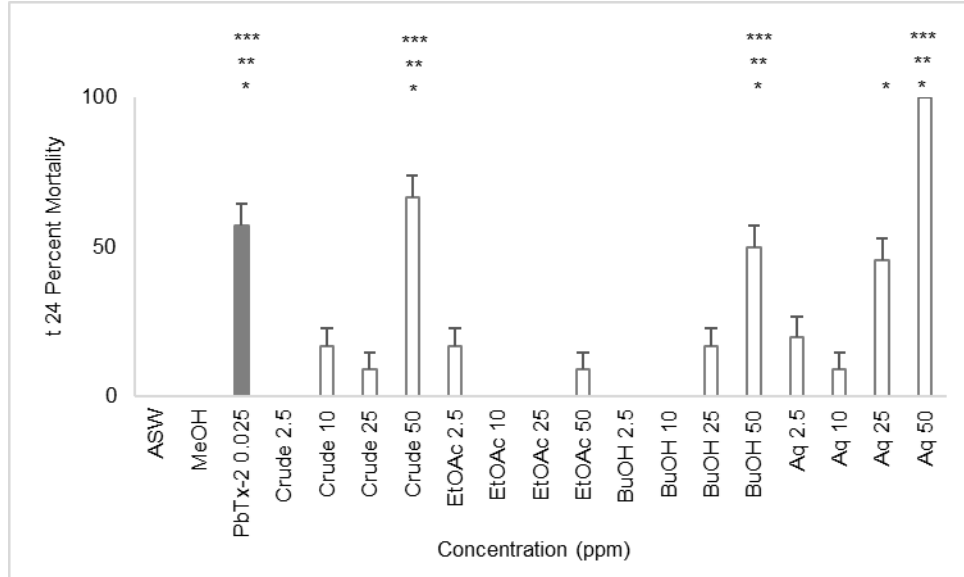


Figure 5.36 Lethality of acute larval exposures to the cyanobacteria extracts compared to controls with error bars indicating \pm SEM ($n = 12$ for extracts and $n = 24$ for controls). Significance levels, $p < 0.05$, $p < 0.01$ and $p < 0.001$, derived from one-way ANOVA followed by the Tukey HSD multiple comparison test, are respectively denoted by *, **, *** relative to untreated ASW control.

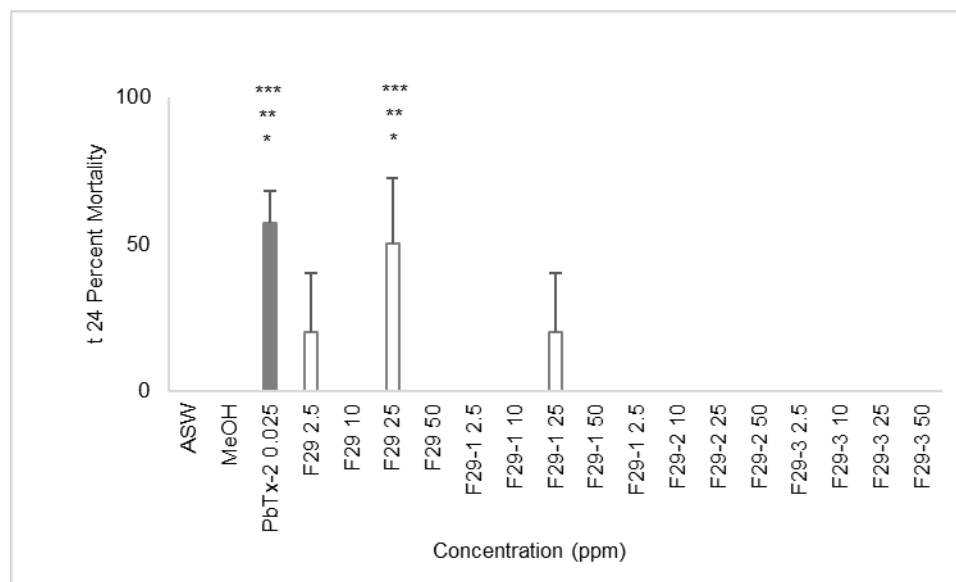


Figure 5.37 Lethality of acute larval exposures to the cyanobacteria lipophilic F29 fractions compared to controls. Error bars indicate \pm SEM ($n = 5$ for fractions and $n = 24$ for controls). Significance levels, $p < 0.05$, $p < 0.01$ and $p < 0.001$, derived from one-way ANOVA followed by the Tukey HSD multiple comparison test, are respectively denoted by *, **, *** relative to untreated ASW control.

Within 1-hpe, all larvae treated with the crude cyanobacteria extracts exhibited swimming issues, qualitatively aligned with the PbTx-2 treatment, suggesting neurotoxicity (see Appendix). However, by 24 hpe, some larvae appeared to have recovered in each of the cyanobacteria extract test conditions compared to the persisting effects from exposure to PbTx-2 (Figure 5.38). Indeed, 24-hpe ED₅₀ values of 4.8 ppm and 17.5 ppm were extrapolated for the crude cyanobacteria and BuOH extracts (Figure 5.39). Although, no other specific dose dependency was observed for the EtOAc and Aqueous cyanobacteria extract treatments, approximately half of the treated larvae appeared to have recovered in each exposure concentration.

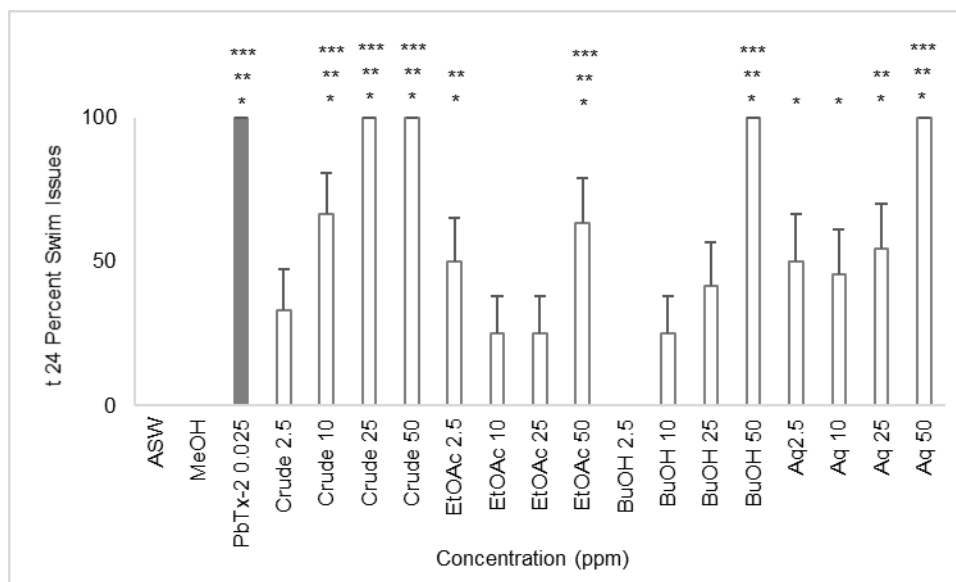


Figure 5.38 Percentages of larvae acutely exposed to cyanobacteria extracts exhibiting swimming issues at 24 hpe (t24) relative to controls. Error bars indicate \pm SEM (n = 12 for extracts n =24 for controls). Significance levels, $p < 0.05$, $p < 0.01$ and $p < 0.001$, derived from one-way ANOVA followed by the Tukey HSD multiple comparison test, are respectively denoted by *, **, *** relative to untreated ASW control.

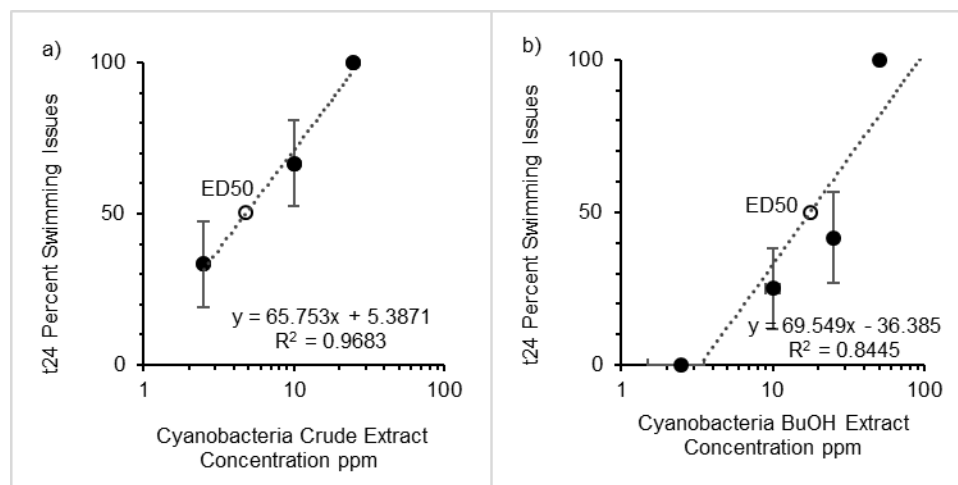


Figure 5.39 Linear regression analysis extrapolation of the 24-hpe (t24) percent swimming issues ED₅₀ values for the cyanobacteria a) crude and b) BuOH extracts with error bars denoting \pm SEM (n = 12).

Generally, larvae exposed to the lipophilic (i.e., EtOAc) F29-related fractions exhibited fewer percentages of swimming issues (SI) compared to the PbTx-2 treatment when examined at 1 hpe (Figure 5.40). Notably, none of the fraction F29-3 treatments

affected larval swimming behaviors in the first hour of exposure. Whereas, dose dependency was observed for fractions F29-1 and F29-2 with respective ED₅₀ values of 12.7 ppm and 14.0 ppm determined at 1 hpe (Figure 5.41). Moreover, the effects from exposure to the lipophilic fraction treatments appeared to peak at 2 hpe, including the 25 and 50 ppm F29-3 test solutions, after which the larvae seemed to begin recovering (See Appendix). Indeed, by 24 hpe, the percentages of larvae exhibiting swimming issues were almost halved in nearly all F29-related test solutions and the affected 25 and 50 ppm F29-3 treated larvae appeared fully recovered (Figure 5.42, Appendix). Moreover, for the F29-2 treatments, the ED₅₀ value, determined by probit analysis to be 238 ppm at 24 hpe (Figure 5.44), a nearly 20-fold increase in exposure concentration relative to the 1-hpe ED₅₀ value of 14.0 ppm, further supported larvae recovery after initial exposure (Figure 5.44). However, this large increase is suspect, due to the low correlation coefficient of 0.8608.

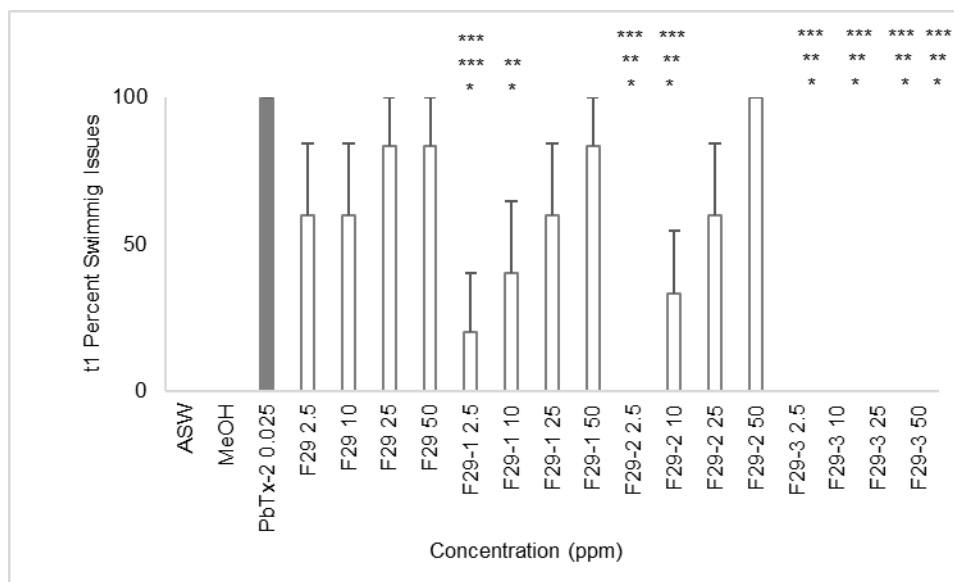


Figure 5.40 Percentages larvae acutely exposed to lipophilic F29 fractions exhibiting swimming issues at 1-hpe (t1) relative to controls. Error bars indicate \pm SEM ($n = 5$ for extracts and $n = 24$ for controls). Significance levels, $p < 0.05$, $p < 0.01$ and $p < 0.001$, derived from one-way ANOVA followed by the Tukey HSD multiple comparison test, are respectively denoted by *, **, *** relative to PbTx-2 control.

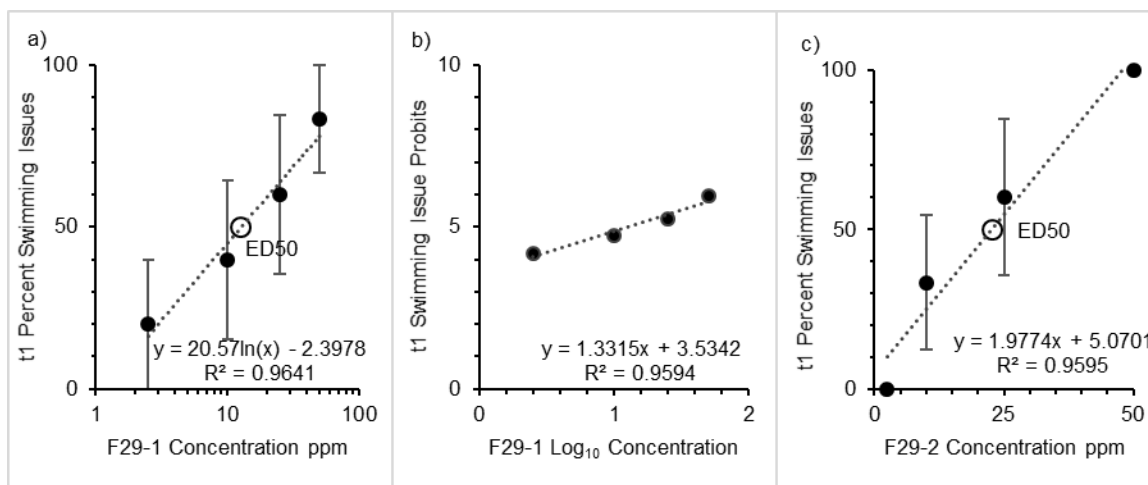


Figure 5.41 Determination of the 1-hpe (t1) percent swimming issues (% SI) ED₅₀ values for acute larval exposures to fractions F29-1 and F29-2: a) F29-1 concentration versus % SI plot, b) F29-1 probit analysis plot and c) F29-2 concentration versus % SI plot. Error bars are \pm SEM ($n = 5$).

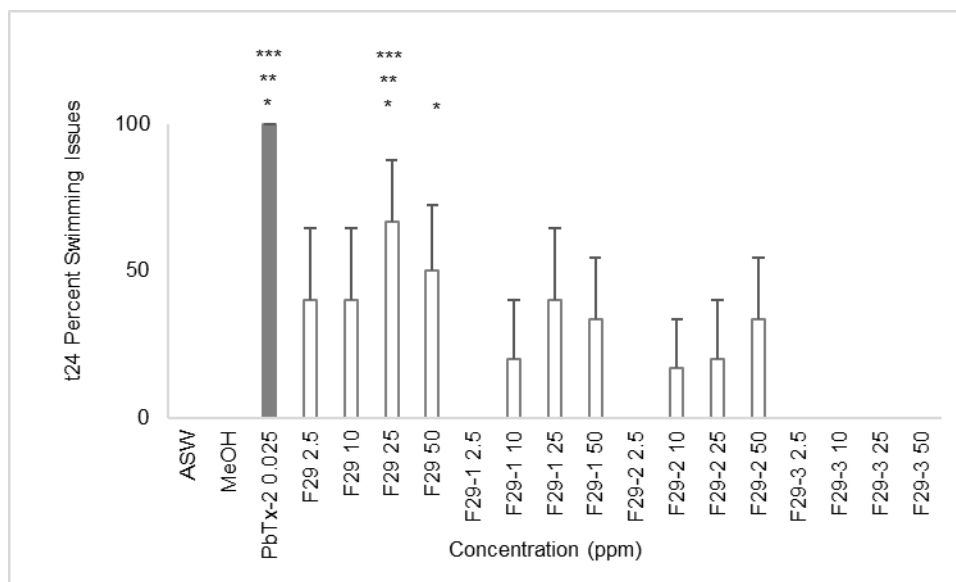


Figure 5.42 Percentages of larvae acutely exposed to lipophilic F29 fractions exhibiting swimming issues at 24 hpe (t24) compared to controls. Error bars indicate \pm SEM (n = 5 for extracts and n = 24 for controls). Significance levels, $p < 0.05$, $p < 0.01$ and $p < 0.001$, derived from one-way ANOVA followed by the Tukey HSD multiple comparison test, are respectively denoted by *, **, *** relative to untreated ASW control.

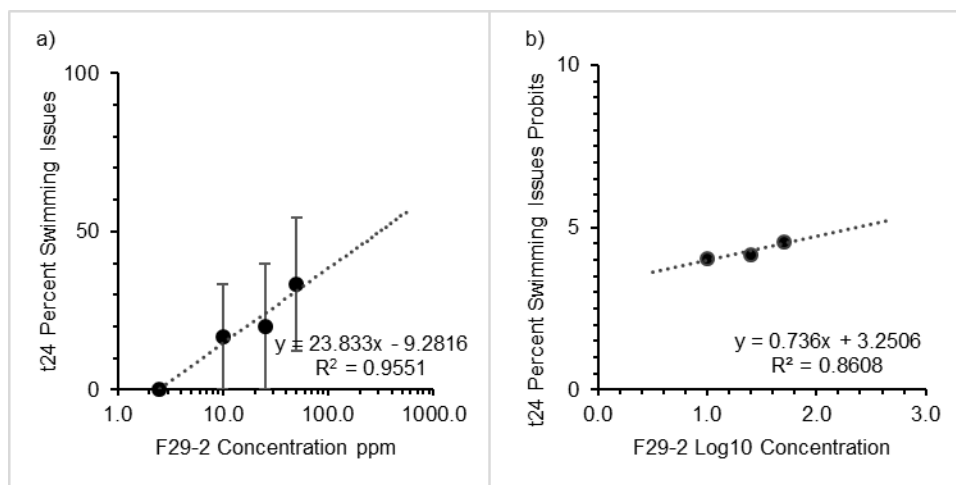


Figure 5.43 Probit analysis determination of the 24-hpe (t24) percent swimming issues ED₅₀ value for acute larval exposure to the lipophilic fraction F29-2 with error bars denoting \pm SEM (n = 5).

5.5 Discussion

Mixed assemblage, marine, filamentous cyanobacteria, initially identified, by morphology, belonging to polyphyletic, HAB-related *Lyngbya s.l.*, were recently

implicated in apparent ingestion related intoxications of captive bottlenose dolphins, managed at a marine mammal zoological facility in the Florida Keys. The dolphins then presented symptoms, seemingly associated with neurotoxicity, including uncoordinated swimming, ataxia, ocular dysfunction and respiratory issues. Under staff veterinarian care, the dolphins generally recovered from each apparent intoxication event within several days. Bounded by the Gulf of Mexico and the Atlantic Ocean, the Florida Bay-Florida Keys watershed is subject to heavy anthropogenic eutrophication leading to HAB events involving neurotoxin-producing organisms including cyanobacteria (e.g., *Lyngbya s.l.*), dinoflagellates (e.g., *Karenia brevis*) and diatoms (e.g., *Pseudo-nitzschia* spp.) within its waterways (Mylavarapu et al., 2017).

Samples of the cyanobacteria mixed assemblage (i.e., mat) were collected from within the captive dolphin enclosures for chemical exploration of known, or otherwise, uncharacterized neurotoxic metabolites. Chemical analysis of a portion of the sampled cyanobacteria mat, conducted by a commercial biotoxins laboratory, concluded the most culpable, marine HAB-related neurotoxins (i.e., ATX-a, STX, PbTx-2, DA), were below detectable limits, affirming the absence of any major blooms. Simultaneously, bioassay-guided fractionation, using the well-established zebrafish embryo-larvae toxicological models, was undertaken, in search of a putative neurotoxin. The neurotoxicological, and teratogenic, effects of PbTx-2 were first profiled in the zebrafish embryo and larval behavioral toxicological models. Neurotoxicity, and teratogenicity, were comparatively assessed, at each cyanobacteria fractionation step, against PbTx-2, used as the positive control. The aims of this research emphasized the use of the zebrafish embryo and larval behaviors as neurotoxicological models to chemically explore cyanobacteria and

characterize the relevant neurotoxicity of extracts and subsequent fractions, toward obtaining a putative metabolite. The chemical exploration of the cyanobacterial mat, associated with captive dolphin intoxications, led to the isolation of a secondary, from the lipophilic extract, exhibiting neurotoxicity in the zebrafish embryo-larval neurotoxicological model, consistent with the neurotoxic effects observed in the positive control, PbTx-2 (Lydon et al., submitted).

Characterization of neurotoxicological and teratogenic effects using PbTx-2 treated zebrafish embryos and larvae led to the selection of a suitable exposure concentration (i.e., 25 ppb [27.9 nM] PbTx-2) to comparatively, and quickly, screen cyanobacteria extracts and subsequent fractions for potential neurotoxicity using the zebrafish embryo-larva neurobehavioral models. The physical and behavioral neurotoxic effects of four PbTx-2 exposure concentrations, profiled against negative controls (i.e., untreated in aquaria system water, methanol solvent) in the zebrafish embryo and larval behavioral models, led to a suitable concentration to quickly and comparatively, guide the fractionation of the cyanobacterial material. The PbTx-2 treatments evaluated in the 5-day embryogenesis study included 2.5, 5, 10 and 25 ppb and normally developed 5-dpf larvae were exposed to 2.5, 10, 25 and 50 ppb PbTx-2 over 24 hours. Normal larval development was defined by fully inflated swim bladders and exhibiting typical beat-and-glide swimming behaviors and buoyancy regulation (i.e., upright orientation). The PbTx-2 concentrations evaluated during embryogenesis were non-lethal to all developing embryos through 5 dpf, whereas larval treatments with PbTx-2 established an LD₅₀ value of 16.6 ppb (18.5 nM) at 24 hpe, by probit analysis. Whilst, embryos chronically exposed to PbTx-2 during embryogenesis exhibited little to no effects regarding mortality, SCF

and hatch rates, neurotoxicity was particularly evident by the D2 tachycardia and D5 impaired swimming behaviors. Indeed, a D5 ED₅₀ value of 1.0 ppb (1.12 nM) was determined by probit analysis of the percentage of embryos having swim bladder dysfunction. Teratogenicity was implied from the percentages of deformed embryos observed through D5 where an ED₅₀ value was estimated from the nearly 50% deformed embryos associated with the 10 ppb (11.2 nM) PbTx-2 treatment. Interestingly, the 10 ppb PbTx-2 treated embryos exhibited significantly decreased average SCF relative to controls, indicative of neurotoxicity. The variable results observed during the embryogenesis study may be attributed to the mode of action of PbTx-2 as a neuromodulator and the fact that developing zebrafish can undergo neuronal regeneration (Villegas et al., 2012).

Neurotoxicity-related effects (e.g., swim bladder deformations, erratic swim behaviors) in otherwise normally developed 5-dpf larvae treated with PbTx-2 were observed within one hour and persisted through the end of the 24-hour study. Notably, PbTx-2 treatments adversely impacted swim bladder morphology and function, affecting buoyancy regulation. Erratic swimming behaviors (e.g., corkscrew patterns), hyperkinesis (e.g., convulsions, twitching), and general inactivity (e.g., laying on side). Moreover, the lethality of PbTx-2 to zebrafish larvae established a 24-hour LD₅₀ value of 18.5 nM (16.6 ppb). A previous ichthyotoxicity study by Rein et al. (1994) quantified a 24-hour LD₅₀ value of 14.3 nM of PbTx-2 in exposed female mosquitofish (*Gambusia affinis*), a North American subtropical, freshwater species akin to zebrafish.

Most abundant in nature, PbTx-2 is readily metabolized into the PbTx-3 congener and bioaccumulates in the visceral (e.g., liver, stomach) and muscle tissues of several

marine fish species exposed via contaminated prey, particularly shellfish (e.g., oysters, clams) and HAB producing phytoplanktons (Naar et al., 2007). A recent developmental toxicity study with PbTx congeners, by Colman and Ramsdell (2003), microinjected PbTx-3 directly into fertilized eggs of freshwater Japanese rice fish, medaka (*Oryzias latipes*), defining an LD₅₀ value of 4 ng PbTx-3 per egg. Tachycardia was evident with PbTx-3 exposure, whilst exposure to PbTx-1 caused bradycardia, further supporting different modes of action for these voltage-gated sodium channel agonists. The lipophilicity of PbTx-2 allows entry into cell membranes and across the blood-brain barrier, overstimulating nerve, skeletal and heart muscle cells, resulting in ataxia (e.g., uncontrolled tremors, twitching, ocular dysfunction). The neurotoxicological results presented herein demonstrated that PbTx-2 can cross the zebrafish chorion membrane during development as evidenced by the deformities observed at 1 dpf including yolk and pericardial edemas (not shown) continuing through 5 dpf manifested as bent body axis, deficient swim bladder development and aberrant swimming behaviors (see Figure 5.32). Thus, based on the overall developmental and behavioral neurotoxicity effects profiled in the 5-day embryogenesis and 24-hour larval studies, the 25 ppb (0.028 µM) PbTx-2 exposure concentration was chosen as the positive control treatment to guide the fractionation of the cyanobacteria material towards a putative metabolite.

The cyanobacteria crude extract displayed sublethal bioactivity in the range of 2.5 to 50 ppm consistent with PbTx-2. The crude extracts (i.e., EtOAc, BuOH, Aq), obtained from the initial fractionation of the cyanobacteria material, continued to exhibit neurotoxic and teratogenic bioactivity analogous to PbTx-2 within the tested concentrations. The EtOAc extract most aligned with effects observed for the

cyanobacteria crude extract and PbTx-2 whilst the BuOH extract proved lethal and the Aq extract displayed inconsistent results. Indeed, an LD₅₀ value of 36 ppm was established at D1 of the embryogenesis study, persisted through D5. Thus, fractionation of the EtOAc crude extract was undertaken by normal-phase (i.e., silica gel) automated, flash chromatography, with a mobile phase gradient of n-hexanes:EtOAc:MeOH (H-E-M) of increasing polarity from 95:5:0 to 0:0:100, resulting in 74 fractions. A semi-pure fraction eluted with 50:50:0 H-E-M (i.e., F29), exhibiting biological activity aligned most with that of PbTx-2 in the five-day developmental neurotoxicity and the 24-hour larval neurobehavioral assays. Particularly, treatments with F29 were not lethal, the percentages of deformed embryos and observed larval swimming issues at D5 and 24 hours were consistent with those of PbTx-2. An orthogonal approach used reverse-phase (i.e., C₁₈) column chromatography with an aqueous MeOH mobile phase gradient from 20-0%, to further separate F29. The first of three eluted fractions, F29-1, displayed neurotoxicity effects most consistent with PbTx-2 including average SCF, deformed embryos, and swimming issues. Purification of F29-1 via C₁₈ column chromatography with an isocratic 20% aqueous methanol mobile phase isolated the compound of interest in the first eluent as F29-1A (see Figure 5.1). As reported in Chapter Six (see section 6.4.2 Structural Elucidation of Eudesmacarbonate), structural elucidation and characterization of F29-1A identified the neurotoxic metabolite from F29-1A to be eudesmacarbonate, a cyclic carbonate ester of the sesquiterpene eudesmane, exhibiting neurotoxicity in the zebrafish neurotoxicity models used during the fractionation of the cyanobacterial material described herein.

In comparison to PbTx-2, the developmental neurotoxicity, and teratogenicity, of the cyanobacteria extracts (i.e., EtOAc) and subsequent fractions (i.e., F29, F29-1), manifested as decreased SCF at 24 hpf, increased deformities, bradycardia and delayed hatching rates observed at D2 and D3, and swimming issues at D5 related to irregular swim bladders and aberrant swimming behaviors compared to the ASW and MeOH negative controls (see Figure 5.33). Indeed, the swimming issues observed were well aligned with those elicited by PbTx-2 exposures, including head-up passive drifting, erratic corkscrew swim patterns and swim bladder deformations (e.g., shrunken) affecting buoyancy regulation, in both the embryogenic and larval studies (see Appendix). Interestingly, altered heart rhythms of bradycardia and tachycardia are both neurotoxicity-specific effects owing to potentially different modes of action. Thus, the bradycardia observed with embryonic exposure to cyanobacterial extracts and fractions may hint of neurotoxicity induced by a different mechanistic action than the tachycardia effects expressed by PbTx-2 exposure. Moreover, during the 24-hour larval neurobehavioral studies, some of the larvae exposed to the cyanobacteria extracts and fractions appeared to recover from the effects of these treatments also implying a different, mode of action than that of PbTx-2. Indeed, approximately half of the larvae in the each of the cyanobacteria (i.e., extracts, fractions) treatment conditions, appeared to recover within 24 hours. For the F29-2 treatments, the 17-fold increase in ED₅₀ values from 14.0 to 238 ppm after 1 and 24 hours of exposure suggested larval recoveries. However, the correlation coefficient was lower than desired at 0.8608.

Application of PbTx-2 as a positive control in the zebrafish developmental toxicological model afforded reliable characterization of teratogenic and neurotoxic

effects to quickly assess the cyanobacteria extracts and subsequent fractions for neurotoxicity. The differences in observed effects between PbTx-2 and cyanobacteria samples such as tachycardia versus bradycardia also hinted at the potential to discern the mechanistic action involved. Moreover, comparative assessment of larval zebrafish behaviors as a neurotoxicological model using PbTx-2, rapidly guided the identification of potentially neurotoxic cyanobacteria extracts and fractions to the ultimate purification of a neurotoxic metabolite. The larval neurobehavioral studies also implied the potential for neuroregeneration as observed by the apparent recovery of larvae exposed to the cyanobacteria extracts and fractions. However, neuroregeneration was not evident in the chronic embryogenic study as no embryo recoveries were observed, suggesting the adverse exposure effects impaired neural development. More importantly, these findings show that cyanobacteria fractionation leading to a previously undocumented eudesmane-type sesquiterpene aligned well the apparent transient nature of the captive dolphin intoxications, potentially related to ingesting the mixed assemblage of marine filamentous cyanobacteria assemblage.

5.6 Conclusions

The present study utilized the zebrafish embryo and larva as neurobehavioral models of neurotoxicity to characterize, for the first time, the neurobehavioral toxicity, and teratogenicity, of the known HAB neurotoxin, PbTx-2. The PbTx-2 standard was then applied in this study, as a positive control in the zebrafish embryo and larva neurobehavioral toxicity models, to guide the fractionation of cyanobacterial material toward the subsequent isolation, purification and chemical characterization of eudesmacarbonate from a mixed assemblage of marine filamentous cyanobacteria, in the

Florida Keys. This neurotoxic metabolite may contribute – along with the diversity of recognized neurotoxins affiliated with the previously classified and ubiquitous, polyphyletic, aquatic genus *Lyngbya* - to the available chemical defenses of marine cyanobacteria now including *Neolyngbya* spp. Indeed, eudesmacarbonate may be the putative molecule associated with recently observed apparent intoxications, seemingly neurotoxic, of captive bottlenose dolphins, subsequent to grazing cyanobacteria, including *Neolyngbya* spp., growing within their Florida Keys habitats. Considering marine cyanobacteria, particularly *Lyngbya s.l.*, are currently undergoing reclassifications via phylogenetic advances, the resulting taxa warrant further investigation of previously identified bioactive metabolites, including neurotoxins and their biosynthetic origins. Likewise, neurotoxicity testing may be prudent during chemical inquiries of marine cyanobacteria species in relation to climate change, increasing eutrophication and HAB formations, adversely impacting aquatic organisms and perhaps human health. Moreover, this study showed the use of developing and larval zebrafish behaviors to be reliable models to assess neurotoxic effects in the bioassay-guided isolation of a novel, natural product derived from a marine cyanobacteria, consistent with the known HAB neurotoxin, PbTx-2. The zebrafish toxicological model continues to provide a cost-effective, rapid means to assess biological activity, including neurotoxicity, during natural product chemical explorations of marine cyanobacteria.

5.7 Acknowledgments

Support for this research was provided, in part, by FIU Teaching Assistance Grants and a Dissertation Year Fellowship. Chemical isolation, purification and characterizations and phylogenetic inferences of the cyanobacterial mat were obtained

through the altruistic charity of Valerie Paul with Sarath Gunasekera, Thomas Sauvage and Larissa dos Santos of the Smithsonian Marine Station at Fort Pierce, Fort Pierce, FL. Collections of cyanobacteria, investigated in the study, were kindly provided by Johanna Fava-Mejia, D.V.M, Ph.D., and staff at Dolphins Plus Inc., Key Largo, FL. Morphology-based taxonomic identifications of macrophytes and filamentous cyanobacteria were assisted by Kevin Montenegro and Ligia Collado-Vides at the FIU Marine Macroalgae Research Laboratory, Miami Fl.

5.8 References

Aráoz, R., Molgó, J., de Marsac, N.T., 2010. Neurotoxic cyanobacterial toxins. *Toxicon* 56, 813-828. doi:10.1016/j.toxicon.2009.07.036

Berry, J.P., Gantar, M., Gibbs, P.D.L., Schmale, M.C., 2007. The zebrafish (*Danio rerio*) as a model system of identification and characterization of developmental toxins from marine and freshwater microalgae. *Comp. Biochem. Physiol. C Toxicol Pharmacol.* 145(1), 61-72. doi:10.1016/j.cbpc.2006.07.011

Bossart, G.D., 2011. Marine mammals as sentinel species for oceans and human health. *Vet. Pathol.* 48(3), 676-690. doi:10.1177/0300985810388525

Brown, A., Foss, A., Miller, M.A., Gibson, Q., 2018. Detection of cyanotoxins (microcystins/nodularins) from estuarine and coastal bottlenose dolphins (*Tursiops truncatus*) from Northeast Florida. *Harmful Algae* 76, 22-34. doi:10.1016/j.hal.2018.04.011

Bukaveckas, P.A., Franklin, R., Tassone, S., Trache, B., Egerton, T., 2018. Cyanobacteria and cyanotoxins at the river-estuarine transition. *Harmful Algae* 76, 11-21. doi:10.1016/j.hal.2018.04.012

Burns, J., 2008. Toxic cyanobacteria in Florida waters. In *Cyanobacterial harmful algal blooms: state of the science and research needs.* 127-137. Springer, New York, NY.

Caires, T.A., de Mattos Lyra, G., Hentschke, G.S., de Gumão Pedrini, A., Sant'Anna, C.L., de Castro Nunes, J.M., 2018a. *Neolyngbya* gen. nov. (Cyanobacteria, Oscillatoriaceae): A new filamentous benthic marine taxon widely distributed along the Brazilian coast. *Mol. Phylogenet. Evol.* 120, 196-211. doi:10.1016/j.ympev.2017.12.009

Caires, T.A., de Lyra, G.M., Hentschke, G.S., de Silva, A.M.S., de Araújo, V.L., Anna, C.L.S., de Nunes, J.M.C., 2018b. Polyphasic delimitation of a filamentous marine genus,

Capillus gen. nov. (Cyanobacteria, Oscillatoriaceae) with the description of two Brazilian species. *Algae* 33(4), 291–304. doi:10.4490/algae.2018.33.11.25

Caires, T.A., Sant’Anna, C.L., Nunes, J.M., 2019. *Capilliphycus* gen. nov.; validation of “*Capillis* T.A.Caires, Sant’Anna & J.M.Nunes”, inval. (Oscillatoriaceae, Cyanobacteria). *Notulae Algarum*, 95, 1-2.

Capper, A., Erickson, A.A., Ritson-Williams, R., Becerro, M.A., Arthur, K.A., Paul, V.J., 2016. Palatability and chemical defences of benthic cyanobacteria to a suite of herbivores. *J. Exp. Mar. Biol. Ecol.* 474, 100–108. doi:10.1016/j.jembe.2015.09.008

Carmichael, W.W., Evans, W.R., Yin, Q.Q., Bell, P., Moczydlowski, E., 1997. Evidence for paralytic shellfish poisons in the freshwater cyanobacterium *Lyngbya wollei* (Farlow ex Gomont) comb. nov. *Appl. and Environ. Microbiol.* 63(8), 3104-310.

Colman, J.R., Ramsdell, J.S., 2003. The type B brevetoxin (PbTx-3) adversely affects development, cardiovascular function, and survival in medaka (*Oryzias latipes*) embryos. *Environ. Health Persp.* 111, 1920-1925. doi:10.1289/ehp.6386

Davis, D.A., Mondo, K., Stern, E., Annor, A.K., Murch, S.J., Coyne, T.M., Brand, L.E., Niemeyer, M.E., Sharp, S., Bradley, W.G., Cox, P.A., Mash, D.C., 2019. Cyanobacterial neurotoxin BMAA and brain pathology in stranded dolphins. *PLoS One* 14(3), e0213346. doi:10.1371/journal.pone.0213346

Fire, S.E. Flewelling, L.J., Stolen M., Durden, W.N., de Wit, M., Spellman, A.C., Wang, Z., 2015. Brevetoxin-associated mass mortality event of bottlenose dolphins and manatees along the east coast of Florida, USA. *Mar. Ecol. Prog. Ser.* 526, 241-251. doi:10.3354/meps11225

Fire, S.E. Flewelling, L.J., Wang, A., Naar, J., Henry, M.S., Pierce, R.H., Wells, R.S., 2008. Florida red tide and brevetoxins: Association and exposure in live resident bottlenose dolphins (*Tursiops truncatus*) in the eastern Gulf of Mexico, U.S.A. *Mar. Mammal Sci.* 24(4), 831-844. doi:10.1111/j.1748-7692.2008.00221.x

Foss, A.J., Philips, E.J., Yilmaz, M., Chapman, A., 2012. Characterization of paralytica shellfish toxins from *Lyngbya wollei* dominated mats collected from two Florida springs. *Harmful Algae* 16, 98-107. doi:10.1016/j.hal.2012.02.004

Hall, M.O., Madley, K., Durako, M.J., Zieman, J.C., Robblee, M.B., 2007. Florida Bay In Seagrass Status and Trends in the Northern Gulf of Mexico: 1940-2002, eds. Handley, L., Altsman, D., DeMay, R., U.S. Geological Survey Scientific Investigations Report 2006-5287, 243-254. doi:10.3133/sir20065287

Henry, T.R., Spitsbergen, J.M., Hornung, M.W., Abnet, C.C., Peterson, R.E., 1997. Early life stages toxicity of 2,3,7,8-tetrachlorodibenzo-*p*-dioxin in zebrafish (*Danio rerio*). *Toxicol. Appl. Pharm.* 142, 56-68.

- Jones, A.C., Monroe, E.A., Podell, S., Hess, W.R., Klages, S., Esquanazi, E., Niessen, S., Hoover, H., Rothmann, M., Lasken, R.S., Yates, J.R., Reinhardt, R., Kube, M., Burkart, M.D., Allen, E.E., Dorrestein, P.C., Gerwick, G.W., Gerwick, L., 2011. Genomic insights into the physiology of and ecology of the marine filamentous cyanobacterium *Lyngbya majuscula*. PNAS 108(21), 8815-8820.
- Kalueff, V., Gebhardt, M., Stewart, A.M., Cachat, J.M., Brimmer, M., Chawla, J.S., Craddock, C., Kyzar, E.J., Roth, A., Landsman, S., Gaikward, S., Robinson, K., Baatrup, E., Tierney, K., Shamchuk, A., Norton, W., Miller, N., Nicolson, T., Braubach, O., Gilman, C. P., Pittman, J., Rosemberg, D.B., Gerlai, R., Echevarria, D., Lamb, E., Neuhauss, S.C.F., Weng, W., Bally-Cuif, L., Schneider, H., 2013. Towards a comprehensive catalog of zebrafish behavior 1.0 and beyond. Zebrafish 10(1), 70-86. doi:10.1089/zeb.2012.0861
- Komárek, J., Zapomelova, E., Smarda, J., Kopecky, J., Rejmankova, E., Woodhouse, J., Neilan, B.A., Komarkova, J., 2013. Polyphasic evaluation of *Limnoraphis robusta*, a water-bloom forming cyanobacterium from Lake Atitlan, Guatemala, with a description of *Limnoraphis* gen. nov. Fottea 13 (1): 39–52. doi:10.5507/fot.2013.004
- Landsberg, J.H., Hall, S., Johannessen, J.N., White, K.D., Conrad, S.M., Abbott, J.A., Flewelling, L.J., Richardson, R.W., Dickey, R.W., Jester, E.L.E., Etheridge, S.M., Deeds, J.R., Van Dolah, F.M., Leighfield, T.A., Zou, Y., Beaudry, C.G., Benner, R.A., Rogers, P.L., Scott, P.S., Kawabata, K., Wolny, J.L., Steidinger, K.A., 2006. Saxitoxin Pufferfish Poisoning in the United States, with the First Report of *Pyrodinium bahamense* as the Putative Toxin Source. Environ. Health Persp. 114, 1502-1507. doi:10.1289/ehp.8998
- Lapointe, B.E., Clark, M.W., 1992. Nutrient Inputs from the Watershed and Coastal Eutrophication in the Florida Keys. Estuaries 15(4), 465-476.
- Lapointe, B.E., Herren, L.W., Debortoli, D.D., Vogel, M.A., 2015. Evidence of sewage-driven eutrophication and harmful algal blooms in Florida's Indian River Lagoon. Harmful Algae 43, 82-102. doi:10.1016/j.hal.2015.01.004
- Legradi, J., el Abdellaoui, N., van Pomeran, M., Legler, J., 2015. Comparability of behavioral assays using zebrafish larvae to assess neurotoxicity. Environ. Sci. Pollut. Res. 22, 16277-16289. doi:10.1007/s113586-014-3805-8
- Lydon, C.; Mathivathanan, L., Sanchez, J., dos Santos, L.A.H., Sauvage, T., Gunasekera, S., Paul, V., Berry, J.P., (submitted). Eudesmacarbonate, an eudesmane-type sesquiterpene from marine filamentous cyanobacterial mat (Oscillatoriales) in the Florida Keys. J. Nat. Prod.
- McGregor, G.B., Sendall, B.C., Lindell, D., 2015. Phylogeny and toxicology of *Lyngbya wollei* (Cyanobacteria, Oscillatoriales) from north-eastern Australia, with a description of *Microseira* gen. nov. J. Phycol. 51 (1), 109–119. doi:10.1111/jpy.12256

- Méjean A., Perraud-Thomas, C., Kerbrat, A.S., Golubic, S., Pauillac, S., Chinain, M., Laurent, D., 2010. First identification of the neurotoxin homoanatoxin-a from mats of *Hydrocoleum lyngbyaceum* (marine cyanobacterium) possibly linked to giant clam poisoning in New Caledonia. *Toxicon* 56, 829-835. doi:10.1016/j.toxicon.2009.10.029
- Milbrandt, E.C., Bartleson, R.D., Coen, L.D., Rybak, O., Thompson, M.A., DeAngelo, J.A., Stevens, P.W., 2012. Local and regional effects of reopening a tidal inlet on estuarine quality, seagrass habitat, and fish assemblages. *Cont. Shelf Res.* 41, 1-16. doi:10.1016/j.csr.2012.03.012
- Mylavarapu, R., Hines, K., Obreza, T., Means, G., 2017. Watershed of Florida: Understanding a Watershed Approach to Water Management. <https://edis.ifas.ufl.edu/ss568#FIGURE%202> (last accessed 08OCT2019)
- Naar, J.P., Flewelling, L.J., Lenzi, A., Abbott, J.P., Granholm, A., Jacocks, H.M., Gannon, D., Henry, M., Pierce, R., Baden, D.G., Wolny, J., Landsberg, J.H., 2007. Brevetoxins, like ciguatoxins, are potent ichthyotoxic neurotoxins that accumulate in fish. *Toxicon* 50(5) 707–723. doi:10.1016/j.toxicon.2007.06.005.
- Peacock, M.B., Gobble, C.M., Senn, D.B., Cloern, J.E., Kudela, R.M., 2018. Blurred lines: Multiple freshwater and marine algal toxins at the land-sea interface of San Francisco Bay, California. *Harmful Algae* 73, 138-147. doi:10.1016/j.hal.2018.02.005
- Phlips, E.J., Badylak, S., Christman, M., Wolny, J., Brame, J., Garland, J., Hall, L., Hart, J., Landsberg, J., Lasi, M., Lockwood, J., Paperno, R., Scheidt, D., Staples, A., Steidinger, K., 2011. Scales of temporal and spatial variability in the distribution of harmful algae species in the Indian River Lagoon, Florida, USA. *Harmful Algae* 10, 277-290. doi:10.1016/j.hal.2010.11.001
- Rein, K.S., Lynn, B., Gawley, R.E., Baden, D.G., 1994. Brevetoxin B: Chemical modifications, synoptosome binding, toxicity, and an unexpected conformational effect. *J. Org. Chem.* 59 (8), 2107-2113. doi:10.1021/jo00087a028
- Rodgers, K.J., Main, B.R., Samardzic, K., 2018. Cyanobacterial neurotoxins: Their occurrence and mechanisms of toxicity. *Neurotox. Res.* 33, 168-177. doi:10.1007/s12640-017-9757-2
- Sarmah, S., Marrs, J.A., 2016. Zebrafish as a Vertebrate Model to Evaluate Effects of Environmental Toxicants on Cardiac Development and Function. *Int. J. Mol. Sci.* 17, 2123-2139. doi:10.3390/ijms17122123
- Sigua, G.C., Steward, J.S., Tweedale, W.A., 2000. Water-Quality Monitoring and Biological Integrity Assessment in the Indian River Lagoon, Florida: Status, Trends, and Loadings (1988-1994). *Environ. Manage.* 25(2), 199-209. doi:10.1007/s002679910016

- Swain, S.S., Padhy, R.N., Singh, P.K., 2015. Anticancer compounds from cyanobacterium *Lyngbya* species: a review. *Antonie Leeuwenhoek* 108, 223-265. doi:10.1007/s10482-015-0487-2
- Twiner, M.J., Fire, S., Schwacke, L., Davidson, L., Wang, Z., Morton, S., Roth, S., Balmer, B., Rowles, T.K., Wells, R.S., 2011. Concurrent Exposure of Bottlenose Dolphins (*Tursiops truncatus*) to Multiple Algal Toxins in Sarasota Bay, Florida, USA. *PLoS One* 6(3), e17394. doi:10.1371/journal.pone.0017394
- Villegas, R., Martin, S.M., O'Donnell, K.C., Carillo, S.A., Sagasti, A., Allende, M.L., 2012. Dynamics of degeneration and regeneration in developing zebrafish peripheral axons reveals a requirement for extrinsic cell types. *Neural Dev.* 7, 19. doi:10.1186/1749-8104-7-19
- Wang, P.F., Martin, J., Morrison, G., 1999. Water Quality and Eutrophication in Tampa Bay, Florida. *Estuar. Coast. Shelf S.* 49, 1-20.
- Wang, K.R., Payne, P.M., Thayer, C.G., (compilers), 1994. Coastal Stock(s) of Atlantic Bottlenose Dolphin: Status Review and Management: Proceedings and recommendations from a workshop held in Beaufort, North Carolina, 13-14 September 1993. U.S. Dep. Commer., NOAA Tech. Memo. NMFS-OPR-4, 121.

**6. EUDESMACARBONATE AN EUDESMANE-TYPE SESQUITERPENE
FROM MARINE FILAMENTOUS CYANOBACTERIAL MAT
(OSCILLATORIALES) IN THE FLORIDA KEYS (Submitted, Journal of
Natural Products)**

6.1 Abstract

Marine filamentous cyanobacteria were recently implicated in apparent ingestion-related intoxications of captive bottlenose dolphins in the Florida Keys.

Eudesmacarbonate (1), a novel, cyclic carbonate eudesmane-type sesquiterpene, was isolated, as the putative compound, from filamentous cyanobacterial mats (Sample CAL-V) collected from within the dolphin habitation. Sequencing of 16S rDNA data revealed that the mats were composed of closely related Oscillatoriacean species possibly dominated by a previously undocumented *Neolyngbya* sp. and two species, including *Neolyngbya arenicola* and a representative found in a poorly supported clade, including the genera *Limnoraphis* and *Capilliphycus*. The structure of 1 was elucidated by its (+)-HRESIMS, 1D and 2D NMR, single-crystal X-ray diffraction (XRD) and vibrational circular dichroism (VCD) data. Using the zebrafish (*Danio rerio*) embryo-larval model to assess neurotoxicity, 1 (9.4 μM) exhibited developmental and neurobehavioral impairments consistent with those observed for the known marine HAB-neurotoxin brevetoxin-2 (PbTx-2) at 0.0223 μM .

6.2 Introduction

Marine cyanobacteria produce a wealth of noxious (Paerl and Otten, 2013; Tamele et al., 2019) and therapeutically exploitable (Singh et al., 2017; Shah et al., 2017) natural products with diverse structural and biological activities including neurotoxins.

Historically, the genus *Lyngbya sensu lato (s.l.)* has afforded potent neurotoxic secondary metabolites with a range of structural classes such as peptides, polyketides, alkaloids and a disputed non-essential amino acid (Aráoz et al., 2010; Delcourt et al., 2018; Lance et al., 2018). Previously classified *Lyngbya* spp. including the toxigenic *L. majuscula* are now recognized as taxonomically complex, polyphyletic, mixed assemblages (Jones et al., 2011; Soares et al., 2015). Indeed, recent molecular-based phylogenetic investigations of *Lyngbya s.l.* have identified newly accepted genera including *Neolyngbya* (Caires et al., 2018a). Marine filamentous, polyphyletic assemblages continue to yield biologically active secondary metabolites from increasingly diversified taxa (Cai et al., 2016). Captive bottlenose dolphins (*Tursiops truncatus*), managed in a marine mammal zoological facility in the Florida Keys, were recently observed grazing on macroalgae and filamentous cyanobacteria growing within their enclosures. Subsequently, the dolphins presented apparent intoxications expressed by neurological symptoms of uncoordinated swimming behaviors (i.e., ataxia), ocular dysfunctions (i.e., blepharospasms) and respiratory issues. Each case of apparent intoxication was addressed and resolved, generally within several days, by the facility's veterinarian.

Representative samples of the filamentous, marine cyanobacterial mat, associated with grazing by the captive dolphins, were collected from within their enclosure for taxonomic and chemical characterizations. The mat comprised a mixed assemblage of filamentous cyanobacteria morphologically resembling the formerly classified, toxigenic genus *Lyngbya*. Molecular-based phylogenetic techniques were employed to genetically identify the cyanobacteria members comprising the mat. Traditional bioactivity-guided fractionation utilized the widely accepted zebrafish (*Danio rerio*) toxicological models

(Beekhuijzen et al., 2015; Nishimura et al., 2015) to chemically investigate the mat leading to a putative neurotoxic metabolite described herein.

6.3 Methods

6.3.1 Biological Material

The cyanobacteria samples for this study were collected by snorkeling at a depth of 2-5 m (8-16 ft) at the marine mammal zoological facility in the Florida Keys, Florida, United States (25.084192° N, 80.442295° W), in January 2016 and resampled in December 2018 for phylogenetic characterization using 16S rDNA techniques (see 6.3.2. DNA Sequencing and Phylogenetics). A voucher specimen (CAL-V) is maintained at the Smithsonian Marine Station, Fort Pierce, FL and 16S rDNA sequences obtained via cloning of the PCR products were deposited under GenBank accession MN845141-MN845143. Voucher specimen preparations were previously described in Chapter Two (see 2.2.1.2 Taxonomic Reference Samples).

6.3.2 DNA Sequencing and Phylogenetics

The CAL-V isolate (approximate 0.5 mg) was preserved in 1.5 mL of *RNAlater* (Ambion, Austin, Texas, USA) and stored at -80 °C until analysis. Nucleic acids from a subsample of the December 2018 preserved isolate (approximately 0.1 mg) were extracted with a DNeasy Plant Mini Kit (Qiagen, Hilden, Germany) and subjected to PCR amplification of the 16S ribosomal gene (16S rDNA) with cyanobacterial primers 106F and 781R from Nubel et al. (1997). The PCR products were cloned with a pGEM-T Easy Vector Systems (Promega Corporation, Madison, WI, USA) according to the manufacturer's protocol. Clones were grown on LB agar plates containing 100 µg/mL Ampicillin 0.1 mM IPTG and 40 µg/mL X-Gal (GOLDBIO, St Louis, MO, USA) and

PCR performed on white colonies with M13 primers. Colony PCR products of the correct size (≥ 1 mm diameter) were then Sanger sequenced at the Laboratory of Analytical Biology (LAB, Smithsonian Institution, Washington DC) and resulting chromatograms assembled in Sequencher v5.1. Following BLASTn searches (Alstchul et al., 1997) to retrieve closely related matches to CAL-V for phylogenetic context, phylogenetic reconstruction with RAxML (Stamatakis, 2014) was performed to find the best tree out of 1000 tree search restarts and branch support was assessed with 1000 bootstrap replicates. The remainder of the CAL-V isolate is maintained at the Smithsonian Marine Station as a voucher.

6.3.3 Extraction and Isolation of Eudesmacarbonate

Lyophilized cyanobacterial biomass (50 g), from the January 2016 cyanobacteria collection, was exhaustively extracted with EtOAc-MeOH (1:1) and dried in vacuo (15 g). A 13 g portion of the crude extract was partitioned (3 \times) between EtOAc-H₂O (3:1). The EtOAc layer was dried in vacuo (2.4 g) and exhibited biological activity in the zebrafish developmental neurotoxicity and neurobehavioral assays. A 500 mg portion of the bioactive EtOAc extract was then fractionated by normal-phase semi-preparative flash chromatography (Büchi Reveleris HP silica gel, 40 g, 60-75 Å mesh, 16-24 µm; flow rate 20 mL/min) using a stepwise solvent gradient of hexanes-EtOAc-MeOH from 95:5:0 to 0:0:100 over 80 min on a Büchi Reveleris X2 automated flash chromatography system equipped with UV/ELSD detection. The bioactive fraction eluted with 50:50:0 hexanes-EtOAc-MeOH, was dried in vacuo (39 mg), and further separated using reversed-phase C₁₈ (Varian BondElut, 1.6 g) vacuum-assisted column chromatography with a step gradient elution of 80-100% MeOH in H₂O. The bioactive fraction eluted

with 80% MeOH and was purified using Varian BondElut octadecyl-functionalized silica gel (C₁₈) column chromatography with 80% MeOH isocratic elution to afford eudesmacarbonate (11.3 mg) as an amorphous, white solid in the first eluent. The solid was recrystallized in MeOH yielding 10.2 mg of compound 1. All solvents were HPLC or LC-MS grade (Fisher Scientific, OmniSolv).

The lyophilized sample (3.2 mg) of the second batch of cyanobacterial material, collected in December 2018 and representative of CAL-V, was thrice extracted with EtOAc-MeOH (1:1) and dried in vacuo (0.3mg). The residue was reconstituted with MeOH to approximately 2 mg/mL and analysis by low-resolution LC-MS attributed the production of 1 by the cyanobacteria genera associated herein with *Neolyngbya*, *Capilliphycus*, and *Limnoraphis* (see below).

6.3.4 Chemical Characterization of Eudesmacarbonate

Optical rotation data was measured on a Rudolph Research Analytical Autopol III automatic polarimeter. The VCD spectra were acquired using a BioTools dualPEM ChiralIR spectrophotometer (Jupiter, FL, USA). The X-ray data were collected on a Bruker D8 Quest diffractometer. The IR spectroscopic data were recorded with a Thermo Scientific Nicolet iS FTIR spectrometer. The 1D and 2D NMR experiments were performed on a JEOL ECA-600 spectrometer operating at 600.17 MHz for ¹H and 150.9 MHz for ¹³C. Chemical shift assignments were referenced to (CD₃)₂CO ($\delta_{\text{H}} = 2.04$, $\delta_{\text{C}} = 29.8$ and 206.3). The low-resolution LC-MS data were obtained using an LC electrospray ionization MS system equipped with an LTQ Advantage Max spectrometer (Thermo Finnegan). The high-resolution mass spectrum (HRMS) data was acquired on an Agilent 6210 LC-TOF mass spectrometer equipped with an APCI/ESI multimode ion source-

detector at the Mass Spectrometer Facility at the University of California, Riverside, California. Normal-phase chromatographic separation was performed on a 40 g Büchi Reveleris HP silica gel cartridge using a Büchi Reveleris X2 Flash Chromatography/Preparative Purification system equipped with ELSD/UV detection. Varian BondElut octadecyl-functionalized silica gel (C₁₈) was used for column chromatography. All solvents were HPLC (Fisher Scientific) or LC-MS grade (OmniSolv).

6.3.5 X-ray Crystallographic Analysis

Translucent-white, orthorhombic crystals were obtained by slow evaporation of a solution of 4 mg of compound 1 in 1 mL MeOH. Single crystal X-ray data were collected at 296 K on a Bruker D8 Quest diffractometer equipped with a CMOS detector (Mo K α radiation, $\lambda = 0.71073$). Data were collected with APEX3 and integrated with SAINT (Bruker 2018). The crystal structure was solved by intrinsic phasing methods available with ShelXT (Sheldrick, 2015) and refined by full-matrix, least-squares on F^2 using ShelXL using the Olex2 interface (Sheldrick, 2015; Dolomanov et al., 2009). Multi-scan absorption correction was performed using SADABS (Krause et al, 2015). The geometrically positioned hydrogen atoms were refined using riding models with fixed $U_{\text{iso}}(\text{H}) = 1.2U_{\text{eq}}(\text{CH}, \text{CH}_2)$ and $1.5U_{\text{eq}}(\text{CH}_3)$. The ternary CH were refined with riding coordinates C5(H5), C6(H6), C7(H7) and C11(H11). The secondary CH₂ were refined with riding coordinates C1(H1A, H1B), C2(H2A, H2B), C3(H3A, H3B), C8(H8A, H8B), and C9(H9A, H9B). The methyl groups were idealized and refined as rotating groups for C12(H12A, H12B, H12C), C13(H13A, H13B, H13C), C14(H14A, H14B, H14C) and C15(H15A, H15B, H15C). The relative/absolute configuration was assigned based on

data obtained from NMR data for 1. Graphics were drawn using CrystalMaker9 (Palmer, 2014). The structural data of compound 1 were deposited in the Cambridge Crystallographic Data Center (CCDC No. 1945948). Copies of the X-ray data can be obtained free of charge via the Internet at <https://www.ccdc.cam.ac.uk/>.

6.3.6 Experimental VCD Analysis

The experimental IR and VCD spectra were measured using a BioTool dualPEM ChiralIR spectrophotometer, optimized at 1400 cm^{-1} . A 4 mg sample of 1 was dissolved in 0.15 mL CDCl_3 and placed in a BaF_2 cell with a fixed pathlength of $100\ \mu\text{m}$. Data were acquired for 12 hours at a resolution of 4 cm^{-1} . The spectra for the solvent were acquired for the same conditions then subtracted from the IR-VCD spectra of the compound. The geometry of the conformers was optimized using the Gaussian09 (Gaussian, Inc., Wallingford, CT, USA) software with the DFT at the B3LYP/6-31G(d). The experimental and calculated IR and VCD spectra for the (4*S*,5*R*,6*R*,7*S*,10*S*) configuration were then numerically compared for similarity in the $1100\text{-}1800\text{ cm}^{-1}$ region using the BioTools CompareVOA software. The calculated Boltzmann-averaged spectra for the enantiomer (4*R*,5*S*,6*S*,7*R*,10*R*) configuration and experimental spectra were also compared.

6.3.7 Zebrafish Neurotoxicity Assays

Zebrafish (*Danio rerio*), wild-type AB (i.e., embryos, larvae), were purchased from the Zebrafish Core Facility, University Miami, Miami, FL. Experiments were completed under approved animal protocols (Florida International University IACUC protocol number 16-075-CR02 entitled “The Zebrafish (*Danio rerio*) Embryo as a Model for Cyanobacterial Toxins (Using Embryos)” and 18-059 entitled “Larval Zebrafish as a

Behavioral Model for Neurotoxicity”; PI: John P. Berry) (See Appendix). Developing zebrafish were exposed to eudesmacarbonate (1) or brevetoxin-2 standard (positive control) or aquarium system water (negative control) and housed at 28 °C with a 16-h light and 8-h dark photoperiod over the respective five-day (embryonic) or 24-hour (larval) study duration. The zebrafish embryo-larva development and behavior, associated with neurotoxicity (Kalueff et al., 2013), were recorded at selected timepoints during the studies using a Spot Imaging Solutions TLB-4000 equipped with a Fisher Bioblock Scientific Carl Zeiss Microimaging STEMI 2000-C stereomicroscope and an Optronics Microcast HD Studio 3CCD 1080P 2MP digital camera. Exposure conditions included three different concentrations of compound 1, brevetoxin-2 (PbTx-2) standard (Sigma-Aldrich, St. Louis, MO, USA) as the positive control and aquarium system water (ASW) as the negative control. Compound 1 exposure concentrations were 9.4, 38 and 94 μM . Exposure concentrations of PbTx-2 included 0.0045 and 0.0223 μM . Solvent-resistant, polypropylene 24-well and 96-well plates were used to conduct the biological assays (Evergreen Scientific, Caplugs CA, Rancho Domingo, CA, USA). Replicate exposure concentrations were added to individual wells and dried prior to the addition of test subjects described for each assay.

6.3.7.1 Zebrafish Embryogenic Neurotoxicity Assay

The developmental toxicity assay previously described by Berry et al. (2007) was modified to assess the neurotoxicity effects of 1 in developing zebrafish embryos from 1-5 days post-fertilization (dpf). Five embryos, between 4-6 hpf, were added, in a 1-mL volume of aquarium system water, to each well of a polystyrene, 24-well plate, pre-treated with triplicate test concentrations of 1 or PbTx-2. The developing embryos were

monitored daily for percentages of adverse neurotoxic and developmental effects including mortality, atypical 24-hpf spontaneous coiling frequencies, abnormal growth and hatching rates, and irregular heart rhythms through 5 dpf.

6.3.7.2 Zebrafish Larval-Behavioral Neurotoxicity Assay

The larval-behavioral neurotoxicity assay, adapted from Legradi et al. (2015) used normal 5-6 dpf zebrafish larvae with inflated swim bladders (e.g., exhibiting normal beat-and-glide, upright orientation) to evaluate the neurobehavioral toxicity effects of exposures to compound 1 over 24 hours. One larva per 100 μ L of aquarium system water was added to each well of a polystyrene, 96-well plate, pre-treated with test concentrations of 1 or PbTx-2 (positive control) and untreated (negative control) Twelve replicates of each exposure condition were tested. Neurotoxicity endpoints assessed included percentages of mortality, aberrant swimming behaviors and swim bladder irregularities compared to the negative controls.

6.3.7.3 Statistical Analysis of Zebrafish Biological Assay Data

Data were analyzed by one-way ANOVA followed by Tukey's HSD test. A p value of ≤ 0.05 was considered statistically significant. Statistical analyses were generated using the Real Statistics Resource Pack software (Release 5.4.2). Copyright (2013-2019) Charles Zaiontz. www.real-statistics.com (last accessed 23JAN2018).

6.4 Results and Discussion

The grazed filamentous marine cyanobacteria, collected from within the captive dolphin enclosure, comprised a mixed assemblage morphologically resembling the formerly classified, toxigenic genus *Lyngbya s.l.* Cloning of 16S rDNA PCR products and their Sanger sequencing revealed three closely related members of the family

Oscillatoriaceae (Oscillatoriales) in the sampled cyanobacterial mat CAL-V, including a previously undocumented *Neolyngbya* sp. as the dominant taxa (represented by the largest number of clones) along with *Neolyngbya arenicola* (Caires et al., 2018a) and an unknown taxon found in a poorly resolved clade comprising the genera *Limnoraphis* (Komárek et al., 2013) and *Capilliphycus* (Caires et al., 2018b; Caires et al., 2019) as shown in Figure 6.1.

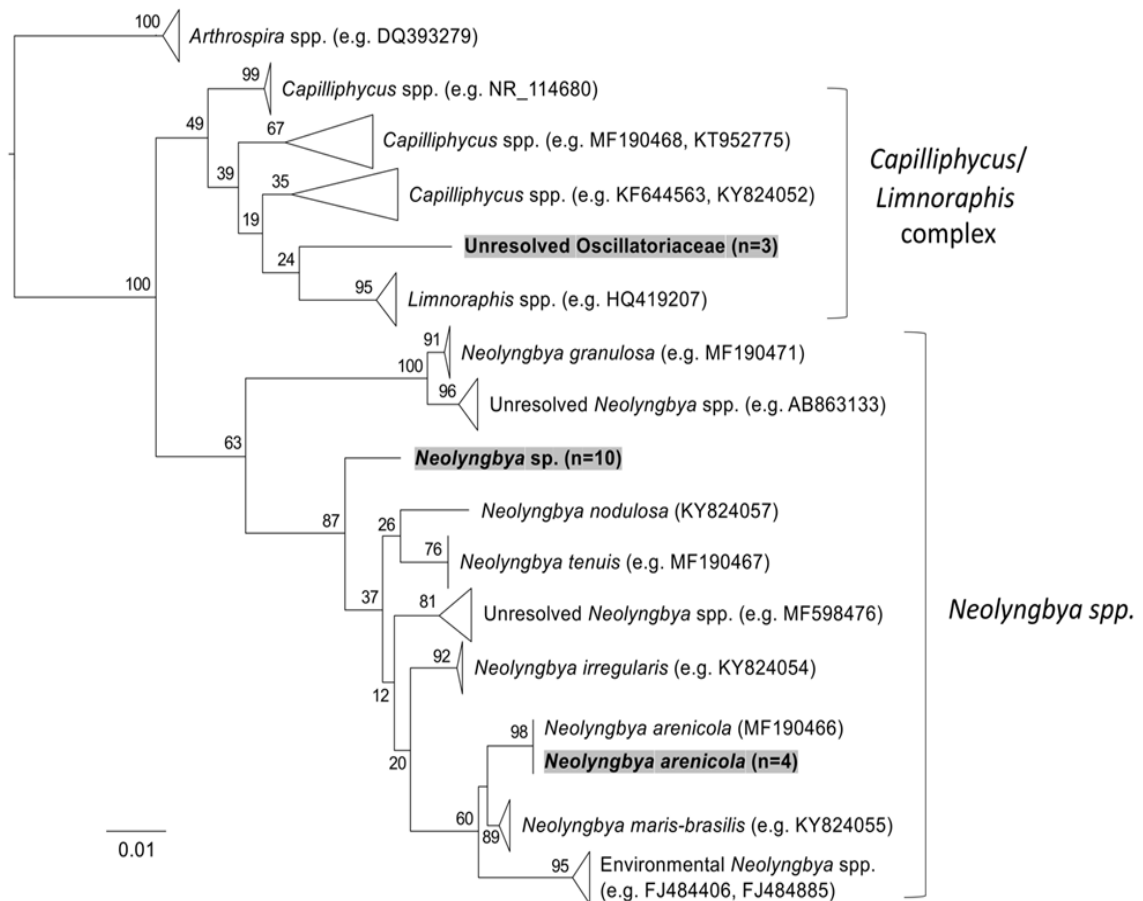


Figure 6.1 The 16S rDNA maximum likelihood tree showing the phylogenetic position of three Oscillatoriacean species found in the eudesmacarbonate-producing cyanobacterial mat CAL-V (shaded in grey and with clone abundance in parenthesis). Note the overall lack of the backbone of the tree for clarity.

Bioactivity-guided chemical investigation of the sampled cyanobacteria using the widely accepted zebrafish embryo-larvae toxicological models, led to the identification of

eudesmacarbonate (1), a novel, six-membered, cyclized carbonate eudesmane-type sesquiterpene (Figure 6.2), isolated from the lipophilic extract, as a putative neurotoxic metabolite.

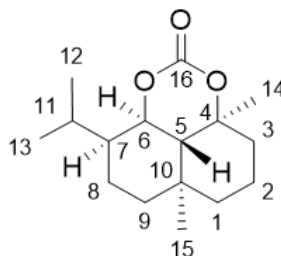


Figure 6.2 The molecular structure of eudesmacarbonate (1).

Various marine organisms, including the red macroalgae genus *Laurencia* and the invertebrate (i.e., “sea hare”) genus *Aplysia*, produce eudesmane-type sesquiterpenes (formerly selinane) with antifeedant activities (Al-Massarani, 2014; Pereira et al., 2016). However, cyanobacteria production of eudesmanoids has been sparsely reported (Pattanaik and Lindberg, 2015). Notably, Todd and Gerwick (1995) previously isolated a novel, five-membered, cyclic carbonate substituted diacetate, lyngbya carbonate, from *Lyngbya majuscula*. Herein, the isolation, structural elucidation and neurotoxic effects of eudesmacarbonate (1) are discussed.

6.4.1 Purification of Eudesmacarbonate by Bioassay-Guided Fractionation

Wet samples of the grazed cyanobacteria, collected in January 2016, from within the captive dolphin habitat, were stored frozen, and lyophilized prior to solvent extraction. Exhaustive extraction of the lyophilized material in EtOAc-MeOH (1:1), then partitioning with EtOAc-H₂O (3:1) afforded the bioactive EtOAc-soluble extract, exhibiting neurotoxicity in the zebrafish embryogenesis-larval toxicological models (see Experimental Section). Semipreparative fractionation of the EtOAc-soluble extract with

n-hexane-EtOAc-MeOH gradient using normal-phase automated flash chromatography, followed by aqueous MeOH gradient reversed-phase column chromatography, and recrystallization in MeOH, led to the purification of eudesmacarbonate (1). The structure of 1 (see Figure 6.2), was elucidated by spectroscopic data analysis, single-crystal X-ray diffraction data and vibrational circular dichroism data.

6.4.2 Structural Elucidation of Eudesmacarbonate

Eudesmacarbonate (1) was obtained as translucent, white crystals with a specific rotation of $[\alpha]_D^{25} -46.7$ (*c* 0.27, MeOH). The molecular formula $C_{16}H_{26}O_3$ was determined by the (+)-HRESI/TOFMS ion at m/z 267.1965 $[M+H]^+$ (calcd for 267.1960), implying four indices of hydrogen deficiency (IHDs). Also observed in the HRMS mass spectrum (Figure 6.3) were the apparent $M+23$, sodium adduct $[M+Na]^+$ observed at m/z 289.1785, and the fragmentation ion at m/z 205.1966 $[M+H-62]^+$, where 62 m/z represents the loss of the carbonate moiety as H_2CO_3 , accounting for one IHD.

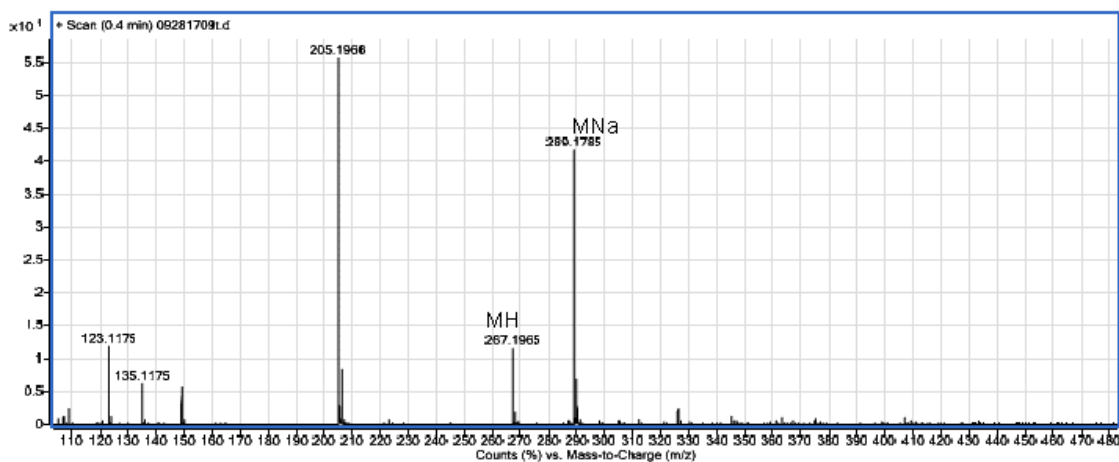


Figure 6.3 High-resolution LC-MS spectrum of eudesmacarbonate (1) with MH indicating the $[M+H]^+$ peak and MNa indicating the $[M+Na]^+$ peak.

The FTIR absorption bands indicated the presence of a carbonyl group (1734 cm^{-1}), sp^3 oxygenated carbons (1095 cm^{-1}) and aliphatic 5-7 membered ring structures (1158

and 1082 cm^{-1}) supporting the carbonate function and accounting for the remaining three IHDs (Figure 6.4).

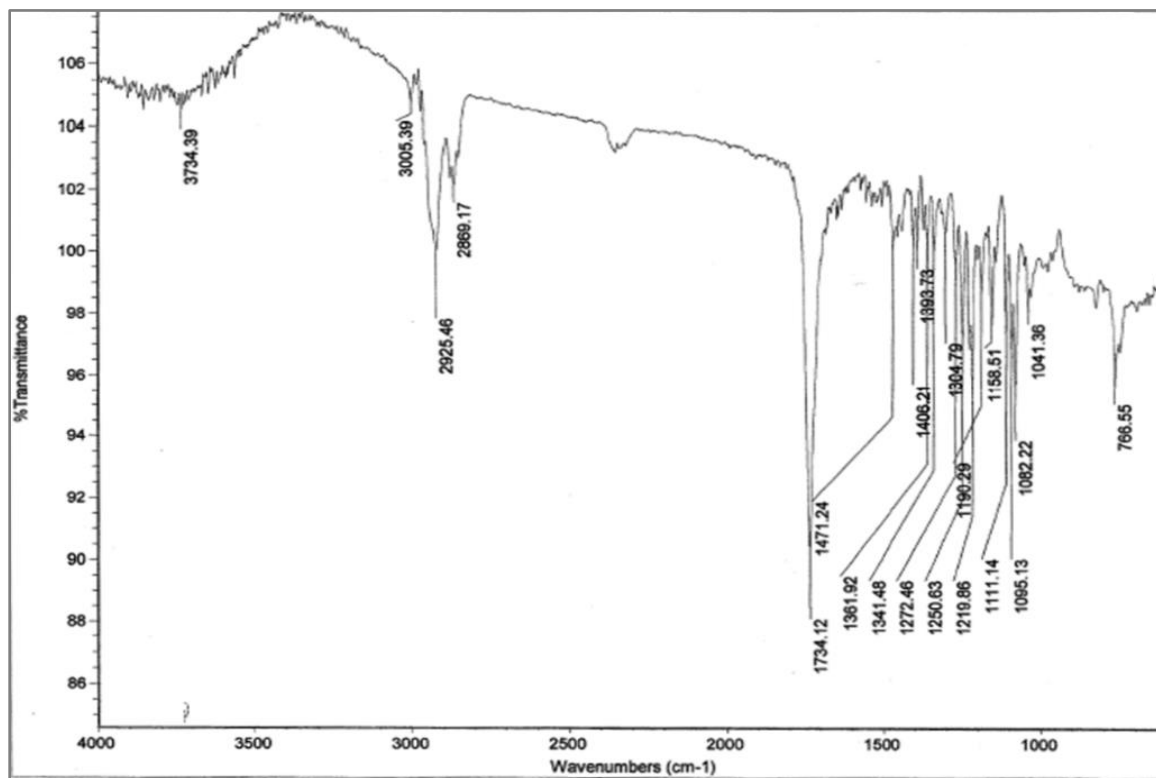


Figure 6.4 FTIR spectrum of eudesmacarbonate (1).

The molecular formula was confirmed by the ^1H NMR and ^{13}C NMR experiments as shown in Figures 6.5 and 6.6, respectively.

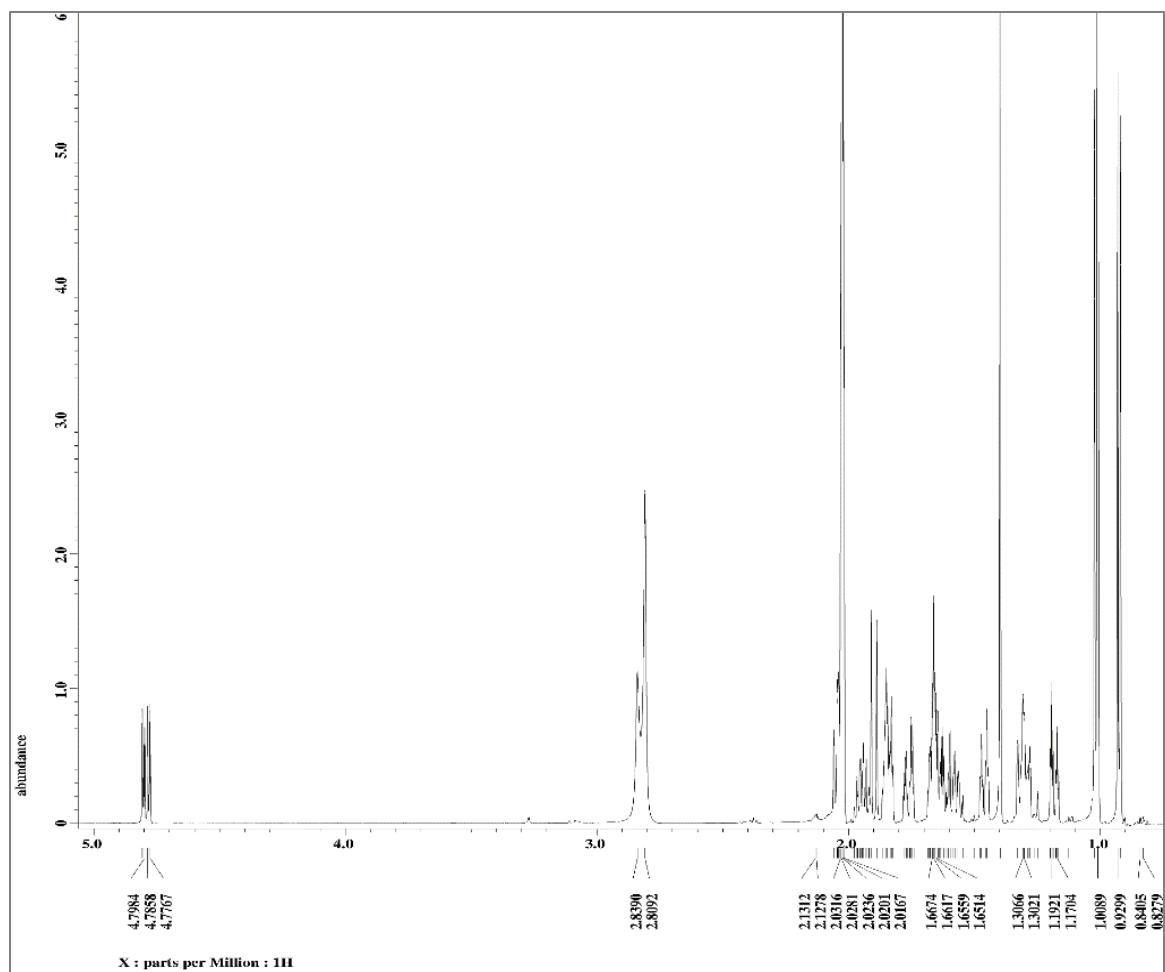


Figure 6.5 The ¹H NMR spectrum of eudesmacarbonate (1). The peaks observed between 2.01 and 2.05 ppm, respectively indicate the (CD₃)₂CO solvent. Water contamination is indicated by the peaks at 2.81 and 2.84 ppm respectively.

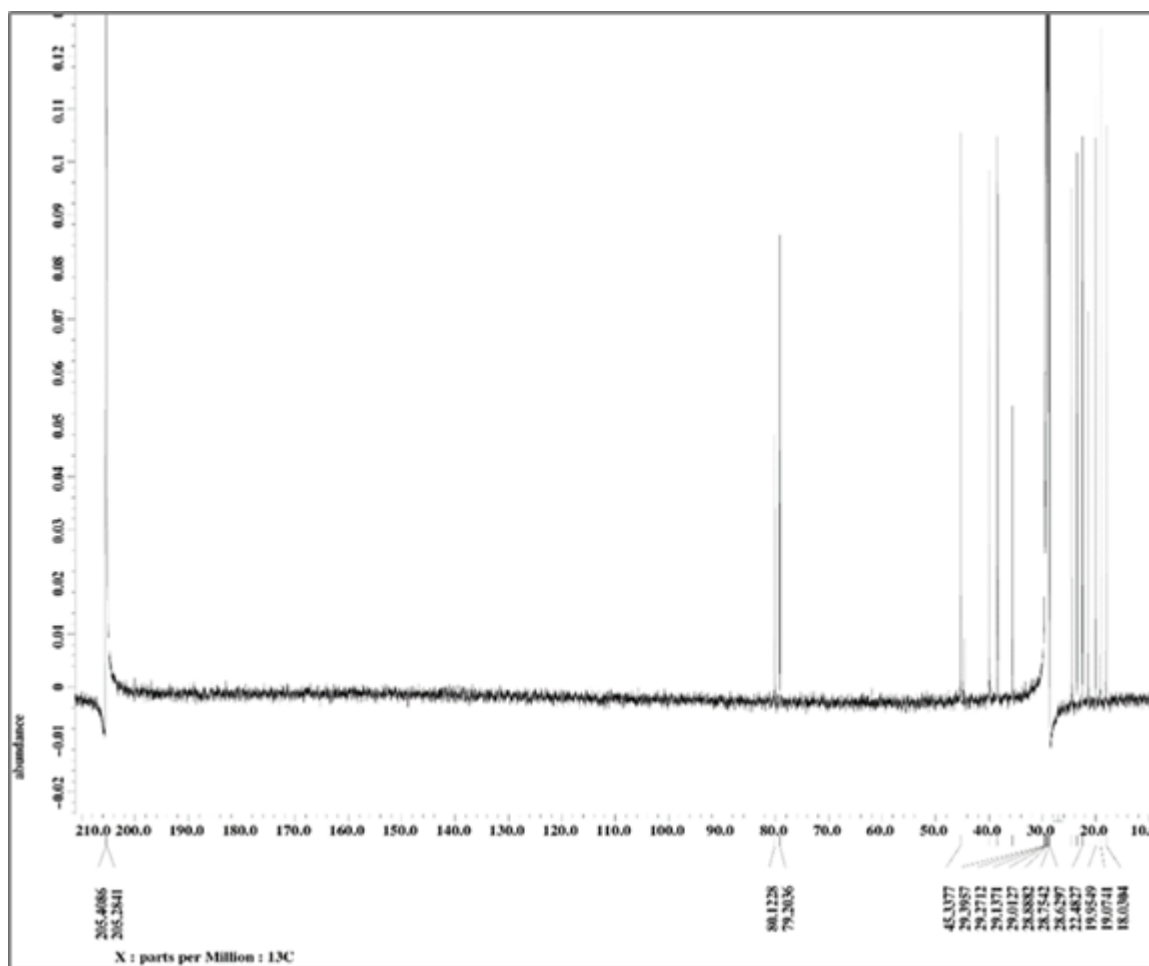


Figure 6.6 The ^{13}C NMR spectrum of eudesmacarbonate (1). The $(\text{CD}_3)_2\text{CO}$ solvent peaks are indicated between 28.6-29.4 ppm and at 205.3 and 205.4 ppm, respectively.

The ^{13}C NMR spectrum displayed 16 carbon signals (Table 6.1), including a carbonyl (δ_{C} 148.0) and two oxygenated carbons (δ_{C} 80.1 and δ_{C} 79.2), corroborating the presence of a carbonate substituent. No other signals indicating double bonds were observed in either the IR or ^{13}C NMR spectra. The ^1H NMR data (Table 6.1) displayed signals associated with an isopropyl group [δ_{H} 0.92 (d, $J = 6.9$ Hz), 1.02 (d, $J = 8.2$ Hz), and 1.94 (m)], two methyl groups [δ_{H} 1.01 (s) and 1.40 (s)], two methines [δ_{H} 1.90 (d, $J = 13.0$ Hz), and 4.79 (dd, $J = 13.1, 5.5$ Hz)] and several aliphatic multiplets, of which, three

were resolved [δ_{H} 1.18 (1H, dt, $J = 13.0, 3.5$ Hz), 1.46 (1H, dt, $J = 13.0, 3.4$), 1.76 (1H, dq, $J = 14.8, 3.4$)].

Table 6.1 NMR spectroscopic data for eudesmacarbonate (1) in $(\text{CD}_3)_2\text{CO}$ (^1H 600 MHz, ^{13}C 151MHz).

C/H #	δ_{C} , type	δ_{H} (J in Hz)	COSY ^a	HMBC ^b	NOESY ^c
1	39.9, CH ₂	1.30, m	2	3, 9, 10, 15	1, 2, 3, 5
		1.46, dt (13.0, 3.4)	2	3, 5, 9	1, 2
2	19.1, CH ₂	1.66, m	1, 3	1, 3, 4, 10	1, 15
		1.66, m	1, 3	1, 3, 4, 10	1, 15
3	38.4, CH ₂	1.58, m	2	4, 14	2, 3, 5
		1.83, m	2	1, 2, 4, 5	2, 3, 14
4	80.1, C	-	-	-	-
5	45.3, CH	1.90, d (13.0)	6	1, 3, 4, 7, 9, 10, 14, 15	1, 6, 9, 12, 13
6	79.2, CH	4.79, dd (13.1, 5.5)	5, 7	7, 11, 16	5, 11, 12, 14, 15
7	44.8, CH	1.85, m	6, 8, 11	5	8, 11, 12, 13
8	22.5, CH ₂	1.63, m	7, 9	9, 10	7, 8, 9, 12
		1.76, dq (14.8, 3.4)	7, 9	6, 9, 10	8, 9, 13
9	38.3, CH ₂	1.18, dt (13.0, 3.5)	8	5	8, 9
		1.30 m	8	1, 8, 10, 15	5, 8, 9
10	35.6, C	-	-	-	-
11	24.4, CH	1.94, m	7, 12, 13	6, 7, 12, 13	12, 13
12	23.5, CH ₃	1.02, d (8.2) ^d	11	7, 11, 13	13
13	21.4, CH ₃	0.92, d (6.9)	11	7, 11, 12	12
14	20.0, CH ₃	1.40, s	-	3, 4, 5	3, 6, 7, 11, 12, 13
15	18.0, CH ₃	1.01, s	-	1, 5, 9, 10	7, 11, 13, 14
16	148.0, C	-	-	-	-

^a COSY correlations are from proton(s) stated to the indicated proton(s). ^b HMBC correlations are from proton(s) stated to the indicated carbon. ^c NOESY correlations are from proton(s) stated to the indicated proton(s). ^d The 1.02 doublet signal is overlapped by the 1.01 singlet signal.

Interpretation of the DQF-COSY, edited HSQC, and HMBC data allowed the ^1H and ^{13}C signal assignments for four methyls, five methylenes, four methines, one carbonyl and two unprotonated carbons (Table 6.1, Appendix). The DQF-COSY spectrum (Figure 6.7) indicated the methine proton, H-5 (δ_{H} 1.90, δ_{C} 45.3), was coupled to the H-6 (δ_{H} 4.79, δ_{C} 79.2) proton of one sp^3 oxygenated carbon of the presumptive carbonate moiety. The large coupling constant ($J = 13.0$ Hz) inferred a *trans* axial arrangement between H-5 and H-6. The DQF-COSY spectrum displayed coupling from the H-7 (δ_{H} 1.85, δ_{C} 44.8) methine proton to H-6, the isopropyl proton, H-11 (δ_{H} 1.94, δ_{C} 24.4), and the methylene

protons, H₂-8 (δ_{H} 1.63, 1.76; δ_{C} 22.5), in turn, coupled to the methylene protons, H₂-9 (δ_{H} 1.30, 1.18; δ_{C} 38.3). A partial structure of an aliphatic chain, connecting H-5 through H-9, was substituted with an isopropyl group at H-7 and a carbonate group at H-6. A second aliphatic chain linked the remaining methylene groups H₂-1 [δ_{H} 1.30, 1.46; δ_{C} 39.9] to H₂-2 [δ_{H} 1.66, 1.66; δ_{C} 19.2) and to H₂-3 (δ_{H} 1.58, 1.83; δ_{C} 38.4).

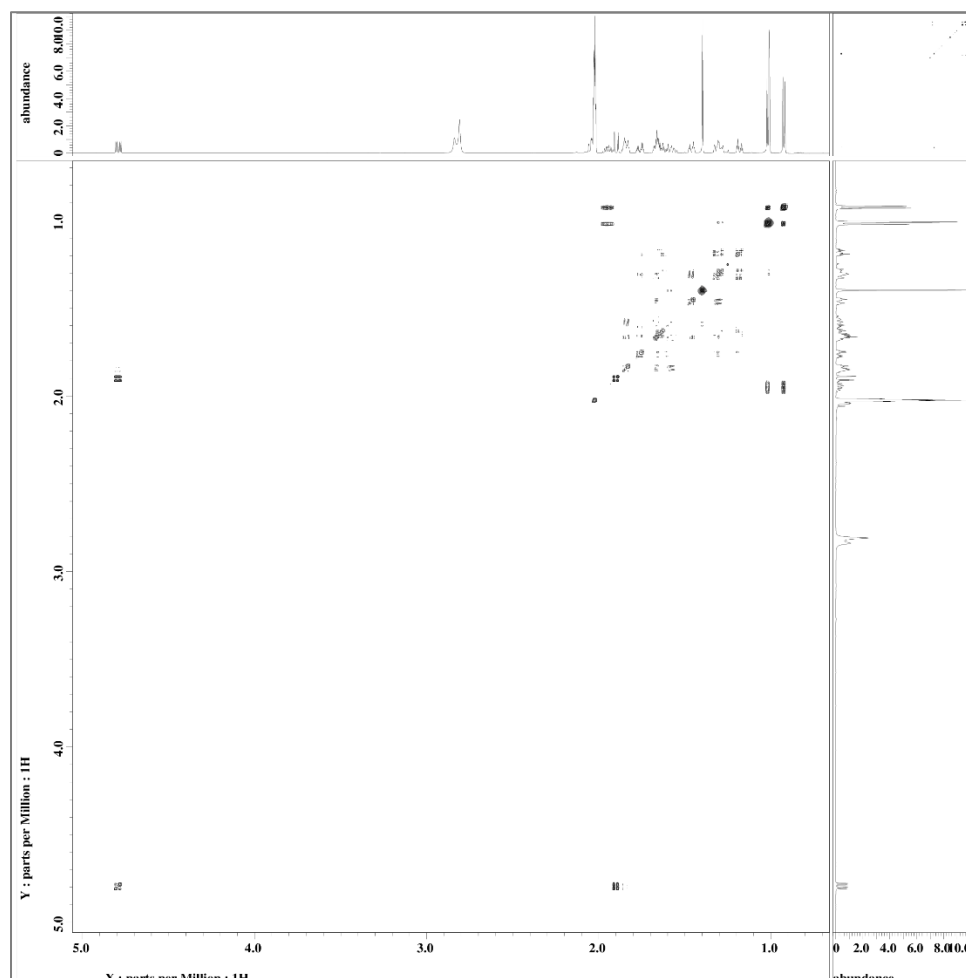


Figure 6.7 The DQF-COSY 2D-NMR spectrum of eudesmacarbonate (1).

The HMBC spectrum (Figure 6.8) displayed correlations for the unprotonated, sp^3 oxygenated carbon, C-4 (δ_{C} 80.1), to the H-5 proton, the H₂-3 methylene protons and the methyl group, H₃-14 (δ_{H} 1.40, δ_{C} 20.0), suggesting the carbonate substituent was cyclized,

attached to C-4 and C-6. The single HMBC correlation of the carbonyl carbon to the H-6 proton confirmed the cyclic substitution of the carbonate moiety, accounting for two of the four IHDs. The HMBC correlations observed for the unprotonated carbon, C-10 (δ_C 35.6) to the H-5 proton, the methylene protons of H₂-1 and H₂-9, and the methyl group, H₃-15 (δ_H 1.01, δ_C 18.0) inferred a bicyclic, aliphatic, six-membered ring structure, resolving the remaining two IHDs. A fused, bicyclic ring structure emerged as a 7-isopropyl-4,10-dimethyl decalin scaffold with the carbonate moiety adducted in 1,3 dioxan-2-one fashion to C-4 and C-6. Specifically, an eudesmane-type sesquiterpene skeleton featuring five stereocenters was deduced from the arrangements of the isopropyl and angular methyl substituents.

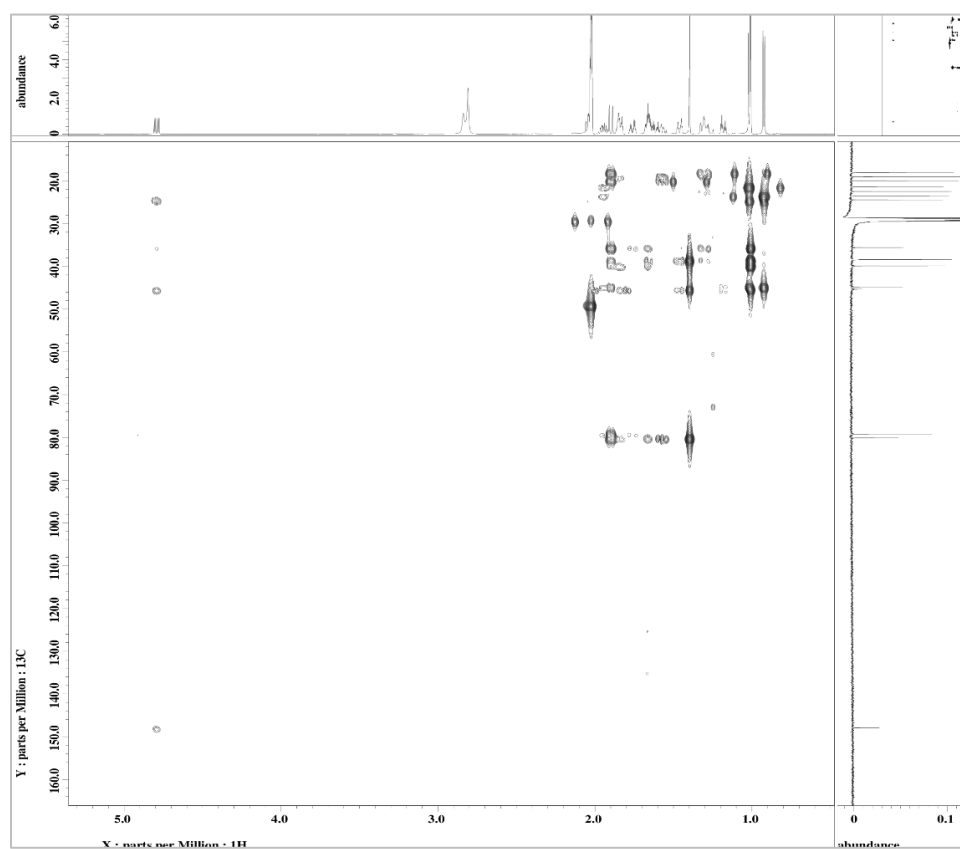


Figure 6.8 The HMBC 2D-NMR spectrum of eudesmacarbonate (1).

The NOESY spectrum (Figure 6.9) indicated long-range coupling between the H-5 proton and the methyl protons H₃-12, and H₃-13 as well as the methylene protons, H-1a and H-9a, inferring a *trans*-fused eudesmane skeleton. Long-range coupling between the H-6 proton and the two angular methyl groups, H₃-14 and H₃-15, was inferred from the NOESY spectrum. The angular methyl group, H₃-14, displayed NOE interactions with the H-6, H-7, H-11 and H₂-3 protons. The H₃-15 angular methyl group showed NOE correlations with the H-7 and H-11 protons and the methyl protons of H₃-13 and H₃-14. Axial (α) orientations were ascribed to the two angular methyl groups and the H-6 proton while the H-5 proton and the isopropyl group were axial (β) oriented. The relative configuration of 1 (Figure 6.10) was established as (4*S*,5*R*,6*R*,7*S*,10*S*) via NOESY interpretation.

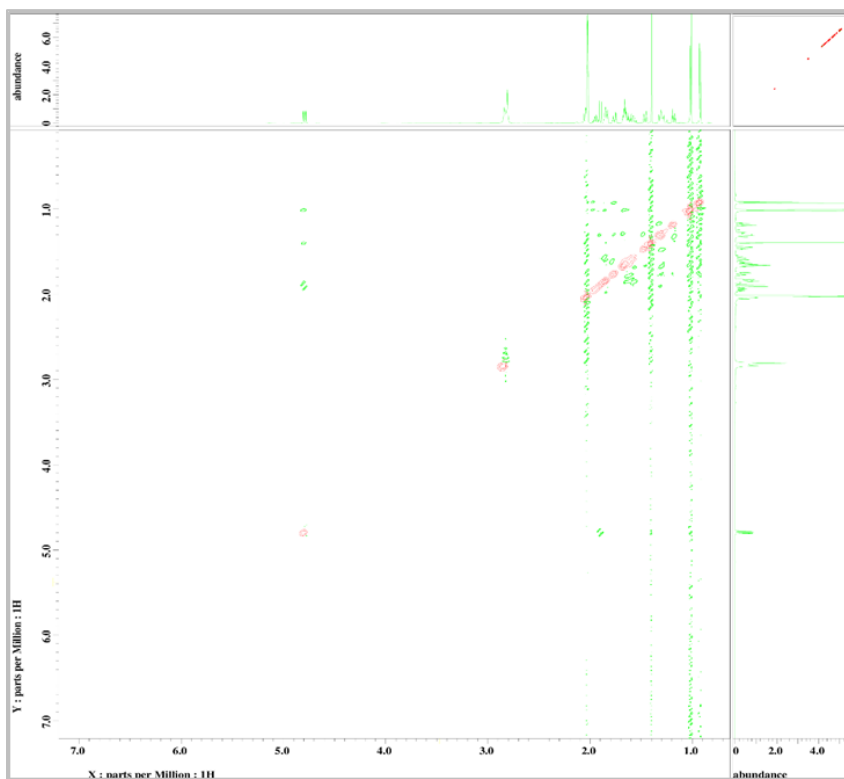


Figure 6.9 The NOESY 2D-NMR spectrum of eudesmacarbonate (1).

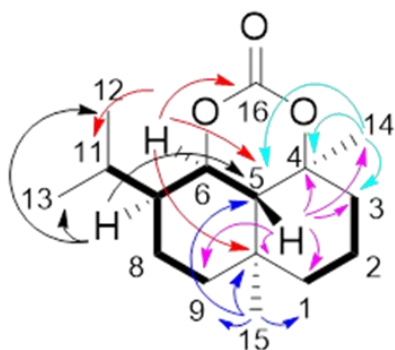


Figure 6.10 Key ^1H - ^1H COSY (bold lines) and HMBC (arrows) correlations of eudesmacarbonate (1).

The X-ray crystal and molecular structures (Figures 6.11 and 6.12) of eudesmacarbonate were constructed from the collected X-ray crystallographic data and structure refinement parameters (Table 6.2) with the relative configuration assignment based on the NMR data. The structural data of eudesmacarbonate were deposited in the Cambridge Crystallography Data Center (CCDC Number 1945948). Copies of these data can be obtained free of charge via the Internet at www.ccdc.cam.ac.uk/conts/retrieving.html.

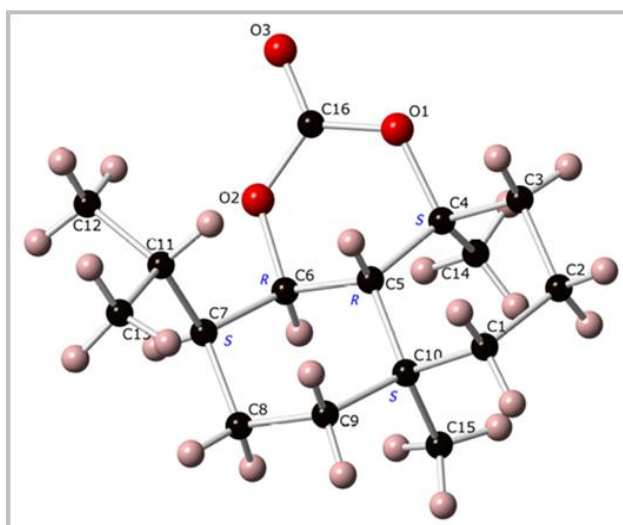


Figure 6.11 The single crystal X-ray structure of eudesmacarbonate (1).

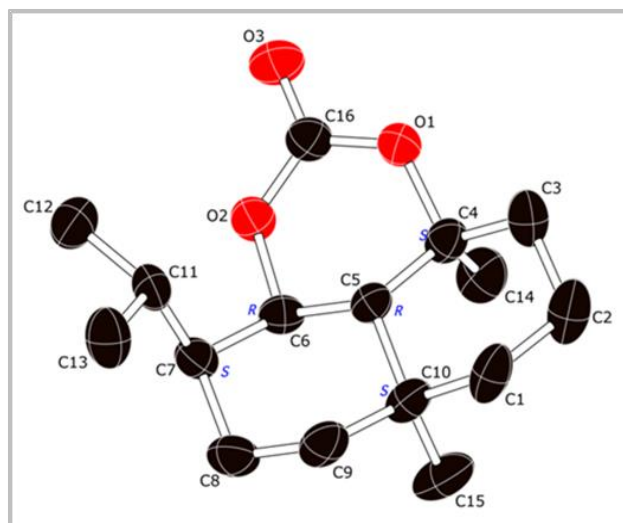


Figure 6.12 The molecular structure of eudesmacarbonate (1) with assigned relative configuration.

Table 6.2 Crystallographic data and structure refinement of eudesmacarbonate (1).

Empirical formula	$C_{16}H_{26}O_3$
Formula Weight (amu)	266.37
Temperature (K)	296
Size (mm ³)	$0.221 \times 0.178 \times 0.08$
Crystal System	orthorhombic
Space Group	$P2_12_12_1$
<i>a</i> (Å)	8.3643(4)
<i>b</i> (Å)	9.9485(4)
<i>c</i> (Å)	17.7102(8)
α (°)	90
β (°)	90
γ (°)	90
Volume (Å ³)	1473.71(11)
<i>Z</i>	4
ρ_{calc} (g cm ⁻³)	1.201
μ (mm ⁻¹)	0.0081
<i>F</i> (000)	584.0
Total Data or Reflections Collected	34690
Unique Data or Independent Reflections	3038 ($R_{\text{int}} = 0.0433$, $R_{\text{sigma}} = 0.0273$)
Data/Restraints/Parameters	3038/0/176
Theta Range (°)	6.16 - 52.846
Completeness (%)	1.72/1.00
Goodness of Fit (GOF) on F^2	1.049
Index Ranges	$-10 \leq h \leq 10$, $-12 \leq k \leq 12$, $-22 \leq l \leq 22$
R_1/wR_2 [$I \geq 2\sigma(I)$]	0.0440/0.0854
R_1/wR_2 (all data)	0.0634/0.0925
Largest diff. peak/hole / e Å ⁻³	0.12/-0.17

The absolute configuration of eudesmacarbonate was determined by numerical comparison (Table 6.3) of its experimental and simulated IR and VCD spectra in the range of 1100-1800 cm^{-1} for the (4*S*,5*R*,6*R*,7*S*,10*S*) enantiomer using the B3LYP/6-31G(d) basis set density functional theory method (see Chapter Six Section 6.36 Experimental VCD Analysis). The confidence level of 99% was based on the degree of congruence between the calculated and measured spectra.

Table 6.3 Numerical comparison between the calculated IR and VCD spectra for the (4*S*,5*R*,6*R*,7*S*,10*S*) enantiomer of eudesmacarbonate (1).

Calculated (1000-1600 cm^{-1})	Numerical Comparison	Observed eudesmacarbonate
(4 <i>S</i> ,5 <i>R</i> ,6 <i>R</i> ,7 <i>S</i> ,10 <i>S</i>)	Scaling factor	0.975
	IR similarity (%)	77.4
	^a Σ (%)	75.462
	^b Δ (%)	69.696
	Confidence Level (%)	99
^a Σ : single VCD similarity, gives the similarity between the calculated and observed VCD spectra. ^b Δ : enantiomeric similarity index, gives the difference between the values of Σ for both enantiomers of a given diastereomer.		

The experimental IR and VCD spectra (Figure 6.13) were consistent with those calculated for the (4*S*,5*R*,6*R*,7*S*,10*S*)-enantiomer, indicating that eudesmacarbonate possessed the same absolute configuration.

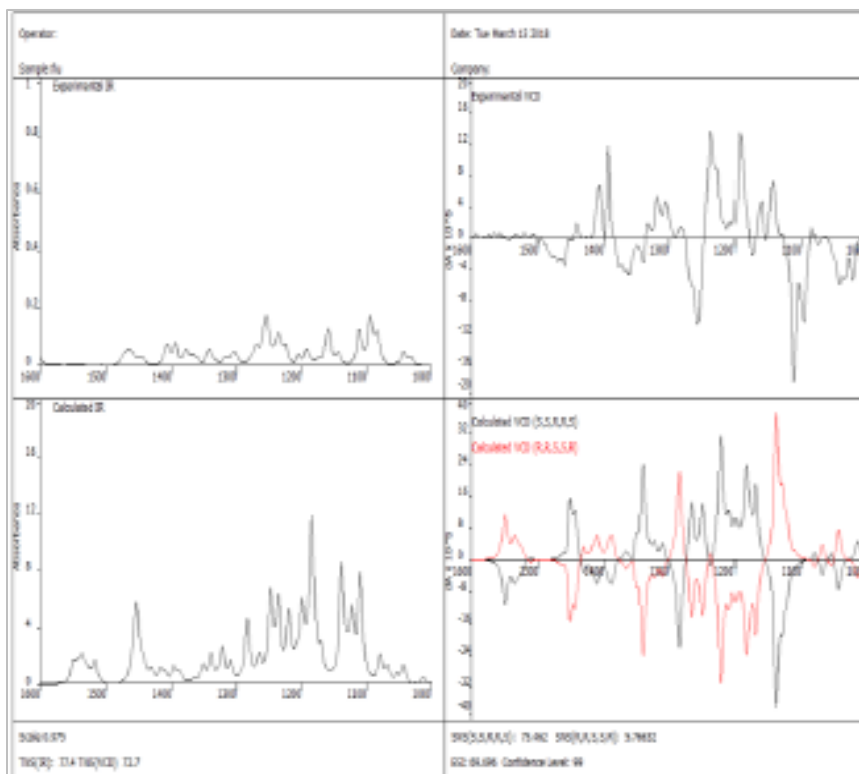


Figure 6.13 Comparison of experimental and calculated VCD and IR spectra of eudesmacarbonate (1) and the respective enantiomers for (4*S*,5*R*,6*R*,7*S*,10*S*) in black and (4*R*,5*S*,6*S*,7*R*,10*R*) in red, obtained from the CompareVOA software.

The molecular structure was determined from the lowest-energy conformer of the three total conformers calculated (Figure 6.14). Thus, the structure of eudesmacarbonate was unambiguously determined to be (4*S*,5*R*,6*R*,7*S*,10*S*)-eudesman-(4*S*,6*R*)-cyclocarbonate. The trivial name eudesmacarbonate was given as tribute to the associated structural class of eudesmane-type sesquiterpenes.

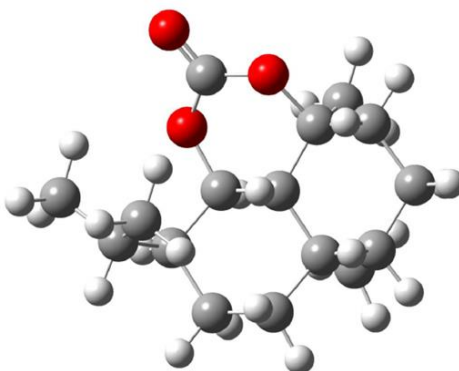


Figure 6.14 The molecular structure of the lowest-energy conformer of eudesmacarbonate (1).

Compound 1 may be the first reported eudesmane-type sesquiterpene isolated from filamentous, marine cyanobacteria. The few reports of eudesmanoids detected in cyanobacteria are limited to freshwater species (Höckelmann et al., 2009; Agger et al., 2008). Moreover, this is the first reported cyclic carbonate identified in this family of sesquiterpenes. Previously, Toyota and Asakawa (1990) isolated the antipodal enantiomer diol of 1, (+)-5 α ,7 β (H)-eudesm-4 α ,6 α -diol (2), from the methanolic extract of the terrestrial liverwort *Frullania tamarisci* subsp. *obscura* (Jubulaceae) and prepared the cyclic sulfurous ester (3) via thionyl chloride in pyridine (Figure 6.15). Srivastava and Alam (2005), subsequently, reported a symbiotic relationship between *F. tamarisci* and its epiphytic, filamentous cyanobacteria, *Stigonema cf. minutum* (Stigonemaceae). Initially, Kariyone and Majima (1935) isolated the sesquiterpenes, torilen (4), now known as germacrene-D, and the cyclized sulfate ester (5), torilensulfat, from the terrestrial plant *Torilis japonica* (Apiaceae) (Figure 6.15). Itokawa et al. (1988) corroborated these findings, during their investigations of *T. japonica*, by synthesizing 5 as “eudesmane cyclic sulfate” (formerly torilensulfat) via sulfuric acid catalysis of 4. While no biological data were available for 2, 3 and 5, 4 acted as a moth pheromone

attractant and a potent insect deterrent (Mozuraitis et al., 2002; Noge and Becerra, 2009).

Moreover, Bülow and König (2000) established 4 as a precursor for sesquiterpene biosynthesis, including eudesmanes, via acid catalyzed rearrangement.

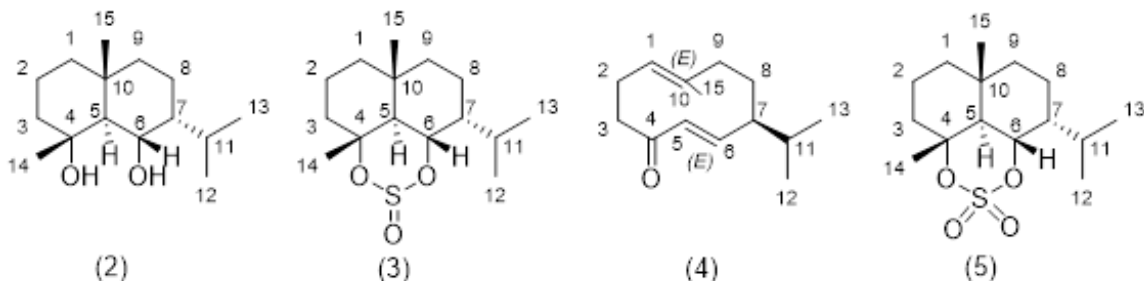


Figure 6.15 The structures of referenced compounds (2)–(5). The structures of (+)-5 α ,7 β (H)-eudesma-4 α ,6 α -diol (2) and its sulfurous ester (3) were adapted from Toyota and Asakawa (1990). The structures of torilen (4), now known as germacrene-D, and torilensulfat (5), now known as eudesmane-4,6-diol cyclic sulfate, were adapted from Itokawa et al. (1988).

6.4.3 Biological Activity of Eudesmacarbonate

Eudesmacarbonate (1) was tested against the recognized marine algal neurotoxin, brevetoxin-2 standard (PbTx-2), using available zebrafish embryotoxicity-larval models to assess developmental neurotoxicological and neurobehavioral effects through five dpf. The low and high exposure concentrations of PbTx-2 corresponded to 0.0045 μ M (4 ppb) and 0.0223 μ M (20 ppb), respectively. Exposure concentrations of 1 were evaluated at 9.4 μ M (2.5 ppm), 37.5 μ M (10 ppm) and 93.8 μ M (25 ppm), respectively representing the low, mid and high treatments. Negative controls were treated with aquarium system water (ASW) without any compounds. Exposure to 9.4 μ M of 1 elicited neurotoxicity and neurobehavioral effects in developing zebrafish, through five dpf, and in 5-dpf larvae, over 24-hpe, consistent with those of 0.0223 μ M of PbTx-2, evinced by abnormal 24-hpf spontaneous coiling responses, cardiac arrhythmias, swim bladder irregularities and aberrant swimming behaviors associated with ataxia (e.g., laying on side, motor

incoordination, seizure-like behaviors, spasms, tilting) as characterized by Henry et al. (1997) and Kalueff et al. (2013). The LD₅₀ value was not established in this study due to the paucity of 1 (see Appendix).

Spontaneous coiling frequencies (SCF), quantified as the number of spontaneous coils per minute at 24 hpf for each embryo of the three replicate test solutions per exposure condition, were used to compare developmental neurotoxicity effects between treated embryos and controls (see Appendix). Results were plotted as a box diagram and analyzed using one-way ANOVA followed by the Tukey HSD multiple comparison test (Figure 6.16). Significance levels were evaluated for $p < 0.05$ (*), $p < 0.01$ (**), and $p < 0.001$ (***). All measured SCF data for the different exposure concentrations, except 0.0045 μM PbTx-2, were normally distributed using the d'Agostino-Pearson test for normality. The untreated embryos, averaging 5.5 ± 0.5 SCF per minute (SEM, $n = 15$ total embryos for the 3 negative control replicates), were used to compare the embryos treated with the relevant replicate exposure concentrations (Table 6.4, Figure 6.16). Embryos exposed to the 0.0045 and 0.0223 μM PbTx-2 replicate test solutions and the lowest test concentration replicates of 1, (9.4 μM), respectively exhibited an average SCF of 4.1 ± 0.6 cpm (SEM, $n = 15$), 3.9 ± 0.5 cpm (SEM, $n = 14$) and 3.9 ± 0.5 cpm (SEM, $n = 14$), and were not significantly different than the average SCF of the untreated embryos (Table 6.4, Figure 6.16). The average SCF 3.9 ± 0.3 cpm (SEM, $n = 15$), displayed by the embryos treated with 38 μM of 1, was significantly lower compared to the negative controls (Table 6.4, Figure 6.16). Treatment with the highest concentration (94 μM) of 1 completely suppressed the SCF of all embryos relative to the untreated ASW controls (Table 6.4, Figure 6.16).

Table 6.4 Average 24-hpf embryo SCF as coils per minute (cpm) per exposure condition.

Exposure	Negative Control	PbTx-2		Compound 1		
Concentration (μM)	0	0.0045	0.0223	9.4	38	94
Average SCF (cpm)	5.5	4.1	3.9	3.9	1.9	0
SD (cpm)	1.8	2.2	1.7	1.2	1.7	0
SEM (\pm cpm)	0.48	0.58	0.45	0.32	0.43	0
n	15	15	14	14	15	15
Maximum SCF (cpm)	9	10	8	6	5	0
Minimum SCF (cpm)	3	0	1	2	0	0
Percent Abnormal SCF (<3 cpm)	0.0	0.0	14.3	14.3	60.0	100.0

n = total number of embryos per treatment for 3 replicate test solutions

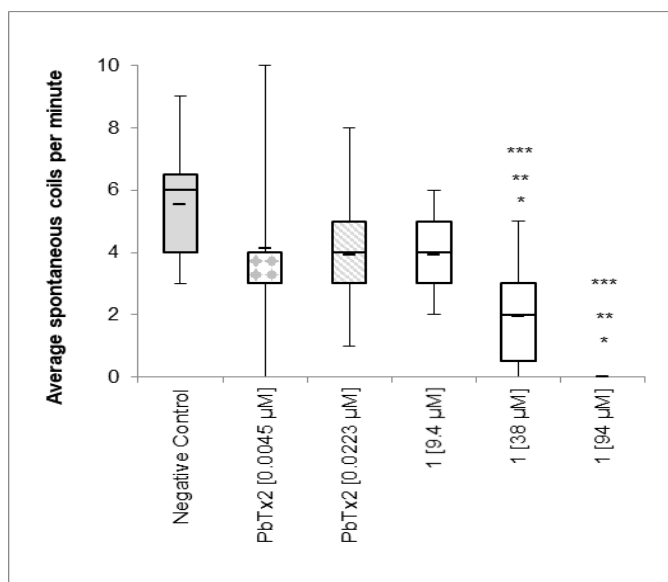


Figure 6.16 Comparative results of average 24-hpf spontaneous coils per minute. Data are the mean and SD of the total number of embryos for three replicate samples. Respectively, the *, **, *** denote $p < 0.05$, $p < 0.01$ and $p < 0.001$ significance derived by one-way ANOVA followed by the Tukey HSD multiple comparison test relative to the negative control.

The average spontaneous coiling frequencies (SCF) of embryos exposed to 1, quantified at 24 hpf, were then plotted against the exposure concentrations of 1. A logarithmic increase in concentration of 1 resulted in decreased embryonic SCF measurements (Figure 6.17). The untreated embryos SCF averaged 5.5 cpm ranging from 3-9 cpm. Embryos exhibiting SCF less than 3 cpm were considered abnormal. Probit

analysis of the percent of embryos exposed to 1 displaying abnormal SCF inferred an ED₅₀ value of 28.9 μM (7.7 ppm) for 1 (see Appendix). Representative embryos of each treatment, staged at 24-hpf, are shown in Figure 6.18.

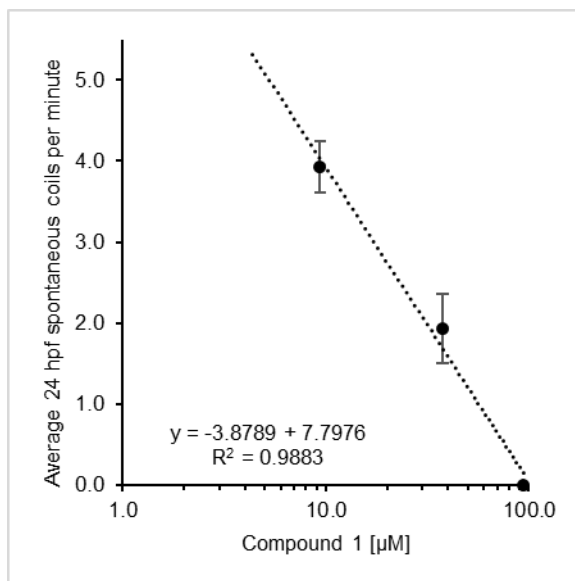


Figure 6.17 Logarithmic dose dependence of eudesmacarbonate (1) with respect to spontaneous coiling frequency per minute. Error bars are ± SEM for the total number of embryos of three replicate test solutions with n = 14,15 and 14, respectively, for the low, mid and high treatments.

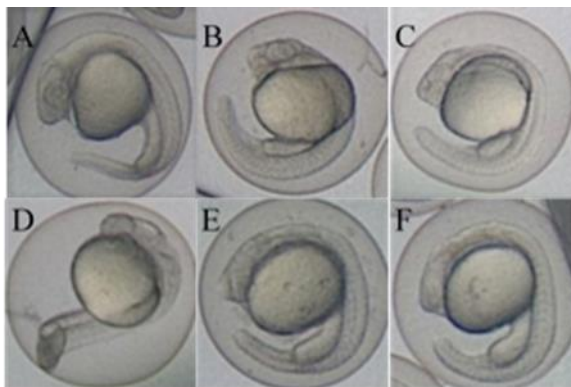


Figure 6.18 Comparative embryo morphologies observed at 24-hpf for untreated control (A) versus PbTx-2 treatments of 0.0045 μM (B) and 0.0223 μM (C) and treatment with eudesmacarbonate (1) at 9.4 μM (D), 38 μM (E) and 94 μM (F), respectively.

Average heart rates (HR), quantified as beats per minute (bpm) for each embryo of the three replicate test solutions, on Day 2 (D2) and Day 3 (D3), were used to compare developmental neurotoxicity effects between treated embryos and controls (see Appendix). Results were plotted as a box diagram and analyzed using one-way ANOVA followed by the Tukey HSD multiple comparison test (Figure 6.19, Figure 6.21). Significance was assessed for $p < 0.05$ (*), $p < 0.01$ (**) and $p < 0.001$ (***)).

The d'Agostino-Pearson test for normality indicated all experimental D2 HR measurements were normally distributed. The D2 HR of the untreated embryos averaged 146.7 ± 1.1 bpm (SEM, $n = 15$), shown in Table 6.5 and Figure 6.19. The average D2 HR of embryos exposed to both the low ($0.0045 \mu\text{M}$) and high ($0.0223 \mu\text{M}$) PbTx-2 concentrations, were respectively 160.3 ± 1.4 bpm (SEM, $n = 15$) and 154.0 ± 1.4 bpm (SEM, $n = 14$), significantly higher than the negative controls HR (Table 6.5, Figure 6.19) and implying neurotoxicity. Notably, the low PbTx-2 concentration elicited more rapid heart rates in embryos than the higher PbTx-2 treatment. Exposure to the low and high PbTx-2 treatments, respectively induced tachycardia in 80% and 50% of the embryos compared to untreated embryos (see Appendix). The average D2 HR of 150.9 ± 1.4 bpm (SEM, $n = 14$) for embryos exposed to the low concentration ($9.4 \mu\text{M}$) of 1 was significantly higher than the ASW negative control, suggesting neurotoxic effects (Table 6.5, Figure 6.19). Whilst, the mid ($38 \mu\text{M}$) and high ($94 \mu\text{M}$) concentrations of 1, significantly reduced the average D2 HR, respectively to 141.9 ± 1.1 bpm (SEM, $n = 15$) and 210.9 ± 2.1 (SEM, $n = 14$) (Table 6.5, Figure 6.19). Moreover, a linear dose dependent suppression of average HR was observed during embryonic exposure to 1, compared to the untreated embryos (Figure 6.20), further supporting neurotoxicity. The

ED₅₀ value for 1 could not be established by probit analysis of the percentages of treated embryos with abnormal D2 HR to untreated embryos (see Appendix).

Table 6.5 Average D2 HR (bpm) data of embryos per exposure condition.

Exposure Condition	Negative Control	PbTx-2		Compound 1		
Concentration (μM)	0	0.0045	0.0223	9.4	38	94
Average D2 HR (bpm)	146.7	160.3	154.0	150.9	141.9	120.9
SD (bpm)	4.5	5.5	5.1	5.3	4.2	7.7
SEM (± bpm)	1.1	1.4	1.4	1.4	1.1	2.1
n	15	15	14	14	15	14
Maximum D2 HR (bpm)	152	168	164	156	148	132
Minimum D2 HR (bpm)	140	152	148	140	132	108

HR = heart rate
bpm = beat per minute
n = total number of embryos per treatment for 3 replicate test solutions

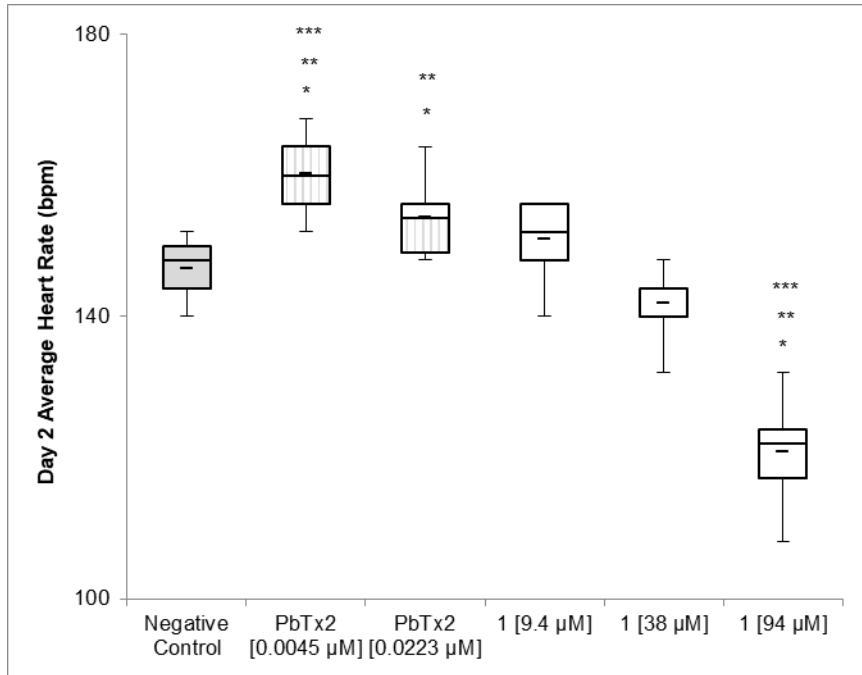


Figure 6.19 Comparative results of Day 2 average heart rates measured as beats per minute (bpm). Data are the mean and SD of the total number of embryos for the three replicate samples. The *, ** and ***, respectively denote $p < 0.05$, $p < 0.01$ and $p < 0.001$ significance derived by one-way ANOVA followed by the Tukey HSD multiple comparison test relative to the negative control.

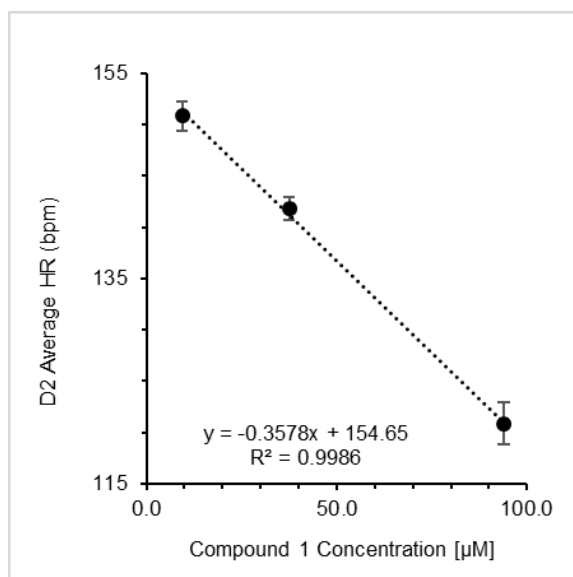


Figure 6.20 Dose dependence of eudesmacarbonate (1) with respect to D2 average heart rates (HR) in bpm. Error bars are \pm SEM of the total number of embryos per exposure concentration of 1 (n = 14, 15 and 14 for the respective low, mid and high treatments).

All D3 HR exposure data, except the 0.0223 μ M PbTx-2 test concentration, were normally distributed using the d'Agostino-Pearson test for normality. An average D3 HR of 194.5 ± 1.1 (SEM, n = 15) bpm was observed for the ASW negative control embryos (Table 6.6, Figure 6.21). Both PbTx-2 treatments induced significant bradycardia in \geq 90% of the exposed embryos compared to the untreated group, indicative of neurotoxic effects (Figure 6.21, Appendix). Notably, the D3 HR for embryos exposed to 0.0045 μ M PbTx-2, averaging 170.5 ± 2.0 bpm (SEM, n = 15), was slower than the 174.8 ± 3.2 bpm (SEM, n = 10) average HR observed for the 0.023 μ M PbTx-2 exposure concentration. Moreover, five of the 0.023 μ M PbTx-2 exposed embryos were deceased by the D3 monitoring interval (see Appendix). Embryos exposed to the mid and high concentrations of 1 exhibited significant bradycardia, relative to the ASW negative controls, when respectively quantified on D3 (Figure 6.21, Appendix). Whilst, exposure to the low

concentration of 1 did not significantly affect the D3 average HR (201.4 ± 3.2 bpm, SEM, n = 14) of the treated embryos. The D3 average HR at the lowest test concentration (9.4 μ M) of 1 was not statistically different that of the untreated group. However, chronic exposure to 1 at the mid (38 μ M) and high (94 μ M) treatments significantly suppressed average D3 HR, respectively 152.5 ± 0.7 bpm (SEM, n = 15) and 121.0 ± 1.5 bpm (SEM, n = 14), compared to the ASW negative controls, suggesting neurotoxic effects (Table 6.6, Figure 6.21). A decreasing logarithmic, dose-dependent trend was observed for the D3 average HR of embryos exposed to 1, further supporting neurotoxicity (Figure 6.22). At the 9.4 μ M (2.5 ppm) PbTx-2 exposure concentration, 50% of the embryos exhibited abnormal HR compared to the untreated embryos, thus establishing the ED₅₀ value of 1 (see Appendix). Representative D3 embryo developments are shown in Figure 6.23.

Table 6.6 Average D3 HR (bpm) data of embryos per exposure condition.

Exposure Condition	Negative Control	PbTx-2		Compound 1		
Concentration (μ M)	0	0.0045	0.0223	9.4	38	94
Average D3 HR (bpm)	194.5	170.5	174.8	201.4	152.5	121.0
SD (bpm)	4.4	7.6	10.3	7.9	2.9	5.6
SEM (\pm bpm)	1.1	2.0	3.2	2.1	0.7	1.5
n	15	15	10	14	15	14
Maximum D3 HR (bpm)	202	188	200	212	158	132
Minimum D3 HR (bpm)	188	158	164	186	148	114
HR = heart rate Bpm = beats per minute n = total number of embryos per treatment for 3 replicate test solutions						

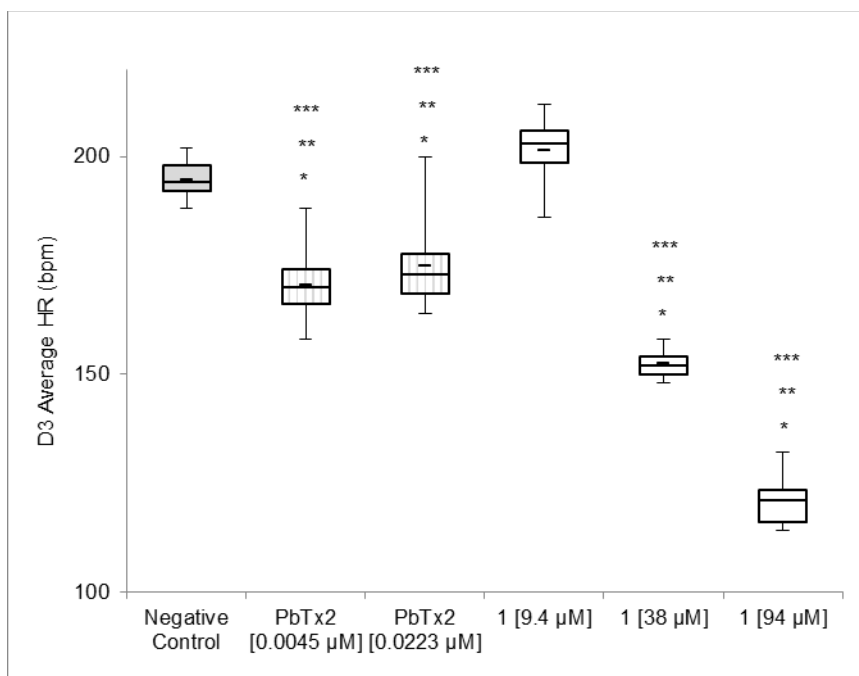


Figure 6.21 Comparative results of D3 average heart rates measured as beats per minute (bpm). Data are the mean and SD of the total number of embryos for three replicate samples. The *, **, and *** respectively denote $p < 0.05$, $p < 0.01$ and $p < 0.001$ significance derived by one-way ANOVA followed by the Tukey HSD multiple comparison test relative to the negative control.

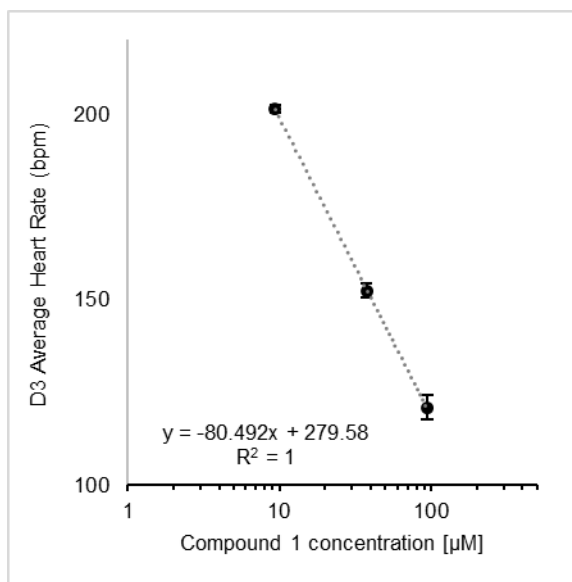


Figure 6.22 Logarithmic dose dependence of eudesmacarbonate (1) with respect to D3 average heart rates (HR) in bpm with error bars denoting \pm SEM for the total number of embryos per treatment ($n = 14$, $n = 15$ and $n = 14$ for the respective low, mid and high treatments).



Figure 6.23 Comparative embryo development observed at D3 for untreated control (A) versus PbTx-2 treatments of 0.0045 μM (B) and 0.0223 μM (C) and treatment with eudesmacarbonate (1) at 9.4 μM (D), 38 μM (E) and 94 μM (F), respectively.

Examination of swim bladder inflation and swimming behaviors occurred on Day 5 (D5) when, during normal embryogenesis, larvae typically exhibit fully inflated swim bladders and beat-and-glide swimming behaviors (Kalueff et al., 2013). Swim bladder dysfunction (SBD) was quantified by the percentage of embryos with swim bladder irregularities (e.g., under-inflated, uninflated, undeveloped) compared to the untreated ASW (i.e., normal) subjects (Table 6.7). Aberrant swimming behaviors (ASB) were quantified as the percentage of embryos displaying ataxia-related swimming patterns including laying on the side, titling, and spasms, relevant to the ASW negative controls (Table 6.8). Results were analyzed using one-way ANOVA followed by the Tukey HSD multiple comparison test. None of the measured percent SBD or ASB data were considered normally distributed by the d'Agostino-Pearson test for normality. No significant swim bladder irregularities (Table 6.7, Figure 6.24) or aberrant swimming behaviors (Table 6.8, Figure 6.25) were observed for any of the untreated ASW embryos at D5 of the developmental neurotoxicity study. Comparatively, all embryos, chronically exposed to the PbTx-2 test concentrations, exhibited significant irregularities with swim bladder inflation, indicating neurotoxicity (Table 6.7, Figure 6.24). Significant aberrant swimming behaviors were observed in 40% of the 0.0045 μM PbTx-2 exposed embryos

and all embryos exposed to 0.0223 μM PbTx-2, compared to the negative controls, further evincing neurotoxic effects (Table 6.8, Figure 6.25). Chronic exposure to 1, through D5, also resulted in larvae with significantly irregular swim bladder inflation (Table 6.7, Figure 6.24) and aberrant swimming behaviors (Figure Table 6.8, Figure 6.25), relevant to the negative controls, inferring qualitatively similar neurotoxic effects to PbTx-2. Moreover, an increasing, logarithmic, dose dependent trend was observed for embryos treated with 1, during embryogenesis, with respect to the percent SBD and ASB data when examined on D5 (Figure 6.26). The D5 percent SBD and ASB ED₅₀ values for 1 were, respectively, extrapolated to be 12.9 μM and 6.8 μM from the linear regression analysis of the pertinent log₁₀ concentration plotted data (Figure 6.26, Appendix). The representative D5 embryonic development of each treatment is depicted in Figure 6.27.

Table 6.7 Average D5 percent SBD of embryos per exposure condition.

Exposure Condition	Negative Control	PbTx-2		Compound 1		
Concentration (μM)	0	0.0045	0.0223	9.4	38	94
Average D5 percent SBD (%)	0.0	100.0	100.0	43.3	73.3	100.0
SD (% SBD)	0.0	0.0	0.0	5.8	11.5	0.0
SEM (\pm % SBD)	0.0	0.0	0.0	3.3	6.7	0.0
Number of replicate test solutions	3	3	3	3	3	3
Number of Day 5 surviving embryos	15	15	10	14	15	14
Number of Day 0 test subjects	15	15	15	14	15	15
SBD = swim bladder dysfunction SD = standard deviation SEM = standard error of the mean Note: The number of abnormal D5 embryos, including dead embryos, were compared to the number of Day 0 normal test subjects for each replicate exposure condition.						

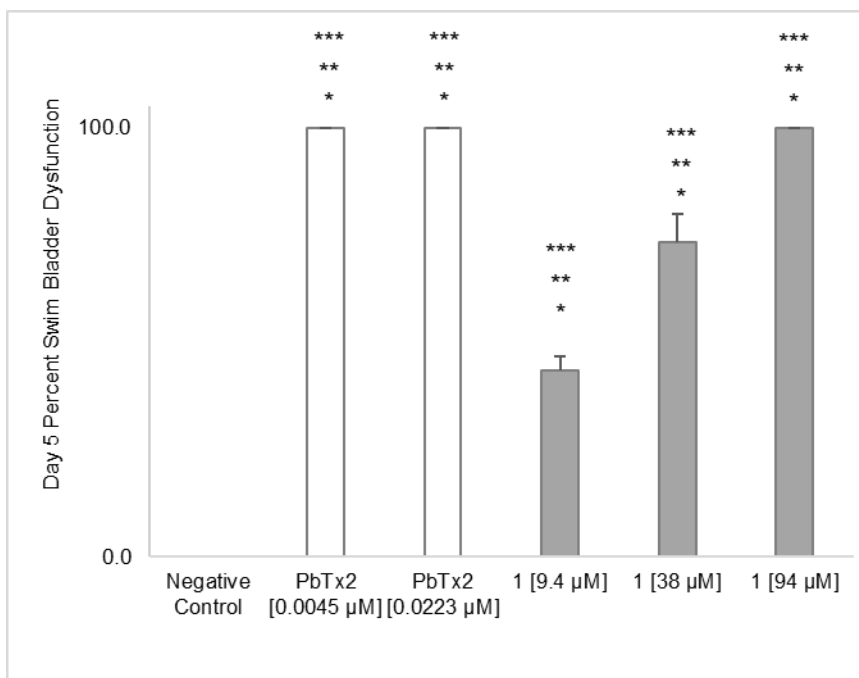


Figure 6.24 Comparative results of D5 average percent swim bladder dysfunction per chronic exposure concentration. Data are the mean and SEM of three replicate samples. Respectively, the *, **, and *** denote $p < 0.05$, $p < 0.01$ and $p < 0.001$ significance derived by one-way ANOVA followed by the Tukey HSD multiple comparison test relative to the negative control.

Table 6.8 Average D5 percent ASB of embryos per exposure condition.

Exposure Condition	Negative Control	PbTx-2		Compound 1		
Concentration (μM)	0	0.0045	0.0223	9.4	38	94
Average Day 5 percent ASB (%)	0.0	40.0	100.0	56.7	80.0	100.0
SD (% ASB)	0.0	0.0	0.0	5.8	0.0	0.0
SEM (\pm % ASB)	0.0	0.0	0.0	3.3	0.0	0.0
Number of replicate test solutions	3	3	3	3	3	3
Number of Day 5 surviving embryos	15	15	10	14	15	14
Number of Day 0 test subjects	15	15	15	14	15	15

ASB = aberrant swimming behaviors
SD = standard deviation
SEM = standard error of the mean
Note: The number of abnormal Day 5 embryos, including dead embryos, were compared to the number of Day 0 normal test subjects for each replicate exposure condition.

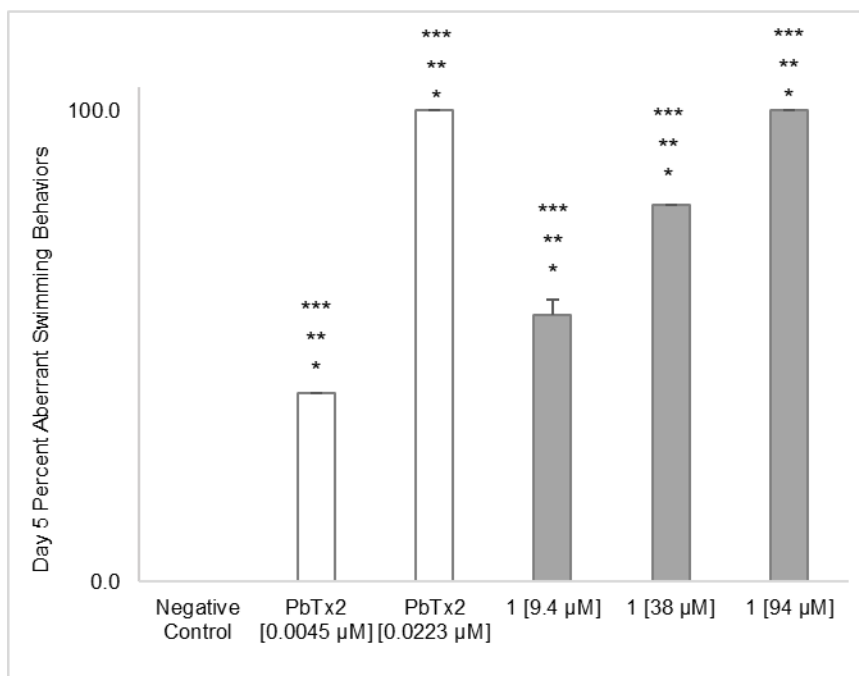


Figure 6.25 Comparative results of D5 average percent aberrant swimming behaviors per chronic exposure concentration. Data are the mean and SEM of three replicate samples. The *, **, and *** denote the respective $p < 0.05$, $p < 0.01$, and $p < 0.001$ significance derived by one-way ANOVA followed by the Tukey HSD multiple comparison test relative to the negative control.

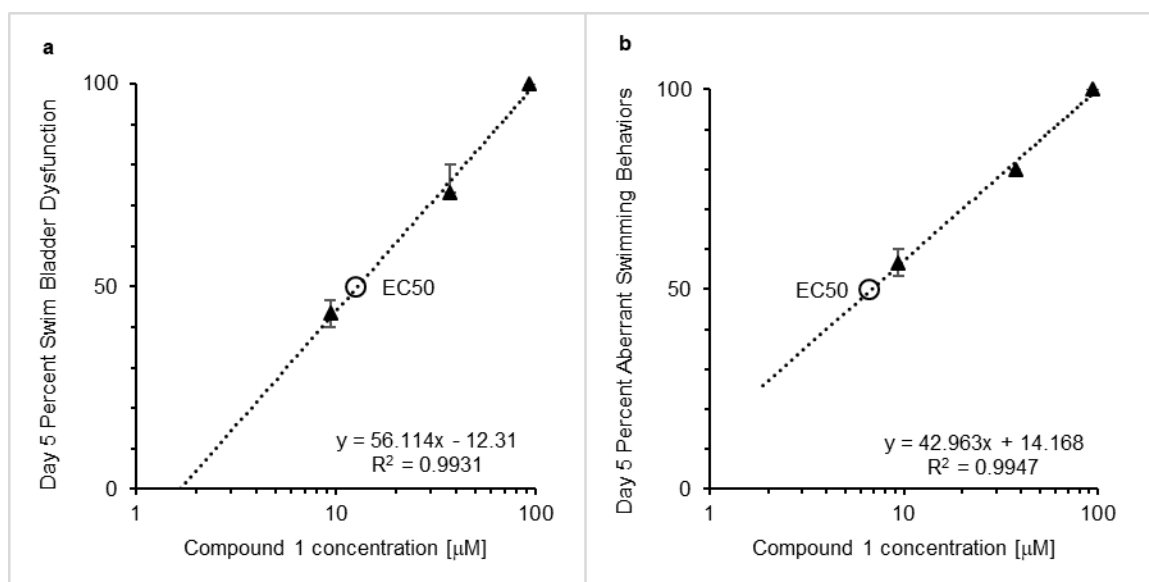


Figure 6.26 Day 5 logarithmic dose dependency of eudesmacarbonate (1) with respect to a) average percent swim bladder dysfunction and b) average aberrant swimming behaviors with error bars denoted as \pm SEM ($n = 3$ replicate test solutions).

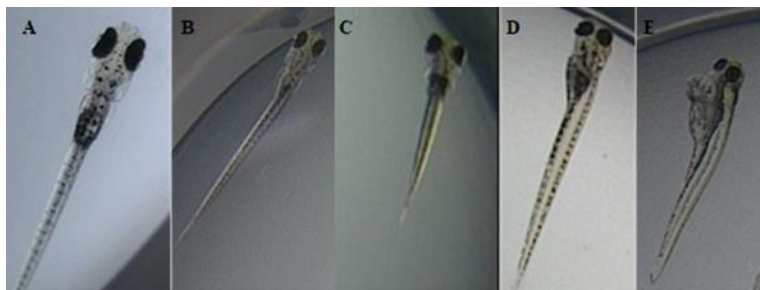


Figure 6.27 Comparative embryo development observed at D5 for untreated control (A) versus chronic exposure to 0.0045 μM PbTx-2 (B) and eudesmacarbonate (1) at 9.4 μM (C), 38 μM (D) and 94 μM (E), respectively.

The average ataxia-related swimming behaviors (XSB) were quantified by the number of embryos, per replicate test solution, exhibiting atypical mobility, and used to compare neurotoxicity effects between treated embryos and untreated controls in the 24-hour acute larval exposure study. The swimming behaviors of each larva were evaluated at two-hours and twelve-hours post-exposure (hpe). The untreated larvae continued to exhibit normal beat-and-glide swimming behaviors and maintained upright orientation at both observation intervals (Figure 6.28, Table 6.9, Table 6.10). All treated larvae displayed 100% XBS at 2 hpe, manifested by motor incoordination, head butting and spasms, compared to the untreated controls, indicating neurotoxic effects (Figure 6.28, Table 6.9). At 12 hpe, 50% of the 0.0045 μM PbTx-2 treated larvae appeared normal compared to the ASW negative controls, suggesting recovery (Figure 6.29, Table 6.10). Whilst, all larvae treated with 1 and 0.0223 μM PbTx-2 displayed 100% XBS through 12 hpe relative to the untreated controls, confirming neurotoxic effects (Figure 6.28, Table 6.10). No larval mortalities occurred in any of the test solutions when observed at 2 hpe (Table 6.9). However, at 12 hpe, one deceased larva was observed in the low and high treatments of 1 and could not be directly attributed to neurotoxic effects (Table 6.10). All

deceased larvae were counted as abnormal. Due to the challenges of observing swim bladders in active larvae, especially the untreated controls, the average percent swim bladder irregularities were not quantified at either timepoint.

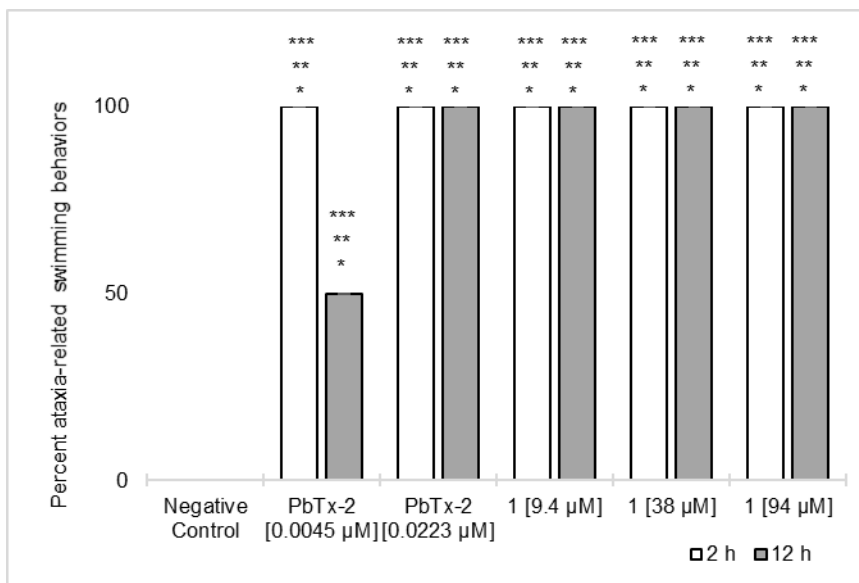


Figure 6.28 Comparative results of the percent ataxia-related swimming behaviors per acute exposure concentration. Data are the mean and SEM of 12 replicate larvae. The *, **, and *** denote the respective $p < 0.05$, $p < 0.01$, and $p < 0.001$ significance derived by one-way ANOVA followed by the Tukey HSD multiple comparison test relative to the negative control.

Table 6.9 Average 2-hpe percent XSB data of larvae per treatment.

Exposure Condition	Negative Control	PbTx-2		Compound 1		
Concentration (μM)	0	0.0045	0.0223	9.4	38	94
Average 2-hpe percent XSB (%)	0.0	100.0	100.0	100.0	100.0	100.0
SD (% XSB)	0.0	0.0	0.0	0.0	0.0	0.0
SEM (\pm % XSB)	0.0	0.0	0.0	0.0	0.0	0.0
Number of replicate larvae at 0-hpe	12	12	12	12	12	12
Number of deceased larvae at 2-hpe	0.0	0.0	0.0	0.0	0.0	0.0
Percent Mortality (%)	0.0	0.0	0.0	0.0	0.0	0.0
SD (% Mortality)	0.0	0.0	0.0	0.0	0.0	0.0
SEM (\pm % Mortality)	0.0	0.0	0.0	0.0	0.0	0.0
XSB = ataxia-related swimming behaviors						
SD = standard deviation						
SEM = standard error of the mean						
Note: Deceased larvae were counted as abnormal when compared to untreated larvae.						

Table 6.10 Average 12-hpe percent XSB data of larvae per treatment.

Exposure Condition	Negative Control	PbTx-2		Compound 1		
Concentration (μM)	0	0.0045	0.0223	9.4	38	94
Average 12-hpe percent XSB (%)	0.0	100.0	100.0	100.0	100.0	100.0
SD (% XSB)	0.0	0.0	0.0	0.0	0.0	0.0
SEM (\pm % XSB)	0.0	0.0	0.0	0.0	0.0	0.0
Number of replicate larvae at 0-hpe	12	12	12	12	12	12
Number of deceased larvae at 12-hpe	0	0	0	1	0	1
Percent Mortality (%)	0.0	0.0	0.0	8.3	0.0	8.3
SD (% Mortality)	0.0	0.0	0.0	0.0	0.0	0.0
SEM (\pm % Mortality)	0.0	0.0	0.0	0.0	0.0	0.0
XSB = ataxia-related swimming behaviors SD = standard deviation SEM = standard error of the mean Note: Deceased larvae were counted as abnormal when compared to untreated larvae.						

Overall, larvae treated with 1 incurred immediate motor incoordination, particularly upside down and side swimming behaviors, associated with neurotoxic effects, at 2 hpe and persisting through 12 hpe. Larvae exposed to sub-lethal concentrations of PbTx-2, up to 0.0223 μM , generally experienced symptoms of neurotoxicity, expressed as hypoactivity, through 12 hpe. Moreover, the neurotoxic effects of the low concentration (0.0045 μM) of PbTx-2 appeared to be transient as observed by the recovery of 50% of the larvae at 12 hpe.

6.5 Conclusions

In summary, compound 1 (i.e., eudesmacarbonate) was identified as a novel, cyclic carbonate ester eudesmane-type sesquiterpene, obtained from a mixed assemblage of filamentous, marine cyanobacteria dominated by an undocumented *Neolyngbya* sp. characterized by 16S rDNA sequencing and obtained clone abundance. However, until further work is conducted to establish monocultures of the three Oscillatoriacean species present in the cyanobacterial mat, the actual producer of the compound cannot be

ascertained with confidence. To date, no secondary metabolites have been reported from *Neolyngbya* spp. and genomic data are also nonexistent for this genus to determine whether it harbors biosynthetic genes. However, genomic data from *Limnoraphis robusta* (CCAP 1446/4) [co-referenced as CS-951 (Willis et al., 2015)] documented the presence of secondary metabolites and biosynthetic genes, suggesting the Oscillatoriacean clustering within the poorly resolved *Limnoraphis* and *Capilliphycus* spp. complex, may produce novel compounds. Future species discovery in these clades with more informative gene markers may improve topological relationships and branch support in order to reassess generic boundaries in this part of the Oscillatoriaceae tree. In association with the observed intoxication events among the captive bottlenose dolphins, compound 1 may function as a putative neurotoxic chemical defense available to marine cyanobacteria, perhaps as a feeding deterrent. These findings emphasize the continued need to explore marine sourced cyanobacteria for biologically active secondary metabolites and the biosynthetic origins of these natural products using molecular and genetic techniques.

6.6 Acknowledgments

This research was charitably supported by the Smithsonian Marine Station. Financial support was provided, in part, by Florida International University Teaching Assistance Grants and a Dissertation Year Fellowship. The Harbor Branch Oceanographic Institute at Florida Atlantic University spectroscopy facility is thanked for donating 600 MHz NMR and LC-MS spectrometer time and the optical rotation measurements. The high-resolution mass spectrometric analysis was performed by the Mass Spectrometer Facility, Department of Chemistry, University of California at

Riverside. BioTools, Inc., generously conducted the VCD/IR experiments and calculations. J. Mejia-Fava and the staff at Dolphins Plus kindly provided the research project and assistance with the cyanobacteria collections.

6.7 References

- Agger, S.A., Lopez-Gallego, F., Hoye, T.R., Claudia Schmidt-Dannert, C., 2008. Identification of Sesquiterpene Synthases from *Nostoc punctiforme* PCC 73102 and *Nostoc* sp. Strain PCC 7120. *J. Bacteriol.* 190(18), 6084-6096. doi:10.1128/jb.00759-08
- Al-Massarani, S.M., 2014. Phytochemical and Biological Properties of Sesquiterpene Constituents from the Marine Red Seaweed *Laurencia*: A Review. *Nat. Prod. Chem. Res.* 2, 5. doi:10.4172/2329-6836.1000147
- Altschul, S.F., Maden, T.L., Schagger, A.A., Zhang, J., Zhang, Z., Miller, W., Lipman, D.J., 1997. Gapped BLAST and PSI-BLAST: a new generation of protein database search programs. *Nucleic Acids Res.* 25(17), 3389-3402. doi:10.1093/nar/25.17.3389
- Aráoz, R., Molgó, J., De Marsac, N.T., 2010. Neurotoxic cyanobacterial toxins. *Toxicon* 56, 813-828. doi:10.1016/j.toxicon.2009.07.036
- Beekhuijzen, M., de Koning, C., Flores-Guillen, M.-E., de Vries-Buitenweg, S., Tobor-Kaplon, M., van de Waart, B., Emmen, H., 2015. From cutting edge to guideline: A first step in harmonization of the zebrafish embryotoxicity test (ZET) by describing the most optimal test conditions and morphology scoring system. *Rep. Toxicol.* 56, 64-76. doi:10.1016/j.reprotox.2015.06.050
- Berry, J.P., Gantar, M., Gibbs, P.D.L., Schmale, M.C., 2007. The zebrafish (*Danio rerio*) embryo as a model system for the identification and characterization of developmental toxins from marine and freshwater microalgae. *Comp. Biochem. Physiol. C Toxicol. Pharmacol.* 145(1), 61-72. doi:10.1016/j.cbpc.2006.07.011
- Bülow, N., König, W.A., 2000. The role of germacrene D as a precursor in sesquiterpene biosynthesis: investigations of acid catalyzed, photochemical and thermally induced rearrangements. *Phytochemistry* 55, 141-168.
- Cai, W., Matthews, J.H., Paul, V.J., Luesch, H., 2016. Pitiamides A and B, Multifunctional Fatty Acid Amides from Marine Cyanobacteria. *Planta Med.* 82, 897-902. doi:10.1055/s-0042-105157

- Caires, T.A., de Mattos Lyra, G., Hentschke, G.S., de Gumão Pedrini, A., Sant'Anna, C.L., de Castro Nunes, J. M., 2018a. *Neolyngbya* gen. nov. (Cyanobacteria, Oscillatoriaceae): A new filamentous benthic marine taxon widely distributed along the Brazilian coast. *Mol. Phylogenet. Evol.* 120, 196-211. doi:10.1016/j.ympev.2017.12.009
- Caires, T.A., de Lyra, G.M., Hentschke, G.S., de Silva, A.M.S., de Araujo, V.L., Anna, C.L.S., de Nunes, J.M.C., 2018b. Polyphasic delimitation of a filamentous marine genus, *Capillus* gen. nov. (Cyanobacteria, Oscillatoriaceae) with the description of two Brazilian species. *Algae* 33(4), 291-304. doi:10.4490/algae.2018.33.11.25
- Caires, T.A., Sant'Anna, C.L.S., Nunes, J.M., 2019. *Capilliphycus* gen. nov.; validation of "Capillus T.A.Caires, Sant'Anna & J.M.Nunes", *inval.* (Oscillatoriaceae, Cyanobacteria). *Notulae Algarum* 95, 1-2.
- Delcourt, N., Claudepierre, T., Maignien, T., Arnich, N., Mattei, C., 2018. Cellular and Molecular Aspects of β -N-Methylamino-L-alanine (BMAA) Mode of Action within the Neurodegenerative Pathway: Facts and Controversy. *Toxins* 10(1), 6. doi:10.3390/toxins10010006
- Henry, T.R., Spitsbergen, J.M., Hornung, M.W., Abnet, C.C., Peterson, R.E., 1997. Early Life Stage Toxicity of 2,3,7,8-Tetrachlorodibenzo-p-dioxin in Zebrafish (*Danio rerio*). *Toxicol. Appl. Pharm.* 142, 56-68. doi:10.1006/taap.1996.8024
- Höckelmann, C., Becher, P.G., Reuss, S.H., Jüttner, F., 2009. Sesquiterpenes of the Geosmin-Producing Cyanobacterium *Calothrix* PCC 7507 and their Toxicity to Invertebrates. *Z. Naturforsch C*, 64, 49 - 55. doi:10.1515/znc-2009-1-209
- Itokawa, H., Matsumoto, H., Nagamine, S., Totsuka, N., Watanabe, K., 1988. Sulfuric Acid-Catalyzed Cyclization of Germacrene-D to Eudesmane-4,6-diol Cyclic Sulfate. *Chem. Pharm. Bull.* 36(8), 3161-3163.
- Jones, A.C., Monroe, E.A., Podell, S., Hess, W.R., Klages, S., Esquanazi, E., Niessen, S., Hoover, H., Rothmann, M., Lasken, R.S., Yates, J.R., Reinhardt, R., Kube, M., Burkart, M.D., Allen, E.E., Dorrestein, P., C., Gerwick, G., W., Gerwick, L., 2011. Genomic insights into the physiology and ecology of the marine filamentous cyanobacterium *Lyngbya majuscula*. *PNAS* 108(21), 8815-8820. doi:10.1073/pnas.1101137108
- Kalueff, A.V., Gebhardt, M., Stewart, A.M., Cachat, J.M., Brimmer, M., Chawla, J.S., Craddock, C., Kyzar, E.J., Roth, A., Landsman, S., Gaikwad, S., Robinson, K., Baatrup, E., Tierney, K., Shamchuk, A., Norton, W., Miller, N., Nicolson, T., Braubach, O., Gilman, C.P., Pittman, J., Rosemberg, D.B., Gerlai, R., Echevarria, D., Lamb, E.,

- Neuhauss, S.C.F., Weng, W., Bally-Cuif, L., Schneider, H., 2013. Towards a Comprehensive Catalog of Zebrafish Behavior 1.0 and Beyond. *Zebrafish* 10(1), 70-86. doi:10.1089/zeb.2012.0861
- Kariyone, T.; Majima, J., 1935. On the ethereal oil of *Torilis anthriscus*. *Yakuga Zasshi* 55, 887-893. doi:10.1248/yakushi1881.55.9_887
- Komárek, J., Zapomelová, E., Smarda, J., Kopecký, J., Rejmanková, E., Woodhaouse, J., Neilan, B.A., Komárková, J., 2013. Polyphasic evaluation of *Limnorphis robusta* a water-bloom forming cyanobacterium from Lake Atitlán, Guatemala, with a description of *Limnorphis* gen. nov. *Fottea* 13(1): 39-52. doi:10.5507/fot.2013.004
- Lance, E., Arnich, N., Maignien, T., Biré, R., 2018. Occurrence of β -N-Methylamino-L-alanine (BMAA) and Isomers in Aquatic Environments and Aquatic Food Sources for Humans. *Toxins* 10(2), 83. doi:10.3390/toxins10020083
- Legradi, J., el Abdellaoui, N., van Pomerén, M., Legler, J., 2015. Comparability of behavioural assays using zebrafish larvae to assess neurotoxicity. *Environ. Sci. Pollut. Res.* 16277-16289. doi:10.1007/s11356-014-3805-8
- Mozuraitis, R., Strandén, M., Borg-Karlson, A.-K., Mustaparta, H., 2002. (-)-Germacrene D Increases Attraction and Oviposition by the Tobacco Budworm Moth *Heliothis virescens*. *Chem. Senses* 27, 505-509.
- Nishimura, Y., Murakami, S., Ashikawa, Y., Sasagawa, S., Umemoto, N., Shimada, Y., Tanaka, T., 2015. Zebrafish as a systems toxicology model for developmental neurotoxicity testing. *Cogenit. Anom.* 55, 1-16. doi:10.1111/cga.12079
- Noge, K., Becerra, J.X., 2009. Germacrene D, A Common Sesquiterpene in the Genus *Bursera* (Burseraceae). *Molecules* 14, 5289-5297. doi:10.3390/molecules14125289
- Paerl, H.W., Otten, T.G., 2013. Harmful Cyanobacterial Blooms: Causes, Consequences, and Controls. *Microb. Ecol.* 65, 995-1010. doi:10.1007/s00248-012-0159-y
- Pattanaik, B., Lindberg, P., 2015. Terpenoids and Their Biosynthesis in Cyanobacteria. *Life* 5, 269-293. doi:10.3390/life5010269
- Pereira, R.B., Andrade, P.B., Valentão, P., 2016. Chemical Diversity and Biological Properties of Secondary Metabolites from Sea Hares of the *Aplysia* Genus. *Mar. Drugs* 14, 39. doi:10.3390/md14020039

- Shah, S.A. A., Akhter, N., Auckloo, B.N., Khan, I., Lu, Y., Wang, K., Wu, B., Guo, Y.-W., 2017. Structural Diversity, Biological Properties and Application of Natural Products from Cyanobacteria. A Review. *Mar. Drugs* 15, 354-383. doi:10.3390/md15110354
- Singh, R., Parihar, P., Singh, M., Bajguz, A., Kumar, J., Singh, S., Singh, V.P., Prasad, S.M., 2017. Uncovering Potential Applications of Cyanobacteria and Algal Metabolites in Biology, Agriculture and Medicine: Current Status and Future Prospects. *Front. Microbiol.* 8, 515. doi:10.3389/fmicb.2017.00515
- Soares, A.R., Engene, N., Gunasekera, S.P., Sneed, J.M., Paul, V.J., 2015. Carriebowlinol, an Antimicrobial Tetrahydroquinolinol from an Assemblage of Marine Cyanobacteria Containing a Novel Taxon. *J. Nat. Prod.* 78, 534-538. doi:10.1021/np500598x
- Srivastava, S.C., Alam, A., 2005. *Frullania tamarisci* (L.) Dum. – A new phorophyte for *Stigonema cf. minutum* (C.A. Agardh) Hassall. *Indian J. For.* 29(4), 429-432.
- Stamatakis, A., 2014. RAxML version 8: a tool for phylogenetic analysis and post analysis of large phylogenies. *Bioinformatics* 30(9), 1312-1313. doi:10.1093/bioinformatics/btu033
- Tamele, I.J., Silva, M., Vasconcelos, V., 2019. The incidence of marine toxins and the associated seafood poisoning episodes in the African countries of the Indian Ocean and the Red Sea. *Toxins* 11(1), 58. doi:10.3390/toxins11010058
- Todd, J.S., Gerwick, W.H., 1995. Isolation of a cyclic carbonate, a γ -butyrolactone, and a new indole derivative from the marine cyanobacterium *Lyngbya majuscula*. *J. Nat. Prod.* 58(4), 586-589.
- Toyota, M., Asakawa, Y., 1990. An eudesmane-type sesquiterpene alcohol from the liverwort *Frullania tamarisci*. *Phytochemistry* 29(11), 3664-3665.
- Willis, A., Park, M., Burford, M.A., 2015. Draft genome assembly of filamentous brackish cyanobacterium *Limnoraphis robusta* strain CS-951. *Genome Announc.* 3(5), e008446-15. doi:10.1128/genomeA.00846-15

7 SUMMARY AND PROSPECT

7.1 Summary Results of Research Project

This research project represented an unprecedented opportunity to a) investigate biologically active secondary metabolites from marine cyanobacteria relative to bottlenose dolphins in captivity at a marine mammal zoological facility in the Florida Keys and b) potentially directly observe zoopharmacognosy-related behaviors in human-managed bottlenose dolphins (Mejia-Fava and Colitz, 2014). The marine mammal zoological facility's location and tidal flux from the Atlantic Ocean allowed for a more natural habitat, permitting a mesocosm of native flora (e.g., seaweeds, seagrass, cyanobacteria, microalgae) and fauna (e.g., fish, crustaceans) within the captive dolphin enclosures. Staff observed their captive dolphins occasionally grazing these organisms, particularly sea lettuce (*Ulva* spp.) and mixed assemblage, marine, filamentous cyanobacteria (i.e., mat), characteristic of the previously classified, polyphyletic, toxigenic *Lyngbya* genus. Foremost, bottlenose dolphins, wild or captive, were not previously known to overtly ingest macroalgae or cyanobacteria. However, wild bottlenose dolphins, particularly females of the Western Australian Shark Bay pod, were previously observed using sponges for presumably nutraceutical purposes during periods of pregnancy and lactation (Smolker et al., 1997). Secondly, the captive dolphins appeared to experience transient intoxications related to these ingestion activities. Symptoms manifested as neurological impairments including motor incoordination, blepharospasms and respiratory issues akin to the effects of the marine HAB neurotoxin, PbTx-2, produced by the dinoflagellate, *Karenia brevis*.

A taxonomic survey of the dominant macroalgae growing within the captive dolphin enclosures determined the absence of known toxigenic species (i.e., *Caulerpa taxifolia*). Attempts to qualitatively identify potential HAB microalgae, including *K. brevis* and the domoic acid producing *Pseudo-nitzschia* spp. were inconclusive by light microscopy and FlowCam digital imaging. Moreover, chemical analysis of the cyanobacteria, from selected collection times during the study, concluded the plausible HAB-related neurotoxins ATX-a, BMAA, STX, PbTx-2 and DA were below the detection limits of the respective methods, indicating the associated HAB organisms were not present in bloom forming abundances, and not likely contributing to the captive dolphin intoxications.

Traditional, bioassay-guided investigation of the cyanobacteria mat ensued yielding a potential, associated neurotoxin. The well-established zebrafish toxicological model was adapted to distinguish developmental and larval behaviors associated with neurotoxicity compared to PbTx-2 standard. Herein, the neurotoxicity and teratogenicity of PbTx-2 was profiled, for the first time, using the zebrafish embryo-larva toxicological models. The use of PbTx-2 as a positive control afforded a rapid, reliable tool to guide the fractionation of the cyanobacteria and evaluate extracts and subsequent fractions for neurotoxicity. Consequently, a previously undocumented secondary metabolite was purified from the lipophilic cyanobacteria extract (i.e., EtOAc) and structurally identified as a the cyclic, carbonate ester of an eudesmane-type sesquiterpene. This new compound elicited neurotoxicity in developing zebrafish aligned with PbTx-2, including decreased spontaneous coiling frequencies at 24-hpf, bradycardia during the second and third days of development and swimming-related issues (i.e., irregular swim bladder development,

ataxia-related swimming behaviors) observed in embryos and larvae at day five of development in chronically and acutely exposure conditions. Whilst, developmental exposure to PbTx-2 induced tachycardia at Day 2 through Day 3, chronic embryo exposure to the cyanobacteria metabolite caused bradycardia symptoms, portending a possible different mode of action than PbTx-2.

Phylogenetic inquest of the cyanobacteria mat revealed an undocumented new species of the newly described *Neolyngbya* genus in addition to *Neolyngbya arenicola* and a third undocumented species clustering in a poorly resolved clade between the newly accepted genera *Limnoraphis* and *Capilliphycus*. The characterized compound, potentially isolated from this undescribed *Neolyngbya* sp., was given the corresponding trivial name, eudesmacarbonate, relative to the molecular classification.

7.2 Prospects of Cyanobacteria Biological and Chemical Diversity

Cyanobacteria range from unicellular individuals to dense, communal aggregates. These microbial bacteria, formerly termed “blue-green algae”, are ubiquitous in Earth’s biosphere, capable of surviving in extreme and unique habitats. Archaic organisms that have been credited with oxygenating Earth’s atmosphere by their ability to photosynthesize, cyanobacteria have a long evolutionary history. Consequently, cyanobacteria have proven to be a rich, exploitable source of biologically active secondary metabolites.

Previous taxonomic classification relied on traditional morphology-based characterizations. Since the onset of molecular and genomic-based approaches, taxonomic reclassifications have ensued, using 16S rRNA genes and other molecular markers. New genera and species of cyanobacteria continue to be catalogued via

phylogenetic and molecular analysis. Indeed, the putative metabolite was tracked throughout the fractionation process by low-resolution LC-MS. The metabolite of interest was consistently identified by its characteristic protonated molecular ion and sodiated adduct ion in conjunction with biological activity akin to that of PbTx-2 in the versatile zebrafish embryo and larva models of neurotoxicity.

The discoveries in this research confirm that marine cyanobacteria require continued investigation to detect new species and biologically active secondary metabolites. This research also shows the need to explore the biosynthetic origins of these metabolites. Previously, eudesmane-type sesquiterpenes have been isolated primarily from higher organisms including the red macroalgae (e.g., *Laurencia* spp.), sea hares (e.g., *Aplysia* spp.) and terrestrial plants including liverworts (e.g., *Frullania* spp.) and asterids (e.g., *Torilis japonica*). Reviews of eudesmanoid production are limited to terrestrial plants (Zhang et al., 2014) and particularly from asterids (Wu et al., 2006). However, biosynthetic genes related to the production of the malodorous sesquiterpene geosmin have been detected and studied in *Lyngbya* spp. (Zhang et al., 2009, 2014, 2016). The discovery of a novel, cyclic carbonate ester derivative of an eudesmane, isolated from a new species of marine cyanobacteria (i.e., *Neolyngbya* sp.), exemplifies the need to explore the biosynthetic origin of eudesmacarbonate compared to the other biological sources of eudesmanes, particularly from *Laurencia* spp. and *Aplysia* spp. Sea hares are known grazers of marine cyanobacteria and cyanobacteria are often epiphytic to macroalgae. Moreover, the eudesmane-type sesquiterpene biosynthesis in marine cyanobacteria should be investigated relative to the biosynthetic origins of eudesmanoids

in *Laurencia* spp. and *Aplysia* spp. to define the functional roles of these secondary metabolites (e.g., antifeedants).

7.3 Future Directions

Next steps to progress the findings of this research should include continued monitoring of the captive dolphins grazing behaviors and future intoxication events. Foremost, the project provides an unprecedented opportunity to investigate the zoopharmacognosy hypothesis, in a controlled setting, to explain why the captive dolphins are ingesting the macroalgae and cyanobacteria within their enclosure. Prudently, analysis of biological samples (e.g., blood, urine, faecal) for the presence of the HAB-related neurotoxins (i.e., ATX-a, BMAA, DA, PbTx-2, STX), and eudesmacarbonate, should be considered during any future intoxication event. Moreover, additional collection and culturing of the *Neolyngbya* sp. and unidentified filamentous species from the marine mammal zoological facility should be conducted to fully describe this new species. A comprehensive toxicological profile of eudesmacarbonate's biological activity and mode of action is warranted to assess its role as a neurotoxic secondary metabolite. Organic synthesis should be considered to derive more material and a chemical standard. Lastly, the biosynthetic pathway of eudesmacarbonate deserves investigation to gain insight into how and why this novel, neurotoxic marine cyanobacteria is produced.

In conclusion, this research project emphasized the absolute need for collaboration to realize results of unique origins. The project itself was a unique opportunity to investigate cyanobacteria potentially involved with ingested-related intoxications of dolphins living in a human managed habitat. The dolphins provided

unique insight into their feeding behaviors; no one has witnessed wild dolphins foraging macroalgae or cyanobacteria. Cyanobacteria, as some of the oldest life forms known, may uniquely be adapting to increasing eutrophic conditions and climate change. The advent of phylogenetic characterization techniques enables more precise taxonomic identification of morphologically similar, yet distinctly unique cyanobacteria members. Advances in chemical characterizations (i.e., MALDI-TOF/TOF, XRD, VCD) and separation techniques (Büchi Reveleris automated flash chromatography) afford more rapid and conclusive analysis techniques to identify unique biological molecules. In a nutshell, it literally did take a scientific village to achieve the results herein and I am extraordinarily indebted to everyone who supported and progressed this unique endeavor.

7.4 References

Mejia-Fava, J., Colitz, C.M.H., 2014. Supplements for Exotic Pets. *Vet. Clin. North Am. Exot. Anim. Pract.* 17(3), 503-525. doi:10.1016/j.cvex.2014.05.001

Wu, Q.-X., Shi, Y.-P., Jia, Z.-J., 2006. Eudesmane sesquiterpenoids from the Asteraceae family. *Nat. Prod. Rep.* 23, 699-734. doi:10.1039/b606168k

Zhang, H., Liu, H.B., Yue, J.-M., 2014. Organic Carbonates from Natural Sources. *Chem. Rev.* 114, 883-898. doi:10.1021/cr300430e

Zhang, T., Li, L., Song, L., Chen, W., 2009. Effects of temperature and light on the growth and geosmin production of *Lyngbya kuetzingii* (Cyanophyta). *J. Appl. Phycol.* 21, 279-285. doi:10.1007/s10811-008-9363-z

Zhang T., Li, D., Wang, G., Song, L., Li, L., 2014. Identification and expression analysis of the gene associated with geosmin production in *Lyngbya kuetzingii* UTEX 1547 (cyanobacteria). *Harmful Algae* 39, 127-133. doi:10.1016/j.hal.2014.07.005

Zhang, T., Li, L., Zheng, L., Song, L., 2016. Effects of nutritional factors on the geosmin production of *Lyngbya kuetzingii* 1547 (Oscillatoriales, Cyanobacteria). *Phycologia* 56(2), 221-229. doi:10.2216/16-98.1

APPENDICES

Appendix 1.1 IACUC-16-075-CR02 Protocol “The Zebrafish (*Danio rerio*) Embryo as a Model for Cyanobacterial Toxins (Using Embryos)”



MEMORANDUM

To: Dr. John Berry
CC: File
From: Mario E. Sánchez, Research Integrity Coordinator
Date: December 13, 2018
Protocol Title: "The Zebrafish (*Danio rerio*) Embryo as a Model for Cyanobacterial Toxins (Using Embryos)".

The Institutional Animal Care and Use Committee has renewed your protocol application.

Protocol Approval #: IACUC-16-075-CR02
TOPAZ Reference #: 200701
Approval Date: 12/04/18 **Expiration Date:** 12/01/19
Special Conditions: N/A

As a requirement of IACUC re-approval, you are required to:

1. Submit an IACUC amendment application for all proposed additions or changes to your protocol. All changes and additions must be reviewed and approved by the IACUC prior to implementation.
2. Promptly submit an Event Form that will notify the IACUC regarding any unanticipated deaths, adverse events, unexpected study results or a phenotype that negatively impacts the welfare of an animal. As well as, any deviations from the approved protocol. Notification must still occur even if the issue has been identified and corrected. Notification must be timely, to minimize the effect on animal welfare
3. Receive annual review and re-approval of your study prior to your IACUC expiration date. Please submit the IACUC renewal form at least 30 days in advance of the study's expiration date. As a reminder, if your protocol has reached its third year, please submit a new application prior to your expiration date.
4. Submit an IACUC Project Completion Report Form when the study is finished or discontinued.

For further information, you may visit the FIU IACUC website at:
<http://research.fiu.edu/iacuc/index.html>.

Appendix 1.2 IACUC-18-059 Protocol “Larval Zebrafish as a Model for Neurotoxicity”



MEMORANDUM

To: Dr. John Berry
CC: File
From: Barbara L. Rodriguez, MBA, Associate Director for Research Integrity
Date: October 24, 2018

Protocol Title: "Larval Zebrafish as a Behavioral Model for Neurotoxicity."

The Institutional Animal Care and Use Committee has approved your protocol application.

Protocol Approval #: IACUC-18-059
TOPAZ Reference #: 200926
Approval Date: 09/19/18 **Expiration Date:** 09/19/19
Special Conditions: N/A

As a requirement of IACUC approval, you are required to:

1. Submit an IACUC amendment application for all proposed additions or changes to your protocol. All changes and additions must be reviewed and approved by the IACUC prior to implementation.
2. Promptly submit an Event Form that will notify the IACUC regarding any unanticipated deaths, adverse events, unexpected study results or a phenotype that negatively impacts the welfare of an animal. As well as, any deviations from the approved protocol. Notification must still occur even if the issue has been identified and corrected. Notification must be timely, to minimize the effect on animal welfare
3. Receive annual review and re-approval of your study prior to your IACUC expiration date. Please submit the IACUC renewal form at least 30 days in advance of the study's expiration date.
4. Submit an IACUC Project Completion Report Form when the study is finished or discontinued.

For further information, you may visit the FIU IACUC website at <http://research.fiu.edu/iacuc/index.html>.

Appendix 3.1: Observed algal ingestion and intoxication symptoms data compiled from staff logs between 2011 through 2016.

2011:	Observations	JAN	FEB	MAR	APR	MAY	JUN	JUL	AUG	SEP	OCT	NOV	DEC
M	Symptom Date(s)	NR	NR	NR	22	NR	6	16-25	NR	NR	NR	18	NR
	Symptomatic Days	0	0	0	1	0	1	10	0	0	0	1	0
D	Symptom Date(s)	NR	NR	NR	NR	NR	NR	NR	NR	NR	NR	18	NR
	Days Symptomatic	0	0	0	0	0	0	0	0	0	0	1	0
Total	Days Symptomatic	0	0	0	1	0	1	10	0	0	0	2	0
Note: Algal ingestions were observed but not formally documented.													

2012:	Observations	JAN	FEB	MAR	APR	MAY	JUN	JUL	AUG	SEP	OCT	NOV	DEC
M	Symptom Date(s)	NR	NR	NR	18	25	12-22	17-19	31	NR	22	NR	NR
	Days Symptomatic	0	0	0	1	1	11	3	1	0	1	0	0
D	Symptom Date(s)	NR	15	16	NR	NR	NR	NR	NR	NR	NR	NR	NR
	Days Symptomatic	0	1	1	0	0	0	0	0	0	0	0	0
Total	Days Symptomatic	0	1	1	1	1	11	3	1	0	1	0	0
Note: Algal ingestions were observed but not formally documented.													

2013:	Observations	JAN	FEB	MAR	APR	MAY	JUN	JUL	AUG	SEP	OCT	NOV	DEC
M	Symptom Date(s)	28	NR	NR	NR	NR	NA	NA	NR	NA	NA	NA	NR
	Days Symptomatic	1	0	0	0	0	0	0	0	0	0	0	0
	<i>Ulva</i> . spp.	NR	4-15, 20	3-7, 29	1,10,19	7,12	NR	NR	NR	NR	NR	NR	16,19,29
	Days Ingested	0	13	6	3	2	0	0	0	0	0	0	3
	Rhodophyta	NR	NR	11	NR	NR	NR	NR	NR	NR	NR	NR	NR
	Days Ingested	0	0	1	0	0	0	0	0	0	0	0	0
	Cyanobacteria	NR	NR	NR	NR	23	NR	NR	14	NR	NR	NR	NR
	Days Ingested	0	0	0	0	1	0	0	1	0	0	0	0
	<i>T. Testudinum</i>	NR	NR	NR	NR	NR	NR	NR	17	NR	NR	NR	1,4
	Days Ingested	0	0	0	0	0	0	0	1	0	0	0	2
“Unobserved”	1	0	0	0	0	0	0	0	0	0	0	0	
D	Symptom Date(s)	NA	NR	NR	NR	NR	NR	NR	NR	27,29	NR	NR	NR
	Days Symptomatic	0	0	0	0	0	0	0	0	2	0	0	0
	<i>Ulva</i> spp.	NR	5,15-17,20	7	NR	NR	NR	14	NR	NR	NR	NR	7,18,29
	Days Ingested	0	4	1	0	0	0	1	0	0	0	0	3
	Rhodophyta	NR	5,15,20	NR	NR	NR	NR	24	NR	NR	NR	NR	NR
	Days Ingested	0	3	0	0	0	0	1	0	0	0	0	0
	cyanobacteria	NR	NR	NR	NR	NR	NR	11		27	3-4	NR	NR
	Days Ingested	0	0	0	0	0	0	1	0	1	2	0	0
	<i>T. testudinum</i>	NR	NR	NR	NR	NR	NR	NR	19	11	NR	NR	1
Days Ingested	0	0	0		0	0	0	1	1	0	0	1	
“unobserved”	NA	NA	NA	NA	NA	NA	NA	NA	NA	NA	NA	NA	
total	Days Symptomatic	1	0	0	0	0	0	0	0	2	0	0	0

2014:	Observations	JAN	FEB	MAR	APR	MAY	JUN	JUL	AUG	SEP	OCT	NOV	DEC	
M	Symptom Date(s)	NR	NR	NR	NR	NA	5-22, 30	1-8, 28-31	1,12	12	2-3	NA	NR	
	Days Symptomatic	0	0	0	0	0	19	11	2	1	2	0	0	
	<i>Ulva</i> spp.	12,15,26	26	3,9,11,12,22,24,26	4,9,12	0	29	0	0	0	0	0	0	16,19,29
	Days Ingested	3	1	7	3	0	1	0	0	0	0	0	3	
	Rhodophyta	NR	4	19	NR	NR	NR	NR	NR	NR	NR	NR	NR	
	Days Ingested	0	1	1	0	0	0	0	0	0	0	0	0	
	cyanobacteria	NR	NR	NR	NR	NR	NR	NR	14	NR	NR	NR	NR	
	Days Ingested	0	0	0	0	0	0	0	1	0	0	0	0	
	<i>T. testudinum</i>	15	NR	NR	NR	NR	0	0	17	NR	NR	NR	1,4	
	Days Ingested	1	0	0	0	0	0	0	1	0	0	0	2	
“unobserved”	NA	NA	NA	NA	NA	18	11	NA	1	2	NA	NA		
D	Symptom Date(s)	NR	4	11, 21-28	15,23	NA	5-15	31	8-12	NA	NA	NA	NA	
	Days Symptomatic	0	1	9	2	0	11	1	5	0	0	0	0	
	<i>Ulva</i> spp.	5,15,26,30	4	11,18	24	NR	NR	NR	NR	NR	NR	NR	NR	
	Days Ingested	4	1	2	1	0	0	0	0	0	0	0	0	
	Rhodophyta	15	4	NR	NR	NR	NR	10	NR	NR	NR	NR	NR	
	Days Ingested	1	1	0	0	0	0	1	0	0	0	0	0	
	cyanobacteria	NR	NR	NR	NR	NR	NR	NR	13	NR	NR	NR	NR	
	Days Ingested	0	0	0	0	0	0	0	1	0	0	0	0	
	<i>T. testudinum</i>	5,30	NR	NR	NR	NR	NR	NR	NR	NR	NR	NR	NR	
	Days Ingested	2	0	0	0	0	0	0	0	0	0	0	0	
“unobserved”	NA	NA	NA	NA	NA	11	1	NA	NA	NA	NA	NA		
Total	Days Symptomatic	0	1	9	2	0	30	12	7	1	2	0	0	
2015:	No intoxication symptoms were observed for either captive dolphin. Algal ingestions were observed but not formally documented.													
2016:	No intoxication symptoms were observed for either captive dolphin. Algal ingestions were observed but not formally documented.													
M = mother captive (Sarah, 30 years old)														
D = daughter captive dolphin (Grace, 6 years old)														
NR = Not data reported														
NA = No data available														

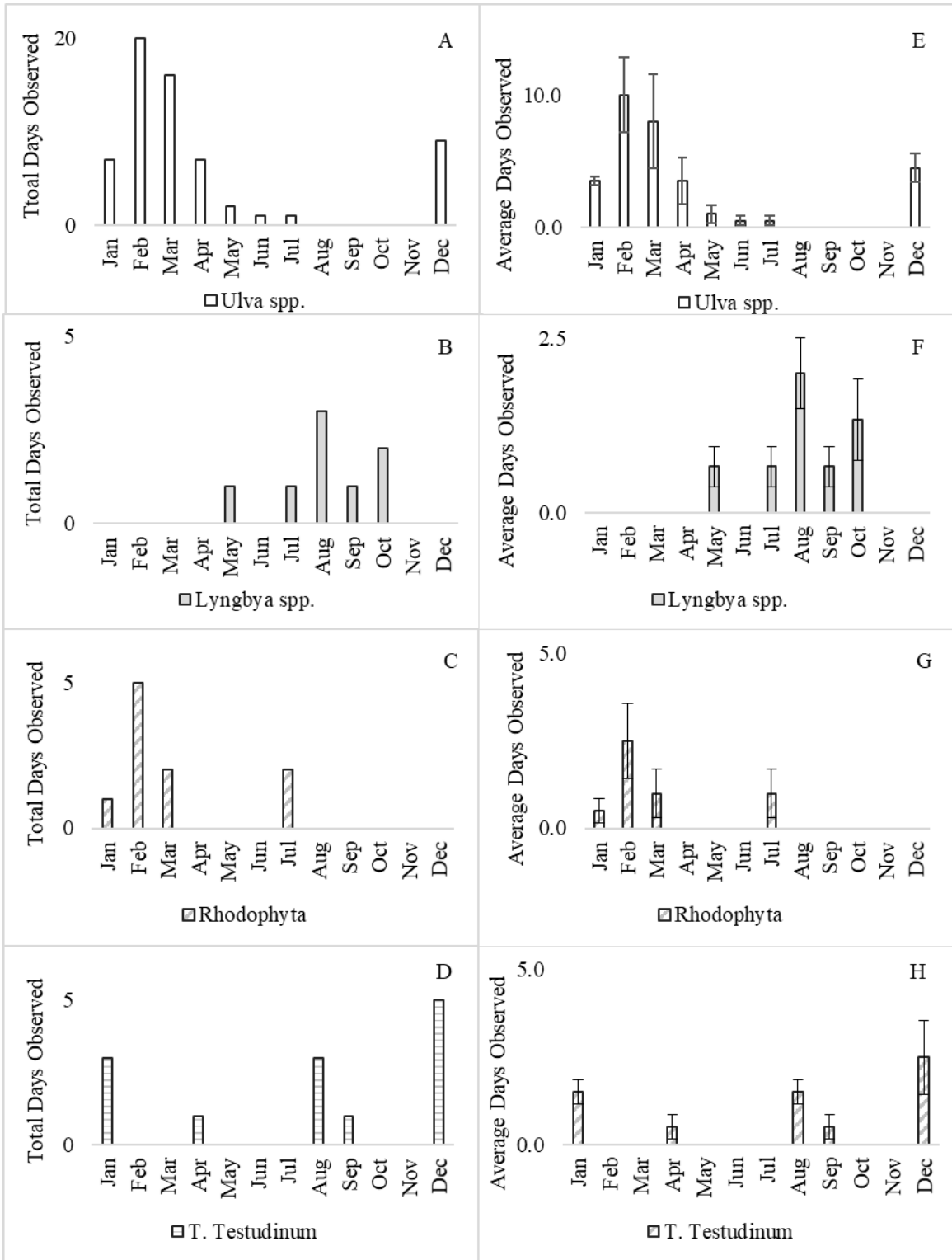
Appendix 3.2: 2011-2014 Observed intoxication event (IE) data for mother (M) and daughter (D) captive dolphins.

IE	Jan	Feb	Mar	Apr	May	Jun	Jul	Aug	Sep	Oct	Nov	Dec
M 2011	0	0	0	1	0	1	10	0	0	0	1	0
M 2012	0	0	0	1	1	11	3	1	0	1	0	0
M 2013	1	0	0	0	0	0	0	0	0	0	0	0
M 2014	0	0	0	0	0	19	12	2	1	2	0	0
D 2011	0	0	0	0	0	0	0	0	0	0	1	0
D 2012	0	1	1	0	0	0	0	0	0	0	0	0
D 2013	0	0	0	0	0	0	0	0	2	0	0	0
D 2014	0	1	9	2	0	11	1	5	0	0	0	0
4-year averaged data for mother captive dolphin, n = 4												
Total	1	0	0	2	1	31	25	3	1	3	1	0
Average	0.25	0	0	0.5	0.25	7.75	6.25	0.75	0.25	0.75	0.25	0
SD	0.5	0	0	0.58	0.50	9.00	5.68	0.96	0.50	0.96	0.5	0
SEM	0.25	0	0	0.29	0.25	4.50	2.84	0.48	0.25	0.48	0.25	0
4-year averaged data for daughter captive dolphin, n = 4												
Total	0	2	10	2	0	11	1	5	2	0	1	0
Average	0	0.5	2.5	0.5	0	2.75	0.25	1.25	0.5	0	0.25	0
SD	0	0.58	4.36	1	0	5.5	0.5	2.5	1	0	0.5	0
SEM	0	0.29	2.18	0.5	0	2.75	0.25	1.25	0.5	0	0.25	0
4-year averaged data for both mother and daughter captive dolphins, n = 8												
Total	1	2	10	4	1	42	26	8	3	3	2	0
Average	0.125	0.25	1.25	0.5	0.125	5.25	3.25	1	0.375	0.375	0.25	0
SD	0.35	0.46	3.15	0.76	0.35	7.40	4.92	1.77	0.74	0.74	0.46	0
SEM	0.13	0.16	1.11	0.27	0.13	2.62	1.74	0.63	0.26	0.26	0.16	0
IE = Intoxication Event, expressed as days observed symptomatic												
M = Mother captive dolphin (Sarah, 30 years old)												
D = Daughter captive dolphin (Grace, 6 years old)												
SD = Standard Deviation												
SEM = Standard Error of the Mean												

Appendix 3.3: Summary of monthly 2013-2014 algal ingestion (AI) data observed for both captive dolphins.

2013-2014 AI totals		Jan	Feb	Mar	Apr	May	Jun	Jul	Aug	Sep	Oct	Nov	Dec
<i>Ulva</i> spp.	Mother	3	14	13	6	2	1	0	0	0	0	0	6
	Daughter	4	6	3	1	0	0	1	0	0	0	0	3
	both	7	20	16	7	2	1	1	0	0	0	0	9
	average	3.5	10.0	8.0	3.5	1.0	0.5	0.5	0	0	0	0	4.5
	SD	0.7	5.7	7.1	3.5	1.4	0.7	0.7	0	0	0	0	2.1
	SEM	0.4	2.8	3.5	1.8	0.7	0.4	0.4	0	0	0	0	1.1
Rhodophyta	Mother	0	1	2	0	0	0	0	0	0	0	0	0
	Daughter	1	4	0	0	0	0	2	0	0	0	0	0
	both	1	5	2	0	0	0	2	0	0	0	0	0
	average	0.5	2.5	1.0	0	0	0	1.0	0	0	0	0	0
	SD	0.7	2.1	1.4	0	0	0	1.4	0	0	0	0	0
	SEM	0.4	1.1	0.7	0	0	0	0.7	0	0	0	0	0
<i>Lyngbya</i> spp.	Mother	0	0	0	0	1	0	0	2	0	0	0	0
	Daughter	0	0	0	0	0	0	1	1	1	2	0	0
	both	0	0	0	0	1	0	1	3	1	2	0	0
	average	0	0	0	0	0.7	0	0.7	2.0	0.7	1.3	0	0
	SD	0	0	0	0	0.6	0	0.6	1.0	0.6	1.2	0	0
	SEM	0	0	0	0	0.3	0	0.3	0.5	0.3	0.6	0	0
<i>T. Testudinum</i>	Mother	1	0	0	0	0	0	0	2	0	0	0	4
	Daughter	2	0	0	1	0	0	0	1	1	0	0	1
	both	3	0	0	1	0	0	0	3	1	0	0	5
	average	1.5	0	0	0.5	0	0	0	1.5	0.5	0	0	2.5
	SD	0.7	0	0	0.7	0	0	0	0.7	0.7	0	0	2.1
	SEM	0.4	0	0	0.4	0	0	0	0.4	0.4	0	0	1.1

AI = Algal Ingestion
SD = Standard Deviation
SEM = Standard Error of Mean
n = 4 (years)



Appendix 3.4: Summary plots of combined monthly algal ingestion data observed for both captive dolphins, from 2013 through 2014. A-D total number of observed ingestion days per month by algae type and E-H average observed ingestion days per month by algae type.

Appendix 3.5 IBM SPSS Pearson's Chi-Squared tests for independence report.

```

CROSSTABS
/TABLES=ingestionsarah BY intoxsarah
/FORMAT=AVALUE TABLES
/STATISTICS=CHISQ PHI
/CELLS=COUNT ROW COLUMN TOTAL
/COUNT ROUND CELL
/BARCHART.
    
```

Crosstabs - Sarah

Notes

Output Created		29-APR-2019 21:18:...
Comments		
Input	Data	/Users/holliresearch/Desktop/Lydon SPSS Intoxication and Ingestion.sav
	Active Dataset	DataSet1
	Filter	< none >
	Weight	< none >
	Split File	< none >
	N of Rows in Working Data File	24
Missing Value Handling	Definition of Missing	User-defined missing values are treated as missing.
	Cases Used	Statistics for each table are based on all the cases with valid data in the specified range(s) for all variables in each table.
Syntax		CROSSTABS /TABLES=ingestionsarah BY intoxsarah /FORMAT=AVALUE TABLES /STATISTICS=CHISQ PHI /CELLS=COUNT ROW COLUMN TOTAL /COUNT ROUND CELL /BARCHART.
Resources	Processor Time	00:00:00.22
	Elapsed Time	00:00:00.00

Notes

Dimensions Requested	2
Cells Available	524245

Case Processing Summary

	Valid		Missing		Total	
	N	Percent	N	Percent	N	Percent
ingestionsarah * intoxsarah	23	95.8%	1	4.2%	24	100.0%

ingestionsarah * intoxsarah Crosstabulation

		intoxsarah		Total
		1.00	2.00	
ingestionsarah 0	Count	4	9	13
	% within ingestionsarah	30.8%	69.2%	100.0%
	% within intoxsarah	80.0%	50.0%	56.5%
	% of Total	17.4%	39.1%	56.5%
1	Count	1	9	10
	% within ingestionsarah	10.0%	90.0%	100.0%
	% within intoxsarah	20.0%	50.0%	43.5%
	% of Total	4.3%	39.1%	43.5%
Total	Count	5	18	23
	% within ingestionsarah	21.7%	78.3%	100.0%
	% within intoxsarah	100.0%	100.0%	100.0%
	% of Total	21.7%	78.3%	100.0%

Chi-Square Tests

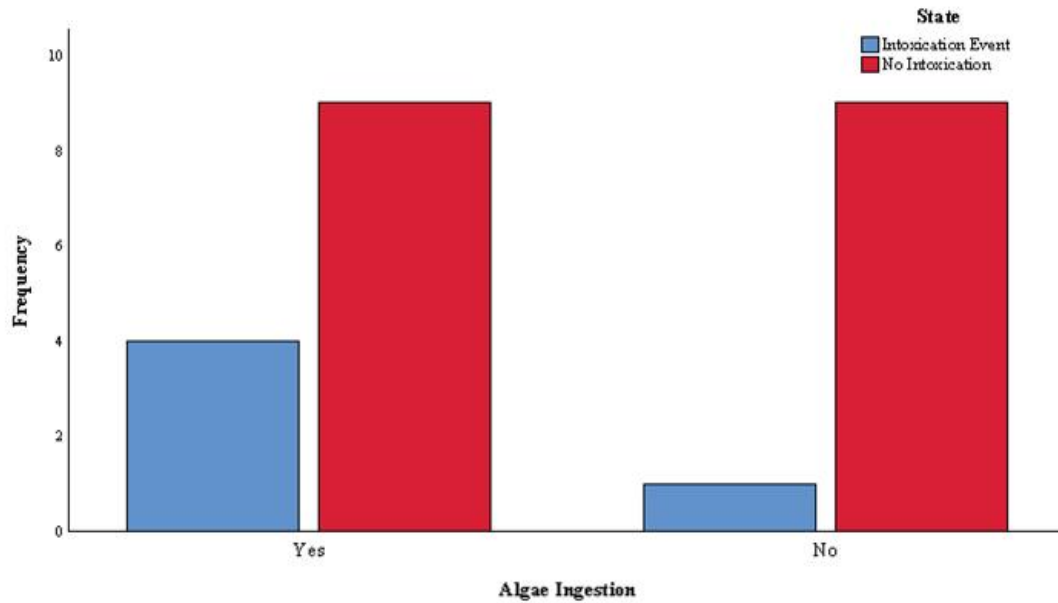
	Value	df	Asymptotic Significance (2-sided)	Exact Sig. (2- sided)	Exact Sig. (1- sided)
Pearson Chi-Square	1.433 ^a	1	.231		
Continuity Correction ^b	.472	1	.492		
Likelihood Ratio	1.535	1	.215		
Fisher's Exact Test				.339	.251
N of Valid Cases	23				

a. 2 cells (50.0%) have expected count less than 5. The minimum expected count is 2.17.

b. Computed only for a 2x2 table

Symmetric Measures

		Value	Approximate Significance
Nominal by Nominal	Phi	.250	.231
	Cramer's V	.250	.231
N of Valid Cases		23	



```
DATASET ACTIVATE DataSet1.
```

```
SAVE OUTFILE='/Users/holliresearch/Desktop/Lydon SPSS Intoxication and Ingestion.sav'  
/COMPRESSED.
```

```
DATASET ACTIVATE DataSet1.
```

```
SAVE OUTFILE='/Users/holliresearch/Desktop/Lydon SPSS Intoxication and Ingestion.sav'  
/COMPRESSED.
```

```
CROSSTABS  
/TABLES=ingestiongrace BY intoxgrace  
/FORMAT=AVALUE TABLES  
/STATISTICS=CHISQ PHI  
/CELLS=COUNT ROW COLUMN TOTAL  
/COUNT ROUND CELL  
/BARCHART.
```

Notes

Output Created		29-APR-2019 21:45:...
Comments		
Input	Data	/Users/holliresearch/Desktop/Lydon SPSS Intoxication and Ingestion.sav
	Active Dataset	DataSet1
	Filter	< none >
	Weight	< none >
	Split File	< none >
	N of Rows in Working Data File	24
Missing Value Handling	Definition of Missing	User-defined missing values are treated as missing.
	Cases Used	Statistics for each table are based on all the cases with valid data in the specified range(s) for all variables in each table.
Syntax		CROSSTABS /TABLES=ingestiongrace BY intoxgrace /FORMAT=AVALUE TABLES /STATISTICS=CHISQ PHI /CELLS=COUNT ROW COLUMN TOTAL /COUNT ROUND CELL /BARCHART.
Resources	Processor Time	00:00:00.21
	Elapsed Time	00:00:01.00
	Dimensions Requested	2
	Cells Available	524245

Case Processing Summary

	Valid		Cases Missing		Total	
	N	Percent	N	Percent	N	Percent
ingestiongrace ^ intoxgrace	24	100.0%	0	0.0%	24	100.0%

ingestiongrace ^ intoxgrace Crosstabulation

			intoxgrace		Total
			1.00	2.00	
ingestiongrace 0	Count		1	9	10
	% within ingestiongrace		10.0%	90.0%	100.0%
	% within intoxgrace		14.3%	52.9%	41.7%
	% of Total		4.2%	37.5%	41.7%
1	Count		6	8	14
	% within ingestiongrace		42.9%	57.1%	100.0%
	% within intoxgrace		85.7%	47.1%	58.3%
	% of Total		25.0%	33.3%	58.3%
Total	Count		7	17	24
	% within ingestiongrace		29.2%	70.8%	100.0%
	% within intoxgrace		100.0%	100.0%	100.0%
	% of Total		29.2%	70.8%	100.0%

Chi-Square Tests

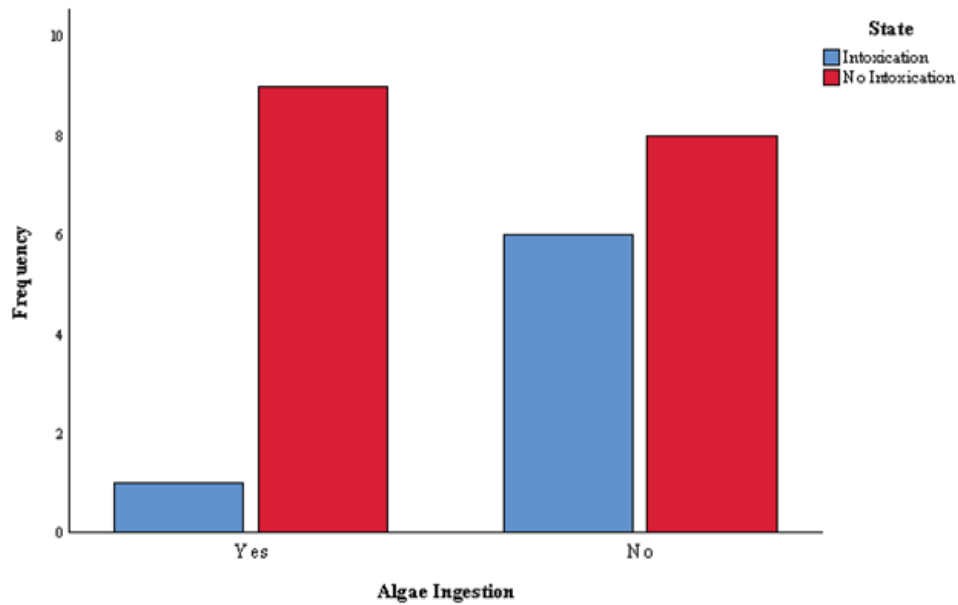
	Value	df	Asymptotic Significance (2-sided)	Exact Sig. (2-sided)	Exact Sig. (1-sided)
Pearson Chi-Square	3.048 ^a	1	.081		
Continuity Correction ^b	1.665	1	.197		
Likelihood Ratio	3.352	1	.067		
Fisher's Exact Test				.172	.097
N of Valid Cases	24				

a. 2 cells (50.0%) have expected count less than 5. The minimum expected count is 2.92.

b. Computed only for a 2x2 table

Symmetric Measures

		Value	Approximate Significance
Nominal by Nominal	Phi	-.356	.081
	Cramer's V	.356	.081
N of Valid Cases		24	



```

CROSSTABS
/TABLES=Season BY intoxgrace
/FORMAT=AVALUE TABLES
/STATISTICS=CHISQ PHI
/CELLS=COUNT ROW COLUMN TOTAL
/COUNT ROUND CELL
/BARCHART.
    
```

Crosstabs - Intoxication and Season Grace

Notes

Output Created		29-APR-2019 21:49:...
Comments		
Input	Data	/Users/holliresearch/Desktop/Lydon SPSS Intoxication and Ingestion.sav
	Active Dataset	DataSet1
	Filter	< none >
	Weight	< none >
	Split File	< none >
	N of Rows in Working Data File	24
Missing Value Handling	Definition of Missing	User-defined missing values are treated as missing.
	Cases Used	Statistics for each table are based on all the cases with valid data in the specified range(s) for all variables in each table.
Syntax		<pre> CROSSTABS /TABLES=Season BY intoxgrace /FORMAT=AVALUE TABLES /STATISTICS=CHISQ PHI /CELLS=COUNT ROW COLUMN TOTAL /COUNT ROUND CELL /BARCHART. </pre>
Resources	Processor Time	00:00:00.17
	Elapsed Time	00:00:00.00
	Dimensions Requested	2
	Cells Available	524245

Case Processing Summary

	Cases					
	Valid		Missing		Total	
	N	Percent	N	Percent	N	Percent
Season * intoxgrace	24	100.0%	0	0.0%	24	100.0%

Season * intoxgrace Crosstabulation

		intoxgrace		Total	
		1.00	2.00		
Season	Winter	Count	1	5	6
		% within Season	16.7%	83.3%	100.0%
		% within intoxgrace	14.3%	29.4%	25.0%
		% of Total	4.2%	20.8%	25.0%
	Spring	Count	2	4	6
		% within Season	33.3%	66.7%	100.0%
		% within intoxgrace	28.6%	23.5%	25.0%
		% of Total	8.3%	16.7%	25.0%
	Summer	Count	3	3	6
		% within Season	50.0%	50.0%	100.0%
		% within intoxgrace	42.9%	17.6%	25.0%
		% of Total	12.5%	12.5%	25.0%
	Fall	Count	1	5	6
		% within Season	16.7%	83.3%	100.0%
		% within intoxgrace	14.3%	29.4%	25.0%
		% of Total	4.2%	20.8%	25.0%
Total	Count	7	17	24	
	% within Season	29.2%	70.8%	100.0%	
	% within intoxgrace	100.0%	100.0%	100.0%	
	% of Total	29.2%	70.8%	100.0%	

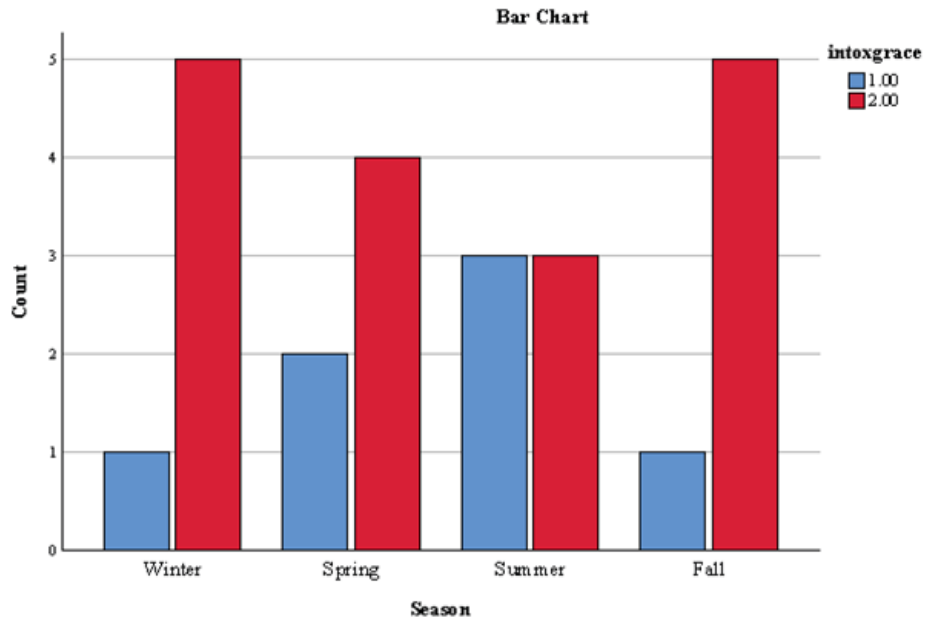
Chi-Square Tests

	Value	df	Asymptotic Significance (2-sided)
Pearson Chi-Square	2.218 ^a	3	.528
Likelihood Ratio	2.205	3	.531
Linear-by-Linear Association	.039	1	.844
N of Valid Cases	24		

a. 8 cells (100.0%) have expected count less than 5. The minimum expected count is 1.75.

Symmetric Measures

		Value	Approximate Significance
Nominal by Nominal	Phi	.304	.528
	Cramer's V	.304	.528
N of Valid Cases		24	



```

CROSSTABS
/TABLES=Season BY intoxsarah
/FORMAT=AVALUE TABLES
/STATISTICS=CHISQ PHI
/CELLS=COUNT ROW COLUMN TOTAL
/COUNT ROUND CELL
/BARCHART.
    
```

Crosstabs - Intoxication and Season Sarah

Notes

Output Created		29-APR-2019 21:49:...
Comments		
Input	Data	/Users/holliresearch/Desktop/Lydon SPSS Intoxication and Ingestion.sav
	Active Dataset	DataSet1
	Filter	< none >
	Weight	< none >
	Split File	< none >
	N of Rows in Working Data File	24
Missing Value Handling	Definition of Missing	User-defined missing values are treated as missing.
	Cases Used	Statistics for each table are based on all the cases with valid data in the specified range(s) for all variables in each table.
Syntax		<pre> CROSSTABS /TABLES=Season BY intoxsarah /FORMAT=AVALUE TABLES /STATISTICS=CHISQ PHI /CELLS=COUNT ROW COLUMN TOTAL /COUNT ROUND CELL /BARCHART. </pre>
Resources	Processor Time	00:00:00.19
	Elapsed Time	00:00:01.00
	Dimensions Requested	2
	Cells Available	524245

Case Processing Summary

	Cases					
	Valid		Missing		Total	
	N	Percent	N	Percent	N	Percent
Season * intoxsarah	24	100.0%	0	0.0%	24	100.0%

Season * intoxsarah Crosstabulation

		intoxsarah		Total	
		1.00	2.00		
Season	Winter	Count	1	5	6
		% within Season	16.7%	83.3%	100.0%
		% within intoxsarah	16.7%	27.8%	25.0%
		% of Total	4.2%	20.8%	25.0%
	Spring	Count	0	6	6
		% within Season	0.0%	100.0%	100.0%
		% within intoxsarah	0.0%	33.3%	25.0%
		% of Total	0.0%	25.0%	25.0%
	Summer	Count	3	3	6
		% within Season	50.0%	50.0%	100.0%
		% within intoxsarah	50.0%	16.7%	25.0%
		% of Total	12.5%	12.5%	25.0%
	Fall	Count	2	4	6
		% within Season	33.3%	66.7%	100.0%
		% within intoxsarah	33.3%	22.2%	25.0%
		% of Total	8.3%	16.7%	25.0%
Total	Count	6	18	24	
	% within Season	25.0%	75.0%	100.0%	
	% within intoxsarah	100.0%	100.0%	100.0%	
	% of Total	25.0%	75.0%	100.0%	

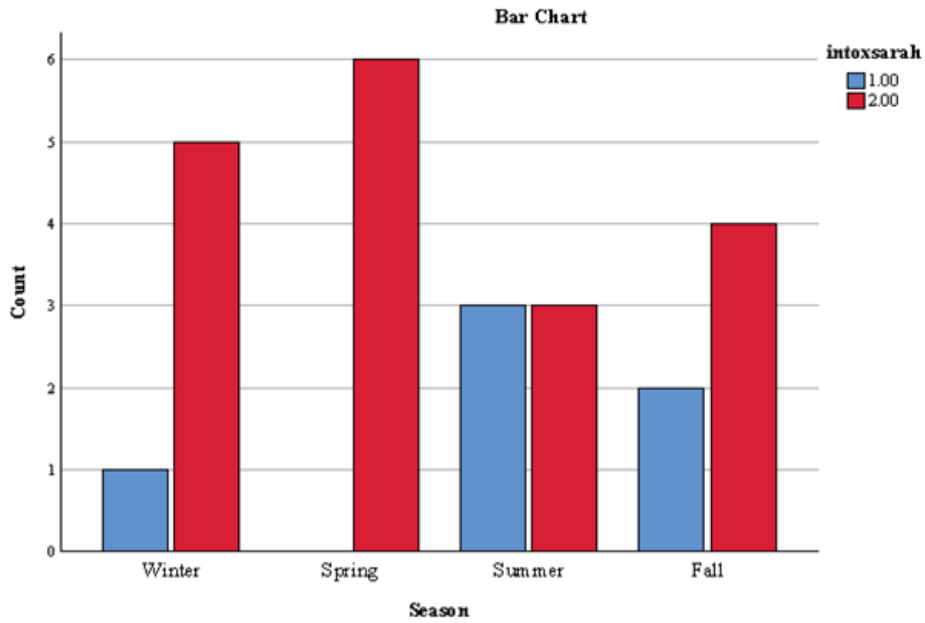
Chi-Square Tests

	Value	df	Asymptotic Significance (2-sided)
Pearson Chi-Square	4.444 ^a	3	.217
Likelihood Ratio	5.629	3	.131
Linear-by-Linear Association	1.533	1	.216
N of Valid Cases	24		

a. 8 cells (100.0%) have expected count less than 5. The minimum expected count is 1.50.

Symmetric Measures

		Value	Approximate Significance
Nominal by Nominal	Phi	.430	.217
	Cramer's V	.430	.217
N of Valid Cases		24	



```

CROSSTABS
/TABLES=SarahLettuce BY intox Sarah
/FORMAT=AVALUE TABLES
/STATISTICS=CHISQ PHI
/CELLS=COUNT ROW COLUMN TOTAL
/COUNT ROUND CELL
/BARCHART.
    
```

Crosstabs - Intoxication and Lettuce Ingestion Sarah

Notes

Output Created		29-APR-2019 21:50:...
Comments		
Input	Data	/Users/holliresearch/Desktop/Lydon SPSS Intoxication and Ingestion.sav
	Active Dataset	DataSet1
	Filter	< none >
	Weight	< none >
	Split File	< none >
	N of Rows in Working Data File	24
Missing Value Handling	Definition of Missing	User-defined missing values are treated as missing.
	Cases Used	Statistics for each table are based on all the cases with valid data in the specified range(s) for all variables in each table.
Syntax		<pre> CROSSTABS /TABLES=SarahLettuce BY intoxsarah /FORMAT=AVALUE TABLES /STATISTICS=CHISQ PHI /CELLS=COUNT ROW COLUMN TOTAL /COUNT ROUND CELL /BARCHART. </pre>
Resources	Processor Time	00:00:00.18
	Elapsed Time	00:00:01.00
	Dimensions Requested	2
	Cells Available	524245

Case Processing Summary

	Valid		Cases Missing		Total	
	N	Percent	N	Percent	N	Percent
SarahLettuce ^ intoxsarah	24	100.0%	0	0.0%	24	100.0%

SarahLettuce * intoxsarah Crosstabulation

		intoxsarah		Total	
		1.00	2.00		
SarahLettuce	.00	Count	5	8	13
		% within SarahLettuce	38.5%	61.5%	100.0%
		% within intoxsarah	83.3%	44.4%	54.2%
		% of Total	20.8%	33.3%	54.2%
SarahLettuce	1.00	Count	1	10	11
		% within SarahLettuce	9.1%	90.9%	100.0%
		% within intoxsarah	16.7%	55.6%	45.8%
		% of Total	4.2%	41.7%	45.8%
Total		Count	6	18	24
		% within SarahLettuce	25.0%	75.0%	100.0%
		% within intoxsarah	100.0%	100.0%	100.0%
		% of Total	25.0%	75.0%	100.0%

Chi-Square Tests

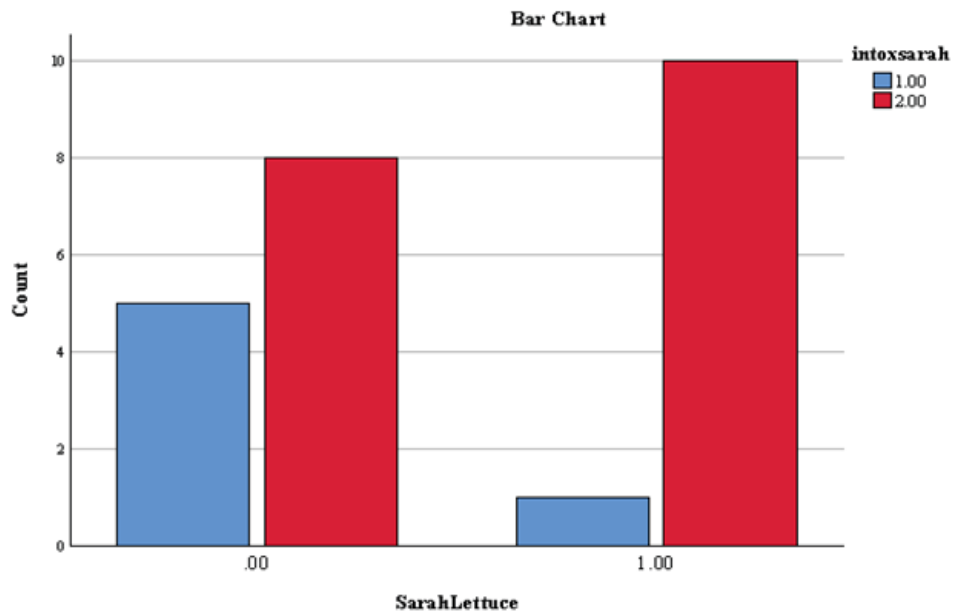
	Value	df	Asymptotic Significance (2-sided)	Exact Sig. (2-sided)	Exact Sig. (1-sided)
Pearson Chi-Square	2.741 ^a	1	.098		
Continuity Correction ^b	1.399	1	.237		
Likelihood Ratio	2.967	1	.085		
Fisher's Exact Test				.166	.118
Linear-by-Linear Association	2.627	1	.105		
N of Valid Cases	24				

a. 2 cells (50.0%) have expected count less than 5. The minimum expected count is 2.75.

b. Computed only for a 2x2 table

Symmetric Measures

		Value	Approximate Significance
Nominal by Nominal	Phi	.338	.098
	Cramer's V	.338	.098
N of Valid Cases		24	



```

CROSSTABS
/TABLES=SarahLettuce BY intoxgrace
/FORMAT=AVALUE TABLES
/STATISTICS=CHISQ PHI
/CELLS=COUNT ROW COLUMN TOTAL
/COUNT ROUND CELL
/BARCHART.

```

Crosstabs Intoxication and Lettuce Ingestion Grace

Notes

Output Created		29-APR-2019 21:51:...
Comments		
Input	Data	/Users/holliresearch/Desktop/Lydon SPSS Intoxication and Ingestion.sav
	Active Dataset	DataSet1
	Filter	< none >
	Weight	< none >
	Split File	< none >
	N of Rows in Working Data File	24
Missing Value Handling	Definition of Missing	User-defined missing values are treated as missing.
	Cases Used	Statistics for each table are based on all the cases with valid data in the specified range(s) for all variables in each table.
Syntax		CROSSTABS /TABLES=SarahLettuce BY intoxgrace /FORMAT=AVALUE TABLES /STATISTICS=CHISQ PHI /CELLS=COUNT ROW COLUMN TOTAL /COUNT ROUND CELL /BARChart.
Resources	Processor Time	00:00:00.19
	Elapsed Time	00:00:00.00
	Dimensions Requested	2
	Cells Available	524245

Case Processing Summary

	Valid		Cases Missing		Total	
	N	Percent	N	Percent	N	Percent
SarahLettuce * intoxgrace	24	100.0%	0	0.0%	24	100.0%

SarahLettuce * intoxgrace Crosstabulation

		intoxgrace		Total	
		1.00	2.00		
SarahLettuce	.00	Count	3	10	13
		% within SarahLettuce	23.1%	76.9%	100.0%
		% within intoxgrace	42.9%	58.8%	54.2%
		% of Total	12.5%	41.7%	54.2%
	1.00	Count	4	7	11
		% within SarahLettuce	36.4%	63.6%	100.0%
		% within intoxgrace	57.1%	41.2%	45.8%
		% of Total	16.7%	29.2%	45.8%
Total		Count	7	17	24
		% within SarahLettuce	29.2%	70.8%	100.0%
		% within intoxgrace	100.0%	100.0%	100.0%
		% of Total	29.2%	70.8%	100.0%

Chi-Square Tests

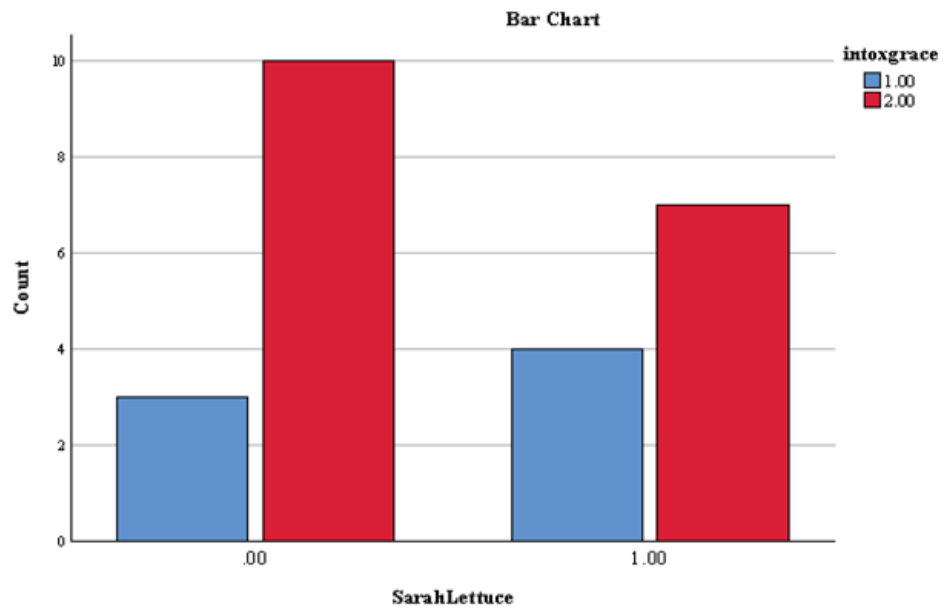
	Value	df	Asymptotic Significance (2-sided)	Exact Sig. (2-sided)	Exact Sig. (1-sided)
Pearson Chi-Square	.509 ^a	1	.476		
Continuity Correction ^b	.069	1	.793		
Likelihood Ratio	.509	1	.476		
Fisher's Exact Test				.659	.395
Linear-by-Linear Association	.488	1	.485		
N of Valid Cases	24				

a. 2 cells (50.0%) have expected count less than 5. The minimum expected count is 3.21.

b. Computed only for a 2x2 table

Symmetric Measures

		Value	Approximate Significance
Nominal by Nominal	Phi	-.146	.476
	Cramer's V	.146	.476
N of Valid Cases		24	



```

CROSSTABS
/TABLES=allintox BY allingestion
/FORMAT=AVALUE TABLES
/STATISTICS=CHISQ PHI
/CELLS=COUNT ROW COLUMN TOTAL
/COUNT ROUND CELL
/BARCHART.

```

Crosstabs - Intoxication and Ingestion Sarah and Grace Combined

Notes

Output Created		29-APR-2019 22:01:...
Comments		
Input	Data	/Users/holliresearch/Desktop/Lydon SPSS Intoxication and Ingestion.sav
	Active Dataset	DataSet1
	Filter	< none >
	Weight	< none >
	Split File	< none >
	N of Rows in Working Data File	49
Missing Value Handling	Definition of Missing	User-defined missing values are treated as missing.
	Cases Used	Statistics for each table are based on all the cases with valid data in the specified range(s) for all variables in each table.
Syntax		<pre> CROSSTABS /TABLES=allintox BY allingestion /FORMAT=AVALUE TABLES /STATISTICS=CHISQ PHI /CELLS=COUNT ROW COLUMN TOTAL /COUNT ROUND CELL /BARCHART. </pre>
Resources	Processor Time	00:00:00.20
	Elapsed Time	00:00:00.00
	Dimensions Requested	2
	Cells Available	524245

Case Processing Summary

	Valid		Cases Missing		Total	
	N	Percent	N	Percent	N	Percent
allintox * allingestion	48	98.0%	1	2.0%	49	100.0%

allintox * allingestion Crosstabulation

		allingestion		Total	
		.00	1.00		
allintox	1.00	Count	7	6	13
		% within allintox	53.8%	46.2%	100.0%
		% within allingestion	20.6%	42.9%	27.1%
		% of Total	14.6%	12.5%	27.1%
	2.00	Count	27	8	35
		% within allintox	77.1%	22.9%	100.0%
		% within allingestion	79.4%	57.1%	72.9%
		% of Total	56.3%	16.7%	72.9%
Total		Count	34	14	48
		% within allintox	70.8%	29.2%	100.0%
		% within allingestion	100.0%	100.0%	100.0%
		% of Total	70.8%	29.2%	100.0%

Chi-Square Tests

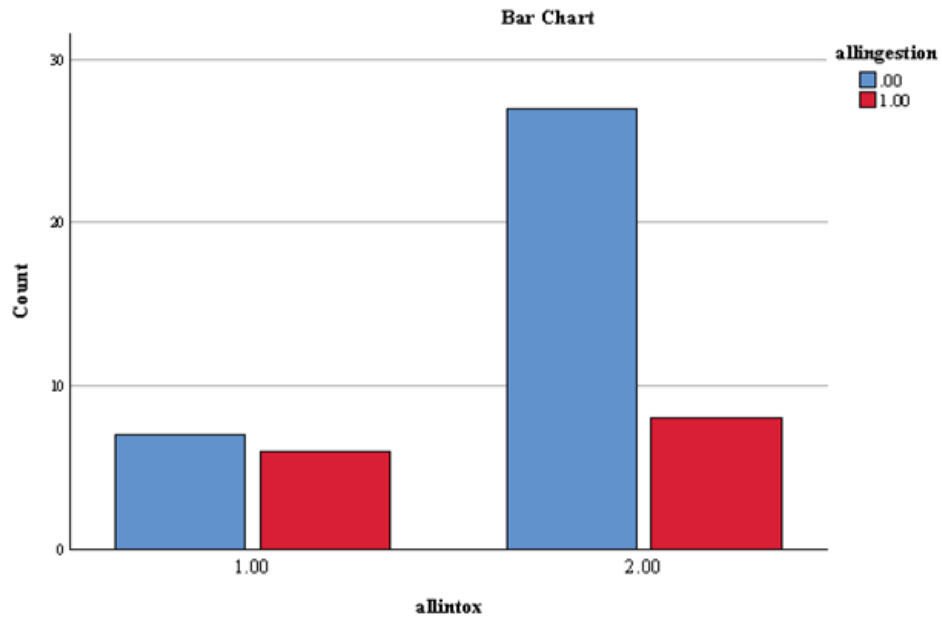
	Value	df	Asymptotic Significance (2-sided)	Exact Sig. (2-sided)	Exact Sig. (1-sided)
Pearson Chi-Square	2.490 ^a	1	.115		
Continuity Correction ^b	1.490	1	.222		
Likelihood Ratio	2.376	1	.123		
Fisher's Exact Test				.157	.113
Linear-by-Linear Association	2.438	1	.118		
N of Valid Cases	48				

a. 1 cells (25.0%) have expected count less than 5. The minimum expected count is 3.79.

b. Computed only for a 2x2 table

Symmetric Measures

		Value	Approximate Significance
Nominal by Nominal	Phi	-.228	.115
	Cramer's V	.228	.115
N of Valid Cases		48	



```

CROSSTABS
/TABLES=allintox BY alllettuce
/FORMAT=AVALUE TABLES
/STATISTICS=CHISQ PHI
/CELLS=COUNT ROW COLUMN TOTAL
/COUNT ROUND CELL
/BAR.CHART.

```

Crosstabs - Intoxication and Lettuce Ingestion Sarah and Grace Combined

Notes

Output Created		29-APR-2019 22:02:...
Comments		
Input	Data	/Users/holliresearch/Desktop/Lydon SPSS Intoxication and Ingestion.sav
	Active Dataset	DataSet1
	Filter	< none >
	Weight	< none >
	Split File	< none >
	N of Rows in Working Data File	49
Missing Value Handling	Definition of Missing	User-defined missing values are treated as missing.
	Cases Used	Statistics for each table are based on all the cases with valid data in the specified range(s) for all variables in each table.
Syntax		<pre> CROSSTABS /TABLES=allintox BY alllettuce /FORMAT=AVALUE TABLES /STATISTICS=CHISQ PHI /CELLS=COUNT ROW COLUMN TOTAL /COUNT ROUND CELL /BARCHART. </pre>
Resources	Processor Time	00:00:00.18
	Elapsed Time	00:00:00.00
	Dimensions Requested	2
	Cells Available	524245

Case Processing Summary

	Valid		Cases Missing		Total	
	N	Percent	N	Percent	N	Percent
allintox * alllettuce	48	98.0%	1	2.0%	49	100.0%

allintox * allettuce Crosstabulation

		allettuce		Total	
		.00	1.00		
allintox	1.00	Count	6	7	13
		% within allintox	46.2%	53.8%	100.0%
		% within allettuce	22.2%	33.3%	27.1%
		% of Total	12.5%	14.6%	27.1%
	2.00	Count	21	14	35
		% within allintox	60.0%	40.0%	100.0%
		% within allettuce	77.8%	66.7%	72.9%
		% of Total	43.8%	29.2%	72.9%
Total		Count	27	21	48
		% within allintox	56.3%	43.8%	100.0%
		% within allettuce	100.0%	100.0%	100.0%
		% of Total	56.3%	43.8%	100.0%

Chi-Square Tests

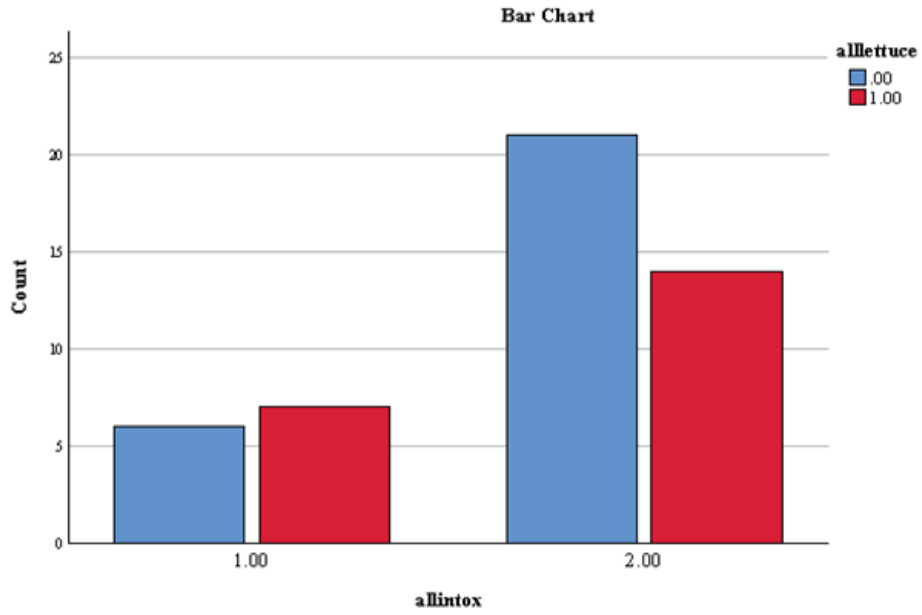
	Value	df	Asymptotic Significance (2-sided)	Exact Sig. (2-sided)	Exact Sig. (1-sided)
Pearson Chi-Square	.738 ^a	1	.390		
Continuity Correction ^b	.283	1	.595		
Likelihood Ratio	.735	1	.391		
Fisher's Exact Test				.516	.296
Linear-by-Linear Association	.723	1	.395		
N of Valid Cases	48				

a. 0 cells (0.0%) have expected count less than 5. The minimum expected count is 5.69.

b. Computed only for a 2x2 table

Symmetric Measures

		Value	Approximate Significance
Nominal by Nominal	Phi	-.124	.390
	Cramer's V	.124	.390
N of Valid Cases		48	



```

CROSSTABS
/TABLES=allintox BY AllSeason
/FORMAT=AVALUE TABLES
/STATISTICS=CHISQ PHI
/CELLS=COUNT ROW COLUMN TOTAL
/COUNT ROUND CELL
/BARCHART.

```

Crosstabs - All Intoxication Events and Season Sarah and Grace Combined

Notes

Output Created		29-APR-2019 22:04:...
Comments		
Input	Data	/Users/holliresearch/Desktop/Lydon SPSS Intoxication and Ingestion.sav
	Active Dataset	DataSet1
	Filter	< none >
	Weight	< none >
	Split File	< none >
	N of Rows in Working Data File	49
Missing Value Handling	Definition of Missing	User-defined missing values are treated as missing.
	Cases Used	Statistics for each table are based on all the cases with valid data in the specified range(s) for all variables in each table.
Syntax		<pre> CROSSTABS /TABLES=allintox BY AllSeason /FORMAT=AVALUE TABLES /STATISTICS=CHISQ PHI /CELLS=COUNT ROW COLUMN TOTAL /COUNT ROUND CELL /BARCHART. </pre>
Resources	Processor Time	00:00:00.23
	Elapsed Time	00:00:00.00
	Dimensions Requested	2
	Cells Available	524245

Case Processing Summary

	Cases					
	Valid		Missing		Total	
	N	Percent	N	Percent	N	Percent
allintox * AllSeason	48	98.0%	1	2.0%	49	100.0%

allintox * AllSeason Crosstabulation

			AllSeason				
			1.00	2.00	3.00	4.00	Total
allintox	1.00	Count	2	2	6	3	13
		% within allintox	15.4%	15.4%	46.2%	23.1%	100.0%
		% within AllSeason	16.7%	16.7%	50.0%	25.0%	27.1%
		% of Total	4.2%	4.2%	12.5%	6.3%	27.1%
	2.00	Count	10	10	6	9	35
		% within allintox	28.6%	28.6%	17.1%	25.7%	100.0%
		% within AllSeason	83.3%	83.3%	50.0%	75.0%	72.9%
		% of Total	20.8%	20.8%	12.5%	18.8%	72.9%
Total	Count	12	12	12	12	48	
	% within allintox	25.0%	25.0%	25.0%	25.0%	100.0%	
	% within AllSeason	100.0%	100.0%	100.0%	100.0%	100.0%	
	% of Total	25.0%	25.0%	25.0%	25.0%	100.0%	

Chi-Square Tests

	Value	df	Asymptotic Significance (2-sided)
Pearson Chi-Square	4.536 ^a	3	.209
Likelihood Ratio	4.314	3	.230
Linear-by-Linear Association	1.012	1	.314
N of Valid Cases	48		

a. 4 cells (50.0%) have expected count less than 5. The minimum expected count is 3.25.

Symmetric Measures

		Value	Approximate Significance
Nominal by Nominal	Phi	.307	.209
	Cramer's V	.307	.209
N of Valid Cases		48	

Appendix 3.6: 2011-2014 Maximum fecal coliform units per 100 mL seawater water (FC) data.

Site Seawater FC data	South	North	Canal	Average	SD	SEM (n = 3)	
2011	JAN	-	-	-	-	-	
	FEB	-	7.5	7.5	7.5	0.0	0.0
	MAR	-	-	-	-	-	-
	APR	-	-	-	-	-	-
	MAY	-	-	-	-	-	-
	JUN	-	-	-	-	-	-
	JUL	-	-	-	-	-	-
	AUG	17.5	17.5	17.5	17.5	0.0	0.0
	SEP	-	-	-	-	-	-
	OCT	-	-	-	-	-	-
	NOV	-	-	-	-	-	-
	DEC	-	-	-	-	-	-
2012	JAN	-	-	-	-	-	-
	FEB	-	-	-	-	-	-
	MAR	-	-	-	-	-	-
	APR	-	-	-	-	-	-
	MAY	7.5	2.5	17.5	9.2	7.6	4.4
	JUN	2.0	7.0	1.0	3.3	3.2	1.9
	JUL	5.0	1.0	2.0	2.7	2.1	1.2
	AUG	1.0	1.0	13.0	5.0	6.9	4.0
	SEP	28.0	28.0	34.0	30.0	3.5	2.0
	OCT	17.0	15.0	16.0	16.0	1.0	0.6
	NOV	-	-	-	-	-	-
	DEC	5.0	7.5	2.5	5.0	2.5	1.4
2013	JAN	-	-	-	-	-	-
	FEB	-	-	-	-	-	-
	MAR	3.0	2.0	12.0	5.7	5.5	3.2
	APR	-	-	-	-	-	-
	MAY	-	-	-	-	-	-
	JUN	2.0	2.0	2.0	2.0	0.0	0.0
	JUL	-	-	-	-	-	-
	AUG	-	-	-	-	-	-
	SEP	-	-	-	-	-	-
	OCT	3.0	-	-	3.0	0.0	0.0
	NOV	-	-	-	-	-	-
	DEC	-	-	-	-	-	-
2014	JAN	-	-	-	-	-	-
	FEB	27.0	18.0	14.0	19.7	6.7	3.8
	MAR	9.0	6.0	7.0	7.3	1.5	0.9
	APR	10.0	4.0	38.0	17.3	18.1	10.5
	MAY	45.0	25.0	7.0	25.7	19.0	11.0
	JUN	8.0	4.0	5.0	5.7	2.1	1.2
	JUL	-	5.0	3.0	4.0	1.4	0.8
	AUG	10.0	10.0	6.0	8.7	2.3	1.3
	SEP	7.0	6.0	4.0	5.7	1.5	0.9
	OCT	7.0	10.0	9.0	8.7	1.5	0.9

	NOV	6.0	8.0	9.0	7.7	1.5	0.9
	DEC	1.0	2.0	6.0	3.0	2.6	1.5
FC	Average	SD	SEM	Count	Maximum	Minimum	
All FC	9.8	9.4	1.2	66	45.0	1.0	
North	8.6	7.6	1.6	22	28.0	1.0	

AFC = Average of MFCU/100 mL seawater

SD = Standard Deviation

SEM = Standard Error of the Mean

Appendix 3.7 Descriptive statistical analysis of monthly FC data from 2011 through 2014.

Month:	Jan	Feb	Mar	Apr	May	Jun	Jul	Aug	Sep	Oct	Nov	Dec
Mean	NA	12.8	6.5	17.3	17.4	3.7	3.2	10.4	17.8	11.0	7.7	4.0
SEM	NA	3.6	1.5	10.5	6.4	0.8	0.8	2.2	5.5	2.0	0.9	1.0
Median	NA	10.8	6.5	10.0	12.5	2.0	3.0	10.0	17.5	10.0	8.0	3.8
Mode	NA	7.5	NA	NA	NA	2	5	17.5	28	NA	NA	NA
SD	NA	8.9	3.7	18.1	15.8	2.5	1.8	6.7	13.5	5.2	1.5	2.5
SV	NA	78	14	329	250	6	3	44	183	27.0	2.3	6.5
Kurtosis	NA	-0.05	-0.76	NA	1.09	-0.73	-2.3	-1.3	-2.9	-1.21	NA	-1.79
Skewness	NA	0.72	0.28	1.52	1.22	0.86	-0.05	-0.35	0.09	-0.30	-0.94	0.24
Range	0	24.5	10	34	42.5	7	4	16.5	30	14	3	6.5
Max	NA	27.0	12.0	38.0	45.0	8.0	5.0	17.5	34.0	17.0	9.0	7.5
Mini	NA	2.5	2.0	4.0	2.5	1.0	1.0	1.0	4.0	3.0	6.0	1.0
Sum	NA	77	39	52	105	33	16	94	107	77.0	23.0	24.0
Count	0	6	6	3	6	9	5	9	6	7	3	6
GM	NA	9.9	5.5	11.5	11.7	3.0	2.7	7.0	12.8	9.6	7.6	3.2
HM	NA	7.2	4.5	8.0	7.5	2.4	2.2	3.4	9.1	8.0	7.4	2.5
AAD	NA	6.9	2.8	13.8	11.8	2.1	1.4	5.3	12.2	4.3	1.1	2.2
MAD	NA	5.3	3.0	6.0	7.8	1.0	2.0	7.5	11.0	5.0	1.0	2.0
IQR	NA	9.5	4.8	17.0	16.0	3.0	3.0	11.5	21.8	7.5	1.5	3.6
4-year	Mean	SD	SEM	Count	Maximum	Minimum						
AFC	10.2	5.6	1.6	11*	17.8	3.2						

SEM = Standard Error of the Mean

SD = Standard Deviation

SV = Sample Variance

GM = Geometric Mean

HM = Harmonic Mean

AAD = Average Absolute Deviation

MAD = Median Absolute Deviation

IQR = Inter-Quartile Range

*n = 11 months, no data measured for January of any year

Appendix 3.8: 2011-2014 FC Box Plot analysis data.

Month:	Jan	Feb	Mar	Apr	May	Jun	Jul	Aug	Sep	Oct	Nov	Dec
Minimum	0.0	2.5	2.0	4.0	2.5	1.0	1.0	1.0	4.0	3.0	6.0	1.0
Q1-Minimum	NA	5.0	1.8	3.0	4.6	1.0	1.0	5.0	2.3	5.0	1.0	1.1
Median-Q1	NA	3.3	2.8	3.0	5.4	0.0	1.0	4.0	11.3	2.0	1.0	1.6
Q3-Median	NA	6.3	2.0	14.0	10.6	3.0	2.0	7.5	10.5	5.5	0.5	2.0
Maximum-Q3	NA	10.0	3.5	14.0	21.9	3.0	0.0	0.0	6.0	1.5	0.5	1.8
Mean (x)	NA	12.8	6.5	17.3	17.4	3.7	3.2	10.4	17.8	11.0	7.7	4.0

Appendix 3.9: 2011-2014 Lagoon water temperature (°F) raw data.

Lagoon Water Temperature (°F)		North	South	Canal	Average	SD	SEM (n = 3)
2011	JAN	-	-	-	-	-	-
	FEB	71.0	72.0	71.0	71.5	0.5	0.3
	MAR	-	-	-	-	-	-
	APR	-	-	-	-	-	-
	MAY	-	-	-	-	-	-
	JUN	-	-	-	-	-	-
	JUL	-	-	-	-	-	-
	AUG	85.0	85.0	85.0	85.0	0.0	0.0
	SEP	-	-	-	-	-	-
	OCT	-	-	-	-	-	-
	NOV	-	-	-	-	-	-
	DEC	-	-	-	-	-	-
2012	JAN	-	-	-	-	-	-
	FEB	-	-	-	-	-	-
	MAR	-	-	-	-	-	-
	APR	-	-	-	-	-	-
	MAY	82.0	82.0	82.0	82.0	0.0	0.0
	JUN	85.0	85.0	85.0	85.0	0.0	0.0
	JUL	85.0	85.0	85.0	85.0	0.0	0.0
	AUG	85.0	85.0	85.0	85.0	0.0	0.0
	SEP	85.0	85.0	85.0	85.0	0.0	0.0
	OCT	79.0	79.0	79.0	79.0	0.0	0.0
	NOV	-	-	-	-	-	-
	DEC	74.0	74.0	74.0	74.0	0.0	0.0
2013	JAN	-	-	-	-	-	-
	FEB	-	-	-	-	-	-
	MAR	76.0	77.0	75.0	76.0	1.0	0.6
	APR	-	-	-	-	-	-
	MAY	-	-	-	-	-	-
	JUN	81.0	81.0	81.0	81.0	0.0	0.0
	JUL	-	-	-	-	-	-
	AUG	-	-	-	-	-	-
	SEP	-	-	-	-	-	-
	OCT	-	76.0	-	76.0	0.0	0.0
	NOV	-	-	-	-	-	-
	DEC	-	-	-	-	-	-
2014	JAN	-	-	-	-	-	-
	FEB	71.0	78.0	71.0	74.5	3.5	2.0
	MAR	80.0	78.0	80.0	79.0	1.0	0.6
	APR	79.0	79.0	79.0	79.0	0.0	0.0
	MAY	79.0	79.0	78.0	78.5	0.5	0.3
	JUN	85.4	82.0	82.0	82.0	0.0	0.0
	JUL	85.0	-	85.0	85.0	0.0	0.0
	AUG	86.0	86.0	85.0	85.5	0.5	0.3
	SEP	82.0	84.0	84.0	84.0	0.0	0.0
	OCT	80.0	80.0	79.0	79.5	0.5	0.3

	NOV	75.0	76.0	76.0	76.0	0.0	0.0
	DEC	79.0	79.0	79.0	79.0	0.0	0.0
WT	Average	SD	SEM	Count	Maximum	Minimum	
All WT	80.3	4.4	0.5	66	86.0	71.0	
North	80.4	4.7	1.0	22	86.0	71.0	
SD = Standard Deviation							
SEM = Standard Error of the Mean							

Appendix 3.10: Lagoon water temperature (°C) data analysis.

Lagoon Water Temperature (°C)		North	South	Canal	Average	SD	SEM (n = 3)
2011	JAN	-	-	-	-	-	-
	FEB	21.7	22.2	21.7	21.9	0.3	0.2
	MAR	-	-	-	-	-	-
	APR	-	-	-	-	-	-
	MAY	-	-	-	-	-	-
	JUN	-	-	-	-	-	-
	JUL	-	-	-	-	-	-
	AUG	29.4	29.4	29.4	29.4	0.0	0.0
	SEP	-	-	-	-	-	-
	OCT	-	-	-	-	-	-
	NOV	-	-	-	-	-	-
	DEC	-	-	-	-	-	-
2012	JAN	-	-	-	-	-	-
	FEB	-	-	-	-	-	-
	MAR	-	-	-	-	-	-
	APR	-	-	-	-	-	-
	MAY	27.8	27.8	27.8	27.8	0.0	0.0
	JUN	29.4	29.4	29.4	29.4	0.0	0.0
	JUL	29.4	29.4	29.4	29.4	0.0	0.0
	AUG	29.4	29.4	29.4	29.4	0.0	0.0
	SEP	29.4	29.4	29.4	29.4	0.0	0.0
	OCT	26.1	26.1	26.1	26.1	0.0	0.0
	NOV	-	-	-	-	-	-
	DEC	23.3	23.3	23.3	23.3	0.0	0.0
2013	JAN	-	-	-	-	-	-
	FEB	-	-	-	-	-	-
	MAR	24.4	25.0	23.9	24.4	0.6	0.3
	APR	-	-	-	-	-	-
	MAY	-	-	-	-	-	-
	JUN	27.2	27.2	27.2	27.2	0.0	0.0
	JUL	-	-	-	-	-	-
	AUG	-	-	-	-	-	-
	SEP	-	-	-	-	-	-
	OCT	-	24.4	-	24.4	-	-
	NOV	-	-	-	-	-	-
	DEC	-	-	-	-	-	-
2014	JAN	-	-	-	-	-	-
	FEB	21.7	25.6	21.7	23.0	2.2	1.3

MAR	26.7	25.6	26.7	26.3	0.6	0.4
APR	26.1	26.1	26.1	26.1	0.0	0.0
MAY	26.1	26.1	25.6	25.9	0.3	0.2
JUN	29.7	27.8	27.8	28.4	1.1	0.6
JUL	29.4	-	29.4	29.4	0.0	0.0
AUG	30.0	30.0	29.4	29.8	0.3	0.2
SEP	27.8	28.9	28.9	28.5	0.6	0.4
OCT	26.7	26.7	26.1	26.5	0.3	0.2
NOV	23.9	24.4	24.4	24.3	0.3	0.2
DEC	26.1	26.1	26.1	26.1	0.0	0.0
AWT (°C)	SD	SEM	Count	Maximum	Minimum	
26.9	2.4	0.3	66	30.0	21.7	
SD = Standard Deviation						
SEM = Standard Error of the Mean						

Appendix 3.11 Descriptive statistical analysis of monthly AWT (°C) data from 2011 through 2014.

Month:	Jan	Feb	Mar	Apr	May	Jun	Jul	Aug	Sep	Oct	Nov	Dec
Mean	NA	23.1	25.4	26.1	26.9	28.4	29.4	29.6	29.0	26.0	24.3	24.7
SEM	NA	0.8	0.5	0.0	0.4	0.4	2E-15	0.1	0.3	0.3	0.2	0.6
Median	NA	21.9	25.3	26.1	26.9	27.8	29.4	29.4	29.2	26.1	24.4	24.7
Mode	NA	21.7	26.7	26.1	27.8	29.4	29.4	29.4	29.4	26.1	24.4	23.3
SD	NA	1.9	1.1	0	1.0	1.1	4E-15	0.2	0.6	0.7	0.3	1.5
SV	NA	3.8	1.3	0	1.1	1.2	2E-29	0.1	0.4	0.6	0.1	2.3
Kurtosis	NA	-1.9	-1.7	NA	-2.8	-2.4	-4	0.7	2.6	4.6	NA	-3.3
Skewness	NA	0.9	0.1	NA	-0.2	0.2	-1.49	1.6	-1.6	-1.9	-1.7	0.0
Range	0	3.9	2.8	0	2.2	2.4	0	0.6	1.7	2.2	0.6	2.8
Maximum	0	25.6	26.7	26.1	27.8	29.7	29.4	30.0	29.4	26.7	24.4	26.1
Minimum	0	21.7	23.9	26.1	25.6	27.2	29.4	29.4	27.8	24.4	23.9	23.3
Sum	0	138	152	78	161	255	147	266	174	182	73	148
Count	0	6	6	3	6	9	5	9	6	7	3	6
GM	NA	23.0	25.3	26.1	26.8	28.3	29.4	29.6	29.0	26.0	24.3	24.7
HM	NA	22.9	25.3	26.1	26.8	28.3	29.4	29.6	29.0	26.0	24.3	24.6
AAD	NA	1.7	0.9	0	0.9	1.0	4E-15	0.2	0.5	0.5	0.2	1.4
MAD	NA	0.3	1.1	0	0.8	0.6	0	0	0.3	0	0	1.4
IQR	NA	3.1	1.8	0	1.7	2.2	0	0	0.6	0.3	0.3	2.8
4-year	Mean	SD	SEM	Count	Maximum	Minimum						
AWT (°C)	26.6	2.2	0.6	11*	29.6	23.1						

SEM = Standard Error of the Mean

SD = Standard Deviation

SV = Sample Variance

GM = Geometric Mean

HM = Harmonic Mean

AAD = Average Absolute Deviation

MAD = Median Absolute Deviation

IQR = Inter-Quartile Range

*n = 11 months, no data measured for January of any year

Appendix 3.12: 2011-2014 WT (°C) Box Plot analysis data.

Month:	Jan	Feb	Mar	Apr	May	Jun	Jul	Aug	Sep	Oct	Nov	Dec
Minimum	0	21.7	23.9	26.1	25.6	27.2	29.4	29.4	27.8	24.4	23.9	23.3
Q1-Minimum	NA	0	0.7	0	0.6	0	0	0	1.1	1.7	0.3	0
Median-Q1	NA	0.3	0.7	0	0.8	0.6	0	0	0.3	0	0.3	1.4
Q3-Median	NA	2.8	1.1	0	0.8	1.7	0	0	0.3	0.3	0	1.4
Maximum-Q3	NA	0.8	0.3	0	0	0.2	0	0.6	0	0.3	0	0
Mean (×)	NA	23.1	25.4	26.1	26.9	28.4	29.4	29.6	29.0	26.0	24.3	24.7

NONPAR CORR
/VARIABLES=INTOXICATIONYN WATERQUALITY
/PRINT=SPEARMAN TWOTAIL NOSIG
/MISSING=PAIRWISE.

Nonparametric Correlations

Correlations

			INTOXICATION YN	WATERQUALIT Y
Spearman's rho	INTOXICATIONYN	Correlation Coefficient	1.000	-.139
		Sig. (2-tailed)	.	.176
		N	96	96
	WATERQUALITY	Correlation Coefficient	-.139	1.000
		Sig. (2-tailed)	.176	.
		N	96	96

NONPAR CORR
/VARIABLES=SARAHINTOXICATIONYN SARAHWATERQUALITY
/PRINT=SPEARMAN TWOTAIL NOSIG
/MISSING=PAIRWISE.

Nonparametric Correlations

Correlations

			SARAHINTOXI CATIONYN	SARAHWATER QUALITY
Spearman's rho	SARAHINTOXICATIONYN	Correlation Coefficient	1.000	-.141
		Sig. (2-tailed)	.	.340
		N	48	48
	SARAHWATERQUALITY	Correlation Coefficient	-.141	1.000
		Sig. (2-tailed)	.340	.
		N	48	48

NONPAR CORR
/VARIABLES=GRACEINTOXICATION GRACEWATERQUALITY
/PRINT=SPEARMAN TWOTAIL NOSIG
/MISSING=PAIRWISE.

Nonparametric Correlations

Page 1

Correlations

			GRACEINTOXI CATION	GRACEWATER QUALITY
Spearman's rho	GRACEINTOXICATION	Correlation Coefficient	1.000	-.147
		Sig. (2-tailed)	.	.317
		N	48	48
	GRACEWATERQUALITY	Correlation Coefficient	-.147	1.000
		Sig. (2-tailed)	.317	.
		N	48	48

Page 2

Appendix 3.13 Statistical comparison of north lagoon FC and individual captive dolphin intoxications where Sarah indicates the mother and Grace indicates the daughter.



Advanced Mass Spectrometry Facility

Sample Analysis Report

Date: July 01, 2015

Sample batch description: Four samples were submitted by Christina Lydon on June 24th, 2015, for Saxitoxin analysis by LC-MS/MS. The following samples are included in this report:

1. DP19OCT2014 STX XTN
2. DP24DEC2014 STX XTN
3. DP19JAN2015 STX XTN
4. DP19JAN2015 SPIKED STX

Report contents:

1. LC-MS Report Summary
2. Submission document
3. ESI+ MRM Chromatograms

Methods:

The samples were analyzed as received by hydrophilic interaction chromatography mass spectrometry (HILIC-MS) using a custom-developed method (saxitoxin_MRM_HILIC_v1.6_HR). Saxitoxin was detected by an AB Sciex QTRAP 5500 Triple-Quadrupole mass spectrometer, equipped with a Turbospray ESI source, after a binary gradient separation performed by a Shimadzu Prominence LC-20AD Ultra-Fast Liquid Chromatograph equipped with a customer-provided Phenomenex Kinetex HILIC Column (100x4.6mm, 2.6µm).

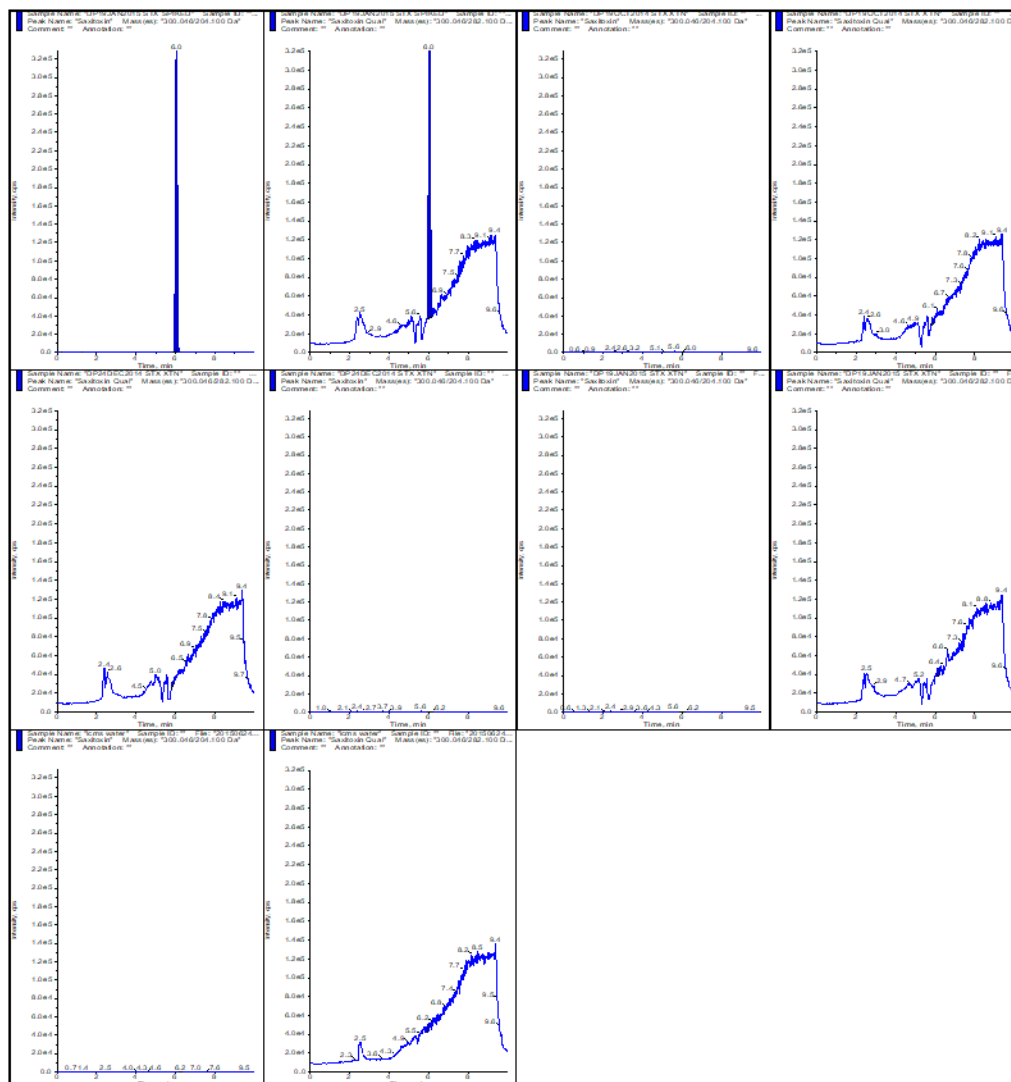
Report summary:

Analyte was successfully detected in the fortified (spiked) vegetal tissue extract sample. However, it was not detected in any of the unspiked samples. The AMSF staff does not have the concentration of saxitoxin in the fortified sample and figures of merit studies have not been performed, therefore limits of detection/quantitation are not currently available. Customer is advised to take this into consideration when interpreting these results.

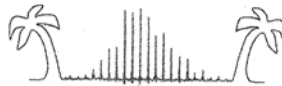
Advanced Mass Spectrometry Facility

Department of Chemistry and Biochemistry, 11200 SW 8th ST, Room CP-174 Miami, FL, 33199.
Phone: 305.348.6656 - Fax: 305.348.3772 - E-mail: cramirez@fiu.edu

*Advanced Mass Spectrometry Facility, CP-174



	Sample Name	Acquisition Date	Vial Position	File Name	Acquisition Method
1	DP19JAN2015 STX SPIKED	6/26/2015 5:48:17 PM	65	20150624_1	Saxitoxin_MRM_HILIC_v1.6_HR.dam
2	DP19JAN2015 STX SPIKED	6/26/2015 5:48:17 PM	65	20150624_1	Saxitoxin_MRM_HILIC_v1.6_HR.dam
3	DP19OCT2014 STX XTN	6/26/2015 5:58:42 PM	62	20150624_1	Saxitoxin_MRM_HILIC_v1.6_HR.dam
4	DP19OCT2014 STX XTN	6/26/2015 5:58:42 PM	62	20150624_1	Saxitoxin_MRM_HILIC_v1.6_HR.dam
5	DP24DEC2014 STX XTN	6/26/2015 6:09:06 PM	63	20150624_1	Saxitoxin_MRM_HILIC_v1.6_HR.dam
6	DP24DEC2014 STX XTN	6/26/2015 6:09:06 PM	63	20150624_1	Saxitoxin_MRM_HILIC_v1.6_HR.dam
7	DP19JAN2015 STX XTN	6/26/2015 6:19:30 PM	64	20150624_1	Saxitoxin_MRM_HILIC_v1.6_HR.dam
8	DP19JAN2015 STX XTN	6/26/2015 6:19:30 PM	64	20150624_1	Saxitoxin_MRM_HILIC_v1.6_HR.dam



FIU Mass Spectrometry Facility

Department of Chemistry & Biochemistry CP-174 Phone: 305-348-6656 or 305-348-3525
 11200 SW 8th Street, MMC Campus Website: http://ms.fiu.edu
 Miami, FL 33199-0001 E-mail: jujeon@fiu.edu or daniel.debord@fiu.edu

Sample Submission Form

Contact Information
 Name: Christina Lydon Date: 06/24/2015
 Phone: 305-919-4016 Dept./Company: Chemistry/FIU-BBC
 Email: chlydo@fiu.edu Account/PO#: 800004120
 PI Signature: Dr. John Berry *[Signature]* Address: MSB-332 3000 NE151st St 33181

Sample Information
 Sample ID: DP-PSP Formula: _____ Monoisotopic Mass: _____
 Attach sample vial within box. Provide chem. structure.

1. DP 19 OCT 2014 STX XTN 2. DP 24 DEC 2014 STX XTN 3. DP 19 JAN 2015 STX XTN 4. DP 19 JAN 2015 SPIKED STX	Estimated Quantity <input type="radio"/> In Solution Solvent _____ Concent. _____ mg/ml <input type="radio"/> Neat Liquid: _____ ml <input type="radio"/> Neat Solid: _____ mg	Solubility <input type="radio"/> Methanol <input type="radio"/> Acetonitrile <input type="radio"/> Chloroform <input type="radio"/> Dichloromethane <input type="radio"/> Water <input type="radio"/> Tetrahydrofuran <input type="radio"/> Other _____	Purity <input type="radio"/> Crude <input type="radio"/> Semi Pure <input type="radio"/> Pure
---	--	---	---

(NOTE: Samples are NOT accepted in DMF or DMSO)

Confidence of Quality <input type="radio"/> Tentative <input type="radio"/> Confident <input type="radio"/> Confirmed by _____	Storage <input type="radio"/> Refrigerate <input type="radio"/> Freeze <input type="radio"/> Keep Dark	Toxicity <input type="radio"/> Safe <input type="radio"/> Toxic <input type="radio"/> Biohazard	Sensitive to <input type="radio"/> Acid <input type="radio"/> Base <input checked="" type="radio"/> Air <input type="radio"/> Light
--	--	---	--

Please provide chemical structure in the space provided above or attach drawing/image on the back of this form.

Analysis Requested

Mass Analysis <input type="radio"/> Unit Mass (Low-Res) <input type="radio"/> TOF Accurate Mass (High-Res) <input type="radio"/> FT-ICR Accurate Mass (High-Res) <input type="radio"/> Fragmentation Pattern Mass Range Desired: From _____ to _____	Ionization <input checked="" type="radio"/> + ESI <input type="radio"/> - ESI <input type="radio"/> + MALDI <input type="radio"/> - MALDI <input checked="" type="radio"/> + APCI <input type="radio"/> - APCI <input type="radio"/> EI, CI <input type="radio"/> Not Sure	<input checked="" type="radio"/> LC/MS Provide the following info. Column: _____ ID: _____ Length: _____ Flow rate: _____ Solvent A: _____ Solvent B: _____ Gradient: _____	<input type="radio"/> GC/MS Provide the following info. Temperature Program _____
--	---	--	--

Acknowledgment Policy . Research carried out in part or in full using FIU/MS facilities with services and/or contributions requires acknowledgements of facility and staff members. See our acknowledgment policy details on our web page.

MS Facility Use Only
 File Name: 20150624-12 to 16 Operator: CR
 Result: Observed Not Observed N/A Theoretical Mass: _____ Accuracy: _____ ppm
 Ionization Method: ESI -ESI +APCI -APCI +MALDI -MALDI EI CI
 Separation: LC GC Zip-Tip Fragmentation: MS/MS
 Instrument: HP-GCMS DECA UltraTOF-Q TOF-TOF FTMS ToF.SIMS⁵ Other: QTRAP 5500
 Matrix Used: DHB THAP CHCA SA HABA IAA Dithranol Other _____ Solvent _____
 Date/Time of Analysis: 06/26/2015
 Comments: Method Saxitoxin-NRM-1111C-v1.6-HR



Advanced Mass Spectrometry Facility

Sample Analysis Report

Report Date: September 22, 2015

Request date: September 3, 2015

Request description: Two samples (SE-014 and CMX-014) were submitted for MALDI-TOF-MS analysis by Christina Lydon on 2015-09-03.

Report contents:

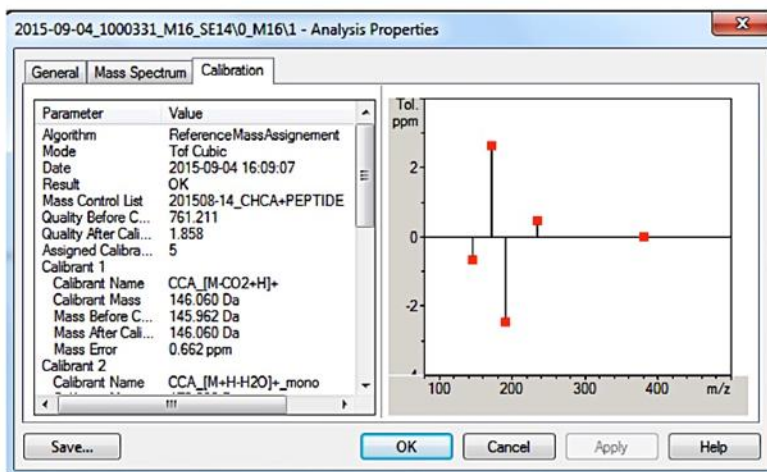
1. Report Summary
2. Submission document
3. Calibration data
4. Overlay of MALDI-TOF-MS data for samples SE-014, CMX-014 and CHCA matrix blank.
5. Mass lists for samples SE-014, CMX-014 and CHCA matrix blank.

Methods: MALDI-TOF-MS analysis was conducted on the Bruker AutoFlex III instrument, utilizing the dried droplet technique. Typically, a 1 μ L droplet of pre-mixed saturated CHCA solution was deposited on the stainless steel plate, and allowed to air dry. Thereafter, a 1 μ L aliquot of the aqueous analyte solution was deposited on top of the dried CHCA spot. The sample was allowed to air dry, and then the MALDI plate was inserted into the MALDI-MS for analysis.

Report summary: The attached mass spectra show the results for the analysis for samples SE-014 and CMX-14. The customer desired to obtain confirmation on the presence of BMAA on the aforementioned samples. BMAA has a molecular formula of $C_4H_{10}N_2O_2$ with a $m/z = 119.0815$ for the $[M+H]^+$ ion. The attached mass spectra show ions at $m/z = 119.0566$ and $m/z = 119.0384$ for samples SE-014 and CMX-014 respectively. The calculated mass error for SE-014 is 209.1 ppm and 361.9 ppm for sample CMX-014 with respect to the m/z of BMMA (119.0815). In addition, the S/N ratio was < 3 for both samples. The blank matrix spectrum is also provided as a reference, showing that the signals at approx. $m/z = 119$ were not detected in the matrix blank. The full mass scan is also included for samples SE-014 and CMX-14. The full mass scan also lets appreciate the dominant signals in the MS data. The calibration data is also attached to this report, together with the mass list for samples SE-014 and CMX-014 and the CHCA blank.

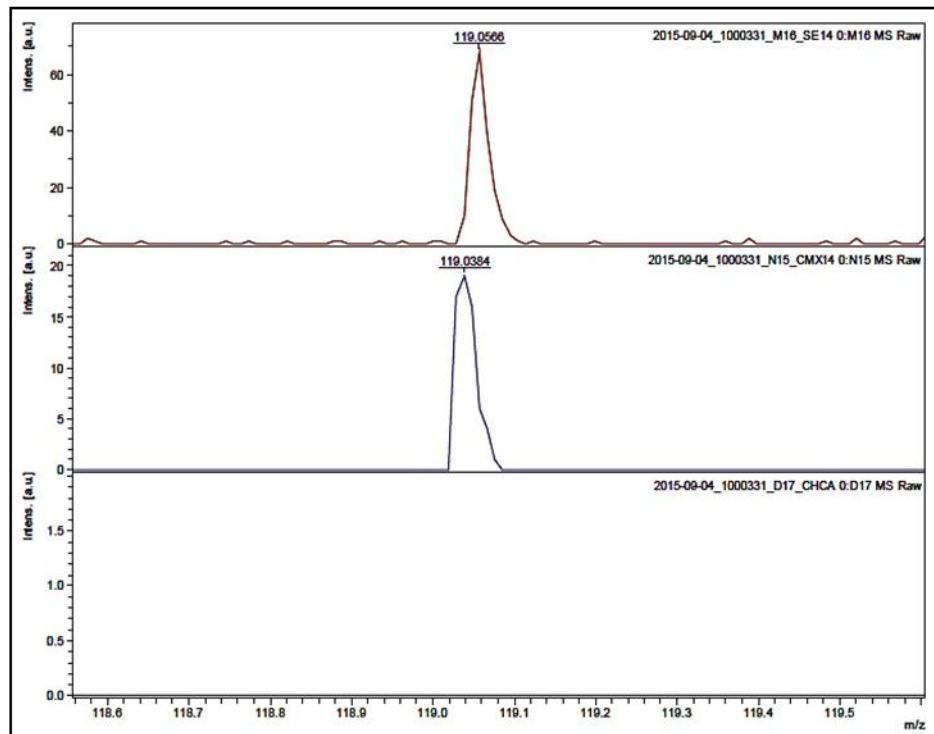
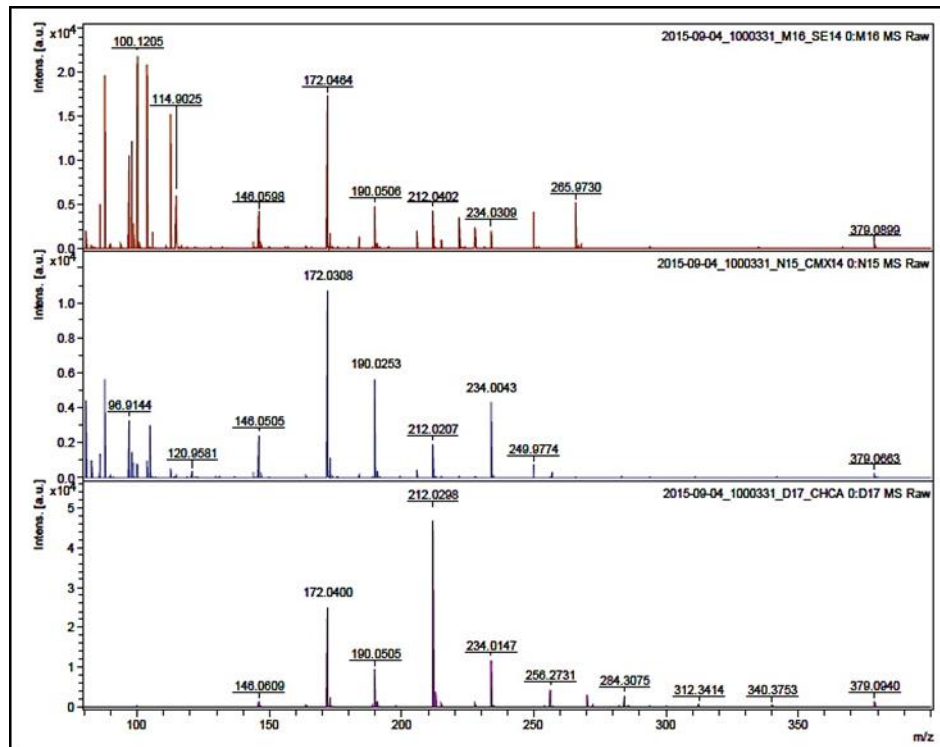
Advanced Mass Spectrometry Facility

Department of Chemistry and Biochemistry. 11200 SW 8th ST. Room CP-174 Miami, FL. 33199.
Phone: 305.348.6656 - Fax: 305.348.3772 - E-mail: cramirez@fiu.edu



Algorithm: ReferenceMassAssignment
 Mode: Tof Cubic
 Date: 2015-09-04 16:09:07
 Result: OK
 Mass Control List: 201508-14_CHCA+PEPTIDE
 Quality Before Calibration: 761.211
 Quality After Calibration: 1.858
 Assigned Calibrants: 5
 Calibrant 1:
 Calibrant Name: CCA_[M-CO2+H]+
 Calibrant Mass: 146.060 Da
 Mass Before Calibration: 145.962 Da
 Mass After Calibration: 146.060 Da
 Mass Error: 0.662 ppm
 Calibrant 2:
 Calibrant Name: CCA_[M+H-H2O]+_mono
 Calibrant Mass: 172.039 Da
 Mass Before Calibration: 171.923 Da
 Mass After Calibration: 172.040 Da
 Mass Error: 2.652 ppm
 Calibrant 3:
 Calibrant Name: CCA_[M+H]+_mono
 Calibrant Mass: 190.050 Da
 Mass Before Calibration: 189.917 Da
 Mass After Calibration: 190.049 Da
 Mass Error: 2.468 ppm
 Calibrant 4:
 Calibrant Name: CCA_[M-H+2Na]+

Calibrant Mass: 234.014 Da
Mass Before Calibration: 233.843 Da
Mass After Calibration: 234.014 Da
Mass Error: 0.493 ppm
Calibrant 5:
Calibrant Name: CCA_[2M+H]⁺_mono
Calibrant Mass: 379.092 Da
Mass Before Calibration: 378.857 Da
Mass After Calibration: 379.092 Da
Mass Error: 0.015 ppm



Spectrum: D:\Data\AMSF service\20150904_Berry\2015-09-04_1000331_M16_SE14\0_M16\1\1SRef

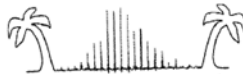
m/z	time	Intens.	SN	Res.	Area	Rel. Intens.	FWHM
80.9540	10555.63	1916.764	69.472	3325.734	52.413	0.087	0.024
82.9507	10683.02	207.072	7.659	4146.543	4.617	0.009	0.020
84.0856	10754.75	101.794	3.336	4487.068	2.144	0.005	0.019
86.1057	10881.22	5263.213	183.650	3498.555	148.872	0.238	0.025
87.9626	10996.17	20244.290	736.303	2725.028	757.935	0.915	0.032
88.1187	11005.78	353.424	12.287	3867.425	9.060	0.016	0.023
94.0715	11365.97	421.724	15.765	5400.061	8.464	0.019	0.017
96.9269	11534.68	10896.850	393.635	3535.443	350.867	0.493	0.027
98.1037	11603.48	12250.622	460.975	3533.760	404.292	0.554	0.028
98.9249	11651.25	3056.255	106.304	3916.810	89.345	0.138	0.025
100.1205	11720.44	22113.109	833.951	3230.736	821.228	1.000	0.031
103.9380	11938.62	21060.667	797.178	3211.360	810.847	0.952	0.032
105.9380	12051.32	1923.425	72.727	4155.948	57.278	0.087	0.025
111.1002	12337.37	224.762	8.525	6013.879	4.696	0.010	0.018
112.9026	12435.66	15680.067	604.982	3683.896	581.963	0.709	0.031
114.9025	12543.81	6255.323	238.502	3940.142	217.897	0.283	0.029
116.9035	12651.07	183.533	7.259	5483.133	4.578	0.008	0.021
119.0566	12765.46	68.000	2.733	4747.666	1.951	0.003	0.025
144.0493	14024.00	710.394	26.660	4532.543	29.248	0.032	0.032
146.0598	14120.28	4069.489	142.720	3644.181	231.699	0.184	0.040
147.0604	14167.95	275.990	10.224	3491.233	13.340	0.012	0.042
164.0753	14954.92	152.140	5.086	6715.779	4.479	0.007	0.024
172.0464	15309.46	17280.909	561.373	4032.581	937.627	0.781	0.043
184.0227	15826.96	1288.413	38.688	6288.421	47.079	0.058	0.029
189.0512	16039.18	113.145	3.063	6462.300	4.023	0.005	0.029
190.0506	16081.03	4840.892	139.586	4605.032	245.517	0.219	0.041
206.0127	16734.88	1938.997	51.414	6666.484	72.871	0.088	0.031
212.0402	16975.12	4309.862	113.572	5797.168	195.022	0.195	0.037
215.1700	17098.52	894.090	23.792	6978.448	33.222	0.040	0.031
221.9881	17364.25	3671.622	89.182	5798.899	176.187	0.166	0.038
228.0098	17595.54	2313.894	59.701	5669.395	115.992	0.105	0.040
234.0309	17823.77	2012.030	45.869	6373.918	90.520	0.091	0.037
249.9993	18415.15	4149.202	97.506	5823.843	222.863	0.188	0.043
265.9730	18988.02	5158.507	124.275	5425.872	324.435	0.233	0.049
367.0822	22270.58	106.781	4.539	5163.220	9.905	0.005	0.071
379.0899	22628.40	454.493	19.278	5381.045	43.251	0.021	0.070

Spectrum: D:\Data\AMSF service\20150904_Berry\2015-09-04_1000331_N15_CMx14\0_N15\1\1SRef

m/z	time	Intens.	SN	Res.	Area	Rel. Intens.	FWHM
80.9424	10554.88	4538.358	66.726	3068.473	139.800	0.406	0.026
82.9401	10682.35	997.069	14.436	3642.342	26.053	0.089	0.023
86.0926	10880.41	1409.615	20.990	3662.766	37.745	0.126	0.024
87.9499	10995.39	5800.976	87.027	3214.207	187.834	0.519	0.027
96.9144	11533.95	3344.124	52.156	3860.892	99.289	0.299	0.025
98.0910	11602.74	1550.794	22.393	4048.736	43.868	0.139	0.024
98.9127	11650.54	857.144	13.732	4329.903	22.993	0.077	0.023
100.1070	11719.66	784.896	12.317	4460.630	20.469	0.070	0.022
103.9237	11937.81	1044.279	16.801	4272.135	30.098	0.093	0.024
104.9838	11997.69	3163.557	51.603	4061.725	97.480	0.283	0.026
112.8891	12434.93	549.023	9.835	5093.635	14.503	0.049	0.022
119.0384	12764.50	18.998	< 1			0.002	
120.9581	12865.62	374.282	7.477	5056.030	10.556	0.034	0.024
144.0352	14023.32	327.806	7.338	4872.424	12.105	0.029	0.030
146.0505	14119.84	2495.178	57.736	5075.006	87.864	0.223	0.029
172.0308	15308.77	11172.31	244.806	4098.297	588.235	1.000	0.042
184.0074	15826.31	179.235	3.448	5987.145	6.852	0.016	0.031
190.0253	16079.97	5920.615	115.133	4043.525	346.516	0.530	0.047
205.9922	16734.05	444.465	8.074	6312.205	17.885	0.040	0.033
212.0207	16974.35	1944.781	34.533	5715.315	90.616	0.174	0.037
234.0043	17822.77	4589.409	84.441	5609.277	243.374	0.411	0.042
249.9774	18414.35	752.472	15.756	6701.156	34.908	0.067	0.037
256.9729	18667.44	340.059	9.201	6417.829	16.912	0.030	0.040
379.0663	22627.71	283.039	8.977	6078.187	24.039	0.025	0.062

Spectrum: D:\Data\AMSF service\20150904_Berry\2015-09-04_1000331_D17_CHCA\0_D17\1\1SRef

m/z	time	Intens.	SN	Res.	Area	Rel. Intens.	FWHM
146.0609	14120.34	1462.052	14.901	5484.607	47.304	0.030	0.027
172.0400	15309.18	25752.731	257.869	4727.202	1194.381	0.522	0.036
190.0505	16081.02	9256.456	98.829	5151.996	423.597	0.188	0.037
212.0298	16974.71	49301.518	475.090	5353.157	2546.052	1.000	0.040
228.0049	17595.36	644.781	6.122	7352.671	24.743	0.013	0.031
234.0147	17823.16	12069.454	113.116	6817.324	537.122	0.245	0.034
256.2731	18642.28	4633.227	43.033	5745.328	265.981	0.094	0.045
270.3255	19141.10	3126.855	32.366	5861.893	184.229	0.063	0.046
284.3075	19624.66	2982.230	33.972	5580.039	195.158	0.060	0.051
312.3414	20559.48	578.192	9.052	5851.856	39.712	0.012	0.053
340.3753	21453.05	513.678	17.941	5517.737	40.849	0.010	0.062
379.0940	22628.52	1339.386	41.785	5445.704	125.652	0.027	0.070



FIU - Advanced Mass Spectrometry Facility
 Department of Chemistry and Biochemistry, 11200 SW 8th ST. Room CP-174 Miami, FL. 33199.
 Phone: 305.348.6656 - Fax: 305.348.3772 - E-mail: gramirez@fiu.edu

Sample Submission Form

Contact Information
 Name: Christina Lydon/John Berry Date: 9/3/2015
 Phone: 305 919 4569 Dept./Company: Chemistry/FIU
 Email: berryj@fiu.edu Account/PO#: 800004120
 PI Signature: *[Signature]* Address: 354 Marine Science, FIU, 3000 151 Street, North Miami, FL 33181

Sample Information
 Sample ID: CMX-D14 Formula: C₄H₁₀N₂O₂ Monoisotopic Mass: 118.14
 Attach sample vial within box. **Estimated Quantity** **Solubility** **Purity**
 Provide chem. structure. In Solution Methanol Crude
 (2) SE-D14 Solvent MeO Acetonitrile Semi Pure
 3/MAA analysis Neat Liquid: _____ ml Chloroform Pure
 Neat Solid: _____ mg Water Dichloromethane
 Tetrahydrofuran
 Other _____
 (NOTE: Samples are NOT accepted in DMF or DMSO)
Confidence of Quality **Storage** **Toxicity** **Sensitive to**
 Tentative Refrigerate Safe Acid/Base
 Confident Freeze Toxic Air
 Confirmed by _____ Keep dark Biohazard Light
 Please provide chemical structure in the space provided above or attach drawing/image on the back of this form.

Analysis Requested **Ionization** **Chromatography info:** **Describe gradient (LC) or temperature (GC) program:**
 Type of analysis Unit (Low-Res) ESI LC Column: _____ Flow rate: _____
 TOF (High-Res) MALDI APCI Solvent A: _____
 FT-ICR (Ultrahigh-Res) EI CI Solvent B: _____
 Fragmentation Pattern Not sure GC Column: _____
Mass Range: Pos (+) Split ratio _____
 Neg (-) Split-less _____
 Both
 (see Laura Concl'n)
 Acknowledgment Policy: Research carried out in part or in full using FIU/MS facilities with services and/or contributions requires acknowledgements of faculty and staff members. See our acknowledgment policy details on our web page.

MS Facility Use Only File Name: 20150904-1000331-MS-CMXH Operator: CR
 Result: Observed Not Observed N/A Theoretical Mass: _____ Accuracy: _____ ppm
 Ionization Method: +ESI -ESI +APCI -APCI +MALDI -MALDI EI CI
 Separation/Cleanup: LC GC Zip-Tip SPE Filtration Fragmentation: MS/MS
 Instrument: Agilent GCMS Thermo LCQ-Decca XP Bruker Ultr-OTOF-Q Bruker Autoflex III
 Bruker Solarix FT-ICR IonToF ToF.SIMS³ AB Sciex QTRAP-5500 Other _____
 Matrix Used: DHB THAP CHCA SA HABA IAA Dithranol Other _____ Solvent _____
 Date/Time of Analysis: 09/04/2015
 Comments: _____
 FIU-AMSF Sample Submission Form, July 2013. Prepared by CR.

Appendix 4.3: FIU-AMSF BMAA LC-MS/MS analysis report



Advanced Mass Spectrometry Facility

Sample Analysis Report

Report Date: December 10, 2015

Request date: November 13, 2015

Request description: Eleven (5) samples were submitted for LC-MS/MS analysis by Christina Lydon on November 13, 2015. Seven (7) extra LC-MS/MS analysis runs were added by the AMSF for calibration and quality control purposes. The following samples are included in this report:

1. BE5A IS
2. CHX d14
3. SE014
4. 21AS
5. 21A
6. SE014, LFM

Report contents:

1. LC-MS Report Summary
2. Submission document
3. Calibration report
4. Results table
5. ESI+ MRM Chromatograms
6. Calibration and sample preparation sheet

Methods:

The samples were diluted and analyzed by hydrophilic interaction liquid chromatography (HILIC) using a modification of a previously developed methodology* (BMAA_DAB_MRM_V2.0_HILIC_v1.6). β -methylamino-L-alanine (BMAA) was quantified using both α,γ -diaminobutyric acid (DAB) as internal standards using an AB Sciex QTRAP 5500 Triple-Quadrupole mass spectrometer equipped with a Turbospray ESI source, after a binary gradient separation performed by a Shimadzu Prominence LC-20AD Ultra-Fast Liquid Chromatograph equipped with a customer-provided Phenomenex Kinetex HILIC Column (100x4.6mm, 2.6 μ m).

*The modification consist in the use of a different pair of MRM transitions for BMAA in order to prevent interference from DAB. In the previous version (method BMAA_DAB_MRM_HILIC_v1.6, see method development report from 08/14/2015) the most

Advanced Mass Spectrometry Facility

Department of Chemistry and Biochemistry. 11200 SW 8th ST. Room CP-174 Miami, FL. 33199.
Phone: 305.348.6656 - Fax: 305.348.3772 - E-mail: cramirez@fiu.edu

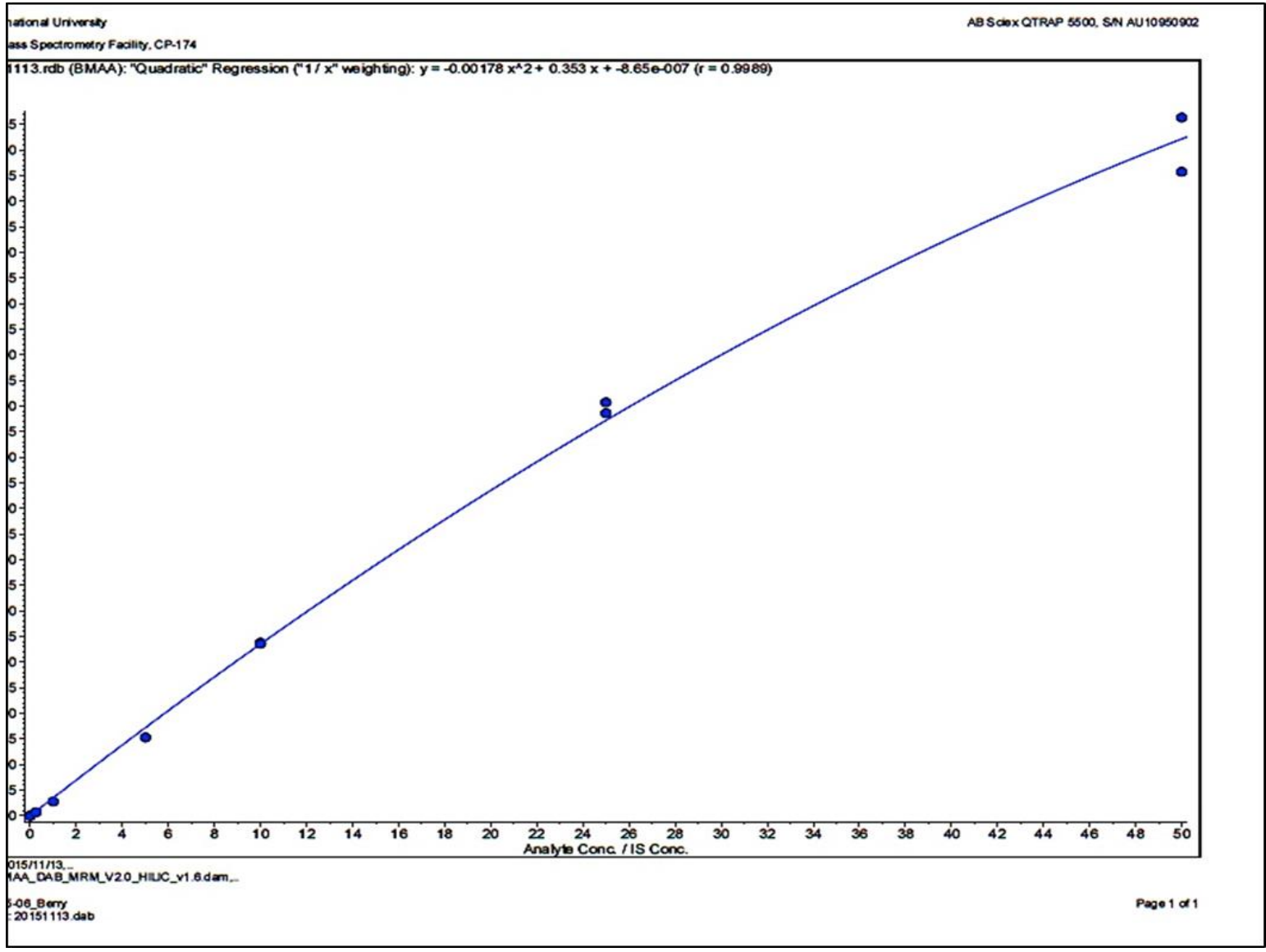
abundant transition of BMAA (119>102) was adopted as quantitative signal. However, this transition is also produced by the fragmentation of DAB (see optimization files, report from 08/14/2015) causing a severe interference if DAB is used as ISTD. Therefore, it was decided to switch to the second and third most abundant transitions of BMAA for analytical purposes. See table 1 for used transitions in this methodology.

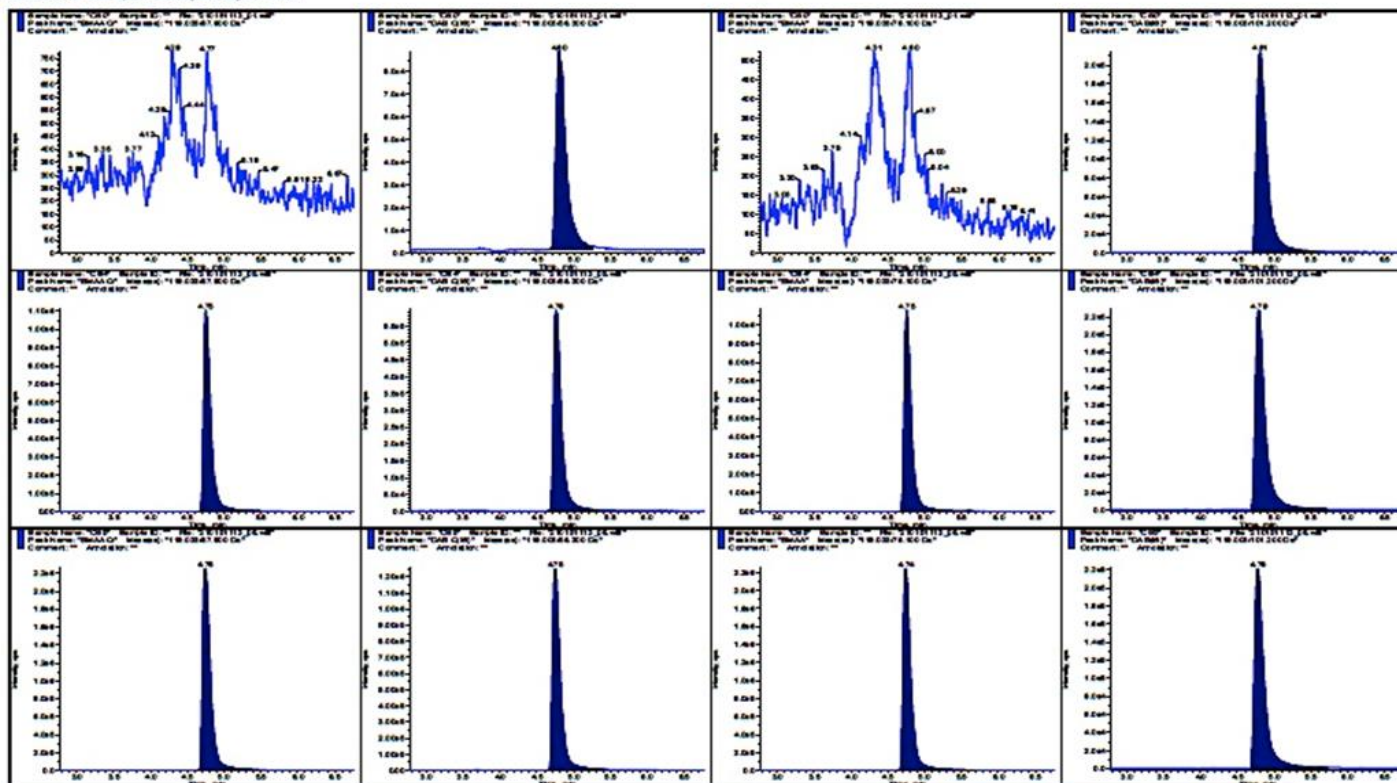
Table 1. Summary of MRM transitions used in this analysis.

Compound	Main MRM	Second MRM
BMAA	119>76	119>88
DAB (IS)	119>101	-

Report summary:

Results can be observed in attached documentation. Quality control consisted in a laboratory fortified matrix (LFM) experiment, performed by adding BMAA to 10 mg/L to sample SE014, in which no BMAA was detected. A recovery of 89% was observed, suggesting that matrix effects are low and the non-detection is caused by the absence of BMAA in the original sample. User has informed the FIU-AMSF staff that these samples underwent extraction procedures. Therefore, users should evaluate the use of a surrogate standard to quantify analytical losses during pre-instrumental analysis steps.

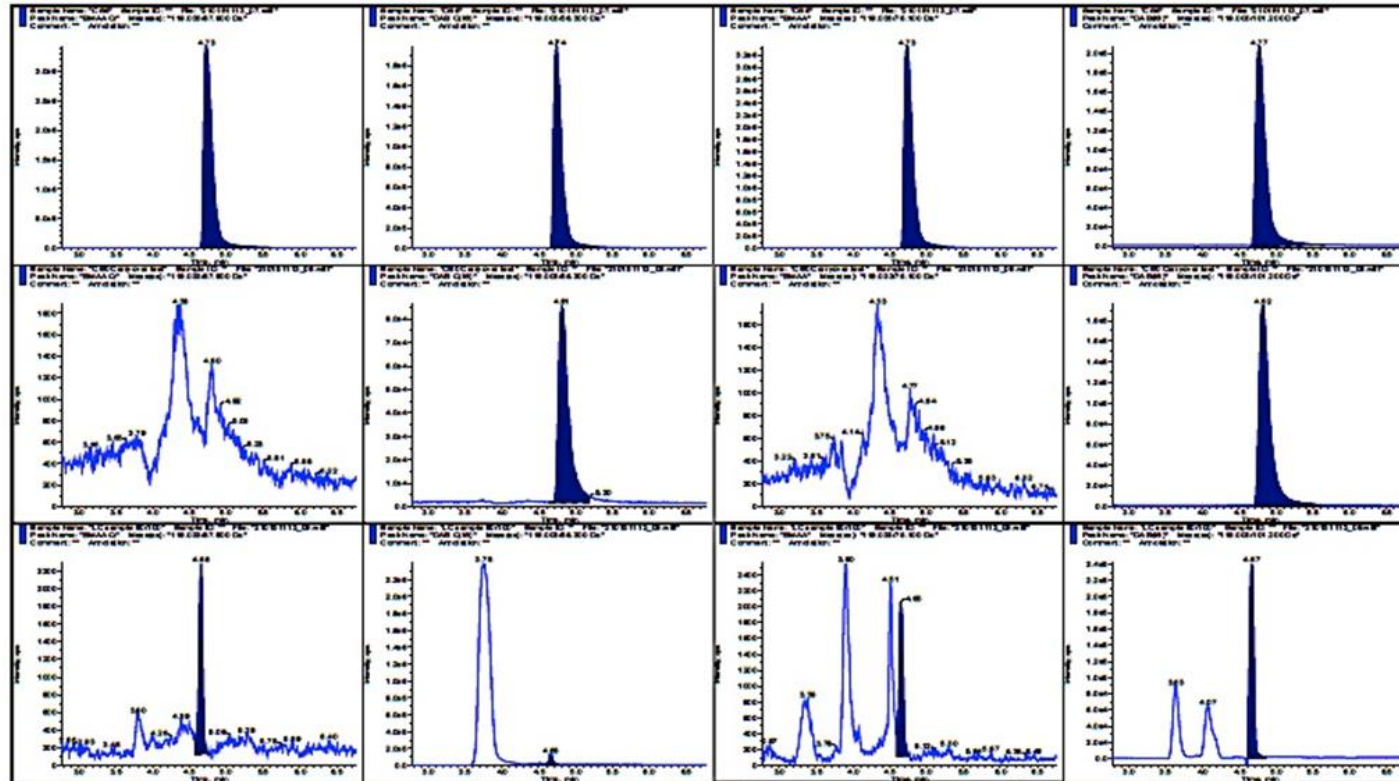




	Sample Name	Sample Type	File Name	Dilution Factor	Analyte Peak Area (counts)	IS Peak Area (counts)	Analyte Concentration (mo/L)
1	CS0	Standard	20151113\210151113_01.wiff	1.00	0.00e+000	8.17e+005	0.00
2	CS0	Standard	20151113\210151113_01.wiff	1.00	0.00e+000	2.03e+006	0.00
3	CS4	Standard	20151113\210151113_05.wiff	1.00	7.13e+006	4.29e+006	10.0
4	CS4	Standard	20151113\210151113_05.wiff	1.00	6.96e+006	2.06e+006	10.0
5	CS5	Standard	20151113\210151113_06.wiff	1.00	1.62e+007	8.97e+006	25.0

Acq. Date: 2015/11/13...
Acq. File: BMAA_DAB_MRM_V2.0_HILIC_v1.6.dam...

Project: 2015-09_Berry
Batch Name: 20151113.dab



	Sample Name	Sample Type	File Name	Dilution Factor	Analyte Peak Area (counts)	IS Peak Area (counts)	Analyte Concentration (mg/L)
7	CS6	Standard	20151113\210151113_07.wiff	1.00	2.68e+007	1.45e+007	50.0
8	CS6	Standard	20151113\210151113_07.wiff	1.00	2.59e+007	1.90e+006	50.0
9	CS0 Canyover test	Unkown	20151113\210151113_08.wiff	1.00	0.00e+000	7.73e+005	N/A
10	CS0 Canyover test	Unkown	20151113\210151113_08.wiff	1.00	0.00e+000	1.92e+006	N/A
11	LC sample 80/100	Unkown	20151113\210151113_09.wiff	1.25	6.95e+003	4.12e+005	N/A

Acq. Date: 2015/11/13...
 Acq. File: BMAA_DAB_MRM_V2.0_HILIC_v1.6.dam...

Project: 2015-08_Berry
 Batch Name: 20151113.dab



**Saxitoxin (Paralytic Shellfish Toxins), Anatoxin-a,
Brevetoxins and Domoic Report
Project: FIU – Christina Lydon**

<u>Sample ID</u>	<u>Site</u>	<u>Date Collected</u>
DP16	FL Keys	1/16/16

Toxins – Saxitoxin (Paralytic Shellfish Toxins, STX), Anatoxin-a (ANTX-A), Brevetoxins (PbX), Domoic Acid (DA)

Sample Preparation

The dried sample was homogenized prior to extraction using a coffee grinder and kept in a freezer in between extractions.

Toxin extraction

STX

Dried algal material was extracted in in 0.500 ± 0.005 gram subsets. A lab fortified matrix (LFM) was prepared by adding 10 ng of STX standard to a duplicate sample (100 ng/g spike). The sample and spike were extracted with 7.5 mL of 0.1 M acetic acid solution and placed in a boiling water bath for 5 minutes. The sample and spike were cooled, centrifuged and the supernatants retained. The pellets were rinsed with an additional 2.5 mL of 0.1 M acetic acid and the supernatants pooled. An aliquot was removed, diluted with ELISA kit diluent and analyzed at a sample concentration of 0.01 g/mL.

ANTX-A

Dried algal material was extracted in 0.100 ± 0.005 gram subsets with 75% acidified methanol solution. A LFM was prepared in the same manner with 1 ng of ANTX-A standard added to a duplicate sample (10 ng/g spike). The sample and spike were sonicated using a water bath for 25 minutes followed by centrifugation at 3,000 RPM for 10 minutes. The supernatant of each sample was collected and the pellet was rinsed with acidified MeOH solution. The supernatants were pooled methanol was removed using heat and N₂. Solid phase extraction (SPE) with Strata-X was used for sample clean-up. Post SPE, the sample and spike were filtered through 0.45 µm PVDF and analyzed at a sample concentration of 0.1 g/mL for ANTX-A.



PbX

Dried algal material was extracted in 0.500 ± 0.005 gram subsets with an 80% methanol solution. A LFM was prepared by adding 500 ng of PbX2 to a duplicate sample (1 $\mu\text{g/g}$ spike). The sample and spike were sonicated via water bath for 25 minutes and centrifuged at 3,000 RPM for 10 minutes. The supernatant of each sample was collected and the pellet was rinsed with 80% MeOH solution. The supernatants were pooled methanol was removed. The extracts were clarified using Strata X SPE and filtered prior to analysis. Samples were analyzed at sample concentration of 0.001 g/mL in 5% MeOH with a PbX ELISA.

DA

Dried algal material was extracted in 0.100 ± 0.005 gram subsets with an 80% methanol solution. A LFM was prepared by adding 50 ng of DA to a duplicate sample (500 ng/g spike). The sample and spike were sonicated via water bath for 25 minutes and centrifuged at 3,000 RPM for 10 minutes. The supernatant of each sample was collected and the pellet was rinsed with 80% MeOH solution. The supernatants were pooled methanol was removed. The extracts were clarified using Strata X SPE and filtered prior to analysis. Samples were analyzed at sample concentrations of 0.1 g/mL with LC-MS/MS.

Analytical Methodology**ELISA****STX**

A saxitoxin ELISA (Abraxis) was utilized for the detection of saxitoxin. The current assay is sensitive down to a detection/quantification limit of 5 ng/g as determined from dilution factors and kit sensitivity (0.05 $\mu\text{g/L}$).

PbX

A brevetoxins ELISA (Abraxis) was utilized for the detection of the neurotoxic shell fish toxins. A PbX3 curve was generated in a 5% MeOH solution and all QC (LFBs, LFM) was conducted using a PbX2 standard. The current assay is sensitive down to a detection/quantification limit of 50 ng/g (0.05 $\mu\text{g/g}$) as determined from dilution factors and kit sensitivity (0.05 $\mu\text{g/L}$).

LC-MS/MS**ANTX-A**

Liquid chromatography- mass spectrometry/ mass spectrometry (LC-MS/MS) was utilized for the determination of ANTX-A. The $[\text{M}+\text{H}]^+$ ion for ANTX-A (m/z 166) was fragmented and the product ions (m/z 43.5, 91.5, 107.3, 131.1) were monitored. The current method detection limit is 10 ng/g for ANTX-A based on the LFM and instrument sensitivity.

DA

LC-MS/MS was utilized for the determination of domoic acid. The $[\text{M}+\text{H}]^+$ ion for DA (312 m/z) was fragmented and the product ions (145.5, 220.3, 248.5, 266.2 m/z) were monitored. The current method detection limit is 50 ng/g for DA, based on the LFM and instrument sensitivity.

Summary of Results
(ng/g - ppb)

<u>Sample</u>	<u>STX</u>	<u>PbX</u>	<u>ANTX-A</u>	<u>DA</u>
DP16	ND	ND	ND	ND
<i>Detection Limits (ng/g)</i>	5	50	10	50

ND = Not detected above the detection limit

ELISA (STX & PbX)


Saxitoxin was not detected above the detection limit using the Abraxis STX ELISA kit. A pre-extraction LFM return was 55%, indicating some spike loss to the matrix or destruction of the saxitoxin spike during extraction. A post extraction spike return was 70%.

Brevetoxins were not detected using the Abraxis brevetoxin kit above 50 ng/g. A pre-extraction spike return was 64%, indicating some spike loss or destruction during extraction. A post extraction spike return of 110% was observed.

LC-MS/MS (ANTX-a & DA)

Anatoxin-a and domoic acid were not detected above the method detection limits utilizing LC-MS/MS. LFM's were used to determine method detection limits.

Submitted by:


Mark T. Aubel, Ph.D.

Date:

February 25, 2016

Submitted to:

Christina Lydon
Chemistry Ph.D. Candidate
Marine Biotoxins/Biochemistry Lab
Florida International University
chlydo@fiu.edu
mobile: 772-418-9358

Appendix 5.1: Bioassay-guided fractionation mortality per embryo raw data.

Test Solution	Concentration (ppm)	count	Day 1	Day 2	Day 3	Day 4	Day 5
ASW	0	5	0	0	0	0	0
		5	0	0	0	0	0
		5	0	0	0	0	0
MeOH	0	5	0	0	0	0	0
		5	0	0	0	0	0
		5	0	0	0	0	0
PbTx-2	0.0025	5	0	0	0	0	0
		5	0	0	0	0	0
		4	0	0	0	0	0
	0.005	5	0	0	0	0	0
		4	0	0	0	0	0
		4	0	0	0	0	0
	0.010	5	0	0	0	0	0
		5	0	0	0	0	0
		5	0	0	0	0	0
	0.025	5	0	0	0	0	0
		5	0	0	0	0	0
		5	0	0	0	0	0
ASW	0	5	0	0	0	0	0
MeOH	0	5	0	0	0	0	0
PbTx-2	0.025	5	0	0	0	0	0
Crude Cyanobacteria	10	5	1	1	1	1	1
	25	5	1	1	1	1	1
	50	5	3	4	5	5	5
Crude Ethyl Acetate Extract (EtOAc)	10	5	0	0	0	0	0
	25	5	2	2	2	2	2
	50	5	3	3	3	3	3
Crude 2-Butanol Extract (BuOH)	10	5	0	0	0	0	0
	25	5	5	5	5	5	5
	50	5	5	5	5	5	5
Crude Aqueous Extract (Aq)	10	4	1	1	1	1	1
	25	5	0	0	0	0	0
	50	5	1	1	1	1	1
EtOAc Fraction F29	10	5	0	0	0	0	0
	25	5	0	0	0	0	0
	50	5	0	0	0	0	0
EtOAc Fraction F29-1	10	5	0	0	0	0	0
	25	5	0	0	0	0	0
	50	5	0	0	0	0	0
EtOAc Fraction F29-2	10	5	0	0	0	0	0
	25	5	0	0	0	0	0
	50	5	1	1	5	5	5
EtOAc Fraction F29-3	10	5	0	0	0	0	0
	25	5	0	0	0	0	0
	50	5	0	0	0	0	0

ASW = Aquarium System Water (negative control)
MeOH = Methanol Solvent Control (negative control)
PbTx-2 = brevetoxin-2 standard (positive control)

Appendix 5.2: Bioassay-guided fractionation deformed embryos raw data.

Test Solution	Concentration (ppm)	count	Day 1	Day 2	Day 3	Day 4	Day 5
ASW	0	5	0	0	0	0	0
		5	0	0	0	0	0
		5	0	0	0	0	0
MeOH	0	5	0	0	0	0	0
		5	0	0	0	0	0
		5	0	0	0	0	0
PbTx-2	0.0025	5	0	0	2	2	2
		5	0	0	2	2	2
		4	0	0	1	1	1
	0.005	5	2	2	2	2	2
		4	1	1	1	1	1
		4	1	1	1	1	1
	0.010	5	1	1	2	2	2
		5	2	2	2	2	2
		5	1	1	2	3	3
	0.025	5	2	2	3	5	5
		5	2	2	2	4	5
		5	1	1	1	5	5
ASW	0	5	0	0	0	0	0
MeOH	0	5	0	0	0	0	0
PbTx-2	0.025	5	2	2	2	5	5
Crude Cyanobacteria	10	5	2	3	4	5	5
	25	5	3	5	5	5	5
	50	5	5	5	5	5	5
Crude Ethyl Acetate Extract (EtOAc)	10	5	1	1	2	2	2
	25	5	4	5	5	5	5
	50	5	5	5	5	5	5
Crude 2-Butanol Extract (BuOH)	10	5	0	2	2	2	2
	25	5	5	5	5	5	5
	50	5	5	5	5	5	5
Crude Aqueous Extract (Aq)	10	4	2	3	3	3	3
	25	5	1	3	3	3	3
	50	5	1	2	2	4	4
EtOAc Fraction F29	10	5	1	1	1	1	1
	25	5	2	2	2	2	2
	50	5	2	2	2	2	2
EtOAc Fraction F29-1	10	5	0	0	1	1	1
	25	5	1	1	2	2	2
	50	5	1	2	2	2	2
EtOAc Fraction F29-2	10	5	0	1	1	1	1
	25	5	2	2	2	3	3
	50	5	5	5	5	5	5
EtOAc Fraction F29-3	10	5	0	0	1	1	1
	25	5	0	0	1	2	2
	50	5	2	2	2	2	2
ASW = Aquarium System Water (negative control)							
MeOH = Methanol Solvent Control (negative control)							
PbTx-2 = brevetoxin-2 standard (positive control)							

Appendix 5.3: Bioassay-guided fractionation hatched embryos raw data.

Test Solution	Concentration (ppm)	count	Day 1	Day 2	Day 3	Day 4	Day 5
ASW	0	5	0	2	5	5	5
		5	0	3	5	5	5
		5	0	2	5	5	5
MeOH	0	5	0	3	5	5	5
		5	0	1	5	5	5
		5	0	2	5	5	5
PbTx-2	0.0025	5	0	5	5	5	5
		5	0	4	5	5	5
		4	0	1	4	4	4
	0.005	5	0	0	5	5	5
		4	0	2	4	4	4
		4	0	2	4	4	4
	0.010	5	0	2	5	5	5
		5	0	3	5	5	5
		5	0	3	5	5	5
	0.025	5	0	3	5	5	5
		5	0	3	5	5	5
		5	0	3	5	5	5
ASW	0	5	0	3	5	5	5
MeOH	0	5	0	3	5	5	5
PbTx-2	0.025	5	0	3	5	5	5
Crude Cyanobacteria	10	5	0	0	4	4	4
	25	5	0	0	0	0	0
	50	5	0	0	0	0	0
Crude Ethyl Acetate Extract (EtOAc)	10	5	0	4	5	5	5
	25	5	0	0	2	3	3
	50	5	0	0	2	2	2
Crude 2-Butanol Extract (BuOH)	10	5	0	1	5	5	5
	25	5	0	0	0	0	0
	50	5	0	0	0	0	0
Crude Aqueous Extract (Aq)	10	4	0	1	3	3	3
	25	5	0	0	5	5	5
	50	5	0	1	4	4	4
EtOAc Fraction F29	10	5	0	3	5	5	5
	25	5	0	3	5	5	5
	50	5	0	1	5	5	5
EtOAc Fraction F29-1	10	5	0	5	5	5	5
	25	5	0	2	5	5	5
	50	5	0	2	5	5	5
EtOAc Fraction F29-2	10	5	0	2	5	5	5
	25	5	0	1	5	5	5
	50	5	0	0	0	0	0
EtOAc Fraction F29-3	10	5	0	4	5	5	5
	25	5	0	3	5	5	5
	50	5	0	0	5	5	5
ASW = Aquarium System Water (negative control)							
MeOH = Methanol Solvent Control (negative control)							
PbTx-2 = brevetoxin-2 standard (positive control)							

Appendix 5.4 Bioassay-guided fractionation subfraction F29-1A deformed embryos raw data.

Test Solution	Concentration (µM)	count	Day 1	Day 2	Day 3	Day 4	Day 5
Aquaria System Water (untreated control)	0	5	0	0	0	0	0
		5	0	0	0	0	0
		5	0	0	0	0	0
PbTx-2 Standard (positive control)	0.0045	5	0	3	1	1	1
		5	0	3	3	3	2
		5	0	2	1	1	0
	0.0223	5	0	3	3	NA	NA
		5	0	3	5	NA	NA
		5	0	3	5	NA	NA
EtOAc derived F29-1A (pure metabolite)	9.4	4	0	2	2	2	2
		5	0	0	1	1	2
		5	0	2	2	2	2
	38	5	0	3	3	3	3
		5	0	2	2	2	3
		5	0	2	2	2	3
	94	5	0	3	5	5	5
		5	0	4	4	4	4
		5	0	3	3	3	5
NA = not applicable, deceased embryos							

Appendix 5.5 Bioassay-guided fractionation subfraction F29-1A hatched embryos raw data.

Test Solution	Concentration (µM)	count	Day 1	Day 2	Day 3	Day 4	Day 5
Aquaria System Water (untreated control)	0	5	0	5	5	5	5
		5	0	3	5	5	5
		5	0	1	5	5	5
PbTx-2 Standard (positive control)	0.0045	5	0	1	5	5	5
		5	0	0	5	5	5
		5	0	1	5	5	5
	0.0223	5	0	3	5	NA	NA
		5	0	2	5	NA	NA
		5	0	1	0	NA	NA
EtOAc derived F29-1A (pure metabolite)	9.4	4	0	0	4	4	4
		5	0	4	5	5	5
		5	0	3	5	5	5
	38	5	0	2	5	5	5
		5	0	1	5	5	5
		5	0	2	5	5	2
	94	5	0	0	0	1	2
		5	0	0	0	0	0
		5	0	0	4	4	4
NA = not applicable, deceased embryos							

Appendix 5.6: 24 hours post-fertilization spontaneous coiling frequency raw data for control embryos.

Test Solution	ASW	MeOH	PbTx-2			
Concentration (nM)	0	0	2.79	5.59	11.2	27.9
24 hpf SCF (cpm) per embryo	4	2	2	6	0	4
	2	2	0	4	0	2
	4	4	2	2	4	2
	2	2	2	4	0	2
	6	4	4	2	0	0
	4	4	4	4	2	4
	6	2	4	2	2	4
	4	4	2	4	2	2
	2	2	0	2	2	0
	2	4	2	2	0	0
	4	2	0	4	2	2
	2	2	6	4	2	2
	4	6	4	2	2	2
	4	4	0	-	2	2
	2	4	-	-	0	0
Mean SCF (cpm)	3.5	3.2	2.3	3.2	1.3	1.9
Standard Deviation (cpm)	1.4	1.3	1.9	1.3	1.2	1.4
Standard Error of Mean (cpm)	0.4	0.3	0.5	0.4	0.3	0.4
Number of Embryos	15	15	14	13	15	15
ASW	= Aquarium System Water (negative control)					
MeOH	= Methanol Solvent Control (negative control)					
PbTx-2	= brevetoxin-2 standard (positive control)					
SCF (cpm)	= spontaneous coiling frequency measured as coils per minute (cpm) at 24 hours post fertilization (hpf)					
-	= no embryo					

Appendix 5.7: 24 hours post-fertilization spontaneous coiling frequency raw data for the crude cyanobacteria extracts.

Test Solution	ASW	MeOH	PbTx-2	Crude Extract			EtOAc Extract			BuOH Extract			Aqueous Extract		
Concentration (ppm)	0	0	0.025	10	25	50	10	25	50	10	25	50	10	25	50
24 hpf SCF (cpm) per embryo	6	4	4	6	2	0	4	4	10	2	0	0	2	2	4
	4	4	2	6	0	0	4	4	0	4	0	0	2	0	2
	6	6	2	4	0	0	0	6	0	4	0	0	0	2	2
	4	4	2	6	0	0	0	0	0	2	0	0	0	4	2
	2	4	0	0	0	0	0	0	0	2	0	0	-	4	0
Mean (cpm)	4.4	4.4	2.0	4.4	0.4	0.0	1.6	2.8	2.0	2.8	0.0	0.0	1.0	2.4	2.0
Standard Deviation (cpm)	1.7	0.9	1.4	2.6	0.9	0.0	2.2	2.7	4.5	1.1	0.0	0.0	1.2	1.7	1.4
Standard Error of Mean (cpm)	0.7	0.4	0.6	1.2	0.4	0.0	1.0	1.2	2.0	0.5	0.0	0.0	0.6	0.7	0.6
Number of Embryos	5	5	5	5	5	5	5	5	5	5	5	5	4	5	5
ASW	= Aquarium System Water (negative control)														
MeOH	= Methanol Solvent Control (negative control)														
PbTx-2	= brevetoxin-2 standard (positive control)														
SCF (cpm)	= spontaneous coiling frequency measured as coils per minute (cpm) at 24 hours post-fertilization (hpf)														
-	= no embryo														

Appendix 5.8 24 hours post-fertilization spontaneous coiling frequency raw data for the EtOAc derived fraction F29 and its subfractions.

Test Solution	ASW	MeOH	PbTx-2	F29 crude			F29-1			F29-2			F29-3		
Concentration (ppm)	0	0	0.025	10	25	50	10	25	50	10	25	50	10	25	50
24 hpf SCF (cpm) per embryo	6	4	4	2	0	0	2	2	2	2	2	0	0	6	2
	4	4	2	0	0	0	4	0	0	0	2	2	4	2	4
	6	6	2	2	0	2	4	2	2	2	2	0	4	4	2
	4	4	2	0	0	2	2	4	4	4	2	0	2	0	2
	2	4	0	0	0	0	2	2	4	4	2	0	0	0	6
Mean (cpm)	4.4	4.4	2.0	0.8	0.0	0.8	2.8	2.0	2.4	2.4	2.0	0.4	2.0	2.4	3.2
Standard Deviation (cpm)	1.7	0.9	1.4	1.1	0.0	1.1	1.1	1.4	1.7	1.7	0.0	0.9	2.0	2.6	1.8
Standard Error of Mean (cpm)	0.7	0.4	0.6	0.5	0.0	0.5	0.5	0.6	0.7	0.7	0.0	0.4	0.9	1.2	0.8
Number of Embryos	5	5	5	5	5	5	5	5	5	5	5	5	5	5	5
ASW	= Aquarium System Water (negative control)														
MeOH	= Methanol Solvent Control (negative control)														
PbTx-2	= brevetoxin-2 standard (positive control)														
SCF (cpm)	= spontaneous coiling frequency measured as coils per minute (cpm) at 24 hours post-fertilization (hpf)														

Appendix 5.9 Day 2 heart rate measurements for the control embryos.

Test Solution	ASW	MeOH	PbTx-2			
Concentration (nM)	0	0	2.79	5.59	11.2	27.9
Day 2 Heart Rate (bpm)	138	126	184	180	178	152
	136	128	170	166	170	148
	136	128	172	168	184	140
	132	120	180	176	174	154
	140	132	178	174	180	146
	142	136	176	182	174	188
	146	138	182	186	166	180
	134	134	186	188	178	168
	144	140	174	176	184	174
	138	138	182	172	182	176
	136	140	182	178	180	186
	140	136	176	174	176	184
	136	132	180	182	174	176
	142	130	172	-	178	182
136	126	-	-	184	180	
Mean (bpm)	138.4	132.3	178.1	177.1	177.5	168.9
SD (bpm)	3.9	5.9	4.9	6.5	5.3	16.3
SEM (bpm)	1.0	1.5	1.3	1.8	1.4	4.2
Embryo Count	15	15	14	13	15	15
ASW	= Aquarium System Water (negative control)					
MeOH	= Methanol Solvent Control (negative control)					
PbTx-2	= brevetoxin-2 standard (positive control)					
bpm	= beats per minute					
SD	= Standard Deviation					
SE	= Standard Error Mean					
-	= no embryo					

Appendix 5.10 Day 3 heart rate measurements for the control embryos.

Test Solution	ASW	MeOH	PbTx-2			
Concentration (nM)	0	0	2.79	5.59	11.2	27.9
Day 3 Heart Rate (bpm)	168	174	180	180	174	186
	180	186	180	186	180	180
	168	180	180	186	186	186
	174	168	174	180	174	192
	162	180	186	186	186	180
	186	168	186	180	180	174
	192	174	186	186	186	186
	180	174	180	180	186	168
	174	162	174	186	174	174
	174	180	180	186	180	180
	186	168	186	186	174	180
	168	174	180	186	186	186
	162	186	180	180	186	186
	180	192	174	-	174	180
	174	174	-	-	186	174
Mean (bpm)	175.2	176.0	180.4	183.7	180.8	180.8
SD (bpm)	8.8	8.1	4.4	3.0	5.5	6.4
SEM (bpm)	2.3	2.1	1.2	0.8	1.4	1.6
Embryo Count	15	15	14	13	15	15
ASW	= Aquarium System Water (negative control)					
MeOH	= Methanol Solvent Control (negative control)					
PbTx-2	= brevetoxin-2 standard (positive control)					
bpm	= beats per minute					
SD	= Standard Deviation					
SEM	= Standard Error of Mean					
-	= no embryo					

Appendix 5.11 Day 2 heart rate measurements per embryo for the crude cyanobacteria extracts.

Test Solution	ASW	MeOH	PbTx-2	Crude Extract			EtOAc Extract			BuOH Extract			Aqueous Extract		
Concentration (ppm)	0	0	0.025	10	25	50	10	25	50	10	25	50	10	25	50
Day 2 Heart Rate (bpm)	136	126	148	126	54	24	116	76	92	120	0	0	110	126	130
	140	128	168	118	54	0	114	102	84	112	0	0	92	122	118
	134	132	180	118	40	0	108	106	0	108	0	0	106	124	120
	144	136	176	124	72	0	110	0	0	106	0	0	0	122	114
	136	140	184	0	0	0	112	0	0	116	0	0	-	126	0
Mean (bpm)	138.0	132.4	171.2	97.2	44.0	4.8	112.0	56.8	35.2	112.4	0.0	0.0	77.0	124.0	96.4
SD (bpm)	4.0	5.7	14.3	54.5	27.1	10.7	3.2	53.1	48.3	5.7	0.0	0.0	51.9	2.0	54.2
SEM (bpm)	1.8	2.6	6.4	24.4	12.1	4.8	1.4	23.8	21.6	2.6	0.0	0.0	26.0	0.9	24.2
Embryo Count	5	5	5	5	5	5	5	5	5	5	5	5	4	5	5
ASW	= Aquarium System Water (negative control)														
MeOH	= Methanol Solvent Control (negative control)														
PbTx-2	= brevetoxin-2 standard (positive control)														
bpm	= beats per minute														
SD	= Standard Deviation														
SEM	= Standard Error of Mean														
-	= no embryo														

Appendix 5.12 Day 3 heart rate measurements per embryo for the crude cyanobacteria extracts.

Test Solution	ASW	MeOH	PbTx-2	Crude Extract			EtOAc Extract			BuOH Extract			Aqueous Extract		
Concentration (ppm)	0	0	0.025	10	25	50	10	25	50	10	25	50	10	25	50
Day 3 Heart Rate (bpm)	186	168	180	180	12	0	186	174	126	168	0	0	174	168	174
	168	174	186	174	24	0	180	168	138	174	0	0	180	180	180
	162	186	186	180	30	0	174	180	0	168	0	0	168	174	168
	180	192	180	186	18	0	174	0	0	162	0	0	0	168	174
	174	174	174	0	0	0	180	0	0	180	0	0	-	162	0
Mean (bpm)	174.0	178.8	181.2	144.0	16.8	0.0	178.8	104.4	52.8	170.4	0.0	0.0	130.5	170.4	139.2
SD (bpm)	9.5	9.9	5.0	80.6	11.5	0.0	5.0	95.4	72.4	6.8	0.0	0.0	87.1	6.8	77.9
SEM (bpm)	4.2	4.4	2.2	36.0	5.2	0.0	2.2	42.7	32.4	3.1	0.0	0.0	43.6	3.1	34.9
Embryo Count	5	5	5	5	5	5	5	5	5	5	5	5	4	5	5
ASW	= Aquarium System Water (negative control)														
MeOH	= Methanol Solvent Control (negative control)														
PbTx-2	= brevetoxin-2 standard (positive control)														
bpm	= beats per minute														
SD	= Standard Deviation														
SEM	= Standard Error of Mean														
-	= no embryo														

Appendix 5.13 Day 2 heart rate measurements per embryo for the EtOAc derived fraction F29 and its subfractions.

Test Solution	ASW	MeOH	PbTx-2	F29 crude			F29-1			F29-2			F29-3		
Concentration (ppm)	0	0	0.025	10	25	50	10	25	50	10	25	50	10	25	50
Day 2 Heart Rate (bpm)	136	126	148	138	138	142	144	146	144	148	134	116	132	126	132
	140	128	168	150	152	144	132	140	152	140	138	104	126	138	132
	134	132	180	132	144	142	138	150	150	146	144	100	138	132	126
	144	136	176	144	140	140	138	148	140	142	146	108	126	120	126
	136	140	184	138	146	142	132	142	142	144	140	0	120	132	132
Mean (bpm)	138.0	132.4	171.2	140.4	144.0	142.0	136.8	145.2	145.6	144.0	140.4	85.6	128.4	129.6	129.6
SD (bpm)	4.0	5.7	14.3	6.8	5.5	1.4	5.0	4.1	5.2	3.2	4.8	48.2	6.8	6.8	3.3
SEM (bpm)	1.8	2.6	6.4	3.1	2.4	0.6	2.2	1.9	2.3	1.4	2.1	21.6	3.1	3.1	1.5
Embryo Count	5	5	5	5	5	5	5	5	5	5	5	5	5	5	5
ASW	= Aquarium System Water (negative control)														
MeOH	= Methanol Solvent Control (negative control)														
PbTx-2	= brevetoxin-2 standard (positive control)														
bpm	= beats per minute														
SD	= Standard Deviation														
SEM	= Standard Error of Mean														

Appendix 5.14 Day 3 heart rate measurements per embryo for the EtOAc derived fraction F29 and its subfractions.

Test Solution	ASW	MeOH	PbTx-2	F29 crude			F29-1			F29-2			F29-3		
Concentration (ppm)	0	0	0.025	10	25	50	10	25	50	10	25	50	10	25	50
Day 3 Heart Rate (bpm)	186	168	180	186	180	162	186	168	150	186	168	0	186	174	174
	168	174	186	192	186	156	192	162	162	192	180	0	180	180	186
	162	186	186	186	180	168	186	162	168	192	186	0	174	168	192
	180	192	180	180	174	180	180	174	180	180	174	0	192	192	180
	174	174	174	186	180	174	180	180	174	174	174	0	198	180	180
Mean (bpm)	174.0	178.8	181.2	186.0	180.0	168.0	184.8	169.2	166.8	184.8	176.4	0.0	186.0	178.8	182.4
SD (bpm)	9.5	9.9	5.0	4.2	4.2	9.5	5.0	7.8	11.5	7.8	6.8	0.0	9.5	8.9	6.8
SEM (bpm)	4.2	4.4	2.2	1.9	1.9	4.2	2.2	3.5	5.2	3.5	3.1	0.0	4.2	4.0	3.1
Embryo Count	5	5	5	5	5	5	5	5	5	5	5	5	5	5	5
ASW	= Aquarium System Water (negative control)														
MeOH	= Methanol Solvent Control (negative control)														
PbTx-2	= brevetoxin-2 standard (positive control)														
Bpm	= beats per minute														
SD	= Standard Deviation														
SEM	= Standard Error of Mean														

Appendix 5.15 Day 5 swim bladder dysfunction and aberrant swimming behavior per embryo raw data.

Test Solution	Concentration (ppm)	Embryo Count	Day 5	
			Swim Bladder Dysfunction	Aberrant Swimming Behavior
Aquaria System Water (ASW)	0	5	0	0
		5	0	0
		5	0	0
Methanol Solvent Control (MeOH)	0	5	0	0
		5	0	0
		5	0	0
Brevetoxin-2 Standard (PbTx-2)	0.0025	5	3	3
		5	3	4
		4	2	2
	0.005	5	3	3
		4	3	2
		4	2	3
	0.010	5	4	4
		5	3	3
		5	3	3
	0.025	5	5	5
		5	5	5
		5	5	5
ASW	0	5	0	0
MeOH	0	5	0	0
PbTx-2	0.025	5	5	5
Crude Cyanobacteria	10	5	5	5
	25	5	5	5
	50	5	5	5
Crude Ethyl Acetate Extract (EtOAc)	10	5	3	2
	25	5	4	5
	50	5	5	5
Crude 2-Butanol Extract (BuOH)	10	5	4	4
	25	5	5	5
	50	5	5	5
Crude Aqueous Extract (Aq)	10	4	3	4
	25	5	3	3
	50	5	5	5
EtOAc Fraction F29	10	5	4	4
	25	5	2	3
	50	5	2	3
EtOAc Fraction F29-1	10	5	2	3
	25	5	5	5
	50	5	5	5
EtOAc Fraction F29-2	10	5	3	4
	25	5	3	4
	50	5	5	5
EtOAc Fraction F29-3	10	5	5	5
	25	5	3	3
	50	5	4	4

Appendix 5.16 Acute larval exposure neurobehavioral toxicity study percent mortality raw data.

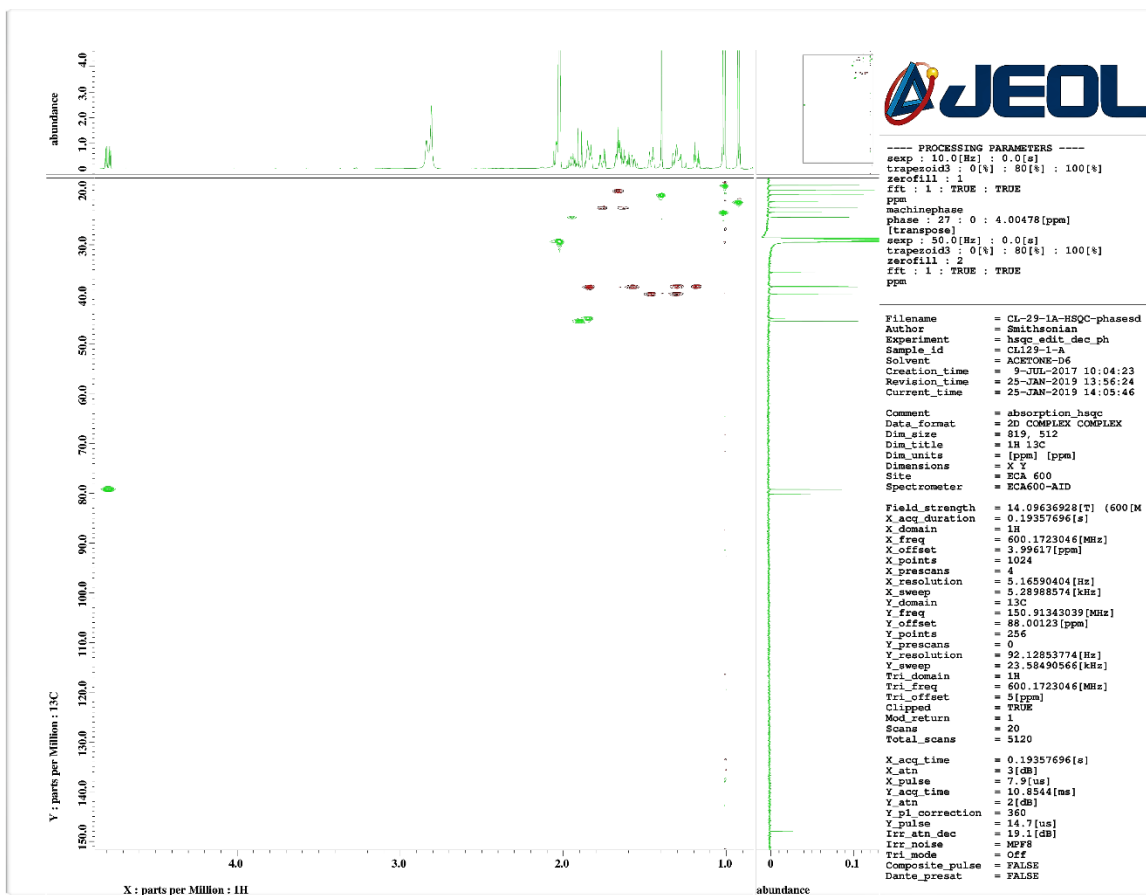
Test Solution	Concentration (ppm)	count	Hour 1	Hour 2	Hour 6	Hour 12	Hour 24
ASW	0	24	0	0	0	0	0
MeOH	0	24	0	0	0	0	0
PbTx-2	0.0025	20	0	0	0	0	0
	0.010	21	0	3	3	3	9
	0.025	21	0	0	5	7	12
	0.050	24	0	0	1	6	15
Crude Cyanobacteria	2.5	12	0	0	0	0	0
	10	12	0	0	0	2	2
	25	11	0	1	1	1	1
	50	12	3	4	6	6	8
Crude Ethyl Acetate Extract (EtOAc)	2.5	12	1	2	2	2	2
	10	12	0	0	0	0	0
	25	12	0	0	0	0	0
	50	11	0	1	1	1	1
Crude 2-Butanol Extract (BuOH)	2.5	11	0	0	0	0	0
	10	12	0	0	0	0	0
	25	12	0	1	2	2	2
	50	12	0	1	2	4	6
Crude Aqueous Extract (Aq)	2.5	10	2	2	2	2	2
	10	11	0	1	1	1	1
	25	11	1	1	1	3	5
	50	12	0	2	2	4	12
EtOAc Fraction F29	2.5	5	0	0	0	1	1
	10	5	0	0	0	0	0
	25	6	0	3	3	3	3
	50	6	0	0	0	0	0
EtOAc Fraction F29-1	2.5	5	0	0	0	0	0
	10	5	0	0	0	0	0
	25	5	0	1	1	1	1
	50	6	0	0	0	0	0
EtOAc Fraction F29-2	2.5	3	0	0	0	0	0
	10	6	0	0	0	0	0
	25	5	0	0	0	0	0
	50	6	0	0	0	0	0
EtOAc Fraction F29-3	2.5	5	0	0	0	0	0
	10	5	0	0	0	0	0
	25	5	0	0	0	0	0
	50	5	0	0	0	0	0

ASW = Aquarium System Water (negative control)
MeOH = Methanol Solvent Control (negative control)
PbTx-2 = brevetoxin-2 standard (positive control)

Appendix 5.17 Acute larval exposure neurobehavioral toxicity study percent swimming issues raw data.

Test Solution	Concentration (ppm)	count	Hour 1	Hour 2	Hour 6	Hour 12	Hour 24
ASW	0	0	1	2	6	12	24
MeOH	0	24	0	0	0	0	0
PbTx-2	0.0025	24	0	0	0	0	0
	0.010	20	20	20	20	20	20
	0.025	21	21	21	21	21	21
	0.050	21	21	21	21	21	21
Crude Cyanobacteria	2.5	12	12	8	12	12	4
	10	12	12	8	12	12	8
	25	11	11	8	11	11	11
	50	12	12	10	12	12	12
Crude Ethyl Acetate Extract (EtOAc)	2.5	12	12	12	12	3	6
	10	12	12	12	12	2	3
	25	12	12	12	12	3	3
	50	11	11	11	11	4	7
Crude 2-Butanol Extract (BuOH)	2.5	11	11	11	11	1	3
	10	12	12	12	12	7	5
	25	12	12	12	12	12	5
	50	12	12	12	12	12	12
Crude Aqueous Extract (Aq)	2.5	10	10	4	3	4	5
	10	11	11	9	3	5	5
	25	11	11	9	3	11	6
	50	12	12	12	4	12	12
EtOAc Fraction F29	2.5	5	3	5	2	2	2
	10	5	3	5	3	2	2
	25	6	5	6	5	4	4
	50	6	5	6	4	2	3
EtOAc Fraction F29-1	2.5	5	1	2	1	0	0
	10	5	2	4	2	1	1
	25	5	3	5	2	2	2
	50	6	5	6	5	3	2
EtOAc Fraction F29-2	2.5	3	0	1	3	0	0
	10	6	2	3	3	1	1
	25	5	3	5	4	2	1
	50	6	6	4	5	3	2
EtOAc Fraction F29-3	2.5	5	0	0	0	0	0
	10	5	0	0	0	0	0
	25	5	0	3	2	1	0
	50	5	0	5	3	2	0

ASW = Aquarium System Water (negative control)
MeOH = Methanol Solvent Control (negative control)
PbTx-2 = brevetoxin-2 standard (positive control)



Appendix 6.1 The HSQC 2D-NMR spectrum of eudesmacarbonate (1).

Appendix 6.2: Day 1 percent mortality data for eudesmacarbonate (1) and controls.

Exposure Condition	Negative Control	PbTx-2		Compound 1		
Concentration (μM)	0.0	0.0045	0.0223	9.4	38	94
Number of dead embryos in Replicate a	0	0	0	0	0	0
Number of dead embryos in Replicate b	0	0	0	0	0	0
Number of dead embryos in Replicate c	0	0	1	0	0	0
N* (total embryos on Day 0)	15	15	15	14	15	15
% M in Replicate a	0.0	0.0	0.0	0.0	0.0	0.0
% M in Replicate b	0.0	0.0	0.0	0.0	0.0	0.0
% M in Replicate c	0.0	0.0	20.0	0.0	0.0	0.0
Average % M	0.0	0.0	6.7	0.0	0.0	0.0
SD (% M)	0.0	0.0	11.5	0.0	0.0	0.0
SEM (\pm % M)	0.0	0.0	6.7	0.0	0.0	0.0
n (number of replicates test solutions)	3	3	3	3	3	3
% M = Percent Mortality SD = Standard Deviation SEM = Standard Error of the Mean						

Appendix 6.3: Day 2 percent mortality data for eudesmacarbonate (1) and controls.

Exposure Condition	Negative Control	PbTx-2		Compound 1		
Concentration (μM)	0.0	0.0045	0.0223	9.4	38	94
Number of dead embryos in Replicate a	0	0	0	0	0	0
Number of dead embryos in Replicate b	0	0	0	0	0	1
Number of dead embryos in Replicate c	0	0	1	0	0	0
N* (total embryos on Day 0)	15	15	15	14	15	15
% M in Replicate a	0.0	0.0	0.0	0.0	0.0	0.0
% M in Replicate b	0.0	0.0	0.0	0.0	0.0	20.0
% M in Replicate c	0.0	0.0	20.0	0.0	0.0	0.0
Average % M	0.0	0.0	6.7	0.0	0.0	6.7
SD (% M)	0.0	0.0	11.5	0.0	0.0	11.5
SEM (\pm % M)	0.0	0.0	6.7	0.0	0.0	6.7
n (number of replicates test solutions)	3	3	3	3	3	3
% M = Percent Mortality SD = Standard Deviation SEM = Standard Error of the Mean						

Appendix 6.4: Day 3 percent mortality data for eudesmacarbonate (1) and controls.

Exposure Condition	Negative Control	PbTx-2		Compound 1		
Concentration (μM)	0.0	0.0045	0.0223	9.4	38	94
Number of dead embryos in Replicate a	0	0	0	0	0	0
Number of dead embryos in Replicate b	0	0	0	0	0	1
Number of dead embryos in Replicate c	0	0	5	0	0	0
N* (total embryos on Day 0)	15	15	15	14	15	15
% M in Replicate a	0.0	0.0	0.0	0.0	0.0	0.0
% M in Replicate b	0.0	0.0	0.0	0.0	0.0	20.0
% M in Replicate c	0.0	0.0	100.0	0.0	0.0	0.0
Average % M	0.0	0.0	33.3	0.0	0.0	6.7
SD (% M)	0.0	0.0	57.7	0.0	0.0	11.5
SEM (\pm % M)	0.0	0.0	33.3	0.0	0.0	6.7
n (number of replicates test solutions)	3	3	3	3	3	3
% M = Percent Mortality SD = Standard Deviation SEM = Standard Error of the Mean						

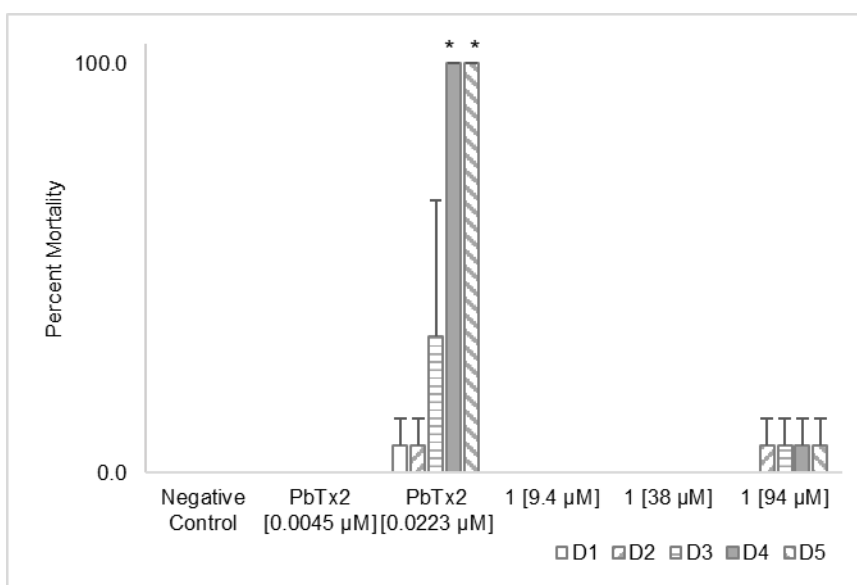
Appendix 6.5: Day 4 percent mortality data for eudesmacarbonate (1) and controls.

Exposure Condition	Negative Control	PbTx-2		Compound 1		
Concentration (μM)	0.0	0.0045	0.0223	9.4	38	94
Number of dead embryos in Replicate a	0	0	5	0	0	0
Number of dead embryos in Replicate b	0	0	5	0	0	1
Number of dead embryos in Replicate c	0	0	5	0	0	0
N* (total embryos on Day 0)	15	15	15	14	15	15
% M in Replicate a	0.0	0.0	100.0	0.0	0.0	0.0
% M in Replicate b	0.0	0.0	100.0	0.0	0.0	20.0
% M in Replicate c	0.0	0.0	100.0	0.0	0.0	0.0
Average % M	0.0	0.0	100.0	0.0	0.0	6.7
SD (% M)	0.0	0.0	0.0	0.0	0.0	11.5

SEM (\pm % M)	0.0	0.0	0.0	0.0	0.0	6.7
n (number of replicates test solutions)	3	3	3	3	3	3
% M = Percent Mortality SD = Standard Deviation SEM = Standard Error of the Mean						

Appendix 6.6: Day 5 percent mortality data for eudesmacarbonate (1) and controls.

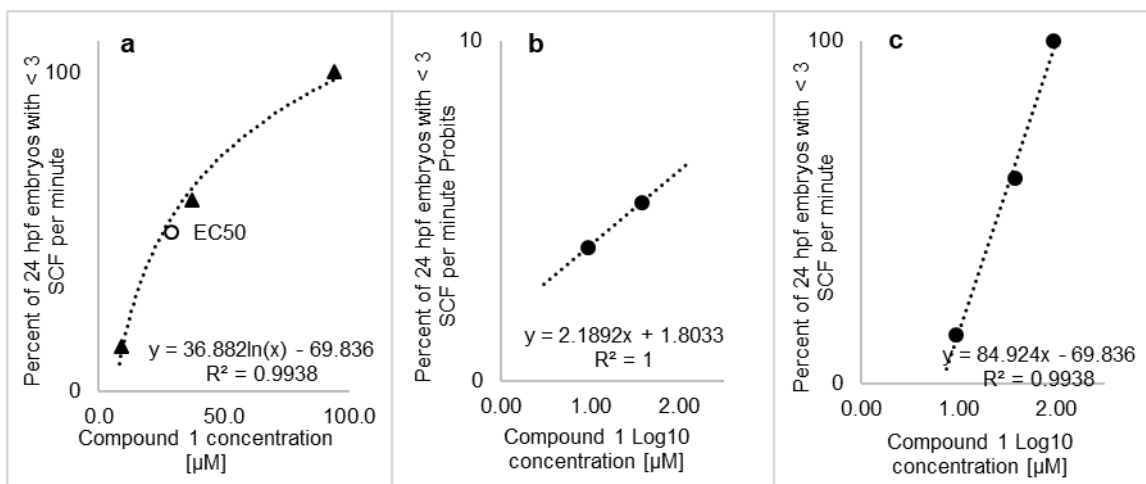
Exposure Condition	Negative Control	PbTx-2		Compound 1		
Concentration (μ M)	0.0	0.0045	0.0223	9.4	38	94
Number of dead embryos in Replicate a	0	0	5	0	0	0
Number of dead embryos in Replicate b	0	0	5	0	0	1
Number of dead embryos in Replicate c	0	0	5	0	0	0
N* (total embryos on Day 0)	15	15	15	14	15	15
% M in Replicate a	0.0	0.0	100.0	0.0	0.0	0.0
% M in Replicate b	0.0	0.0	100.0	0.0	0.0	20.0
% M in Replicate c	0.0	0.0	100.0	0.0	0.0	0.0
Average % M	0.0	0.0	100.0	0.0	0.0	6.7
SD (% M)	0.0	0.0	0.0	0.0	0.0	11.5
SEM (\pm % M)	0.0	0.0	0.0	0.0	0.0	6.7
n (number of replicates test solutions)	3	3	3	3	3	3
% M = Percent Mortality SD = Standard Deviation SEM = Standard Error of the Mean						



Appendix 6.7 Percent mortality of embryos per exposure condition of 1 and controls from Day 1 through Day 5. Error bars are \pm SEM (n = 3 replicates). The * denotes $p < 0.05$ significance derived by one-way ANOVA followed by the Tukey HSD multiple comparison test.

Appendix 6.8: 24-hpf spontaneous coiling frequency (SCF) data measured as the number of spontaneous coils per minute (cpm) observed per embryo for eudesmacarbonate (1) and controls.

Exposure Condition	Negative Control	PbTx-2		Compound 1			
Concentration (μM)	0.0	0.0045	0.0223	9.4	38	94	
Replicate a	embryo 1	6	6	5	5	3	0
	embryo 2	4	7	4	4	1	0
	embryo 3	3	10	1	6	0	0
	embryo 4	4	0	8	5	5	0
	embryo 5	4	4	5	-	2	0
Replicate b	embryo 1	4	4	4	5	0	0
	embryo 2	6	3	3	4	1	0
	embryo 3	6	4	5	2	3	0
	embryo 4	4	3	2	3	4	0
	embryo 5	4	3	3	2	2	0
Replicate c	embryo 1	9	4	4	4	3	0
	embryo 2	7	3	3	3	1	0
	embryo 3	6	3	3	4	0	0
	embryo 4	8	4	5	5	4	0
	embryo 5	8	4	-	3	0	0
Average SCF per minute	5.53	4.1	3.9	3.9	1.9	0	
SD (SCF per minute)	1.8	2.2	1.7	1.2	1.7	0	
SEM (\pm SCF per minute)	0.48	0.58	0.45	0.32	0.43	0	
n (total number of embryos)	15	15	14	14	15	15	
Number of abnormal embryos (< 3 SCF per minute)	0	0	2	2	9	15	
Percent abnormal embryos	0.0	0.0	14.3	14.3	60.0	100.0	
Probit values	NA	NA	3.93	3.93	5.25	NA	
ED ₅₀ by probit analysis (μM)	NA	NA		28.9			
ED ₅₀ by linear regression (μM)*	NA	NA		25.8			
SCF = Spontaneous Coiling Frequency SD = Standard Deviation SEM = Standard Error of the Mean *The ED ₅₀ value was extrapolated from the linear regression analysis of the Log ₁₀ concentration versus % abnormal (< 3 SCF per minute) plot.							



Appendix 6.9: Linear regression analysis of the percent of embryos exhibiting abnormal SCF per minute (% SCF) per treatment with 1 used to determine the ED₅₀ value: a Concentration versus % SCF, b Probit analysis and c Log₁₀ concentration versus % SCF.

Appendix 6.10: Day 2 heart rate (HR) data measured as beats per minute (bpm) for 1 and controls.

Exposure Condition		Negative Control	PbTx-2		Compound 1		
Concentration (μM)		0.0	0.0045	0.0223	9.4	38	94
Replicate a	embryo 1	140	160	148	144	144	132
	embryo 2	140	164	148	140	144	132
	embryo 3	148	168	148	144	144	108
	embryo 4	152	160	152	148	140	112
	embryo 5	148	152	156	148	136	116
Replicate b	embryo 1	144	156	152	152	140	108
	embryo 2	148	164	148	156	132	120
	embryo 3	152	152	156	156	140	124
	embryo 4	144	164	156	152	144	124
	embryo 5	148	168	160	156	148	128
Replicate c	embryo 1	140	164	164	152	148	120
	embryo 2	148	152	152	156	144	124
	embryo 3	144	160	160	152	144	124
	embryo 4	152	156	156	156	140	120
	embryo 5	152	164	-	-	140	-
Average Day 2 HR (bpm)		5.53	146.7	160.3	154.0	150.9	141.9
SD (bpm)		1.8	4.5	5.5	5.1	5.3	4.2
SEM (\pm bpm)		0.48	1.1	1.4	1.4	1.4	1.1
n (total number of embryos)		15	15	14	14	15	14
Number of abnormal embryos (D2 HR bpm <140, >152)		0	12	7	5	2*	15
Percent abnormal embryos		0.0	80.0	50.0	35.7	13.3*	100.0
Probit values		NA	5.84	5.0	NA	NA	NA
ED ₅₀ by probit analysis (μM)		NA	0.0223		NA*		
HR = Heart Rate SD = Standard Deviation SEM = Standard Error of the Mean NA = Not Applicable *The observed data were too variable to determine the ED ₅₀ value of 1.							

Appendix 6.11: Day 3 heart rate (HR) data measured as per minute (bpm) for 1 and controls.

Exposure Condition	Negative Control	PbTx-2		Compound 1		
Concentration (μM)	0.0	0.0045	0.0223	9.4	38	94
Replicate a	embryo 1	194	160	148	144	132
	embryo 2	188	164	148	140	132
	embryo 3	190	168	148	144	108
	embryo 4	192	160	152	148	112
	embryo 5	196	152	156	148	116
Replicate b	embryo 1	200	156	152	152	108
	embryo 2	198	164	148	156	120
	embryo 3	202	152	156	156	124
	embryo 4	192	164	156	152	124
	embryo 5	194	168	160	156	128
Replicate c	embryo 1	188	164	164	152	120
	embryo 2	192	152	152	156	124
	embryo 3	198	160	160	152	124
	embryo 4	194	156	156	156	120
	embryo 5	200	164	-	-	140
Average Day 3 HR (bpm)	5.53	194.5	160.3	154.0	150.9	141.9
SD (bpm)	1.8	4.4	5.5	5.1	5.3	4.2
SEM (\pm bpm)	0.48	1.1	1.4	1.4	1.4	1.1
n (total number of embryos)	15	15	15	14	15	14
Number of abnormal embryos (D3 HR bpm <188, >202)	0	14	9	7	15	14
Percent abnormal embryos	0.0	93.3	90.0	50.0	100.0	100.0
Probit values	NA	6.50	6.28	5.0	NA	NA
ED ₅₀ by probit analysis (μM)	NA	NA*		9.4		
HR = Heart Rate SD = Standard Deviation SEM = Standard Error of the Mean NA = Not Applicable *The data were too limited and variable to determine the ED ₅₀ value of PbTx-2.						

Appendix 6.12: Day 5 percent swim bladder dysfunction (SBD) measured as the number of embryos exhibiting irregular swim bladder inflation per exposure condition of eudesmacarbonate (1) and controls.

Exposure Condition	Negative Control	PbTx-2		Compound 1		
Concentration (μM)	0.0	0.0045	0.0223	9.4	38	94
Number abnormal embryos Replicate a	0	5	5	2	4	5
Number abnormal embryos Replicate b	0	5	5	2	3	5
Number abnormal embryos Replicate c	0	5	5	2	4	5
N (total number of embryos Day 0)	15	15	15	14	15	15
% SBD Replicate a	0.0	100.0	100.0	50.0	80.0	100.0
% SBD Replicate b	0.0	100.0	100.0	40.0	60.0	100.0
% SBD Replicate c	0.0	100.0	100.0	40.0	80.0	100.0
Average Percent SBD (%)	0.0	100.0	100.0	43.3	73.3	100.0
SD (% SBD)	0.0	0.0	0.0	5.8	11.5	0.0
SEM (\pm % SBD)	0.0	0.0	0.0	3.3	6.7	0.0
n (number of replicates test solutions)	3	3	3	3	3	3
Probit values	NA	NA	NA	4.83	5.62	NA

ED ₅₀ by probit analysis (μM)	NA	NA	12.7
ED ₅₀ by linear regression analysis (μM)	NA	NA	12.9
SBD = Swim Bladder Dysfunction SD = Standard Deviation SEM = Standard Error of the Mean *The ED ₅₀ value was extrapolated from the linear regression analysis of the Log ₁₀ concentration versus % SBD plot. Note: Dead embryos observed on Day 5 were assessed as abnormal for comparative analysis against the number of normal test subjects at Day 0.			

Appendix 6.13: Day 5 percent of embryos exhibiting aberrant swimming behaviors (ASB) data for eudesmacarbonate (1) and controls.

Exposure Condition	Negative Control	PbTx-2		Compound 1		
Concentration (μM)	0.0	0.0045	0.0223	9.4	38	94
Number abnormal embryos Replicate a	0	5	5	2	4	5
Number abnormal embryos Replicate b	0	5	5	2	3	5
Number abnormal embryos Replicate c	0	5	5	2	4	5
N (total number of embryos Day 0)	15	15	15	14	15	15
% ABS Replicate a	0.0	40.0	100.0	50.0	80.0	100.0
% ABS Replicate b	0.0	40.0	100.0	60.0	80.0	100.0
% ABS Replicate c	0.0	40.0	100.0	60.0	80.0	100.0
Average Percent ASB (%)	0.0	40.0	100.0	56.7	80.0	100.0
SD (% ASB)	0.0	0.0	0.0	5.8	0.0	0.0
SEM (± % ASB)	0.0	0.0	0.0	3.3	0.0	0.0
n (number of replicates test solutions)	3	3	3	3	3	3
Probit values	NA	4.75	NA	5.17	5.84	NA
ED ₅₀ by probit analysis (μM)	NA	NA*		6.6		
ED ₅₀ by linear regression analysis (μM)**	NA	NA*		6.6		
ASB = Aberrant Swimming Behaviors SD = Standard Deviation SEM = Standard Error of the Mean *The data were too limited to determine the ED ₅₀ value for PbTx-2. **The ED ₅₀ value was extrapolated from the linear regression analysis of the Log ₁₀ concentration versus % ABS plot. Note: Dead embryos observed on Day 5 were assessed as abnormal for comparative analysis against the number of normal test subjects at Day 0.						

VITA

CHRISTINA A. LYDON

Born: Hackensack, New Jersey

- 1995 B.S., Chemistry, cum laude
University of Massachusetts-Dartmouth
North Dartmouth, Massachusetts
- 1997 M.S., Chemistry
University of Massachusetts-Dartmouth
North Dartmouth, Massachusetts
- 1997-2007 Pfizer, Inc. Associate Scientist II
Groton, Connecticut
- 2005 Regulatory Affairs/Quality Assurance Graduate Certificate
Temple University Graduate School of Pharmacy
Philadelphia, Pennsylvania
- 2008-2010 Educator Preparative Institute Graduate Certificate
Indian River State College
Fort Pierce, Florida
- 2008-2012 Adjunct Professor, Chemistry
Indian River State College
Fort Pierce, Florida
- 2012-2020 Doctoral Candidate, Teaching Assistant, Research Assistant
Florida International University
Miami, Florida

AWARDS

Indian River State College Instructional Certificate CHEMISTRY (2023 expiry)
FIU UGS Dissertation Year Fellowship Award (Spring 2018)
Indian River State College Adjunct of the Year Nominee (2012)
Pfizer Outstanding Leadership, Teamwork and Community Values Impact Award (2005)
UMassDartmouth-Chemistry Graduate Teaching Assistant Award (1997)
UMassDartmouth-Chemistry Academic Achievement Award (1993, 1994, and 1995)

PUBLICATIONS AND PRESENTATIONS

Lydon CA, Eskelinen HC, Mejia-Fava JC, Collado-Vides L, Berry JP. (in preparation)
Bioassay-guided inquest of a marine filamentous cyanobacterial assemblage associated

with intoxications of captive bottlenose dolphins (*Tursiops truncatus*) in the Florida Keys using zebrafish (*Danio rerio*) models of neurotoxicity. *Harmful Algae*

Lydon CA, Sanchez J, Mathivathanan L, dos Santos L, Sauvage T, Gunasekera S, Paul VJ, Berry JP. (submitted) Eudesmacarbonate an eudesmane-type sesquiterpene from marine cyanobacterial mat (Oscillatoriales) in the Florida Keys. *Journal of Natural Products*

Haq M, Gonzalez N, Mintz K, Jaja-Chimedza A, De Jesus CL, Lydon C, Welch AZ, Berry JP. Teratogenicity of Ochratoxin A and the Degradation Product, Ochratoxin α , in the Zebrafish (*Danio rerio*) Embryo Model of Vertebrate Development. *Toxins*. 2016; 8(2):40. doi:10.3390/toxins802004

Lydon CA. 2015. A Grim Reaper? Ochratoxin. Oral presentation at: Science and Suds Club of the FIU Marine Science Program at Biscayne Bay Campus; October 30, 2015; FIU-BBC, North Miami, FL.

Lydon CA, Liu S, Brand L, Berry JP. Identification of cyanobacterial toxins involved in the apparent intoxication of dolphins in the Florida Keys. Poster presented at: 7th Symposium on Harmful Algae in the US; October 27-31, 2013; Sarasota, FL.

Lydon C, Schenk E, DeBord JD, Smotherman M, Fernandez-Lima F. MSI MALDI-MS for Direct Lipid Profiling of Intact Tissues. *Microscopy and Microanalysis*. 2013; 19(S2):682-683. doi:10.1017/S1431927613005400

Lydon C, DeBord JD, Fernandez-Lima F. Analysis of complex mixtures of heteroatom hydrocarbons using TIMS-MS. *Preprints - American Chemical Society, Division of Energy & Fuels*. 2013;58(1):949.

Lydon C, Schenk E, DeBord JD, Smotherman M, and Fernandez-Lima F. MSI MALDI-MS for Direct Lipid Profiling of Intact Tissues. Poster presented at: Microscopy and Microanalysis 2013. A07 Mass Spectrometry Imaging (MSI): Applications, Current Challenges and Perspectives; August 4-8, 2013; Indianapolis, IN.

Schenk E, DeBord JD, Lydon C, McKenzie A, Fernandez-Lima F. High resolution gas-phase, MS-based post-ionization separation for molecular imaging and conformational dynamics. Poster presented at: FIU Forensic Workshop 2013; March 13-15, 2013; FIU, Miami, FL.

Wood CA, Lee K, Vaisberg AJ, Kingston DG, Neto CC, Hammond GB (2001) "A Bioactive Spirolactone Iridoid and Triterpenoids from *Himatanthus Sucuuba*." *Chem. Pharm. Bull.* 2001;49(11):1477-1478.